THE ZERO CAVITY AND DPV WALL PROJECT

Canada Mortgage and Housing Corporation, the Federal Government's housing agency, is responsible for administering the National Housing Act.

This legislation is designed to aid in the improvement of housing and living conditions in Canada. As a result, the Corporation has interests in all aspects of housing and urban development and growth and development.

Under Part IX of the Act, the Government of Canada provides funds to CMHC to conduct research into the social, economic and technical aspects of housing and related fields, and to undertake the publishing and distribution of the results of this research. CMHC therefore has a statutory responsibility to make available information that may be useful in the improvement of housing and living conditions.

This publication is one of the many items of information published by CMHC with the assistance of federal funds.

Disclaimer

This study was conducted by the Building Engineering Group, University of Waterloo, for Canada Mortgage and Housing Corporation under Part IX of the National Housing Act. The analysis, interpretation, and recommendations are those of the consultants and do not necessarily reflect the views of Canada Mortgage and Housing Corporation or those divisions of the Corporation that assisted in the study and its publication.

Executive Summary

Background

In cold climates multi-layer wall systems are almost mandatory if an effective building envelope is desired. Multi-layer wall systems, especially for low-rise residential buildings, often employ a brick veneer as the outermost screen against environmental factors such as the rain and sun.

One of the most important and problematic functions of walls is the control of moisture penetration. Various strategies are used for moisture control in exterior walls. The popular brick veneer "rainscreen" wall system uses an exterior brick wythe to resist water and a cavity and water barrier to drain any water that penetrates the brick screen. The provision of a clear cavity and effective drainage in this form of construction is an important, if not critical, issue for moisture control. In field surveys it has been found that many cavities are obstructed by mortar dams and crossed by mortar bridges. Ensuring a clear cavity presently depends largely on the mason and the level of quality control during construction. If this issue is to be resolved it is essential that the masons' job be made easier and that the quality control requirements be rendered feasible.

This project is a full-scale, field assessment of two alternative solutions to ensuring a clear cavity. One alternative involves filling the cavity with an air and water permeable fibrous insulation to reduce the effect of mortar droppings and mortar dams on the cavity (called the Zero-Cavity approach). The other alternative is to avoid blockage by preventing the mortar from entering the cavity space while at the same time ensuring the drainage, pressure-moderation, and ventilating capabilities of the cavity (called the DPV approach). A prototype of a unique insulated sheathing being developed by Dow Chemical Canada in conjunction with the Building Engineering Group was used in the DPV wall system. To provide a comparison with standard construction techniques, a Datum wall system with a clear cavity was also included in the study.

The report is a record of the project. The construction, instrumentation, and installation of the panels are documented. The data is collated and analyzed, and the results and their implications are then reported. At this stage it should be noted that this overall project, jointly funded by CMHC and Dow, turned out to be somewhat more ambitious and instructive than initially intended. The findings go well beyond the issue of mortar blockage and clear cavities.

Test Facility and Set-up

The project involved constructing and installing three pairs of full-scale panels in the Building Engineering Group's (BEG) natural exposure test facility (Beghut) located on the University of Waterloo campus. The panel locations and orientations in the Beghut are shown in Figure 1. Common to all panels was a gypsum board interior sheathing, a polyethylene vapour retarder, and a 2x4 wood stud frame filled with fiberglass batt insulation. Insulating sheathing was used in all three pairs of panels. Fiberglass insulating board and Tyvek™ housewrap were used in the Datum and Zero-Cavity panels. In the DPV panels, specially modified extruded polystyrene was placed over building paper. All the panels were clad with a face brick veneer. Figure 1 presents a horizontal cross section of each of the three panel types.

Test Program

Each panel was typically instrumented with 12 to 15 thermocouples for sensing temperature, 4 Delmhorst pins for measuring the wood moisture content of the framing, 6 relative humidity transmitters, and 7 to 9 pressure taps for sampling pressures (Figure 2). The panels were installed in July of 1991, three facing east and three facing west, and exposed to the environment of South-Western Ontario. After acclimatization, the panels and their environments were continuously monitored for fourteen months from November 1991. The interior conditions were maintained at 50 % relative humidity and 21 °C.

To establish specific characteristics of the performance of each panel, air leakage, water penetration, and pressure equalization tests were conducted using standard ASTM and CSGB procedures, where ever possible. The drainage of water within the wall assembly after it had penetrated the brickwork was studied in laboratory mockup tests.

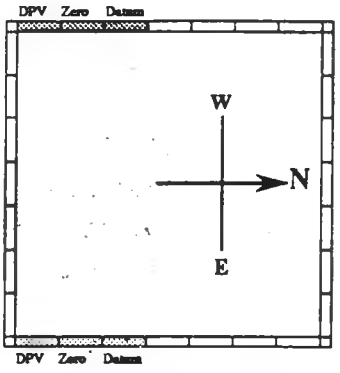

Panel Locations in Test Hut

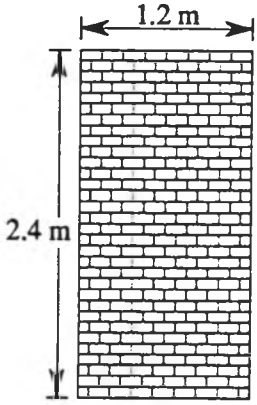

Panel Dimensions

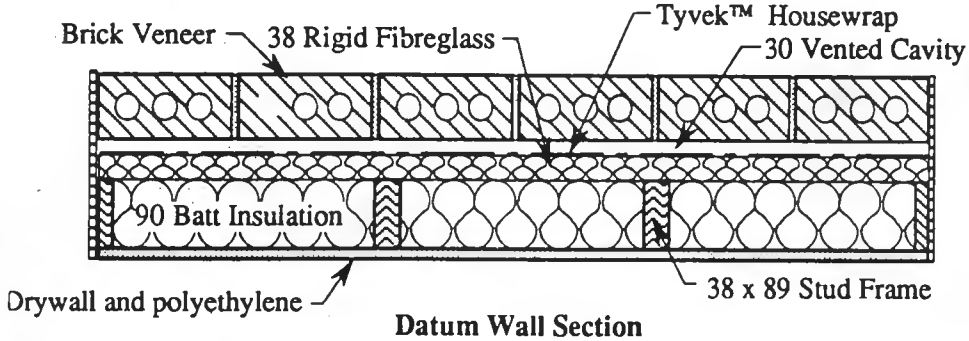

Datum Wall Section

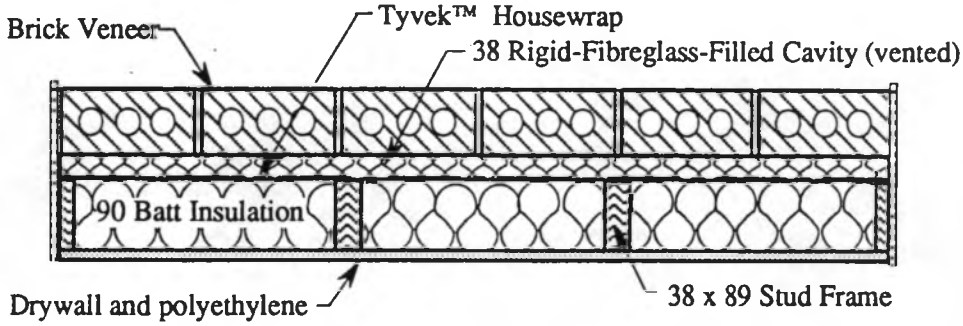

Zero-Cavity Wall Section

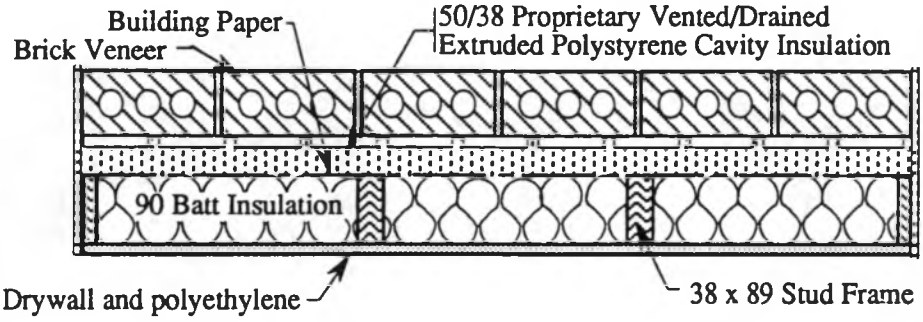

Drained-Pressure Equalized-Vented (DPV) Wall Section

Figure 1: Test Panels

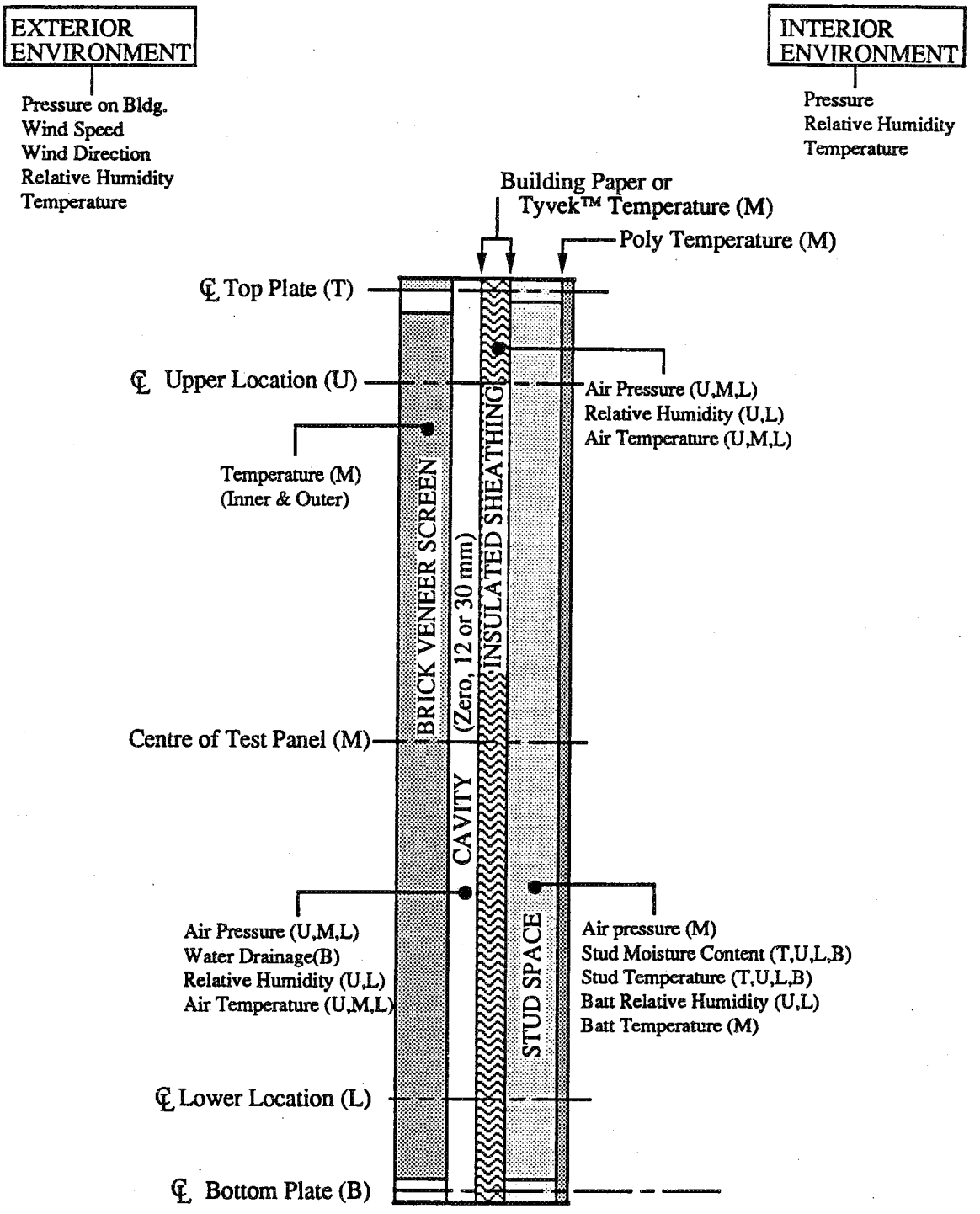

Note: Not to Scale. For precise dimensions and details see body of report.

Figure 2: Type and Location of Sensors

Results

In this project, the **Zero-Cavity** panel performed poorly. As is the case in typical walls, the brickwork veneer allowed significant amounts of rain water to penetrate into the cavity. The untreated glass fibre insulation retained some of this water by capillary action at its base. Solar-driven inward vapour drives during the summer and fall transported this retained moisture from the glass fibre cavity fill through the vapour-permeable Tyvek™ and resulted in saturated wood framing in the bottom of the stud space within the first year.

However, these problems were the result of the combination of the water permeability of the brick screen, the capillary retention characteristics of the glass fibre cavity fill, the very high vapour permeability of the Tyvek™, and the solar-induced inward vapour drive. Two of these factors can be easily resolved. The moisture retention characteristics of the glass fibre fill can be easily controlled by applying a hydrophobic treatment during the manufacture of the product; this is the case for all European products. An exterior layer of housewrap, sheathing, or building paper with less vapour permeance than the Tyvek™ can be used on the inside of the cavity fill to control inward vapour drives.

The performance of the **Datum** panels was often dominated by solar effects. The vapour drive from the cavity through the Tyvek™ and glass fibre insulating sheathing into the stud space created high wood moisture levels in late summer. Instrumentation indicated moisture contents of more than 20%, and temperatures over 15 °C for two weeks in the upper portion of one stud. Slight mold growth was subsequently found at this location when the panels were inspected at the end of the project. Drying of the framing occurred through the fall and winter. The use of the vapour-permeable Tyvek™ resulted in wall performance quite different from what one would expect if building paper had been used. The air barrier in the Datum panels was practically perfect; air leakage must be expected in typical walls and this will influence these conclusions.

The **DPV** panels performed very well. The restriction of water vapour transfer inwards by the less vapour-permeable EXPS sheathing in the DPV panels resulted in considerably more stable and lower stud space relative humidity levels in the summer, and more stable and slightly higher winter relative humidity levels than the other two pairs of panels. Physical inspection of the two panels (conducted after monitoring ended) found the general condition of the DPV panels to be excellent. As for all of the test panels, the air

barrier in the DPV panels was practically perfect. In reality, air leakage must be expected in typical walls and this will influence the above conclusions.

Some more general, wide-ranging conclusions which apply to the performance of many wall systems are presented below.

Mortar Control

Inspection after opening up of the panels revealed that the base of the Zero-Cavity panels was completely clean of mortar droppings and would allow unhindered drainage of any water reaching the base flashing of the panel. Despite the extraordinary precautions taken during construction, mortar projections occurred and mortar dropping were found at the base of the Datum panel cavities. While in this case the limited mortar blockage did not greatly impair drainage nor cause damage to the wall, it did highlight how difficult it is to provide a clear clean cavity in normal wall construction.

Drainage

The drainage system in all six panels performed well under the water penetration test conditions. The brickwork allowed a significant amount of water to penetrate through into the cavity. The application of a static pressure *across the wall* and the open vents had no noticeable effect on the water leakage. In the water penetration tests, the presence of the fibreglass cavity fill did not appear to effect the drainage of water in the Zero-Cavity panels. While the fibreglass cavity fill used in the Zero-Cavity wall was also found to drain water well in laboratory tests, capillary forces retained a small amount of water in the lower 50 to 75 mm. It took some time for this stored water to be removed by evaporation. The use of hydrophobic coatings is recommended to control this potentially damaging moisture storage.

Brick Veneer Water Permeance

Water penetration testing (using a modified ASTM standard) showed that the brick veneer screen on all six panels was, as confirmed by other field research, quite water permeable even when no pressure difference is applied across the screen. Drainage of water both outside and within the panels appeared to function well. It was established that, in spite of the fact that all panels were pressure-equalized rainscreen systems, significant amounts of moisture penetrated the brick veneer. In these tests, the presence of the fiberglass cavity fill did not appear to effect the drainage of water in the Zero-

Cavity panels. Special water penetration tests indicate that the penetration through the vent holes did not make a disproportionate contribution to the total penetration.

Thermal Performance

If exposed to the sun, the brick veneer screen undergoes large temperature changes during the course of the day during all times of the year. In the winter, the brick will tend to have an average temperature not far below freezing, with significant daily excursions above and below zero due to solar effects. Over both the summer and winter, the temperature of the east/west facing panels was about 5-7 °C higher than the average ambient temperature. This temperature difference has a dramatic effect on the inner layers of each wall and affects condensation potential, moisture storage and transmission, energy consumption, material durability, and thermal conditions.

The air in the cavity of all panels remained warmer than the brick and at least 6 °C warmer than the average ambient temperature. There was also no pattern of measurable vertical temperature stratification within the cavity. The cavity temperature closely followed the temperature of the back of the brick, even during fast, solar-induced, temperature changes. As suggested by theory, it is practically impossible for sufficient air flow through the masonry vents to remove solar heat gains from the cavity. The amount of water vapour in the cavity was not strongly related to the moisture content of the exterior air. As the temperature increased, the amount of moisture in the cavity air increased, indicating evaporation and desorption of moisture. No conclusions could be made regarding the influence of ventilation on the moisture content of the air in the cavity (and hence its drying ability) because ventilation flow could not be measured with the test setup.

Pressure Moderation Performance

The effectiveness of the moderation of pressure differences across the screen in one-storey buildings, as well as low and high-rise construction, needs further study. Many more pressure moderation measurements using repeatable, quantitative test procedures are necessary. The wind pressures experienced by exposed low-rise construction are generally quite low (less than 20 Pa) and higher pressures (greater than 50 Pa) occur very rarely. The variation in wind pressure with height had a relatively large effect on pressures and pressure moderation in the test panels. Spatial variations near building corners were found to result in significantly different pressure conditions. Based on the

data we recorded, none of the panels were fully pressure equalized for any record at any frequency.

The wind can be considered as being composed of the addition of a mean component and a rapidly varying component. The Datum and Zero-Cavity panels moderated from 20 to 50% of the variable pressure differences across the screen, i.e., they were 20 to 50% "pressure equalized", at 0.2 Hz. The degree of pressure moderation decreased with increasing frequency. The mean values (of one minute records) indicated that the panels moderated more than 90% of the difference across the screen. It also appears that mean pressures or mean pressure differences have limited relevance to the actual response of the cavity pressure to the wind. Both the water permeance of brick veneer screens, especially under dynamically-varying, low-pressure differences, and the incidence and coincidence of rain and wind effects need to be given more study and attention.

Housewrap / Building Paper

As far as the housewrap / building paper is concerned, placing it between the insulated sheathing and the batt insulation protects it from temperature extremes and large variations in all seasons. Support given to an air barrier, housewrap, or building paper by attachment to rigid insulation or placement between two relatively stiff layers was found to have a significant beneficial effect on airtightness. Relatively air tight housewrap and building paper layers are desirable because they reduce convective heat losses from the low-density batt insulation, reduce the effective volume of the pressure equalization chamber, and provide a second plane of airflow resistance in the event the primary air barrier is or becomes defective. Housewrap should only be used when well adhered to a stiff substrate and fully taped. It is strongly recommended that the use of housewrap, in particular its location, vapour permeance, and intended purpose, be carefully considered in the future.

Mean Values

It is clear from this field monitoring that consideration of mean values does not reflect the effect of daily variations, especially those due to solar radiation, in lightweight framed wall assemblies. Daily peak values may play an important role in the actual performance of the wall. As has been found in other studies, hourly readings are important for a full understanding of the behaviour of the lightweight framed wall assemblies typically used in North American residential construction.

Conclusions and Recommendations

In this project, the Zero-Cavity panel performed poorly. Spring and summer diffusion of moisture from the fiberglass-filled cavity produced saturated wood framing in the bottom of the stud space. However, this was the result of the combination of the water permeability of the brick screen, the moisture retention characteristics of the fiberglass cavity fill, the vapour permeability of the Tyvek™, and the solar-induced inward vapour drive. Two of these factors can be easily resolved. It is recommended that only hydrophobically-treated fibrous insulations and sheathing or sheathing paper with sufficient vapour resistance be used in the future.

Despite the problems caused by the use of standard materials in a non-standard way, this work confirmed that the zero-cavity concept is essentially sound and offers benefits such as better assurance of drainage, thinner wall sections, support and protection of the sheathing paper / housewrap, and possibly better pressure moderation. Decades of successful and widespread use of this form of construction in Scandinavia and Europe provides some assurance that, with proper materials and construction, fibrous cavity fills can improve the field performance of multi-wythe rainscreen walls.

Acknowledgments

Thanks are due to many individuals and organizations for their participation and cooperation during this project. Canada Mortgage and Housing Corporation and Dow Chemical Canada Inc. for their initiative, financial support and patience. In particular, Mr. Jacques Rousseau has been a supportive and constructive project manager for CMHC. David Greely, Cecile Mutton, and Linda Kenworthy of Dow have also contributed.

Dr. Ewart Brundrett has been a continual source of assistance and information and his consulting involvement is greatly appreciated. Special thanks are extended to Peter Sloof for his great contribution during the construction and installation of the test panels. Peter also wrote the first interim report and the Construction and Installation report which forms the basis of Chapter 2.

The following individuals at the University of Waterloo need to be thanked for their willing assistance:

Mr. Ralph Korchensky	-Structures Laboratory, University of Waterloo
Ms. Amanda Reynolds	-Graduate Student, University of Waterloo
Mr. Terry Ridgeway	-Structures Laboratory, University of Waterloo
Mr. David Walsh	-Structures Laboratory, University of Waterloo
Mr. Oscar Szoczei	-Structures Laboratory, University of Waterloo
Mr. Jeff Dibattista	-Research Assistant, University of Waterloo

Special thanks are also due to:

Fiberglass Canada	-who supplied insulation materials
G&A Masonry Ltd.	-who undertook the masonry work

The Ontario Masonry Industries Promotion Fund provided supplementary funding to cover brick-related labour costs. Garth Miller's assistance is appreciated.

Résumé

Contexte

En climat froid, les murs multicouches sont presque essentiels pour que l'enveloppe d'un bâtiment soit efficace. Les murs multicouches, surtout ceux qui sont destinés aux bâtiments résidentiels de faible hauteur, ont souvent le placage de brique comme ultime revêtement extérieur faisant écran entre l'intérieur et des éléments climatiques comme la pluie et le soleil.

L'une des fonctions les plus importantes et les plus complexes des murs extérieurs est d'empêcher l'infiltration d'humidité. Diverses stratégies sont utilisées pour y parvenir. Le très populaire «écran pare-pluie» est composé d'un placage de brique extérieur qui résiste à l'eau ainsi que d'une cavité et d'un pare-pluie qui favorisent l'évacuation de l'eau qui parvient à traverser l'écran de brique. Pour bien maîtriser l'humidité avec ce genre de construction, il est important, voire essentiel, que la cavité soit libre et que l'évacuation de l'eau soit efficace. Lors d'études en service, on s'est aperçu que les cavités sont souvent obstruées partiellement ou totalement par des bavures de mortier. Pour que la cavité soit libre, il revient donc au maçon d'abord et aux inspecteurs de chantier ensuite de prendre les précautions qui s'imposent dès la construction. Il est primordial que le travail du maçon soit facilité et que les exigences en matière de contrôle de la qualité soient réalistes.

Cette étude sur le terrain à grande échelle porte sur deux solutions de rechange permettant de réaliser des cavités exemptes de tout obstacle. L'une de ces solutions consiste à remplir la cavité avec un isolant fibreux perméable à l'air et à l'eau dans le but de réduire les problèmes causés par les éclaboussures de mortier (une méthode dite «sans cavité»). L'autre consiste à éviter l'obturation en empêchant le mortier de pénétrer dans la cavité tout en conservant à la cavité ses propriétés de drainage, de modération de la pression et de ventilation (la méthode DMV). Le prototype d'un revêtement d'ossature isolant unique en cours de développement par Dow Chemical Canada en collaboration avec le Building Engineering Group a été utilisé pour réaliser le mur DMV. L'étude a aussi porté sur un mur de référence, doté d'une cavité libre, afin d'effectuer des comparaisons avec les techniques de construction standards.

Le présent rapport fait état de cette étude comparative. La construction et la pose des panneaux ainsi que la mise en place d'instruments y sont documentées. Les données sont rassemblées et analysées et les résultats ainsi que leurs incidences sont commentés. Il faut noter à ce stade que cette étude, financée conjointement par la SCHL et la société Dow, s'est avérée plus ambitieuse et

instructive que prévu. Les conclusions qu'il est possible d'en tirer vont bien au-delà de la seule obstruction des cavités.

Installation d'essai et préparation

Cette étude a nécessité la construction et la mise en place de trois paires de panneaux en vraie grandeur dans l'installation d'essai en exposition naturelle du Building Engineering Group située sur le campus de l'université de Waterloo. L'emplacement et l'orientation des panneaux dans l'installation d'essai sont illustrés à la Figure 1. Tous les panneaux avaient en commun un revêtement de finition intérieur en plaques de plâtre, un pare-vapeur en polyéthylène et une ossature en poteaux de 2 x 4 po entre lesquels on avait placé un isolant de fibre de verre en matelas. Un revêtement d'ossature isolant a été employé pour les trois paires de panneaux. Des panneaux isolants en fibre de verre et une membrane d'étanchéité Tyvek™ ont été utilisés pour les panneaux de référence et sans cavité. Dans le cas des panneaux DMV, on a placé du polystyrène extrudé spécialement modifié par-dessus le papier de construction. Tous les panneaux ont été revêtus d'un placage de brique. La Figure 1 présente une coupe horizontale de chacun des trois types de panneau.

Programme d'essai

Chaque panneau a été équipé de 12 à 15 thermocouples destinés à capter la température, de 4 pointes Delmhorst pour mesurer l'humidité du bois d'ossature, de 6 transmetteurs d'humidité relative et de 7 à 9 prises de pression permettant l'échantillonnage des pressions (Figure 2). Les panneaux ont été mis en place au mois de juillet 1991, trois donnant sur l'est, trois donnant sur l'ouest, et ils ont été exposés au climat du sud-ouest de l'Ontario. Après une période d'acclimatation, les panneaux et le milieu dans lequel ils se trouvaient ont fait l'objet d'un contrôle constant pendant 14 mois à compter de novembre 1991. Les conditions intérieures ont été maintenues à une humidité relative de 50 % et à une température de 21 °C.

Afin d'établir des caractéristiques de performance précises pour chaque panneau, des essais de perméabilité à l'air, d'infiltration d'eau et d'équilibrage de pression ont été menés, chaque fois que c'était possible, conformément aux méthodes standards de l'ASTM et de l'ONGC. L'évacuation de l'eau à l'intérieur des murs après qu'elle ait traversé le placage de brique a été étudiée lors de simulations en laboratoire.

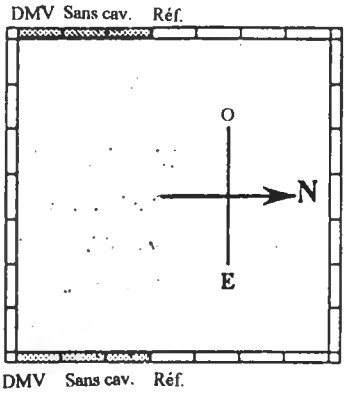

Emplacement des panneaux dans l'installation d'essai

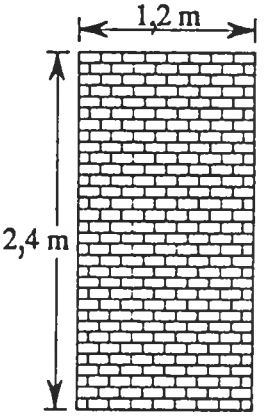

Dimensions des panneaux

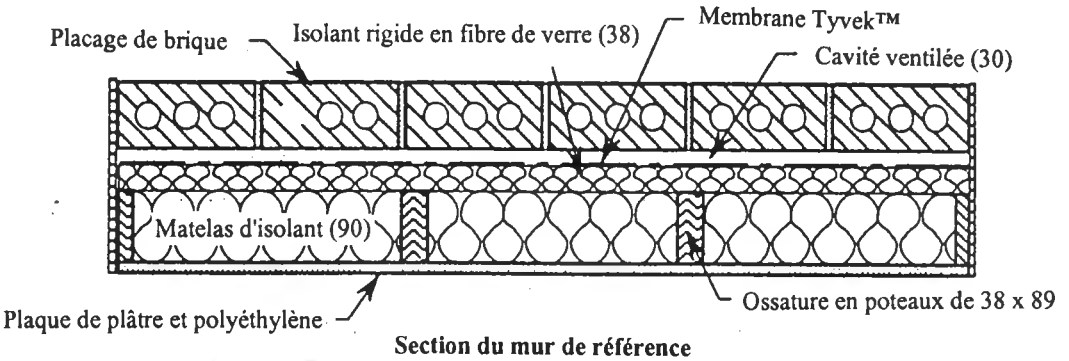

Section du mur de référence

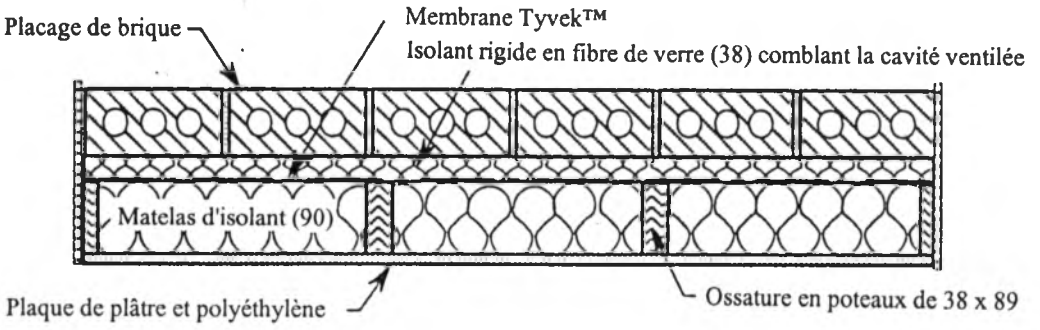

Section du mur sans cavité

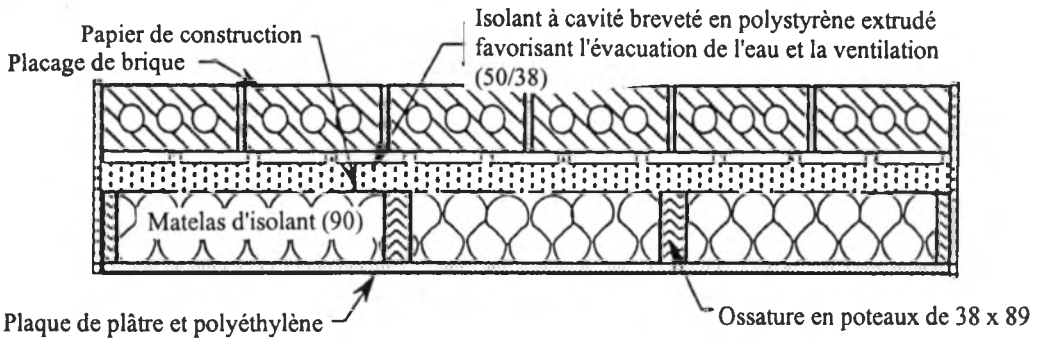

Section du mur de drainage, de régulation de la pression et de ventilation (DMV)

Figure 1 : Panneaux d'essai

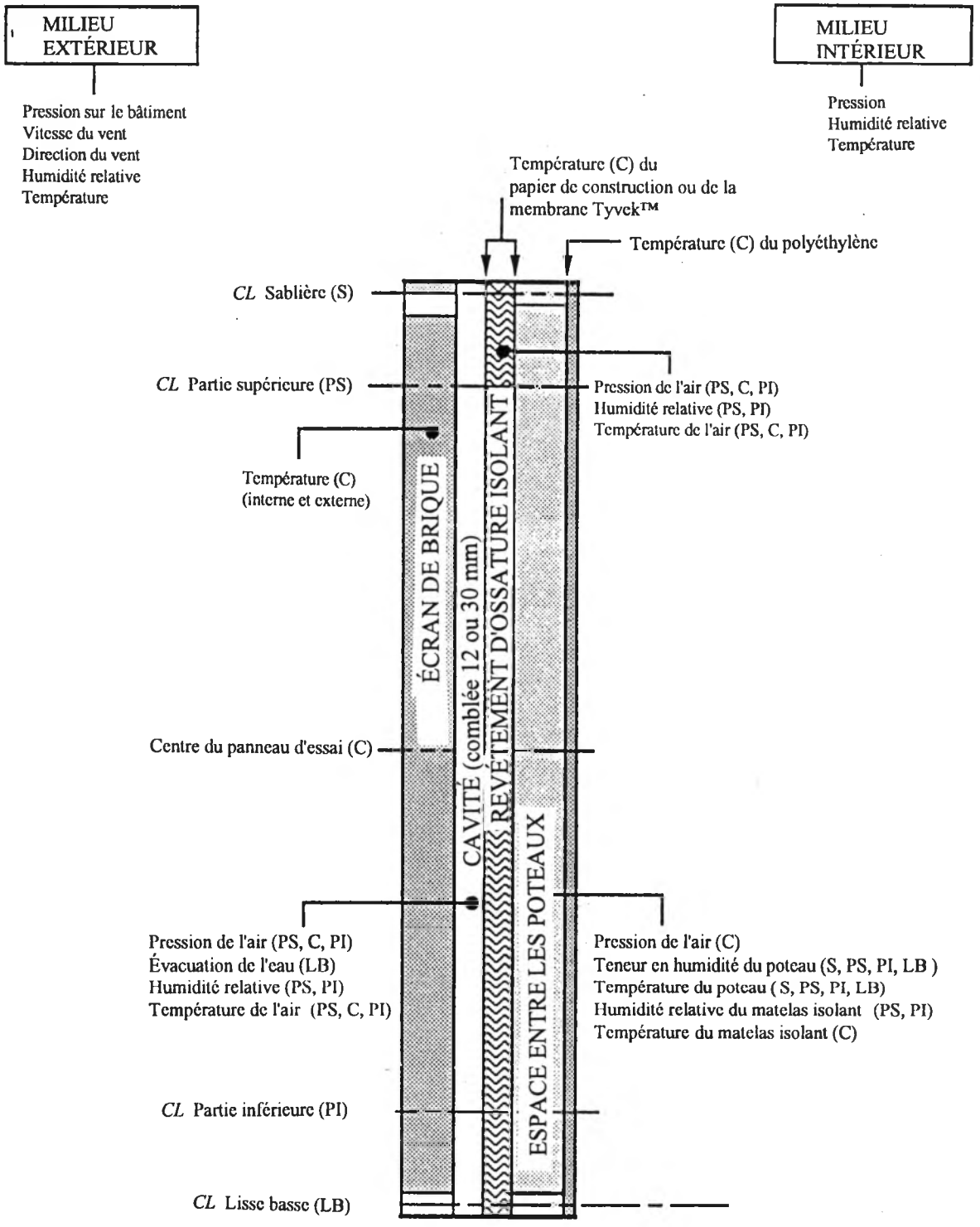

Nota : N'est pas à l'échelle. Pour connaître les dimensions et les détails précis, voir le corps du rapport.

Figure 2 : Type et emplacement des capteurs

Résultats

Au cours de cette étude, le **panneau sans cavité** a été peu efficace. Comme c'est le cas pour la plupart des murs ordinaires, le placage de brique a permis l'infiltration d'une quantité appréciable d'eau de pluie dans la cavité. L'isolant de fibre de verre non traité a retenu une partie de cette eau à sa base, par action capillaire. Au cours de l'été et de l'automne, la vapeur qui s'est formée à l'intérieur du mur par suite du rayonnement solaire a fait passer cette humidité emprisonnée de l'isolant de fibre de verre comblant la cavité à travers la membrane Tyvek™ perméable à la vapeur, ce qui a occasionné une saturation de l'ossature de bois, au bas de l'espace entre les poteaux, durant la première année.

Toutefois, ces problèmes découlaient d'un ensemble de facteurs, à savoir la perméabilité à l'eau de l'écran de brique, les caractéristiques de rétention capillaire de l'isolant de fibre de verre remplissant la cavité, la haute perméabilité à la vapeur de la membrane Tyvek™ et la production de vapeur par le rayonnement solaire. Deux de ces problèmes peuvent facilement être résolus. Les caractéristiques de rétention d'humidité de la fibre de verre comblant la cavité peuvent être modifiées aisément par l'application d'un traitement hydrophobe lors de la fabrication du produit. C'est d'ailleurs le cas de tous les produits européens. On peut également appliquer une membrane d'étanchéité, un revêtement d'ossature ou du papier de construction moins perméable à la vapeur que la membrane Tyvek™ sur la surface interne de la fibre de verre remplissant la cavité afin de prévenir l'infiltration de vapeur.

La performance des **panneaux de référence** a souvent été dominée par les effets du soleil. La vapeur produite dans la cavité et qui traverse la membrane Tyvek™ et le revêtement d'ossature isolant en fibre de verre pour aboutir entre les poteaux d'ossature a entraîné une élévation du taux d'humidité du bois à la fin de l'été. Les instruments ont indiqué un taux d'humidité de plus de 20 % et des températures de plus de 15 °C pendant deux semaines dans la partie supérieure d'un poteau. À la fin de l'étude, on a constaté une légère présence de moisissure à cet endroit lorsque les panneaux ont été inspectés. L'ossature a séché durant l'automne et l'hiver. La performance des murs revêtus de la membrane perméable à la vapeur Tyvek™ a été très différente de celle que l'on aurait pu obtenir avec du papier de construction. Le pare-air des panneaux de référence était pratiquement parfait; des fuites d'air sont toutefois normales dans le cas de murs typiques et cette caractéristique va influer sur les conclusions de cette étude.

Les **panneaux DMV** ont offert une très bonne performance. Comme la membrane en polystyrène extrudé utilisée pour ces panneaux est moins perméable à la vapeur d'eau, elle l'empêche d'atteindre les poteaux d'ossature et, de ce fait, favorise des taux d'humidité relative plus stables et moins élevés en été et des taux d'humidité relative plus stables et légèrement plus élevés en hiver que les deux autres paires de panneaux. Une inspection des deux panneaux (menée après la phase de contrôle) a permis de constater que les panneaux DMV étaient en excellent état. Comme pour tous les panneaux d'essai, le pare-air des panneaux DMV était pratiquement parfait. Dans la réalité, il est normal d'observer des infiltrations d'air dans les panneaux courants, un facteur qui devra être pris en considération dans l'analyse des conclusions précédentes.

Nous présentons ci-dessous des conclusions générales de plus grande portée susceptibles de s'appliquer à la performance d'un bon nombre de murs.

Application du mortier

L'inspection qui a suivi le démontage des panneaux a révélé que la base des panneaux sans cavité était complètement exempte d'éclaboussures de mortier et permettait une évacuation tout à fait libre de l'eau qui avait pu parvenir jusqu'au solin de base du panneau. Toutefois, malgré les précautions extraordinaires prises lors de la construction, les bavures de mortier n'ont pu être évitées dans les panneaux de référence et l'on a retrouvé des éclaboussures de mortier au bas de leurs cavités. Bien que, dans ce cas particulier, les éclaboussures n'aient pas trop nui à l'évacuation de l'eau ou endommagé le mur, elles ont montré à quel point il était difficile de réaliser une cavité totalement libre dans des conditions normales de construction.

Évacuation de l'eau

Le système d'évacuation utilisé pour les six panneaux s'est bien comporté lors de l'essai d'infiltration d'eau. La maçonnerie de brique a laissé entrer une importante quantité d'eau dans la cavité. L'application d'une pression statique *sur toute la surface du mur* et la présence d'orifices de ventilation libres n'ont eu aucun effet notable sur le passage de l'eau. Lors des essais d'infiltration d'eau, la fibre de verre remplissant la cavité n'a pas semblé modifier l'évacuation de l'eau à l'intérieur des panneaux sans cavité. Même si ce matériau a aussi favorisé l'évacuation de l'eau lors des essais en laboratoire des mêmes panneaux, des pressions d'ordre capillaire ont retenu une petite quantité d'eau au bas de la cavité sur une hauteur de 50 à 75 mm. Il a fallu un certain temps

pour que cette eau accumulée disparaisse par évaporation. L'usage d'un revêtement hydrophobe est suggéré afin de prévenir cette accumulation d'eau qui pourrait entraîner des dommages.

Perméance à l'eau du placage de brique

L'essai d'infiltration d'eau (effectué à partir d'une norme de l'ASTM modifiée) a montré que l'écran de brique des six panneaux muraux était, comme l'ont confirmé d'autres études en service, très perméable à l'eau même lorsque l'écran ne subissait aucune différence de pression. L'évacuation de l'eau, tant à l'extérieur qu'à l'intérieur des panneaux a semblé être efficace. On a établi que, en dépit du fait que tous les panneaux étaient des écrans pare-pluie à pression équilibrée, d'importantes quantités d'eau pouvaient s'infiltrer dans le placage de brique. Lors de ces essais, la présence de fibre de verre dans la cavité des panneaux sans cavité n'a pas semblé agir sur l'évacuation de l'eau. Des essais d'infiltration d'eau spéciaux ont révélé que l'infiltration par les orifices de ventilation n'a pas contribué de façon disproportionnée à l'infiltration totale.

Performance thermique

Lorsqu'il est exposé au soleil, le placage de brique est soumis, tout au long de l'année, à d'importantes fluctuations de températures durant le jour. En hiver, la température moyenne de la brique est habituellement un peu inférieure au point de congélation, mais fluctue considérablement au-dessus et au-dessous du point de congélation en raison de l'effet du soleil. Au cours de l'été et de l'hiver, la température des panneaux placés face à l'ouest ou à l'est a été d'environ 5 à 7 °C supérieure à la température ambiante. Cette différence de température a un effet spectaculaire sur les couches internes de chaque mur et agit sur le potentiel de condensation, l'accumulation et la transmission d'humidité, la consommation d'énergie, la durabilité des matériaux et les conditions thermiques.

L'air présent dans la cavité de tous les panneaux est demeuré plus chaud que la brique et au moins 6 °C plus chaud que la température ambiante moyenne. De plus, on n'a mesuré aucune stratification verticale de la température à l'intérieur de la cavité. La température de la cavité a suivi de près la température de la surface interne de la brique, même lors des changements rapides de température provoqués par le soleil. Théoriquement, il est pratiquement impossible d'assurer un mouvement d'air suffisant dans les orifices de ventilation de la maçonnerie pour évacuer l'excès de chaleur solaire accumulé dans la cavité. On n'a pas établi de rapport évident entre la quantité de vapeur d'eau présente dans la cavité et la teneur en humidité de l'air extérieur. À mesure que la température grimpait, la quantité d'humidité dans l'air de la cavité a augmenté aussi, un signe de

l'évaporation et de la désorption de l'humidité. Aucune conclusion n'a toutefois pu être tirée en ce qui concerne l'effet de la ventilation sur le taux d'humidité de l'air dans la cavité (et donc de sa capacité de séchage) parce que la ventilation n'a pas pu être mesurée à cause de la façon dont l'essai avait été organisé.

Modération de la pression

Des études additionnelles s'imposent pour déterminer dans quelle mesure les différences de pression ont été modérées à la surface de l'écran des bâtiments d'un étage et des bâtiments de faible et de grande hauteur. Il faudra en outre procéder à de nombreux autres essais quantitatifs répétables destinés à mesurer la modération de la pression. Les pressions dues au vent que subissent les bâtiments de faible hauteur exposés sont généralement très faibles (moins de 20 Pa) et des pressions plus élevées (supérieures à 50 Pa) sont très rares. La pression du vent variant en fonction de la hauteur a eu un effet relativement important sur les pressions et sur la modération de la pression dans le cas des panneaux d'essai. Il s'est avéré que les variations spatiales à proximité des angles des bâtiments entraînaient par des conditions de pression très différentes. Selon les données enregistrées, aucun des panneaux n'a atteint l'équilibre complet sur le plan de la pression pour toute mesure et à n'importe quelle fréquence.

On peut considérer que le vent est constitué d'une composante moyenne et d'une composante à variation rapide. Les panneaux de référence et les panneaux sans cavité ont permis une modération de 20 à 50 % des différences de pression variables sur toute la surface de l'écran, c'est-à-dire qu'ils présentaient une «pression équilibrée» s'échelonnant entre 20 et 50 % à 0,2 Hz. Le degré de modération de pression diminuait lorsque la fréquence augmentait. Les valeurs moyennes (pour des mesures d'une minute) indiquaient que les panneaux permettaient une modération de plus de 90 % de la différence sur la surface de l'écran. Il semble également que les pressions moyennes ou que les différences de pression moyennes soient peu pertinentes par rapport à la réponse réelle qu'offre la pression de la cavité au vent. Il faudra donc étudier plus à fond la perméance à l'eau des écrans formés par des placages de maçonnerie, surtout dans des conditions de différences de pression faibles à variation dynamique, ainsi que l'incidence et la coïncidence des effets de la pluie et du vent.

Membrane d'étanchéité / Papier de construction

En ce qui a trait à la membrane d'étanchéité et au papier de construction, le fait de placer ces éléments entre le revêtement d'ossature isolant et le matelas d'isolant les protège en toute saison

contre les températures extrêmes et les écarts prononcés. Sur le plan de l'étanchéité à l'air, il est très avantageux de fournir un appui au pare-air, à la membrane d'étanchéité ou au papier de construction en le fixant à l'isolant rigide ou en le plaçant entre deux couches relativement rigides. Il est souhaitable que la membrane d'étanchéité ou le papier de construction soient relativement étanches à l'air, puisque ces couches réduisent les déperditions thermiques par convection que subit l'isolant en matelas à faible densité, qu'elles diminuent le volume effectif de la chambre d'équilibrage des pressions et qu'elles procurent un second plan de résistance au mouvement d'air dans l'éventualité où le premier pare-air serait ou deviendrait défectueux. La membrane d'étanchéité ne doit être utilisée que lorsqu'elle est solidement fixée à un support rigide et qu'elle est entièrement rubanée. On recommande fortement de bien prendre en considération l'emploi de cette membrane dans le futur, surtout pour ce qui est de son emplacement, de sa perméance à la vapeur et de l'usage auquel elle est destinée.

Valeurs moyennes

Cette étude en service démontre clairement que les valeurs moyennes ne sauraient refléter l'effet des écarts quotidiens, surtout ceux qui sont provoqués par le rayonnement solaire, dans les assemblages muraux à ossature légère. Les valeurs quotidiennes de pointe peuvent jouer un rôle important dans la performance réelle du mur. Comme l'ont démontré d'autres études, les lectures horaires sont importantes pour pouvoir comprendre à fond le comportement des assemblages muraux à ossature légère employés couramment dans les bâtiments résidentiels d'Amérique du Nord.

Conclusions et recommandations

Dans le cadre de cette étude, le panneau sans cavité s'est révélé peu performant. La diffusion, au printemps et en été, de l'humidité issue de la cavité remplie de fibre de verre a saturé l'ossature de bois au bas de l'espace formé par les poteaux. Toutefois, ce phénomène résulte de la perméabilité à l'eau de l'écran de brique, des caractéristiques de rétention d'humidité de la fibre de verre remplissant la cavité, de la perméabilité à la vapeur de la membrane Tyvek™ et de la production interne de vapeur par le rayonnement solaire. Deux de ces problèmes peuvent facilement être résolus. Il s'agit de n'utiliser, à l'avenir, que des isolants fibreux traités avec un revêtement hydrophobe ou un revêtement intermédiaire ou un papier de construction possédant une résistance à la vapeur suffisante.

En dépit des problèmes qu'entraîne l'utilisation non standard de matériaux standards, cette étude confirme que le concept du mur sans cavité est essentiellement bon et offre des avantages tels qu'une meilleure évacuation de l'eau, des murs plus minces, le support et la protection du papier de revêtement ou de la membrane d'étanchéité et sans doute aussi une meilleure modération de la pression. Utilisée largement et avec succès pendant des décennies dans les pays scandinaves et en Europe, cette forme de construction offre une certaine assurance que, pourvu que les matériaux et les méthodes de construction employés soient appropriés, le remplissage de la cavité par un matériau fibreux peut améliorer la tenue en service des murs-écrans pare-pluie à parois multiples.

CMHC SCHL

Helping to house Canadians

Question habitation, comptez sur nous

National Office

700 Montreal Road
Ottawa, Ontario
K1A 0P7

Bureau national

700 chemin de Montréal
Ottawa (Ontario)
K1A 0P7

Puisqu'on prévoit une demande restreinte pour ce document de recherche, seul le sommaire a été traduit.

La SCHL fera traduire le document si la demande le justifie.

Pour nous aider à déterminer si la demande justifie que ce rapport soit traduit en français, veuillez remplir la partie ci-dessous et la retourner à l'adresse suivante :

Le Centre canadien de documentation sur l'habitation
La Société canadienne d'hypothèques et de logement
700, chemin de Montréal, bureau C1-200
Ottawa (Ontario)
K1A 0P7

TITRE DU RAPPORT : _____

_____

Je préférerais que ce rapport soit disponible en français.

NOM _____

ADRESSE _____
rue app.

_____
ville province code postal

No de télephone ( ) _____

TEL: (613) 748-2000

Canada Mortgage and Housing Corporation Société canadienne d'hypothèques et de logement

Canada

Table of Contents

List of Tables

List of Figures

1. Introduction

1.1 Background

In cold climates multi-layer wall systems are almost mandatory if an effective building envelope is desired. Multi-layer wall systems, especially for residential buildings, often employ a non-load-bearing brick veneer as the outermost screen against environmental factors such as rain and the sun. One of the most important and problematic functions of walls, particularly masonry veneer walls, is the control of moisture penetration.

Various strategies are used for moisture control.. One strategy is to employ the mass of the enclosure to ensure that any water that does penetrate the exterior is absorbed and subsequently drained and evaporated without ever reaching the interior of the enclosure. A second strategy requires a perfect barrier to water at the exterior surface. A third strategy employs the so-called "rainscreen principle." A classification system based on these three approaches is presented in Figure 1.1 (a). This classification has been extended to show the focus of this project in Figure 1.1 (b).

The primary components of the screened portion of a wall system employing the 'rainscreen principle' are:

1) the screen,

2) the air space or cavity,

3) the gravity drain,

4) the venting capability, and

5) the pressure equalization chamber.

The rainscreen approach acknowledges that the brick wythe or screen is only an imperfect barrier and that water may penetrate the screen. It follows that an additional, second line of defense is essential. This second system should incorporate a capillary break, a drainage system, and some type of water barrier which controls further inward moisture movement.

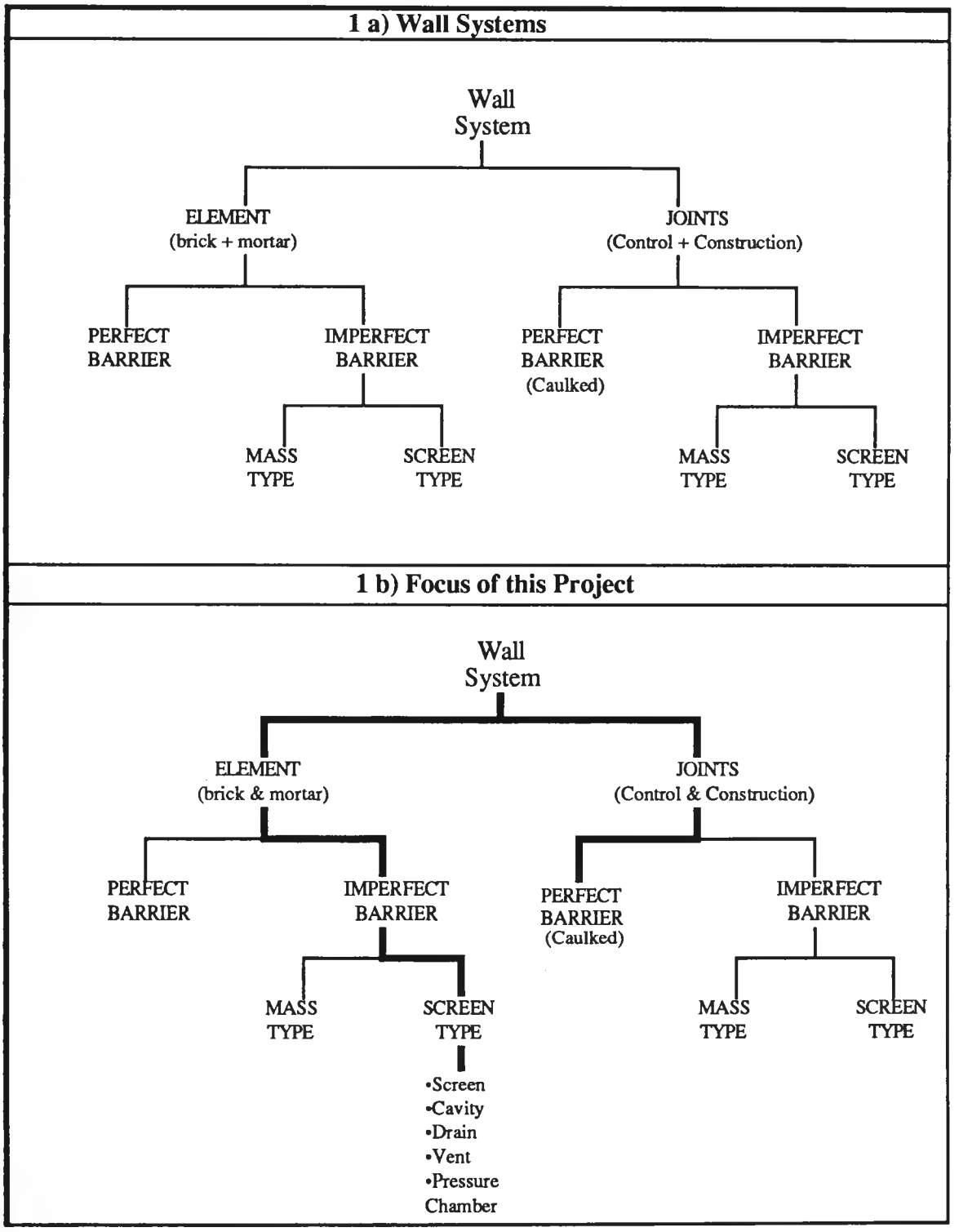

Figure 1.1: Classification of Wall Systems

A clear air cavity is customarily used and it is variously presumed that:

- a clear air space provides the capillary break
- drainage down and then out of the wall will remove free liquid water
- ventilation flow through the cavity contributes to drying behind the veneer.

As a precaution it is also customary to apply a building paper (or similar) to the inside face of the cavity to provide an extra measure of moisture control.

Unfortunately, the draining and venting characteristics of the air cavity are frequently compromised by the inadvertent creation of mortar dams and mortar bridges across the cavity and accumulations of mortar at the base of the cavity. Mortar dams and bridges can direct water running down the inside face of the brick screen across the cavity and wet the inner wythe. Accumulations of mortar droppings at the base of the air space can completely block the drainage path, i.e., the cavity and weep hole, allowing very little or no water to flow. The result can be moisture-related discolourations and deterioration, water leakage, corrosion, and a reduction in thermal performance.

A number of approaches can be taken to resolve the mortar problem. One, not particularly practical, method is to mandate, in codes or project specifications, that mortar dams, bridges, and droppings are to be avoided. Alternatively, an appropriate filler component which fulfills the same functions as a clear cavity (i.e. one that acts as a capillary break and allows drainage and air flow) could be developed and used in lieu of an air cavity. Two types of filler have been studied in this project and compared to the traditional "clear cavity" approach. One cavity filler uses a semi-rigid glass fibre product and the second fills the cavity with a rigid foam plastic, specially shaped with drainage and ventilation grooves protected from mortar intrusion by a fabric mesh.

1.2 Project Objectives

The main objective of this project was to monitor and assess the performance of two alternatives to the traditional brick veneer cavity wall system. A secondary and related objective was to assess the merits of using two different forms of insulating sheathing in BV wall systems. The first form of sheathing used a glass fibre board to fill the cavity (hence the zero cavity option). The other sheathing was a collaborative effort by Dow and BEG to develop a thermal/weather barrier that facilitated drainage, ventilation and

also attempted to satisfy the recommendations for obtaining "instantaneous pressure equalization".

Insofar as the insulation manufacturer's were concerned, the intent of the project was to assess the possibility of using versions of their existing products to best meet the need for improving the performance of walls with brick veneer facings by enhancing thermal, moisture, and air leakage control, reducing the overall width of the wall, and, most importantly, eliminating or avoiding mortar problems while at the same time enhancing pressure equalization performance.

Specific requirements of CMHC were the evaluation of the effect (relative to current construction practice) of using an insulating fibrous cavity fill behind a brick veneer on:

1. the buildability of the veneer,
2. pressure equalization,
3. the brick temperature, and
4. the ability of the walls to drain and dry.

Dow Canada was particularly interested in the development of a hybrid insulated sheathing that would also act as a cavity filler and ensure that drainage, pressure equalization and venting were encouraged.

1.3 Scope and Approach

Three pairs of full-scale wall panels were built, exposed to the environment and monitored comprehensively for more than one year. The wall systems were called the Datum, Zero Cavity, and DPV panels and each pair was identical

One pair of test panels (called the Datum panels) were built using current, accepted practices for wood frame housing. The veneer of the Datum panels was built with great care to ensure that the cavity was kept clear. The intent in building the Datum panels was to establish a drained and vented rainscreen of known quality to which the other panels could be compared. A pair of panels (called the Zero-Cavity panels) were built with a standard high-density (52 kg/m^3) fibrous-glass board filling the cavity. The fibrous glass board was intended to ensure that both water (drainage) and air flow (pressure equalization) was possible while avoiding the potential blockage by mortar droppings and dams. A third pair of panels sponsored by Dow Canada used a special

proprietary drained, pressure-equalized, and vented (DPV) extruded polystyrene (EXPS) board.

The panels were built in a laboratory installed during July 1991 in the Building Engineering Group's natural exposure and test facility, the Beghut. The performance of the masons was closely observed and they were interviewed to assess buildability.

Each panel was instrumented in order to measure temperature, wood moisture content, relative humidity and static air pressure at many different locations. After the panels acclimatized, the sensors were monitored from November 1, 1991, to December 31, 1992 to assess the effect of daily and seasonal variations. The interior of the Beghut was maintained at close to 21°C and 50% relative humidity (RH) throughout the monitoring period. The temperature across the wall, particularly in the brick and at the interface of brick and insulation, the relative humidity in the cavity, and the moisture content of the framing was monitored. The pressure distribution across the wall and inside the cavity was monitored during steady, gusting, and calm conditions. The signals from these sensors were read regularly, stored, and later processed to produce graphical and statistical information of the thermal and moisture behaviour of the panels.

Air leakage and water penetration tests were conducted during August to October of 1992. Water penetration tests were used to assess the relative permeability of the brickwork screens and the drainage capability of the cavities. Air leakage tests defined the panels' resistance to airflow to help assess the pressure-equalization ability, air movement, and energy efficiency. Pressure equalization measurements were taken over the period January to August of 1993. Field pressure-equalization measurements were used to compare and quantify the panels' performance in this aspect. More than two years after the panels were installed, they were opened and physically inspected.

Full-scale mockups of the three different wall assemblies were constructed and tested in the laboratory to investigate the drainage behaviour of the cavities, and the moisture retention characteristics of the filler materials.

1.4 Commentary

For a variety of reasons, the scope of the initial project, the extent of the work, the amount of data collected, and the depth of the analysis required, was far greater than initially intended or contracted. Rather than this single, all-purpose report, perhaps two or three, with different audiences in mind, may have been more appropriate.

The Zero-Cavity panels exhibited high wood moisture content readings from the start of monitoring. Careful and detailed analysis was necessary to understand and explain the reasons for the wetting observed. The issue of pressure equalization was poorly understood at the time the Request For Proposals was drafted (in 1990). It has since become clear that measuring and understanding the complex behaviour of wind and the response of pressure equalized walls is quite difficult, especially in the field. A considerable effort was necessary to develop and demonstrate a reasonable pressure equalization test procedure. CMHC and the National Research Council of Canada have since sponsored several much larger studies into the topic of pressure equalization which are still continuing. In the meantime, BEG has conducted a number of studies that complement the work in this project.

1.5 Scope and Approach of this Report.

This report is a summary record of the work done during this project.

In Chapter 2 the test facility, the construction and installation details of the panels, the instrumentation, data acquisition, and subsequent manipulation and presentation of the data are described. In Chapter 3, the panel performance over the fourteen month monitoring period is discussed. The influence of the major parameters measured, namely temperature, relative humidity and wood moisture is quantified and discussed. The air leakage, water penetration, pressure-equalization and mockup testing are described and the results presented and discussed in Chapters 4 through 7 respectively. Chapter 8 reviews the observations when the panels were opened for inspection at the end of the project, Chapter 9 presents the major conclusions. Basic experimental data and supporting documentation are included in the appendices.

2. Test Program and Setup

2.1 The Beghut Test Facility

The test panels were installed in the Building Engineering Group's outdoor, full-scale permanent test and demonstration facility (the Beghut) located on the University of Waterloo campus. This facility is a square building approximately 10.5 m x 10.5 m in plan and 3.0 m high on the interior. The walls are oriented in the four cardinal directions. The roof is peaked to the centre with a slope of 1-in-3. A pipe mast rising from the central peak of the roof supports a weather station at 10 m above grade.

An air-to-air heat pump heating and air conditioning unit, together with humidification units, controls the interior climate to 21 °C and 50% relative humidity. A floor-mounted air distribution system is used to distribute the conditioned air evenly, and four symmetrically mounted ceiling fans are used to prevent vertical and horizontal stagnation

The structure is of wood post-and-beam construction with a trussed roof. The foundation is a 1.2 m high, 250 mm thick, unreinforced concrete wall on a 500 mm wide, 300 mm deep, strip footing. The floor consists of a 100 mm thick concrete slab-on-grade placed on a polyethylene moisture barrier and 150 mm of granular fill. The corner columns and ring beam are sheathed with plywood, insulated with 150 mm fibreglass batts, and clad with aluminum siding. The roof is insulated to RSI 5.4 and conventionally constructed from prefabricated trusses. The roof system comprises asphalt shingles, building paper, and plywood sheathing, with an additional ice and water shield extending 600 mm up from the eaves. Figure 2.1 provides some additional construction details and dimensions.

The method of framing allows for seven panels in each side (28 total) of approximately 1.2 m width and 2.4 m height to be installed and removed at any time. This project used only six of the panel spaces, three on the west side and three on the east. The other panels were the subject of on-going studies for the IRC/NRC, CMHC, and the housing industry.

The test hut is sited on relatively flat land and is fully exposed to winds from most directions. A two-storey office building is located approximately 30 m to the north-west and substantially shelters this direction. Figure 2.2 provides photographs taken from the Beghut looking exactly west and exactly east (the view seen by the panels in this project). The roof overhang is sized to prevent shading from the sun under all conditions. The

small overhang and the drip-edge, in lieu of eavestroughs, provide very little direct protection from rainfall.

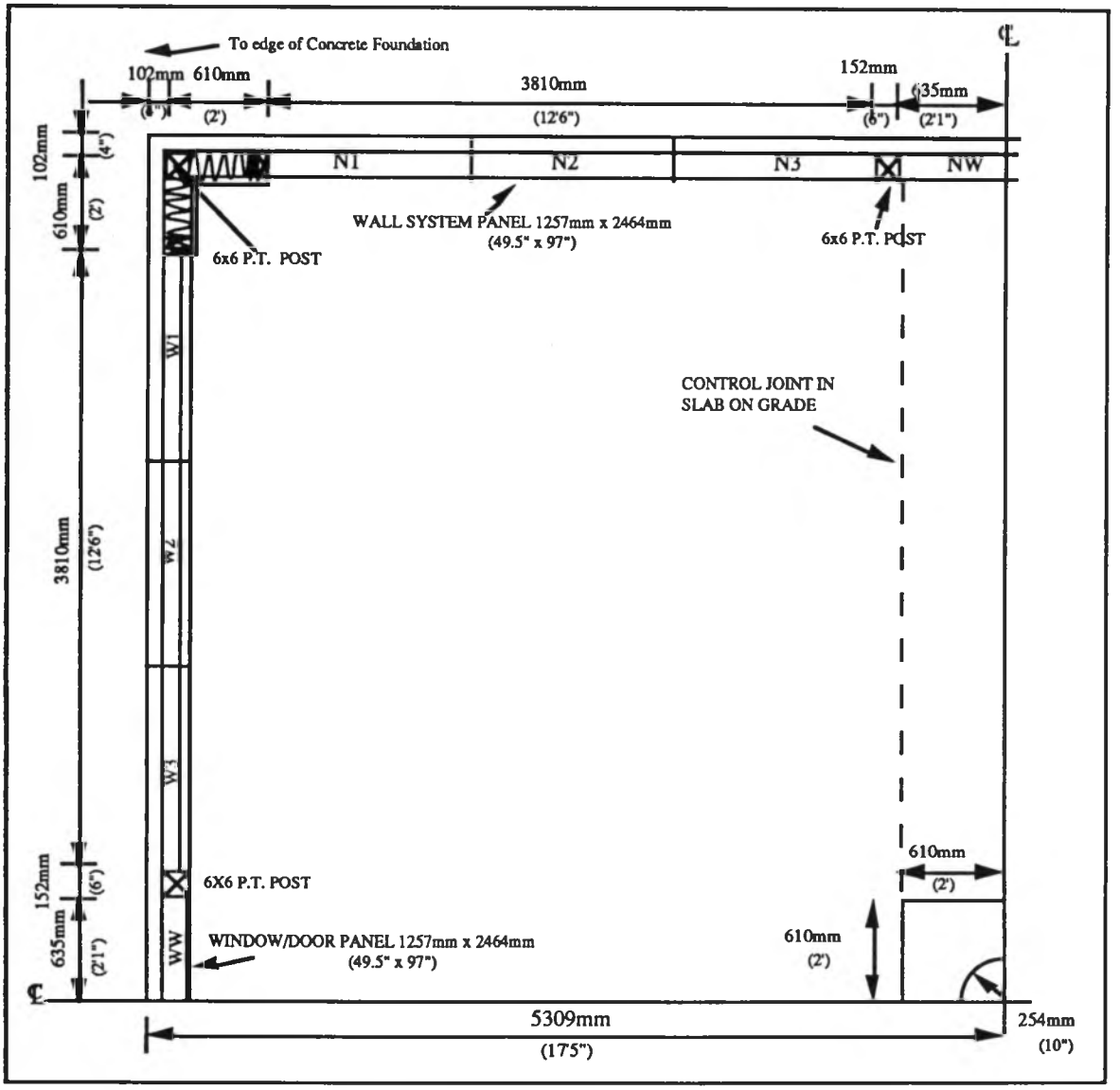

Figure 2.1: Construction Plan of Beghut

Figure 2.2: Photos From Beghut Looking East and West

2.2 Panel Construction and Installation

2.2.1 Panel Construction

All panels were built with a wood-frame structural inner wythe, an exterior insulated sheathing, an air and water barrier, and a brick-veneer screen similar to most Canadian low-rise residential construction. Figure 2.3 is a detailed horizontal section of the three different panels tested.

The wood frame was made of 38x89 (2x4) studs on 400 mm (16") centres and insulated with 90 mm (3 1/2") thick RSI 2.11 (R12) friction-fit fibreglass batts. The interior was finished with unpainted 12.5 mm (1/2") gypsum drywall and a 0.15 mm (6 mille) polyethylene vapour barrier. An 85 mm (3 1/4") thick brickwork veneer formed the exterior screen. The screen was constructed with two open head joints that act as weep holes in the bottom brick course and two open head joints in the second course from the top that act as vents.

The Datum panel used 38 mm (1 1/2") thick RSI 1.18 (R7) rigid fibreglass (Glasclad™ with the Tyvek™ removed, donated by Fiberglas Canada) as the insulating sheathing. The air and water barrier was a 5 mille spun-bonded polyolefin film (tradename Tyvek™) attached to the exterior by large plastic-headed nails at approximately 400 mm horizontally and 800 mm vertically. A 30 mm (1 1/4") cavity separated the Tyvek™ and the brickwork.

The Zero-Cavity panels employed the same insulated fibreglass sheathing as the Datum panels, but the Tyvek™ was placed on the inner face of the sheathing and stapled to the wood studs. The bricks were laid directly against the sheathing during construction.

The DPV panels used specially produced 50 mm thick extruded polystyrene (tradename Styrofoam SM™, produced and donated by Dow Canada) as the insulated sheathing. Grooves 12 mm deep and 100 mm wide provided a small drainage cavity and left 38 mm of full insulating sheathing. The bricks were laid tight against this proprietary board product, and a plastic mesh protected the grooves from mortar droppings. Behind the extruded polystyrene (EXPS), 15 lb building paper was attached to the wood studs. The EXPS and the building paper were intended to act together to resist water penetration and air leakage.

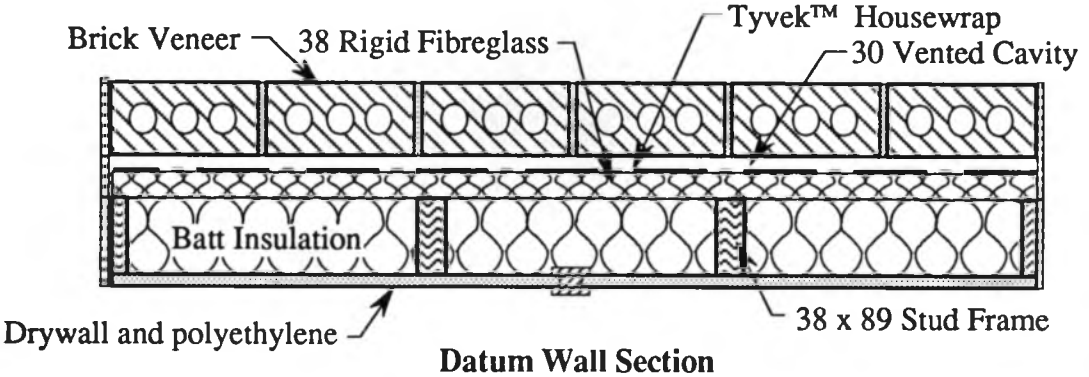

Datum Wall Section

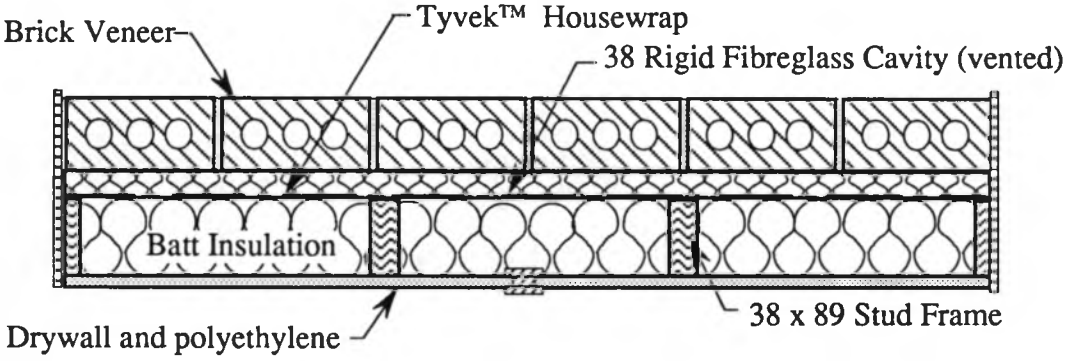

Zero-Cavity Wall Section

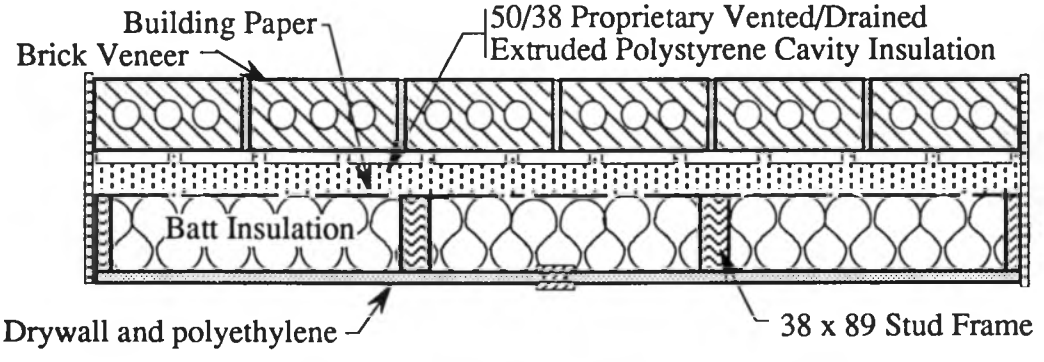

Drained-Pressure Equalized-Vented (DPV) Wall Section

Figure 2.3: Detailed Panel Sections

2.2.2 Material Properties

All of the materials used for the construction of the panels were purchased at building material retailers in the Kitchener-Waterloo area. With the exception of the wood used for framing, no attempt was made to select extraordinary materials or products. Wood stud requirements were such that selectivity regarding quality would reduce variability in wood moisture response due to the absence of knots and wood density differentials. Furthermore, top quality lumber would be less prone to warping and shrinkage. Our lumber supplier (Honsberger Lumber Inc.) assured us that the Ontario White Pine supplied was:

i) of the best quality, i.e.,, free of knots,

ii) grown in one geographic region, and

iii) harvested at approximately the same time.

The proprietary rigid fibreglass insulation used in two of the panels (Glasclad™) normally has a spun-bonded polyolefin air barrier fully adhered to one side. The manufacturer, Fibreglass Canada, generously donated sheets of this insulation without the air barrier.

Table 2.1 contains a complete listing of materials used in the panels and their associated properties (from published data).

Material	Thickness		Thermal resistance	Vapour resistance	Coefficient of expansion	Density
	S.I. mm	imp. inch	$W/m^2 \cdot °C$	Pa s m^2/ng (10^{-4})	$°C \cdot 10^{-6}$	kg/m^3
Gypsum board	12.5	1/2	0.079	3.5	18	800
Polyethylene	0.15	6 mil	0	3000	-	-
Ontario White Pine	38x89	2 x 4	0.82	115-1515	-	600
Fibreglass batt insul.	89	3 1/2	2.11	5.25	-	10
Rigid fibreglass	38	1 1/2	1.18	3.28	5	52
Styrofoam SM™	50/38	2/1 1/2	1.25	214	70	30
Tyvek™ air barrier		-	-	2.52	-	-
15# Building Paper		-	-	30-180	-	-
Brick	90	3-1/2	0.074	189		2000

Table 2.1 Material Properties

2.2.3 Sections, Elevations and Details

Each of the figures on the following pages shows construction drawings of the Datum, Zero-Cavity, and DPV panels. The figures and their titles are listed here to identify the pertinent figures:

Figure 2.4 Elevation and Horizontal Section of Panel Group

Figure 2.5 Typical Airtight Panel Edge Details

Figure 2.6 Typical Instrumentation Details

Figure 2.7 Typical Bottom Plate Details

Figure 2.8 Typical Top Plate Detail

2.2.4 Special Features

Several steps were taken to enhance the performance of the experiment and the quality of the data. The following is a list of these features.

i) Use of plastic conduits to collect and lead wires and tubes out of the panel readily permitted tight seals to be constructed at points of entry (see Figure 2.6).

ii) Half-width studs (19 mm, not 38 mm) were used for the end studs of each panel. This still allowed the full amount of insulation to be placed within the two side cavities, but also permitted the placement of a separating layer of extruded polystyrene (EXPS) insulation between panels (see Figure 2.5), which helped to thermally isolate each panel from neighbouring conditions. To reduce vapour diffusion and air leaks at the edges, a vinyl strip (FR-40) was wrapped completely around each panel (see Figures 2.5 and 2.6).

iii) The brickwork rested on pressure-treated plywood base plates which were formed so that low points were directly below the weep holes; copper water leaders with connecting plastic tubing were placed at these points so that any water running through the weep hole would be led into a collecting vessel inside the Beghut (see Figure 2.7).

iv) Each panel had two bricks that were set in place with foam shims. This allowed the bricks to be removed at any time. The bricks were later sealed and fixed in place with silicone sealant. The locations of these bricks is shown in Figure 2.4.

v) A special mounting device was designed and manufactured to allow the two different types of relative humidity sensors to be positioned in line. Details of this device are shown in Figure 2.6.

vi) A plastic fitting was also installed 500 mm from the bottom of the panel to allow air leakage testing on each panel. The fitting is similar to the upper instrumentation conduit except that it has a screw-in plug (Figure 2.6).

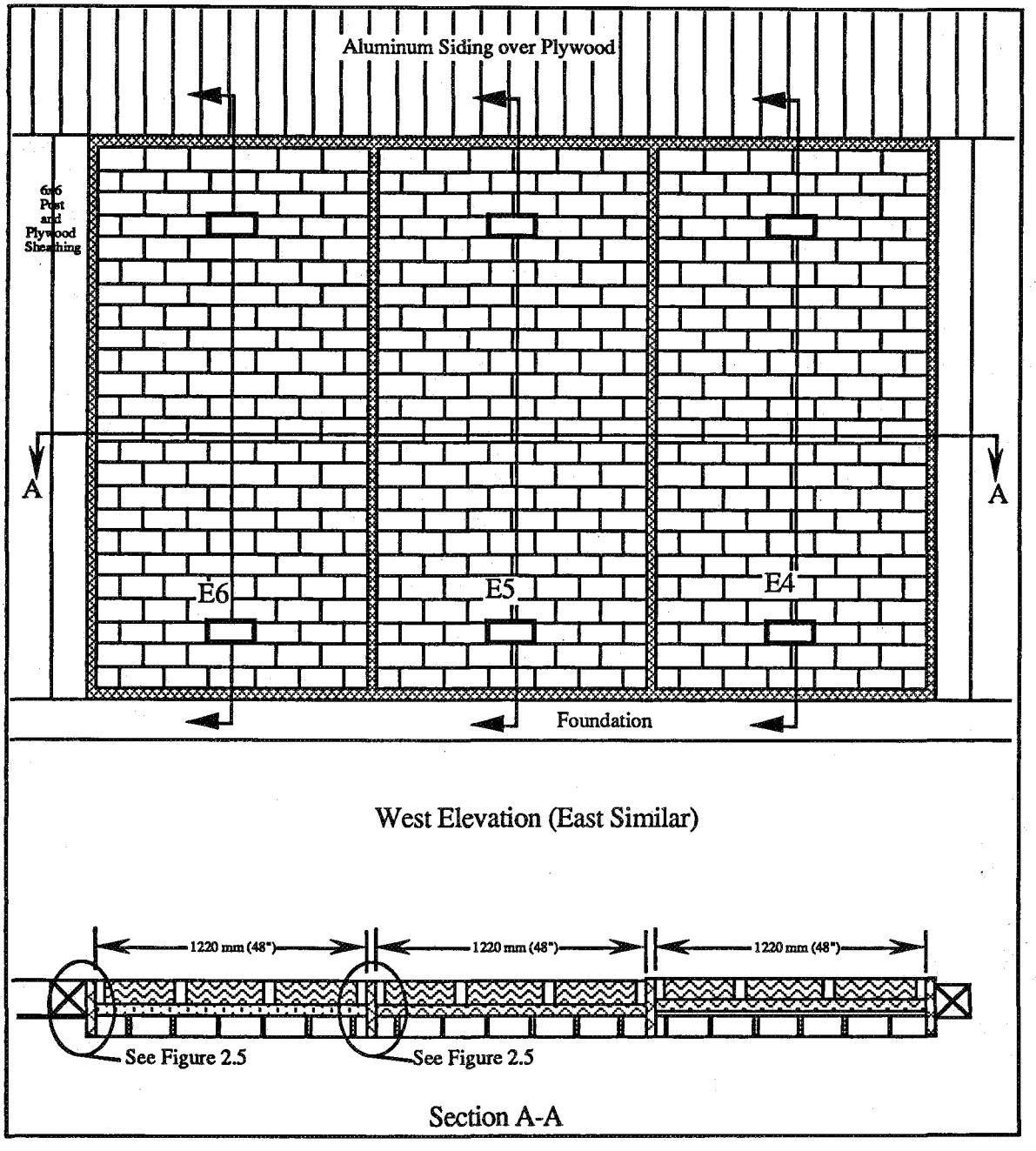

Figure 2.4: Elevation and Horizontal Section of Panel Group

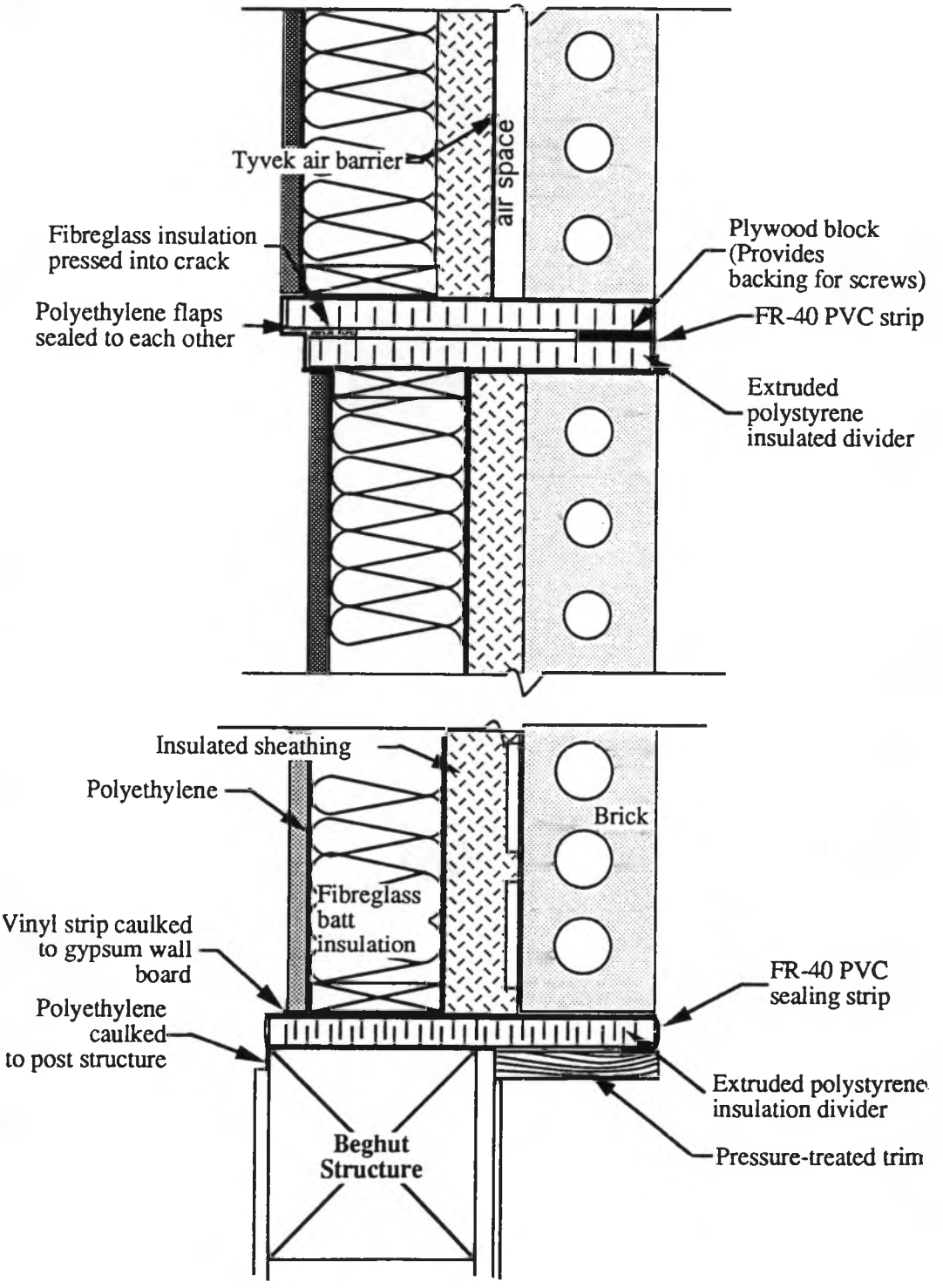

Figure 2.5: Airtight Panel-Edge Details

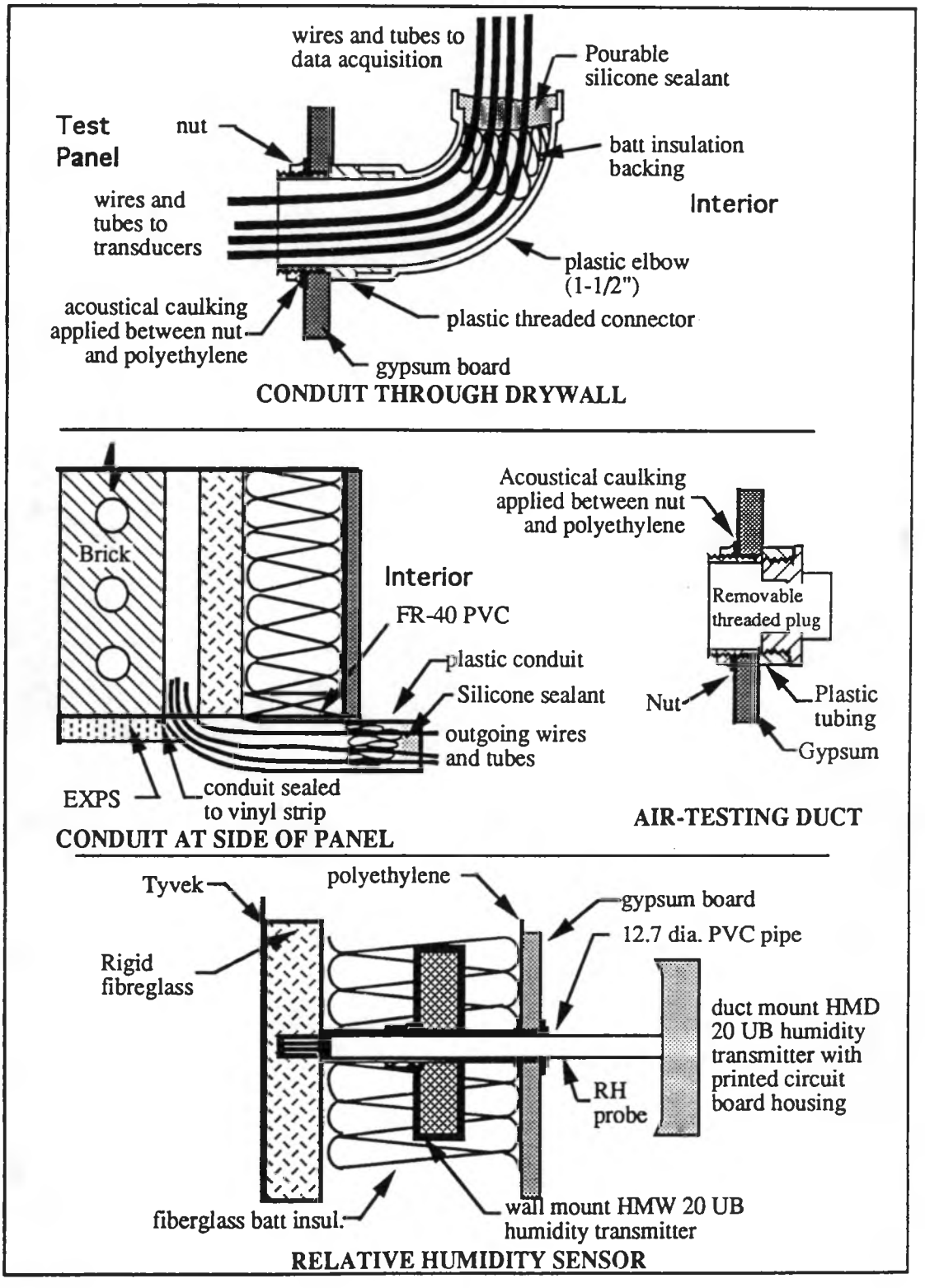

Figure 2.6: Typical Instrumentation Details

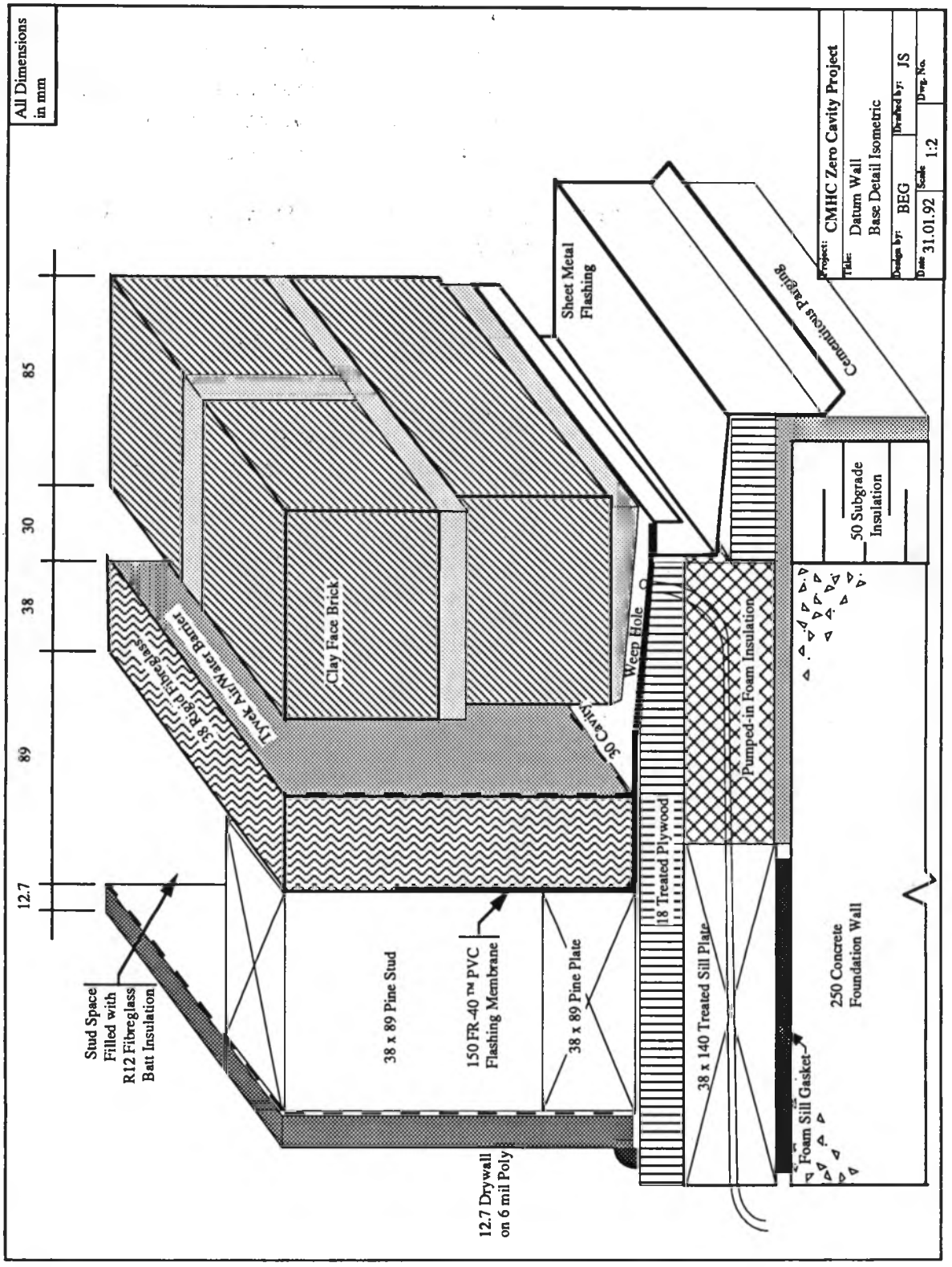

Figure 2.7: Typical Base Detail Isometric

2.2.5 Construction Procedures

The entire panel, excluding the brick veneer, was assembled in the Structures Laboratory of the University of Waterloo on an elevated working surface. The steps in constructing each panel are listed below in sequential order.

i) The studs and plates were cut to the correct length and joined using two #10 x 3 1/2" zinc-coated wood screws (instead of nails) at each intersection.

ii) A 1-1/2" hole was drilled through the drywall 500 mm (20") down from the top and 610 mm (2') from the either edge. A corresponding hole was cut through the polyethylene, and the threaded portion of the conduit was fixed to the polyethylene/drywall assembly using the nut. Caulking was used to ensure a seal between the conduit and the polyethylene. This assembly was then attached to the stud frame using 1 1/4" drywall screws. The panels were then laid cavity side up on the elevated working surface to receive subsequent materials.

iii) All instrumentation was placed within the stud cavity, and the main bundle of wires and tubes was fed out through the upper conduit and coiled and stored beneath the panel.

iv) Brick-bearing plates were formed from pressure-treated plywood. Two low points were created to facilitate collection of water from the weep holes. The bearing plates were fixed to the bottom plate of the panels with 6 #8x2" wood screws. A strip of vinyl (FR-40) was sandwiched between the plates. The remaining edges of each panel were then wrapped with vinyl strips; acoustic caulking was used to ensure continuity at the joints. Extruded polystyrene strips were attached to the sides of each panel with about a dozen drywall screws.

v) The rigid fibreglass and the Tyvek were then attached to the frame. A vertical joint in the fibreglass was located on an inner stud. The edges of the Tyvek were sealed to the vinyl with acoustic caulking. A slot was cut through the EXPS to accommodate the side conduit, and the conduit was attached to the edge of the panel with a plastic strap. Caulking was used to seal around the conduit/vinyl strip intersection.

The remaining instrumentation was placed, and the wires and tubes were fed out through the conduit.

vi) A 1/2" plywood cap was fastened to the top of each panel to provide backing for the vinyl strip and sheet metal flashing. At this time any corners, joints, etc., that remained unsealed were caulked with acoustic sealant.

A crew of five men installed the panels. In order, panels W4, W5, and W6 were installed, followed by E4, E5, and E6. The panels were tilted up onto their bases and fixed temporarily to the header beam with metal straps. After all panels were in place, they were aligned and plumbed into the correct position. Gaps around each panel were filled with expanding urethane foam insulation. This technique provided an excellent air and water seal, good thermal protection, and also wedged the panel into the opening, eliminating the need for fastening devices which might penetrate the vapour barriers.

The final task involved installing the flashing at the top and bottom of the panel and sealing any other unwanted penetrations. Before the brickwork was installed, the base flashing (FR-40 vinyl) was carried horizontally along the treated plywood base plate and approximately 200 mm vertically upward along the wood studs. In the DPV and Zero-Cavity panels the water barrier (building paper and Tyvek respectively) was lapped over the flashing. In the Datum panel, the Tyvek on the face of the sheathing ended at the bottom of the sheathing.

2.2.6 Masonry Work

The brick was installed on three panels on each side simultaneously. The 85 mm thick brick was installed by G & A Masonry. BEG personnel were present during the masonry work to observe and provide quality control. Verticality was not a consideration for either the Zero-Cavity or the DPV panels, since the board insulation was plumb and the bricks could be placed directly against the rigid surface. HRT 60 x 195 Helifix masonry ties were used to tie the brick wythe to the wood studs. All ties were installed using a special driving device that permitted the tie to be screwed in.

2.2.7 Masons' Feedback

Since the masons were using a tie system that was new to them and two building techniques that were developmental, their opinions regarding each system were important. A summation of their feedback follows.

Datum System

The masons felt that their speed was severely affected by having to make a clean, flush surface on the backside of the brick. They said that one mason could lay approximately 600 bricks per day using conventional methods, but ensuring an absolutely flush inner surface and a cavity free of mortar droppings might reduce this number to about 350 bricks per day. They recommended that some device should be available to catch and permit removal of mortar droppings from the air cavity. They also thought that a slightly higher, second level of holes might ensure ventilation if the weep holes became blocked.

Zero-Cavity Wall System

Because of the lack of any finger space, the masons felt that their speed would be seriously affected by this system. Their estimate of bricks laid per day using this system was 300 to 400. One mason felt that his normal style of brick laying was seriously affected. Instead of being able to keep a good grip on the brick at all times, the mason was required to release the brick and let it drop into place or pick up and place bricks using the holes. This reduced his control over initial placement, but, since the mortar remains workable for about five minutes, manipulation of the brick into its correct position is possible.

Break-away fibres from the fibrous insulation did not seem to cause irritation to these masons' hands; however, they seemed to think that some other masons might be affected. They thought that wearing gloves to protect their hands against irritation from the glass fibres would severely hamper their ability to lay bricks accurately and at an acceptable pace. They said that the holes in the bricks could be used for a grip but that they opted not to use them.

The masons considered control over verticality as a problem since the plumbness of the brick wythe is highly dependent upon the plumbness of the rigid fibreglass. They thought that a less dense material might help to overcome this problem while also being less abrasive.

DPV System

The masons felt that their speed was severely affected by having to place the bricks up against the polyester mesh which covered the grooves. They said that having to place bricks against the mesh might reduce their productivity

to about 400 bricks per day. The masons complained that their fingers got caught in the mesh.

The masons cited verticality, or more correctly, control over verticality, to be a problem since the plumbness of the brick wythe is highly dependent upon the plumbness of the EXPS board.

General Comments Made by the Masons

- Increasing the amount of handling of the brick increases the amount of skin abrasion.

- It is virtually impossible to keep the air cavity clean of mortar droppings and this raises the question, "How clear is clear enough?"

- Generally, solid bricks are easier to handle and less abrasive than those with holes (the edges of the holes are usually sharp).

- Altering the consistency of the mortar slightly might ease placement of bricks.

Recommendations Made by the Masons

Recommendations regarding improvements to the fibrous insulation revolved around reducing the density of the material, making it softer, easier to compress, and less "rough" on the hands.

Recommendations regarding improvements to the grooved EXPS insulation board were intended to avoid getting the mason's fingers caught in the polyester mesh. More specifically, the masons recommended that the amount of mesh overlap at the seams be reduced, the mesh be stretched more tightly, and the holes in the mesh be made smaller.

2.2.8 Mockup Panel Construction

As a supplement to the in-situ testing of the six wall panels, laboratory tests were conducted on the insulation material and on a mockup of the building assemblies. To allow for exploratory comparative testing of the Zero-Cavity, DPV, and Datum wall assemblies, three 1220 mm x 1220 mm panels were constructed. Figures 2.8 shows the elevation and sections of the Datum mockup; the others are similar. The materials and

construction of the mockup panels were similar to the panels undergoing long-term testing but with several significant changes.

To allow for visual inspection of the backside ("interior") of the assembly and to ensure a water resistant interior surface, the drywall and 6 mille polyethylene of the full-scale panels were replaced with a sheet of 3 mm acrylic. The studs were also protected with three coats of marine-grade urethane to prevent the wood from absorbing and storing any moisture. The fibreglass insulation in the stud space was prevented from sliding down by a steel wire mesh attached to the bottoms of the studs.

The tops of the wall assemblies were left completely open. Raising the panels on their own supporting frame made it possible to have easy access to the underside and the top at the same time.

In the mockup test setups,three galvanized sheet metal troughs aligned under the stud space, exterior insulation, and exterior face respectively, as shown in Figure 2.8. This arrangement allowed the amount of water which flowed out of the bottom of each of these layers to be collected and measured. The troughs were sloped toward the middle (about a 50 mm drop over a 610 mm run) to collect the water and direct it through a 12 mm diameter hole into 12.7 mm copper tubing and via plastic tubing into a measuring beaker.

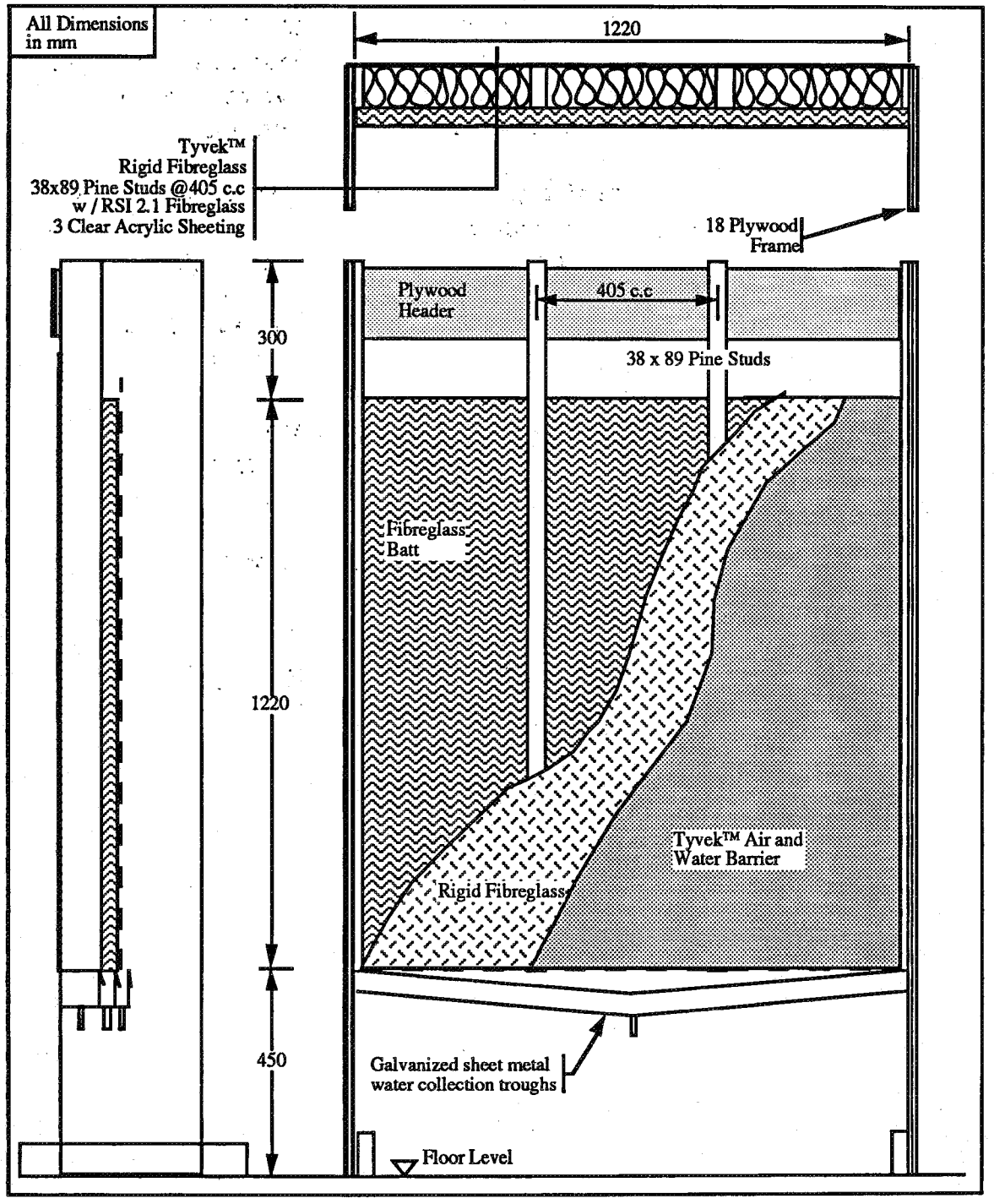

Figure 2.8: Datum Panel Mockup Elevation and Sections

2.3 Instrumentation

All test panels were instrumented to measure moisture content of the framing lumber, temperature, and relative humidity at numerous locations. Pressure taps were also included to allow the measurement of pressure within the batt insulation and at various locations within the air cavity during air leakage and pressure-equalization testing. A diagram showing this instrumentation and its location is given in Figures 2.9 to 2.11. Appendix C contains additional technical information on most of the instrumentation described below.

2.3.1 Relative Humidity Measurement

Relative humidity within a wall assembly is probably one of the more important parameters to monitor. A knowledge of relative humidity and temperature permits the determination of the actual amount of moisture present in the air (via the water vapour pressure), and the condensation potential.

All relative humidity sensors (RH) were placed within each panel 400 mm below the top and 400 mm above the bottom of the panel along the centre of the panel's width. The RH sensor for the batt space was suspended in the middle of the batt insulation with vinyl straps attached to the sides of the middle studs.

Two types of RH sensor/transmitters were used within each panel. Both were made by Vaisala Sensor Systems. Selection of the type of unit was based upon sensitivity, accuracy, and size-related criteria. Type 1 [HMW 20(30) UB] was a wall-mounted type with the sensor and printed circuit board encased in a plastic shell. Type 2 (HMD 20(30) UB) is a duct-mount type; the sensor is mounted at the end of a long probe (300 mm long x 12 mm diameter), which is attached to a plastic box containing the transmitter. The sensors are effective over a range of 0 to 100% relative humidity with an accuracy of ±2% RH. The duct-mounted type is accurate between -20 to +80 °C and the wall mounted sensor between -5 to +55 °C.

In order to place the sensors at the same location within different wall layers, a device was manufactured from 12.5 mm poly-vinyl chloride (PVC) pipe (see Figure 2.6) and assorted fittings which acted as a support for both the wall mount and duct mount sensor.

A Vaisala HMK 20 single-point calibrator was used to calibrate each sensor. This calibrator registers the difference in RH reading between it and a sensor. This difference is adjusted to read zero with the dials provided; a difference of approximately +/- 0.1% was considered satisfactory.

The transmitters returned a 4 to 20 milli-ampere current which was converted to a voltage difference using a simple circuit. The measured voltage was then converted to relative humidity percentage by the software using the following equation:

$$RH\% = (\text{volts} - 2) \cdot 100 / 8 \qquad (2.1)$$

2.3.2 Temperature Measurement

The temperatures within the test panels were monitored using type T (copper and constantan) thermocouples with an operating range of -30 to 150 °C. Temperatures outside this temperature range are inaccurate and would generate an error message. Thermocouple ends were twisted, soldered and clipped so that approximately one full twist or pitch made up the "hot junction." The thermocouple wires were fed back to the data acquisition system. The temperature measurement function of the data acquisition software measured the DC voltage of the thermocouple and linearized it .

The thermocouples were positioned at various locations within each panel. Four of these locations correspond to the moisture content pins (see Section 2.3.3 below) to allow for the accurate determination of wood moisture. These thermocouples were placed at the centre of the stud about 25 mm above or below the pair of wood moisture pins (see also Figure 2.12). The remaining thermocouples were placed at strategic points within the panels, as shown in Figures 2.9 to 2.11.

Before each monitoring cycle commenced, the reference or "cold junction" temperature was read and the thermocouple voltage corrected accordingly. The maximum error for the type T thermocouple is 0.064 °C at a temperature of -30 °C. The average error is 0.012 °C. System accuracy is estimated at better than 0.5 °C but relative readings are likely accurate to about 0.1 °C. For a more detailed discussion on temperature measurement, the reader may review the Sciemetric Operating Manual [1] (page A.6).

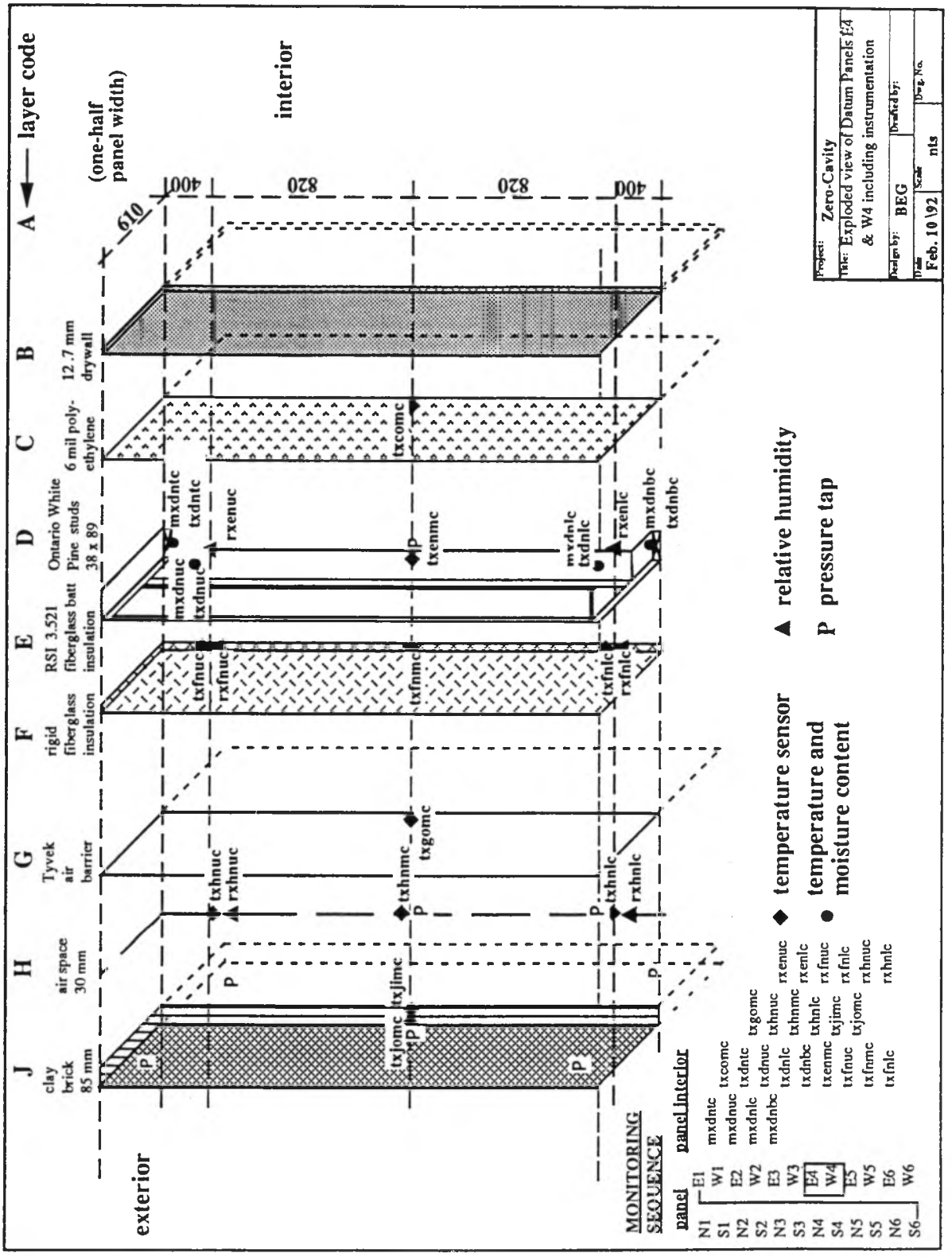

Figure 2.9: Exploded View of Datum Panel Construction

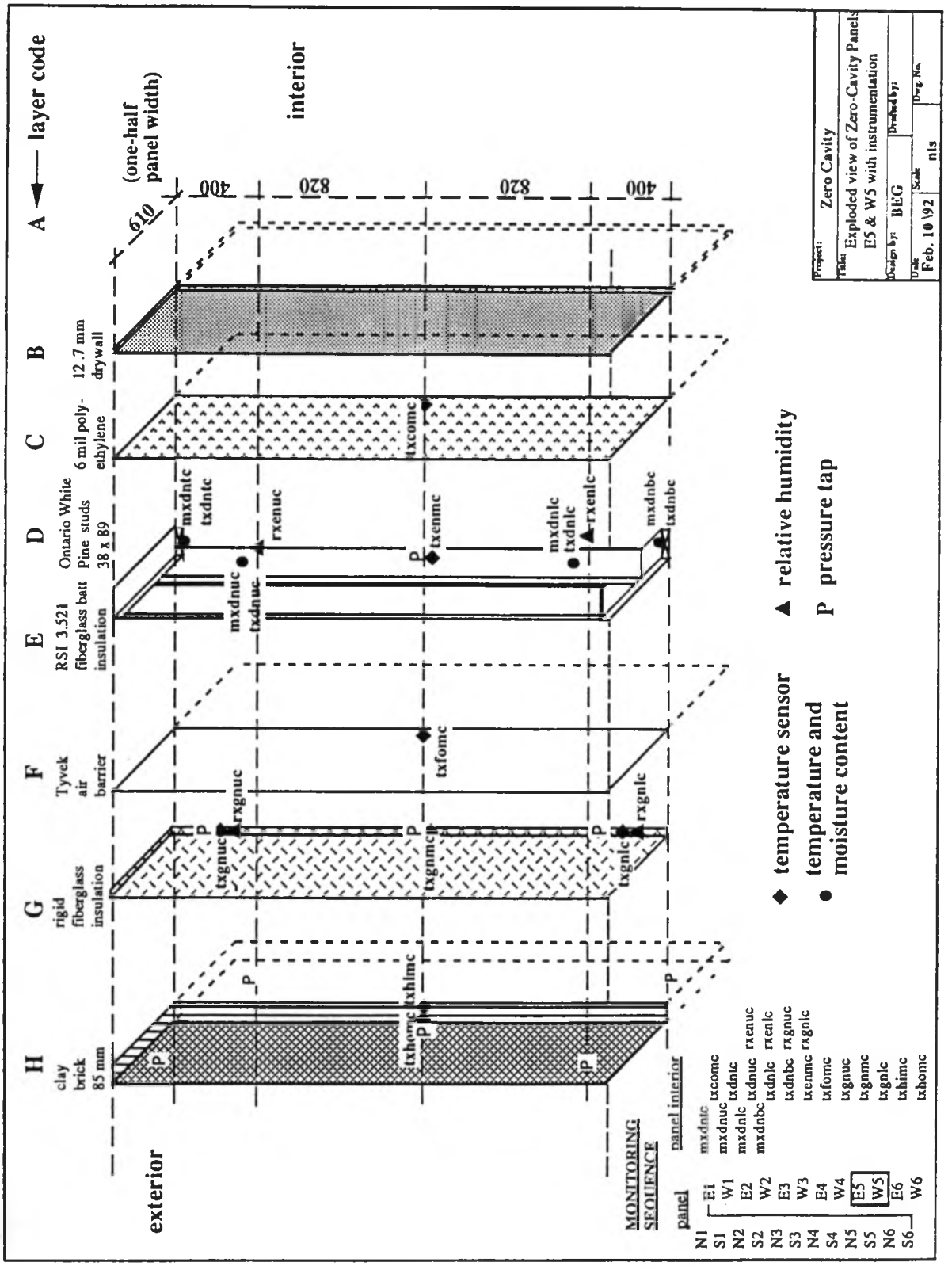

Figure 2.10: Exploded View of Zero-Cavity Panel Construction

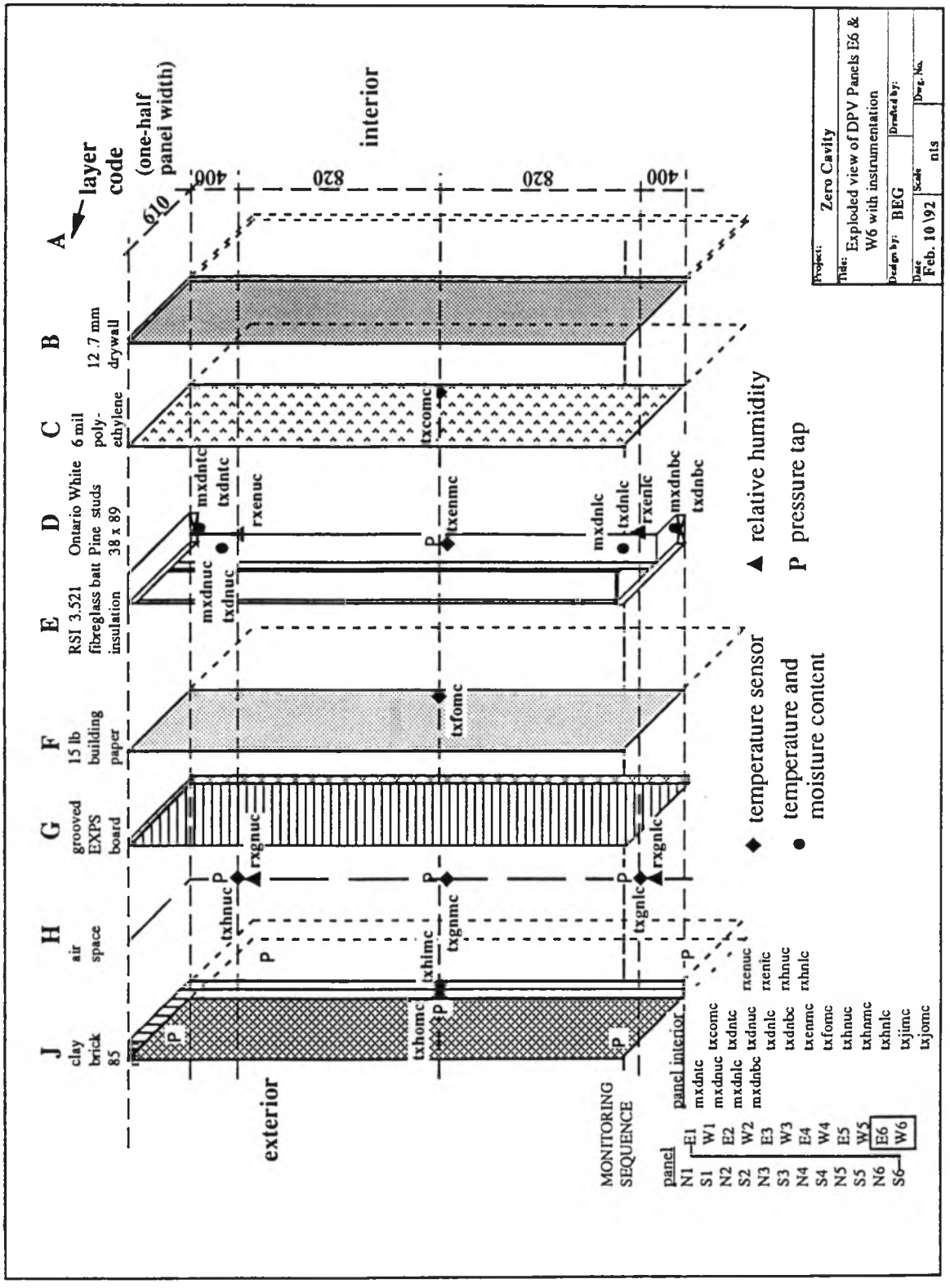

Figure 2.11: Exploded View of DPV Panel Construction

2.3.3 Wood Moisture Measurement

The moisture content in the wood framing was measured by passing a 25 volt direct current difference between two metal pins, 25 mm (1") apart. The voltage was applied for about one second so that the readings would stabilize to the correct level. Output (voltage difference) to the data acquisition system was then converted into a resistance. The resistance values were correlated with readings from a Delmhorst (model RC-1D) moisture meter before installation. The software stored the voltage readings, and these readings were later corrected for temperature and wood species by a separate, custom program.

The moisture pins for the wood frame structure of the wall panels were positioned at five different locations in each panel, as shown in Figures 2.9 to 2.11. All moisture contact pins are located at the middle of the larger, inward-facing side of the stud or plate and placed parallel to the wood grain. For consistency, the instrumented stud was the most northerly of the centre pair of studs.

The moisture pins penetrated the stud to a depth of about 10 mm (3/8"). Since each stud was 38 mm (1-1/2") thick and will, theoretically, dry equally from both 89 mm (3-1/2") faces, the average moisture content of the lumber is likely to be at 1/4 the depth, or approximately 10 mm (3/8"), as shown in Figure 2.12. The moisture pins penetrated the top and bottom plates to a depth of about 19 mm (3/4"). Since the in-place conditions on either face of the plate are not the same, it cannot be assumed that drying will be the same from both 89 mm (3-1/2") faces. Drying is largely towards the inner surface and, for this reason, the average moisture content was assumed to occur at the middle of each plate. The complete method of determining the moisture content in wood using temperature and species corrections is described in Appendix C.

The moisture measurements are the least accurate of all of the readings. The recorded moisture content does not necessarily represent the average moisture content of the wood. Moisture gradients are present through the wood as a result of drying/wetting of the wood and the environmental conditions that promote it, as well as wet pockets that might not represent the average moisture content. The actual accuracy of the resistance-type meters used is estimated as ±2% within the range of 6 to 25%; a considerable loss in accuracy can be expected outside this range. Above fibre saturation (25 to 30%) the meter will generally return lower values than actually exist, whereas below 6%, the resistance becomes so high it cannot be properly measured.

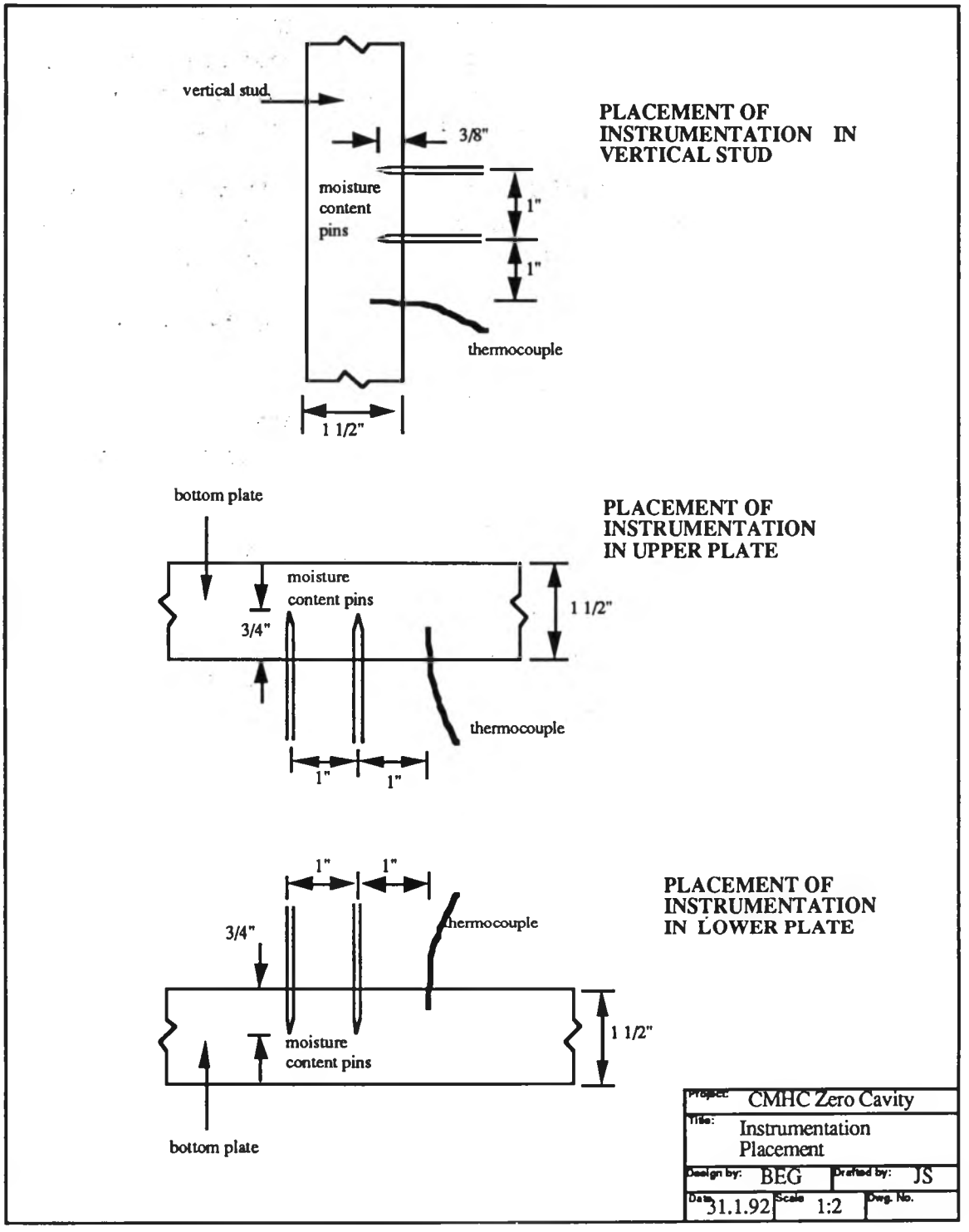

Figure 2.12: Wood Framing Instrumentation Placement

2.3.4 Air Pressure Measurement

The set-up and equipment used to measure pressures was based on, and is practically the same as, the Texas Tech University Wind Engineering Research Field Laboratory (WERFL).

Several pressure taps were installed in each panel. The taps were connected to pressure transducers by 3.5 metre long, 3 mm inner diameter Tygon™ tubing. To ensure that only static air pressure would be measured, the exposed ends of the tubes was designed to avoid the problem of the wind 'ramming' into the open end. A detail of the end design is given in Figure 2.13, and pressure tap locations are given in each panels' exploded view. The taps allowed pressure to be measured at the middle of the exterior of each panel, at each of the four vent/drains, in the middle of the cavity, and in the stud space. Although the length and diameter of the tubing are large relative to what is considered normal in scale-model wind tunnel testing (length of less than 1m, diameter less than 3 mm), the test panels were built at full scale. Relatively flat frequency response was calculated for frequencies of up to 30 Hz.

To convert air pressure to a voltage, Honeywell Micro-Switch PX163 very low pressure transducers were used. These transducers can measure pressures over a range of -1250 to +1250 Pa with an accuracy of approximately 1% of the full scale output. By individually calibrating each transducer over the smaller pressure ranges actually experienced, this accuracy was improved to better than 0.5% (approximately ± 2-5 Pa) and the linearity over the range of pressures measured (±100 Pa) is better than 0.5 Pa. The transducers are based on a piezoresistive silicon diaphragm with a response time of approximately 1 millisecond. The displacement of the pressure transducer is quite small (0.133 cc); this limits resonance and increases response time. Automatic temperature compensation is provided within each unit's circuitry.

The transducers output a voltage which varies linearly with the applied pressure. To provide the high-speed measurements required to determine pressure-equalization and frequency response, a 12-bit high-speed analogue-to-digital converter (Sciemetric Model 236 A/D) and custom software was used. The A/D converter could accurately read the pressure measurements to a resolution of ±0.6 Pascals. The voltage was converted to a pressure by using the individually measured calibration equations for each transducer. While the exterior wind speed and direction were read at the same rate as the pressures, all readings of temperature, wood moisture, and relative humidity were suspended while the pressure measurements were taken.

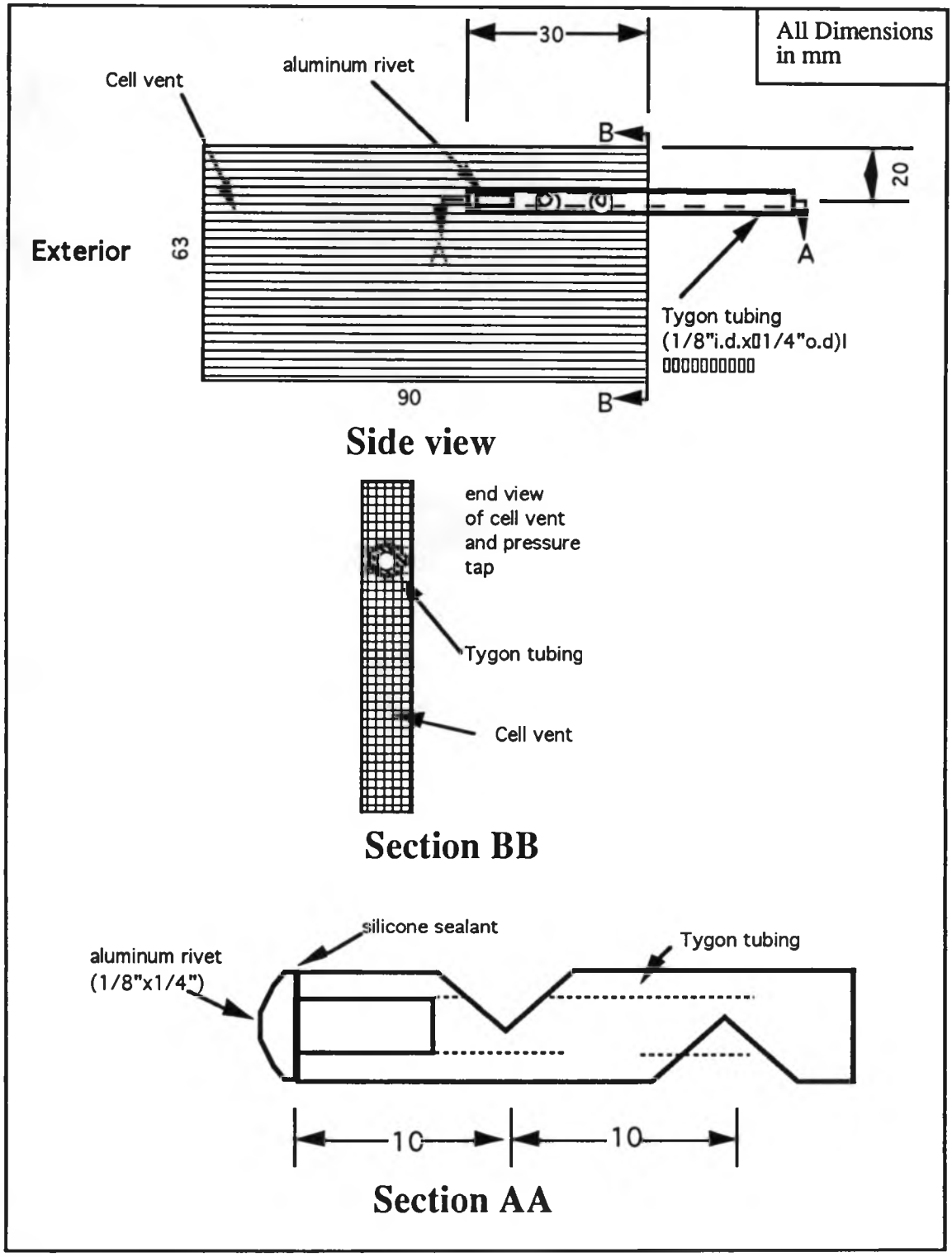

Figure 2.13 : Air Pressure Taps

2.3.5 Weather Station

A weather station was mounted 10 m above the ground on a tower attached to the peak of the Beghut roof. This weather station consisted of a relative humidity and temperature sensor and a wind monitor to measure wind speed and direction.

The relative humidity and temperature probe used was a Vaisala HMP 35A with an integral solar radiation and precipitation shield. This instrument uses a HUMICAP® sensor similar to the other Vaisala RH sensors and a platinum Pt 100 thermistor to sense temperature. The RH sensors have a range of 0 to 100% RH and an accuracy of approximately ± 2% RH and repeatability of better than 1% RH per year. The temperature sensor has a range of -20 to +60 °C with an accuracy of ±0.3 °C. The relative humidity sensor produced a linearly-varying output in the range of 0 to 1 VDC which was directly measured by the hardware and calculated as relative humidity by the software. The temperature sensor varies in resistance at about 0.38 Ohms/°C; the voltage drop of a small current flow across this resistance was measured by the Sciemetric hardware and converted to a temperature by software.

A Young Model 05103 Wind Monitor measured horizontal wind speed and direction through a propeller mounted on the front of a vane. The monitor provides a linear DC voltage proportional to direction and a linearly increasing magnitude AC voltage as wind speed increases. The instrument has a speed range from 1.0 m/s (3.6 km/h) to 100 m/s (360 km/h) with a distance constant of 2.7 m for 63% recovery (this means that in a 2.7 m/s wind, 63% of an instantaneous wind speed change will be measured within 1 second). The direction is accurate to within 5 degrees in wind speeds over 1.5 m/s (5.4 km/h).

2.4 Data Acquisition System

The data acquisition system comprised Sciemetric hardware, two personal computers, and Copilot software. This system allowed continuous monitoring of the data. The following section describes the hardware as well as the routines required to run the system.

2.4.1 Hardware

The monitoring system used was the "System 200" manufactured by Sciemetric Instruments Inc. Each sensor was connected to one of 32 channels on a Model 252 multiplexer card. Each group of seven slave 252 multiplexer cards had one "master" card. This master card permitted communication with a 386-based PC through an analogue-to-digital (A/D) converter (Model 231 or 236) via a Model 802 interface card. Four master cards are associated with monitoring temperature and moisture content and are connected to the PC via the 231 A-to-D converter. One master card drove the RH and weather "slave" card and communicated to a second PC through the Model 236 A/D converter. The computers used to drive the Sciemetric hardware were DTK Personal Computers with 80386 processors. Each had two external disk drives for 3-1/2" floppy disks. The data acquisition software used to run the hardware resided on the hard drives.

A complete scan of all sensors was completed every 5 minutes, and the hourly average was saved to a floppy disk at the top of each hour. Because of the one-second pause used to allow the wood moisture readings to stabilize, the scan of all channels by the 231 A/D required approximately 3 minutes. The wind speed and direction was scanned every ten seconds to improve the accuracy of the average because the high-speed 236 A/D completed its scan in under ten seconds.

2.4.2 Software

An integrated data acquisition software package called Copilot was used to manage data collection. All linearization and data reduction were performed automatically by the program after the user initialization. For further information, the reader may refer to the Copilot User's Manual.

2.4.3 Sensor Codes

A system using six alphabetic characters was devised to code the elements within each panel. Each six-character code is preceded by the panel identification code. A flow chart of how the element codes were configured and the order in which elements were read is presented in Figure 2.14. The system collected the data during each 5 minute cycle in the following order:

i) All of the moisture content (mx) values were read first, starting with panel N1 (Figures 2.9 to 2.11 lists the order of the moisture-content readings) and ending with W6.

ii) The temperature (tx) values were read next, following the same order as moisture content readings.

iii) Relative humidity, weather and interior micro-climate readings were taken by the 236 analogue-to-digital converter which began reading at the same time as i) and followed the same panel order.

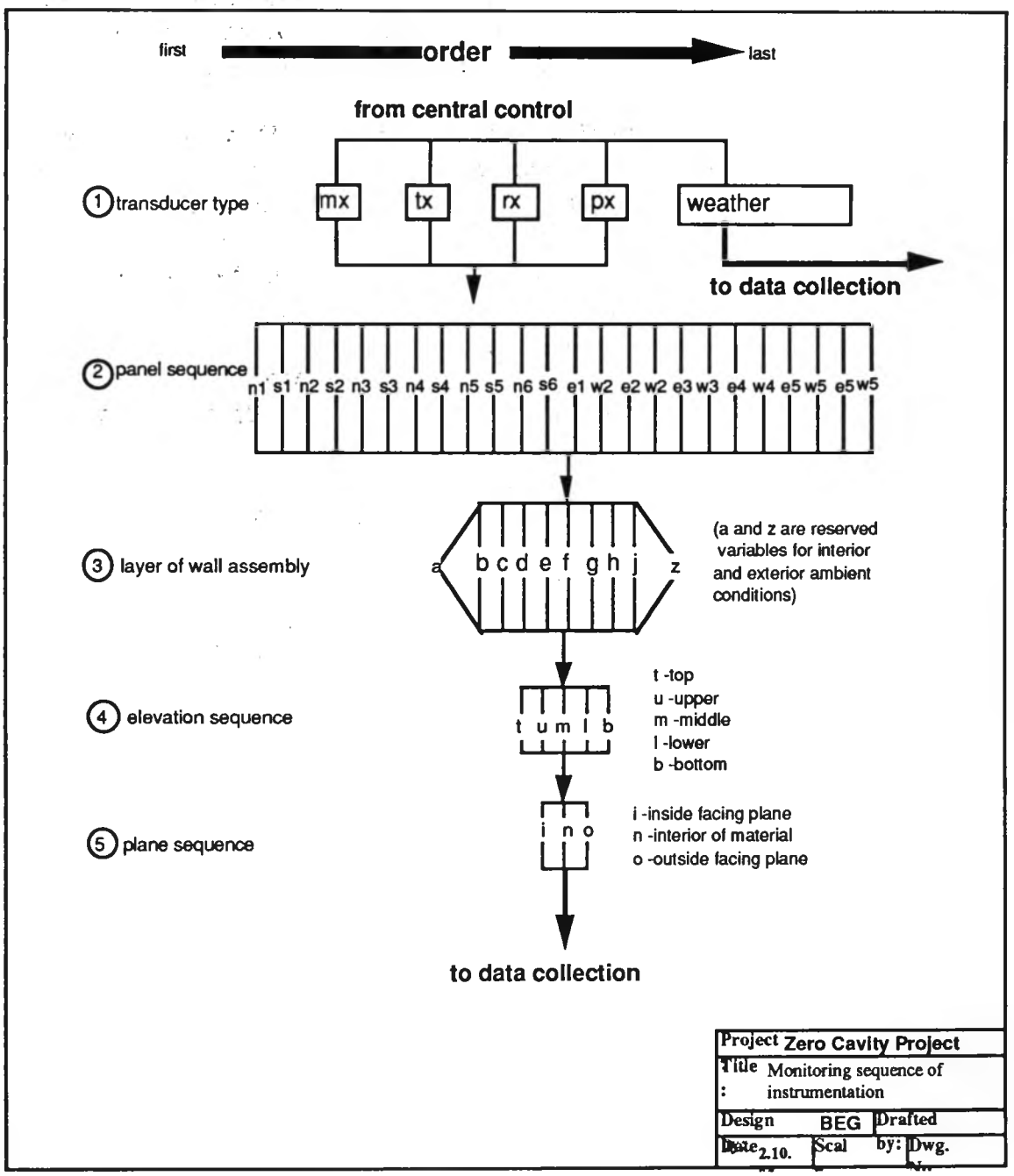

Figure 2.14: Sensor Coding and Monitoring Sequence

2.5 Test Results: Manipulation, Presentation and Documentation

All hourly average data stored on floppy disks were later exported to files in text-readable format by the Copilot software. The data were then processed by a custom program. This program converted the wood moisture voltages to a percentage moisture content by weight and saved the daily averages to a spreadsheet-readable file. Batch files then drove a series of spreadsheet macros which read the daily averages from files and automatically printed graphs. If more than 12 hours of any day's data were lost or incorrect, this day's data were ignored in graphing and in compiling statistics.

Because of the large number of sensors per panel, a graph was produced for each panel for temperature, relative humidity, and wood moisture. The same scale was used for all graphs to facilitate comparisons; the temperature graphs range from -20 °C to +30 °C, relative humidity from 0% to 100%, and wood moisture from 0% to 60%. All graphs for the period November 1, 1992 to November 1, 1993, are reproduced in Appendix A.

Statistical data were compiled from another custom program which used the daily average values and were manually transferred to a spreadsheet for presentation. Appendix C contains tables of the raw summary statistics.

2.6 Timetable of Events

1991	March	- contract awarded
	May	- strategy planning, design of special features, ordering material and instrumentation
	June	- panel assembly
	July 15-19	- panel and masonry installation in Beghut
	July 22-26	- flashing, sealing, and caulking around panels completed
	August 19-23	- connection of instrumentation to the data acquisition system
	September	- troubleshooting, final checks on instrumentation and data acquisition system, panel acclimatization
	October	- panel acclimatization
	November 1	- monitoring and data collection began
1992		
	July -Sept.	- water and air leakage tests
	December	- commissioning of pressure-equalization instrumentation
	December 31	- end of data analysis; collection continues
1993		
	Jan. - August	- pressure-equalization data collection and analysis
	September 2	- panels opened and inspected. Monitoring discontinued.

3. In-Place Panel Performance

3.1 Purpose

Wood moisture content, relative humidity, and temperature were recorded continuously at several locations in the panels in order to permit an assessment of thermal gradients and cycling, condensation potential, and moisture accumulation over both a full calendar year (1992) and four complete seasons.

All the readings are documented and analyzed over five different time periods, namely over the entire year (Section 3.4), representative winter and summer periods (Sections 3.5 and 3.6) and for representative winter and summer days (Sub-sections 3.5.5. and 3.6.5). Using statistical measures, trends, and patterns, the performance of the three wall systems are compared within each of the relevant time periods. The significance of the results are discussed and panel performance is compared in Section 3.7.

3.2 Results: Reduction and Documentation

The panels were continuously monitored from November 1, 1991, to December 31, 1992, with interruptions due to equipment or power failures only. The type and number of instruments used in each panel are described fully in Section 2. Sensors were read every 5 minutes and the hourly average was stored on disk. The hourly values were later averaged over the day for seasonal and annual analysis.

3.2.1 Data Reduction and Presentation

Because of the large number of readings, some reduction and averaging was required. However, possibly significant and recurring short-term variations can be masked by averaging. To deal with this problem and to allow for meaningful analysis, the yearly variation, the steady-state performance over a winter and summer period, and typical daily variations have been prepared and presented in different ways.

The variation of interior and exterior temperatures over the year is shown in Figure 3.1; the variation of RH and vapour pressure is presented in Appendix A. To evaluate the yearly values and variations, the daily average reading for every sensor was calculated

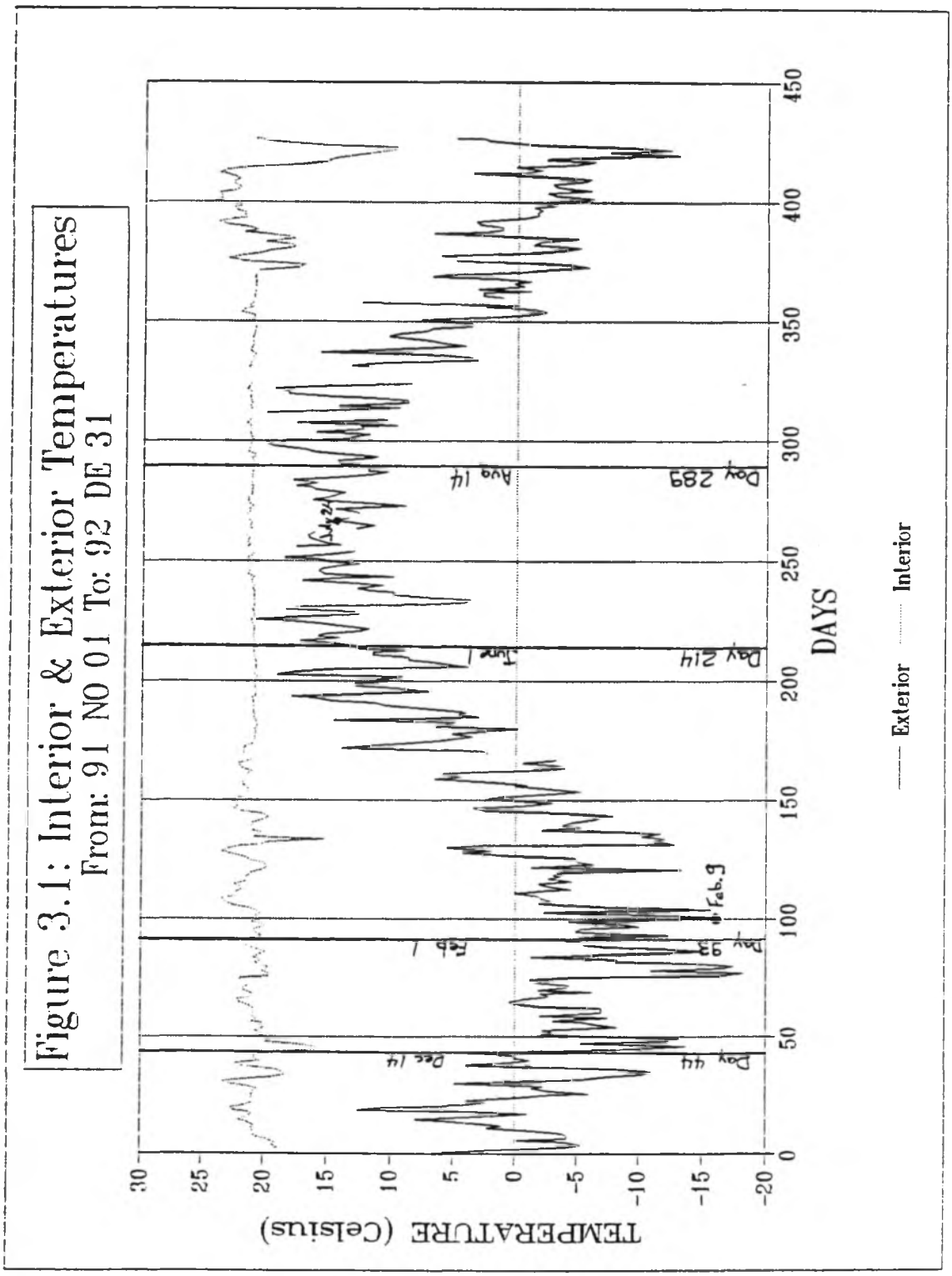
Figure 3.1: Interior & Exterior Temperatures
From: 91 NO 01 To: 92 DE 31
TEMPERATURE (Celsius)
DAYS
Exterior
Interior
30
25
20
15
10
5
0
-5
-10
-15
-20
0
50
100
150
200
250
300
350
400
450
Day 44
Day 289
Day 214
Day 93
Feb. 9
Dec 14
Nov 14
June 1
Feb 1

and plotted for the entire monitoring period. For each panel the five or six graphs were prepared for each of the following:

- temperatures

  i) through the panel mid point,

  ii) within the sheathing,

  iii) within the wood framing, and

  iv) within the cavity (for the Datum and DPV panels only),

- relative humidity

  v) within the stud space, sheathing (Datum only), and cavity, and

- wood moisture content

  vi) in the framing.

All of the resulting graphs can be found in Appendix A.

Relatively constant periods of weather were chosen to be representative of seasonal behaviour. Through an examination of the yearly variation of the daily mean exterior temperature (Figure 3.1), two periods were selected where the temperature changed little over several weeks. The winter period chosen was 49 days long (from December 14, 1991 to February 2, 1992) and the summer period was 75 days long (from June 1, 1992 to August 14, 1992). These periods are shown in Figure 3.1.

The average and standard deviation of the mean daily values were calculated for both representative periods for all sensors over both the summer and winter periods. These statistical measures are presented in tables in Appendix C. These values were further modified by averaging some sensors which were not on the panel centreline (i.e., the wood framing and sheathing) or by averaging sensors not on the panel centreline to provide an average panel value. The resulting tables for the east and west orientations are presented in Tables 3.1 and 3.2. For further simplification, the east and west sides were averaged and these results are contained in Table 3.3.

Significant variations and trends can be discerned by reviewing the hourly data. A complete evaluation of all hourly data involves almost two million readings. To make

Winter Period

Monitoring From: December 14, 1991 to February 1, 1992

	Datum				Zero Cavity				Dow			
Temperatures	W4		E4		W5		E5		W6		E6	
Degrees Celsius	Mean	S.D.	Mean	S.D.	Mean	S.D.	Mean	S.D.	Mean	S.D.	Mean	S.D.
Exterior	-6.9	*4.8*	-6.9	*4.4*	-6.9	*4.8*	-6.9	*4.4*	-6.9	*4.8*	-6.9	*4.4*
Outer Brick	-3.2	*4.3*	-2.7	*4.4*	-2.8	*4.3*	-2.7	*4.4*	-2.9	*4.3*	-2.6	*4.4*
Inner Brick	-2.5	*4.3*	-2.2	*4.3*	-2.1	*4.2*	-2.1	*4.3*	-2.3	*4.3*	-2.2	*4.3*
Cavity	-1.3	*4.0*	-0.9	*4.2*	Not Applicable		Not Applicable		-1.1	*4.1*	-0.8	*4.0*
Sheathing	5.4	*3.4*	6.8	*3.1*	-0.3	*4.0*	1.0	*3.8*	Not Measured		Not Measured	
Tyvek/Bldg Paper	-1.2	*4.1*	-0.5	*4.0*	7.0	*2.9*	6.2	*3.0*	6.8	*2.9*	6.6	*2.9*
Wood Framing	13.6	*2.0*	13.1	*1.9*	12.7	*2.1*	12.7	*1.9*	12.5	*2.0*	13.5	*1.8*
Batt	15.6	*1.7*	16.7	*1.4*	16.5	*1.6*	16.7	*1.5*	16.4	*1.5*	16.0	*1.6*
Vapour Barrier	18.8	*1.4*	18.3	*1.3*	19.1	*1.3*	19.0	*1.3*	18.7	*1.3*	19.0	*1.3*
Interior	20.4	*1.3*	20.4	*1.3*	20.4	*1.3*	20.4	*1.3*	20.4	*1.3*	20.4	*1.3*
Wood Moisture	W4		E4		W5		E5		W6		E6	
Percent	Mean	S.D.	Mean	S.D.	Mean	S.D.	Mean	S.D.	Mean	S.D.	Mean	S.D.
Top Plate	10.7	*0.1*	10.4	*0.1*	11.0	*0.1*	10.8	*0.1*	10.9	*0.1*	10.6	*0.1*
Upper Stud	10.6	*0.1*	10.4	*0.1*	10.6	*0.1*	10.6	*0.1*	10.8	*0.1*	10.6	*0.1*
Lower Stud	10.7	*0.1*	10.7	*0.1*	10.6	*0.1*	10.6	*0.1*	10.8	*0.1*	10.7	*0.1*
Bottom Plate	10.9	*0.1*	10.9	*0.1*	13.9	*1.0*	23.1	*6.5*	10.9	*0.1*	10.4	*0.0*
Relative Humidity	W4		E4		W5		E5		W6		E6	
Percent	Mean	S.D.	Mean	S.D.	Mean	S.D.	Mean	S.D.	Mean	S.D.	Mean	S.D.
Exterior	81.0	*6.8*	81.0	*6.8*	81.0	*6.8*	81.0	*6.8*	81.0	*6.8*	81.0	*6.8*
Upper Cavity	81.2	*4.2*	82.5	*2.3*	Not Applicable		Not Applicable		51.4	*4.7*	43.5	*6.3*
Lower Cavity	79.2	*4.1*	80.4	*4.7*	Not Applicable		Not Applicable		51.9	*5.3*	55.3	*6.2*
Upper Sheathing	35.0	*4.7*	38.2	*4.6*	46.5	*8.4*	48.5	*5.1*	Not Measured		Not Measured	
Lower Sheathing	30.1	*7.9*	26.2	*6.3*	52.5	*5.9*	28.4	*7.5*	Not measured		Not Measured	
Upper Batt	24.4	*5.1*	27.7	*5.4*	26.4	*6.0*	28.8	*4.9*	29.3	*6.1*	27.4	*3.2*
Lower Batt	25.9	*5.2*	25.4	*5.1*	31.0	*5.5*	28.5	*5.7*	28.5	*3.5*	30.6	*2.2*
Interior	48.2	*2.4*	48.2	*2.4*	48.2	*2.4*	48.2	*2.4*	48.2	*2.4*	48.2	*2.4*

Table 3.1: Winter Period Statistics

Summer Period

Monitoring From: June 1, 1992 to August 14, 1992

	Datum				Zero Cavity				Dow			
Temperatures	W4		E4		W5		E5		W6		E6	
Degrees Celsius	Mean	S.D.	Mean	S.D.	Mean	S.D.	Mean	S.D.	Mean	S.D.	Mean	S.D.
Exterior	14.0	3.0	14.0	3.0	14.0	3.0	14.0	3.0	14.0	3.0	14.0	3.0
Outer Brick	20.5	3.5	21.5	4.1	20.7	3.5	21.4	4.1	20.6	3.6	21.6	4.2
Inner Brick	20.4	3.7	21.5	4.0	20.8	3.4	21.5	3.9	20.7	3.5	21.6	4.1
Cavity	20.3	3.4	21.7	3.8	Not Applicable		Not Applicable		20.8	3.3	21.8	3.8
Sheathing	22.6	2.6	22.6	2.7	21.2	3.2	21.5	3.5	Not Measured		Not Measured	
Tyvek/Bldg Paper	20.5	3.3	21.2	3.7	20.9	2.1	21.1	2.6	20.7	2.2	21.4	2.5
Wood Framing	21.0	1.2	20.6	1.3	21.1	1.4	21.0	1.5	20.4	1.2	21.3	1.3
Batt	20.7	0.8	20.1	0.5	21.1	1.0	21.1	1.0	21.0	0.7	20.9	1.2
Vapour Barrier	21.0	0.5	20.5	0.8	20.6	0.6	20.8	0.6	20.7	0.4	20.8	0.4
Interior	21.2	0.2	21.2	0.2	21.2	0.2	21.2	0.2	21.2	0.2	21.2	0.2
Wood Moisture	W4		E4		W5		E5		W6		E6	
Percent	Mean	S.D.	Mean	S.D.	Mean	S.D.	Mean	S.D.	Mean	S.D.	Mean	S.D.
Top Plate	9.8	0.2	11.6	0.7	18.8	2.0	13.8	0.9	10.0	0.1	9.9	0.1
Upper Stud	10.8	0.6	13.0	1.4	23.3	2.6	14.8	14.3	10.1	0.1	10.0	0.1
Lower Stud	11.3	0.9	11.1	0.8	21.9	2.3	51.7	92.8	10.2	0.2	9.8	0.1
Bottom Plate	10.2	0.3	10.8	0.4	19.9	1.7	35.6	1.8	10.0	0.1	9.8	0.1
Relative Humidity	W4		E4		W5		E5		W6		E6	
Percent	Mean	S.D.	Mean	S.D.	Mean	S.D.	Mean	S.D.	Mean	S.D.	Mean	S.D.
Exterior	69.7	13.9	69.7	13.9	69.7	13.9	69.7	13.9	69.7	13.9	69.7	13.9
Upper Cavity	71.0	15.0	62.9	13.2	Not Applicable		Not Applicable		55.0	13.5	57.3	12.0
Lower Cavity	53.1	8.9	66.0	14.5	Not Applicable		Not Applicable		60.8	12.9	54.0	12.7
Upper Sheathing	54.0	9.2	53.6	8.8	87.2	4.4	72.4	6.5	Not Measured		Not Measured	
Lower Sheathing	49.9	8.1	54.5	11.9	86.0	3.2	49.5	38.7	Not Measured		Not Measured	
Upper Batt	55.4	8.5	55.8	9.4	85.4	5.9	70.3	7.8	46.7	4.9	46.7	4.9
Lower Batt	66.2	13.6	53.0	9.1	82.4	4.7	83.1	4.5	42.3	4.2	42.3	4.2
Interior	50.2	2.3	50.2	2.3	50.2	2.3	50.2	2.3	50.2	2.3	50.2	2.3

Table 3.2: Summer Period Statistics

	Summer Period Monitoring Period: June 1, 1992 to August 14, 1992						Winter Period Monitoring Period: Dec. 14, 1991 to Feb. 1, 1992					
Temperatures	**Datum**		**Zero Cavity**		**Dow**		**Datum**		**Zero Cavity**		**Dow**	
Degrees Celsius	Mean	S.D.	Mean	S.D.	Mean	S.D.	Mean	S.D.	Mean	S.D.	Mean	S.D.
Exterior	14.0	*3.0*	14.0	*3.0*	14.0	*3.0*	-6.9	4.8	-6.9	4.8	-6.9	4.8
Outer Brick	20.9	*3.9*	21.1	*3.8*	21.1	*3.9*	-2.9	*4.4*	-2.7	*4.3*	-2.8	*4.3*
Inner Brick	21.0	*3.7*	21.2	*3.7*	21.1	*3.8*	-2.3	*4.3*	-2.2	*4.3*	-2.2	*4.3*
Cavity	21.0	*3.6*	Not Applicable		21.3	*3.6*	-1.2	*4.1*	Not Applicable		-1.0	*4.1*
Sheathing	22.6	*2.6*	21.4	*3.4*	Not Measured		6.1	*3.3*	0.3	*3.9*	Not Measured	
Tyvek/Bldg Paper	20.8	*3.5*	21.0	*2.3*	21.0	*2.3*	-0.8	*4.0*	6.6	*2.9*	6.7	*2.9*
Wood Framing	20.8	*1.2*	21.1	*1.5*	20.9	*1.2*	13.4	*1.9*	12.7	*2.0*	13.0	*1.9*
Batt	20.4	*0.7*	21.1	*1.0*	20.9	*1.0*	16.1	*1.6*	16.6	*1.6*	16.2	*1.6*
Vapour Barrier	20.8	*0.7*	20.7	*0.6*	20.8	*0.4*	18.6	*1.3*	19.0	*1.3*	18.9	*1.3*
Interior	21.2	*0.2*	21.2	*0.2*	21.2	*0.2*	20.4	*1.3*	20.4	*1.3*	20.4	*1.3*
Wood Moisture	**Datum**		**Zero Cavity**		**Dow**		**Datum**		**Zero Cavity**		**Dow**	
Percent	Mean	S.D.	Mean	S.D.	Mean	S.D.	Mean	S.D.	Mean	S.D.	Mean	S.D.
Top Plate	10.7	*0.4*	16.3	*1.4*	9.9	*0.1*	10.5	*0.1*	10.9	*0.1*	10.7	*0.1*
Upper Stud	11.9	*0.0*	19.0	*2.0*	10.0	*0.1*	10.5	*0.1*	10.6	*0.1*	10.7	*0.1*
Lower Stud	11.2	*0.8*	36.8	*47.5*	10.0	*0.1*	10.7	*0.1*	10.6	*0.1*	10.8	*0.1*
Bottom Plate	10.5	*0.3*	27.7	*1.8*	9.9	*0.1*	10.9	*0.1*	18.5	*3.7*	10.7	*0.1*
Relative Humidity	**Datum**		**Zero Cavity**		**Dow**		**Datum**		**Zero Cavity**		**Dow**	
Percent	Mean	S.D.	Mean	S.D.	Mean	S.D.	Mean	S.D.	Mean	S.D.	Mean	S.D.
Exterior	69.7	*13.9*	69.7	*13.9*	69.7	*13.9*	81.0	*6.8*	81.0	*6.8*	81.0	*6.8*
Cavity	63.2	*12.9*	Not Applicable		56.8	*12.8*	80.8	*3.8*	Not Applicable		50.5	*5.6*
Sheathing	53.0	*9.5*	73.8	*13.2*	Not Measured		32.4	*5.9*	44.0	*6.0*	Not Measured	
Batt Insulation	57.6	*10.1*	80.3	*5.7*	46.1	*4.4*	25.8	*5.2*	28.8	*5.5*	29.1	*3.7*
Interior	50.2	*2.3*	50.2	*2.3*	50.2	*2.3*	20.4	*1.3*	20.4	*1.3*	20.4	*1.3*

Table 3.3: Averaged Summer and Winter Statistics

this task manageable, several individual periods of one to three days have been examined during specific weather conditions. A cold, sunny, and calm winter day (February 9, 1992) and a typical sunny/hazy calm summer day (July 24, 1992) preceded and followed by a day with similar weather were selected to describe the daily variations. For each panel the following hourly values for these two days have been plotted:

- temperature
- relative humidity
- water vapour pressure, and
- exterior surface layer temperature rise above ambient (the sol-air effect).

Both the water vapour pressure and solar-induced temperature rise were calculated from the recorded temperature and RH values. Wood moisture content changed so little over a span of 24 hours that it was not analyzed on an hourly basis. All of the resulting plots for these daily periods can be found in Appendix B.

3.2.2 Accuracy of Results

Each of the values presented in Tables 3.1 and 3.2 are averages of from 12 000 to 22 000 individual readings. This large sample permits confidence in the consistency of the values. Section 2 of this report outlines the level of accuracy that can be expected of the various sensors. To review, the temperature sensors are able to read within about ±0.1 °C, the RH sensors within ±2%, and the wood moisture within ±2%. A possible source of error is the placement of the sensors in the wall section. One can only monitor the status at a limited number of location in the wall, and the shape of the gradients (because of thermal stratification, material variability, etc.) between points can only be implied. The measured values will also be a function of location. Although care was taken, it is possible that a sensor was not placed exactly in the middle of a layer, whereas it may have been in the other paired panel. This will result in differences in the long-term averages even if the two walls performed in exactly the same manner.

3.2.3 Missing Data

There were a number of equipment failures and several power outages which resulted in data being lost for a few hours at a time. The failure of a major board in the data acquisition equipment resulted in intermittently inaccurate temperature readings over a 38 day period during April and May. These readings were discarded. Any day for which

less than 12 reliable hourly readings were recorded was not plotted or included in the statistical analysis. A diary which lists all days during which data were lost is provided in Appendix F.

3.3 Exterior and Interior Climate

The average exterior temperature over the entire monitoring period was 3.2 °C, and the average exterior relative humidity was 73.8%. The 30-year normal value of mean daily temperature at the Waterloo-Wellington Airport is 6.7 °C and the value for 1992 was 5.0 °C. The monthly averages of the daily means of exterior temperatures are presented for 1992 and compared to the 30-year average in Figure 3.2. The winter period compares quite well with the 30-year average value, but the summer of 1992 was exceptionally wet and cool, with monthly mean temperatures up to 5 °C colder than the 30-year average. The underlying sinusoidal variation of the temperature over a year can clearly be seen in Figures 3.1 to 3.2.

The interior temperature and humidity were kept relatively constant at an average of 20.9°C and 48.9% throughout the monitoring period. For the 12 months of 1992, the average temperature was 21.1 °C and the RH was 50.0%. In the chosen summer period, the interior temperature was 0.8 °C higher and the RH 2% higher than during the winter period. The standard deviation of the interior summer temperature and the graph of the entire monitoring period indicate that the temperature was quite stable relative to the winter period. Although deviations from the mean of 2 °C were experienced for some days, the standard deviation of temperatures for the winter period (1.25 °C) and summer period (0.2 °C) was small. At the end of the monitoring period, an HVAC failure caused the temperature to fall for several days; this is considered to have no effect on the results.

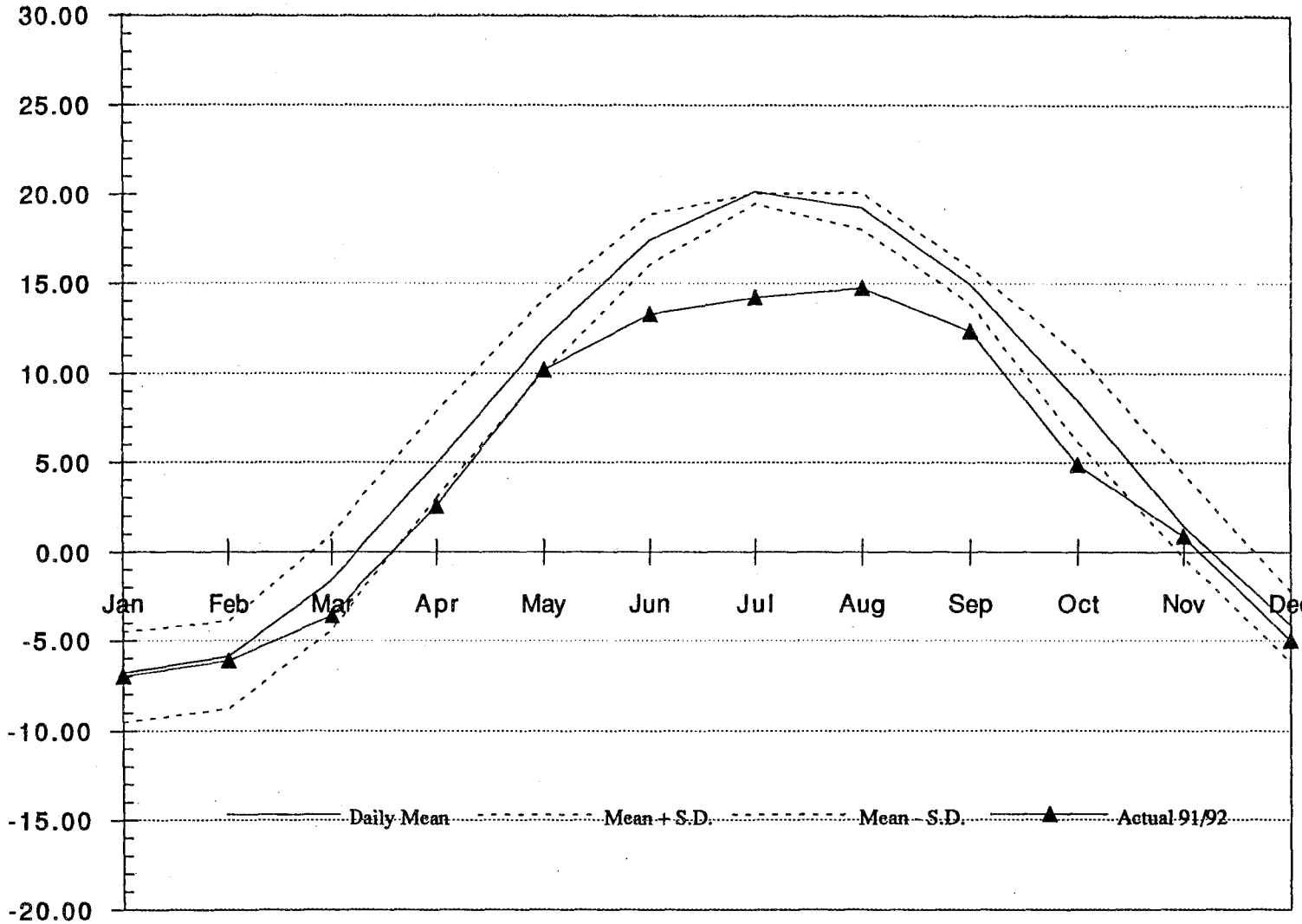

Figure 3.2: 30 Year Normal Mean Values of Daily Temperatures (Waterloo, Ontario)

3.4 Year-Long Performance

The graphed data from the fourteen-month-long monitoring period can be found in Appendix A. Based on the study of these graphs of average daily readings, observations, trends, and patterns are discussed below.

3.4.1 Temperature

The exterior daily mean temperature varies as a sinusoid about the mean of 7 °C over the year; the warmest mean temperatures occur in July (20 °C) and the coldest occur in January (-7°C) (Figure 3.2). The underlying sinusoidal variation of the exterior temperature drives the temperature variations in all layers of all the wall systems. The closer a layer is to the interior (where the temperature is almost constant), the smaller the amplitude of the temperature variation and the closer its value approaches the value of the interior temperature (21 °C). The daily average temperature variation of the walls was always less than the variation of the exterior ambient temperature. In all panels, daily spikes of exterior temperature were clearly reflected in the outer layers. These same short-term changes were also measured in the inner layers but with a much smaller amplitude. In general, the effect of the variation of the exterior air temperature on the inner layers was very small. However, the sun's energy resulted in *hourly* temperature variations in the exterior layers which could be much larger than the exterior ambient air temperature variations.

Each layer in each wall assembly tended to have distinct temperatures, although this distinction was least in the summer because of the smaller driving temperature difference. The hierarchy of the average daily layer temperatures did not change over the entire monitoring period except for the outermost layers, which became warmer than the interior temperature on some summer days.

The brick screen and the cavity temperatures (the fibreglass sheathing behaved as a cavity in the Zero-Cavity panels) were grouped together and followed the exterior sinusoidal variation quite closely. The amplitude and phase of the variation of these outer layers was very close to the exterior temperature, but the mean annual temperature was about 5°C higher than the exterior average because of the influence of solar radiation.

The Tyvek™ and building paper temperature in the Zero-Cavity and DPV panels respectively was elevated about 6 °C above the temperature of the exterior layers (because the air/moisture barrier is protected by significant amounts of insulation in these

panels) but otherwise followed the exterior variations closely (with a smaller magnitude because of the damping effect of the insulated sheathing). The Tyvek™ in the Datum panel, however, followed the cavity temperatures very closely since it was directly exposed to the cavity air.

The wood framing was generally 10 °C below the interior air temperature during the winter period but was almost the same as the interior in the summer (20 °C). The framing temperature readings were very similar between panels and within each panel. No pattern to the variation of framing temperature over the height of the panel was evident. This suggests that significant convection did not occur in the stud space.

The batt and polyethylene temperatures in all the panels remained within 5°C of the interior temperature throughout the monitoring period. The poly and batt temperatures were similar, and exterior temperature variations had much less effect on their temperatures than on the temperature of the outer layers. In the summer period the grouping of the temperatures by layer was only evident when longer term spikes in temperature created a significant temperature difference across the wall.

3.4.2 Relative Humidity

The daily average exterior RH varies greatly from day to day, and while it does not exhibit a strong sinusoidal pattern over the year like the exterior temperature, it does drop by about 10% in the summer. Within the wall systems there is also a large daily variation but with an underlying sinusoidal pattern. This behaviour indicates that the temperatures in the wall directly affect the relative humidity measurements. Compared to the exterior, the temperatures are relatively stable within the wall, and the vapour permeability of the materials tends to reduce the size of the RH variations. Together, these factors explain the observed sinusoidal pattern over the year and the small daily variation (small relative to the exterior) exhibited in all of the walls. The RH was consistently higher in all panels during the summer and lowest during late winter. Little difference was evident between sensors placed in the same layer of the wall (i.e., upper and lower sensors within the same layer) as compared to the grouping of values found in different layers of the wall systems (i.e., inner vs. outer layers).

The Datum panel RH values tended to separate into two distinct groups: the relatively stable and higher cavity RH, and the lower sheathing and batt RH values which followed a sinusoidal variation. The effects of temperature and differences in material vapour permeability account for these results.

The Zero-Cavity panels had much less stratification of RH values across the wall because the cavity and the insulated sheathing are the same. Nevertheless, RH values within the insulated sheathing and batt responded differently: the sheathing exhibited a higher mean RH value and lower amplitude sinusoidal variation than within the batt insulation. One difference between the east and west orientations was that the lower sheathing RH followed the batt RH values until the fall, after which it followed the upper sheathing. All of the Zero-Cavity panel sensors recorded values of over 80% for several weeks during the late spring and early summer. This indicates a high probability of condensation during this time or water vapour evaporating from saturated materials. The batt RH values were similar to the Datum panel values except over the summer when they are consistently higher by as much as 20%.

Relative humidity values within the DPV panel also exhibited a sinusoidal pattern but with the smallest amplitude and lowest mean RH values. The lower amplitude and mean RH values are likely due to the much higher vapour resistance of the exterior sheathing which impedes vapour diffusion between the cavity and the stud space. Of the three pairs of panels, the DPV panels' stud space was the driest over the monitoring period.

3.4.3 Wood Moisture

The wood moisture content of the framing lumber exhibited some considerable variation between panel pairs. In general, there was a consistent gain in wood moisture during the summer and a strong drying trend in the fall. Equilibrium values were around 11 - 12% during the winter.

The Datum panels had very stable wood moisture contents through to the end April. Moisture gain occurred through the summer and ended in October. The framing then dried rapidly to the equilibrium level by the start of December. At no time did the wood approach fibre saturation but it did briefly exceed 20%. The bottom plate remained the driest in both panels, but the other three sensors did not follow the same order as in both panels. The sensor in the upper stud, however, registered the highest moisture content in both Datum test panels.

Relative to the Datum and DPV panels, the Zero-Cavity panels had high moisture content values at the start of the monitoring period (about 3 months after their installation). The east panel bottom plate measurements indicated full saturation, and the west panel bottom plate Delmhorst pins returned a moisture content of over 20%. The other three moisture content sensors in each of these panels indicated typical equilibrium values of about 12%.

Both panels dried quickly during the winter, but the east panel's bottom plate was still at 15% MC by the end of the winter. As in the Datum panel, the moisture content increased over the summer period, driving the east panel's bottom plate moisture content to well above fibre saturation. The western Zero Cavity panel, which began the monitoring period with all wood moisture readings well below 15%, gained considerable moisture, and the bottom plate moisture content peaked at over 25%. Although the moisture content of the bottom plate of the eastern Zero Cavity panel climbed to a level indicative of fibre saturation during the summer, at all other locations behaviour was similar to that of the other Datum panels and the moisture content remained below 20%. Starting in December, both panels dried quickly, but the bottom plate of the east panel still had about 20% moisture content.

The DPV panels exhibited very stable wood moisture content. Although the framing did gain moisture during the summer period, the change was at most 3%, and in all cases the moisture content remained below 14%. The winter equilibrium value was approximately 11%, slightly lower than in the Datum panels.

Both the Datum and the DPV panels behaved in a similar and satisfactory manner, with the DPV panels performing somewhat better than the Datum panels. The bottom plates of the Zero-Cavity panels exhibited much greater fluctuations of both wetting and drying. As the moisture content levels were in excess of both 19% (the maximum allowed by the National Building Code) and fibre saturation, this is not satisfactory and cause for concern. This concern is warranted, as the panel opening later confirmed that a considerable amount of mould had grown in the Zero-Cavity panels.

3.5 Winter Period Performance

The winter period extended from December 14, 1991, to February 1, 1992. Mean thermal and vapour gradients for the three wall systems have been calculated for the winter period using the material properties listed in Table 2.1. These gradients are compared to the measured values in Figure 3.3 and 3.4. Several assumptions were made in the calculations and presentation:

- steady-state thermal conditions with no heat storage,
- steady-state vapour conditions and properties with non-hygroscopic materials (Glaser's Method),

- exterior and interior conditions equal to the mean values measured over the defined winter period,
- measured values from the panel centreline at mid-height were used, and
- all sensors were assumed to be placed exactly as described in Section 2.

From the gradients, it can be expected that the three panels will have very similar performance. However, the measured values show a distinct increase in temperature at the exterior surface; this significant difference is due to the daily influence of the sun.

The behaviour of each layer of the wall assemblies during this period is described below for all three pairs of panels in terms of the temperature, relative humidity, and wood moisture content (if applicable).

3.5.1 Exterior Screen

The average outer brick temperature over the representative period was between -2.9 °C and -2.7 °C for all panels; this is 4.1 °C above the average ambient temperature. This difference could be caused by three factors:

- heat from the interior of the building that is flowing outward,
- the fact that heat is not easily transferred to the exterior by convection and radiation, and
- the sun usually provides considerable heat to the face of the brick for some part of each day (at least on the east/west faces being considered).

By observing the daily screen temperature variation presented in Section 3.5.5, it can be concluded that the sun is the major factor causing the elevated temperature. Only late at night, when the energy stored in the brick from the day was dissipated, did the brick temperature approach the exterior temperature). The temperature of the west side was consistently lower for the outer layers of all wall panels (by 0.4 °C for the outer brick), probably due to the prevailing winds from the northwest (i.e., higher convection losses).

The standard deviation of the daily mean brick face temperature is also less than that for the ambient temperature value; this indicates that the brickwork screen's thermal mass tends to damp out daily temperature fluctuations. Due to solar effects the hourly variation of brick temperature over a day is, however, usually quite high.

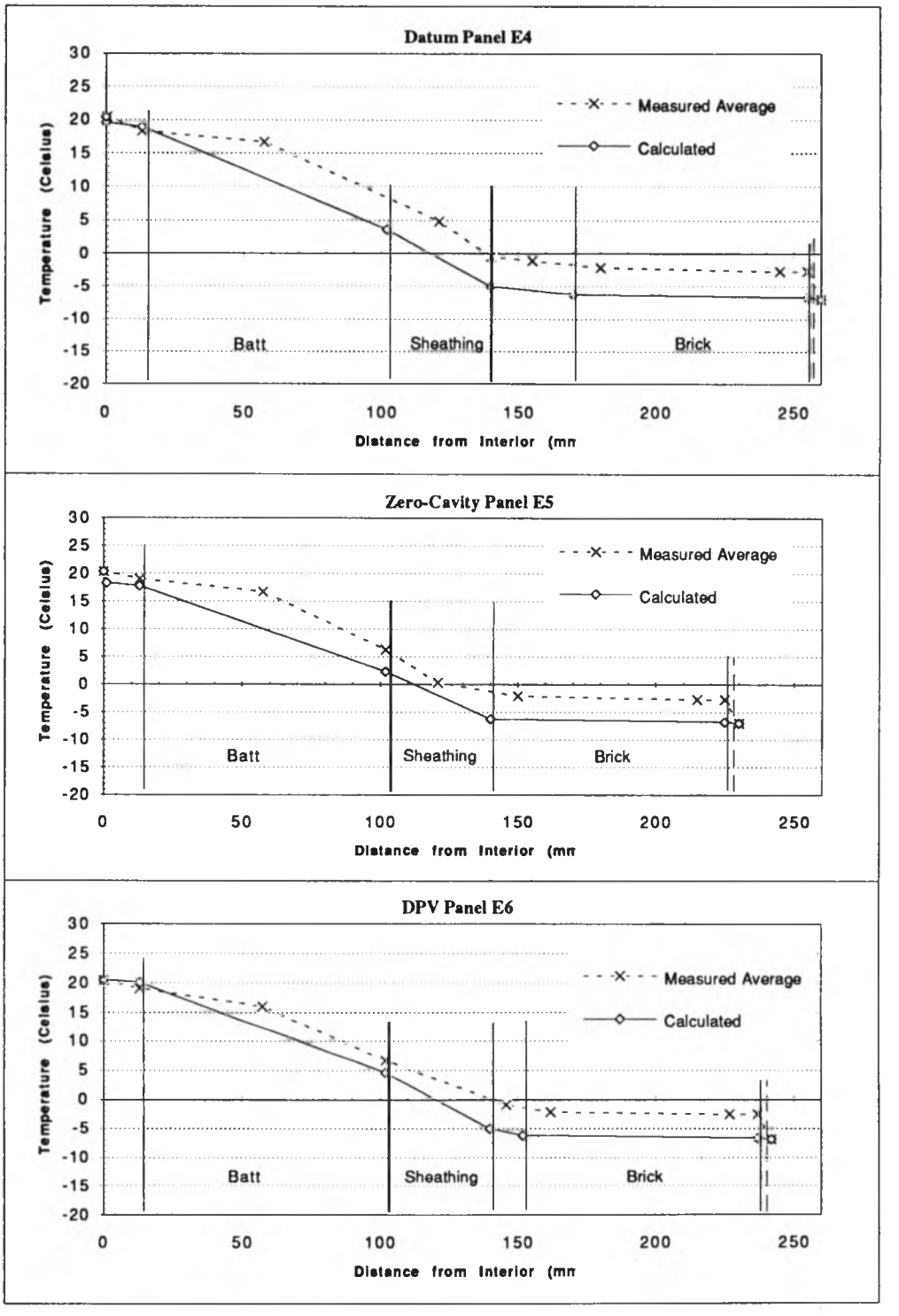

Figure 3.3: Calculated & Measured Winter Period Thermal Gradients

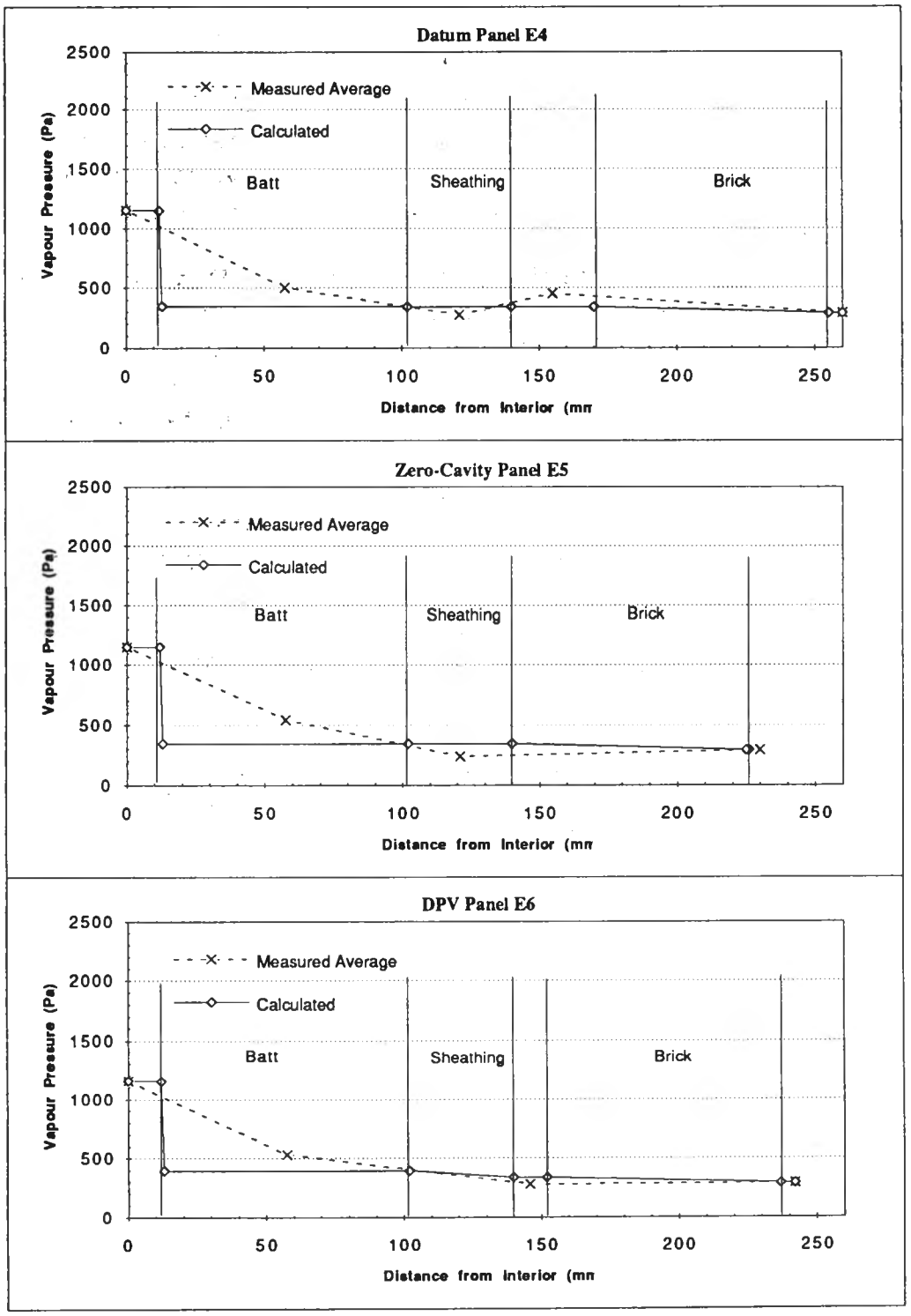

Figure 3.4: Calculated & Measured Winter Period Vapour Pressure Gradients

3.5.2 Cavity

The "cavity" in all six panels had remarkably similar temperatures. The Datum and DPV panels performed comparably, with a difference of approximately 0.25 °C, whereas the average temperature in the middle of the fibreglass sheathing of the Zero-Cavity panel was about 1.5 °C warmer. This is probably because the insulating sheathing in the cavity was in contact with the brickwork. No consistent pattern of vertical temperature stratification was evident on the basis of the lower, middle, and upper cavity temperature sensor readings, indicating little ventilation cooling was occuring.

The standard deviations of the daily mean of the upper, middle, and lower cavity temperatures were found to be very similar for the DPV and the Datum panels, whereas the Zero-Cavity panel had less variation. The variability of all of the panel cavity temperatures was less than that of the ambient air temperature.

The cavity temperatures in the Zero-Cavity panels were expected to be warmer and more stable since the sensor is in the middle of the insulating sheathing, i.e., it was more thermally protected and buffered from air flow. However, if air movement through the insulation was significant enough, the temperatures recorded by the sensor could be as low or lower than in the Datum panel. Since the temperature in the Zero-Cavity sheathing was warmer than in the Datum cavity, it is likely that little air flow occurred and the sheathing acted to insulate the sensor.

The relative humidities in the DPV and Zero-Cavity panel cavities were significantly lower and had significantly higher variations than the RH in the Datum panel. This is partly due to the slightly warmer temperatures experienced in these cavities (as temperature increases 1 °C the relative humidity drops by about 5 - 10% over the temperature range being discussed). The relative humidity in the Datum panel cavity was, on average, very similar to the exterior relative humidity but less variable; this indicates that sufficient ventilation was occuring to move water vapour past the relatively vapour impermeable brick veneer.

3.5.3 Sheathing and Tyvek™/Building Paper

The temperature in the middle of the sheathing at the centre of the panel was measured in the Datum and the Zero-Cavity panel only. There was a relatively steep temperature gradient across the insulated sheathing in all panels. Over the winter period, the average

sheathing temperature measured in the Datum panel was 6.1 °C with a standard deviation of 3.3 °C. The average daily mean sheathing temperature in the Zero-Cavity panel over the winter period was almost 6 °C colder and the standard deviation was slightly larger (3.9 °C). Assuming that daily temperature variations are normally distributed, the above facts suggest that the daily mean of the sheathing temperature in the Datum panel was below freezing for only 3.2% of the time, whereas the Zero-Cavity sheathing was below freezing for 47% of the 44 day winter period. This is an important finding since it demonstrates the increased likelihood of the sheathing in the Zero-Cavity panel to store, as frost, condensate from the interior and melted snow or rain from the exterior.

It follows that when the rigid fibreglass in the Zero-Cavity panel is considered as a cavity (Section 3.5.2), the mean temperature is 1.5 °C warmer than the cavity in the other walls. When the fibreglass is considered as insulated sheathing, the temperature is almost 6 °C colder than at the same location in the Datum panel sheathing.

The thermocouple located 10 mm outward of the back face of the brickwork is the closest point of temperature measurement to the exterior of the sheathing in the Zero-Cavity panels. The temperature at the exterior surface of the sheathing may be assessed from the Tyvek™ temperature in the Datum panel. The Tyvek™ housewrap on the exterior face of the Datum panel sheathing had an average daily temperature of -0.8 °C. In the Zero-Cavity panel, the average temperature of the back of the brick was -2.5 °C. Considering the respective standard deviations and assuming normally distributed temperatures, the mean temperature at the face of the sheathing in the Datum panel was below zero for 58% of the days in this period. In the case of the Zero-Cavity panels, a similar situation existed for 70% of the days at the interface between the brickwork and the insulated sheathing. Again, the "cavity" in the Zero-Cavity panel was cooler for longer than the cavity in the Datum panels.

Thus it can be concluded that the mean daily temperature values in the Zero-Cavity panel will be below freezing more often than in the Datum. While this has significance for the storage of condensation as frost in the sheathing (not a concern for the DPV panel), the solar effects evident from the daily observations can raise the temperature of the sheathing considerably above zero for several hours of any clear day for all orientations exposed to the sun. Even the north wall would experience an exterior surface temperature rise of about 5 °C during a winter day. The solar energy should serve to melt and subsequently drain or evaporate any stored frost. Theoretically, there should be very little if any accumulated condensation but, if the wall is poorly constructed, air leakage

and diffusion may make this a significant issue. If poor construction also increases the temperature significantly, the potential for problems will be reduced.

The magnitude and the variation of the temperature of the moisture barrier was quite different in each of the panels. The Tyvek™ in the Datum panel was exposed to the cavity, and thus had a lower mean temperature, with a significantly higher standard deviation than either the DPV or Zero-Cavity panels. Whereas the Tyvek™ in the Datum panel generally had an average daily temperature below zero, both the Zero-Cavity and DPV panels had quite warm Tyvek™ / building paper temperatures (mean values of 6.6 °C and 6.7 °C respectively). The variation in temperature was also much reduced, both diurnally and over the entire monitoring period, as compared to that in the Datum panels. Placing the air / moisture barrier behind the insulated sheathing in both the Zero-Cavity and DPV panels ensured that its temperature was considerably above zero and not exposed to large temperature fluctuations. In contrast, the Tyvek™ temperature in the Datum panel responded much like the temperature within the cavity.

The relative humidity of the sheathing in the Datum panel was lower than that in the sheathing/cavity of the Zero-Cavity panel, and the variability was similar. However, because the Zero-Cavity sheathing/cavity temperature was 6 °C lower than the Datum panel insulated sheathing temperature, the absolute amount of water present as vapour was greater in the Datum sheathing than in the Zero-Cavity sheathing. This difference may be due to the location of the Tyvek™ sheet in front of the insulated sheathing (which has some vapour resistance and will therefore increase the amount of vapour on the interior side during winter) in the Datum panels, whereas the Zero-Cavity panel can more freely vent any water vapour from the inside to the exterior via the brickwork and vents.

3.5.4 Inner Elements

The layers of the wall inside of or upstream of the inner face of the sheathing were all constructed in exactly the same way for all panels. They performed very similarly with respect to temperature and relative humidity.

Within measuring accuracy, the temperatures of the wood studs, the fibreglass batt, and the vapour barrier were essentially comparable between pairs of panels and between all panels. The only significant performance difference was the considerably lower standard deviation of the relative humidity within the batt insulation in the stud space of the DPV panel as compared to the other two panels. The less vapour-permeable extruded polystyrene probably acts to better decouple the stud space from the more extreme

variations in exterior relative humidity. This effect can also be seen in the plots of hourly readings discussed in Section 3.5.5.

Relative humidity values within the stud space of the DPV and Zero-Cavity panels (29 and 26% respectively) and the temperatures of the building paper / Tyvek™ (6.7 and 6.6 °C respectively) precludes the occurrence of condensation and storage as frost within the stud space at even the extreme 1% confidence interval. As discussed above in Section 3.5.3, the same conclusion cannot be reached for the ***sheathing*** in the Datum panels (which had an average sheathing RH of 32% and a temperature of -0.8 °C). While condensation and storage as frost is not expected to be a problem in well-built walls, trapped condensation could result in decreased thermal resistance and increased wood moisture.

The moisture content of the wood framing was very steady in both the Datum and DPV panels. The levels quickly stabilized at about 11 to 12%, indicating dry lumber. The Zero-Cavity panels, however, started at high levels (almost 60% in the west panel) but quickly dropped over the winter period. The upper plate, upper stud and lower stud all dried down to an equilibrium level comparable to the other panels (less than 11%) but the bottom plate remained somewhat higher than this in the west panel (W5) and over 15% in the east panel (E5).

3.5.5 Daily Winter Variations

In all six panels the wood moisture readings do not change significantly over a day. The hourly readings generally exhibit no change or reflect only the long-term trend of drying/wetting.

Figure 3.5 and 3.6 are hourly plots of temperature and relative humidity on a single cold day. February 9, 1992 was chosen since it was very cold, had little wind, and was clear and sunny throughout. The days preceding and following February 9 had similar weather. Only the western Datum panel (W4) is used in this discussion because its behaviour is representative of that in the other panels; refer to the plots for all six panels for this day, which are provided in Appendix B.

Although the ***temperature*** of the exterior face of the brick drops to within 1.5 °C of the ambient temperature at night, during the day the sun heats the brick to almost 25 °C above the ambient temperature for a short period. While the average exterior brick temperature for this particular day was almost 8 °C above the ambient, days with little

sun have average brick temperatures which are closer to the ambient (generally 2 °C above ambient on fully clouded days). On average the mean daily brick temperature was 4.1 °C above the ambient over the winter period.

The effect of the sun on the rest of the wall assembly is dramatic. The cavity, sheathing, and sheathing paper all experience significant temperature variations. Even the studs and batt are noticeably affected, although the thermal effect of solar radiation temperature is less than 5 °C in these components.

The temperature in the upper, middle, and lower portions of the cavity follow the temperature of the backside of the brick very closely during the short-term, rapid heating caused by the sun. Although the temperature difference across the vent holes is greater then 20 °C, the expected buoyancy-driven ventilation is not reflected in lower temperatures (i.e., closer to ambient) in the cavity or in vertical stratification. These observations suggest that there is no sufficient ventilation flow through the cavity by either wind-pressure differences or thermal buoyancy.

The ***relative humidity*** is highly dependent on temperature, and for this reason water vapour pressure (the absolute amount of water vapour present) was also examined. Both the relative humidity and the vapour pressure were greatly influenced by the large solar-induced temperature changes. Panels with different orientations (i.e., east vs. west) behaved differently only in that the solar influence occurred at a different time of the day. None of the sensors in the wall layers recorded RH values high enough to indicate a danger of condensation on this day.

The solar-induced warmer temperatures prompted an increase in the RH (rather than a decrease as would be expected for a constant volume of water vapour). This indicates evaporation of moisture from the constituent materials. The coincident increases in temperature and vapour pressure values are evident in the hourly plots. Since brick and wood are hygroscopic materials, they will store and release moisture in response to changing RH and temperature conditions. For approximately 8 to 12 hours the vapour pressure of all sensors in all walls increased significantly above the exterior value (which remained relatively constant throughout the day). These high vapour pressures show that the potential for drying exists as long as the downstream layers are vapour permeable.

The Datum and Zero-Cavity walls performed in a similar manner except that the Zero-Cavity panels generally exhibited higher RH and vapour pressure values, indicating either greater moisture or less drying potential (since the temperatures are similar). The higher

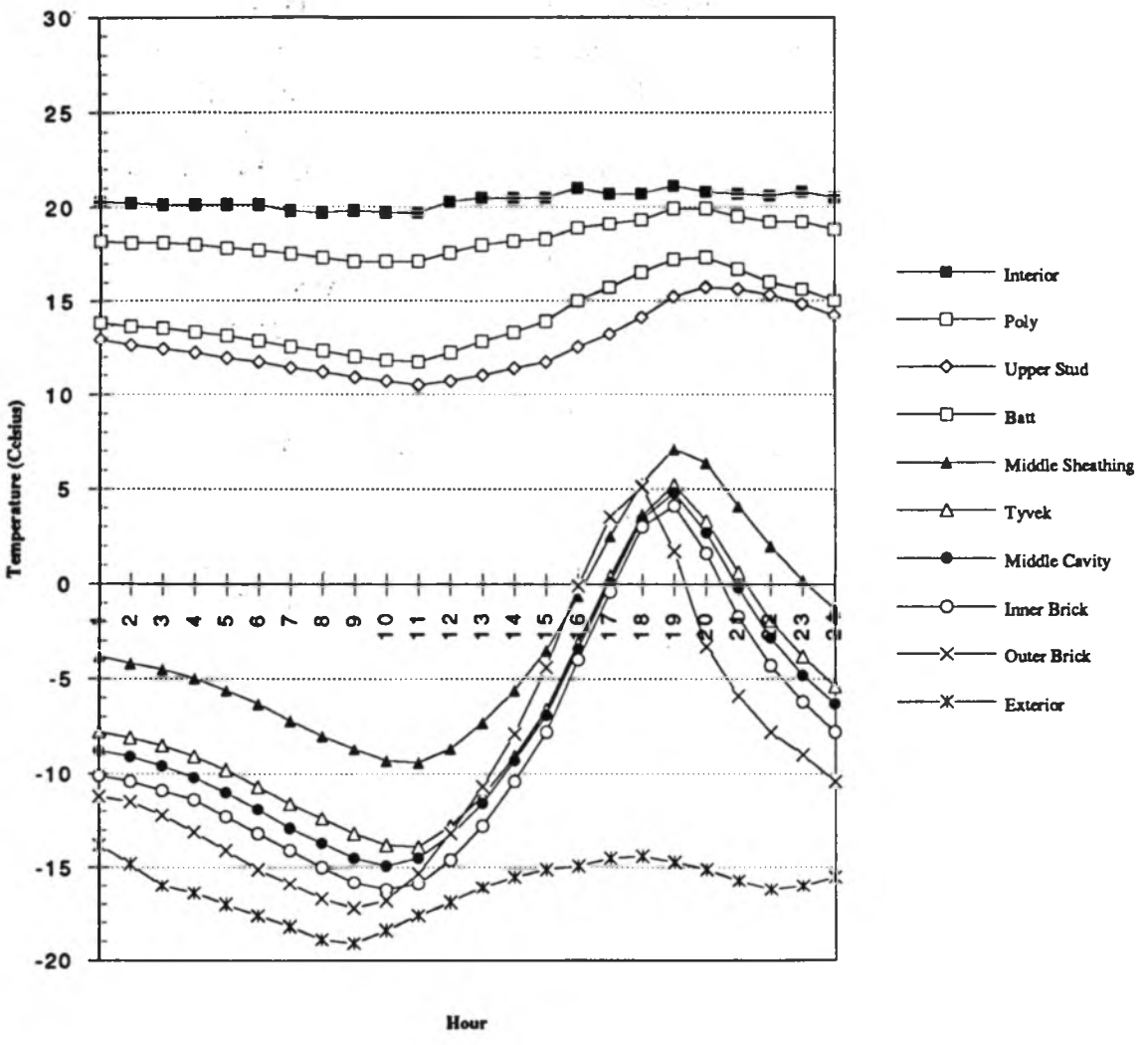

Figure 3.5: Hourly Temperature (Feb. 9, 1992)

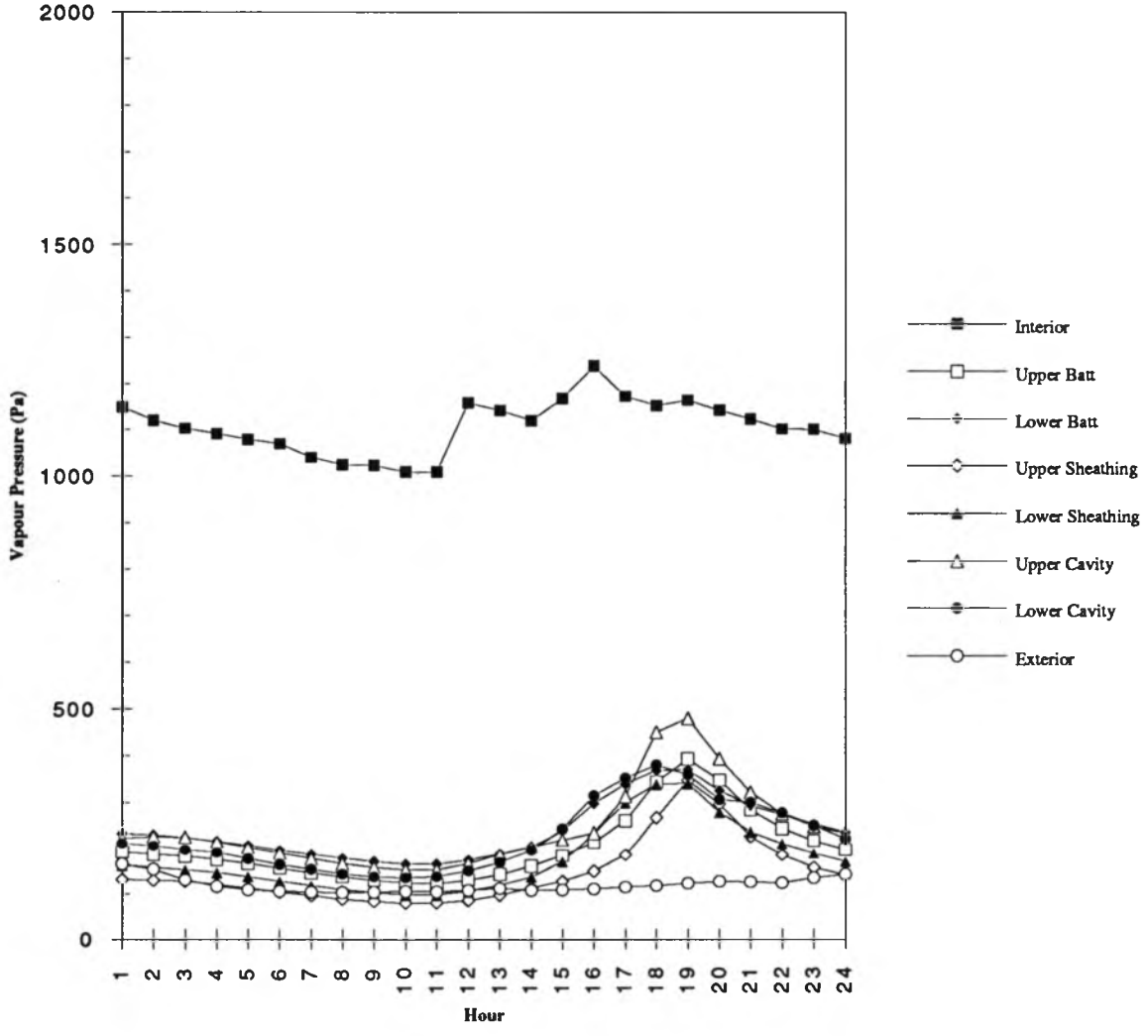

Figure 3.6: Hourly Vapour Pressures (Feb. 9, 1992)

wood moisture values and higher night-time (i.e., no solar influence) RH values suggest that there either is less ability for the Zero-Cavity walls to dry (and thus the moisture remains in the wall longer), or an increased amount of water load is imposed on these panels. The mockup tests reported in Chapter 7 indicate that the Zero-Cavity panels experience a greater moisture load.

The DPV panels behaved with much greater RH and vapour pressure stability than the other two panel pairs. There is a distinct difference between the vapour pressure values of the stud space and the cavity, unlike the datum and Zero-Cavity panels. The Styrofoam™ is much less vapour permeable than the Tyvek™ and fibreglass and is thus less likely to allow any vapour in or out; this accounts for the distinct difference in values between the layers. Because the vapour pressure does remain low and the wood moisture values also indicated the driest framing, it can be concluded that the DPV panels contained the least moisture.

Even the cavity vapour pressure is responsive to the solar influence. It was expected that the cavity vapour pressure in the Datum would closely follow the exterior vapour pressure because of the vent holes in the top and bottom of the brick veneer. However, during periods of peak sun exposure, the amount of water vapour present in the cavity was more than double its stable night-time values. Again, the degree of connection (i.e. ventilation) between the cavity and the exterior was less than expected for the Datum panels.

The high RH levels in the cavity are probably not due to the movement of moisture (by leakage or diffusion) from the inner layers to the cavity because the cavity vapour pressure is often higher than either the batt or sheathing values. Stored moisture (i.e., frost), if any, in the brick veneer may melt and evaporate and thereby add large amounts of vapour to the cavity air, especially when the veneer temperature exceeds the freezing point. It is also possible that moisture within the cavity evaporates and then refreezes during each daily cycle without escaping the assembly.

3.6 Summer Period Performance

The summer period chosen for examination extended from June 1 to August 14, 1992. Although the weather was cooler than normal in South-Western Ontario, the stable mean temperature allowed a longer period to be chosen than for the winter period.

As for the winter period, the summer thermal and vapour gradients were calculated and are compared to the measured values (Figure 3.7 and 3.8). The same assumptions were made as for calculating the winter gradients.

The sun has an even greater influence on the thermal and vapour pressure gradients than in the winter. The actual panel performance is quite different from that calculated using normal procedures (i.e., using the outdoor and indoor temperatures) As will be noted later, the panel behaviour in the summer period is virtually dominated by daily temperature swings induced by the sun rather than the mean daily values (compare Figure 3.7 and 3.9, 3.8 and 3.10).

The measured mean daily behaviour of all panels over the period is presented below for each layer in terms of temperature, relative humidity, and wood moisture. A single summer day is then examined on an hourly basis to provide more insight into the mean daily values.

3.6.1 Outer Screen

The average brick temperature over this representative period was, at 21 °C, almost the same for all panels: some 7 °C above the average ambient temperature. The standard deviation of the average daily brick temperature was similar but greater than the ambient in all six panels. The west side temperature was approximately 1 °C degree cooler than the east because of the prevailing winds and, possibly, because of the increased occurrence of clouds in the afternoon. Solar effects played a significant role in the temperature results, as can be seen from the cloudless and sunny summer day plotted in Figure 3.9.

3.6.2 Cavity

The average daily cavity temperatures in all panels were all of similar magnitude. However, the Zero-Cavity and the DPV panels both had average sheathing/cavity temperatures slightly greater than the brick temperature (by about 0.2 °C). While this difference is relatively and statistically insignificant, it is evident that the temperature in the cavity is essentially the same as that of the brick screen and some 7°C higher than the exterior ambient. It follows that, at least over the summer, these cavities are probably not well ventilated. No cooling of any significance occurs, and this suggests that no large ventilation flows through the cavity occurs. Furthermore, there was no discernible pattern to the order of the upper, middle, and lower cavity temperatures in the panels.

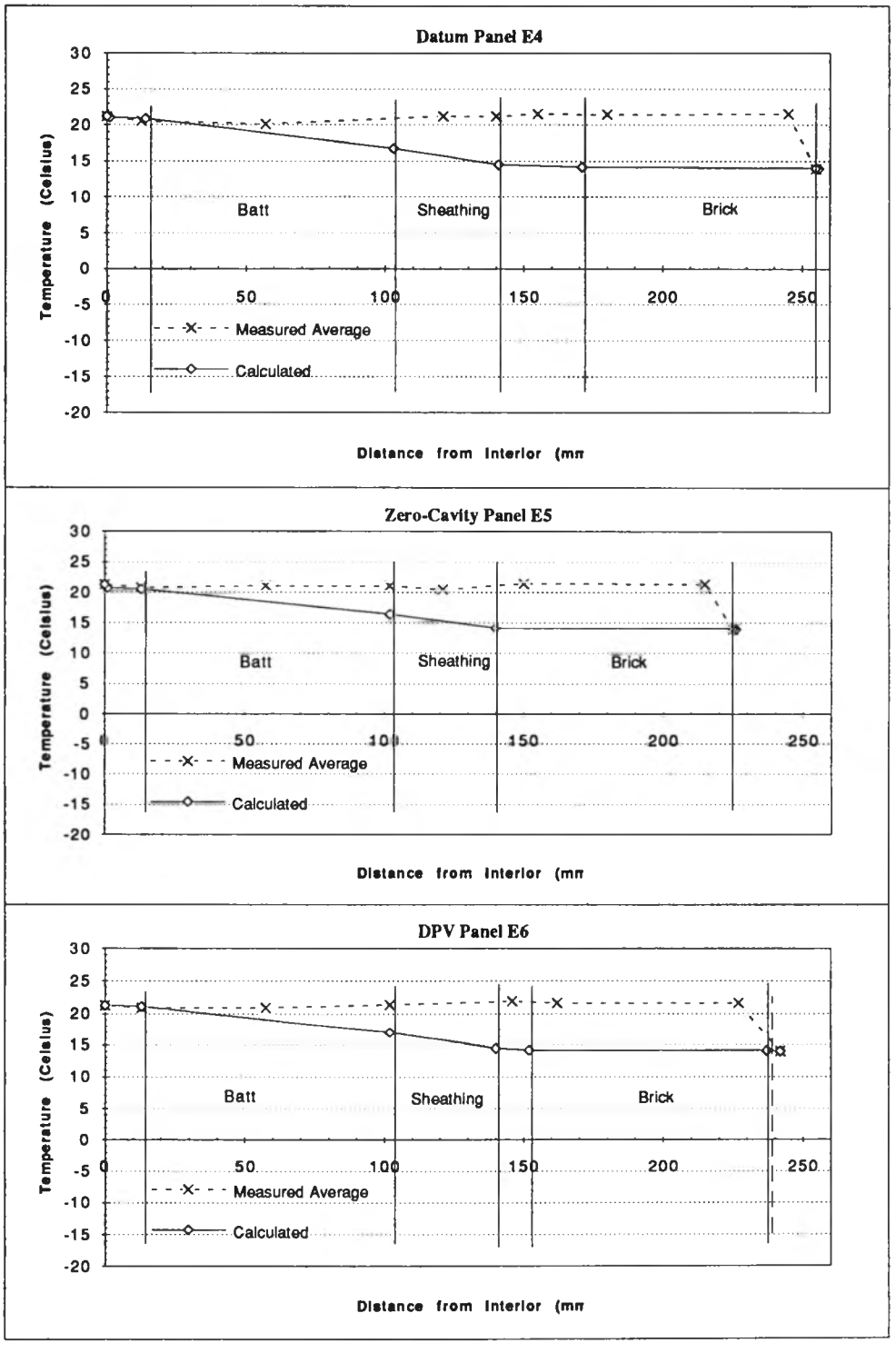

Figure 3.7: Calculated & Measured Summer Period Thermal Gradients

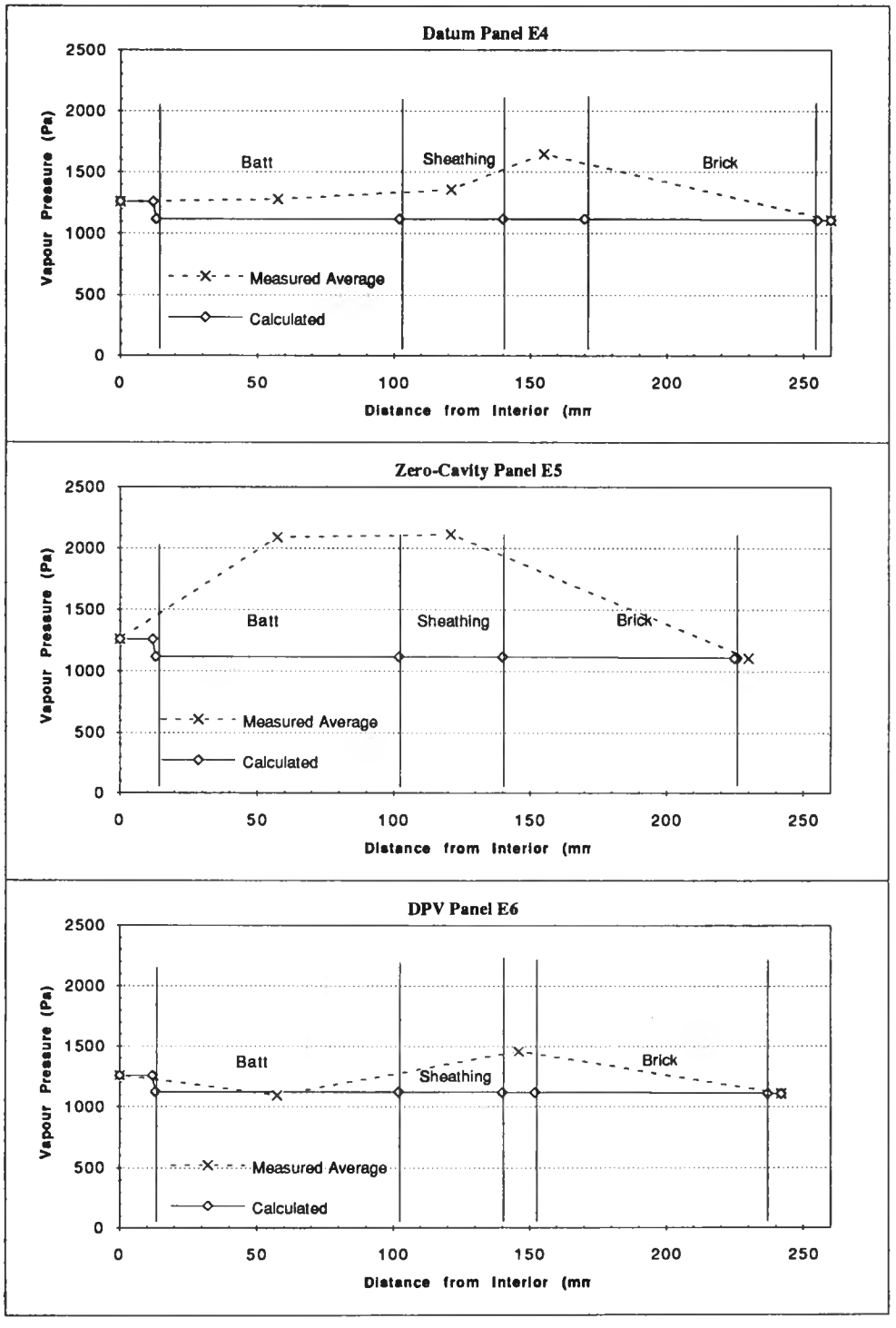

Figure 3.8: Calculated & Measured Summer Period Vapour Gradients

The relative humidity in the Datum and DPV panel cavities was lower than the ambient exterior RH. The Zero-Cavity panel sheathing had higher relative humidity values when compared to the exterior. Since the average exterior temperature was considerably lower than the average rigid fibreglass temperature, this result indicates that more moisture was present in the sheathing than in the exterior environment. The RH sensor within the sheathing of both Zero-Cavity panels gave, at times, readings of about 100%; these sensors were regularly removed and inspected throughout the summer and were found to be wet. The east panel (E5), in particular, had periods of more than a week during which the lower sheathing RH was constantly around 100%.

At the time it could not be ascertained whether the moisture was due to condensation or stored rain moisture which had penetrated the screen and remained in the fibreglass sheathing. Consideration of the temperatures in the fibreglass indicate that condensation *within the sheathing* is unlikely. However, the mockup tests (reported in Chapter 7) indicated that considerable volumes of rainwater penetration through the permeable screen (see Chapter 5) could easily have been retained in the bottom of the sheathing by capillarity.

It is highly likely that the high temperature in the brickwork and sheathing caused the vaporization of large volumes of the moisture trapped in the base of the Zero-Cavity panels' insulated sheathing and resulted in the high RH readings. The water vapour was then transported by vapour diffusion through the Tyvek™ into the stud space. While daily average readings indicate that the mean vapour pressure drive is in the order of 750 Pa (see Figure 3.8), the plot of vapour pressures on an hourly basis (Figure 3.11) shows peak values of 5000 Pa driving vapour inwards and outwards from the sheathing. Because the vapour resistance of the brickwork is relatively much higher than the Tyvek™, vapour will flow inwards.

In complete contrast to both the Datum and DPV panels, the average summer period Zero-Cavity batt/stud space vapour pressure was almost equal to the sheathing values.

3.6.3 Sheathing and Tyvek™/Building Paper

The sheathing in the Zero-Cavity panel was cooler (by 1.2 °C) than in the Datum probably because it contained moisture; the energy required for evaporation of this moisture would keep the sheathing cooler. On a day-to-day basis, the variation of the

Zero-Cavity sheathing temperature was considerably higher, and daily excursions were also generally higher than the Datum.

The Tyvek™ and building paper recorded similar mean temperatures values in the DPV and Zero-Cavity panels; within 0.05 °C. The standard deviation of the Tyvek™ temperatures in the Datum panels, however, was about 50% greater than in the DPV and Zero-Cavity panels because of the greater solar effects on layers closer to the exterior. Therefore, the Tyvek™ in the Datum panels was exposed to greater variations in temperature, which might raise concerns of material durability.

3.6.4 Inner Elements

In all panels, the wood framing and batt experienced similar temperature conditions. The Zero-Cavity panels had slightly higher wood framing temperatures as well as greater variability when compared to the behaviour of the Datum and DPV panels. The batt temperature in both the DPV and Zero-Cavity panels was slightly higher (by about 0.6 °C) and more variable than in the Datum.

The relative humidity of the stud space had similar values in the DPV and Datum panels, but the values in the DPV panel were much more stable; this is because of the relatively low vapour permeability of the sheathing. The Zero-Cavity panel had much higher relative humidities in the stud space because of vapour diffusing inward from the sheathing.

During the summer period, the wood moisture content of the wood framing in the Datum and Zero-Cavity panels increased. In the Datum panels, this increase was relatively modest with a peak in moisture content of around 20% in the third week of September. This peak was followed by a sharp decrease to an equilibrium value of about 12% by the end of October. The increase and decrease were strongly correlated to the measured relative humidities in the upper and lower batt and sheathing. The bottom plate was the least affected; the upper stud the most and the top plate and lower stud were in the middle of this range.

The Zero-Cavity panels, in contrast, registered dangerously high moisture levels in the bottom plate of both panels and in all framing in the west panel. The east panel bottom plate moisture content jumped dramatically from 15% to above fibre saturation over a 5-week period from the end of April to the end of May. The moisture content of the other portions of the wood framing increased sharply but remained below 20%. The moisture

content of all of the framing in the west panel increased at a similar rate, rising from about 12% to about 25% over the 150-day period from April 20 to September 20. The west panel showed fast drying during the month of October, while the east panel dried more slowly. The periods of wetting and drying correspond to the periods of high and low exterior vapour pressure over the year (plotted in Appendix A).

Over the entire summer period, the wood framing in the DPV panels actually experienced some drying and then remained quite stable. A small moisture increase occurred around the beginning of August and this reached a peak of 11.5% on September 17 — at the same time as the Datum panel. The wood had dried down again to an equilibrium of 10.5% by the end of October. The fact that the extruded polystyrene sheathing is externally located and is a relatively vapour impermeable is the reason for this behaviour.

Higher equilibrium wood moisture levels are expected under high humidity conditions and vice versa. Table 3.4 contains the equilibrium moisture content of wood as a function of the relative humidity of the surrounding air. Table 3.4 is valid for a dry bulb temperature of 15 °C. Temperature variations have little effect, whereas a change in RH from 90% to 50% results in the equilibrium moisture content dropping by more than 10%. Thus it is likely that the higher summer RH values in the stud space contributed to the wood moisture increase over the summer and quick drying in the winter. These values are based on stable conditions and a single surface to volume ratio for standard types of wood; deviations from these norms are to be expected for different conditions.

RH	90	80	70	61	52	44	35	27	19
EMC	20.3	16.3	13.6	11.5	9.8	8.3	7.0	5.8	4.5

At a Dry Bulb Temperature of 15 °C

Table 3.4: Equilibrium Wood Moisture Content vs. Relative Humidity

Over the chosen summer period the average wood framing temperature was 21 °C and the average stud space relative humidity in the Datum panels was 60% respectively. One might expect a wood moisture value of 11%, but instead the values were slowly climbing during the period. During the late fall, the RH values in the stud space were approximately 70% and the wood moisture values climbed to 20% in the upper stud. The DPV panel had the lowest and most stable RH values; this is reflected by the lowest and most stable measured wood moisture content values. The Zero-Cavity panels had very high RH values in the stud space (80%) and correspondingly high wood moisture values; much higher than those given in Table 3.4.

Therefore, mechanisms other than adsorption, (i.e., condensation or rain penetration), must have caused the high moisture levels in the framing. The daily results in the next section suggest that condensation is the mostly likely mechanism.

3.6.5 Daily Summer Variations

The hourly variation in temperature and vapour pressure for the Datum panel W4 for July 24, 1992 are plotted in Figures 3.9 and 3.10. The vapour pressure of the Zero-Cavity panel W5 for the same day is plotted in Figure 3.10. This date was chosen because it was clear and sunny, and there was little wind throughout the day. The ambient temperature was typical of the representative period, and the behaviour of the W4 panel is representative of the other panels. The plots includes measurements of all layers (not all sensors) to allow for a qualitative valuation of the complex dynamic variations. Similar plots for all six panels can be found in Appendix B.

It can be seen that the ***temperature*** variation is less for this summer day than for the selected winter day presented in Figure 3.5. Although the solar effect on these east and west walls is similar to the winter case (the solar effect would be less than the winter values for a southern orientation), the ambient temperature is generally very close to the interior temperature. Thus, the driving temperature difference is less affected. The cavity temperature can be seen to vary almost exactly as the temperature of the inner surface of the brick. This is evidence that cooling by convection or other means of air flow is not significant.

The summer-time ***relative humidity*** and vapour pressure conditions were much like those measured in the winter (see 3.5.5), but the volume of water vapour present was as much as ten times higher because of the higher temperatures. The vapour pressures in the cavities (or the sheathing in the Zero-Cavity panels) generally reacted the most to the solar-induced temperature change. The amount of vapour in the stud space was the least and the most constant in the DPV panel. The value of cavity vapour pressure increased by a factor of three to four with the increase in temperature over the day.

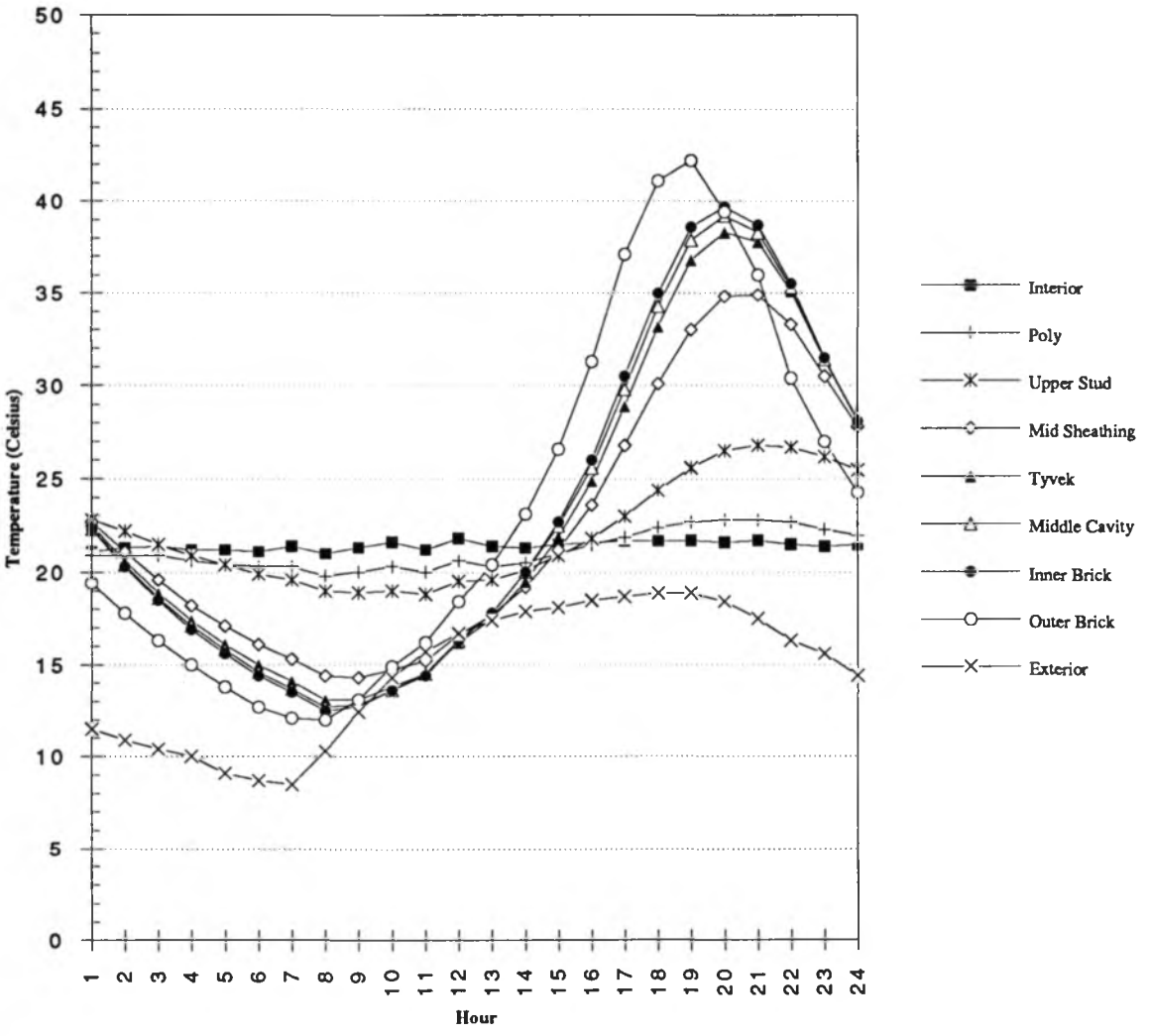

Figure 3.9: Hourly Temperatures (July 24, 1992)

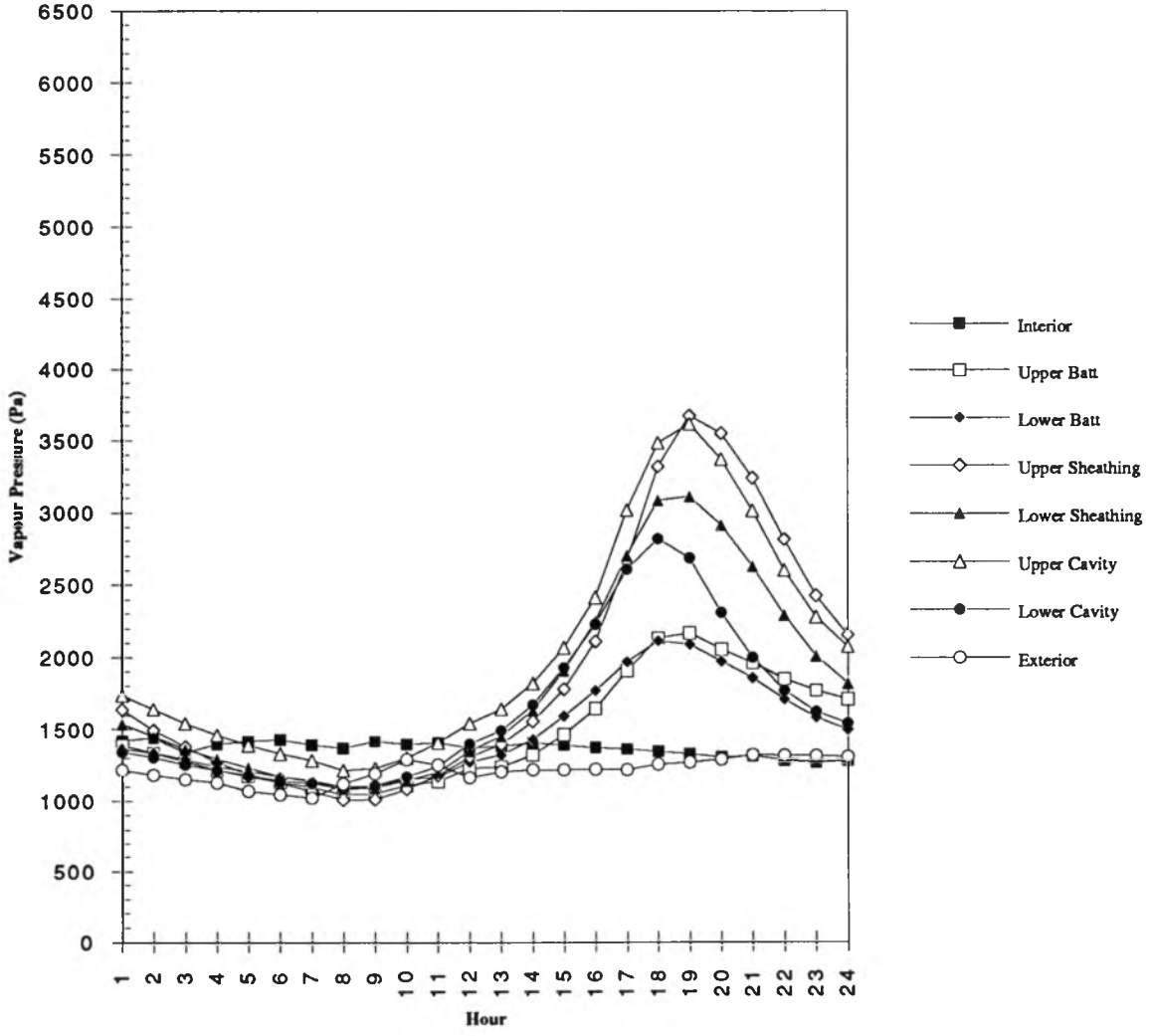

Figure 3.10: Hourly Vapour Pressures (July 24, 1992)

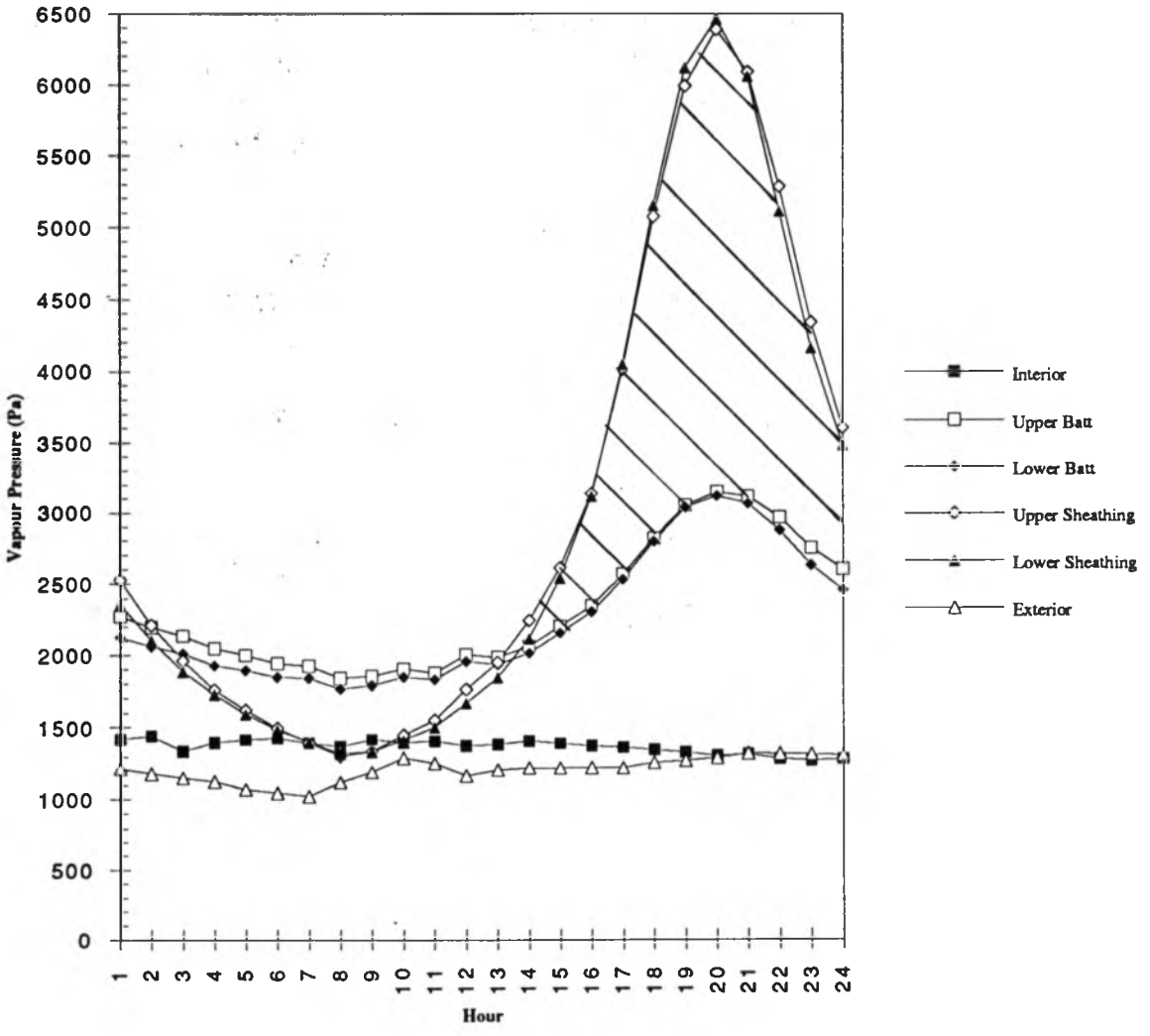

Figure 3.11: Hourly Vapour Pressures (July 24, 1992)

Because the vapour pressure in the cavity was higher than in all other parts of each wall assembly for many hours of each day, vapour will diffuse both outward and inward. In the Datum panel W4, the average pressure difference between the cavity and the stud space over this day was approximately 370 Pa inward (650 in the Zero-Cavity). However, the flow reversed itself for several hours and had a peak difference of almost 1700 Pa (3000 Pa in the Zero-Cavity). By comparison, during the winter day analyzed earlier in Section 3.5.5, the average drive was approximately 100 Pa, with peaks of 200 Pa. The winter day was quite cold, and the overall difference between inside and outside vapour pressures was quite large (1000 Pa). In contrast, the ambient temperatures and relative humidity values on July 24 were quite typical of the summer. Therefore, contrary to common belief, it is clearly evident that the vapour drive inward *from the cavity* is substantially larger in the summer than the outward winter-time vapour drive across the entire wall. This condition exists for a significant portion of each sunny day.

For the Zero-Cavity panel E5 on July 24, an approximate calculation can be made based on the changes in temperature and humidity from the early morning to noon. At 06:00 the air in the sheathing contained 7.5 g of moisture/kg of air (0.89 m^3 of air/kg for 15 °C and 70% RH). By noon the air in the sheathing contained 24.7 g/kg (0.825 m^3/kg for 31 °C and 85%). The difference of 17.2 g of water is the net increase from evaporation, inflows, and outflows. The cavity volume is only 0.11 m^3 so 17 g/m^3· 0.11 m^3 = 1.9 g of water evaporating would result in the upper sheathing changing from 15 °C and 70% RH (at 6 a.m.) to 31 °C and 85% RH (at noon). Such a small amount of moisture could easily be stored in the brick veneer or sheathing itself. There would be some vapour loss from the cavity space (either by mass transfer through the vents to the exterior or by diffusion through the Tyvek™) during this time, so much more vapour may be evaporating. The net deficit is, however, approximately 1.9 grams.

To quantify the vapour drives within the Zero-Cavity panel, the hourly vapour pressures were analyzed (Figure 3.11). The net difference between the interior and exterior on this day was approximately 150 Pa acting toward the outside (i.e., the average difference over 24 hours). However, the vapour actually flows from the insulated sheathing (the cavity fill) to the stud space as well as to the exterior. Between about 14:00 and 02:00 a significant vapour drive occurs from the rigid fibreglass to the stud space. Given the vapour drive from the sheathing to the stud space over the entire day (an average of about 650 Pa) and the vapour permeability of Tyvek™ and brick, an hourly calculation using Glaser's method results in a predicted mass transfer of 225 g of water inward through the Tyvek™ and 7 g outward through the brickwork for this day. Given the mass of the

wood in one panel (13.4 kg @ 400 kg/m^3), only 134 g of water is required to increase the moisture content of the wood by 1%. Therefore, even given the inevitable days of net drying and the reduced rate of absorption as the wood becomes more saturated, a rise of moisture content from 15% (measured winter equilibrium) to 30% (level of wood saturation) would require only nine days similar to the one analyzed.

The calculations presented above are very simplistic. The interaction of temperature and vapour drive is complex, as is the storage and release of water vapour from the building materials. Nevertheless, these calculations are useful in that they show that large vapour flows through the vapour permeable Tyvek™, condensation on the cool polyethylene vapour barrier and studs, and sustained high relative humidities are the likely cause of the moisture and related damage in the Zero-Cavity panels.

3.7 Discussion and Comparisons

The biggest difference between winter and summer performance is that the relative humidity was very high in the Datum and Zero-Cavity panels; saturation was possible for significant lengths of time. The Zero-Cavity sheathing was often wet, probably from rain penetrating the brickwork. The high relative humidity levels in the stud space of the Zero-Cavity panels were likely due to the retained moisture in the base of the fibreglass sheathing diffusing through the vapour permeable Tyvek™ under vapour and temperature gradients. The increased moisture content of the wood studs and top plate in the Datum and Zero-Cavity panels was then caused by the sustained high relative humidity levels and subsequent condensation on cool surfaces in the stud space (the poly and the framing).

Phase 2 of the Ontario Wood Drying Project (OWDP) involved monitoring the temperature, RH, and wood moisture of 12 panels over a one year period after the wood framing had dried to an equilibrium level. The OWDP results demonstarted that panels of similar construction to the Datum panels (but facing north/south and clad with vinyl siding) had stud space relative humidities ranging between 45 to 55% over the summers of 1991 and 1992. The Datum panels in this study had an average relative humidity of 58% over the summer of 1992. This good agreement is surprising since this summer was wetter and cooler than normal. Panels similar to the DPV panels (sheathed with EXPS but clad with vinyl) had relative humidities in the OWDP of 40 to 50%, and in the current study the average summertime RH was 46%.

The wood moisture levels of the Datum-type panel and those sheathed with EXPS increased during the summer to about 15%, and the increase in the DPV-type panels was noticeably less than in the Datum-type panels.

The high moisture content in the wood framing and the high relative humidity in the sheathing of the Zero-Cavity panels for about seven months starting at the beginning of the summer was caused by a number of factors. Throughout the summer, the lower cavity fill was often moist or had a very high amount of water vapour because rain penetrating the brick screen was retained in the base of the fibreglass cavity fill. The retained moisture was transferred to the stud space through the vapour-permeable Tyvek™ by vapour diffusion due largely to solar-induced temperature differences. This resulted in high relative humidity values in the stud space during the summer and occasional condensation on the poly vapour retarder and wood framing. The high relative humidities will cause an increase in moisture in the studs (through adsorption). The condensation probably created free moisture directly in the stud space which ran down the poly and was deposited on the bottom plate. Consequently, the wood moisture level, particularly in the bottom plate, increased through the summer and dried during the winter.

The base detail and flashing in the test panels did not allow for the drainage of water out of the stud space. However, even with several hours of condensation per day, its is very unlikely that enough liquid water collected to drain away. Surface tension forces and the horizontal upper surface of the base plate could retain several hundred ml of liquid water until this moisture was absorbed into the base plate. Daily condensation accumulations of less than 100 ml would likely have formed beads on the poly, been adsorbed onto the glass fibres of the batt insulation, and be absorbed by capillarity into any wood framing. Therefore, the flashing detail employed may have reduced the drying potential of the base plate, but probably did not significantly increase the wetting.

The average exterior daily RH in the summer (70%) was not significantly different from other years. However, the higher than normal amount of rainfall and reduced hours of sun might have led to an increase in rain penetration and RH levels in the cavities. That the same mechanism occured in the summer before monitoring and resulted in the high moisture content of the framing at the start of monitoring lends support to the supposition that the somewhat abnormal weather did not play a significant role in the results. The similar behaviour of the Datum and DPV panels in this study and previous studies also suggests that the weather conditions did not affect the results.

The mechanism of vapour flow under temperature gradient reversals observed in the Zero-Cavity panels has been noted by many other researchers. For example, in a field study of wall sidings under natural exposure, Ten Wolde and Mei[1] reported that moisture moved from the exterior to the interior for many hours of each day. For wall constructions with exterior sheathings, exterior moisture could not move inward if the sheathing had low vapour permeability. Wilson[2] showed that daily vapour and temperature gradient reversals can seriously affect brick veneer wall assemblies. He cites an example of the porous brick cladding of an experimental hut built in Ottawa absorbing water during rainfalls. The subsequent solar exposure caused water vapour to migrate inward and condense on the exterior side of the interior vapour retarder. The wood strapping rotted away in a few years. Andersen[3] provided the example of a wood frame house with wood siding, and Cunningham[4] confirmed that this mechanism is important in roofing as well. These are only a few of the available references. There is, however, little in the readily available literature, e.g. CMHC documents, Canadian Building Digests, for practioners, and little guidance as to what level of exterior vapour permeance is acceptable and necessary.

The sun played a very important role in the temperature and vapour behaviour of all panels in both the summer and winter periods. Little quantitative assistance of this effect is provided for designers in guides to simple analysis (e.g. Canadian Building Digests 37, 50). Even computer packages distributed by CMHC, such as EMPTIED, do not presently account for the influence of the sun, despite its obvious importance and the great deal of information available to assist in the precise prediction of building surface temperatures due to solar radiation.

The average outer brick temperature of the Datum panels over the 49-day winter monitoring period was 4 °C above ambient. The heating degree days (D.D.) based on the exterior ambient temperature and a 18 °C base for the 49-day period is 1222. Based on the elevated brick temperatures, the D.D. total 1024 — a not insignificant 16% reduction.

---

[1].Ten Wolde, A. and Mei, H.T., "Moisture Movement in a Warm Humid Climate", *Proceedings ASHRAE/DOE/BTECC Conference, Thermal Performance of the Exterior Envelopes of Buildings III.* Dec. 2-5, 1985, Clearwater Beach, Fla., pp. 570- 582.

[2]Wilson, A.G., "Condensation in Insulated Masonry Walls in Summer", *RILEM/CIB Symposiuym,* Helsinki, pp.2-7, 1965.

[3]Andersen, N.E.,"Summer Condensation in an Unheated Building", *Proc. of Symposium and Day of Building Physics,* Lund University, August 24-27, 1987, Swedish Council for Building Research, pp. 164-165, 1988.

[4]Cunningham, M.J., Tsongas, G.A., McQuade, D., "Solar-driven Moisture Transfer Through Absorbent Roofing Materials", ASHRAE Transactions, pp. 465 - 472.

3.8 Conclusions

1 All the walls have very similar thermal gradients, but very different vapour pressure gradients, through the wall and within common elements such as the brick veneer, the wood framing, and the batt insulation. However, consideration of mean values does not reflect the effect of daily variations, especially those due to solar radiation.

2 If exposed to the sun, the brick veneer screen undergoes large temperature changes during the course of the day at all times of the year. In the winter, the brick will tend to have an average temperature not far below freezing, with significant daily excursions above and below zero due to solar effects. Over both the summer and winter, the temperature of the east/west facing panels was about 5-7 °C higher than the average ambient temperature.

3 The air in the cavity of all panels remains warmer than the brick and at least 6 °C warmer than the average ambient temperature. There was also no pattern of measurable vertical temperature stratification within the cavity. The cavity temperature closely followed the brick temperature, even during fast, solar-induced, temperature changes. The amount of water vapour in the cavity was weakly related to the vapour in exterior air. These observations suggest that little air circulation through the cavity is occurring, despite the daily temperature differences between the exterior and the cavity.

4 In a South-western Ontario winter the average temperature of the insulated fibrous sheathing within the "cavity" of a zero-cavity brick veneer wall will be lower, by about 5 °C, than in the cavity of a veneer wall with a cavity and insulated sheathing. Moreover, the temperature of the sheathing will often be below 0 °C for longer periods of time (although this does not occur very often) — this would permit the accumulation of moisture as frost. In the summer the sheathing can be expected to be about 1.3 °C warmer in a zero cavity wall than in the cavity in a normally constructed wall.

5 As far as the Tyvek™ / building paper is concerned, placing it between the insulated sheathing and the batt insulation protects it from temperature extremes and large variations in all seasons. In the winter, this thermal protection not only ensures that it remains above freezing but that it remains about 7 °C higher than in the datum wall during the winter. This should improve its durability and performance.

6 The relative humidities and temperatures measured in the stud space indicate very little chance of condensation in the DPV and Zero-Cavity panels in the winter. The higher summer-time RH values in both the sheathing and stud space of the Zero-Cavity wall indicates that moisture can be collected in the sheathing. The less vapour-permeable sheathing in the DPV panels resulted in considerably more stable and lower summer-time relative humidity levels in the studspace, and more stable and slightly higher winter relative humidity levels, than the other two pairs.

7 The wood moisture content of the Zero-Cavity panels is a major concern. Rain penetrating the brick veneer is retained in the fibreglass cavity fill. In the spring and summer this moisture diffuses inward through the relatively vapour permeable Tyvek™. The increased stud space RH results in increased wood moisture content and increases the risk of condensation. This process occurs in the summer, and drying occurs in the winter.

4. Air Leakage Testing

An important function of any wall is the control of air flow. The primary plane of airtightness in a wall is generally labeled the air barrier. No single component of a wall assembly, however, provides all of the resistance to air flow. Out-of-plane, through-envelope air flow is resisted by other layers and materials in the building envelope, intentionally or not, and as such constitute a second plane of airflow resistance.

In most framed, low-rise, residential walls, the primary air barrier is comprised of an inner layer of sealed drywall or polyethylene and drywall. However, outer layers of rigid sheathing, (such as gypsum, waferboard, fibreboard, foam plastic insulation) and house wrap or building paper also provide resistance to out-of-plane air flow. In normal residential construction it can be expected that air leaking past the imperfectly constructed drywall and poly air barrier will then meet resistance in the downstream layers of the assembly. In practice, joints and penetrations in housewraps are sealed with special sheathing tape, and many designers and builders still consider the housewrap as an air barrier despite testing which shows it is not sufficiently airtight to be labeled a primary air barrier. The housewrap or building paper is the only practically significant secondary plane of airflow resistance in the Datum and Zero-Cavity wall assemblies. However, in walls with rigid sheathing, such as the DPV panels, the sheathing can also be a significant contributor to airflow resistance.

The measurement of the flow characteristics of the secondary plane(s) of air flow resistance is important for several reasons:

- the drying rate of moisture that has accumulated or been built into the wall will be influenced by airflow through this secondary plane to the outside.
- from the point of view of pressure equalization performance, the airflow resistance between the cavity and the poly/drywall barrier provided by the secondary plane of air flow resistance can dramatically change predicted performance. If one assumes the poly/drywall is the only plane of resistance to airflow, the pressure moderation chamber is between 125 and 150 mm deep in all of the wall panels. In reality, the effective chamber depth is less because of the resistance to airflow offered by the sheathing and building paper.
- planes of airflow resistance (whether the primary air barrier or not) placed near the outside of an assembly will reduce the loss of heat caused by wind flows over the outside surface of low-density batt insulation (sometimes

called "wind washing"). Natural convection in low-density insulations can also be reduced by facing both faces of the batt with air impermeable materials. To control both types of convective heat losses, Scandinavian researchers have recommended maximum air permeabilities of this secondary air barrier.

- The flow characteristics under exfiltration and infiltration provide an indication of the likely dynamic (i.e. real life) performance, and the actual in-situ effects of the stiffness of the *system.*
- Measurements provide an indication of the effect of time and weather on both wall performance and material performance e.g. under different temperature conditions, after different lengths of time. A change in air flow resistance indicates a change in the wall.

4.1 Purpose

The purpose of the air leakage test program was to determine and compare the relative airtightness of the wall layers downstream of the primary air barrier (the poly/drywall) in the three pairs of test panels. The values obtained can be used to compare the panel constructions, to judge the performance of the tested plane of air flow resistance vis-a-vis the pressure-equalization performance, and to estimate the relative amount of warm air that could leak out from the building interior and condense in the panel during the winter period if the primary air barrier were built imperfectly (generally the case in real buildings). The drywall and polyethylene inner layer was tested and performed as designed, i.e. this plane exhibited practically zero leakage (less than 0.01 l/s/m^2 @ 100 Pa).

4.2 Test Program

The standards ASTM E283-81 and CAN/CGSB-149.1-M86 were used as guides for the testing and subsequent analysis. Figure 4.1 shows sections of each pair of panels and the plane of airtightness tested.

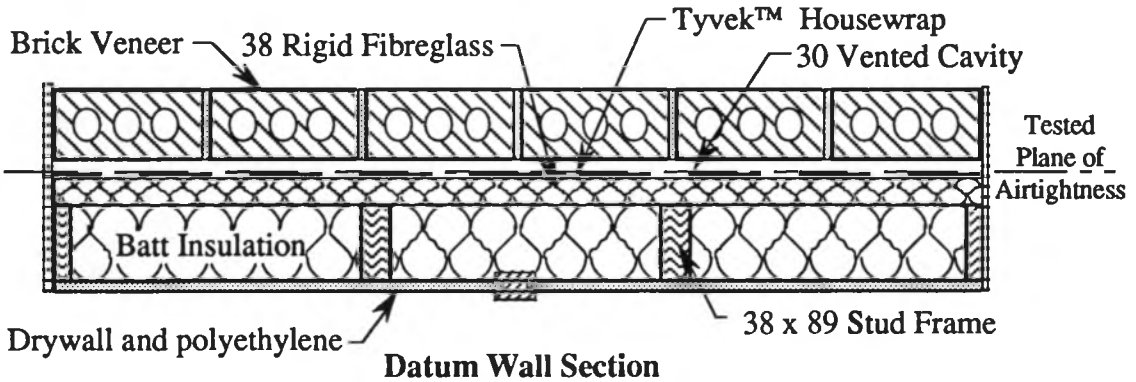

Datum Wall Section

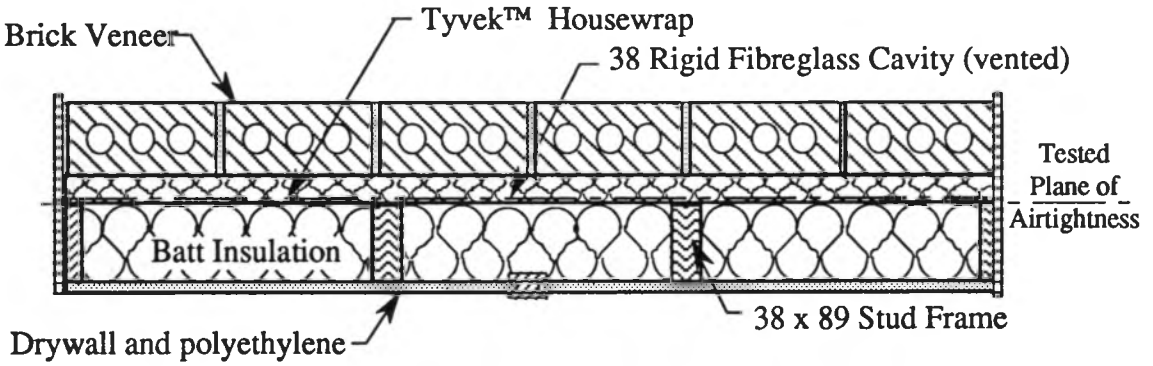

Zero-Cavity Wall Section

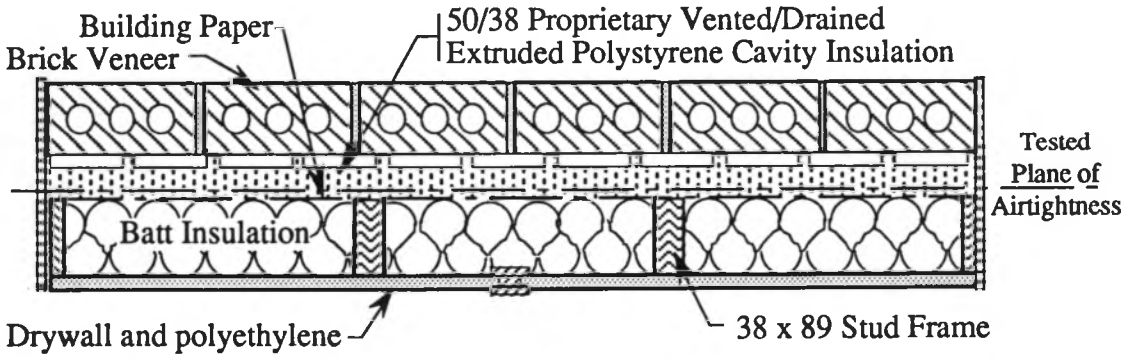

Drained-Pressure Equalized-Vented (DPV) Wall Section

Figure 4.1: Plane of Airtightness Tested

4.2.1 Panels

There was one predominant plane of air flow resistance other than the drywall and polyethylene in the wall panels tested. For the Datum and Zero-Cavity panels, this plane was composed of the Tyvek™ film and its related taped and caulked joints and seals. In the DPV panels, this plane of air flow resistance was composed of the building paper and the Styrofoam SM™ working together.

To avoid testing the airtight inner layer of drywall and polyethylene, the test method by-passed this layer through a special fitting. An airtight port in the centre of the panel (see Figure 2.6) allowed air to be added to, or extracted from, the stud space to create a pressure difference across the plane of airtightness being tested (and the airtight edge seals of the panel). The drywall and polyethylene vapour barrier were built as airtight as possible; all penetrations and edges of representative panels were checked with a smoke pencil at a 100 Pa pressure difference to confirm that this interior plane of airtightness was intact. Figures 2.5 and 2.6 show the various details used to ensure airtightness at all edges and penetrations. The pressure taps that were built into the panel allowed the pressure drop across all layers of interest to be measured.

4.2.2 Apparatus

A CAN-BEST Model 283A200 testing apparatus was used to measure pressure and flow rates, and to apply the pressure difference. Rotometres with a range of 0 to 20 Standard Cubic Feet per Minute (SCFM) (1 SCFM = 0.472 l/s) and a resolution of approximately ±0.01 SCFM and a low-pressure manometre with a range of 0 to 150 Pa and a resolution of ±0.5 Pa were part of the apparatus. A centrifugal fan with variable-speed control provided the air flow.

4.2.3 Procedure

Pressure was applied in approximately 12.5 Pa intervals up to a maximum of either 75 or 100 Pa and then reduced in equal intervals back to zero. The flow rate at each pressure difference was measured after both the flow and pressure had stabilized; flow stabilization was observed to occur within about 10 seconds. The same procedure was repeated for negative pressure (infiltration) and positive pressure (exfiltration). The pressure drop across the central stud space and the exterior was the pressure used for all calculations.

The pressure difference between the stud space and the *cavity* was also measured for representative panels and found to be the same; the pressure difference across the veneer was zero in all cases. The pressure of the side stud space was measured in each panel to ensure that there was no lateral pressure difference in the panels.

4.3 Results

The results of the leakage tests are presented as log-log plots in Figures 4.2 - 4.4, with the best fit linear regression equation and line indicated for each panel under negative and positive pressure differences.

Flow under a pressure difference can be described by the expression:

$$Q = C \cdot (\Delta P)^n \qquad (4.1)$$

where Q is the flow in litres/s,
C is a flow coefficient in (litres/s·Pa)^n,
ΔP is the pressure difference in Pa, and
n is a dimensionless exponent.

The value of the flow exponent n for streamline flow through an orifice is 0.5, and for perfectly laminar flow it is 1.0. Thus, values of the flow exponent close to 0.5 indicate a large opening, and values near one indicate small cracks or high permeability. The value of the flow coefficient C has a wide range depending on the size of the opening. The data for each test was fitted to an equation of this form using units of l/s for flow; the resulting coefficients and exponents are shown in Table 4.1 along with the correlation coefficient (r^2) value from the linear regression analysis.

The leakage behaviour described by Equation 4.1 can be reduced to a single number by assuming all leakage occurs through a single square sharp-edged orifice of a calculated area. This area is called the Equivalent Leakage Area (ELA). The CAN/CGSB standard referenced earlier gives an equation of the form:

$$ELA = 0.01157 \sqrt{\rho} \cdot C \cdot 10^{(n-0.5)} \qquad (4.2)$$

where ρ is the density of air at the reference conditions of 20 °C and 101.3 kPa
C and n are from the flow equation (Eq. 4.1), and
ELA is the equivalent leakage area in mm^2.

The calculated ELA values are presented in Table 4.2. The air leakage rates at a pressure difference of 75 Pa are listed in Table 4.3. The tested air permeance properties of various materials similar to those used in the construction of the panels are shown in Table 4.3 in

terms of the flow equation and ELA for one square metre of material. These values are taken from a CMHC-sponsored report by AIR-INS Inc.[1]

Panel		Exfiltration			Infiltration			Ratio Ex./In.	
		C	n	r^2	C	n	r^2	C	n
Datum	E4	0.305	0.720	0.995	0.149	0.767	0.998	*2.048*	*0.939*
	W4	0.415	0.737	0.999	0.129	0.813	0.946	*3.216*	*0.907*
	Avg.	**0.360**	**0.729**		**0.139**	**0.790**		***2.590***	***0.922***
Zero-Cavity	E5	0.019	1.019	0.996	0.019	0.801	0.989	*0.966*	*1.271*
	W5	0.024	0.951	0.997	0.028	0.819	0.992	*0.856*	*1.161*
	Avg.	**0.021**	**0.985**		**0.023**	**0.810**		***0.901***	***1.216***
DPV	E6	0.014	1.210	0.986	0.016	1.106	0.987	*0.872*	*1.094*
	W6	0.053	0.930	0.995	0.032	1.034	0.998	*1.648*	*0.900*
	Avg.	**0.033**	**1.070**		**0.024**	**1.070**		***1.384***	***1.000***

Table 4.1: Flow Equation Coefficients and Exponents

Panel	Exfiltration ($l/m^2/s$)	Infiltration ($l/m^2/s$)
Datum	2.91	1.46
Zero-Cavity	0.51	0.76
DPV	1.16	0.85

Table 4.3: Calculated Air Leakage at 75 Pa

[1] "Air Permeance of Building Materials", Research Report for CMHC by AIR-INS Inc.,Ottawa, 1988.

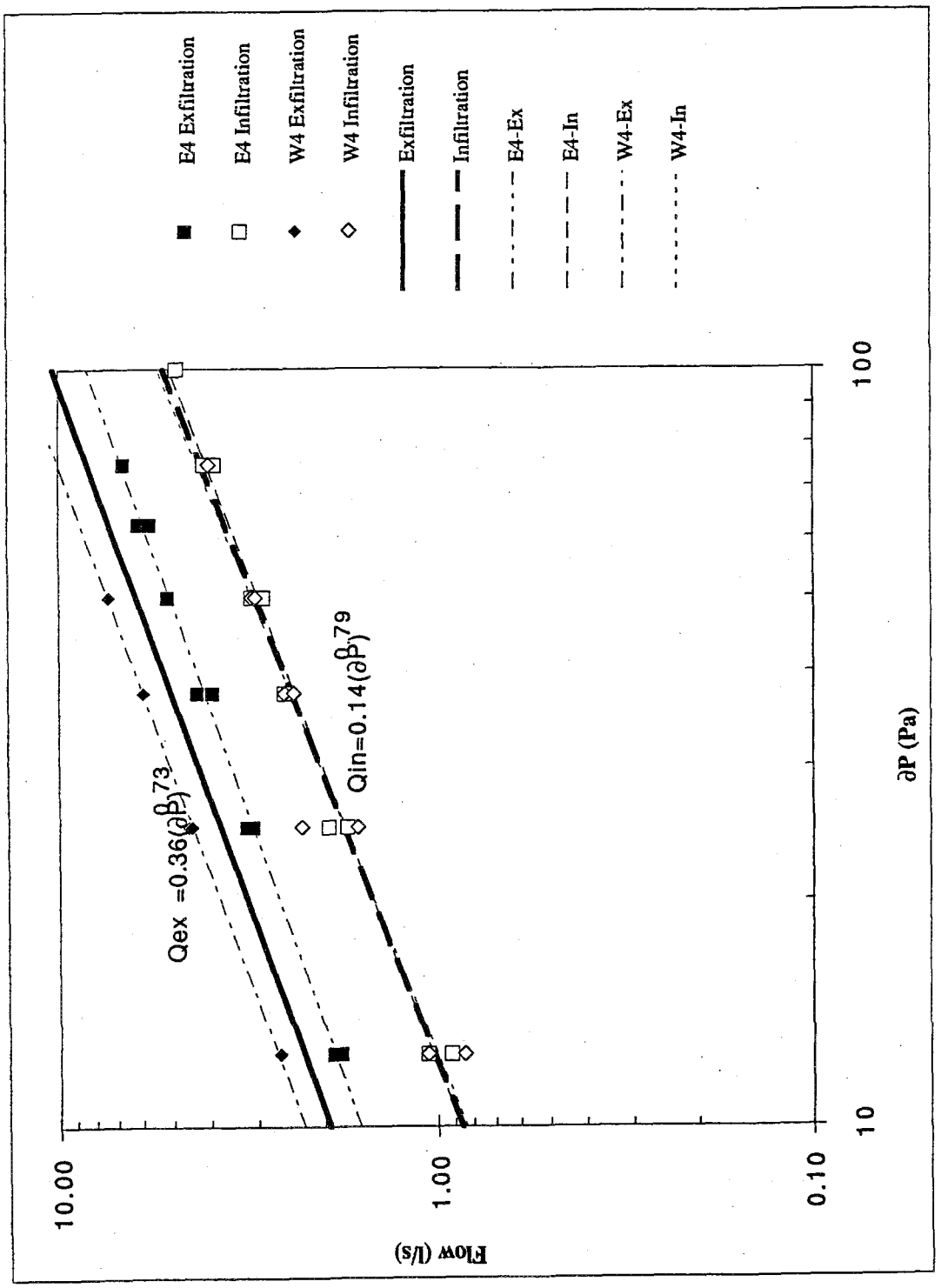

Figure 4.2: Datum Panel Air Leakage Test Results

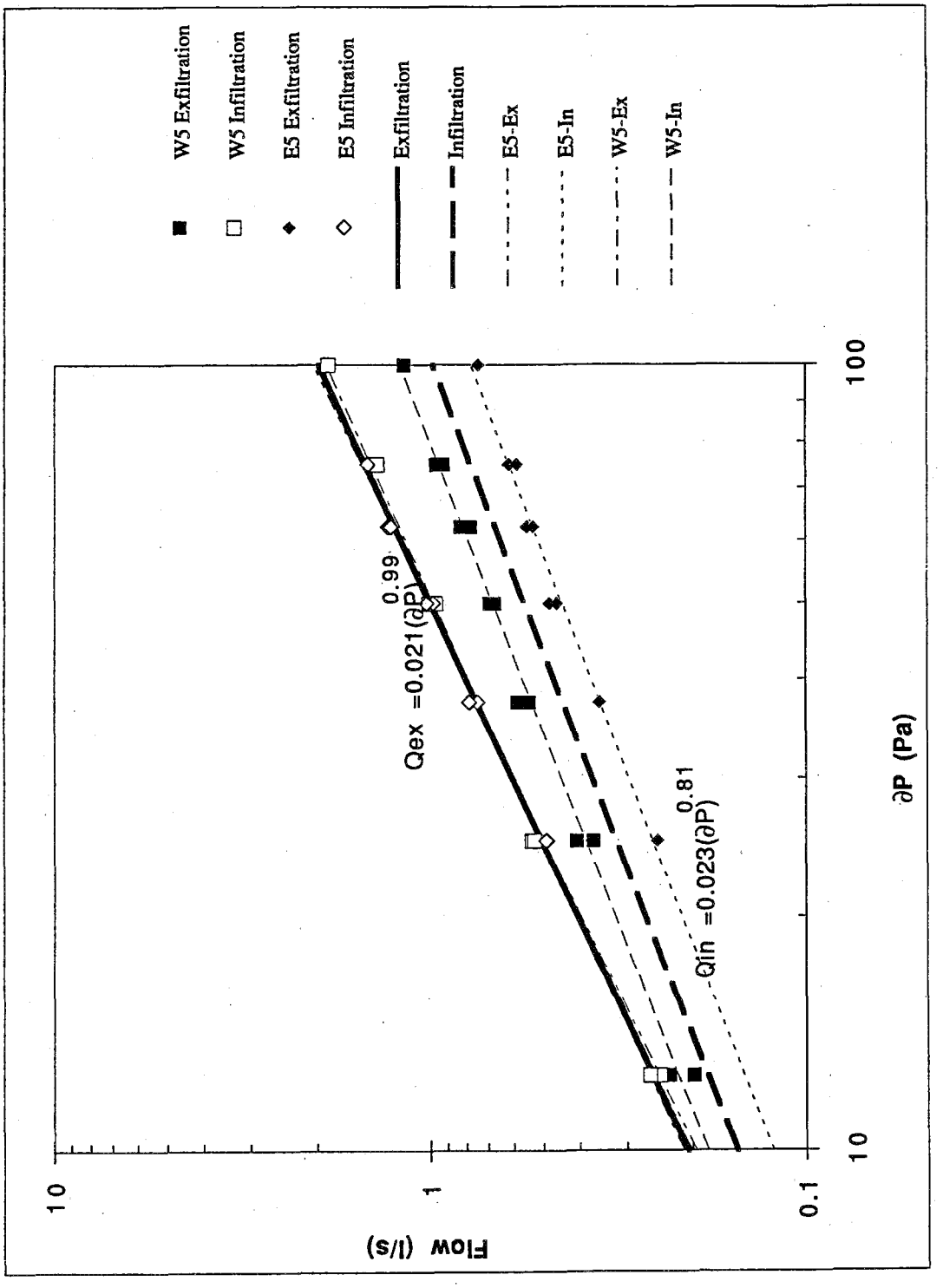

Figure 4.3: Zero-Cavity Panel Air Leakage Test Results

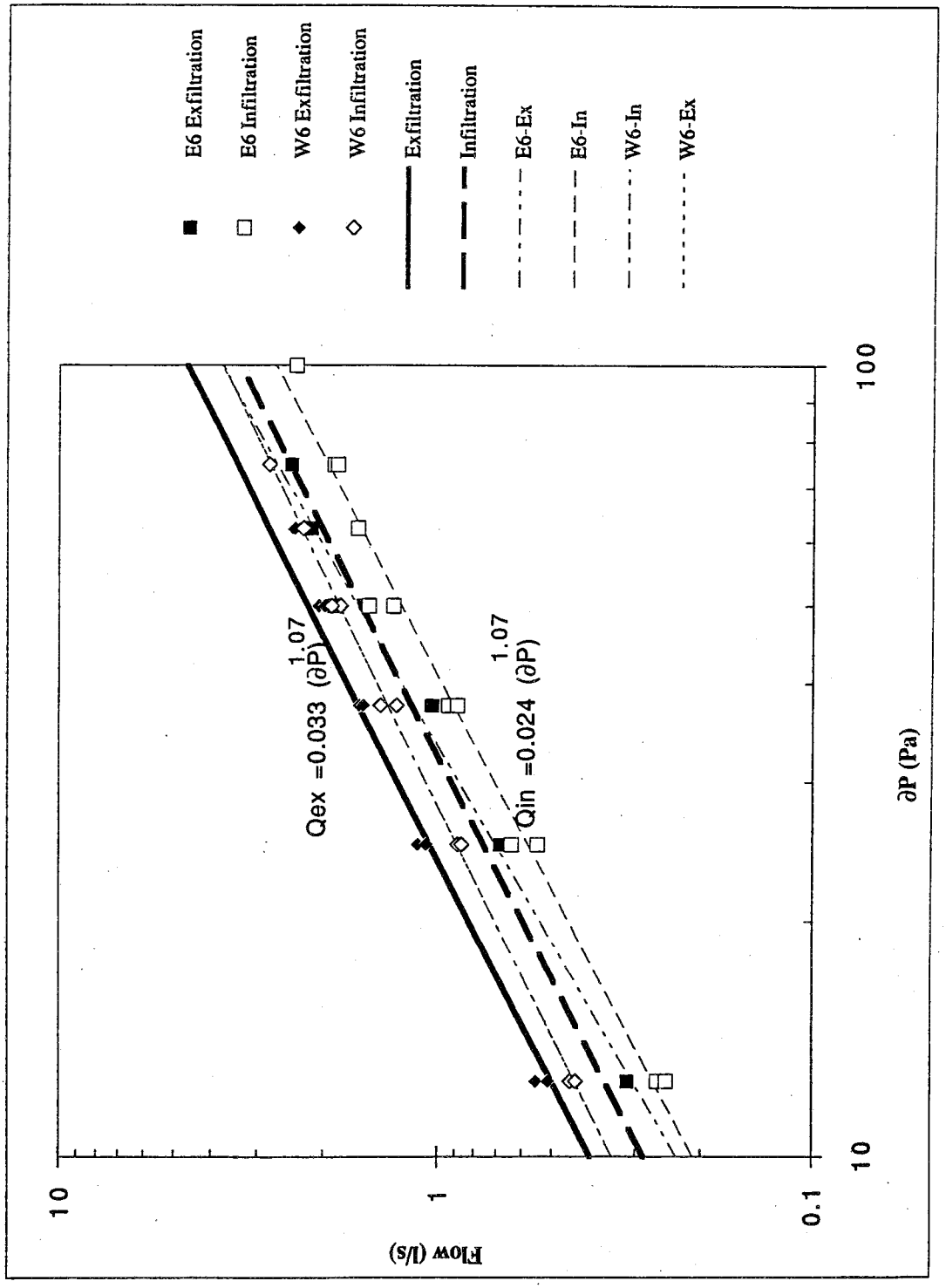

Figure 4.4: DPV Panel Air Leakage Test Results

Panel	**Exfiltration** ELA(mm^2)	**Infiltration** ELA(mm^2)	**Ex./In.** (mm^2/mm^2)
Datum E4	642	349	*1.84*
Datum W4	910	337	*2.70*
Average	**776**	**343**	***2.26***
Zero-Cavity E5	78	49	*1.59*
Zero-Cavity W5	85	73	*1.16*
Average	**82**	**61**	***1.33***
DPV E6	93	84	*1.11*
DPV W6	180	139	*1.30*
Average	**137**	**111**	***1.23***

Table 4.2: Equivalent Leakage Areas

Material	**C**	**n**	**ELA** (mm^2/m^2)
15 lb. building paper	0.0036	1.00	14.48
3 mille spunbonded olefin film	0.0128	1.00	51.35
152 fibreglass batt insulation	0.6110	0.949	2180
5 mille olefin on 25 mm rigid fibreglass	0.0069	0.987	26.81
38 mm EXPS or 6 mille polyethylene	0.00	0.00	0.00
Tyvek™ on 11 mm fibreboard on studs	0.0065	1.00	26.05
25 mm Glasclad™ only on studs	0.0040	1.00	16.03

Table 4.4: Air Permeance Properties of Construction Materials

4.4 Discussion

The test results can be compared to the recommended maximum leakage values of various sources. Building Practice Note 54[2] suggested an allowable leakage rate for buildings with a moderate indoor humidity level of 0.1 litres/second/metre^2 at a 75 Pa pressure difference. Other references suggest levels ranging from 0.02 to 0.3 litres/second/metre^2 at a 75 Pa. The air barrier system in all panels easily met this requirement.

However, in practise the poly/drywall is unlikely to be perfectly built. The downstream layers of all panels failed the criteria of an air barrier; the Datum panels failed by a large margin. The secondary air barriers in the DPV and Zero-Cavity panels, however, would both provide a significant resistance to airflow in the event that the primary air barrier was imperfect.

The Finnish building research establishment, VTT, has recommended a maximum permeability of 25 x10^{-6} m/s/Pa for wind barriers in walls (this is about 1.85 l/s/m^2 @75 Pa). For corners and roof parapets, permeability values of less than 10 x10^{-6} m/s/Pa (0.75 l/s/m^2 @75 Pa) are recommended[3]. The Datum panels would fail both criteria and the DPV and Zero-Cavity panel would meet the first, less stringent, requirement.

There is almost an order of magnitude of difference between the ELA of the Datum panel and the other two panels. The Datum panels were considerably more leaky under a positive pressure than under negative pressure; the average Datum ELA was 2.26 times larger for exfiltration than for infiltration. The other panels also had larger flows under positive pressure than negative, but the differences were much less.

The large value of the C coefficient of the Datum panels relative to the other panels results in a larger equivalent leakage area and hence larger flows at any given pressure difference. The flow exponents of all panels are also quite different, but no trend is evident. The low flow exponent (closest to 0.5) of the Datum panels indicates that air is not flowing through many small cracks, or through the material itself, but rather through larger holes, punctures, and tears. The much smaller flow coefficients of the other two panels indicate their relatively airtight construction, and the large flow exponents suggest many small and

---

[2] Quirouette, R.L., "The Difference Between a Vapour Barrier and an Air Barrier", Building Practice Note No. 54, Division of Building Research, National Research Council Canada, 1985.

[3] Ojanen, T. and Kohonen, "Criteria for the Hygrothermal Performance of Wind Barrier Structures", Proc. of 3rd Symposium of Building Physics in the Nordic Countries, Copenhagen, 13-125 September, 1993, pp. 643-652.

tortuous cracks in the DPV and the Zero-Cavity panels, which increase in size with increasing pressure.

One possible explanation for the higher leakage of the Datum panel is the position of the Tyvek™ housewrap on the exterior of the fibrous insulation, where it receives less support from the insulation and studs. In the Datum panels the Tyvek™ is supported by large-headed nails only and will balloon outwards under exfiltration, causing cracks to stretch open at joints, edges, nail holes, and any accidental rips and tears. Under infiltration, the Tyvek™ is pressed tightly against the relatively stiff rigid fibreglass insulation. This same effect would also explain the big difference between the ratio of exfiltration and infiltration ELA values versus the ratios of the other panels (1.33 and 1.23 for the Zero-Cavity and DPV panels respectively) because of their increased support to the Tyvek™ and building paper. In commercially available products such as Glasclad™, the Tyvek™ is glued to the rigid fibreglass over its entire area; this will improve the stiffness and thus improve airtightness under exfiltration pressures. In the Zero Cavity and DPV panels, the Tyvek™ and building paper was sandwiched between two relatively stiffer layers.

Instrumentation and wiring penetrated the Tyvek™ film at many points in the Datum panels because of its position, whereas both the DPV and Zero-Cavity panels had fewer penetrations. Despite careful attention, more leakage due to this difference must be expected.

The DPV panel, which was sheathed with Styrofoam SM™ extruded polystyrene (EXPS), was expected to be more airtight under exfiltration since the EXPS should provide more support to the building paper under exfiltration than the fibreglass batt insulation in the stud space under infiltration. Contrary to prediction, the panel behaved in a similar manner to the Zero-Cavity panel, although with even less variation between infiltration and exfiltration. However, since all nails are attached to the studs, and even the edge caulking is applied to a firm support which is on the interior face of the air barrier, negative pressure will cause the the building paper and EXPS to attach themselves more firmly to the locations where leakage is occurring. Under positive pressure, the EXPS (and rigid fibreglass insulation in the Zero-Cavity panel) may offer some support to the joints and edges, but not nearly as much as the unyielding studs. The differences in ELA between exfiltration and infiltration for the DPV and the Zero-Cavity panels was an average of 21 and 26 mm^2 respectively; a crack 1 mm wide and 30 mm long would be more than sufficient to cause these measured differences.

The Datum and Zero-Cavity panels both employed Tyvek™ housewrap and had more repeatable results between the respective pairs than did the DPV panel which employed a combination of building paper and shiplapped Styrofoam SM™ insulation. From an examination of Table 4.1, it can be seen that there is considerable variation in the values between the two DPV panels of the same construction (i.e., DPV E6 vs. DPV W6 Exfiltration: C= 0.014 vs. 0.053 and n= 1.21 vs. 0.93). At these low flow rates a small tear or crack can easily account for this difference. The leakage through the DPV panel is expected to be through joints in the EXPS (since the EXPS is essentially air-impermeable) and laps in the building paper (see Table 4.3). The building paper may form a seal at the lapped joint when enough heat is applied to encourage the bitumen to become tacky; this will often occur behind a brick veneer but much more rarely behind the insulating EXPS. Wind-induced pressure differences can break this weak seal but the EXPS may offer enough support to prevent this. Overall, greater variability can be expected. The average value of a pair was calculated merely as a representative value of what might be achieved with very tight quality control during construction.

The flow exponents indicate that the Datum panels experienced a combination of laminar and turbulent flow; air flowed through larger openings (n=0.5) and through small holes and cracks (n=1.0). The Zero-Cavity panels exhibited laminar flow under exfiltration, but combination flow under infiltration. This result is difficult to explain, but it is consistent and distinct. One possible explanation is that the leakage under exfiltration (which was larger) was through a hole and also through many cracks in the joints and edges, as described above. This would result in a laminar flow exponent of almost 1.0. Under infiltration, the small edge cracks could be pulled tightly closed and a greater portion of the reduced total flow occurred through the hole, resulting in a flow exponent closer to the 0.5 of pure orifice flow.

Flow exponents of greater than one are obviously not representative of the nature of the flow, but rather indicate that the size of the opening is changing. As pressures increase during testing, stretching and opening up of initially small cracks and openings in flexible materials and movement of rigid material will increase the leakage area. The area in Equation 4.1 is assumed to be pressure-independent, whereas for some materials and assemblies this is clearly not the case. For example, in the DPV panel, the EXPS sheets will flex and the joint will become larger: there will therefore be a disproportionate increase in flow for an increase in pressure. The ballooning of housewraps and the behaviour of building paper lap joints have already been discussed above.

The Zero-Cavity ELA values can be explained almost entirely by permeance through the building materials. The 5 mille Tyvek™ alone has an ELA of approximately 26.8 mm^2/m^2; this value is taken from Table 4.3. A CMHC-sponsored study carried out by the National Research Council of Canada, Institute for Research in Construction[4], found that a wall built with Tyvek™ fastened with wood strapping to a fibreboard backing had an ELA of 26.0 mm^2/m^2 (Table 4.5). For the 2.88 m^2 panels in the present study, this would give an ELA of 75 mm^2. The other materials of the Zero-Cavity wall (the tape) probably added airtightness. The NRC/IRC found that the Tyvek™ ballooned out and stretched. They also found that the support of the fibreboard did increase the airtightness slightly under negative pressure. It can be concluded from these other, more controlled, material and building assembly tests that the Zero-Cavity panels, as built, are as airtight as practically possible in a controlled setting.

Wall Assembly Description: All systems were installed on a frame of 38x89 studs at 405 centres.	C ($l/m^2/s$)	n	ELA (mm^2/m^2)
Tyvek™ on 11 mm fibreboard, taped joints	0.0065	1.00	26.05
25 mm Glasclad™, taped joints	0.0040	1.00	16.03
38 mm Styrofoam SM™, taped joints	0.000028	0.83	0.08

Table 4.5: Air Permeance of Air Barrier Systems

The DPV panels performed in a similar manner to the Zero-Cavity walls. Whereas the materials alone have much lower air permeances (Table 4.3), this can only be exploited if the shiplapped joints between the sheets are taped. The NRC/IRC found that a wall constructed only of EXPS with taped joints was quite air tight. Because of this significant difference it cannot be expected that the DPV panels, as constructed, should have such low permeance.

The Datum panels performed considerably worse than the comparable assembly tested by the NRC/IRC. However, the exterior sheathing in the Datum panels did not have the Tyvek™ adhered to the fibreglass over its entire area. The panels in this study were also built and tested under more realistic conditions and included penetrations for instrumentation.

4.5 Comparisons

A study of 24 panels of residential assemblies[4] (hereafter called OWDP) with less emphasis on airtight details, tested in the same facility using similar equipment, found flow coefficients and exponents in the range 0.038 to 0.421 and 0.776 to 1.283 respectively. These results match well with the range of 0.014 to 0.415 and 0.720 to 1.210 recorded in this smaller study. The OWDP program tested exfiltration only.

The panels E5, W5, E6, and W6 in the OWDP study were of similar construction as the DPV panel except that in this study the building paper was placed on the interior of the EXPS instead of on the exterior. OWDP Panels N5 and S5 were clad with vinyl siding. Table 4.6 lists the flow equation coefficients and exponents as well as the ELA's of these panels. The edges of the panels in the present study were likely tighter since the details were better with respect to air flow. The flow exponents in this study were larger than in the OWDP study, and the ELA's were 1/3 to 1/6 as large. Whether this result is due to the position of the building paper on the inside of the EXPS or to the improved airtightness of the edge details is unknown. The vinyl siding adds considerable support to the building paper in a manner similar to the EXPS, resulting in the increased airtightness of the vinyl-clad OWDP panels (N5 and N6).

Panels E1 and W1 of the OWDP study were built of the same materials as the Datum panels in this study, while OWDP panel E4 and W4 were built with a cladding of vinyl instead of brick. Improved edge details should have decreased leakage in this area; however, the Datum panels tested returned exponents which were lower and ELA's generally higher (Table 4.7). A major difference between the panels tested in these studies was that the Tyvek™ was adhered to the rigid fibreglass in the OWDP panels (since Glasclad™ was used). This extra Tyvek™ support, and that offered by the vinyl siding, could account for the difference in results. The extra instrumentation added for the present study may also have contributed to the leakiness of the Datum panels.

[4] E.F.P. Burnett and A.J. Reynolds, "The Ontario Wall Drying Project", Report for CMHC by the Building Engineering Group, University of Waterloo, Ottawa, 1991.

Panel	C	n	ELA (mm^2)
OWDP- E5	0.128	0.869	380
OWDP- W5	0.252	0.862	740
OWDP-E6	0.137	0.850	390
OWDP-W6	0.285	0.776	690
OWDP-N5 (vinyl)	0.072	0.975	280
OWDP-S5 (vinyl)	0.049	1.026	210

Table 4.6: OWDP Results for Panels Similar to DPV Panels

Panel	C	n	ELA (mm^2)
OWDP-E1	0.132	1.049	600
OWDP-W1	0.116	1.099	590
OWDP-E4 (vinyl)	0.123	0.911	400
OWDP-W4 (vinyl)	0.201	0.979	770

Table 4.7: OWDP Results for Panels Similar to Datum Panels

4.6 Conclusions

The primary air barrier of the test panels was found to practically airtight.

The secondary air barrier in the Datum panel (the Tyvek™) was much less airtight than the secondary air barrier in either the DPV (the building paper and EXPS) or the Zero-Cavity panels (Tyvek™). The Datum panel was also much leakier under exfiltration than under infiltration. The other panels also exhibited this bi-directional behaviour, but to a much lesser extent.

The leakier and bi-directional nature of the Datum panel is likely due to the lack of support given to the very flexible Tyvek™ housewrap. Based on the results of this study and the Ontario Wood Drying Project it would seem that support given to an air barrier, housewrap, or building paper by attachment to rigid insulation or placement between two relatively stiff layers has a significant beneficial effect on airtightness.

The nature of the flow in the tests indicates that the DPV and Zero-Cavity panels leaked through many small cracks and perforations which opened up under pressure whereas the Datum panel leaked through larger openings and tears.

5. Water Penetration Testing

5.1 Purpose

The purpose of these tests was to conduct standard rain penetration tests to quantify the performance of each wall when subjected to a common, known amount of water from the exterior. In fact, the main variable being studied in these tests was the drainage performance of the cavity, which should act as both a capillary break and a drain. The manner in which the cavity construction drains water passing through the veneer and limits wetting of the interior wythe are both of interest. The brickwork on the exterior of all panels is ostensibly the same, being built by the same masons from the same mortar and bricks at the same time. However, because of the natural variability of the bricks and mortar some difference in behaviour can be expected.

Rainwater striking a brick veneer screen can be:

- repelled and drained down the outside face of the brick,
- absorbed by the brick, or
- transmitted through the screen via joints, cracks, capillarity etc.

Once through the screen, any water is intended to drain and not wet the inner wythe. However, mortar bridges, ties, and other obstructions can cause water to reach the inner wythe and prevent ordinary drainage.

In these tests, measurements were limited to the volume of water applied, the volume that immediately exits the cavity via the drains, and the temperature and moisture conditions within the wall.

Since the cavity is vented to the exterior in the wall systems tested, there should not be any pressure difference across the veneer when a static pressure difference is imposed across the wall. It follows that pressurization or depressurization from the inside should not affect water penetration because the air pressure acts mainly across the air barrier, not the brick screen. However, water can still cross the veneer screen or enter through joints under the forces of gravity and capillarity.

Supplementary tests were employed to ascertain the effect of the leaving vent/drains open, of applying a pressure difference across the wall, and to investigate the behaviour of two panels in more detail.

5.2 Test Program

Testing followed the ASTM Standard E331-83 with some significant modifications. This Standard is a test of water penetration for exterior windows, curtain walls, and doors employing a uniform static air pressure difference. It requires the application of a spray of a minimum 3.4 L/m^2/minute for 15 minutes on the specimen with an induced pressure difference of at least 137 Pa. Any points of water leakage are recorded and described. Because of the wall type being tested (a pressure-equalized rainscreen), the procedure was modified to include one test with no applied pressure difference and one test with a 100 Pa difference after a minimum 2 day drying period. The intent was to establish whether there was any difference due to the applied pressure difference.

The water was applied at a rate of 5.55 liters per m^2 per minute to ensure that a uniform spray was produced over the whole panel and to exceed the minimum required. The volume of water applied over the whole test was, therefore,

total water applied = rate · area · time
= 5.55 l/min/m^2 · 2.88 m^2 · 16 min.
= 256 litres.

The application rate and the amount of water far exceeds what can be directly expected on any single-storey wall. However, if water spilling off a roof or collected and drained by the ten storeys above the wall in question is considered, it may be possible for these conditions to occur. To establish a comparable situation, consider the following. With rain falling at an angle of 10° from vertical, approximately 18% as much water will fall on a vertical area as on the same horizontal area. For the Waterloo area, the 15 minute duration rainfall intensity with a probability of being exceeded once in ten years is 28 mm (28 l/m^2) on a horizontal surface. Thus, for a 1.2 m wide vertical panel to receive 256 litres this severe rainfall must occur and 42 m of wall (with a 10° rain angle) above the panel in question would need to drain to it. Even if the wind speed were high enough to cause the rain to fall at an angle of 45° (found to occur at wind speeds greater than 3.5 m/s in one study), the ten year rainfall would be equivalent to a rate of 1.9 l/m^2. For *low-rise* construction these are obviously extreme conditions and would be very unlikely to occur in actual field situations.

5.2.1 Panels

The test panels were built with a special base detail (Figure 2.7) which collected the water that would normally be drained out the weep holes and directed it through 3 mm inner diameter Tygon™ tubing to the inside where it could be collected and measured. This allowed for quantitative measurement of the water penetration through the brick veneer. By means of the numerous relative humidity (RH), temperature, and wood moisture sensors described in Section 2.3, changes within the wall which might signal water penetration of the inner wythe could be detected.

To limit unrepresentative water penetration, the panel edges were sealed with butyl caulking around the edges, the top edge was covered with duct tape to prevent water from spraying directly into this opening, and the air pressure measuring port was covered with tape. The adjoining panels were protected from the spray by fully covering them with 6 mille polyethylene sheet. The vents were left uncovered so that they would act the same as in service. A test with the vents covered by duct tape was later conducted to evaluate the contribution of the open vents to water penetration.

5.2.2 Apparatus

A CAN-BEST Model 283A200 testing apparatus was used to measure flow rates and to apply and measure the pressure difference. The rotameters have a range of 0 to 20 Standard Cubic Feet per Minute (1 SCFM =0.472 l/s) and a resolution of approximately ±0.01 SCFM. A low-pressure manometer with a range of 0 to 150 Pa and a resolution of ±0.5 Pa is also part of the apparatus. A centrifugal fan with variable-speed control provides the air flow.

A spray rack with 16 nozzles was used to apply a uniform spray of water over the test area. Supply water for the spray rack was regulated by a ball valve and measured using a float-type flowmeter (CalQFlow, 8 to 38 L/min range). Water collected was weighed with a Sartorius Model T12000S electronic scale accurate to ±0.1 grams.

All wall sensors were connected to the standard data acquisition system (Section 2.4). To improve the resolution, data was stored on disk at 3 minute intervals instead of the standard 5 minute intervals. The exterior and interior conditions (wind speed and direction, temperature, RH) were also recorded and saved at this shorter interval.

5.2.3 Test Procedure

The nozzle pattern on the rack was adjusted until the perimeter of the panel was receiving the same amount of water as the center while avoiding excessive loss to the sides. The rack was placed so that the nozzles were 450 mm from the face of the specimen and so that none of the water jets impinged directly on a vent or opening. Water was applied at a rate of 5.55 liters per minute per square meter. This was more than the minimum 3.4 L/m^2 minimum required by the Standard and this rate best produced a uniform spray pattern and surface film over the brick. Normal city water at a measured pressure of approximately 10 psi was used. The water pressure occasionally dropped for short periods because of other users.

The spray was started and the flow and nozzle positions adjusted (while the air pressure difference was applied) in less than one minute. One minute after the spray started, the test was officially started and the first water measurements made. After 15 minutes (16 minutes of water application) the spray was stopped and all sensor readings were recorded and stored for the next 24 hours. The test duration and measuring intervals were strictly controlled to within variations of a few seconds .

The water flowing from the weep hole tubes was collected and weighed during the test and for at least 5 minutes after the spray was stopped. The collection trays were left in place for at least 24 hours to collect any long term drainage from the walls; this was also weighed.

5.2.4 Supplementary Tests

Supplementary tests were carried out on the panels Datum W4 and Zero-Cavity W5 only. The test on panel Zero-Cavity W5 began with the vents covered by tape but with a protected tube providing some air flow to allow pressure-equalization. A pressure difference of 100 Pa was applied for the first ten minutes of water application and then discontinued for the remainder of the test. The vents were sealed in the same manner for Datum panel W4 but these were removed at the tenth minute of the test. In both cases, the change was made during the test to better ascertain the effect of changes while eliminating as many experimental variables as possible.

All tests were preceded by at least 2 days of dry, sunny weather to ensure that the brickwork was relatively dry.

Panels	Date	Weather and Comments
No Pressure Difference		
E4, E5, E6	2-09-92	18-20°C, 50% RH, partially cloudy
W4, W5, W6	4-09-92	20 °C, 50% RH, clear
With Pressure Difference		
E4, E5, E6	24-09-92	22 - 25 °C, 40% RH, clear
W4,W5, W6	25-09-92	19 - 21 °C, 60% RH, cloudy
Supplementary Tests (2-10)		
W4	Pressure applied for 10 minutes, no pressure for remainder	
W5	Vents covered for 10 minutes, then uncovered, no pressure	

Note: All tests were preceded by a least two days of dry sunny weather to ensure that the brickwork was relatively dry.

Table 5.1: Test Program

5.3 Test Results

The cumulative water collected versus time and the collection rate versus time for the panels are plotted in Figures 5.2 to 5.5. The shape of these curves is typical of the results of all the tests. There is an initial lag in the collection rate followed by a stabilization within 3 to 5 minutes. Similar observations on other wall assemblies prompted the relatively short 15 minute test duration required by the ASTM standard[1]. The collection rate remains constant until the water supply is stopped, after which it almost immediately drops at a constant rate for about 3 to 5 minutes. The collection of significant amounts ends within 5 minutes of the water spray being stopped. Practically no water was collected 15 minutes after the water spray had been stopped.

In Table 5.2 the test data is summarized. There are considerable differences in both the total volume collected and the peak rate values between panels of similar construction and between different panel types. Panels W5, E5, E5 (with pressure) and W4 and W4 (with pressure) all performed similarly with values for total collected volume spanning a range of 825 ml to 1303.5 ml and with peak rates between 84.6 ml/minute and 102.8 ml/minute. Panels W6 and E4 with and without pressure performed in the same manner with total collected volumes of 2152.5 ml to 2441.3 ml with rates of 154.8 ml/min to 168.9 ml/min.

Panel W5 with pressure performed fundamentally different, with almost double the maximum amount and rate of the others.

		No Pressure Difference		With Pressure Difference		Ratio ΔP=100 Pa / ΔP=0	
Panel Type	**Panel Code**	**Total** (ml)	**Rate** (ml/min)	**Total** (ml)	**Rate** (ml/min)	**Total** (ml)	**Rate** (ml/min)
Datum	W4	1195.0	84.6	1242.4	95.4	1.04	1.13
	E4	2216.0	161.2	2441.3	168.9	1.10	1.05
Supp. Test	W4	546.6	68.1	Note 1			
Zero-Cavity	W5	825.8	88.2	4470.0	388.3	5.41	4.40
	E5	1303.5	102.8	1252.0	88.3	0.960	0.859
Supp. Test	W5	1776.5	166.5	Note 1			
DPV	W6	2152.5	154.6	2442.0	166.1	1.13	1.07
	E6	Note 2	—	—	—	—	—

Notes: 1. Supplementary tests did not follow same procedure as other tests and hence are not strictly comparable. See Table 5.1 and text.

2. An error during construction prevented any drainage measurements from DPV Panel E6.

Table 5.2: Summary Of Water Penetration Test Results

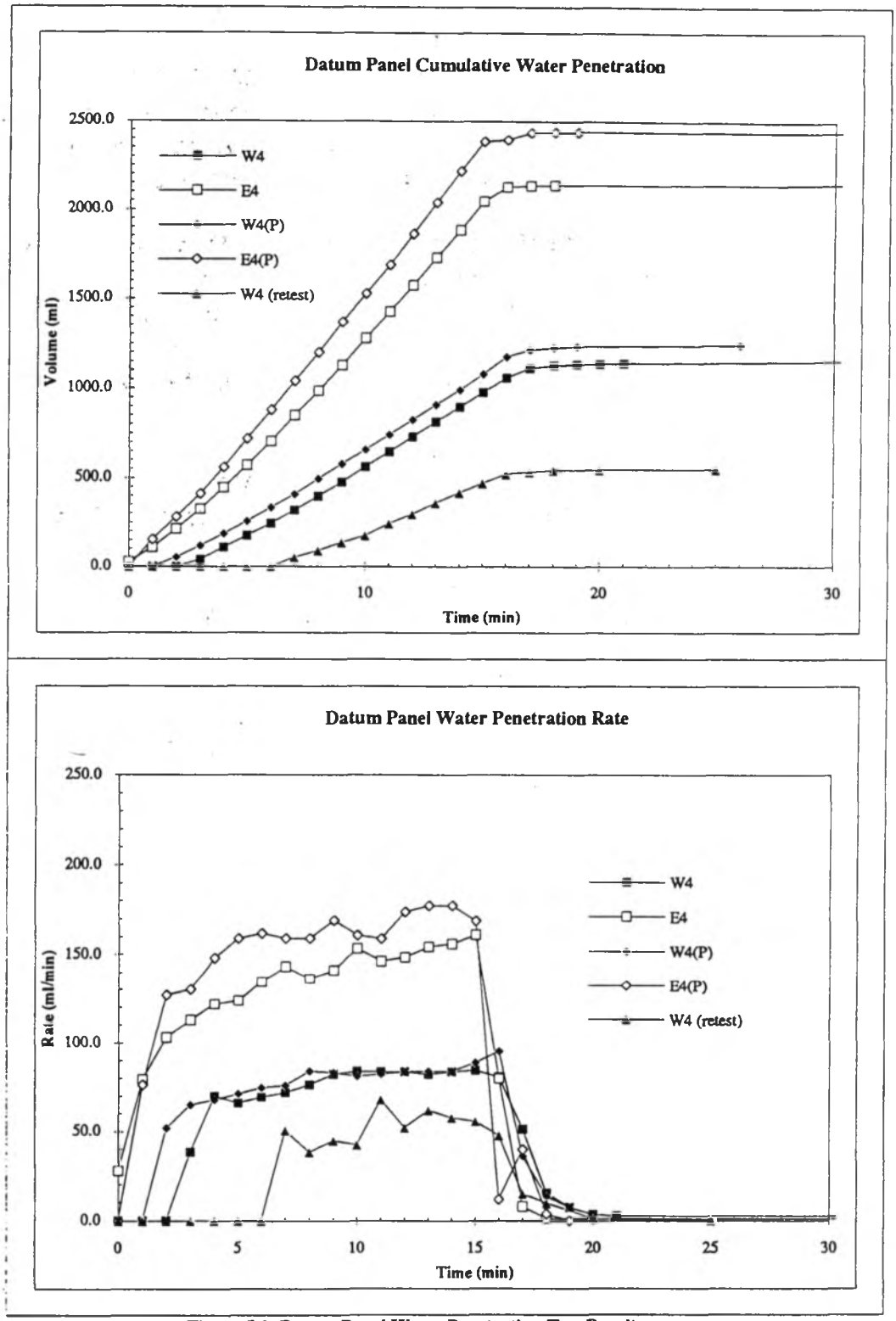

Figure 5.1: Datum Panel Water Penetration Test Results

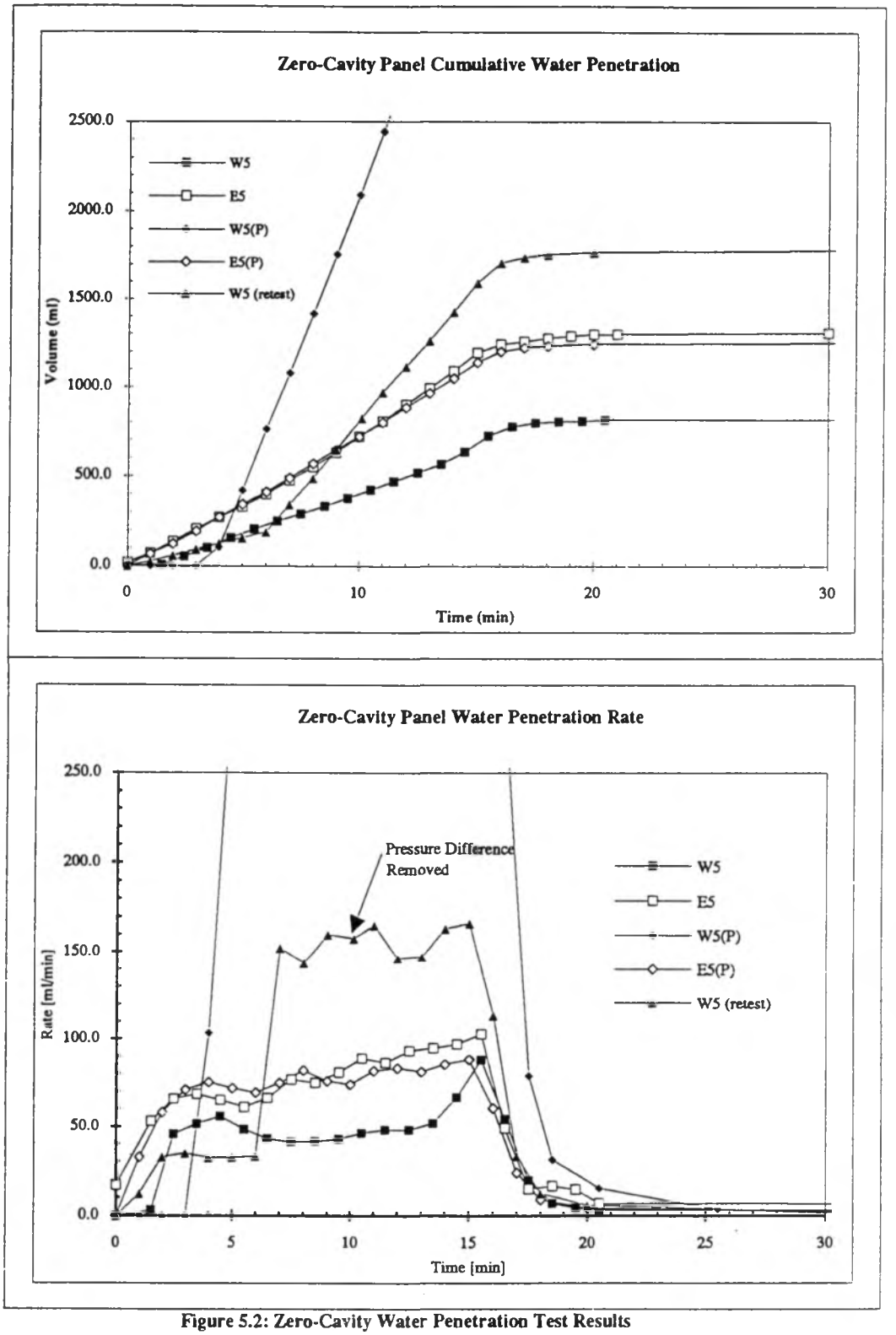

Figure 5.2: Zero-Cavity Water Penetration Test Results

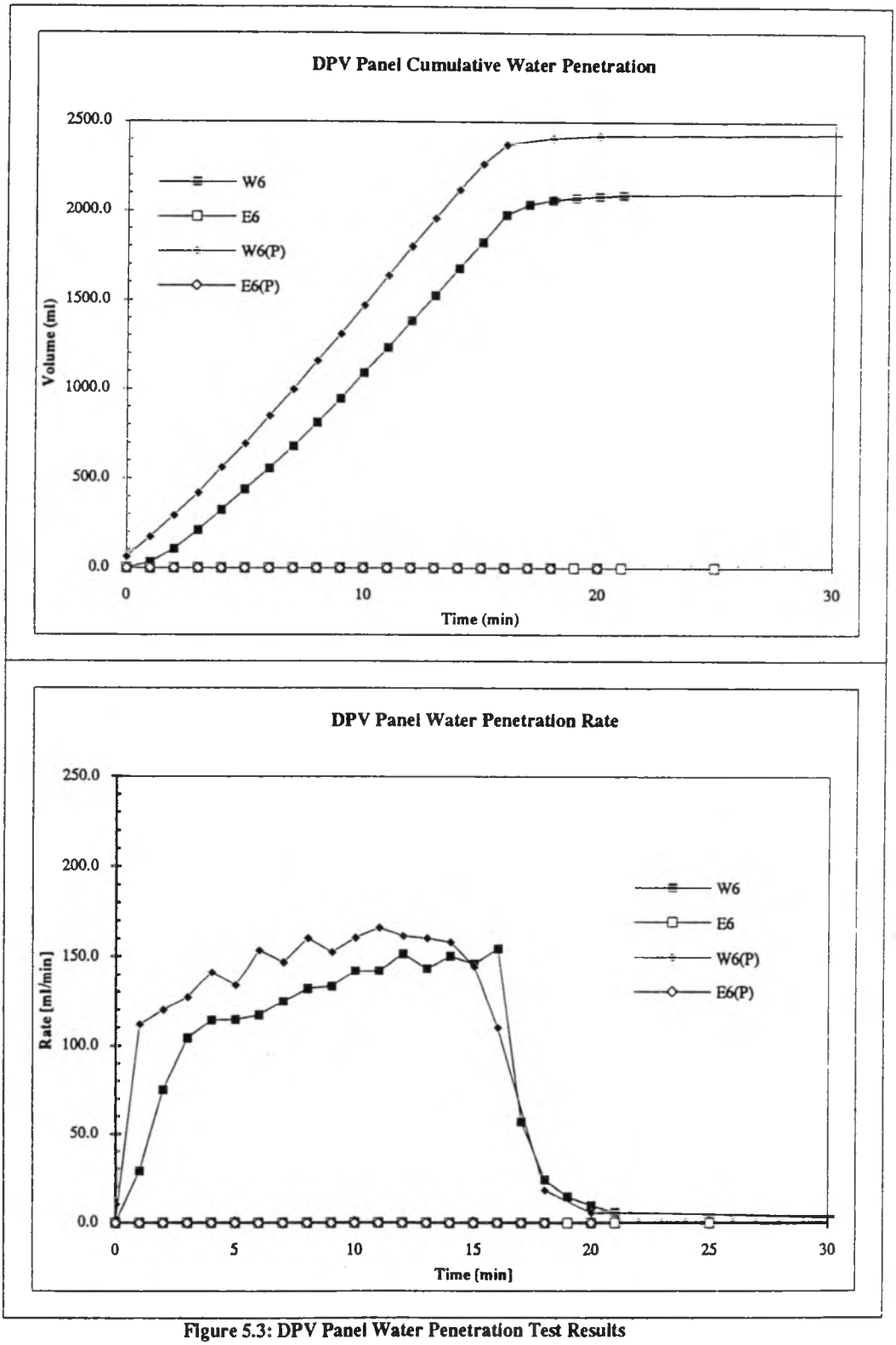

Figure 5.3: DPV Panel Water Penetration Test Results

No water was collected during either test of panel E6, even though the initial test was run 10 minutes longer in an attempt to measure some penetration. An inspection of this panel showed that the collection holes had been completely blocked and could not be cleared without removing the lower course of brickwork. Panel E6 is disregarded in the following discussion because of this problem; a not uncommon problem in practice. The pressurized test of W5 is also an anomaly (for unknown reasons) and is considered separately throughout.

The supplementary test on W4 produced inconsistent data. Although no flow was measured until the seventh minute, the flow rate changed only slightly after the vent covers were removed. Similarly, the test on panel W5 began with a slightly lower rate than in the original non-pressurized test, then jumped to a level more than three times as high by the seventh minute. After the pressure difference was removed the rate did not appear to change.

5.4 Discussion

Despite the severity of the test conditions, all panels appeared to drain the water effectively and protect the interior wythe. This underlines the importance of a clear cavity with no mortar bridges or obstructions.

The two supplementary tests indicated that neither the pressure difference nor the covering of the vents had a significant effect on the test results relative to the variability between tests.

The applied pressure difference resulted in a small but noticeable increase in the water penetration volumes and peak rates for three of the five panels tested. Panel E5, however, had a drop of 51.4 ml with the pressure difference applied. This is a small amount considering the variability of the other results. Although the applied static pressure difference appeared to cause a slight increase, the sample size and variance indicates that this is not a statistically valid conclusion.

Panel W5 reacted fundamentally different to the pressure difference; it had very much higher volumes and flow rates with the pressure difference applied. On retest the panel also performed erratically with a high flow rate but this was not related to the pressure difference since the rate remained high even after the pressure was removed. One explanation for the performance of this panel may be that cracks in the veneer or the drainage tube itself were washed free of accumulated dirt or salts after exposure to water.

Once the initial water had cleaned out the crack, flow would increase. In all three tests on W5, the penetration rate started with one value (50, 0, and 32 ml/min) and changed to another higher value later (75, 350, and 150 ml/min). The first test exhibited the least difference between low and high values and the change occurred latest in the test (indicating that a blockage was removed after exposure to the water and was not fully cleared).

It was expected that the cavity insulation would act as a sponge and slow the drainage response of the Zero-Cavity panels, but, when compared to the Datum panels no lag in response was measured. They also reacted no differently from the Datum in that the drainage rate quickly reached zero only 3 - 5 minutes after the spray stopped.

The total water applied to each panel during the test was 256 liters; the results indicate that from 0.8258/256= 0.32% to 2.442/737= 0.95 % of the applied water penetrated the brick veneer and was collected.

5.5 Comparisons

Initially there was concern because the water penetration rates were higher than expected. This prompted a comprehensive literature search of other water penetration tests on in-situ and laboratory brick veneers.

Some previous CMHC-sponsored research[2] reported much lower rates of water penetration. All of the tests were, however, conducted with brick masonry built in the laboratory and protected from significant temperature changes or other environmental stress.

The British Building Research Establishment has conducted a long-term research program into the water permeance of brick masonry. They have published a number of reports and papers regarding their research and all of the tests conducted on brick veneer walls in the field have resulted in water penetration values quite similar to those measured in the tests reported here. Several other researchers in the U.S. and U.K. have conducted realistic lab and field testing as well. The results of some of these tests are presented in Table 5.6. All of the values have been standardized to milliliters per minute per m^2.

Many tests of solid brick walls have been conducted in the lab (the standard ASTM E514 was developed for this purpose) but the results are not applicable to brick veneers and the procedure is difficult to apply to in-situ walls. Field-modified versions of the E514 are used for many field tests with brick veneers although these test procedures, and thus the

results, almost always involve an induced pressure difference. It has been conclusively shown in many published tests that the application rate is not directly related to penetration rate once a film of water has formed over the surface. The effect of pressure differences have been shown to be approximately linearly related to the zero-pressure leakage rates.

Source (Reference)	Application Rate milliliters/m^2/min	Leakage Rate Range milliliters/m^2/min	Passing %	Comments
BEG Tests	5600	23.6 - 57.8	0.4-1.0	
3. Table 1	50	8.3 - 12.6	17.0-25.0	low application rate, 6 h test
4. Figure 6	5600	20 - 23	0.4	lab test
5. Figure 4	150	1 - 27	0.7-18.0	lab tests
5. Table 1	27	5.74 - 23.9	21.0-88.0	multiple field tests
6. Table 1	27	15.7 - 24.3	58.0-90.0	similar tests as in 3.
7. Figure 1	280	0.1 - 25	0.0 - 9.0	intermittent spray- 50/50 on/off
8. Figure 25 (concrete)	1000 - 3000	50 - 85	5.0 - 2.8	max/min application rate corresponds to max/min leakage

Table 5.6: Comparison of Water Penetration Test Results

Using the existing large data base of E514 tests might permit a better prediction of brick veneer water penetration rates but the correlation and presentation of these and many other tests results is beyond the scope of this report. Suffice it to say that most evidence suggests that the penetration rates recorded in the BEG tests are comparable to other field tests and should be expected for many brick veneer walls presently being built.

Only a small percentage (less than 1 %) of the applied water passed through the screen in the six test panels. Most researchers have found that increasing the application rate decreased the volume of penetration as a percentage of the applied water. Since a very high rate of application was used, the penetration rate is proportionately low.

Other researchers (notably Refs. 3 and 4) have varied the application rate and examined the influence of saturated versus dry performance. Their conclusions indicate that a large percentage (generally in the range of 20 to 80%) of the water applied passed through the

screen when smaller rates of water typical of rainfalls were applied. The BRE has developed a field test procedure where water is applied to the wall at a low rate for 4 hours per day for three consecutive days to relatively accurately mimic rainy spring and fall weather. Tests conducted in this manner have indicated a very high percentage of absorption and penetration (over 80%) and very little face drainage.

5.6 Conclusions

Brick and mortar have quite variable properties and therefore the results of the brickwork assemblage were quite scattered over a large range; repeatability was also poor.

The interior drainage system in all panel types performed well under the high flow test conditions.

The brickwork on all of the panels allowed a significant amount of water to penetrate through into the cavity. Significant amounts of water penetration can be expected through most brickwork veneers.

The fiberglass insulation filling the Zero-Cavity panel did not appear to retard the natural drainage of the cavity in these tests.

The applied pressure and the open vents had no significant effect on the water leakage. The imposed static air pressure difference did not act across the veneer because the walls were well vented. Water penetration through the vents did not provide a significant contribution to the total water penetration because they were protected by inserts, they comprised a small proportion of the area, and the brickwork veneer was also quite leaky.

References

[1]Sakhnovsky, A.A., "Testing for Water Penetration", Window and Wall Testing, ASTM STP 552, American Society for Testing and Materials, 1974, pp. 31-35.

[2]Drysdale, R.G. and Wilson, M.J.,"A Report on Lateral Load and Rain Penetration Tests of Full Scale Brick Veneer/Steel Stud Walls", Research Report, Project Implementation Division, Canada Mortgage and Housing Corporation, Ottawa, July 1990.

[3]Whiteside, A.J., Newman, A.J., Kloss, P.B., Willis, W."Full-Scale Testing of the Resistance to Water Penetration of Seven Cavity Fills", *Bldg. and Environ.*, Vol. 15, pp. 109-118, 1980.

[4]Newman, A.J., and Whiteside, D.,"Water and Air Penetration Through Brick Walls - A Theoretical and Experimental Study", *Trans. J. Br. Ceram. Soc.*, Vol. 80, pp. 17-26, 1981.

[5]Whiteside, A.J., Newman, A.J., Kloss, P.B., Willis, W."Full-Scale Water Penetration Tests on Twelve Cavity Fills- Part I. Nine Retrofit Fills", *Bldg. and Environ.*, Vol. 17, pp. 175-191, 1982.

[6]Whiteside, A.J., Newman, A.J., Kloss, P.B., Willis, W."Full-Scale Water Penetration Tests on Twelve Cavity Fills- Part II. Three Built-in Fills", *Bldg. and Environ.*, Vol. 17, pp. 193-207, 1982.

[7]Newman, A.J., and Whiteside, D.,"Water and Air Penetration Through Masonry Walls - A Device for the Measurement of Air Leakage in-Situ", *Trans. J. Br. Ceram. Soc.*, Vol. 83, pp. 190-195, 1984.

[8]Rathbone, A.J.,*Rain and Air Penetration Performance of Concrete Blockwork*, Technical Report 553, Cement and Concrete Association, Wexham Springs, UK, 1982.

6. Pressure Equalization Testing

Wind-induced pressure difference is one of the forces that contributes to the rain penetration of walls. This force can theoretically be reduced or eliminated by using the "pressure-equalized" rainscreen approach to wall design. This approach entails using a wall system with an air compartment that is located inside the exterior cladding (screen) and vented to the outside to enable the pressure on the inside to balance the wind pressure on the outside. The nature of a so-called pressure-equalized rainscreen wall, or preferably, screened/vented/drained wall system, is shown in Figure 6.1. Since instantaneous pressure-equalization is the basis for the approach, it is important that the air chamber pressure respond quickly to changes in the outdoor air pressure.

6.1 Purpose

The purpose of the series of tests reported in this chapter was to measure the degree of pressure equalization that occurs in each of the test panels. The results obtained for the different panel types are compared with each other and with other research results. Although no standard test for quantifying the degree of pressure equalization exists, a test program was devised to measure the pressure conditions of each wall. Rather than use an artificial pressure, the test panels were exposed to the wind pressures similar to what most low-rise residential walls are exposed to. Methods were also developed to quantify and compare wall systems exposed to the actual, randomly varying wind pressures. The larger and more general issue of defining what level of pressure equalization is necessary or achievable is not addressed in this report.

6.2 Background

6.2.1 Wind and Applied Pressure

Wind speed can be easily and accurately transformed into a pressure (the stagnation pressure) in the centre of a large square plate placed perpendicular to the air flow direction by Bernoulli's equation. This results in:

$$P = \frac{1}{2} \rho V^2, \qquad (6.1)$$

where ρ is the air density, and

V is the air velocity.

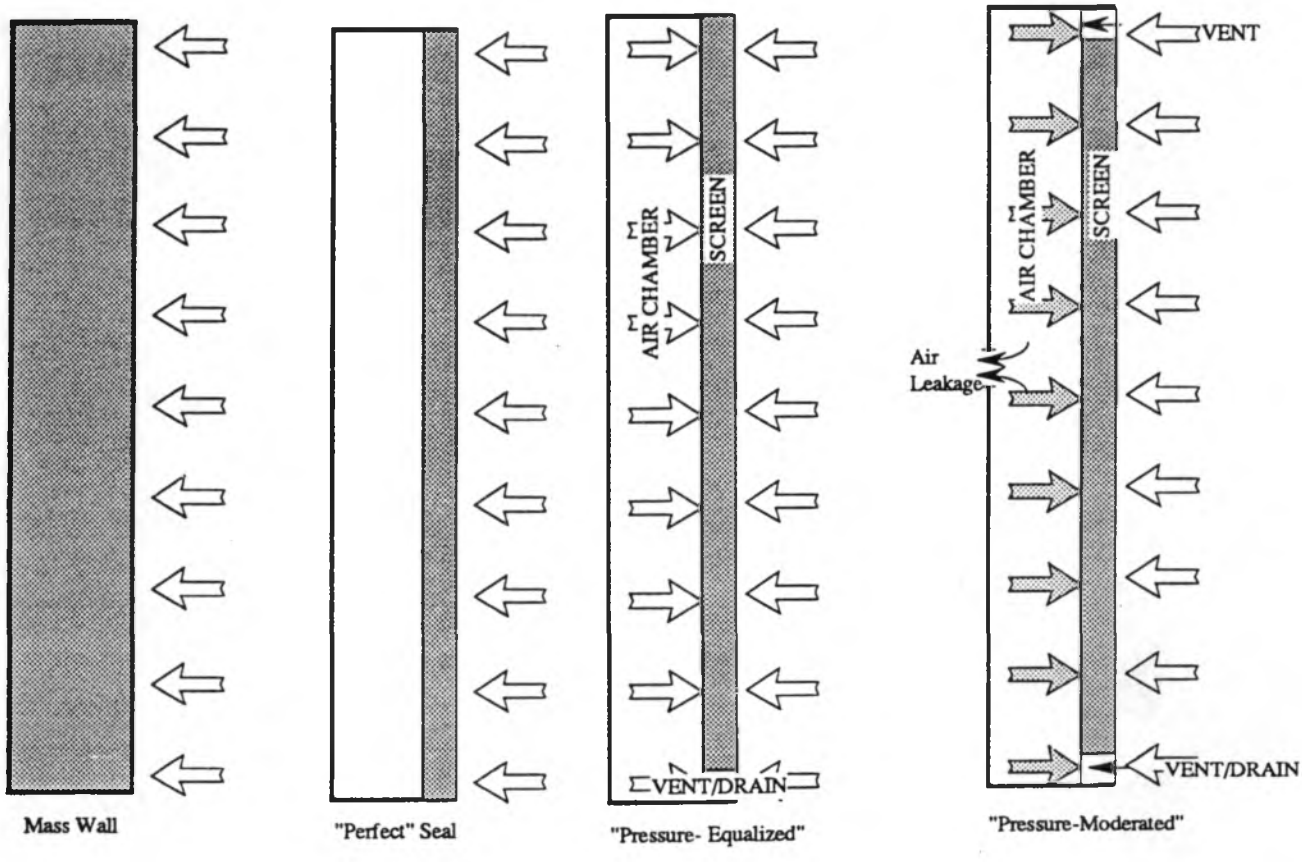

Figure 6.1: Screened/Vented/Drained Wall System

The National Building Code of Canada calculates the design pressure, q, based on long-term records of mean hourly wind velocities measured at 10 metres above grade. An air density of 1.294 kg/m^3 is used, assuming standard temperature and pressure conditions, to generate the design pressure given in the Code:

$$q = \frac{1}{2} \cdot 1.294 \cdot V^2_{10} = 0.647 \cdot V^2_{10} \qquad (6.2)$$

where q is the Code-specified design pressure (Pa), and

V_{10} is the design hourly mean wind speed at 10 m height (m/s).

The pressure acting at any point on a building, however, is drastically affected by the building's location, height, and shape, as well as the wind direction, and local topography. The Code recognizes these variables by modifying the design pressure by means of several factors. The external design pressure or suction on a building surface is given by the equation:

$$p = q \cdot C_e \cdot C_g \cdot C_p \qquad (6.3)$$

where, p is the design *static* pressure (positive or negative i.e. suction) acting normal to the surface,

C_e is the exposure factor which accounts for changes in wind speed with height and terrain,

C_g is the gust factor which is given a value of 2.0 for the structure and 2.5 for cladding, and

C_p is the external pressure coefficient averaged over the area considered.

In the NBCC, values for C_e ,C_g , and C_p are tabulated for many simple building shapes; complicated buildings and/or topographies require wind tunnel testing.

In the Code approach, p is equivalent to a static design pressure. While an equivalent static pressure may be satisfactory for structural design, where safety is a primary concern, it is not a satisfactory means of modelling wind for in-service conditions. The wind is not a steady, smooth-flowing stream of air. The wind velocity and direction are constantly changing, causing short-term pressure variations and gradients on the face of a building. The static code-based extreme design values are the peak long-term (10 or 30-year probability) pressures of wind that, for the vast proportion of the time has a much lower mean pressure with rapidly changing variations. Since even a very small amount

of venting will result in pressure equalization to mean pressures, it is the short-term variations which have the greatest influence on the across-screen pressures in pressure-equalized wall systems.

To establish the wind pressure, some consideration must be given to the fact that the wind velocity (and hence pressure) increases with height. In accordance with the NBCC, the velocity increase with height follows a power law of the following form:

$$V(z) = \left(\frac{z}{10}\right)^{\alpha} \cdot V_{10} \qquad (6.4)$$

where V(z) is the mean velocity at height z (m/s),

z is the height above the ground (m),

α is the gradient exponent, and

V_{10} is the mean velocity at ten metres (m/s).

The term $\left(\frac{z}{10}\right)^{\alpha}$ is incorporated in the C_e factor by the NBCC.

The gradient exponent is given in the NBCC and ANSI standard A58.1-1982 for a variety of terrains. Exposure B (described as suburban and urban areas or wooded terrain) is appropriate for the Beghut site and 2/9 is given as a value for the gradient exponent. Combining equations 6.2 and 6.4 results in a mean pressure gradient described by:

$$P(z) = \left(\frac{z}{10}\right)^{4/9} \cdot P_{10} \qquad (6.5)$$

where P(z) is the mean pressure at z m above the grade (Pa) and

P_{10} is the mean pressure at 10 m (Pa).

6.2.2 Measuring Pressure-Equalization Response

The National Research Council of Canada / Institute for Research in Construction (NRCC/IRC) has conducted some basic research and laboratory testing of cyclic loads and have developed a descriptive equation relating a cyclic pressure (assumed a sinusoid) to the response of the panel[1] . These concepts can be extended to the overall response of a pressure-equalized wall under a random and rapidly varying wind force. Inculet used a

[1]Poirier,G.F. et al., "Pressure Equalization and the Control of Rainwater Penetration", Sixth Conference on Building Science & Technology, Toronto, 1992, pp. 45-65.

similar approach to measure and compare the pressure-equalization performance of wind tunnel models and walls in the field.[2]

Any wind signal can be considered to be composed of a steady component (usually the mean hourly pressure) plus a randomly varying component. Like most random signals, the random component can be considered to be made up of an infinite series of sinusoidal waves, each with a unique frequency, amplitude, and phase shift. Therefore, the wind can be described by the following equation:

$$P_{wind}(t) = P_{mean} + \sum_{0}^{\infty} A_i \cdot \sin(2\pi \cdot f_i \cdot t - \emptyset_i) \qquad (6.6)$$

where P_{mean} is the mean cavity pressure,

A_i and f_i are the amplitude and frequency of the ith component,

t is time,

$\emptyset_i$ is the random phase shift.

The pressure in a pressure-equalized air chamber can lag behind the wind pressure on the building face in time and be smaller in amplitude. This lag may be due to the combined effects of the inertia of the air, the friction of the cavity and vent holes, the flexibility of the screen and the air barrier, and air leakage through the imperfect air barrier and screen.

Pressure-equalized walls have generally been dynamically tested in the laboratory by applying a uniform sinusoidal pressure to the exterior of a mock-up wall and measuring the variation in the cavity pressure. More comprehensive tests include a series of different frequency pressure variations and different amplitude variations.

Figure 6.2 is a typical plot of the pressures recorded during such a test for a single frequency and amplitude wave. The many factors affecting the cavity pressure response can be combined and the cavity pressure for a single-frequency component expressed as:

$$P_{cav}(t) = \overline{P_{cav}} + k_i \cdot A_i \cdot \sin(2\pi \cdot f_i \cdot t - \emptyset_{cav,\,i}) \qquad (6.7)$$

where P_{cav} is the instantaneous cavity pressure contribution of the ith component,

$\overline{P_{cav}}$ is the mean cavity pressure,

A_i and f_i are the amplitude and frequency of the ith component,

[2]Inculet, D.R., "Pressure-Equalization of Rainscreen Cladding", M.Eng.Sc. Thesis, University of Western Ontario, 1990.

t is time,

k_i is the fraction of the ith varying component with respect to A_i,

$\emptyset_{cav,\,i}$ is the phase shift which represents the time lag in response.

The second term of equation 6.7 is usually denotedthe cavity frequency response, or H_{cav}

$$H_{cav} = k_i \cdot A_i \cdot \sin(2\pi \cdot f_i \cdot t - \emptyset_i). \tag{6.8}$$

The values of k and Ø are important since they describe how much amplitude attenuation and time shift has occurred when the pressure wave moves from outside to inside the cavity. The value of k is the ratio of the maximum amplitude of the applied pressure (denoted A in Figure 6.2a) to the amplitude of the cavity pressure:

$$k = \frac{\max(P_{cavity})}{\max(P_{exterior})}. \tag{6.9}$$

The value of Ø is defined as the angular displacement of the cavity pressure wave relative to the applied pressure wave (where 360° or 2π radians are exactly one period in time; see Figure 6.2).

The magnitude of the amplitude attenuation (k) and the phase shift (Ø) are theoretically 1 and 0 respectively for a perfectly pressure-equalized cavity (i.e., one in which the pressure exactly follows the pressure change on the exterior). In practice, the values of k and Ø will not be exactly 1 and 0 because the combined factors of inertia, frictional forces, etc., will always act to retard pressure changes in any real pressure chamber. If the pressure change is fully transmitted to the chamber but delayed in time, k will be 1 and Ø will be some value other than zero (Figure 6.2b). If an exterior pressure change is instantaneously transmitted to the chamber with some loss in amplitude, Ø will be zero and k will be some value less than one (Figure 6.2c). Neither of these extreme situations (i.e. k=1 or Ø=0) will occur in tests on a typical wall assembly.

In any wall exposed to the actual wind, an infinite number of frequencies must be superimposed on one another in order to describe the random nature of the wind. The cavity response described by equation 6.7 can be modified to be a function of these many superimposed pressure waves. For an infinite number of frequency components, equation 6.7 can be written as:

$$P_{cav}(t) = \overline{P_{cav}} + \sum_{0}^{\infty} k(f) \cdot A(f) \cdot \sin(2\pi \cdot f \cdot t + \emptyset(f)) \tag{6.10}$$

The values of k, A, and Ø all vary with the frequency of the pressure change and hence are functions of frequency, f. The corresponding cavity frequency response *function* is therefore:

$$H_{cav}(f) = k(f) \cdot A(f) \cdot \sin(2\pi \cdot f \cdot t + Ø(f)) \tag{6.11}$$

A plot of many amplitudes for different frequency components results in what is called the power spectrum. The power spectrum of many random signals (including the wind) can be approximated by using a Fourier transformation of a record of measurements to calculate an amplitude at many different frequencies. The mathematical foundation of the Fourier technique means N/2 estimates can be calculated from N measurements. This method attempts to approximate any random signal with a series of sinusoidal waves of the following form:

$$X(t) = \sum_{i=1}^{N/2} A_i \cdot \sin(2\pi \cdot f_i \cdot t - Ø_i) \tag{6.12}$$

where $X(t)$ is the estimated value of the random signal at time t,

A_i and f_i are the amplitude and frequency of the ith component,

t is time,

$Ø_i$ is the phase shift, and

N is the number of discrete measurements of the signal.

By mathematically manipulating the Fourier spectrum of a signal (essentially squaring the amplitudes), one can generate the power spectrum and thus the amplitude, A_i, and phase shift, $Ø_i$, can be estimated for each frequency f_i. The power spectrum of the signal X(t) is denoted as $S_X(f)$ in this report. The power spectrum of the wind, the applied pressure, the cavity pressure, and the pressure difference across the screen can all be treated in this way. The plot of A_i versus f_i is the power spectrum. The plot of $Ø_i$ versus f_i is the phase diagram.

Since the definition of k is $A_{cavity} / A_{exterior}$, the $H_{cav}(f)$ function given in equation 6.11 can be calculated for the entire spectrum of frequencies by dividing the pressure spectra of the exterior and cavity pressures:

$$H_{cav}(f) = \frac{S_{cav}(f)}{S_{ext}(f)}, \tag{6.13}$$

$$k(f)^2 = \left|H_{cav}(f)\right| \text{, and } Ø(f) = \tan^{-1}\left(\frac{\text{Im}\,[H_{cav}(f)]}{\text{Re}\,[H_{cav}(f)]}\right) \tag{6.14, 6.15}$$

where, $S_{cav}(f)$ and $S_{ext}(f)$ are the pressure spectra of the cavity and the applied pressure respectively, and

Im[] and Re[] are the real and imaginary parts respectively.

Equation 6.14 is thus merely a restatement of equation 6.9 using power spectra. Although Ø has an obvious meaning for a sinusoidal wave of a single frequency applied to a wall, the physical significance is limited under the full spectrum of the wind. Similarly, k provides an excellent indicator of the pressure attenuation of the wind pressure variations entering the chamber, but the effect of this attenuation is not directly related to the rain penetration force because the resulting force across the screen is difficult to assess without the corresponding lag time (for example, compare Figures 6.2a and 6.2c).

The pressure that is of primary interest is the pressure difference across the screen since this is what might drive water across the screen. The pressure difference across the screen at any time, $P_{\Delta screen}$, is the difference between the air chamber pressure (P_{cavity}) and the applied pressure, ($P_{exterior}$) or the difference between the pressure across the entire wall and across the air barrier ($P_{\Delta air\ barrier}$.); i.e.,

$$P_{\Delta screen} = P_{exterior} - P_{cavity} = P_{exterior} - P_{\Delta air\ barrier}.$$

The average pressure across the rainscreen, $\overline{P_{\Delta screen}}$, varies with the relative air flow resistances of the rainscreen and the air barrier leakage (here average means over a sufficiently long period of time, denoted by the bar over the value). If the air barrier is perfect, no average airflow will occur, and the mean pressure across the rainscreen will, *on average*, be zero, i.e.,

$$\overline{P_{\Delta screen}} = \overline{P_{exterior}} - \overline{P_{\Delta air\ barrier}} = 0.$$

A zero pressure across the rainscreen does not mean that rain penetration will not occur because short term differences in pressure may still cause a driving force. Static air pressure tests of wall mockups will yield the value of $\overline{P_{\Delta screen}}$ and $\overline{P_{\Delta air\ barrier}}$.

The pressure difference across the screen can also be assessed in the same way as the wind and cavity pressures. The pressure spectrum of this pressure difference, $S_{\Delta Scr}(f)$, is a measure of the contribution each frequency component makes to the total driving force across the screen. The magnitude of the frequency response function of the pressure difference across the screen, $k_{\Delta Scr}(f)$, is the ratio of the contribution each frequency makes to the total driving force across the screen relative to the applied pressure. For a single sinusoidal pressure wave:

$$k_{\Delta scr} = \frac{\max(P_{\Delta scr})}{\max(P_{exterior})} \tag{6.16}$$

exactly as for the cavity pressure. For a long record, the Fourier transform method can be used to calculate $k_{\Delta scr}(f)$ and $\emptyset_{\Delta scr}(f)$.

$$H_{\Delta scr}(f) = \frac{S_{\Delta scr}(f)}{S_{ext}(f)} \tag{6.17}$$

$$k_{\Delta scr}(f)^2 = \left|H_{\Delta scr}(f)\right| , \ \emptyset_{\Delta scr}(f) = \tan^{-1}\left(\frac{\text{Im}\,[H_{\Delta scr}(f)]}{\text{Re}\,[H_{\Delta scr}(f)]}\right) \tag{6.18), (6.19}$$

where, $H_{\Delta scr}(f)$ is the frequency response function of the pressure difference across the screen,

$S_{\Delta scr}(f)$ and $S_{ext}(f)$ are the pressure spectrum functions of the difference across the screen and applied pressure respectively, and

Im[], Re[] are the real and imaginary parts respectively.

The function $H_{\Delta scr}(f)$ is an excellent measure of the amount of time that a pressure difference will exist across the screen and the magnitude of this difference. The function $H_{\Delta scr}(f)$ is called a transfer function since it indicates how the exterior pressures are transferred to the cavity.

The $k_{\Delta scr}(f)$ function is in fact, a good measure of the degree of pressure equalization (or, preferably, the degree of pressure moderation). This measure allows quantitative comparisons between different walls measured at different locations under different wind conditions. Since the wind never behaves in exactly the same manner twice, this is an extremely important characteristic and allows for repeatable test results.

Unfortunately, the relationship between $H_{\Delta scr}(f)$ and rainwater penetration has not been investigated. While $H_{\Delta scr}(f)$ measures the effectiveness of the pressure equalization, a different measure of the rain penetration of particular rainscreens under a pressure difference is required to fully assess a PER wall's resistance to rain penetration. This measure will likely also be a function of the frequency and amplitude of the pressure applied across the screen and of the screen properties. Hence, the resistance of a pressure-equalized wall to rainwater penetration could be defined by the combination of the pressure equalization performance ($H_{\Delta scr}(f)$) and water permeance performance of the screen under varying pressures.

Note: The nomenclature and definitions used in frequency-domain analysis are different in the wind engineering, signal processing, and mathematical literature. This report has chosen terms and definitions that provide a simplified (and thus less mathematically rigorous) approach to calculating results from real-time, discretely sampled pressure results, and allows comparison with the NRC-style of single-frequency laboratory tests.

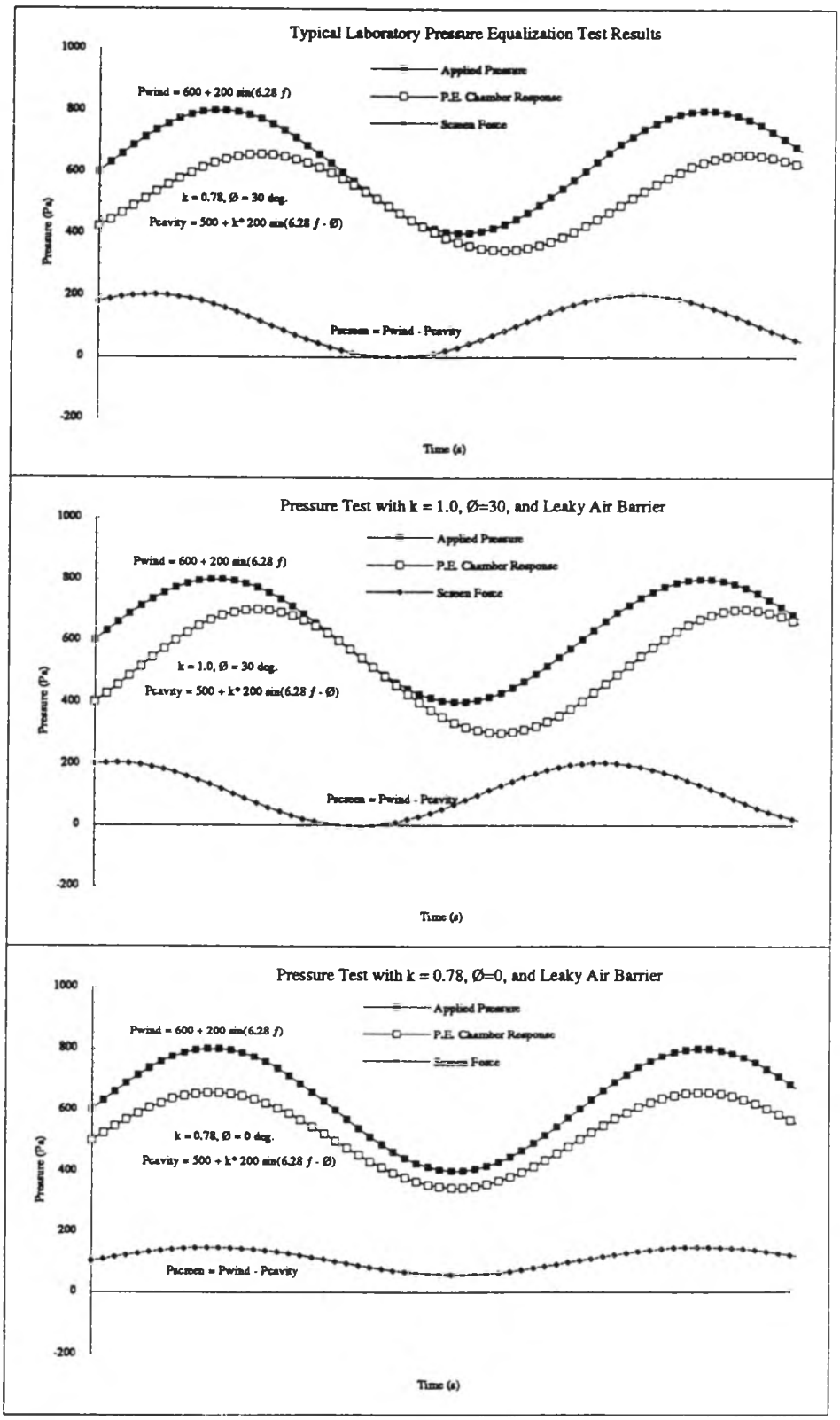

Figure 6.2: Typical Cyclic Pressure-Equalization Test Results

6.2.3 Field Measurement Considerations

The wind pressure on a building face varies in time and in space. The wind is a natural stochastic phenomena and in any field study, the conditions required for simple measurements rarely occur, i.e. high velocity, frontal wind conditions seldom occur. For comparison and uniformity of results, the wind conditions must be similar between tests at different times and on different panels. The wind velocity required to generate significant pressures on a low-rise building neither occur very often nor for long periods of time.

The wind direction greatly affects the pressure acting on a wall. As the wind direction varies significantly from perpendicular, pressures near building corners will drop and air will flow laterally across the building face from the high pressures zone in the middle of the wall to the negative pressure zone on the leeward side of the corner. While these deviations from perpendicular are important to the pressure-equalization performance of walls, the panels that were tested are located at different distances from the Beghut's corner. To ensure equal wind conditions on the face of each test panel, therefore, the wind must be acting almost perpendicularly to the wall. Short records can be collected when the wind direction is close to perpendicular but they may occur during times with significantly different mean wind speeds.

If water penetration resistance is the design goal, pressure equalization is presumably not important for walls under negative pressures (the lee and side walls of most rectangular buildings).

Figure 6.4 provides some indication of the instantaneous effect of pressure variations on a wall high up on a building. While there is some correlation between pressure variations at different points, this correlation is poor over relatively small distances for short-term gusts. If only one vent hole is provided for each pressure-equalized chamber, no through flow is theoretically possible. However, a pressure difference can still develop across the screen because of the spatial variation of exterior pressures, and to a lesser extent, the air chamber pressure gradient.

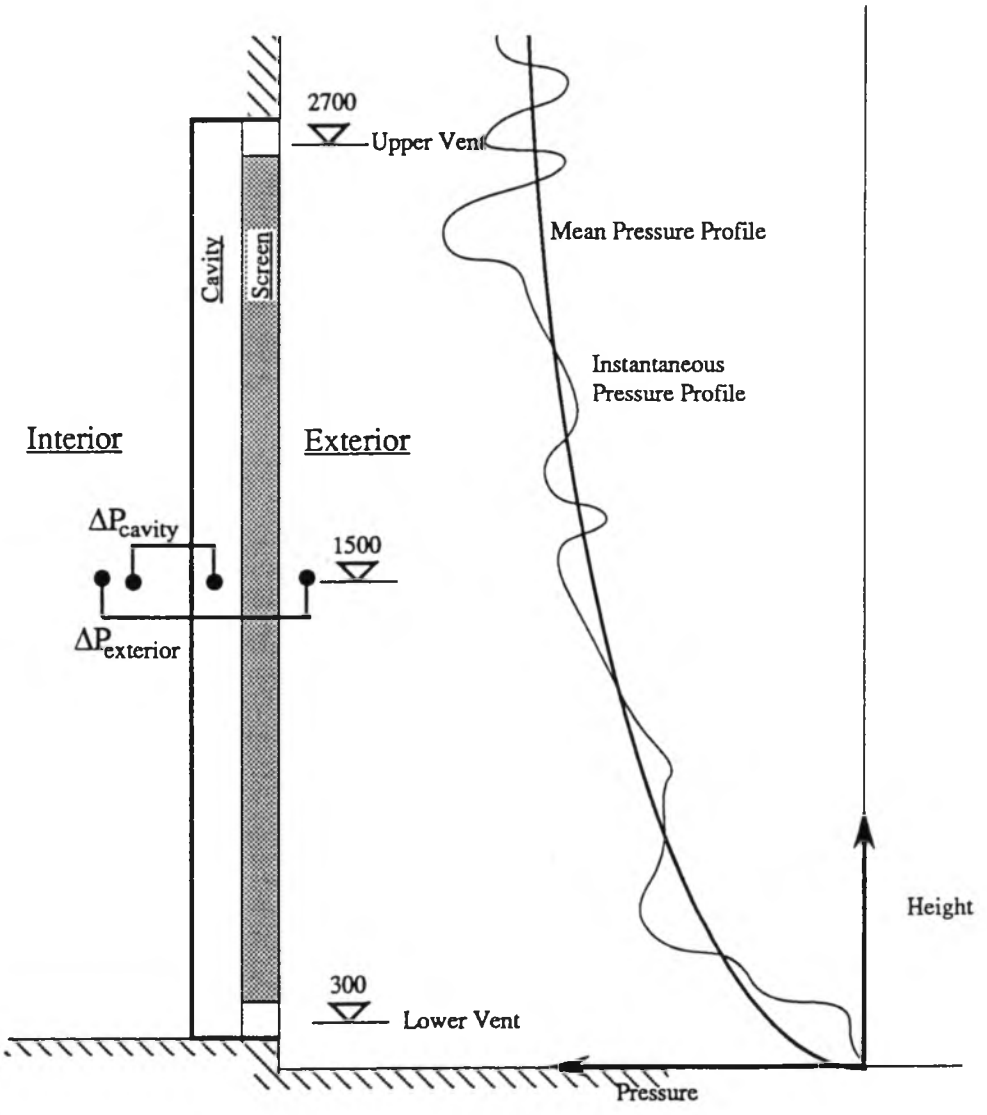

Figure 6.3: Typical Mean and Instantaneous Pressures At Beghut

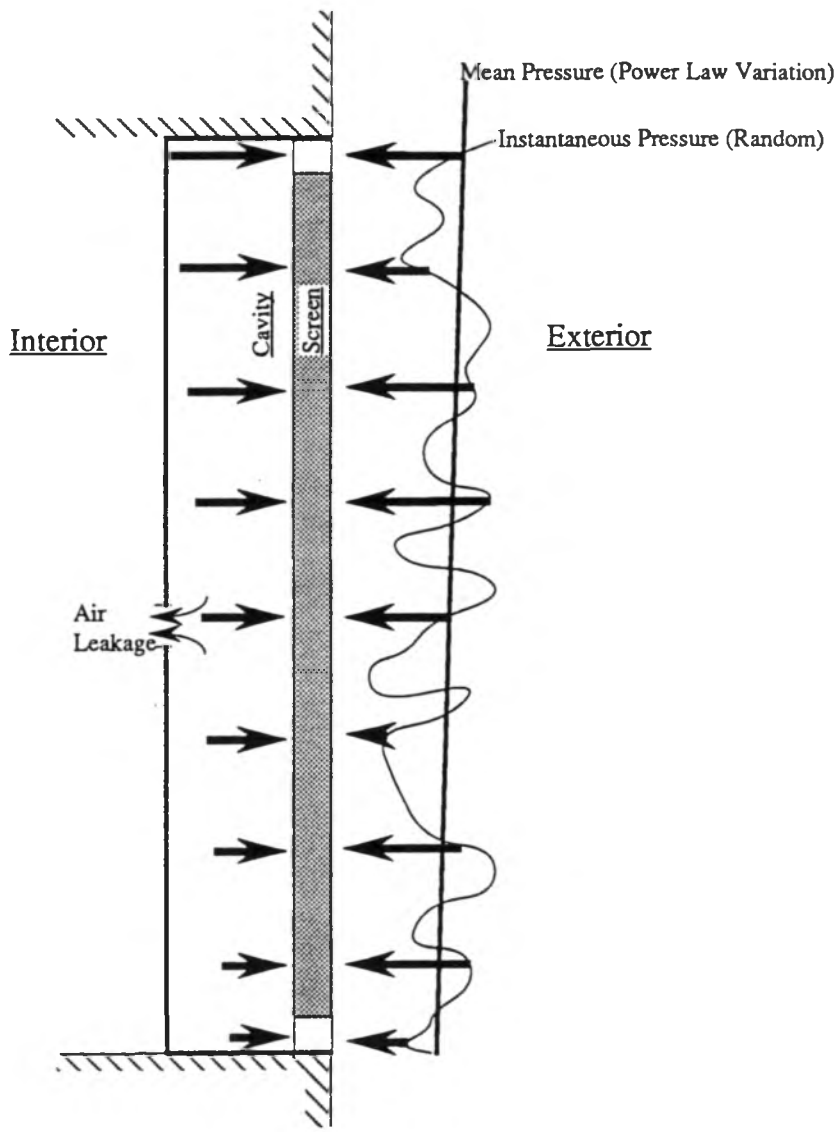

Figure 6.4: Typical Mean and Instantaneous Pressures High on a Building

The spatial variation of pressures over a building face may induce flow through two vent holes connected by a cavity. This flow is likely to change direction rapidly as first one vent hole experiences higher pressure and then the other. Walls with two levels of vent holes can experience net through flow because of a mean difference in pressure acting at the two vents. The increase of mean pressure with height above grade (described by equation 6.5) is superimposed on the short term variations in time and will result in slightly different mean pressures acting at different vent holes.

The panels tested in this study were installed very close to grade (a typical first floor) and each panel was built with 2 vents at approximately 300 mm above grade and 2 vents approximately 2700 mm above grade (Figure 6.3). The two sets of vents are separated horizontally by 600 mm. The likely mean and a hypothetical instantaneous pressure profile are shown in Figure 6.3. The highest mean pressures on the panel can be expected to act on the top vents. This will create some flow from the top of the chamber to the bottom. The horizontal separation of vents will also cause some variation in pressures acting on the exterior, but because these vents are at the same height and separated by only 600 mm, the pressure differences (mean and instantaneous) across these vents should be very close to zero.

6.3 Test Program

The tests carried out on the Beghut panels were directed at finding and comparing the $H_{cav}(f)$ and $H_{\Delta scr}(f)$ functions for each type of panel. Initial investigations have been concerned with the cavity response at the centre of the panel under wind-induced pressure variations on the exterior. The effect of wind direction, wind speed, and the spatial variation of wind are not reported upon here .

6.3.1 Apparatus

The panels were instrumented with pressure taps in at least seven locations. Section 2.3.4 describes the pressure taps, transducers, and data acquisition hardware used.

6.3.2 Procedure

The exterior pressure, cavity pressure, wind speed, and wind direction were read at a rate of 16 times per second. A scan of all 4 sensors could be completed in approximately 12 milliseconds; the exterior pressure and cavity pressure were measured a maximum of 3

milliseconds apart (equivalent to a frequency resolution of about 300 Hz). Data records of at least 64 seconds duration were collected; this resulted in records of 1 024 data points from each sensor. If the average wind speed exceeded a certain minimum threshold speed and the direction was close to perpendicular, the record was saved to disk, if not, the record was discarded and collection restarted. Most of the testing was done on the western panels since the prevailing wind is from the northwest. Some testing was conducted to determine the spatial variation of pressures between vent holes and between panels.

6.3.3 Data Analysis and Manipulation

Each record of collected data was stored individually as voltages and could be analyzed or averaged with other records. The numerical analysis software package Mathcad was used to convert the stored voltages to pressures (using the transducer specific calibration and zero point values) as well as to analyze and plot data. The output from this package is presented in Appendix D.

The wind pressure in Pascals at 10 m was calculated from the wind velocity recorded in kilometres per hour by the wind monitor using the NBCC formula:

$$P_w = 0.647 \cdot \left(\frac{V_{10wind}}{3.6}\right)^2, \tag{6.20}$$

where, P_w is the vector of wind pressures at 10 m,

V_{10wind} is the vector of measured wind velocity in km/h at the 10 m height, and

0.647 converts velocity (m/s) to stagnation pressure (Pa) at standard temperature and pressure.

The raw pressure and wind speed data was later converted to a power spectrum using a fast Fourier transform technique:

$$S_{wind}(f) = \text{fft}\,(P_{wind}) \tag{6.21}$$

Frequencies greater then one half of the collection rate were ignored to avoid aliasing and high frequency AC noise.

Multiplying the numerator by the frequency produces a dimensionless ordinate value to be plotted against the log of the frequency. The advantage of this presentation is that the area under the curve between any two frequencies gives a true measure of the energy in

that frequency range. The 'raw' spectra presented are the calculated pressure spectra multiplied by the frequency, i.e. $f \cdot S_{wind}(f)$ was plotted versus $\log(f)$.

One method of comparing power spectra from different sites, times, and velocities is to divide the spectrum, $S_V(f)$, by the variance of the wind speed, σ_v^2. This normalizes the spectrum since the definition of the spectral density function is:

$$\frac{\int_0^\infty S_v(f) \cdot df}{\sigma_v^2} = 1. \qquad (6.22)$$

Hence, the area under the function will always be unity if spectra are compared in this way. The normalized pressure spectra were calculated in this way, i.e.:

$$S_{wind,n} = \frac{S_{wind}(f)}{\sigma_v^2} \qquad (6.23)$$

where $S_{wind,n}$ is the normalized power spectrum of the wind (or cavity, exterior, difference) pressures, and

σ_v^2 is the variance of the pressure.

The $k_{cav}(f)$ and $\emptyset_{cav}(f)$ functions were calculated from the cavity frequency response function $H_{cav}(f)$ using equations 6.13 to 6.15. The $k_{\Delta scr}(f)$ and $\emptyset_{\Delta scr}(f)$ functions were calculated in the same ways from the frequency response function $H_{\Delta scr}(f)$ using equations 6.17 to 6.19.

The spectral density function calculated using the fast Fourier technique is only an estimate of the actual spectrum. For any individual point calculated, the standard deviation of the estimate can be shown to be equal to the magnitude of the best estimate[3]. Obviously, little value can be placed on any single point. The error can be reduced by using the estimates from neighbouring points to improve individual estimates (this method is called frequency smoothing). Naturally, too much smoothing will result in the loss of real data. Since 1024 data points were recorded, the Fourier transform produced 512 unique estimates of the power. A considerable amount of averaging can be used to produce a better estimate.

Some wind researchers have used weighted averages with 3 terms (weighted 0.25, 0.50,.025) or, for more smoothing, the odd binomial series with five terms (weighted

[3]Lawson, T.V., *Wind Effects on Buildings: Volume 2*, Applied Science Publishers, London, 1980, p.59.

1/16, 1/4, 3/8, 1/4, 1/16) or seven terms (weighted 1/64, 3/32, 15/64, 5/16, 15/64, 3/32, 1/64). Because of the large number of data points, it was found that using simple averaging over 7 terms gave very similar spectra as when the odd binomial weighting was used. The resulting bandwidth becomes 16 / 7 or 2.3 Hz. Any peak in power which occurs with a broader band than 2.3 Hz will clearly be shown, while those peaks considerably less than 2.3 Hz will be smoothed over. To further improve the results, three separate spectra from records within the same measuring period (usually less than an hour) were averaged before any analysis began.

6.4 Results

The results from many records were analyzed and compared. For those panels with at least three records with a consistent mean wind direction almost perpendicular to the panel, mean wind speeds above 25 km/h and similar turbulence intensities, a comprehensive statistical and frequency analysis was conducted. A summary of statistics and relevant charts was created and these data are presented in Appendix D. The output from the data analysis package includes:

- The mean and standard deviations of pressures of the wind, exterior, cavity and difference over each record.

  These measures are useful since they provide an indication of both the mean behavior and the variability of each record and between records.

- The mean and standard deviation of the combined results of the three records.

  Since the three records examined are later averaged in the frequency domain, the statistics for the combined records are necessary.

- The intensity of turbulence (coefficient of variation).

  The intensity of turbulence indicates the amount of variability in the wind signal independent of the mean pressures.

- The raw power spectra for the combined records .

  The spectral density function described in section 6.2.2 provides an excellent indication of how much power exists in each range of frequency. Comparing the different measured pressures indicates

the amount of power each pressure has in a certain pressure i.e. the difference across the screen .

- The smoothed and normalized power spectra for all pressures.

  Normalizing the power spectra allows direct comparisons between different wind events and field measurements at different sites.

- The $k_C(f)$ and $k_{\Delta scr}(f)$ functions plotted with respect to log of the frequency.

  As described earlier, these plots provide the most important and concise indication of pressure equalization performance.

- Plots of the all pressures, the screen pressure difference, and wind direction for each 64 second, 1024 point record.

  The time domain plots provide a visual indication of the pressures and wind direction measured in each of the three records. The pressure difference across the screen is plotted separately for clarity. The ratio of the difference to the applied pressure is a non-dimensional way of expressing the force across the screen.

The nature of the wind at the University of Waterloo site is described below to give some indication as to the applicability of the results to other sites. Pressure moderation performance is then discussed based on time domain statistical measures (average, standard deviation) and the frequency-domain analysis.

6.4.1 Wind Conditions

Mean hourly wind speeds of greater than 30 km/h are recorded in Waterloo between 25 and 50 times per year. While the number of minutes greater than 30 km/h are not recorded at the Beghut, the number should not be substantially greater than 50 hours or 3000 minutes. This means that 30 km/h wind speeds will occur less than 1% of the time. A wind speed of 30 km/h at 10 m corresponds to a pressure of 45 Pa but, under a power law gradient the pressure at 1.5 m will be only 20 Pa. Thus, for most low-rise residential construction in south-western Ontario it is likely that the pressures 1.5 m above grade on a relatively open suburban site will be less than 20 Pa for more than 99% of the time.

These statistical facts are true for most Canadian locations. The results imply that pressure equalized rainscreen walls will usually be exposed to relatively small wind pressures for most of the time.

Mean Wind Pressures and Gradients

The wind pressures and turbulence measured at 10 m above grade are quite different from those measured on the face of the test panel at 1.5 m above grade. As described earlier, wind velocity increases from the earth's surface to the edge of the atmospheric boundary layer under a power law as a function of height. Below 10 m the mean wind pressure gradient changes very rapidly and drops to zero at ground level. All of the wind speed measurements taken at 10 m had calculated pressures (equation. 3.7) approximately twice as high as those measured on the building face at 1.5 m.

Table 6.1 compares the measured pressure at 1.5 m with the pressure calculated using the wind pressure at 10 m and the power law given by equation 6.5. The pressure at the height of the vent holes (2.7 m and 0.3 m) was also calculated and the values are presented in Table 6.1 as well. The shape and size of the Beghut should influence the pressures but, nevertheless, the power law does predict the pressures with surprising accuracy. Apparently, the Datum and Zero-Cavity panels have an effective exposure coefficient (interior minus exterior) of between 0.95 and 1.13.

A review of previous field and wind tunnel studies of buildings with a height and shape similar to the Beghut suggests that the panels near the middle of the Beghut will experience an exterior pressure coefficient of 0.7 to 0.8 and an interior coefficient of 0.2 to 0.3. Therefore the Code-predicted coefficient across the envelope near the middle of the Beghut, $C_{p(in\text{-}out)}$ will be in the range 0.9 to 1.1.

The much lower mean pressures measured on the DPV panel are due to the steep pressure gradient near the Beghut corners. The results suggest a pressure coefficient across the envelope of approximately 0.5 to 0.8 for panel W6, i.e., an exterior coefficient of 0.3 to 0.5. This drop in pressure from the middle of the Beghut indicates a steep pressure gradient near the building corner, as expected.

A	B	C	D	E	F	G
Record	**Measured†**	**Calculated using Power Law**			**Measured**	**Ratio**
	@10m	*@2.7 m*	*@1.5 m*	*@0.3 m*	@1.5m	F÷D
W4_30	39.6	*22.1*	*17.0*	*8.3*	17.0	1.00
W4_31	47.0	*26.3*	*20.2*	*9.9*	20.1	0.99
W4_32	37.7	*21.1*	*16.2*	*7.9*	18.3	1.13
W5_30	38.5	*21.5*	*16.6*	*8.1*	15.7	0.95
W5_31	48.6	*27.1*	*20.9*	*10.2*	20.9	1.00
W5_32	38.5	*21.5*	*16.6*	*8.1*	16.5	1.00
W6_30	35.3	*19.7*	*15.2*	*7.4*	8.5	0.56
W6_31	43.3	*24.2*	*18.6*	*9.1*	9.7	0.52
W6_32	25.6	*14.3*	*11.0*	*5.4*	8.9	0.81

Note: Gradient exponent of 4/9 from NBCC and ANSI A58.1-1982, suburban exposure.

†Pressure at 10 m calculated from velocities using NBCC formula, equation 6.20.

Table 6.1: Comparison of Calculated and Measured Pressures (Pa)

Wind Spectra (Frequency Domain)

The plots in Figure 6.5 are the full and normalized power spectra of the wind averaged from 3 records each of 8 minutes length (sampled at 2 Hz). The spectrum is compared with a generalized shape given by Davenport[4] with a surface drag coefficient using Exposure Category B. Appendix D contains the exact equation and coefficients used. The measured spectrum appears to have slightly less energy in the high frequency regions than the generalized version but otherwise fits quite closely. These results confirm that the wind conditions are similar to those encountered elsewhere in Canada.

[4]Davenport, A.G., "The Spectrum of Horizontal Gustiness Near the Ground in High Winds", *Royal Journal of Meteorology*, 1960, pp. 194- 211.

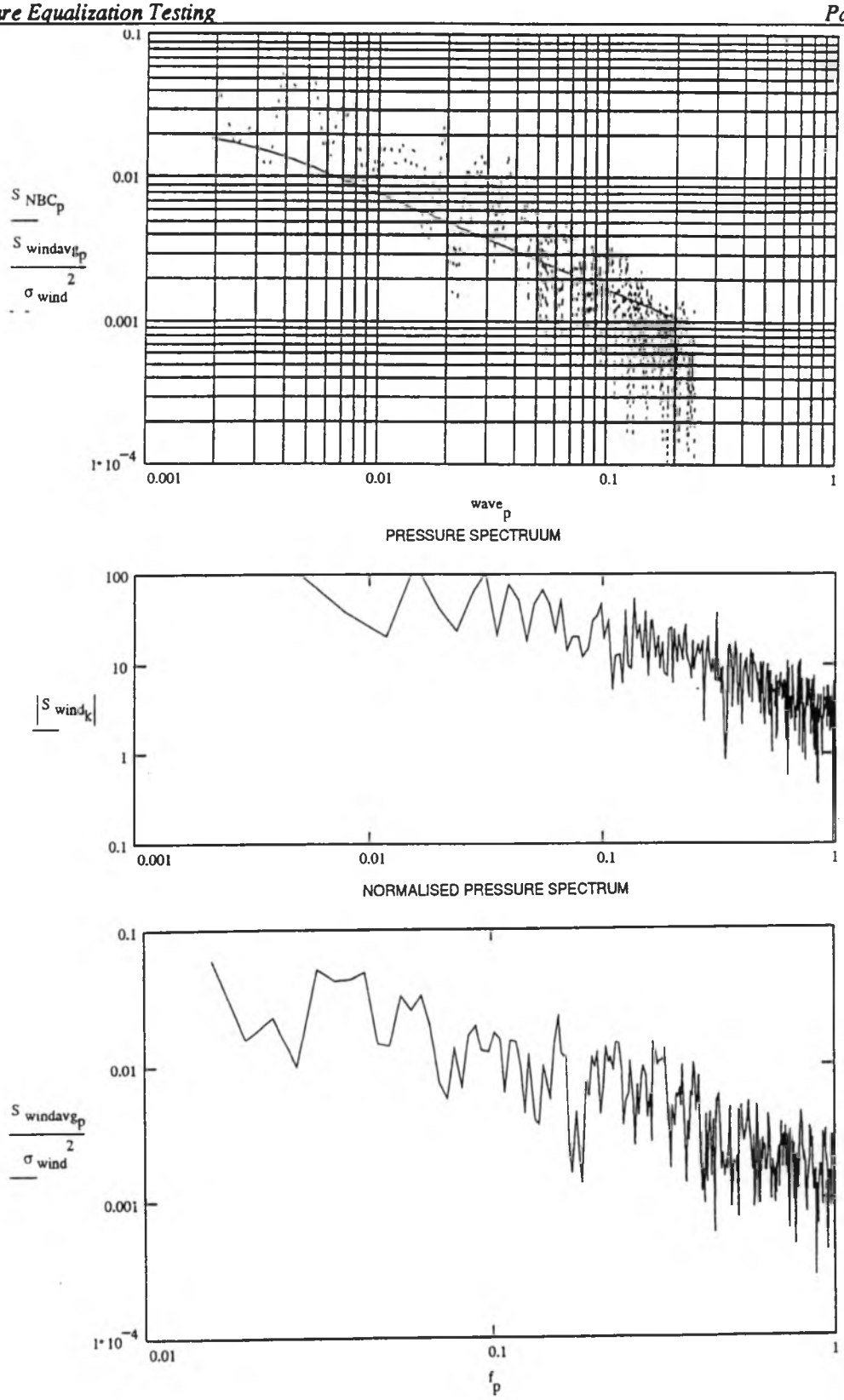

Figure 6.5: Wind Pressure Spectra

6.4.2 Panel Results

General

It has already been noted that wind direction is a critical parameter in pressure moderation response. The ideal condition under which to measure pressure moderation is a steady non-turbulent wind blowing perpendicular to the face of the panel. Unfortunately the real wind does not often oblige and it was necessary to search through numerous records to find records that approximated these ideal conditions. Another concern is that Panels W6 and E6 are the closest to the corner of the building and therefore are subject to larger lateral pressure gradients (and to more turbulence) than the test panels closer to the centre. The frequency-domain measurement method will still allow for some useful comparisons. However, because the pressures are only measured at the centre of the panel (and not at the vent holes) the measured response of the chamber pressure will not be as strongly related to the measured exterior pressure at the centre of the panel as in the Datum and Zero-Cavity.

The results should be considered in light of the known differences in the panel constructions that might affect pressure moderation. The Datum panels have greater air leakage from the chamber to the stud space and less support for this layer than the other two panel types. Both of these factors will theoretically reduce the pressure moderation performance relative to the Zero-Cavity panels. However, the chamber in the Zero-Cavity panels has a larger volume and the fiberglass cavity fill may baffle air flow; both these characteristics will theoretically impair pressure moderation under fast-changing pressure variations. The DPV panels have a small, stiff, and relatively airtight chamber, but the wind conditions near the edge of the Beghut are not conducive to pressure moderation. The vertical grooves in the DPV panel chamber may cause baffling of air flow and thereby reduce the speed of the pressure response of the chamber.

Nine records of the west-facing panels chosen for detailed examination have a mean wind direction within 12° of perpendicular (270° is due west); only record W4-32 had a mean direction of 255° (15° off perpendicular). This nearly perpendicular wind direction should result in a relatively smooth wind force on the panels. The mean wind direction of the three records of the Zero-Cavity panel E5 is 60° (90° is due east). A 30° degree deviation from perpendicular is generally considered the angle where significantly different pressure conditions from a perpendicular angle of attack begin to occur.

Mean Pressures

As described earlier, the wind can be considered to be composed of the addition of a mean component and a varying component. The effect of the variable pressures will be analyzed later using the frequency-domain method described in 6.3.3. Note that the spectral gap in the wind's power spectrum allows the mean to be defined as composed of frequencies of less than about 0.001 Hz. (This also allows the frequency-domain method to include the mean effect if frequencies of less than 0.001 Hz are measured, but requires much longer records than measured in this test program.)

The mean pressures in the chamber of these *vented* walls are expected to be practically equal to the wind-induced mean pressures which act on the wall because, in the tested panels, the leakage through the air barrier is essentially zero. As reported in Chapter 4, the polyethylene and drywall air barrier of all panels was found to be perfectly airtight up to at least 100 Pa. As reported in Chapter 5, the application of a static, spatially uniform pressure will not impose a pressure difference across the brickwork.

The mean pressures and their standard deviation are presented in Table 6.2a for three records for the two panel types installed near the middle of the Beghut (the Zero Cavity and the Datum panels) exposed to wind acting perpendicular to the wall. Table 6.2b and 6.3c present similar results for a panel near the corner of the Beghut (the DPV panel) exposed to wind acting perpendicular to the wall, and a panel near the middle of the Beghut (the Zero-Cavity panel) with a wind direction of 30° from perpendicular. Table 6.3 presents summary and derived statistics of the same pressure records. The average amount of pressure moderation achieved on the basis of a time-domain analysis is presented in the first column of this table. The next two columns present the frequency-domain results for two frequencies, 0.2 Hz (5 seconds) and 1 Hz (1 second). The remaining columns present turbulence intensity results for each of the records.

Consider the results in Table 6.2a. As expected, the average pressure in the centre of the air chamber was only slightly less than the mean pressure on the exterior for most records of panels W4 and W5. Mean pressure differences of -0.8 to 3.2 Pa were recorded in individual records with average exterior pressures of 16 to 21 Pa. For the mean of three records, the differences are 1.2 and 1.5 Pa for the western Datum and Zero-Cavity panels respectively. These mean differences are small in absolute terms, and represent 5 to 10% of the mean applied pressure. Therefore, the Zero-Cavity and Datum panels moderated more than 90% of the mean pressure differences when exposed to perpendicular winds.

Record	Pressures (in Pa)								Wind Direction
	Exterior		Cavity		ΔScreen		Wind @10 m		
	Mean	Std. Dev.	Mean	Std. Dev.	Mean	Std. Dev.	Mean	Std. Dev.	Mean
a) Panels Near the Middle of the Beghut Exposed to Wind Perpendicular to the Wall									
W4-30	17.0	14.0	13.8	12.8	3.2	9.2	39.6	16.5	276.7
W4-31	20.0	16.9	18.8	17.1	1.2	12.6	47.0	22.2	273.3
W4-32	18.3	12.2	19.1	14.6	-0.8	8.7	37.7	19.8	254.7
Mean	**18.4**	**14.4**	**17.2**	**14.9**	**1.2**	**10.1**	**41.4**	**19.5**	**268**
W5-30	15.7	8.8	15.0	8.2	0.8	3.3	38.5	11.8	273.8
W5-31	20.9	14.4	19.5	14.1	1.4	5.9	48.6	21.4	276.4
W5-32	16.5	11.9	14.1	11.5	2.4	3.1	38.5	11.2	275.6
Mean	**17.7**	**11.4**	**16.2**	**11.2**	**1.5**	**4.1**	**41.9**	**14.8**	**275**
b) Panel Near the Corner of the Beghut Exposed to Wind Perpendicular to the Wall									
W6-30	8.5	8.5	7.4	7.3	1.1	7.5	35.3	15.9	280.6
W6-31	9.7	12.4	8.4	9.4	1.3	9.8	43.3	19.5	285.3
W6-32	8.9	9.5	5.7	7.2	3.2	7.5	25.6	10.9	280.8
Mean	**9**	**10.1**	**7.2**	**8**	**1.9**	**8.3**	**34.7**	**15.4**	**282**
c) Panel Near the Middle of the Beghut Exposed to Wind 30° to the Wall									
E5-11	15.3	9.7	10.3	9.0	5.0	5.5	32.0	14.8	52.8
E5-12	20.5	8.7	20.4	9.1	0.1	5.8	32.6	11.5	69.8
E5-13	28.3	13.1	26.2	13.1	2.2	6.9	41.5	17.8	56.1
Mean	**21.4**	**10.5**	**19.0**	**10.4**	**2.4**	**6.1**	**35.4**	**14.7**	**60**

Note: Direction measured in degrees clockwise from North. East winds are at 90° and west winds at 270°. Wind pressure at 10 m has been calculated from the measured wind velocity.

Table 6.2: Statistics of Selected Pressure Records

The records for DPV panel W6 and Zero-Cavity panel E5 are noticeably different. For panel W6, the wind pressure at 10 meters above grade was almost the same as for the other panels but the mean of the exterior pressure was half as large. This is due to the corner location of the panel exacerbated by the 12° off perpendicular wind direction. The mean difference across the screen is, however, approximately the same as for the

other panels. Therefore, while the percentage pressure moderation of mean pressures is lower (approximately 80%, see Table 6.3), the absolute value of the difference is approximately the same. It is likely that a significant mean horizontal and vertical pressure gradient existed across the vent holes. The greater volume of lateral air flow and steeper pressure gradients, as compared to the neighboring panels (i.e. mean spatial pressure gradients), experienced by the DPV panels appear to have negatively impacted on their ability to pressure moderate. It must be borne in mind that these conditions will also affect the frequency-domain analysis results of the DPV panel.

	Pressure Moderation (%)			Turbulence Intensity (in %)		
	Time-Domain	Frequency-Domain				(@ 10 m)
Record	**Mean (64 s)**	**0.2 Hz**	**1 Hz**	**Exterior**	**Cavity**	**Wind**
a) Panels Near the Middle of the Beghut Exposed to Wind Perpendicular to the Wall						
W4-30	81			82	93	42
W4-31	94			85	91	47
W4-32	104			67	76	53
Mean	**93**	**20**	**0**	**78**	**86**	**47**
W5-30	96			56	55	31
W5-31	93			69	72	44
W5-32	86			72	82	29
Mean	**92**	**50**	**45**	**66**	**69**	**35**
b) Panel Near the Corner of the Beghut Exposed to Wind Perpendicular to the Wall						
W6-30	87			100	99	45
W6-31	87			128	112	45
W6-32	64			107	126	43
Mean	**80**	**0**	**0**	**112**	**111**	**44**
c) Panel Near the Middle of the Beghut Exposed to Wind 30° to the Wall						
E5-11	67			63	87	46
E5-12	99			42	45	35
E5-13	93			46	50	43
Mean	**89**	**0**	**0**	**49**	**55**	**42**

Table 6.3: Summary Statistics of Selected Pressure Records

The results of panel W6 indicate that a mean pressure gradient near building corners will reduce the relative degree of pressure moderation. Although the mean pressure drop across the screen is not that large (1.9 Pa), it represents 20% of the mean exterior pressure. Thus the corner panel W6 moderated, on average, 80% of the mean pressures. The lateral pressure gradient and, perhaps, the baffling within the DPV chamber are the likely reasons for the lower degree of pressure moderation relative to the Datum and Zero-Cavity panels. The results of panel E5 indicate that winds striking the Beghut at an angle other than perpendicular will also reduce the pressure moderation of the panels to mean pressures.. The pressure drop across the screen is the largest of all panels in absolute terms (2.4 Pa), although the pressure moderation of the mean pressures was still 89%. Therefore, lateral pressure gradients (because of the corner location for panel W6 and because of the wind direction for panel E5) will negatively affect pressure moderation of the mean pressures.

The turbulent intensity of the cavity and the exterior pressures were much higher than of the wind. This is expected since the pressure at 1.5 m is much lower than at 10 m, whereas the turbulence level should remain the same (see Figure 3.15). However, the standard deviation of the wind was generally in the range of 15 to 20 Pa, whereas the standard deviations of the exterior and chamber pressures was 10 to 15 Pa. The reason for the reduced turbulences is unclear, but may be due to the proximity to the ground.

In Figure 6.6 the time-domain plots of the pressure difference across the screen are plotted for one record of each of the four panels shown in Tables 6.2 and 6.3 (specifically, records W4_30, W5_30 , W6_30, E5_11). The performance of panel W5 is visually better than the others but the difference between W4_30 and W6_30 is not clear. While it is clear that none of the panels are pressure equalized, it is difficult to quantify the extent of pressure moderation in the time domain. It is also clear that while the time-domain average may be almost zero, significant pressure moderation to short pressure changes (5 to 10 seconds) is not occurring. Nevertheless, the effect of wind direction is clearly evident by comparing the plot of the two panels W5 and E5. The influence of the wind conditions on these results are also difficult to ascertain. The plots of all pressures for all records are contained in Appendix D.

To overcome the difficulty of quantifying the pressure moderation performance by use of time-domain statistics alone, the next section presents some frequency-domain analysis results.

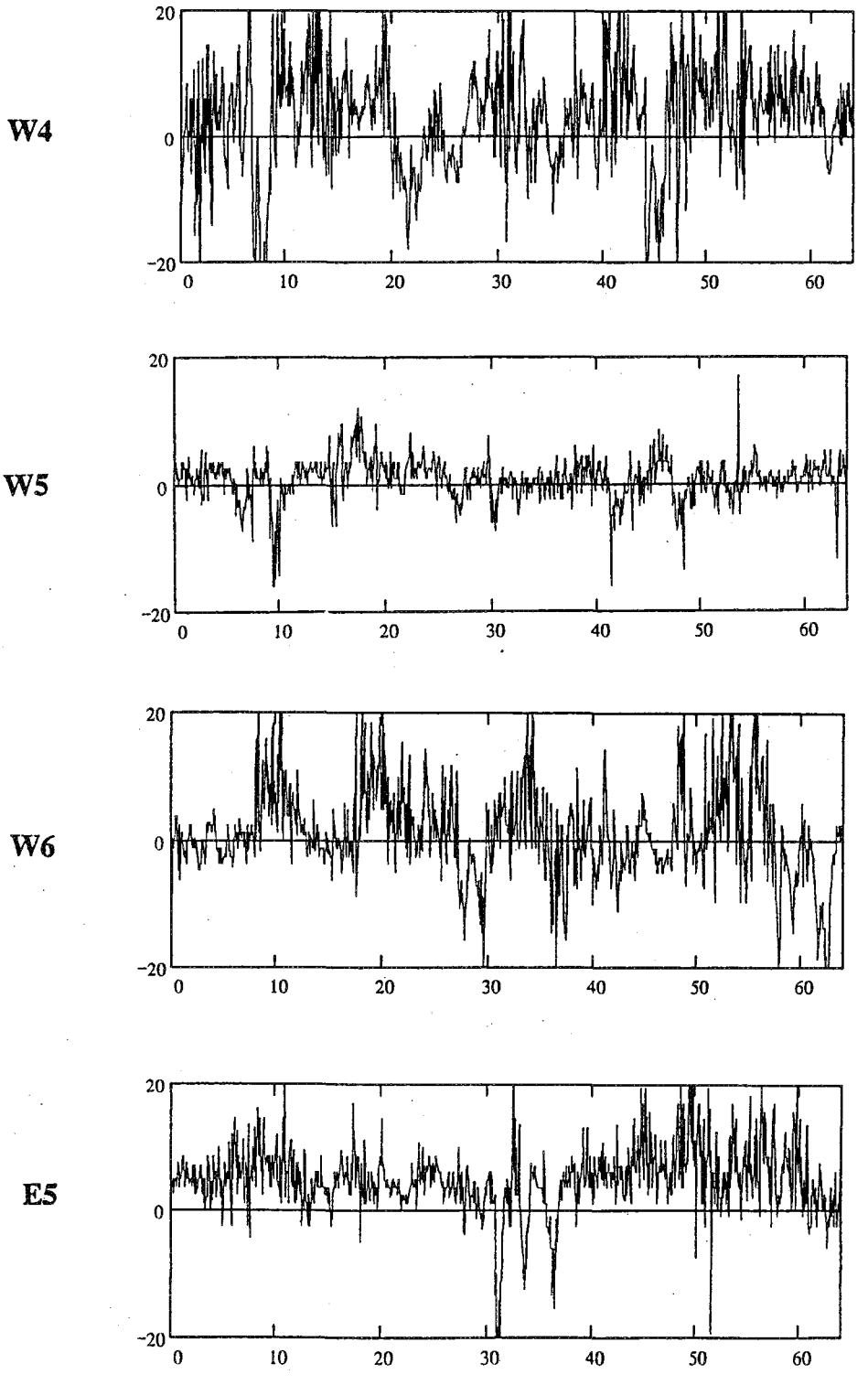

Note: Although the absolute pressure differences are low (±20 Pa), the pressures on the exterior are also low (0-40 Pa). See Appendix D for full plots.

Figure 6.6: Sample 64-Second Plots of Pressure Across Screen (Pa)

Spectra (Frequency Domain)

Comparisons of the important characteristic $k_\Delta(f)$ functions (Figure 6.7) show that pressure equalization was not achieved for any record on any panel at any measured frequency. Only the response to the short-term variations (i.e. variations which take less than about 10 seconds) can be judged because the $k_\Delta(f)$ functions can only be calculated down to a frequency of approximately 0.1 Hz with a 64 second record. As stated earlier, frequency-domain analysis of the response of the wall to the mean pressure would require much longer records, approximately 30 to 60 minutes. It follows that $k_\Delta(f)$ only represents the moderation of the pressure difference across the screen caused by variations in the wind pressure with a period of less than 10 seconds; to obtain the actual pressure drop across the screen the contribution (if any) from the mean pressure would also need to be considered.

Inspection of the power spectrum of the pressure difference is enlightening. Consider the raw and smoothed and normalised pressure spectra for the Zero-Cavity panel W5 presented in Figure 6.8. The peak of this spectrum has almost one-tenth the energy of the exterior at frequencies lower than 0.1 Hz. At higher frequencies, this spectrum has more energy than the applied pressure. This indicates that the majority of the pressure drop across the screen due to pressure variations will be measured in the 0.1 Hz and higher frequency range and any other variations will be due to long term differences i.e. air leakage. This is predicted by the theory in Section 6.2.2 and has been measured in practice[2].

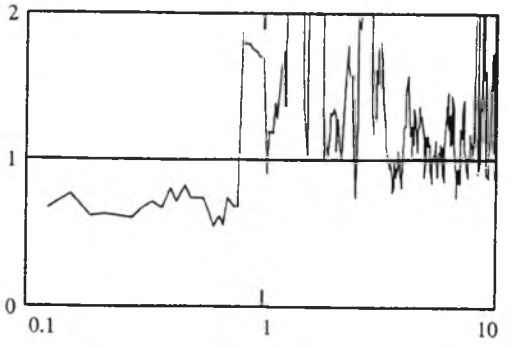

Datum Panel W4

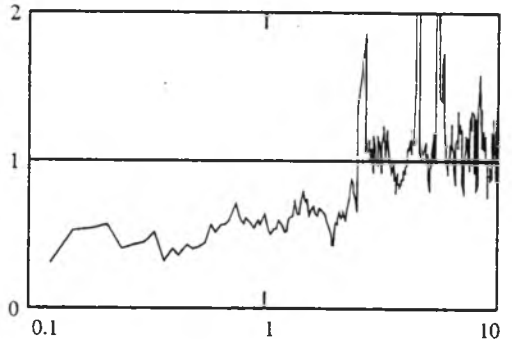

Zero-Cavity Panel W5

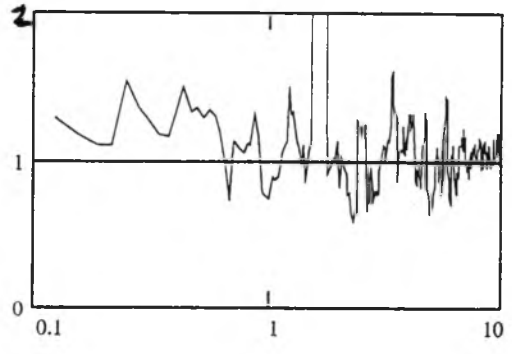

DPV Panel W6

Figure 6.7: $k_{\Delta scr}(f)$ Functions For West-Facing Panels

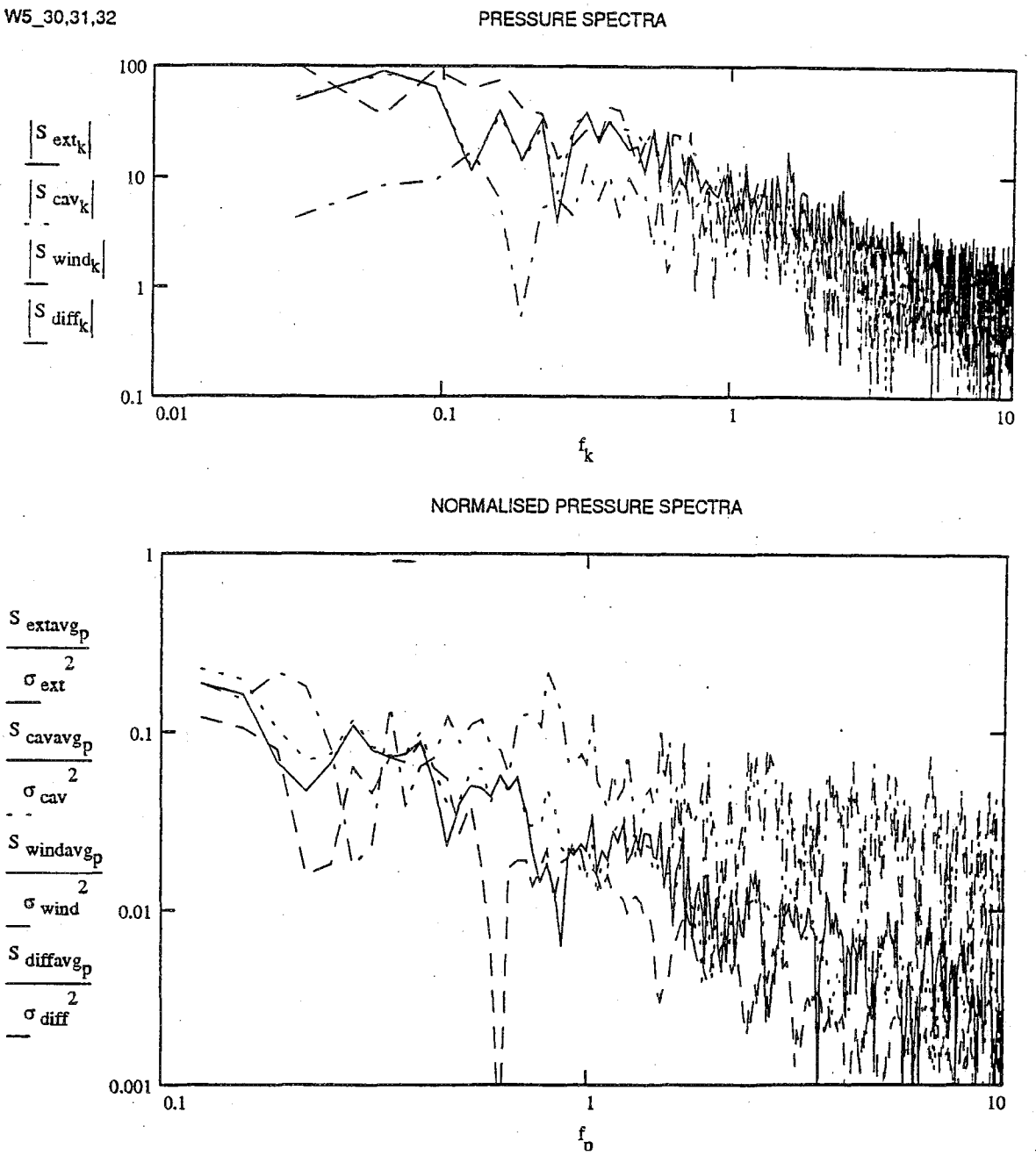

Figure 6.8: Zero-Cavity Pressure Spectra

Panel Results

The Datum panels have greater air leakage and less support for the air barrier. Both of these factors will theoretically reduce the pressure equalization performance relative to the Zero-Cavity panels. However, the cavity in the Zero-Cavity panels has a larger air volume and the fibreglass cavity fill may baffle air flow; both these characteristics will impair good pressure equalization under fast-changing pressure variations. As discussed earlier, the DPV panel has a small, stiff, and relatively airtight chamber, but the wind conditions near the edge of the Beghut are not conducive to good pressure equalization. The vertical grooves in the DPV panel chamber may cause baffling of air flow and thereby reduce the speed of the pressure response of the chamber.

Each set of panel results will be discussed separately and then compared below.

Datum Panel W4

The Datum panel begins to have k_{cav} values of greater than one at frequencies of about 0.5 Hz and drops below one at about 4 Hz. A cavity attenuation value of more than one indicates that pressure from the upper vent is increasing the pressure in the centre of the cavity to values greater than those acting on the exterior at the panel's centre. This may have occurred more readily in the Datum panel because there is less air flow restriction than the Zero-Cavity panel (whose cavity is filled with fibreglass). The low frequency gusts (smaller than 0.5 Hz) do not amplify the measured cavity pressure at the middle since gusts of this frequency will be spatially large enough to envelop the entire panel (or at least the top vents and the centrally located pressure sensor). The smaller (higher frequency) gusts may act over only the upper vent while the lower vent and central pressure tap are experiencing quite low pressures.

Although the $k_{cav}(f)$ indicates a value of one for low frequencies, the actual pressure difference across the screen is greater than for the Zero-Cavity panel. In the frequency range 0.1 Hz to 0.8 Hz, $k_{\Delta scr}$ has a value of about 0.8; indicating that 80% of the exterior pressure changes manifest themselves as a force across the screen. Beyond 0.8 Hz the $k_{\Delta scr}(f)$ function has a value of one or slightly greater than one. The explanation for $k_{\Delta scr}$ values of more than one is that the upper vent is experiencing higher pressures and transmitting these pressures to the centre of the cavity. As frequencies increase above 1 Hz, the value of $k_{\Delta scr}(f)$ approaches one; this indicates that the full magnitude of the pressure changes on the exterior are acting across the screen.

Zero-Cavity Panel W5

The values of $k_{\Delta scr}$ (which directly describes the pressure drop across the screen) remain at approximately 0.5 until about 0.5 Hz and then slowly increase until about 3 Hz when they settle on a value of one. This shows that even for low frequency (long duration) gusts the cavity is poorly pressure equalized. The poor high frequency performance could be caused by a time lag ($\emptyset>0$) due to the mass of the air (inertia), friction, baffling, or a flexible air barrier, or, most likely, spatial pressure variations.

The pressure equalization is poor or non-existent for frequencies greater than 2 Hz. At high frequencies the gust sizes will be spatially small (and thus they may act on the centre of the panel and not on the vents). Since the high frequency gusts are so short in duration, the inertia of the air also likely acts to damp the cavity response. The performance at these high frequencies is not as important since the pressure spectra indicate that there is far more power in the lower frequencies than at frequencies above 2 Hz (note the log-log scale).

The unsmoothed $k_{\Delta scr}(f)$ function (Appendix D) shows that at lower frequencies (which were smoothed over in Figure 6.7) the value approaches zero. This gives further evidence that the panel is almost perfectly pressure-equalized under the mean or very long-term pressure variations (i.e. greater than 60 seconds). This is predicted by theory because of the large vent area, small leakage area, and relatively stiff air barrier.

DPV Panels

The plot of the $k_{\Delta scr}(f)$ function for the DPV panel shows no pressure moderation at any measured frequency. This poor performance is even visible in the time-domain plots of pressure (Appendix D). The low pressures and very variable pressures, lateral air flow, and large pressure gradients are thought to explain these results, although the baffling effect of the special EXPS sheathing may also have contributed. The very different pressures experienced by the DPV panels because of their location is perhaps the most important observation.

Panel Comparison

Insofar as pressure equalization is concerned, the Zero-Cavity panel has measurably better response to the pressure variations in the frequency range investigated. Not only are less of the pressure changes taken by the screen at the lower frequencies (50% vs. 80% for the Datum), the frequency at which pressure equalization ceases (i.e. $k_{\Delta scr}(f)$

=1) is also higher (3 Hz versus 0.8 Hz). One possible reason for these results is that the flexible Tyvek™ is better supported and thus much stiffer in the Zero-Cavity panel. The air leakage tests in Chapter 4 indicated that the cavity delineation in panel W5 is relatively airtight (it is more than ten times as air tight as the Datum panel). However, since the mean value of the exterior pressure difference is so small (18 Pa), the interaction between the stud space air volume and the cavity air volume is unlikely to be a large contributor. Another factor might be that the baffling provided by the fibreglass cavity fill minimizes through flow between the upper and lower vent holes. The DPV panels experienced such different wind conditions that it is difficult to make comparisons.

6.5 Comparisons

The only source of comparison are Inculet's frequency-domain results for the NRC/IRC tests on the Lethbridge Courthouse and Place Air Canada. The panels in Place Air Canada were tightly compartmentalized, and were of similar size as the BEG test panels but had considerably greater venting-to-leakage ratios, vent area, a stiffer air barrier, and a smaller chamber volume. All of these factors should increase the pressure moderation of the wall system. The Lethbridge panels were much larger (in the lateral direction) were very leaky, had a very large cavity volume, poor venting-to-leakage ratio, and poor compartmentalization.

It must be borne in mind that the exposure conditions for Place Air Canada, Lethbridge Court House, and the present measurements are quite different. The different levels of turbulence inherent in different exposures are inherently accounted for in the frequency-domain method. However, the spatial variations have not been directly measured, in these or the Place Air Canada tests, although it has become clear that they can have a large effect on the pressure moderation. The mean spatial pressure variations over the height of the panels were very likely much larger for the BEG panels since the mean pressure changes rapidly from 0.3 to 2.7m whereas the change in mean pressure over the height of the Place Air Canada panels (from 80 to 83 m) is quite small. The mean horizontal pressure gradient is also likely much greater on the BEG panels since the lateral dimension of the Beghut is much less than the Place Air Canada office building. Hence, the negative effect of both vertical and horizontal spatial variations on pressure moderation will be larger for the Beghut exposure than for the Place Air Canada panels which were high up on the middle of a wide building.

Just as in these tests, it was found that strong, perpendicular wind conditions did not often occur in both the Place Air Canada and Lethbridge Court House measurements. In fact, the Place Air Canada results used for comparison had an average exterior pressure of only 17.2 Pa. The Lethbridge Courthouse had fewer records but higher pressures (average of 49.7 Pa). The frequency-domain results of these buildings will be compared to the BEG results.

The Place Air Canada measurements showed excellent equalization up to approximately 0.1 Hz, after which its pressure moderation dropped to almost zero by 1 Hz and remained very small up to the highest measured frequency. The panels measured in this project appeared to moderate the pressure differences poorly from 0.1 Hz to 1 Hz; their pressure moderation in this range was between 20 and 50%. The Zero-Cavity moderated approximately 25% (i.e. 25% pressure equalized) of the pressure changes at 1 Hz and abruptly stopped moderating at frequencies higher than 2 Hz. Interestingly this is slightly better performance than the Place Air Canada panels for the 0.7 to 2 Hz range. However, at low frequencies (from 0.1 to .7 Hz) the Place Air Canada panels performed better than the Zero-Cavity and the Datum panel performed more poorly at all frequencies. At frequencies lower than 0.05 Hz the Place Air Canada panels behaved as fully pressure-equalized; because this frequency range was not measured in these tests, no true comparison can be made.

6.6 Conclusions

- The wind pressures experienced by exposed low-rise construction are generally quite low (less than 20 Pa), and higher pressures (greater than 30 Pa) occur rarely. For inland sites in south-western Ontario, the direction of strong winds is quite variable and unlikely to be perpendicular to a wall for significant proportions of the time.

- Over the time periods considered, none of the panels were fully pressure equalized for any record at any frequency. The Datum and Zero-Cavity panels moderated from 20 to 50% of the variable pressure differences across the screen i.e. they were 20 to 50% 'pressure equalized'. The mean values (of one minute records) indicated that the panels moderated more than 90% of the difference across the screen.

- The variation in pressure with height (vertical gradient) can have a relatively large effect on pressures and pressure moderation in low-rise construction. Spatial variations near building corners and from non-perpendicular wind directions will result in significantly different pressure conditions and generally poorer pressure equalization response.

- Spatial pressure variations are at least as significant to pressure equalization performance as temporal pressure variations. Laboratory tests and computer models which do not account for spatio-temporal variations are unlikely to provide results relevant to field performance.

7. Mockup Testing

7.1 Purpose

As a supplement to the in-situ testing of the six wall panels, laboratory tests were conducted on two full-scale mockups of the building assemblies. The mockup tests were intended to provide an understanding of the differences in drainage capabilities and properties of the various materials and, to some extent, the three wall assemblies. These mockup panels were also useful for demonstration purposes.

7.2 Experimental Program

A controlled amount of water was added to the top of the insulation layer in mockup panels of the Zero-Cavity and DPV panels. The volume of water draining through each layer of the wall was measured, and the behaviour of the drainage was observed.

7.2.1 Panels

The panels were constructed as described in Section 2.8. The panels were exposed at the top to allow for the application of water. Galvanized metal troughs collected any water which exited the bottom of a layer. The bottom of these troughs did not come into contact with the bottom of the insulation; therefore, any liquid water leaving the bottom insulation needed to overcome surface tension forces.

7.2.2 Apparatus

A constant-flow, constant-head device (shown in Figure 7.1) was constructed to evenly distribute a known volume of water along the top of the insulation layer. A centrifugal pump served by a reservoir of approximately 20 litres was used to supply water at approximately 2 litres per minute to the standpipe. Any water in excess of the 150 mm head was drained back to the reservoir. This apparatus allowed for a constant volume of water since the water flowed through an orifice with a constant geometry under a constant head. A 38 mm diameter horizontal pipe distributed the water across the width of the panel and 24 holes (i.e., a spacing of approximately 50 mm) of 1.6 mm diameter allowed the water to flow out. Plastic sheeting was used to ensure the water was distributed only at the top of the insulation and not on the face. The water was distributed along the entire width and depth of the 38 mm thick insulating sheathing.

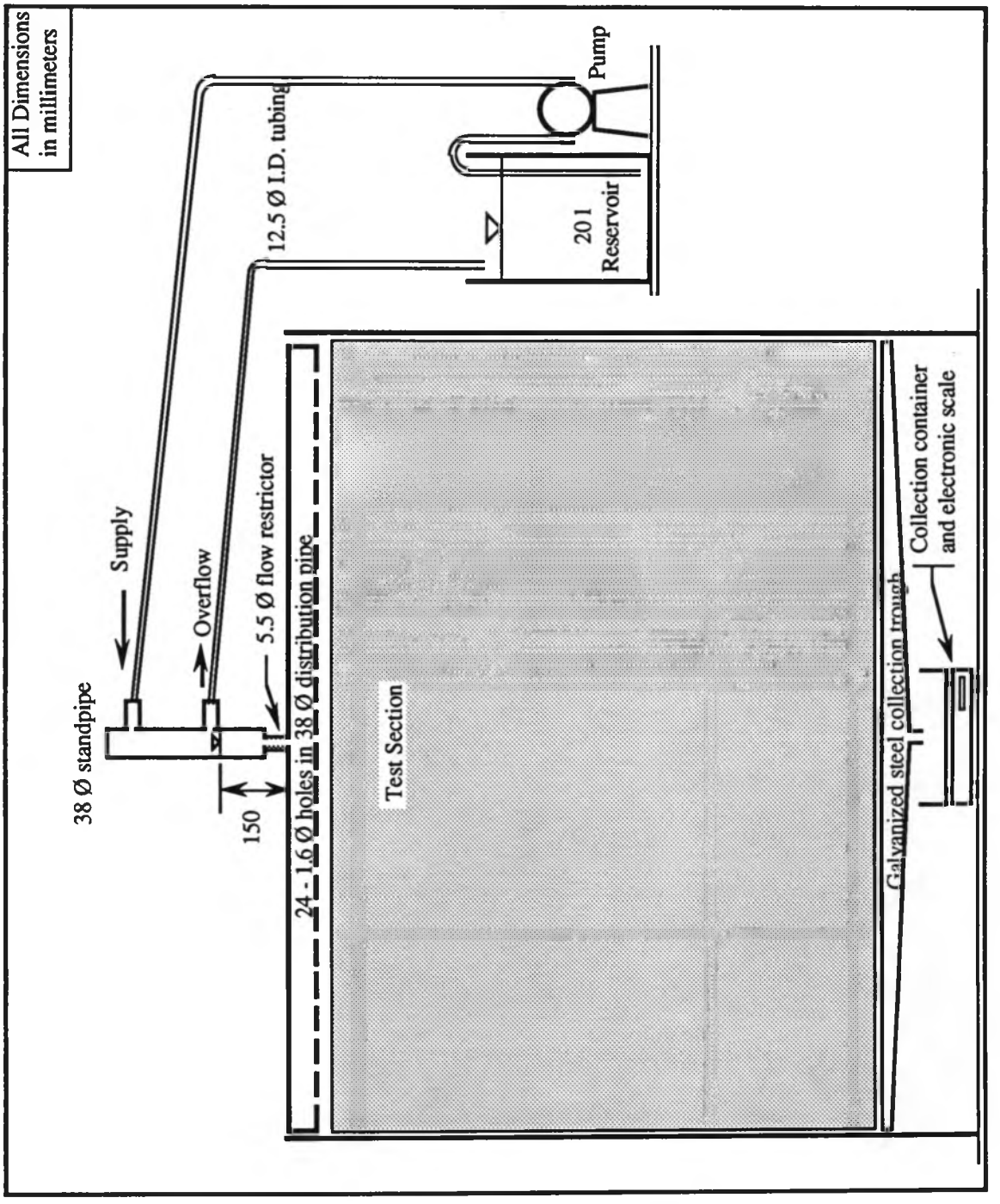

Figure 7.1: Mockup Test Set-up

A Sartorius 12000S digital scale, accurate to ±0.01 g and with a response time of less than 1 second (for an instantaneously applied 1 g load) was used to measure the cumulative weight of water flowing into the collection beaker. Graduated cylinders were used to measure any flow (generally very small) which might occur in the other layers.

7.2.2 Procedure

Initial exploratory tests consisted of pouring various quantities of water into the insulation layer and recording the results. This prompted the development of the special apparatus described above and a test procedure. The procedure consisted of applying 1.5 litres of water per minute into the top of the insulation for approximately 3 to 5 minutes. The application rate varied slightly at the beginning and the end of the test while the standpipe and distribution pipe filled or drained to a constant head condition .

The apparatus was calibrated by measuring the flow through the entire system (including a drainage trough) with no insulation. A typical flow calibration curve which describes the application rate is plotted in Figure 7.2.

The volume of water exiting at the bottom of each panel was measured at regular time intervals by reading the cumulative mass of water in the collection beaker using an electronic scale. A minimum of 3 days was necessary between each Zero-Cavity test to allow for complete draining and drying.

7.3 Results

The results have been plotted in a similar manner to the water penetration tests (Chapter 5). The cumulative volume collected and the drainage rate have been plotted with respect to time.

The DPV mockup drained at the same rate as the water was applied within a few seconds of the start of the test (Figure 7.3). After the water was stopped, the panel drained within a minute except for water droplets which adhered (by surface tension) to the rough-cut surface of the grooves.

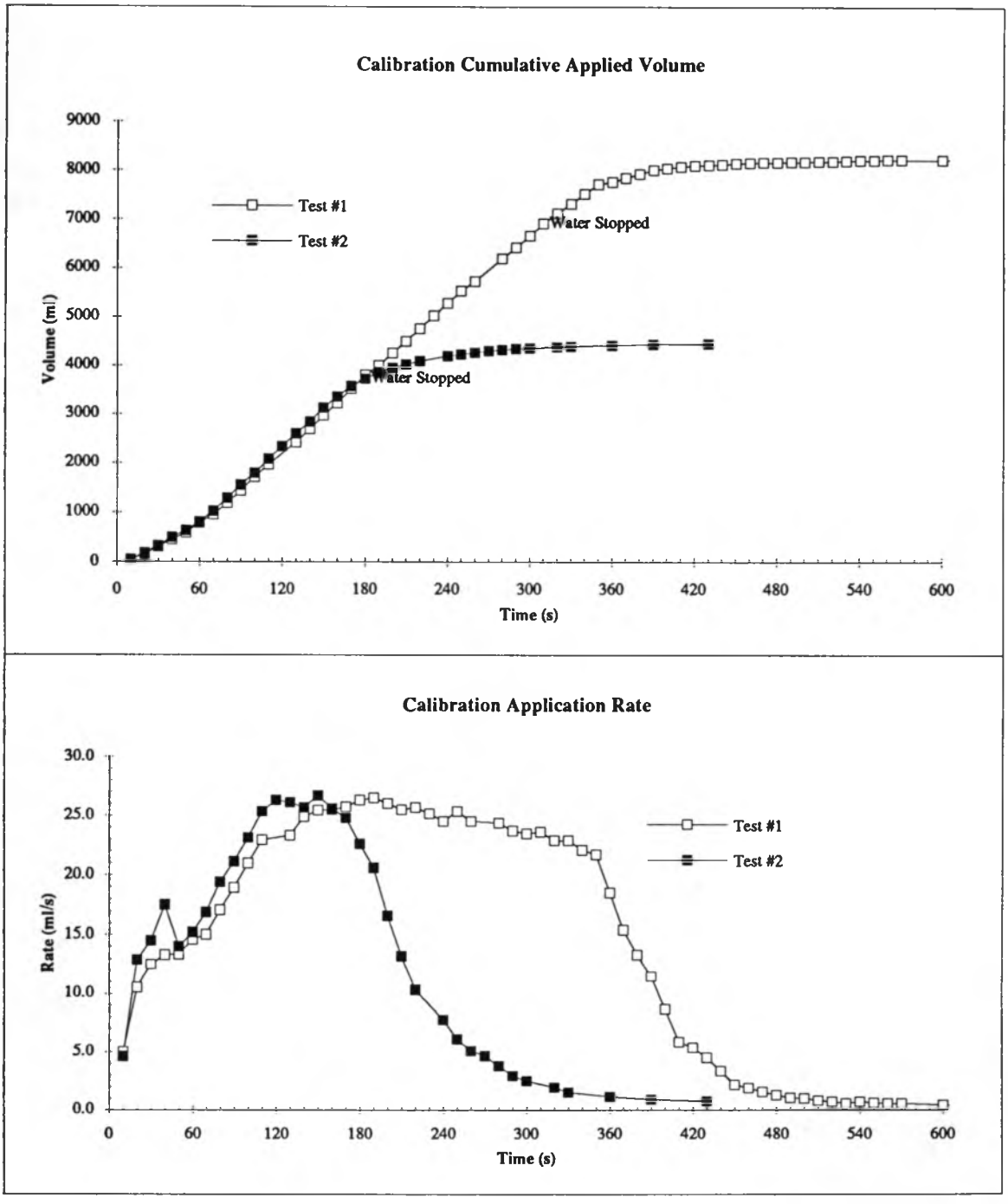

Figure 7.2: Apparatus Calibration Curves

The Zero-Cavity mockup results are shown in Figure 7.4. It can be seen from the plots that there is an initial lag of approximately 2 minutes during which time very little water is collected. The rate of collection then rapidly increases until it equals the rate of application about 4 minutes into the test. After the application of water stops, the rate begins to slow 40 to 60 seconds later. The drainage rate of the remaining water then follows an exponential decay curve (see Figure 7.4).

Approximately 90% of the applied water had drained 12 to 15 minutes after the water application was stopped. After 60 - 90 minutes no water at all was collected. However, a dark orange-coloured, region defined by an irregular line below which the glass fiber sheathing was saturated, remained visible for at least two days.

Figure 7.5 presents a series of photos taken of a Zero-Cavity mockup test conducted in the presence of the same industry representatives who had been present for the panel opening (Chapter 8). The test began shortly after noon and the first photo (dated September 2, 1993) was taken approximately 5 minutes after water application began. The second photo was taken at 2:28 p.m. the same day. The retained moisture in the base of the glass fibre sheathing is clearly evident. The glass fibre sheathing directly above the dark orange areas was dry to the touch. The third photo was taken at 8:37 a.m. the next day. Almost the exact same pattern of wetting is visible, and no water was collected during the 18 hours between photos. The glass fibre sheathing dried over the next two days and no more water was collected.

7.4 Discussion

Because the DPV panels drained the applied water very quickly and retained only a nominal volume, the DPV approach acts as a very effective drainage system. If the fabrication process could be improved and the rough-cut surfaces of the prototype made smoother, even better drainage characteristics can be expected. The extruded polystyrene itself is practically water-impermeable and thus forms a water-resistant inner layer to prevent any small amount of water which does cross the cavity from penetrating further into the wall. The use of ship lap joints is recommended.

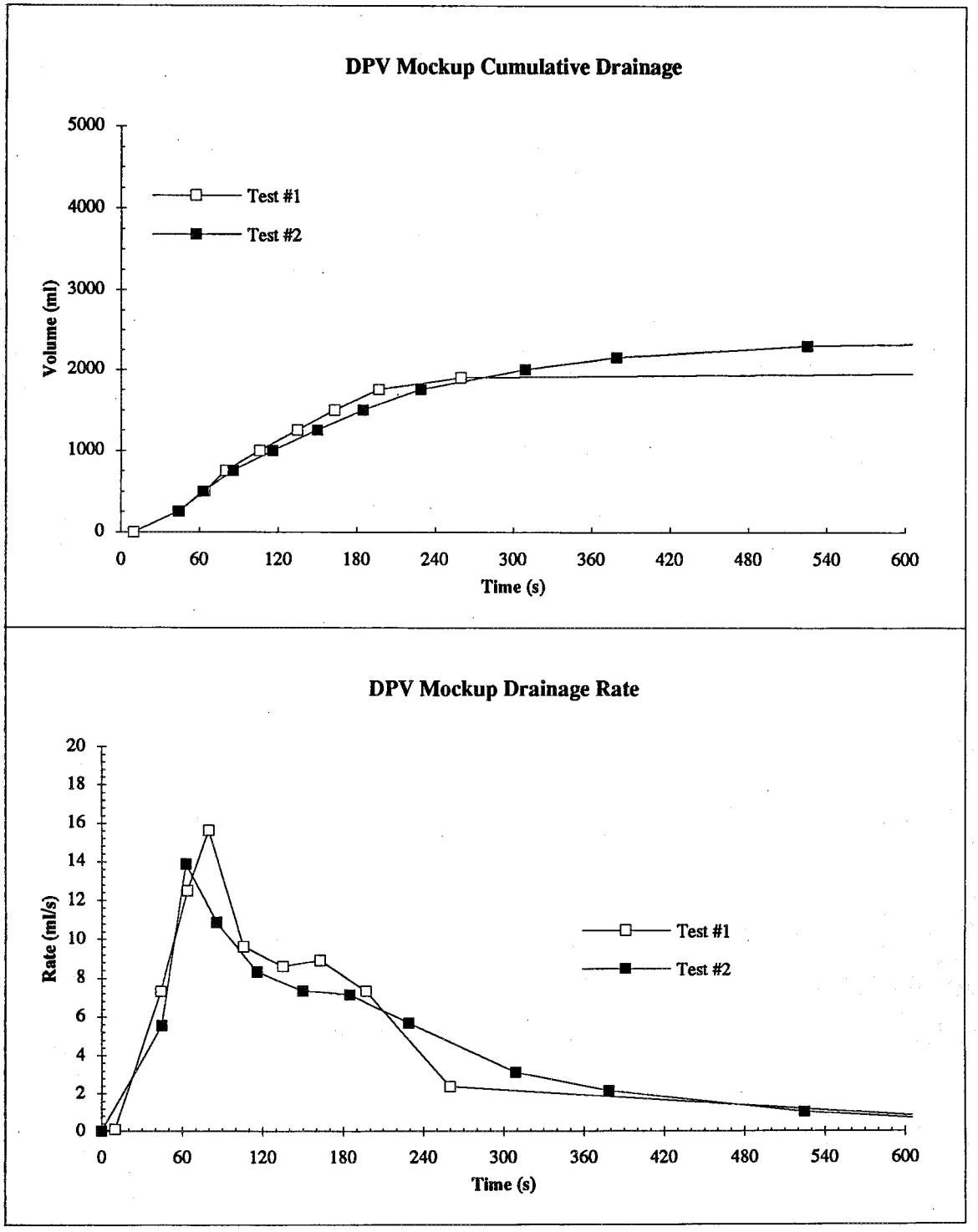

Figure 7.3: DPV Mockup Test Results

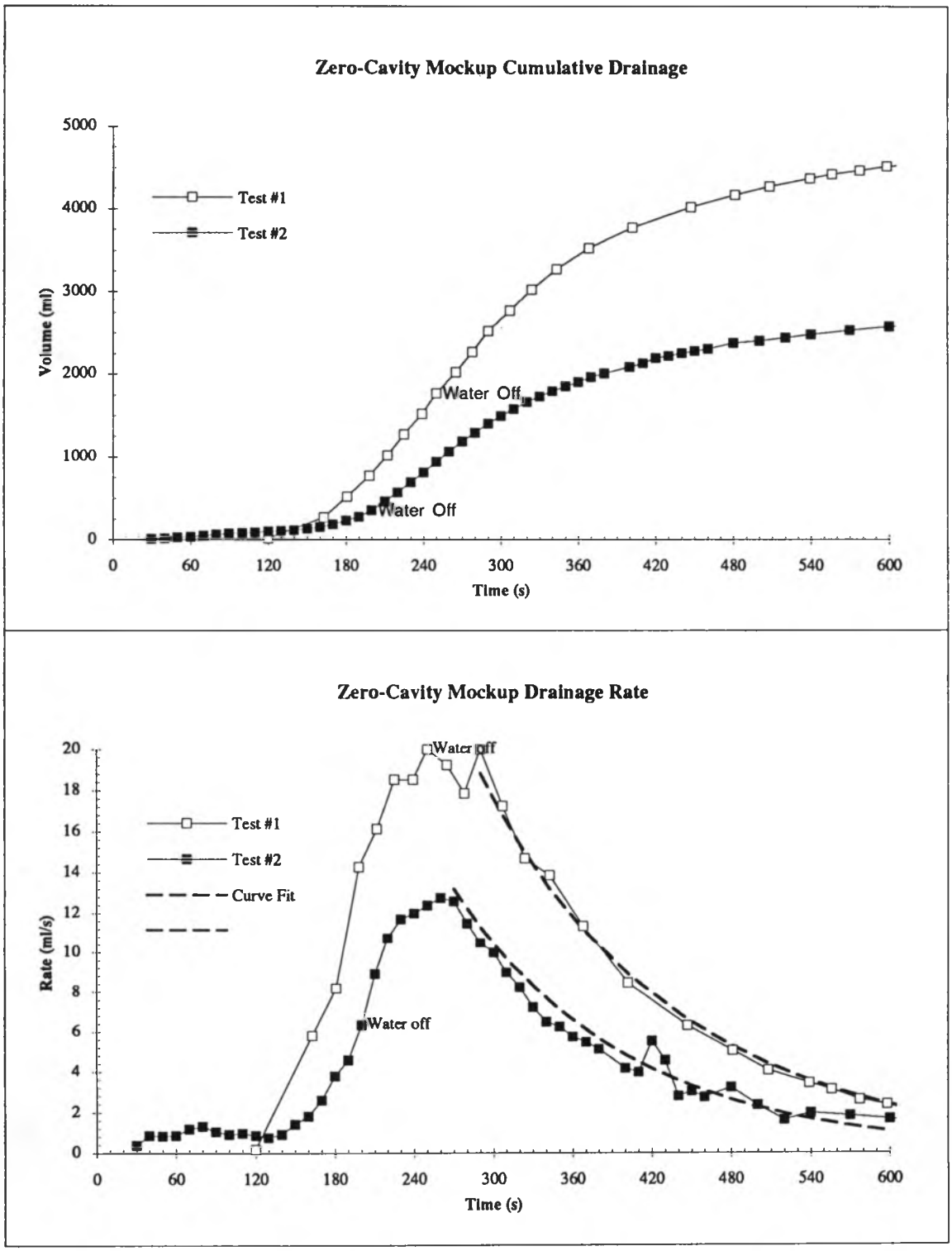

Figure 7.4: Zero-Cavity Mockup Test Results

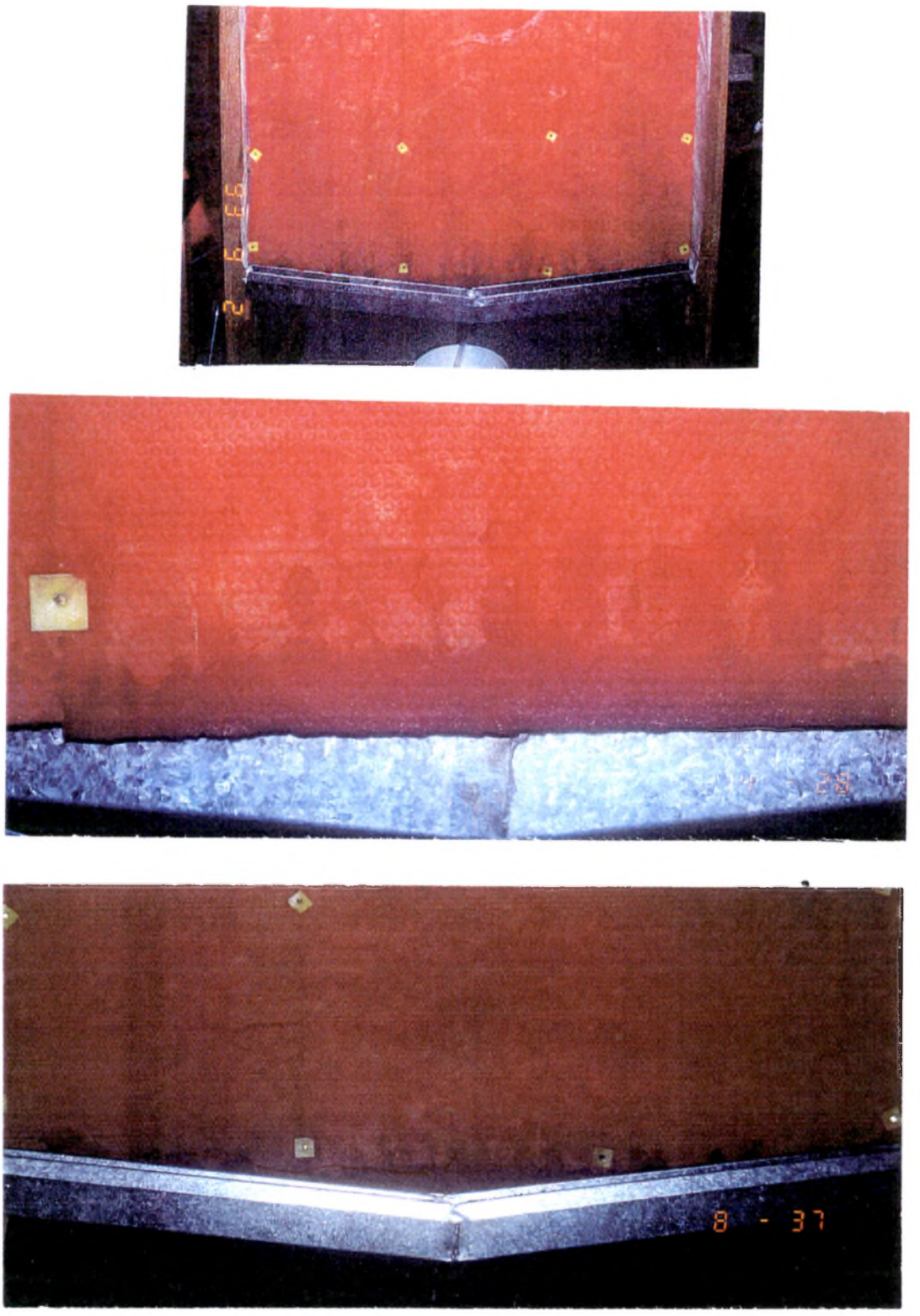

Figure 7.5: Zero-Cavity Mockup Test Photos

The glass fibre sheathing in the Zero-Cavity mockup drained the bulk of the applied water very quickly. While the majority of the insulation quickly dried completely, the water retained in the bottom 25 - 75 mm can cause problems in service. This retention is due to the capillary attraction of the water to the glass fibres. For small pressure heads, gravity forces will overcome these capillary forces but, depending on the density, diameter, and orientation of the fibers, capillary wicking of up to 60 mm has been observed when the base of various fibrous insulations was set in water[1].

The retained water in the base of the fibreglass board could increase the possibility of water penetrating the base flashing and thus the possibility of damage to the wood frame or other inner wythe components. By increasing the moisture level in the bottom bricks, the likelihood of freeze-thaw damage would also be greater. From the measurements reported in Chapter 3, it appears that the retained moisture was evaporated and then transported by diffusion across the vapour-permeable Tyvek™ housewrap,. resulting in elevated moisture levels in the wood framing.

To prevent this moisture retention (which can occur in rock wool as well as in fibreglass), a hydrophobic treatment should be applied to the material. Such a treatment reduces the capillarity of fibrous insulations to such an extent that very little, if any, water is retained. By employing insulation boards with the most of the fibres oriented vertically, the drainage characteristics could be improved even more; this would not, however, reduce moisture retention by capillarity.

Fibrous insulations have been successfully used as draining cavity fills for many years in Europe and Scandinavia and have become standard in the severe climate of Norway[2]. German building authorities have tested and approved several products for high driving rain exposures[3], but all of the products used have undergone a hydrophobic treatment[2,4,5]. Proper material choice would probably result in similar performance in Canada. However, the type and location of different materials used for the inner wythe and different brick quality should always be cause for concern.

---

[1]Timusk, J. and Tenende, L.M., "Mechanism of Drainage and Capillary Rise in Glass Fiber Insulation", Journal of Thermal Insulation, Vol. 11, April, 1988.
[2]Waldum, A.M., "The Performance of Masonry Walls in Wet and Cold Norwegian Climate", Sixth Canadian Masonry Symposium, Saskatoon, Canada, June, 1992.
[3]Institut für Bautechnik Berlin, Zulassung Nr. Z-23.2.2-57 (rockwool) and Nr. Z-23.2.2-39 (fiberglass), and Institut für Ziegelforschung, Essen, Germany.
[4]Deutsche Rockwool Mineralwoll GmbH, Product Bulletin 2.1.2 "Kerndämmung in der Außenwand", Gladbeck, Germany, 1987.
[5]Grünzweig + Hartmann und Glasfaser AG, Technical Information Sheet,"ISOVER Kerndämmplatten KD", Ludwigshafen, Germany, 1988.

7.5 Conclusions

- The DPV mockup panel drained quickly with almost no moisture retention.

- The Zero-Cavity panel drained quickly, but moisture was retained in the bottom 25 - 75 mm of the fiberglass fill because of capillarity. This retention of moisture within the wall could result in problems. It was certainly an important contributor to the problems experienced by the Zero-Cavity panels, as discussed in Chapter 3.

- Orienting the fibres vertically and applying a hydrophobic coating to fibrous cavity fills would improve the drainage and reduce the water-retention characteristics respectively.

8 Panel Inspection

8.1 Purpose

Two years after installation, the panels were opened from the inside to enable the condition of the entire assembly to be physically inspected. This provided the opportunity to confirm construction details, sensor locations and sensor readings. Since most of the sensors were located in the centre of the panel, any differences in performance during monitoring, especially laterally, could only be inferred from physical inspection of each panel. This report presents all of the data monitored up to Dec. 31, 1992. Air leakage and water penetration tests were conducted from July to September 1992. The panels were opened in September 1993 and reflect all of these experiences.

8.2 Procedure

The drywall on the east-facing panels was removed on August 30, 1993, and a preliminary inspection of the wood framing was conducted. On September 2, the remaining panels were opened and a full inspection conducted in the presence of representatives of CMHC (Jacques Rousseau), Dow Canada (Cecile Mutton and David Greely), and Fiberglass Canada (Keith Wilson). Inspection involved removal of the drywall, 6 mille poly, and batt insulation and cutting a hole approximately 300 mm wide and 400 mm high in the exterior sheathing to expose the base of the panel and the inner face of the brickwork.

8.3 Observations

In general, it was established that all panels were properly constructed, and no obvious errors in sensor placement were discovered. No significant differences in visible effects were found laterally across panels, and it could be confirmed that edge observations were similar to centre-line observations.

8.3.1 Datum Panels

Both Datum panels appeared to be dry and showed no rot, sap or water staining (Figure 8.1a). The east panel showed some very slight evidence of prior mould growth on the north-most stud at mid-height (Figure 8.1b); this wood was dry when opened and the

mold indicated a limited period of some sustained moisture. All wood was visibly dry when the panels was opened. The batt insulation was dry and unstained, as was the sheathing and the Tyvek™. The west panel was in excellent condition with only slight sap staining.

Within the cavities the Datum panel, many small particles (3 to 6 mm diameter) and several large chunks (approximately 50 x 20 x 15 mm) of mortar were found on the flashing. A layer of mortar 5 to 25 mm deep covered large portions of the cavity base (Figure 8.1c); this did not fully obstruct the weep holes but would inhibit the lateral flow of water to them. In general, the back of the brickwork was clean, the mortar was flush with the brick, and no mortar bridging the cavity could be seen. However, at some locations the mortar protruded outwards by as much as 10 mm. At other locations some of the head and bed joints were not completely filled. This indicates that even under ideal conditions, it was difficult to ensure a clean, clear cavity without obstructions.

8.3.2 Zero-Cavity Panels

These two panels were confirmed to have been constructed as described in Chapter 2 (the flashing details were scrutinized especially carefully), and all sensors appeared to be properly located and functioning. The bottom plates and adjacent batt insulation in both Zero-Cavity panels were visibly saturated and stained (Figure 8.2a, b). Free water was evident on the sole plates, and the bottom 200 mm to 400 mm of the studs were completely covered in microbiological growth (Figure 8.2c). The bottom 500 to 1000 mm of the east panel's batt insulation was wet and showed considerable staining on both surfaces. The west panel had slightly less free water on the sole plate, but the batt insulation was visibly wet even at the top of the stud space. Water droplets were visible on the outer face of the polyethylene in the upper sections of the west panel.

In both panels (E5 and W5), the sheathing was visibly saturated over the bottom 40 to 60 mm, and the inside face was obviously wet up to the height of the flashing (Figure 8.4a). The insulated sheathing was dry to the touch above the level of the flashing. Obviously, these two panels had not performed satisfactorily with respect to moisture control.

The backside of the brickwork was clean and the mortar was generally flush with the backside of the brick. All mortar joints were completely filled and the base of the cavity was found to be completely clean when the insulated sheathing was removed (Figure 8.3a). No staining, mould, or mortar adhesion was found on the front face of the glass fibre sheathing. It was confirmed that the zero-cavity approach was a particular effective means of avoiding mortar-related blockage of cavity drainage.

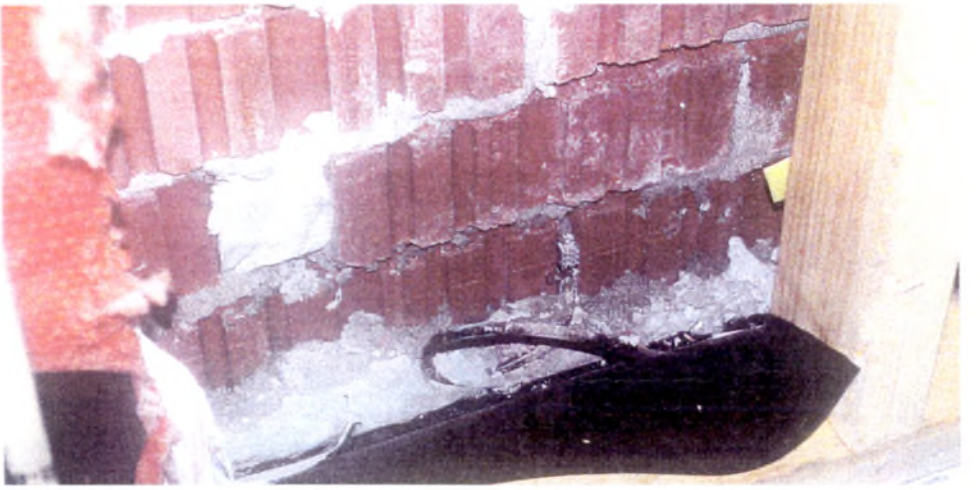

Figure 8.1: Datum Panel

Figure 8.2: Zero-Cavity Panel

Figure 8.3: Zero-Cavity and DPV Panels

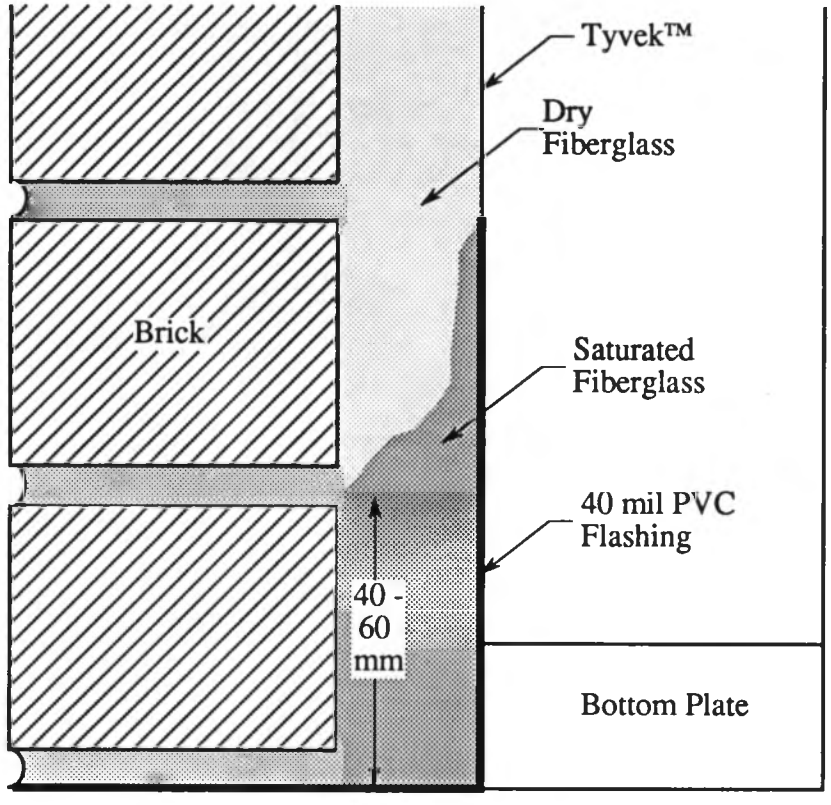

a) Typical Vertical Section of Zero-Cavity Panel Base

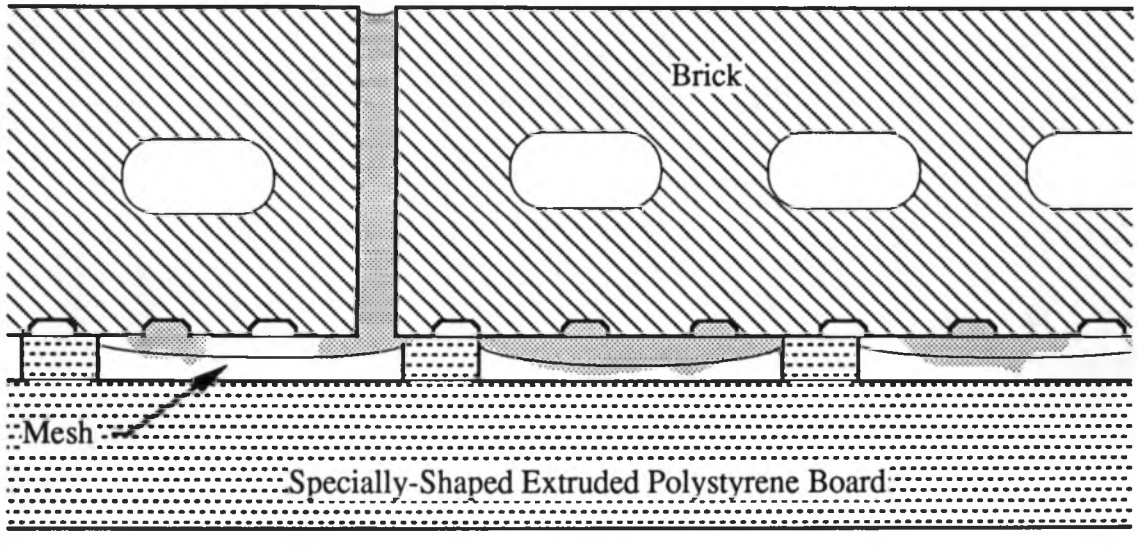

b) Typical Horizontal Section of DPV Panel Cavity

Figure 8.4: Sketch of Zero-Cavity and DPV Panel Conditions

8.3.3 DPV Panels

All layers of materials in both DPV panels, but particularly the batts and studs, were in pristine condition. No mould or sap staining was evident (Figure 8.3b, c). The building paper was still flexible and was not stuck together at any of the overlaps. The extruded polystyrene sheathing and the plastic mesh showed no visible signs of any deterioration.

The backside of the brick was clean and all joints were filled completely. The grooves which formed the cavity in this system were entirely clean. As expected, mortar had adhered to the mesh in many places. Mortar penetration of the mesh was generally limited to 1 or 2 mm but the flexibility of the mesh meant that protrusions, not dams, of mortar, 10 mm from the backside of the brickwork were common at the bed joints (Figure 8.4b). Although the grooves in EXPS were kept clean by the mesh, some mortar had fallen to the base in front of the mesh. These droppings and the sections of protruding EXPS may compromise the lateral drainage capability at the bottom of the wall.

8.4 Discussion

As suggested by the results presented in Chapter 3, the Datum and DPV panels performed well during the more than two years of exposure to the climate of South-western Ontario.

The cause of the slight mould growth on the studs of one Datum panel (E4) is not known. However, this does not indicate a problem. Although the wood was dry when the panel was opened, the presence of mould does suggest that wetting had occurred within the stud space. Temperatures of greater than 15 °C and moisture contents of greater than 20% are considered the minimum requirements for mould growth. The wood moisture measurements of the Datum panels during the monitoring period (Chapter 3) showed that only the upper stud in the east panel exceeded 20% for approximately two weeks at the end of September. This was the only location where evidence of mould growth was found.

Even though great care was taken by the masons, the base of the cavity in the Datum panels was still somewhat obstructed by mortar droppings and not all mortar joints were completely filled. This finding shows that truly clear cavities are exceptionally difficult to achieve, even if there is full-time supervision, skilled workers, and good weather

conditions. Because of the high quality flashing material used, the water which penetrated the screen during the water penetration tests and during rain could be drained or stored in the mortar in the cavity base without causing problems. The brickwork in the Zero-Cavity panels was the cleanest of the three pairs: it had fewer and smaller projections and the base of the cavity was perfectly clear, unlike the Datum and DPV panels. This finding provides clear evidence that the filled cavity concept of ensuring a clear cavity is sound. The back of the brickwork in the DPV panels was relatively clean and the grooves were kept clear. Nevertheless, the protrusions of mortar indicate that grooves of at least 12 mm in depth are necessary with the mesh used. The few mortar droppings in the base of the cavity could inhibit lateral drainage, but, as in the Datum, good flashing would eliminate this as a potential problem. A review of the design of the base detail might provide greater assurance of lateral drainage.

The mortar droppings in the Datum panel explain, to some extent, why the weephole drainage collection system rarely produced any water during the course of the two-year exposure. Since most rainfalls would result in only a small amount of water penetrating the brickwork, this water could be either be stored in the mortar or prevented from draining and be evaporated in the subsequent days. The water penetration tests indicated a similar time lag between water application and drainage measurements in both the Datum and Zero-Cavity panels. Although the rigid fibreglass cavity fill in the Zero-Cavity panel would be expected to slow and absorb the initial penetration, the mortar droppings would have the same effect in the Datum. The Zero-Cavity and Dow panels did collect some water during natural exposure, but only on a few occasions. The higher frequency of collection in the Zero-Cavity panels likely indicates that there was better drainage than either the Datum or DPV panels, not greater rain penetration of the screen.

The lower Zero-Cavity framing was saturated and this water could not have penetrated the Tyvek™ and flashing in liquid form under hydraulic pressure. The saturated base of the stud space suggests that the mechanism of transfer was vapour diffusion through the Tyvek™ under solar-induced vapour pressure differences between the cavity and the stud space. The fact that the interior face of the sheathing was wet only where pressed against the vapour-impermeable flashing also indicates water vapour, rather than water, movement.

8.5 Conclusions

From the physical inspection of the opened wall panels, the following conclusions can be drawn:

- In the Zero-Cavity panels, the base of the rigid fibreglass cavity fill was saturated over the bottom 40 to 60 mm and was the source of the moisture that saturated the sole plate, wet the batt insulation, and caused heavy mould growth. Neither the Zero-Cavity panel base flashing detail nor the instrumentation was improperly constructed. The base of the cavity was completely unobstructed by mortar.

- The base of the Datum panel cavity was not clean and the cavity was not completely clear despite the exceptional precautions taken during construction. Relative to other field studies, the extent of drainage adversely affected as a result of mortar droppings was not severe. The Datum panels were in good condition, but some slight but dry mould growth was found on one stud; this does not constitute a problem.

- The DPV panels were in exceptionally good condition. The base details may need further refinement to ensure perfectly unobstructed drainage.

9. Conclusions

This multi-year, full-scale program of field testing 3 different wall systems has generated much useful information, raised some important issues, and produced some very interesting results. The main conclusions and some recommendations follow.

Test Panel Performance

In this project, the **Zero-Cavity** panel performed poorly. As is the case in typical walls, the brickwork veneer allowed significant amounts of rain water to penetrate into the cavity. The untreated glass fibre insulation retained some of this water by capillary action at its base. Solar-driven inward vapour drives during the summer and fall transported this retained moisture from the glass fibre cavity fill through the vapour-permeable Tyvek™ and resulted in saturated wood framing in the bottom of the stud space within the first year.

However, these problems were the result of the combination of the water permeability of the brick screen, the capillary retention characteristics of the glass fibre cavity fill, the very high vapour permeability of the Tyvek™, and the solar-induced inward vapour drive. Two of these factors can be easily resolved. The moisture retention characteristics of the glass fibre fill can be easily controlled by applying a hydrophobic treatment during the manufacture of the product; this is the case for all European products. An exterior layer of housewrap, sheathing, or building paper with less vapour permeance than the Tyvek™ can be used on the inside of the cavity fill to control inward vapour drives.

Despite the problems caused by the use of standard materials in a non-standard way, this work confirmed that the zero-cavity concept is essentially sound and offers benefits such as better assurance of drainage, thinner wall sections, support and protection of the sheathing paper / housewrap, and possibly better pressure moderation. Decades of use and the popularity of this form of construction in Scandinavia and Europe provides some assurance that, with proper materials and construction, fibrous cavity fills can improve the field performance of multi-wythe rainscreen walls.

The performance of the **Datum** panels was often dominated by solar effects. The vapour drive from the cavity through the Tyvek™ and glass fibre insulating sheathing into the stud space created high wood moisture levels in late summer. Instrumentation indicated moisture contents of more than 20%, and temperatures over 15 °C for two weeks in the upper portion of one stud. Slight mold growth was subsequently found at this location when the panels were inspected at the end of the project. Drying of the framing occurred through the fall and winter. The use of the vapour-permeable Tyvek™ resulted in wall

performance quite different from what one would expect if building paper had been used. The air barrier in the Datum panels was practically perfect; air leakage must be expected in typical walls and this will influence these conclusions.

The **DPV** panels performed very well. The restriction of water vapour transfer inwards by the less vapour-permeable EXPS sheathing in the DPV panels resulted in considerably more stable and lower stud space relative humidity levels in the summer, and more stable and slightly higher winter relative humidity levels than the other two pairs of panels. Physical inspection of the two panels (conducted after monitoring ended) found the general condition of the DPV panels to be excellent. As for all of the test panels, the air barrier in the DPV panels was practically perfect. In reality, air leakage must be expected in typical walls and this will influence the above conclusions.

Some more general, wide-ranging conclusions which apply to the performance of many wall systems are presented below.

Mortar Control

Inspection after opening up of the panels revealed that the base of the Zero-Cavity panels was completely clean of mortar droppings and would allow unhindered drainage of any water reaching the base flashing of the panel. Despite the extraordinary precautions taken during construction, mortar projections occurred and mortar dropping were found at the base of the Datum panel cavities. While in this case the limited mortar blockage did not greatly impair drainage nor cause damage to the wall, it did highlight how difficult it is to provide a clear clean cavity in normal wall construction.

Drainage

The drainage system in all six panels performed well under the water penetration test conditions. The brickwork allowed a significant amount of water to penetrate through into the cavity. The application of a static pressure *across the wall* and the open vents had no noticeable effect on the water leakage. In the water penetration tests, the presence of the fibreglass cavity fill did not appear to effect the drainage of water in the Zero-Cavity panels. While the fibreglass cavity fill used in the Zero-Cavity wall was also found to drain water well in laboratory tests, capillary forces retained a small amount of water in the lower 50 to 75 mm. It took some time for this stored water to be removed by evaporation. The use of hydrophobic coatings is recommended to control this potentially damaging moisture storage.

Thermal Performance

If exposed to the sun, the brick veneer screen undergoes large temperature changes during the course of the day during all times of the year. In the winter, the brick will tend to have an average temperature not far below freezing, with significant daily excursions above and below zero due to solar effects. Over both the summer and winter, the temperature of the east/west facing panels was about 5-7 °C higher than the average ambient temperature. This temperature difference has a dramatic effect on the inner layers of each wall and affects condensation potential, moisture storage and transmission, energy consumption, material durability, and thermal conditions.

The air in the cavity of all panels remained warmer than the brick and at least 6 °C warmer than the average ambient temperature. There was also no pattern of measurable vertical temperature stratification within the cavity. The cavity temperature closely followed the temperature of the back of the brick, even during fast, solar-induced, temperature changes. As suggested by theory, it is practically impossible for sufficient air flow through the masonry vents to remove solar heat gains from the cavity. The amount of water vapour in the cavity was not strongly related to the moisture content of the exterior air. As the temperature increased, the amount of moisture in the cavity air increased, indicating evaporation and desorption of moisture. No conclusions could be made regarding the influence of ventilation on the moisture content of the air in the cavity (and hence its drying ability) because ventilation flow could not be measured with the test setup.

Pressure Moderation Performance

The effectiveness of the moderation of pressure differences across the screen in one-storey buildings, as well as low and high-rise construction, needs further study. Many more pressure moderation measurements using repeatable, quantitative test procedures are necessary. The wind pressures experienced by exposed low-rise construction are generally quite low (less than 20 Pa) and higher pressures (greater than 50 Pa) occur very rarely. The variation in wind pressure with height had a relatively large effect on pressures and pressure moderation in the test panels. Spatial variations near building corners were found to result in significantly different pressure conditions. Based on the data we recorded, none of the panels were fully pressure equalized for any record at any frequency.

The wind can be considered as being composed of the addition of a mean component and a rapidly varying component. The Datum and Zero-Cavity panels moderated from 20 to 50% of the variable pressure differences across the screen, i.e., they were 20 to 50% "pressure equalized", at 0.2 Hz. The degree of pressure moderation decreased with

increasing frequency. The mean values (of one minute records) indicated that the panels moderated more than 90% of the difference across the screen. It also appears that mean pressures or mean pressure differences have limited relevance to the actual response of the cavity pressure to the wind. Both the water permeance of brick veneer screens, especially under dynamically-varying, low-pressure differences, and the incidence and coincidence of rain and wind effects need to be given more study and attention.

Housewrap / Building Paper

As far as the housewrap / building paper is concerned, placing it between the insulated sheathing and the batt insulation protects it from temperature extremes and large variations in all seasons. Support given to an air barrier, housewrap, or building paper by attachment to rigid insulation or placement between two relatively stiff layers was found to have a significant beneficial effect on airtightness. Relatively air tight housewrap and building paper layers are desirable because they reduce convective heat losses from the low-density batt insulation, reduce the effective volume of the pressure equalization chamber, and provide a second plane of airflow resistance in the event the primary air barrier is or becomes defective. Housewrap should only be used when well adhered to a stiff substrate and fully taped. It is strongly recommended that the use of housewrap, in particular its location, vapour permeance, and intended purpose, be carefully considered in the future.

Mean Values

It is clear from this field monitoring that consideration of mean values does not reflect the effect of daily variations, especially those due to solar radiation, in lightweight framed wall assemblies. Daily peak values may play an important role in the actual performance of the wall. As has been found in other studies, hourly readings are important for a full understanding of the behaviour of the lightweight framed wall assemblies typically used in North American residential construction.

Appendix A

Graphed Data

From: November 1, 1991 To: December 31, 1992

Monitoring Day	Date
1	1-Nov-91
31	1-Dec-91
62	1-Jan-92
93	1-Feb-92
122	1-Mar-92
153	1-Apr-92
183	1-May-92
214	1-Jun-92
244	1-Jul-92
275	1-Aug-92
306	1-Sep-92
336	1-Oct-92
367	1-Nov-92
397	1-Dec-92
427	31-Dec-92
428	1-Jan-93
459	1-Feb-93
487	1-Mar-93
518	1-Apr-93
548	1-May-93
579	1-Jun-93

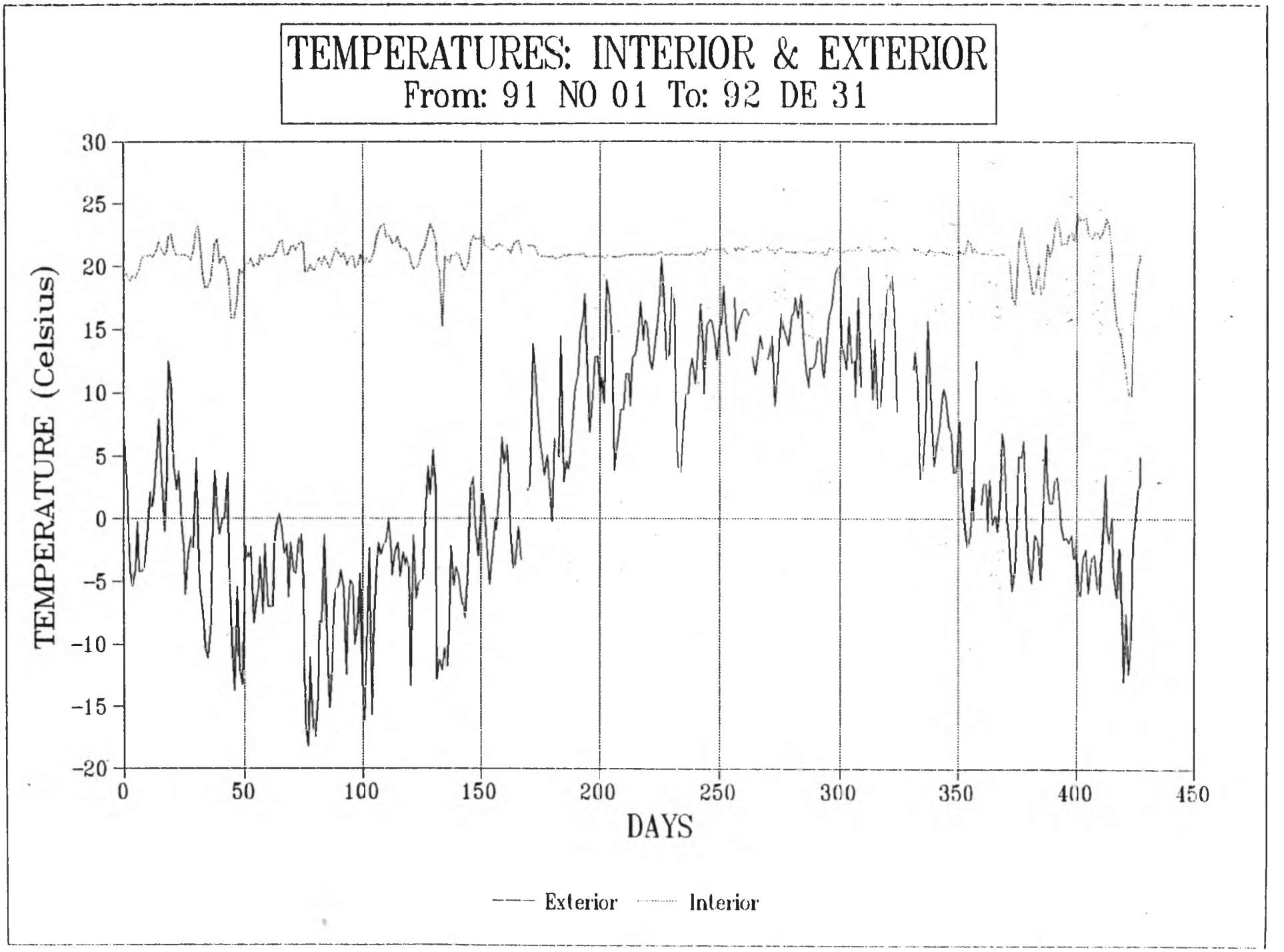
TEMPERATURES: INTERIOR & EXTERIOR
From: 91 NO 01 To: 92 DE 31
TEMPERATURE (Celsius)
30
25
20
15
10
5
0
-5
-10
-15
-20
0
50
100
150
200
250
300
350
400
450
DAYS
Exterior
Interior

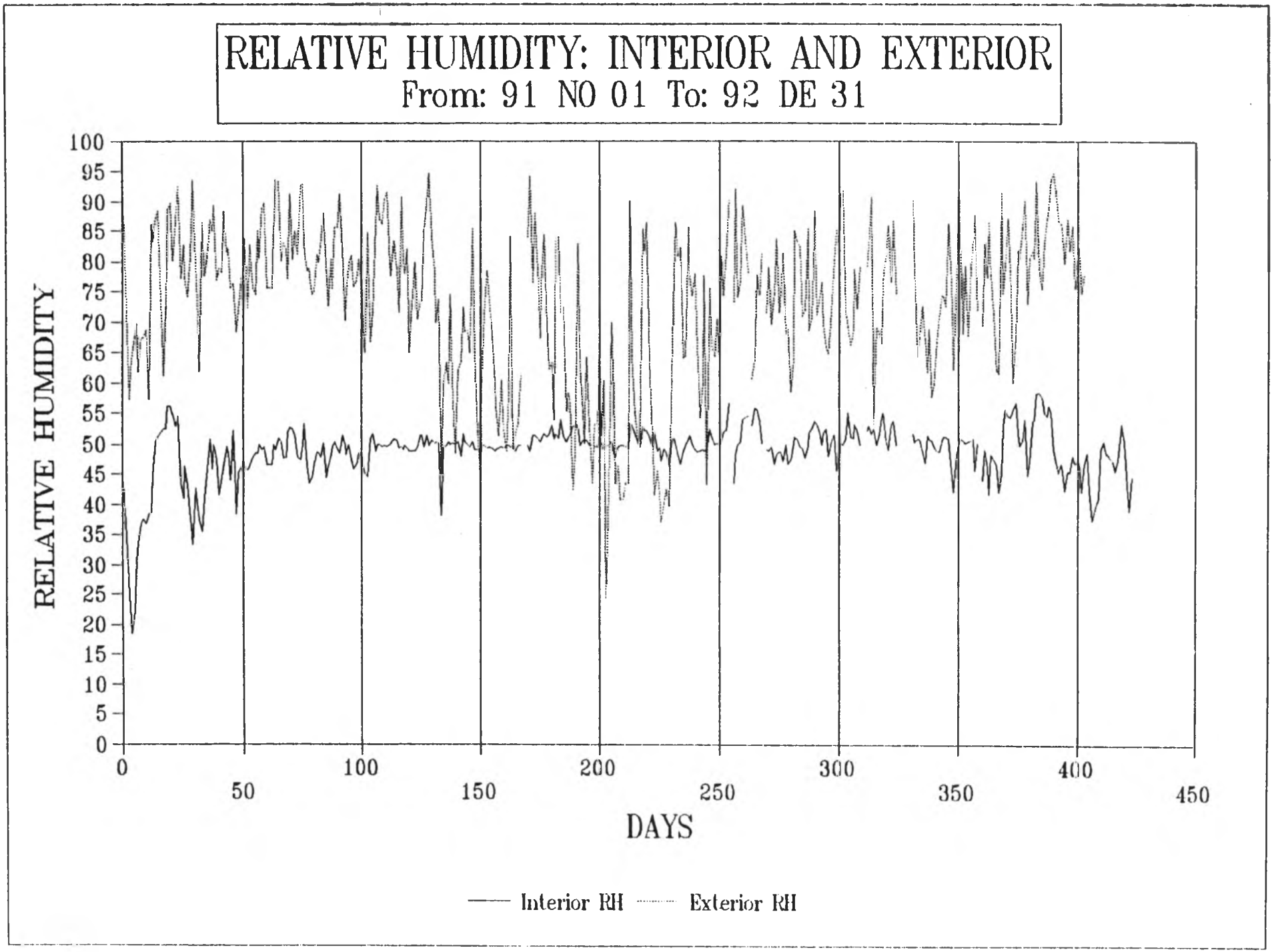
RELATIVE HUMIDITY: INTERIOR AND EXTERIOR
From: 91 NO 01 To: 92 DE 31
RELATIVE HUMIDITY
100
95
90
85
80
75
70
65
60
55
50
45
40
35
30
25
20
15
10
5
0
0
50
100
150
200
250
300
350
400
450
DAYS
Interior RH
Exterior RH

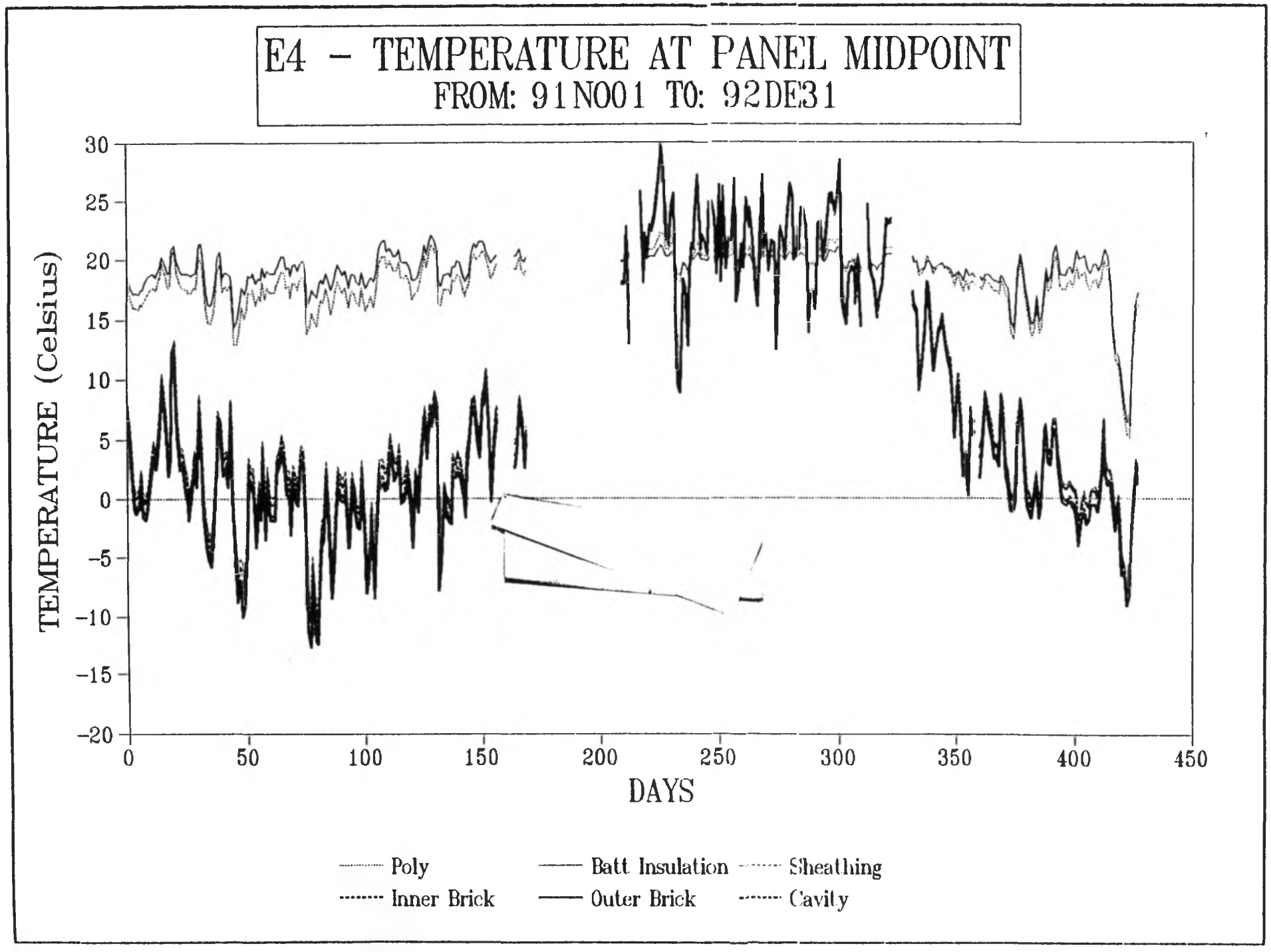
E4 – TEMPERATURE AT PANEL MIDPOINT
FROM: 91N001 TO: 92DE31
TEMPERATURE (Celsius)
30
25
20
15
10
5
0
-5
-10
-15
-20
0
50
100
150
200
250
300
350
400
450
DAYS
Poly
Batt Insulation
Sheathing
Inner Brick
Outer Brick
Cavity

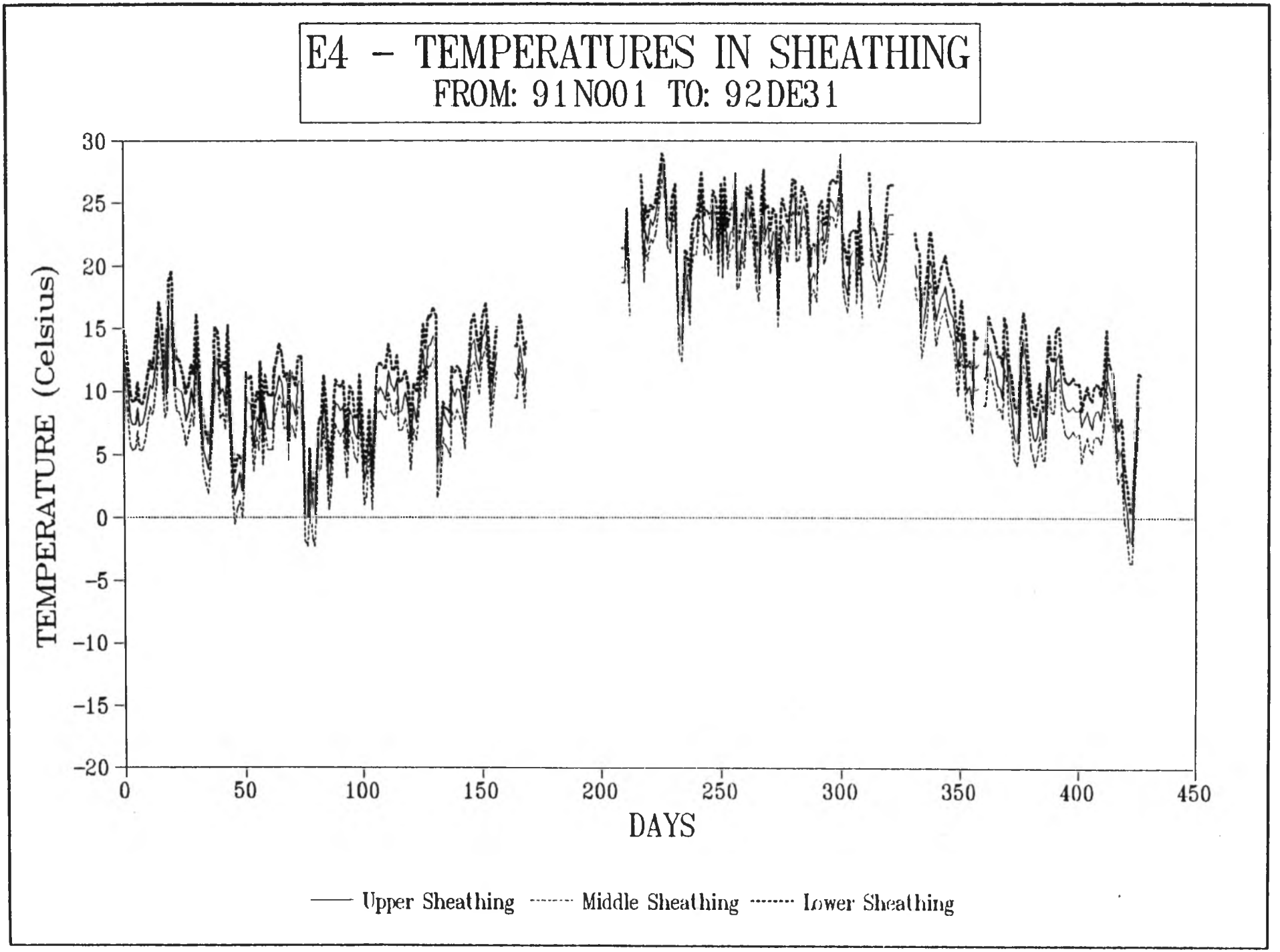
E4 - TEMPERATURES IN SHEATHING
FROM: 91N001 TO: 92DE31
TEMPERATURE (Celsius)
30
25
20
15
10
5
0
-5
-10
-15
-20
0
50
100
150
200
250
300
350
400
450
DAYS
Upper Sheathing
Middle Sheathing
Lower Sheathing

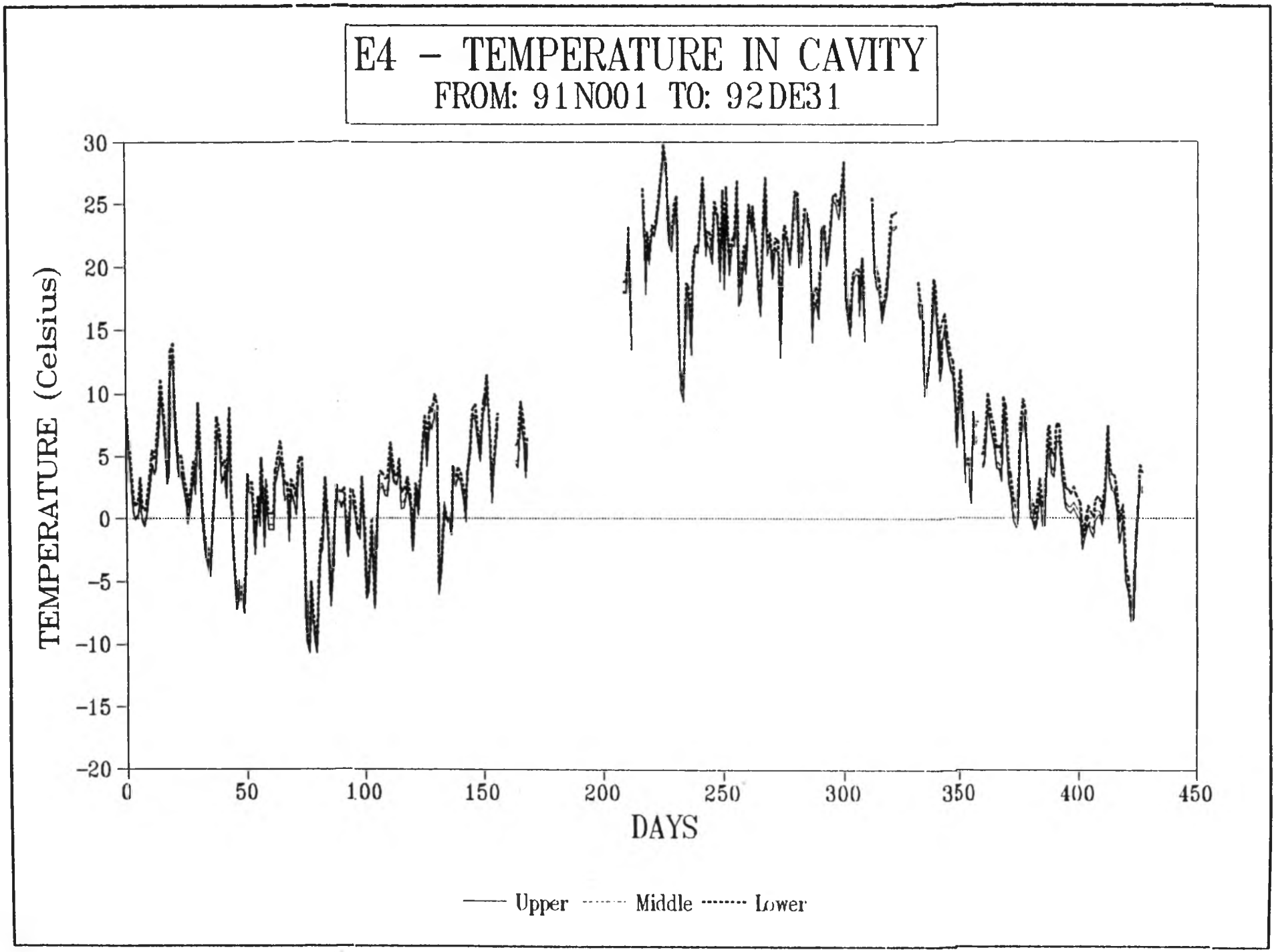
E4 – TEMPERATURE IN CAVITY
FROM: 91N001 TO: 92DE31
TEMPERATURE (Celsius)
30
25
20
15
10
5
0
-5
-10
-15
-20
0
50
100
150
200
250
300
350
400
450
DAYS
Upper
Middle
Lower

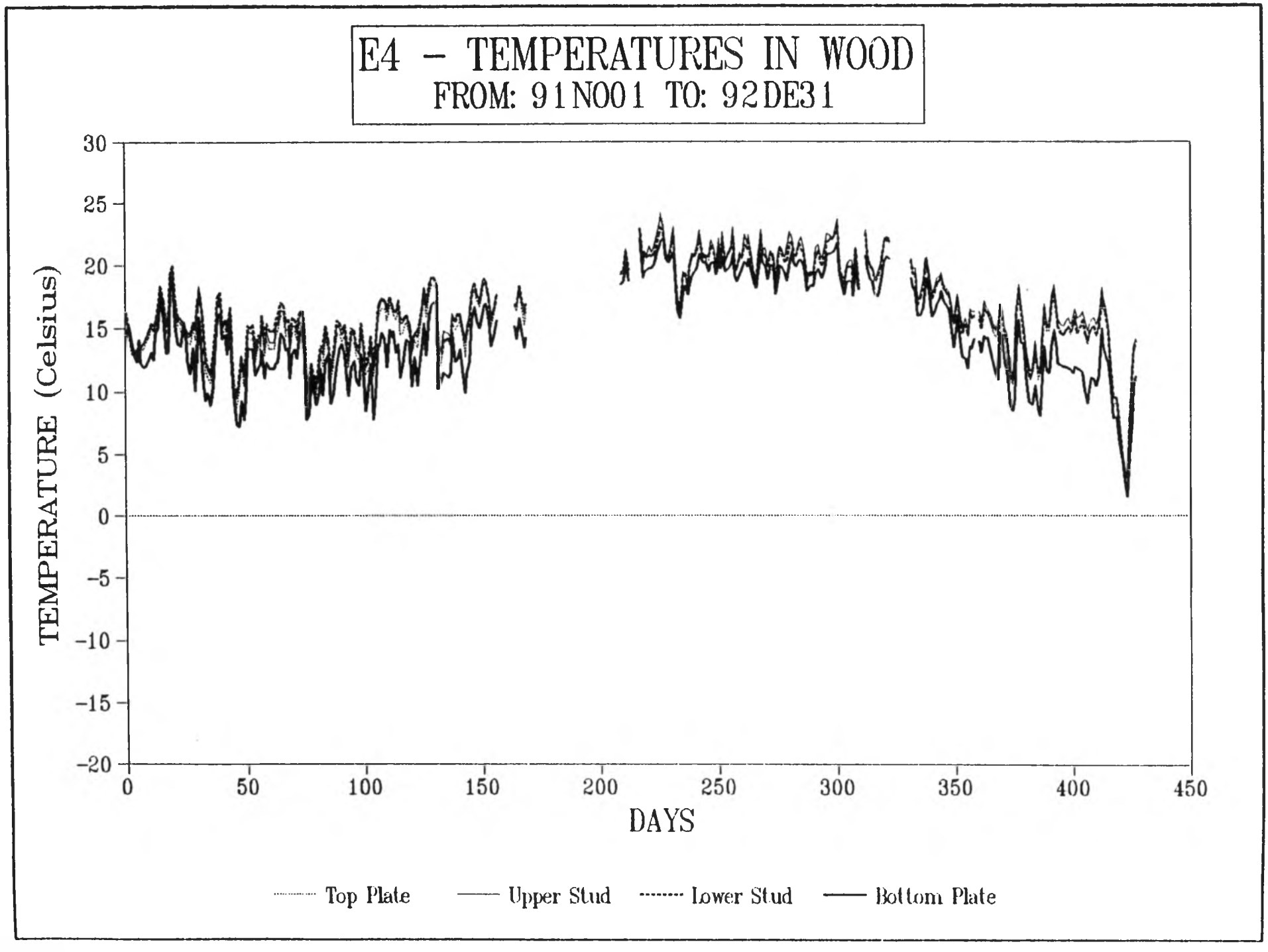
E4 - TEMPERATURES IN WOOD
FROM: 91N001 TO: 92DE31
TEMPERATURE (Celsius)
30
25
20
15
10
5
0
-5
-10
-15
-20
0
50
100
150
200
250
300
350
400
450
DAYS
Top Plate
Upper Stud
Lower Stud
Bottom Plate

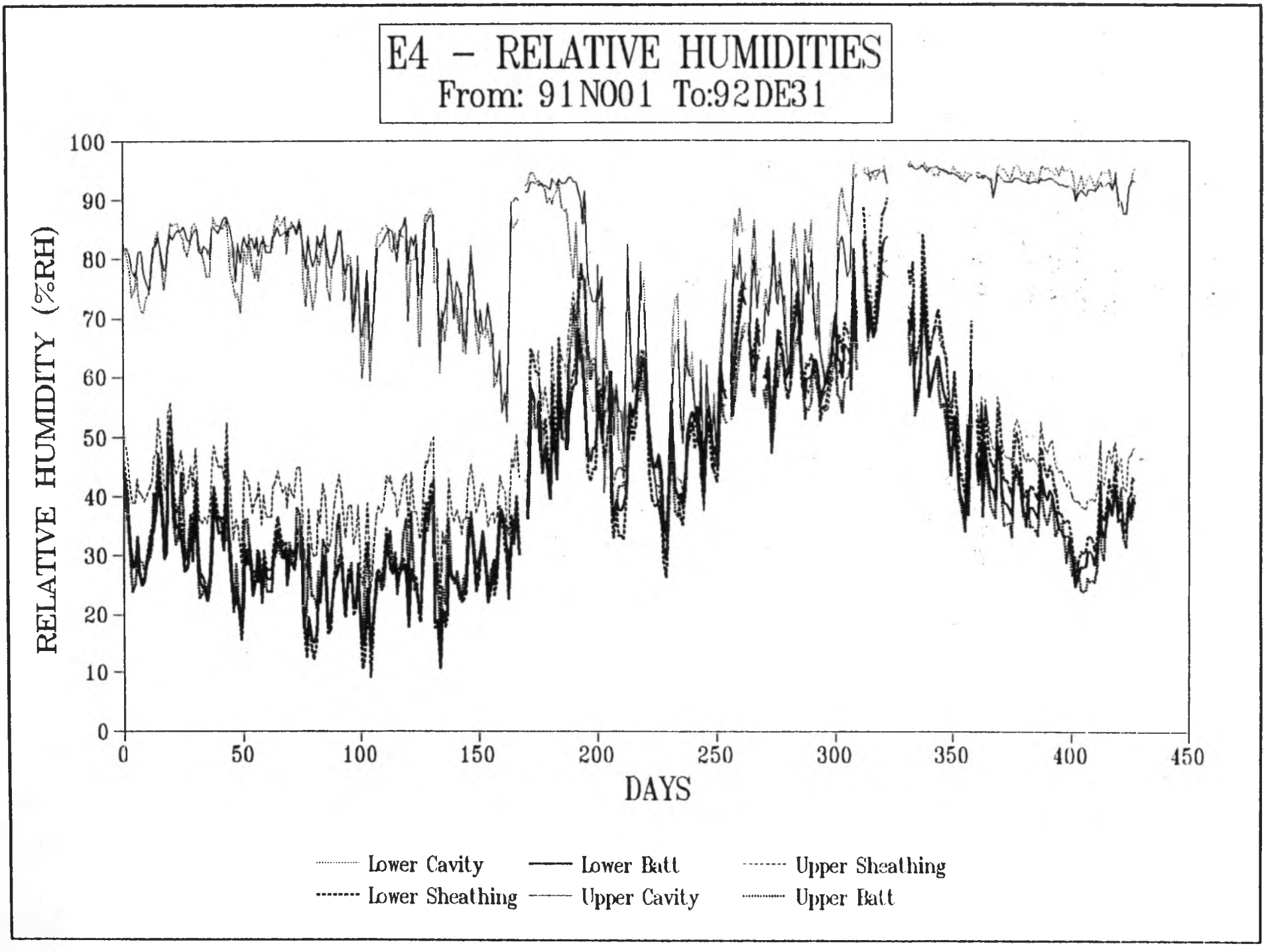
E4 – RELATIVE HUMIDITIES
From: 91N001 To:92DE31
RELATIVE HUMIDITY (%RH)
100
90
80
70
60
50
40
30
20
10
0
0
50
100
150
200
250
300
350
400
450
DAYS
Lower Cavity
Lower Batt
Upper Sheathing
Lower Sheathing
Upper Cavity
Upper Batt

E4 - WOOD MOISTURE CONTENT
From: 91N001 To: 92DE31

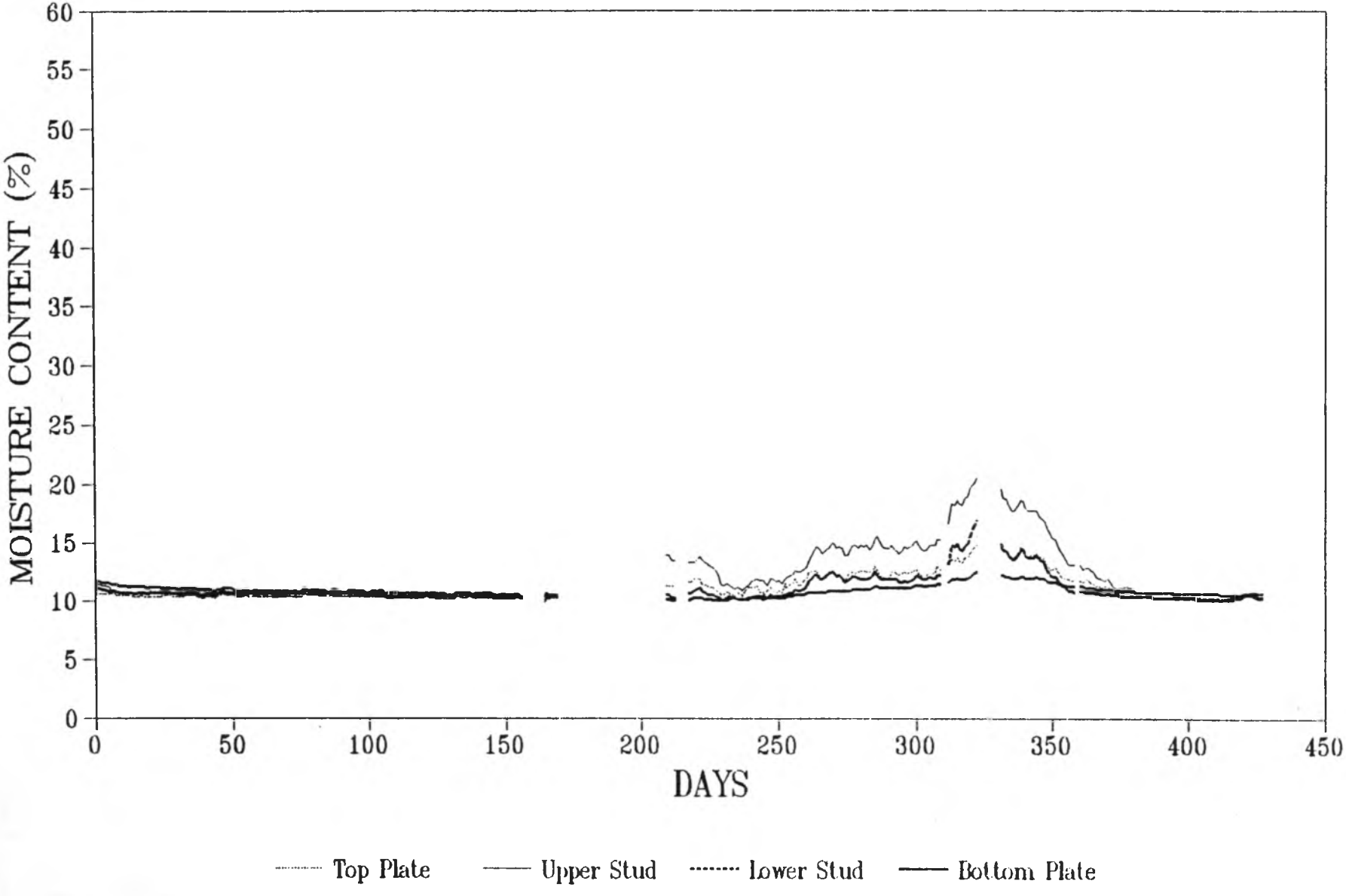

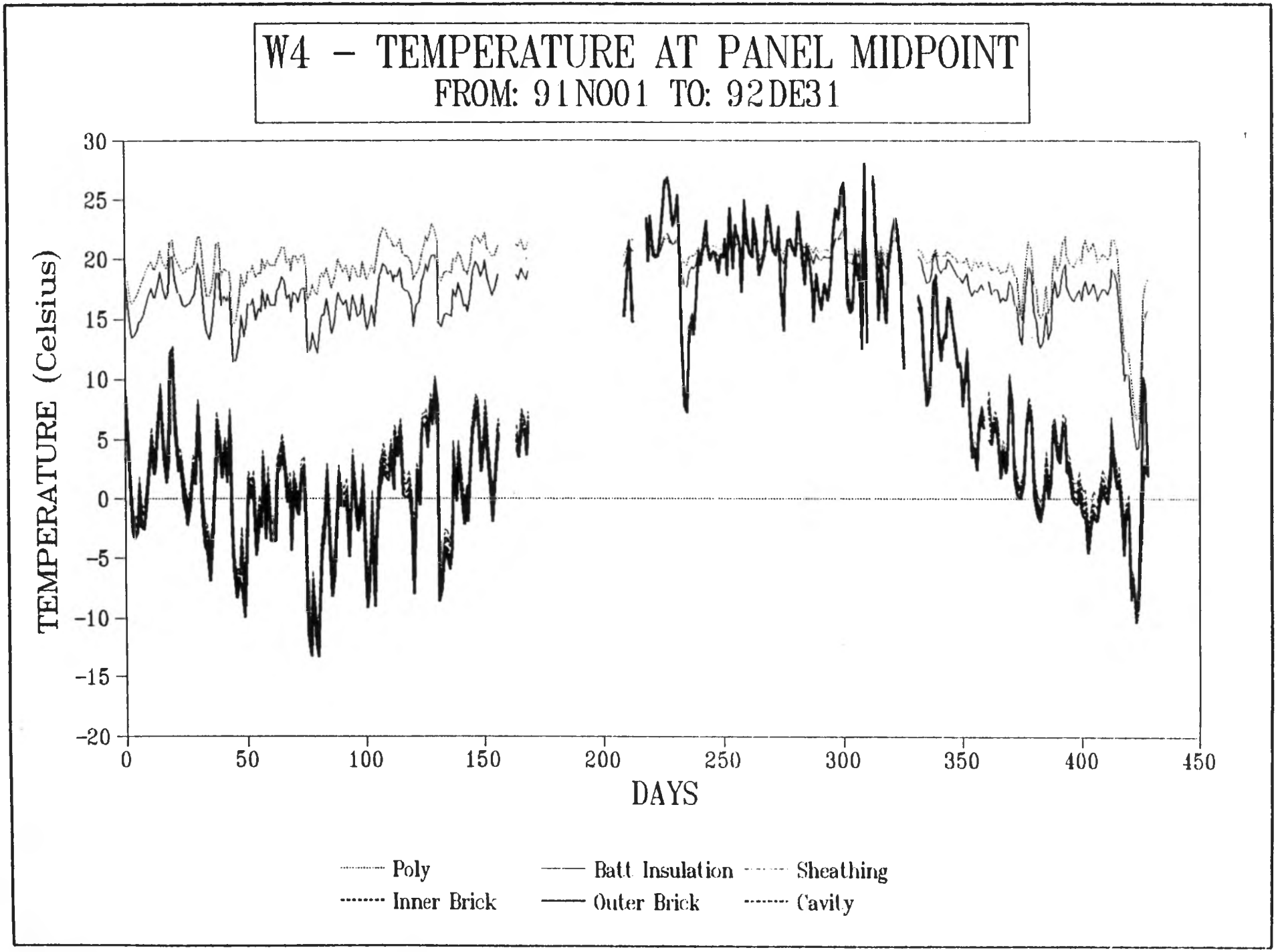
W4 – TEMPERATURE AT PANEL MIDPOINT
FROM: 91N001 TO: 92DE31
TEMPERATURE (Celsius)
30
25
20
15
10
5
0
-5
-10
-15
-20
0
50
100
150
200
250
300
350
400
450
DAYS
Poly
Batt Insulation
Sheathing
Inner Brick
Outer Brick
Cavity

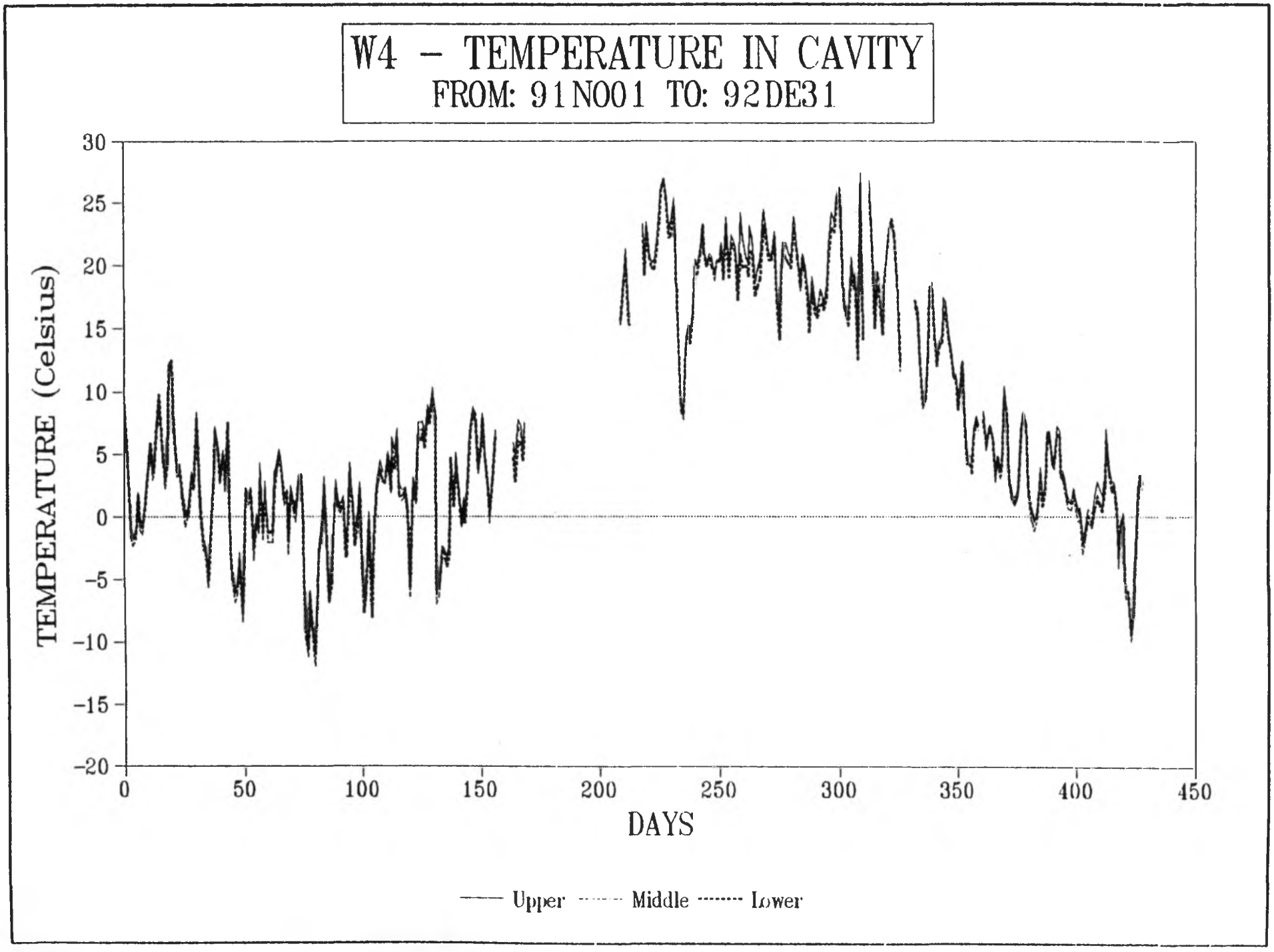
W4 – TEMPERATURE IN CAVITY
FROM: 91N001 TO: 92DE31
TEMPERATURE (Celsius)
30
25
20
15
10
5
0
-5
-10
-15
-20
0
50
100
150
200
250
300
350
400
450
DAYS
Upper
Middle
Lower

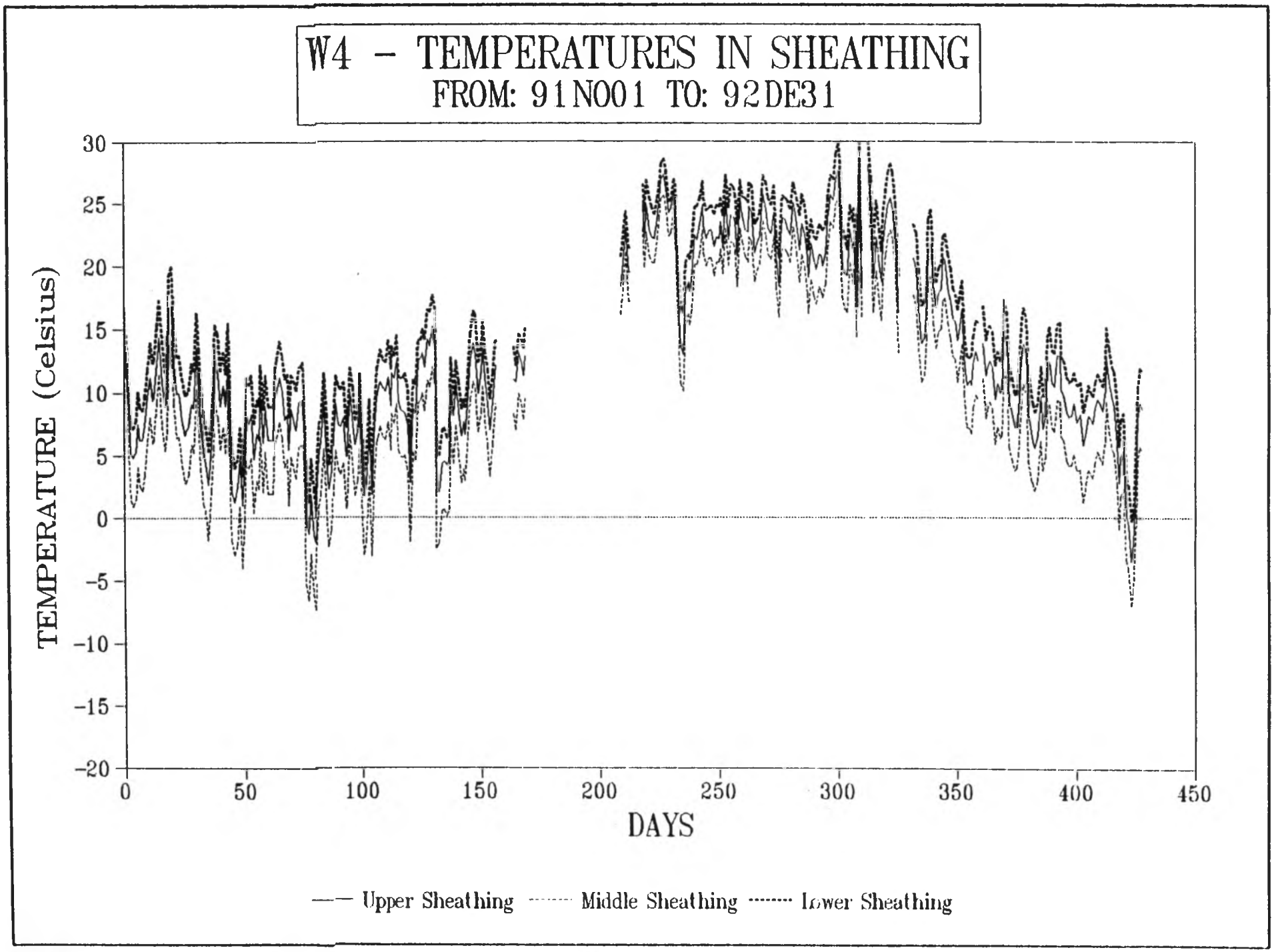
W4 - TEMPERATURES IN SHEATHING
FROM: 91N001 TO: 92DE31
TEMPERATURE (Celsius)
30
25
20
15
10
5
0
-5
-10
-15
-20
0
50
100
150
200
250
300
350
400
450
DAYS
Upper Sheathing
Middle Sheathing
Lower Sheathing

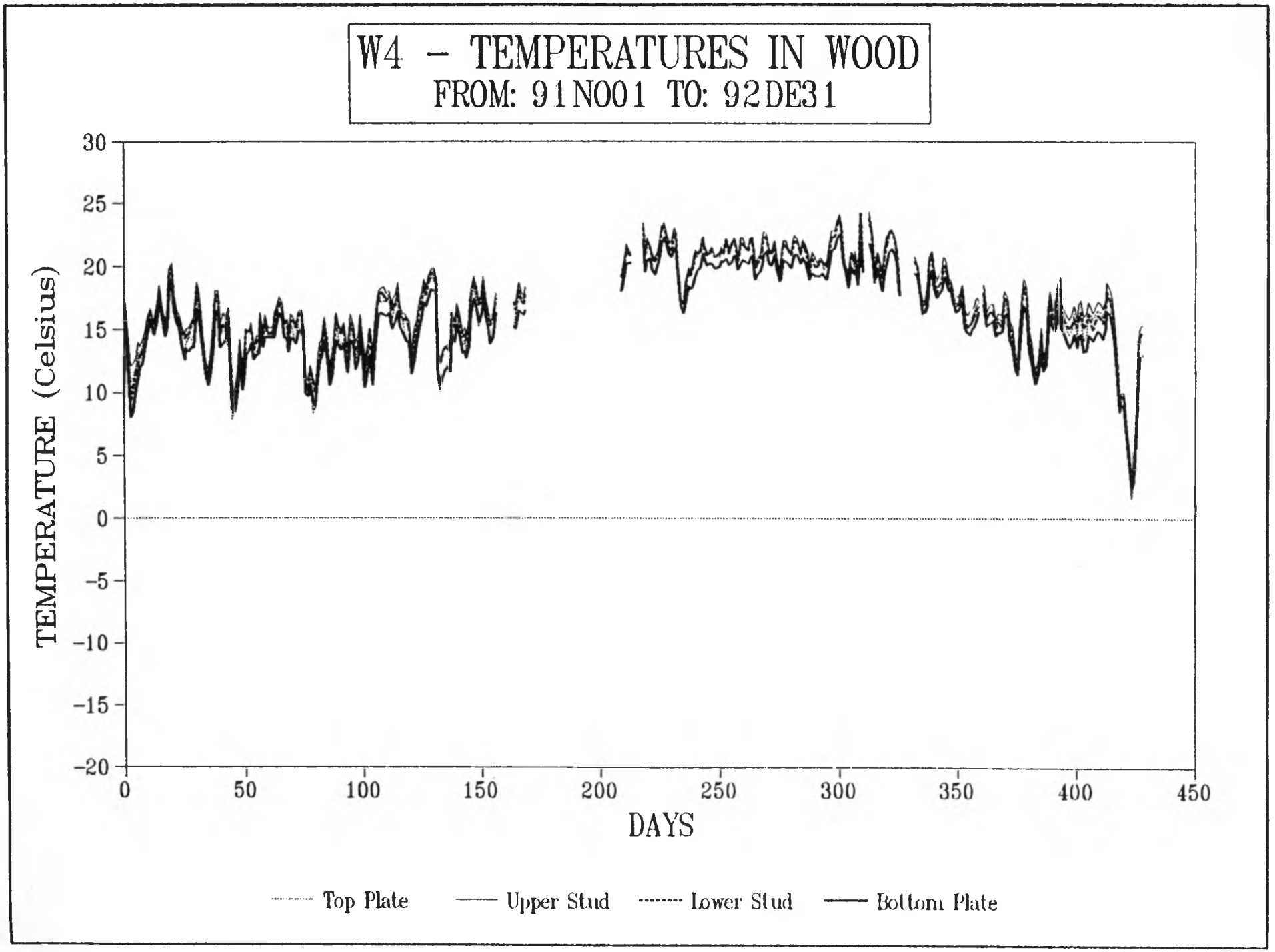
W4 - TEMPERATURES IN WOOD
FROM: 91N001 TO: 92DE31
TEMPERATURE (Celsius)
30
25
20
15
10
5
0
-5
-10
-15
-20
0
50
100
150
200
250
300
350
400
450
DAYS
Top Plate
Upper Stud
Lower Stud
Bottom Plate

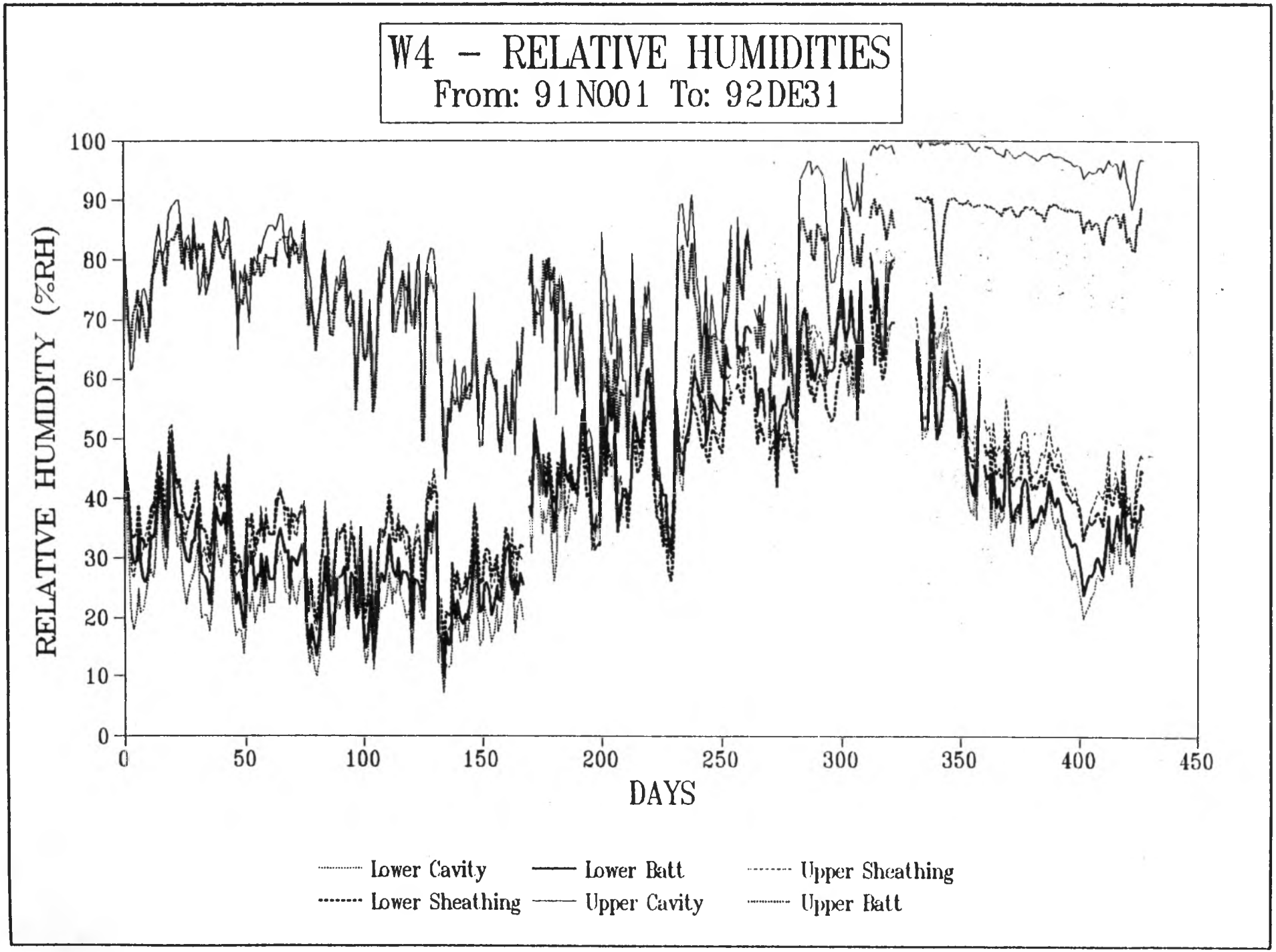
W4 - RELATIVE HUMIDITIES
From: 91N001 To: 92DE31
RELATIVE HUMIDITY (%RH)
100
90
80
70
60
50
40
30
20
10
0
0
50
100
150
200
250
300
350
400
450
DAYS
Lower Cavity
Lower Batt
Upper Sheathing
Lower Sheathing
Upper Cavity
Upper Batt

W4 - WOOD MOISTURE CONTENT
From: 91N001 To: 92DE31

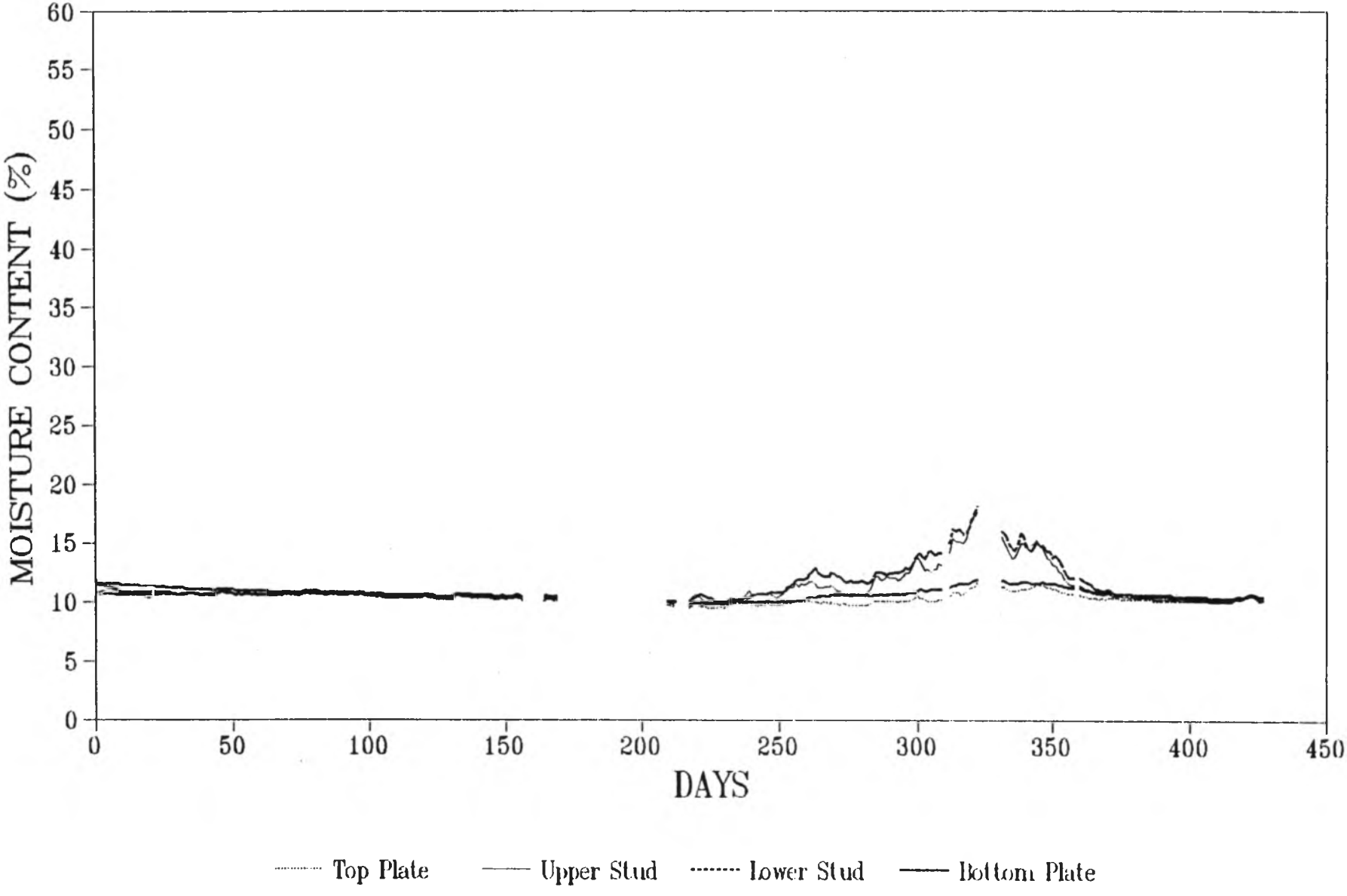

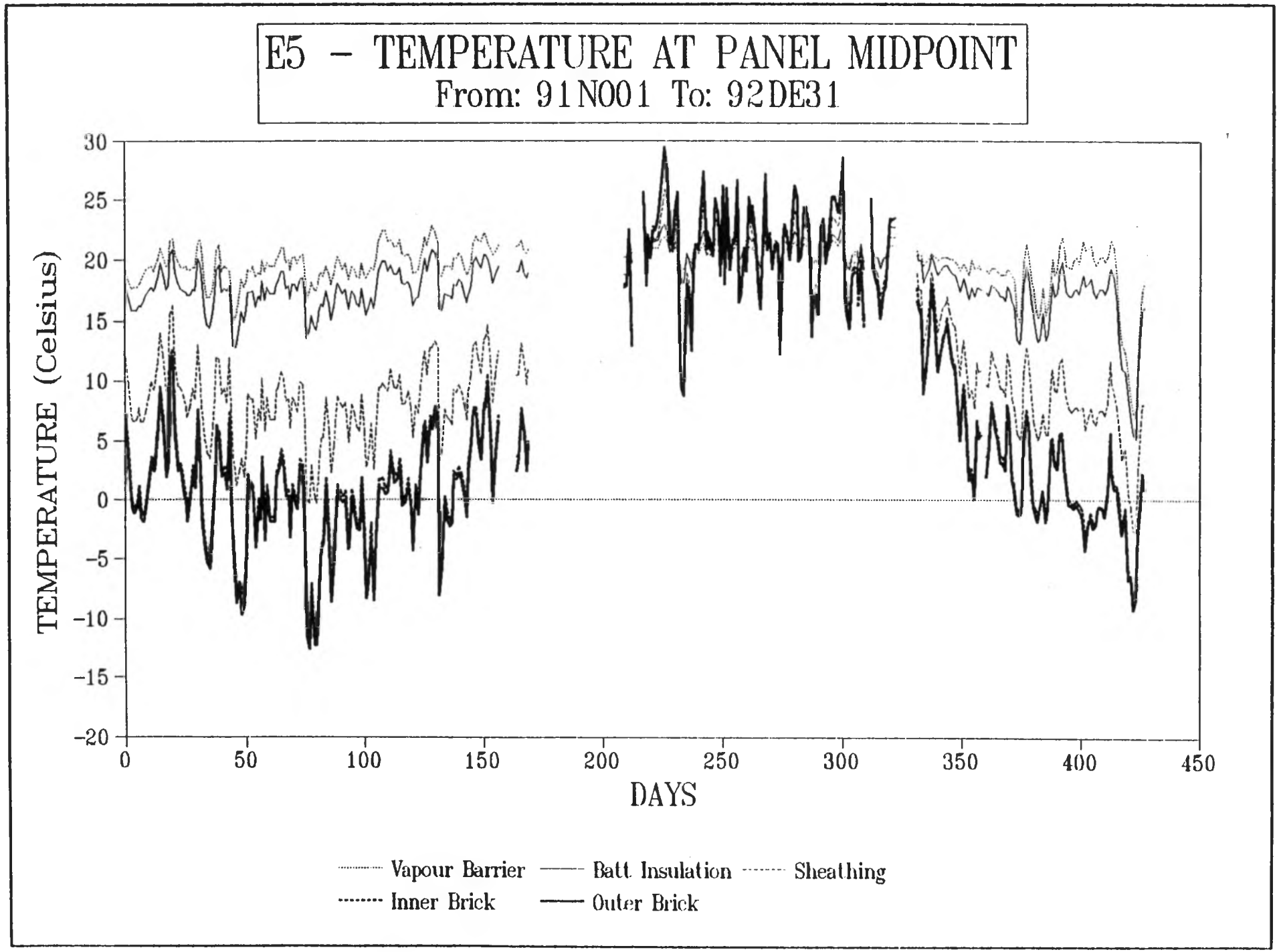
E5 – TEMPERATURE AT PANEL MIDPOINT
From: 91N001 To: 92DE31
TEMPERATURE (Celsius)
30
25
20
15
10
5
0
-5
-10
-15
-20
0
50
100
150
200
250
300
350
400
450
DAYS
Vapour Barrier
Batt. Insulation
Sheathing
Inner Brick
Outer Brick

E5 - TEMPERATURES IN SHEATHING
From: 91N001 To: 92DE31

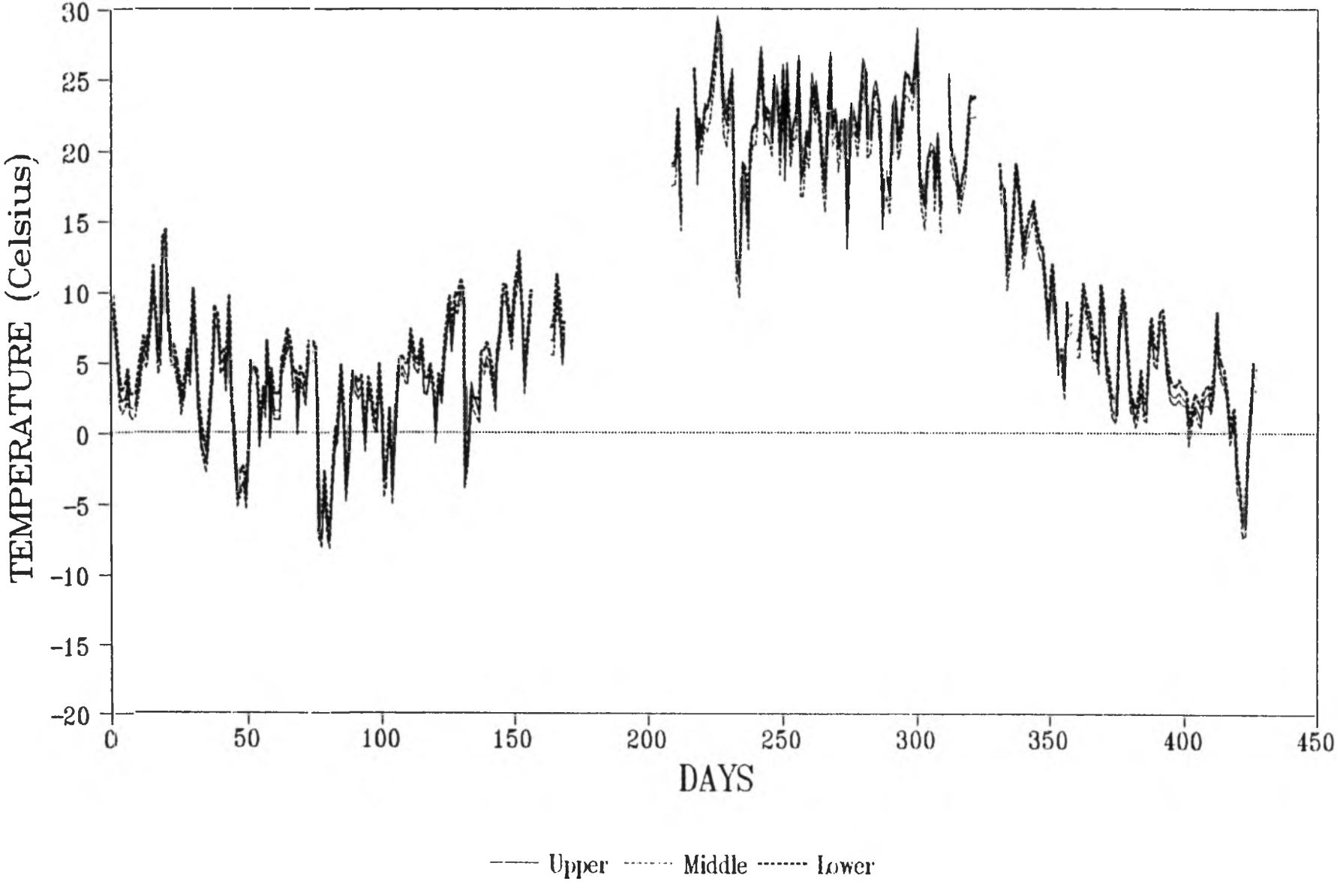

E5 – TEMPERATURES IN WOOD

From: 91N001 To: 92DE31

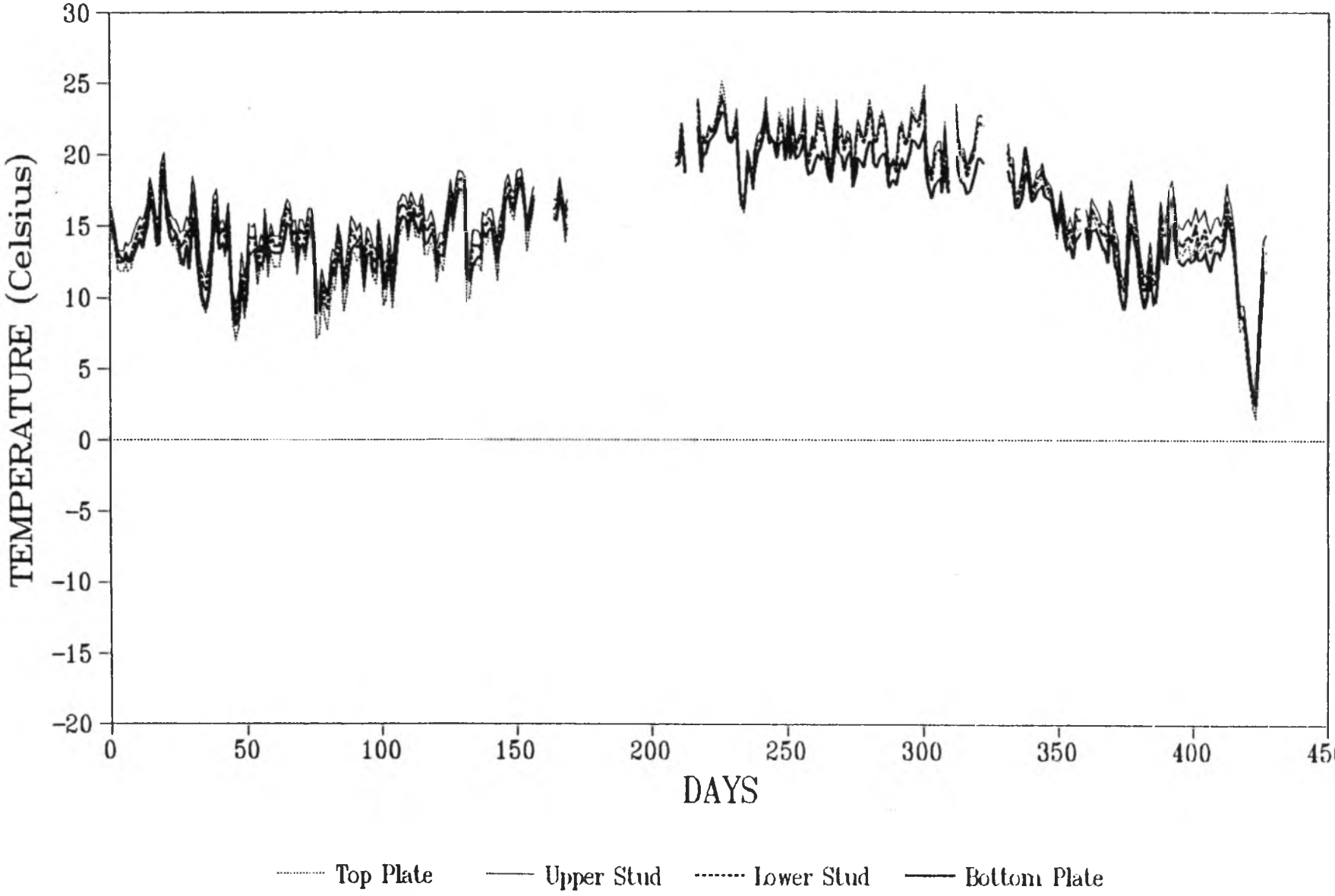

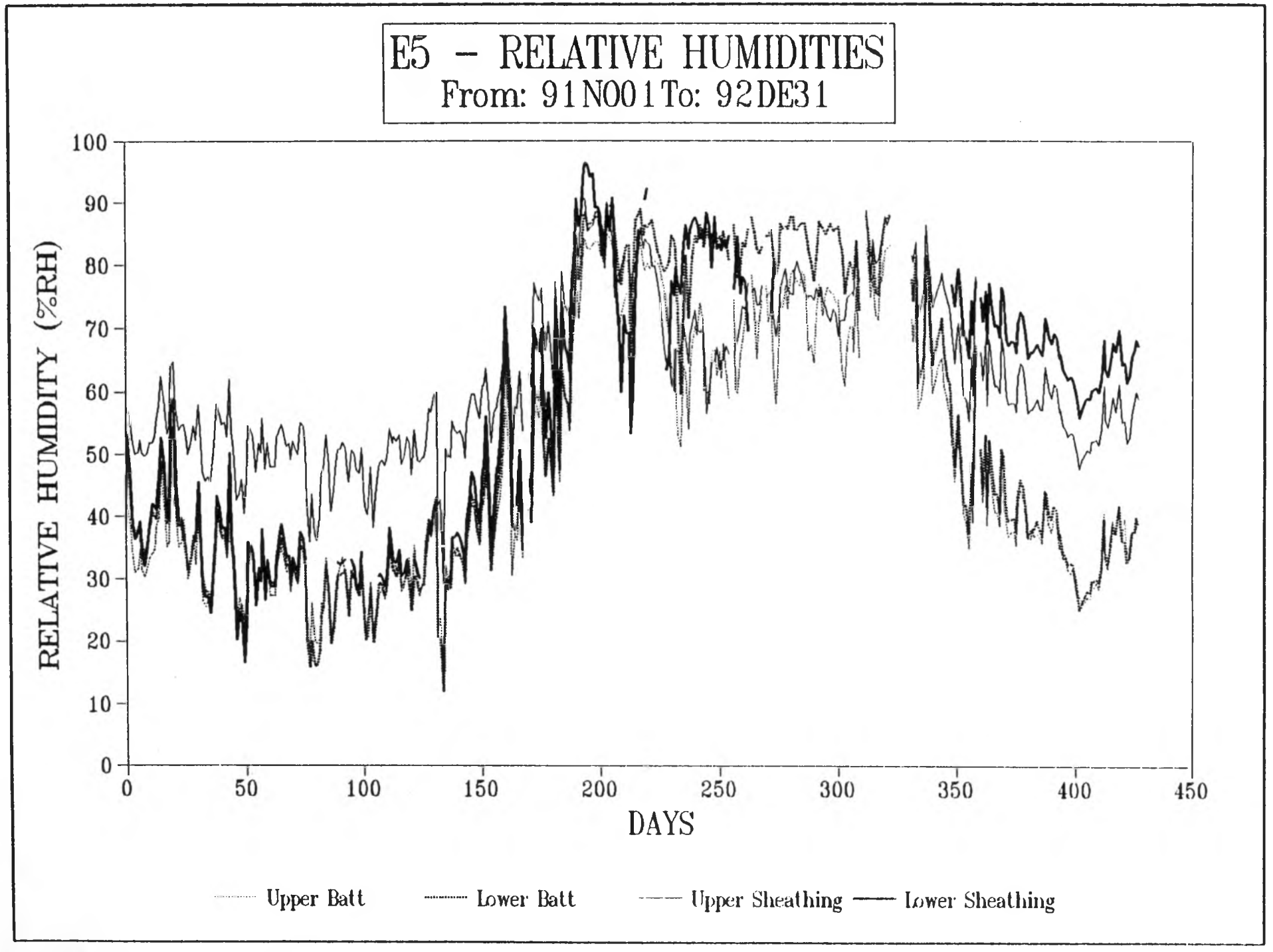
E5 - RELATIVE HUMIDITIES
From: 91N001To: 92DE31
RELATIVE HUMIDITY (%RH)
100
90
80
70
60
50
40
30
20
10
0
0
50
100
150
200
250
300
350
400
450
DAYS
Upper Batt
Lower Batt
Upper Sheathing
Lower Sheathing

E5 - WOOD MOISTURE CONTENT
From: 91N001 To: 92DE31

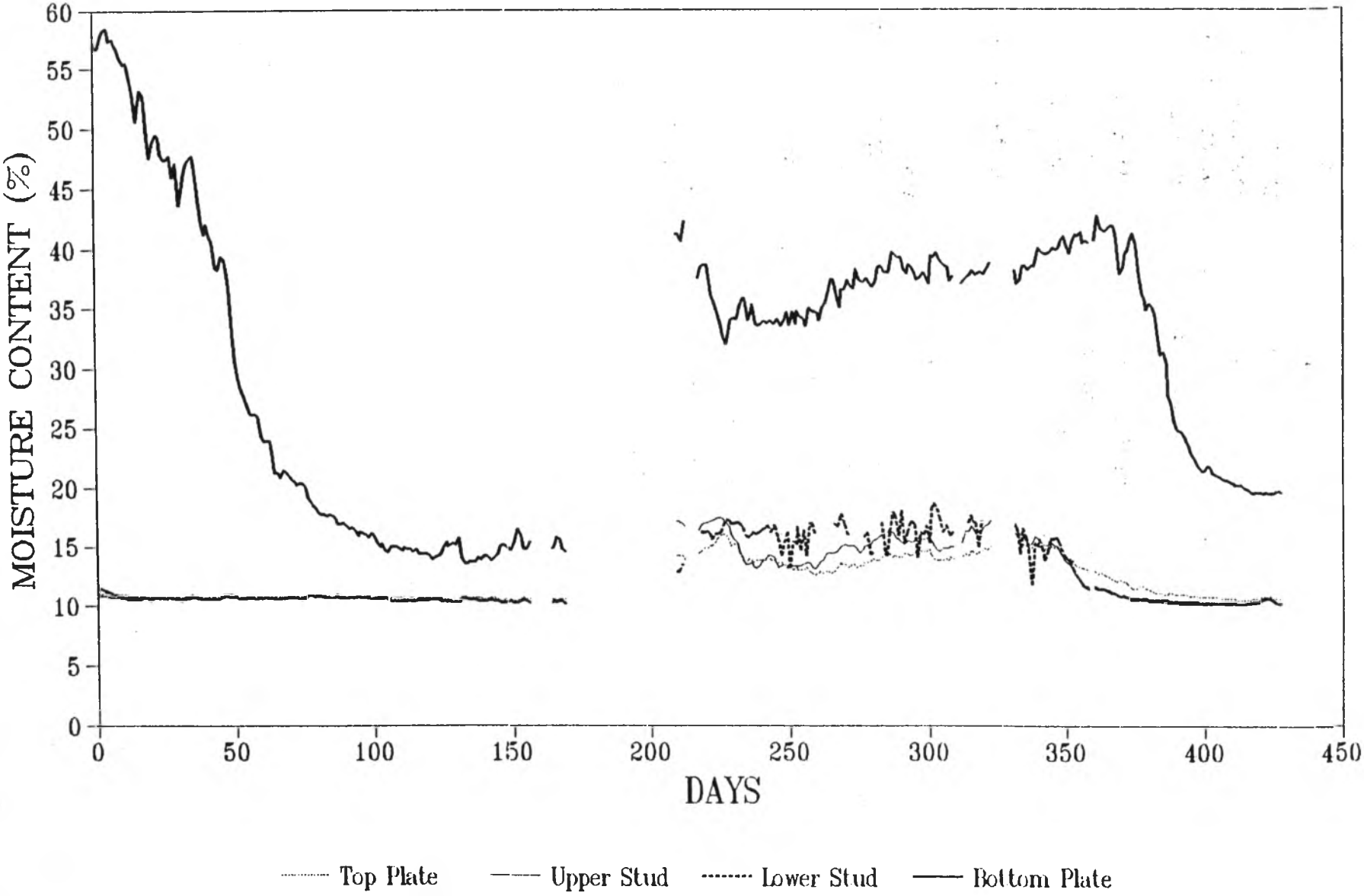

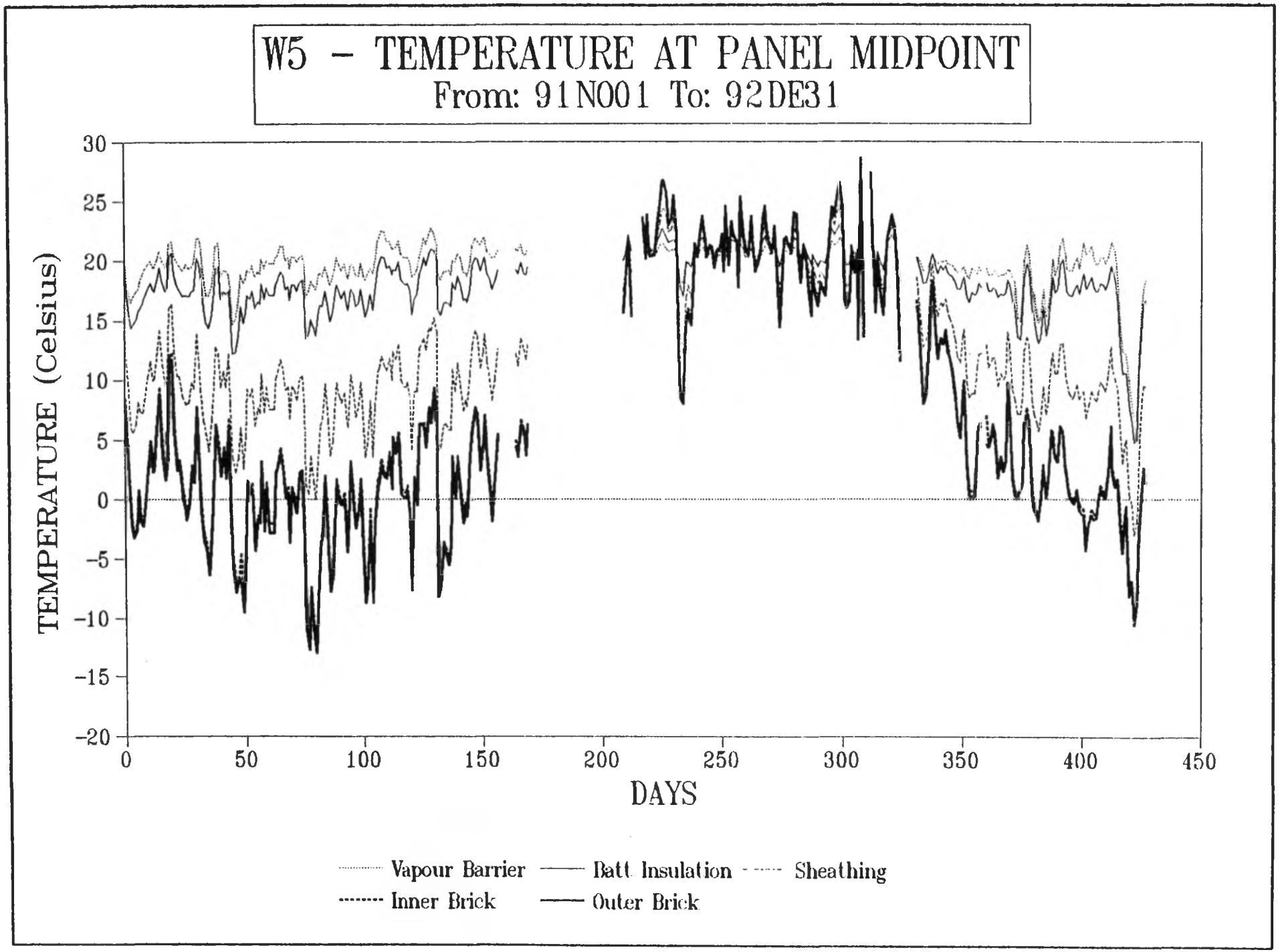
W5 - TEMPERATURE AT PANEL MIDPOINT
From: 91N001 To: 92DE31
TEMPERATURE (Celsius)
30
25
20
15
10
5
0
-5
-10
-15
-20
0
50
100
150
200
250
300
350
400
450
DAYS
Vapour Barrier
Batt Insulation
Sheathing
Inner Brick
Outer Brick

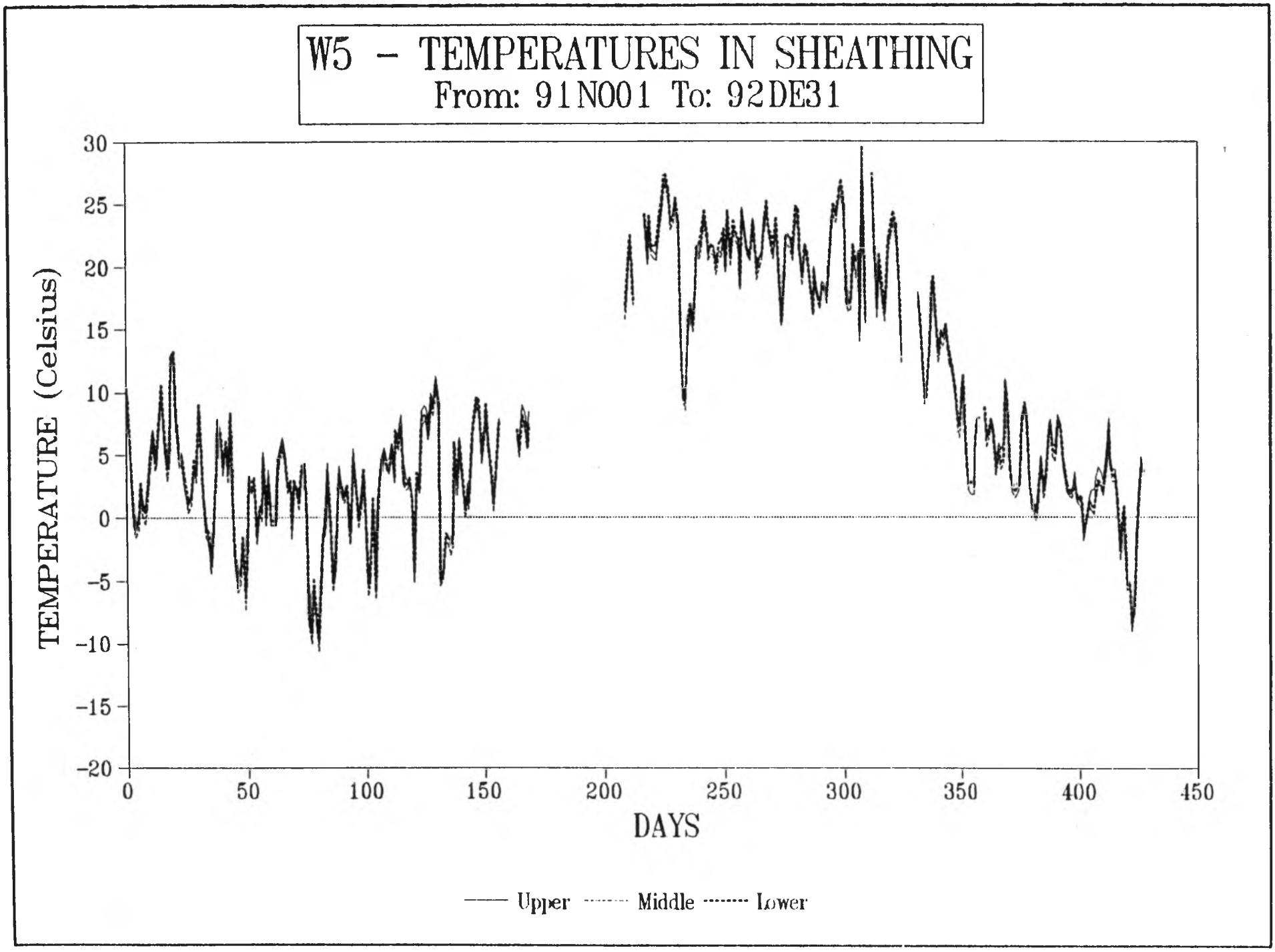
W5 - TEMPERATURES IN SHEATHING
From: 91N001 To: 92DE31
TEMPERATURE (Celsius)
30
25
20
15
10
5
0
-5
-10
-15
-20
0
50
100
150
200
250
300
350
400
450
DAYS
Upper
Middle
Lower

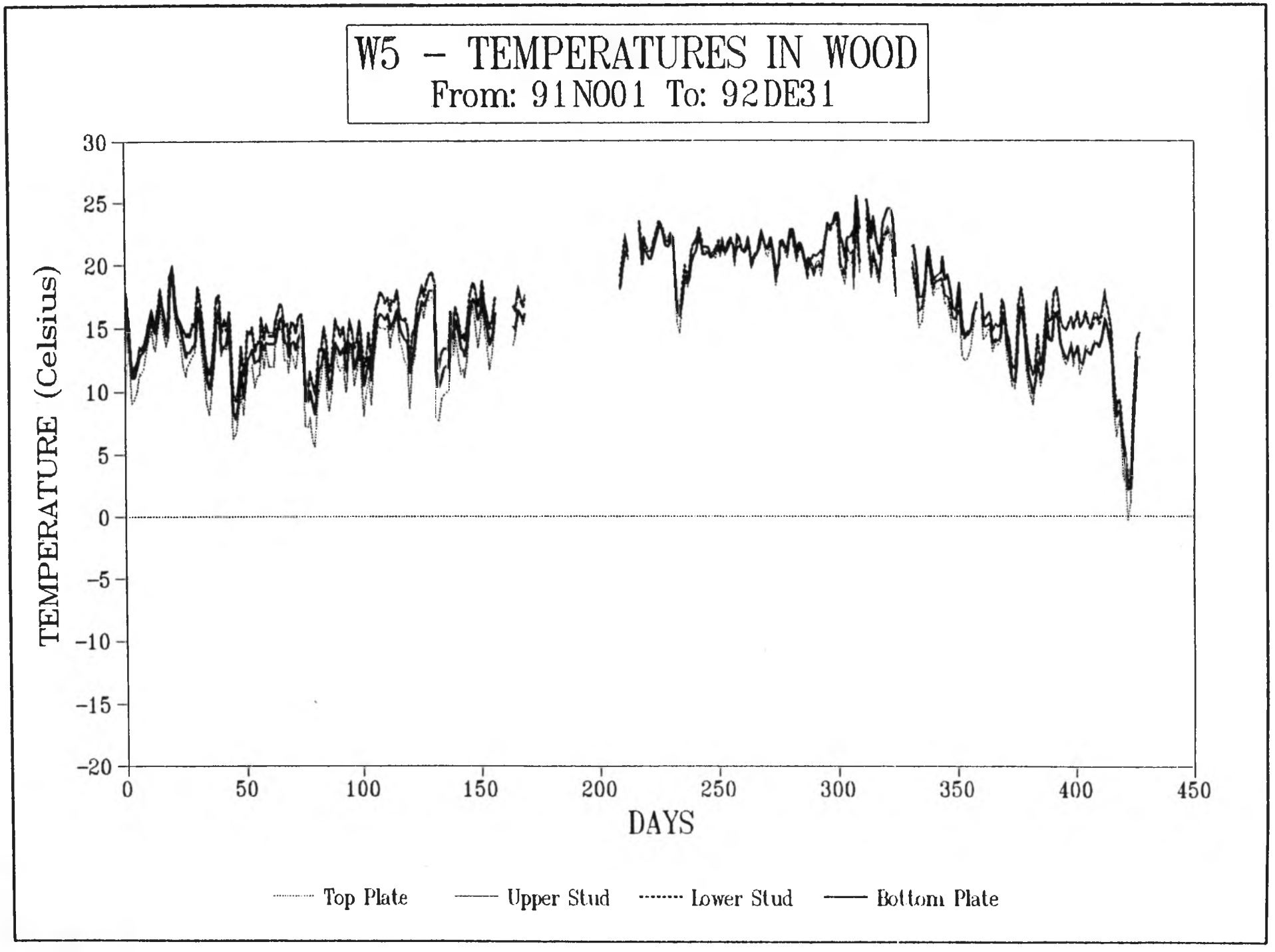
W5 – TEMPERATURES IN WOOD
From: 91N001 To: 92DE31
TEMPERATURE (Celsius)
30
25
20
15
10
5
0
-5
-10
-15
-20
0
50
100
150
200
250
300
350
400
450
DAYS
Top Plate
Upper Stud
Lower Stud
Bottom Plate

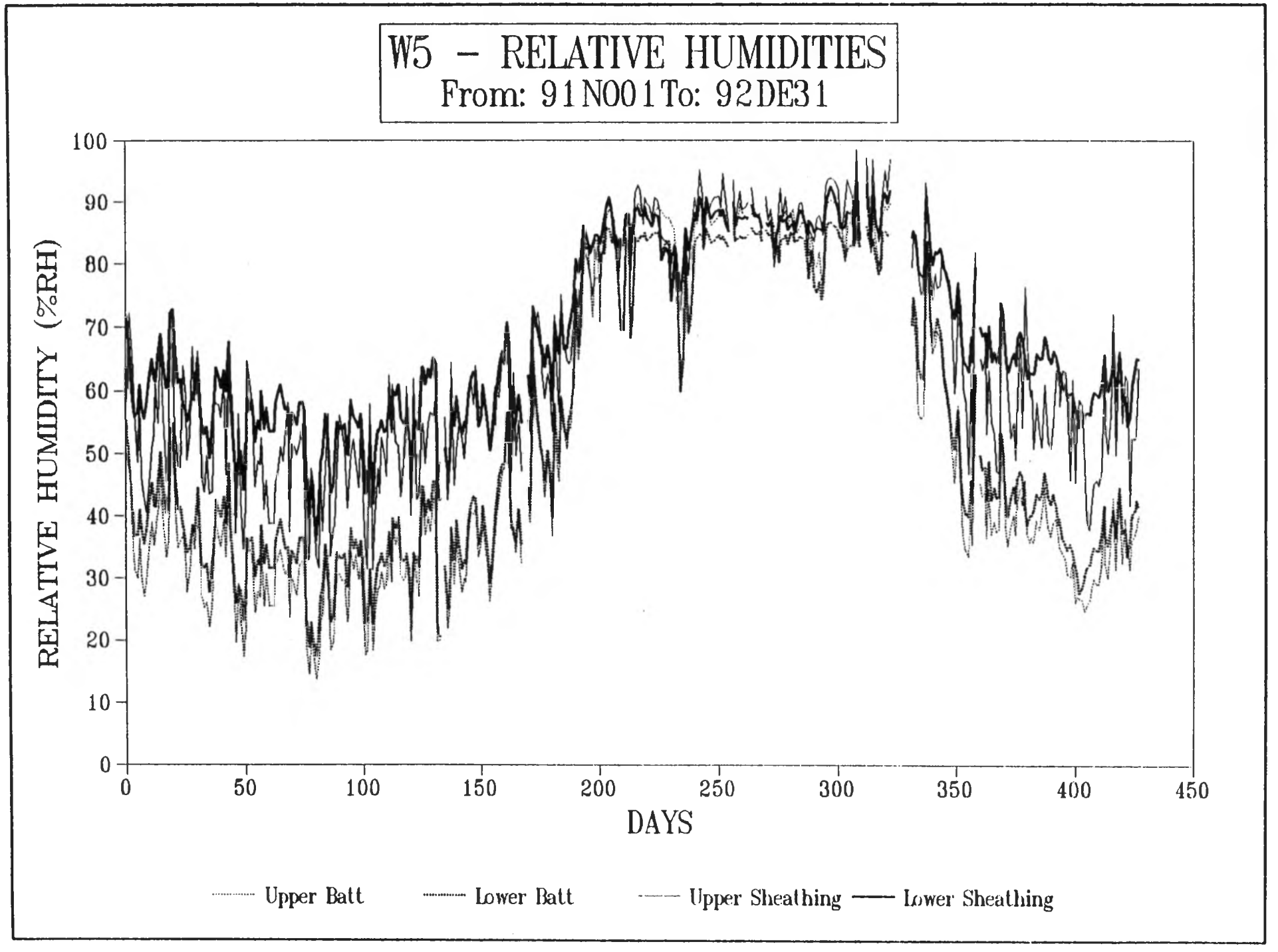
W5 – RELATIVE HUMIDITIES
From: 91N001To: 92DE31
RELATIVE HUMIDITY (%RH)
100
90
80
70
60
50
40
30
20
10
0
0
50
100
150
200
250
300
350
400
450
DAYS
Upper Batt
Lower Batt
Upper Sheathing
Lower Sheathing

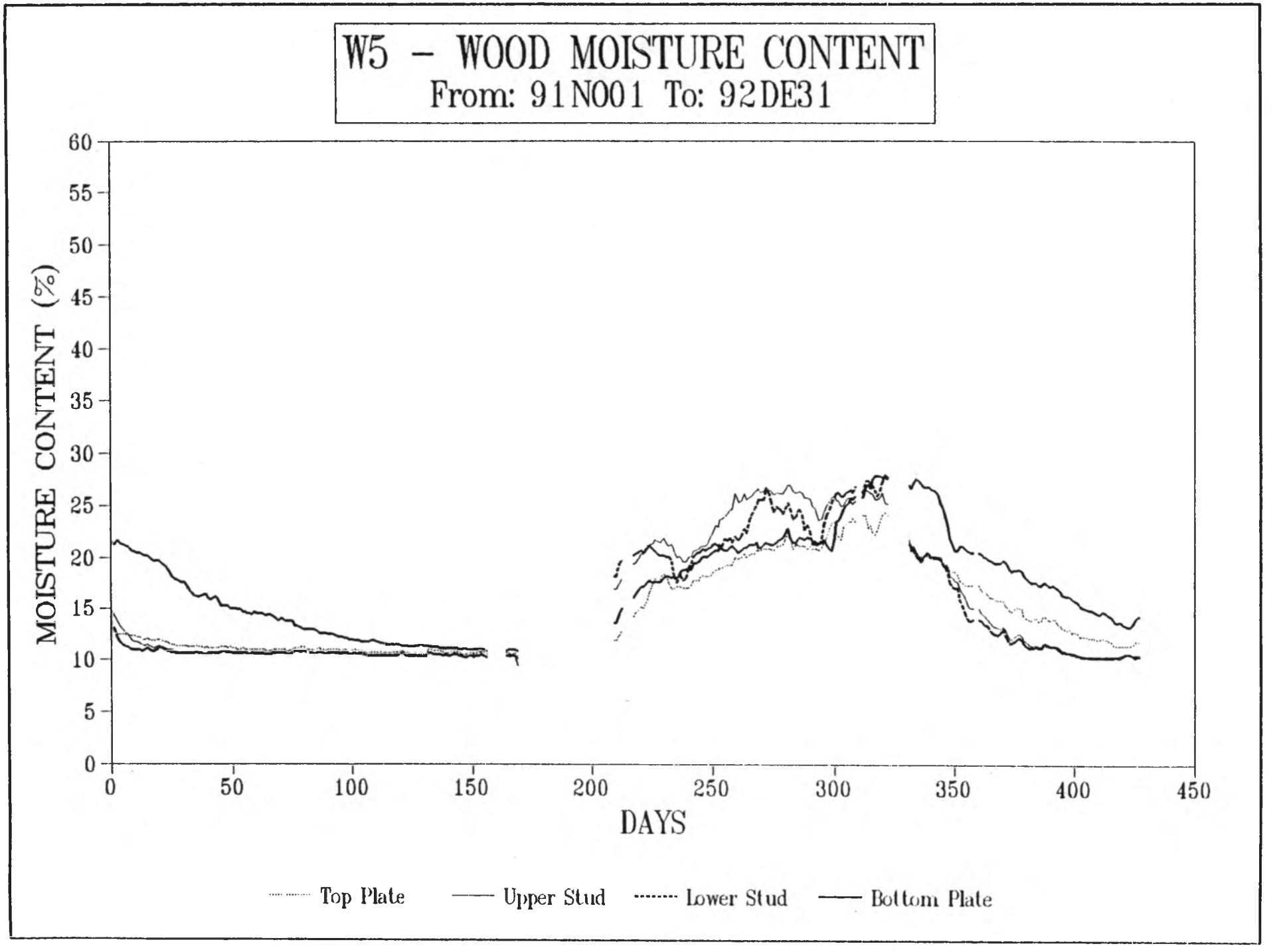
W5 - WOOD MOISTURE CONTENT
From: 91N001 To: 92DE31
MOISTURE CONTENT (%)
60
55
50
45
40
35
30
25
20
15
10
5
0
0
50
100
150
200
250
300
350
400
450
DAYS
Top Plate
Upper Stud
Lower Stud
Bottom Plate

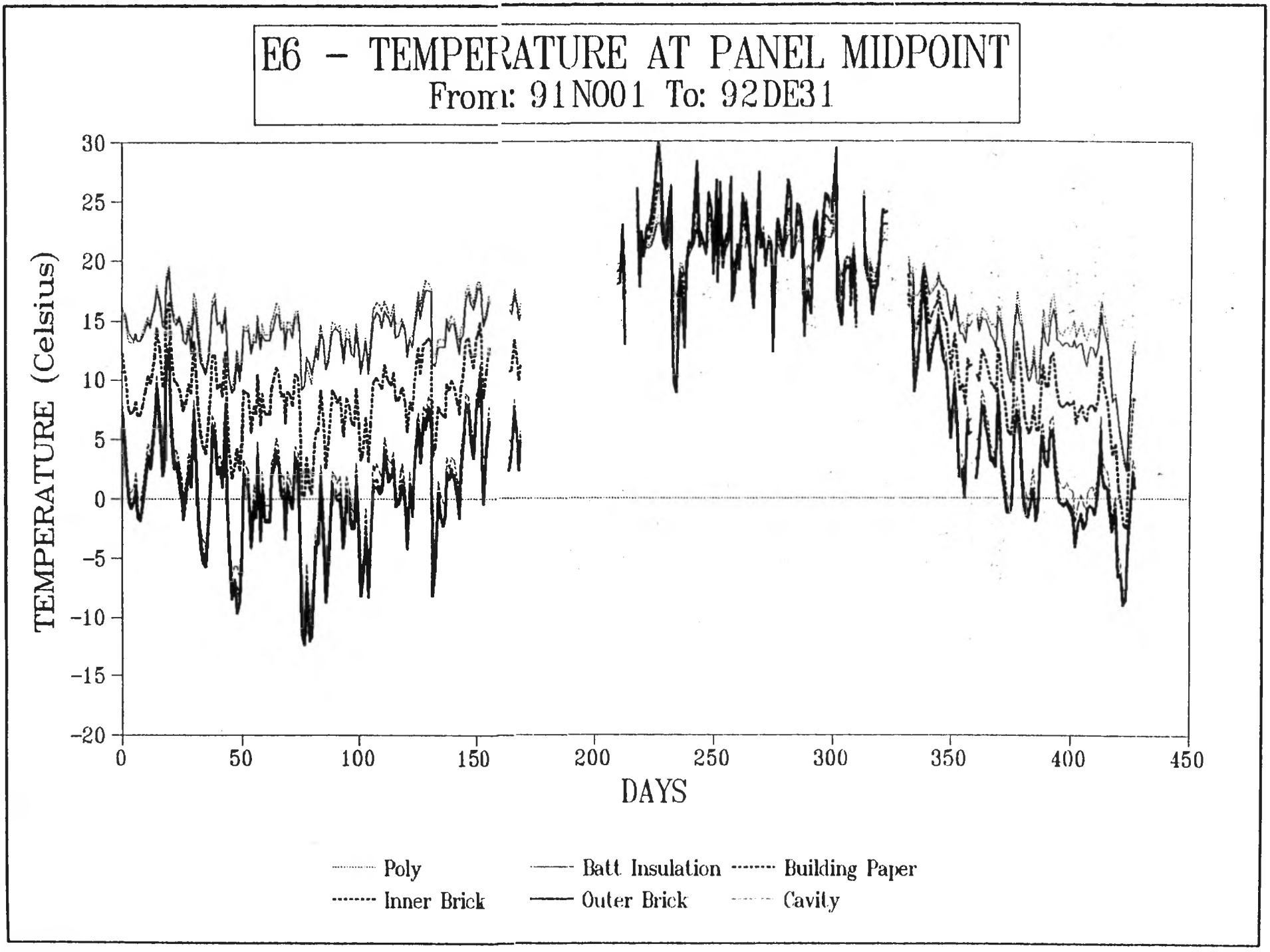
E6 – TEMPERATURE AT PANEL MIDPOINT
From: 91N001 To: 92DE31
TEMPERATURE (Celsius)
30
25
20
15
10
5
0
-5
-10
-15
-20
0
50
100
150
200
250
300
350
400
450
DAYS
Poly
Batt Insulation
Building Paper
Inner Brick
Outer Brick
Cavity

E6 – TEMPERATURES IN SHEATHING
From: 91N001 To: 92DE31

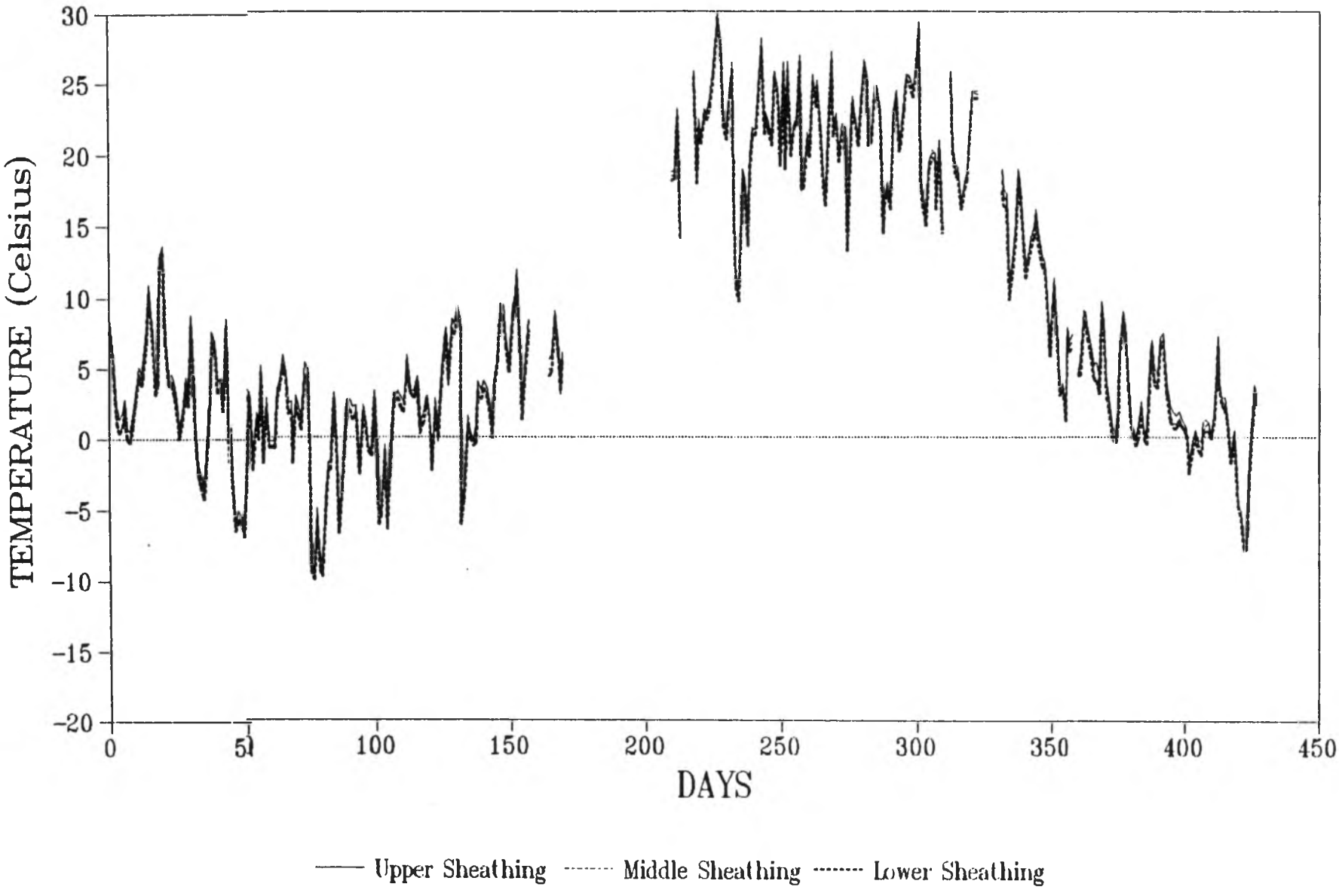

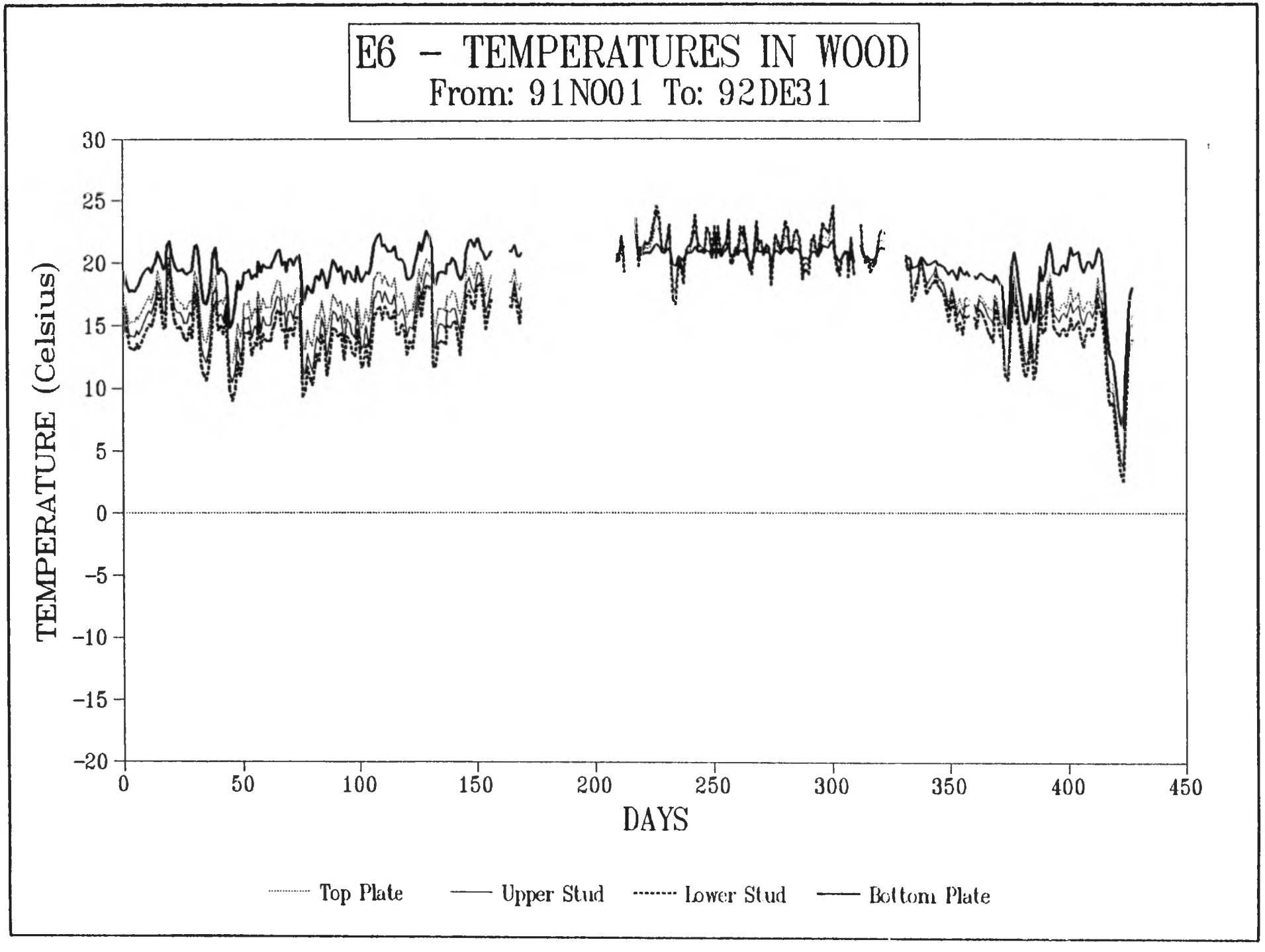
E6 – TEMPERATURES IN WOOD
From: 91N001 To: 92DE31
TEMPERATURE (Celsius)
30
25
20
15
10
5
0
-5
-10
-15
-20
0
50
100
150
200
250
300
350
400
450
DAYS
Top Plate
Upper Stud
Lower Stud
Bottom Plate

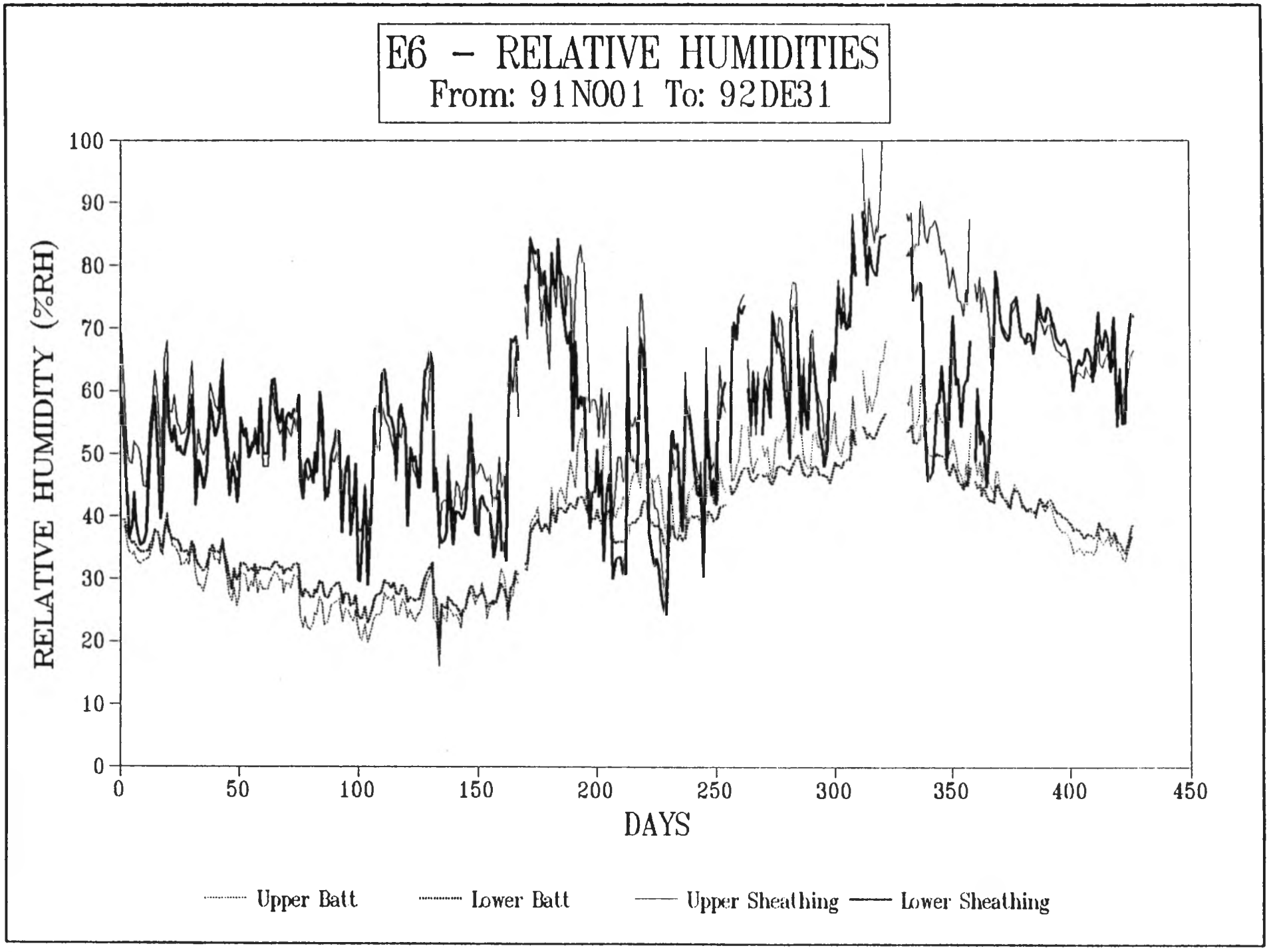
E6 – RELATIVE HUMIDITIES
From: 91N001 To: 92DE31
RELATIVE HUMIDITY (%RH)
100
90
80
70
60
50
40
30
20
10
0
0
50
100
150
200
250
300
350
400
450
DAYS
Upper Batt
Lower Batt
Upper Sheathing
Lower Sheathing

E6 – WOOD MOISTURE CONTENT
From: 91N001 To: 92DE31

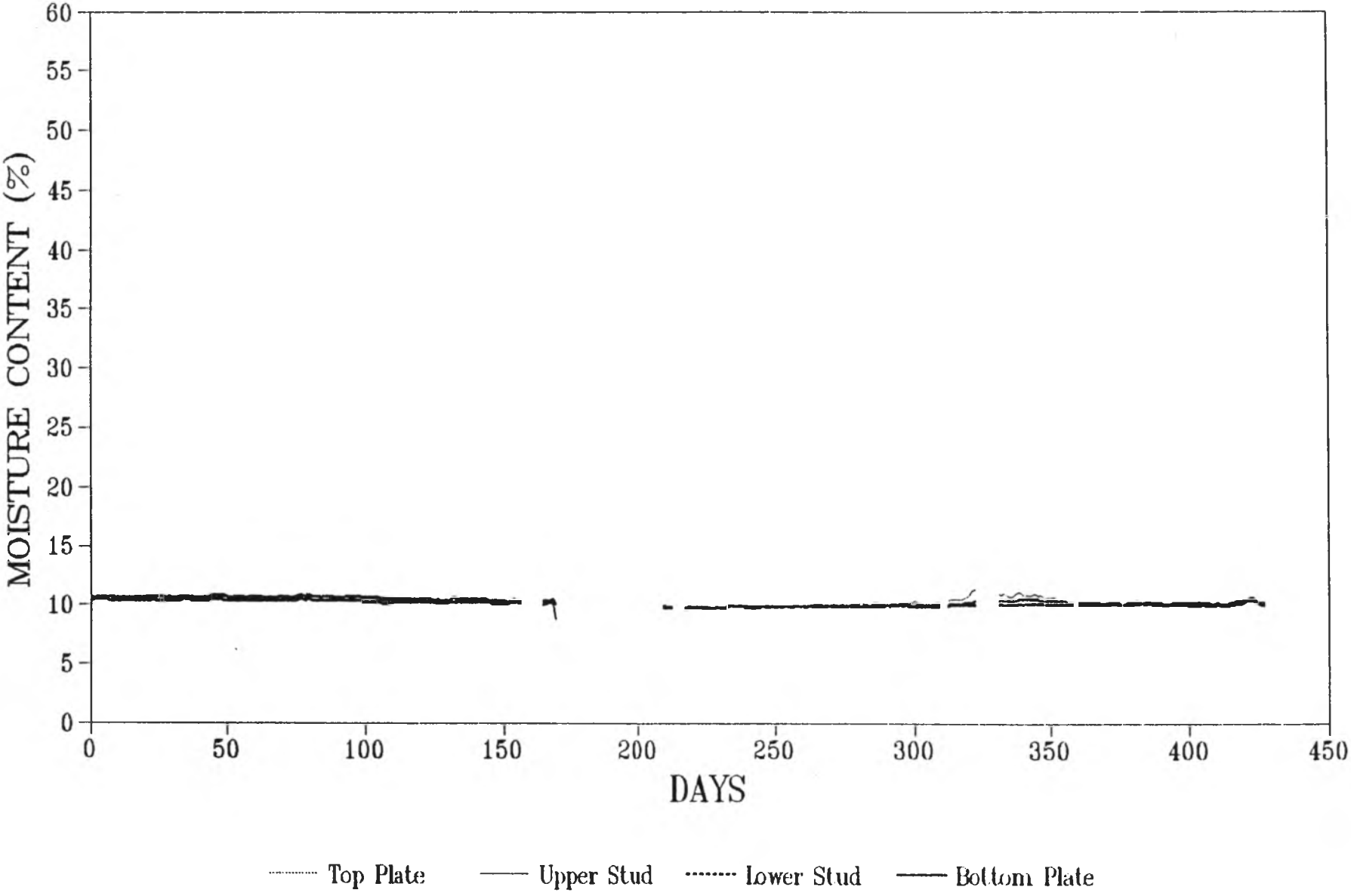

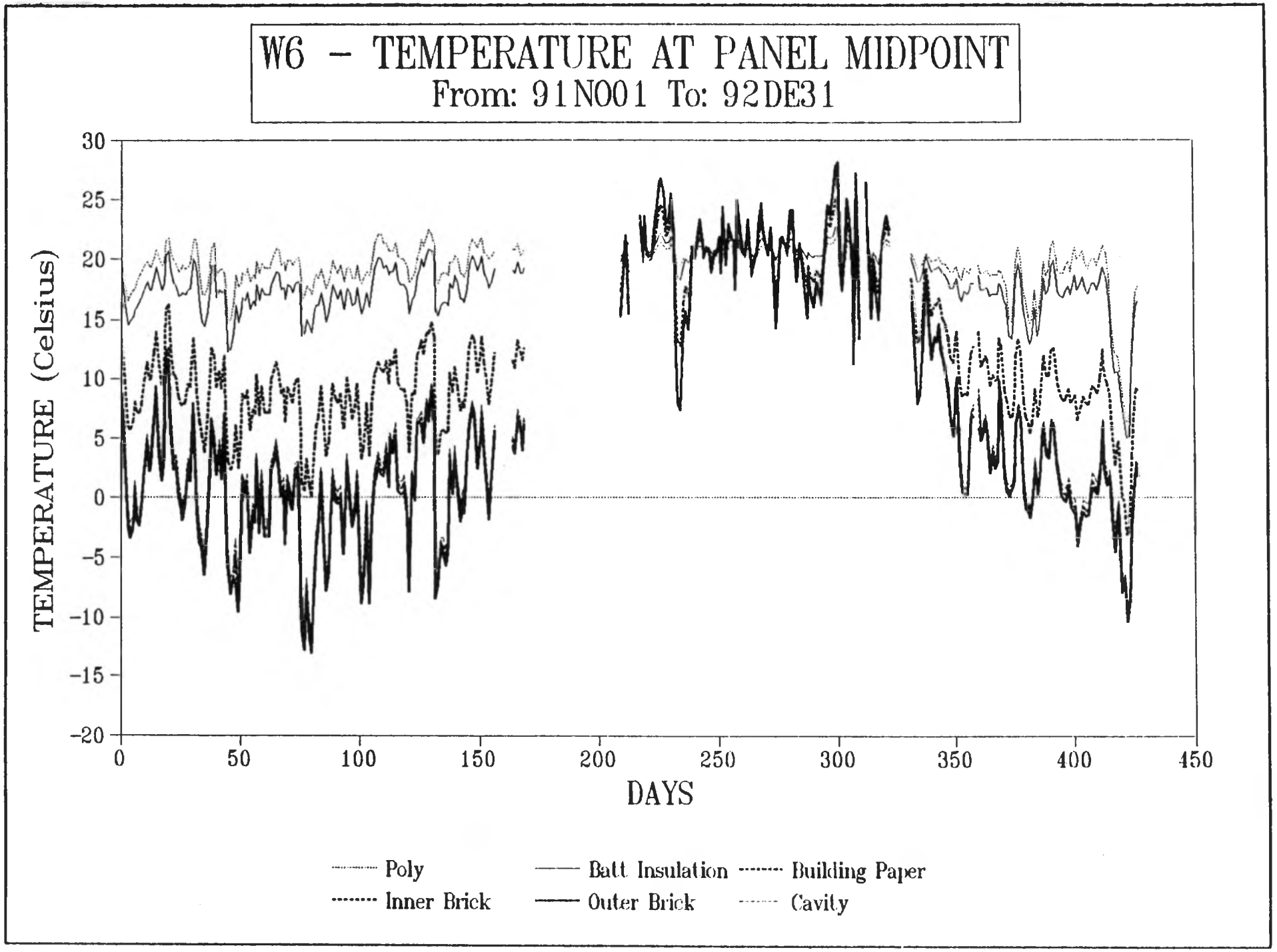
W6 - TEMPERATURE AT PANEL MIDPOINT
From: 91N001 To: 92DE31
TEMPERATURE (Celsius)
30
25
20
15
10
5
0
-5
-10
-15
-20
0
50
100
150
200
250
300
350
400
450
DAYS
Poly
Batt Insulation
Building Paper
Inner Brick
Outer Brick
Cavity

cavity

W6 – TEMPERATURES IN ~~SHEATHING~~

From: 91N001 To: 92DE31

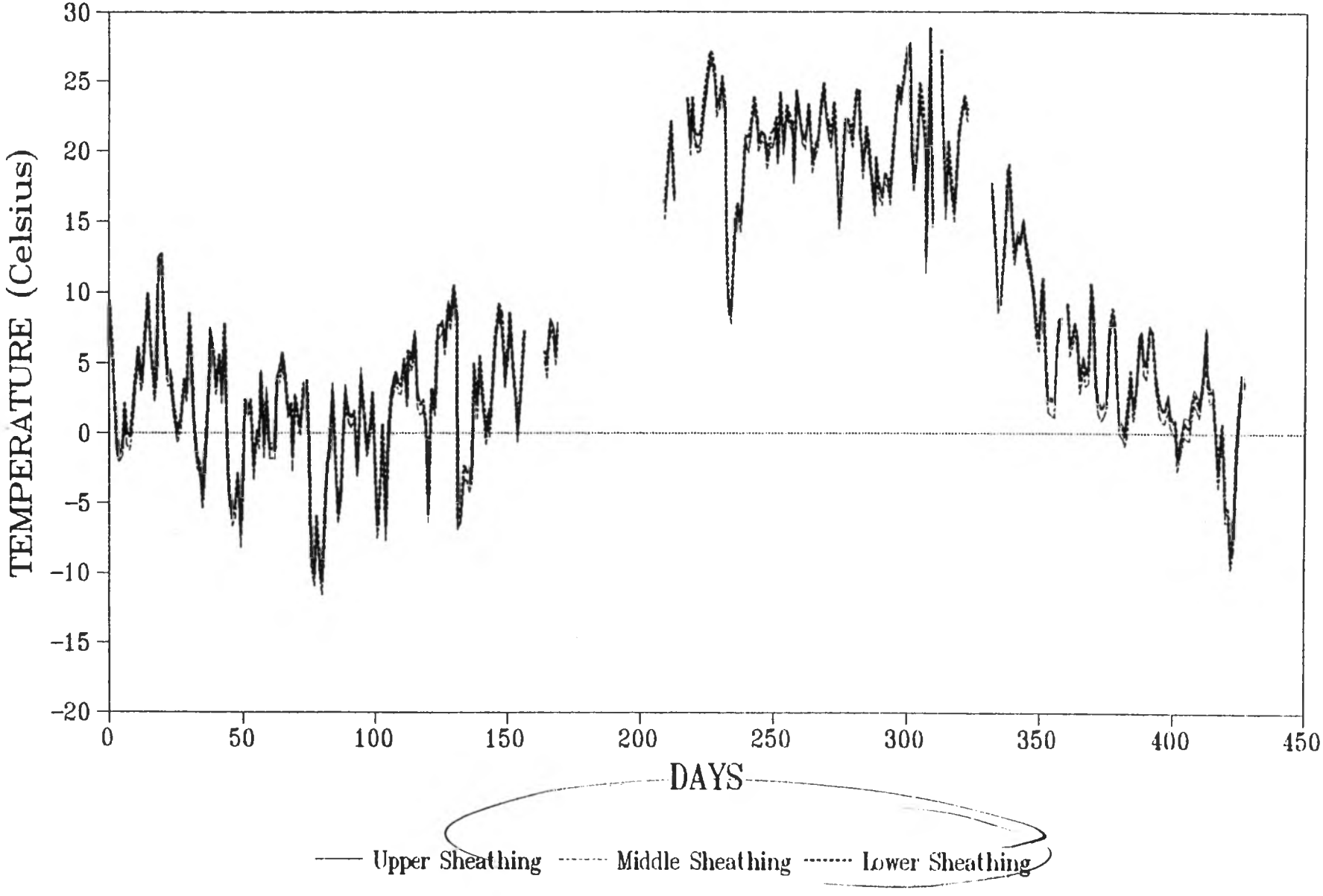

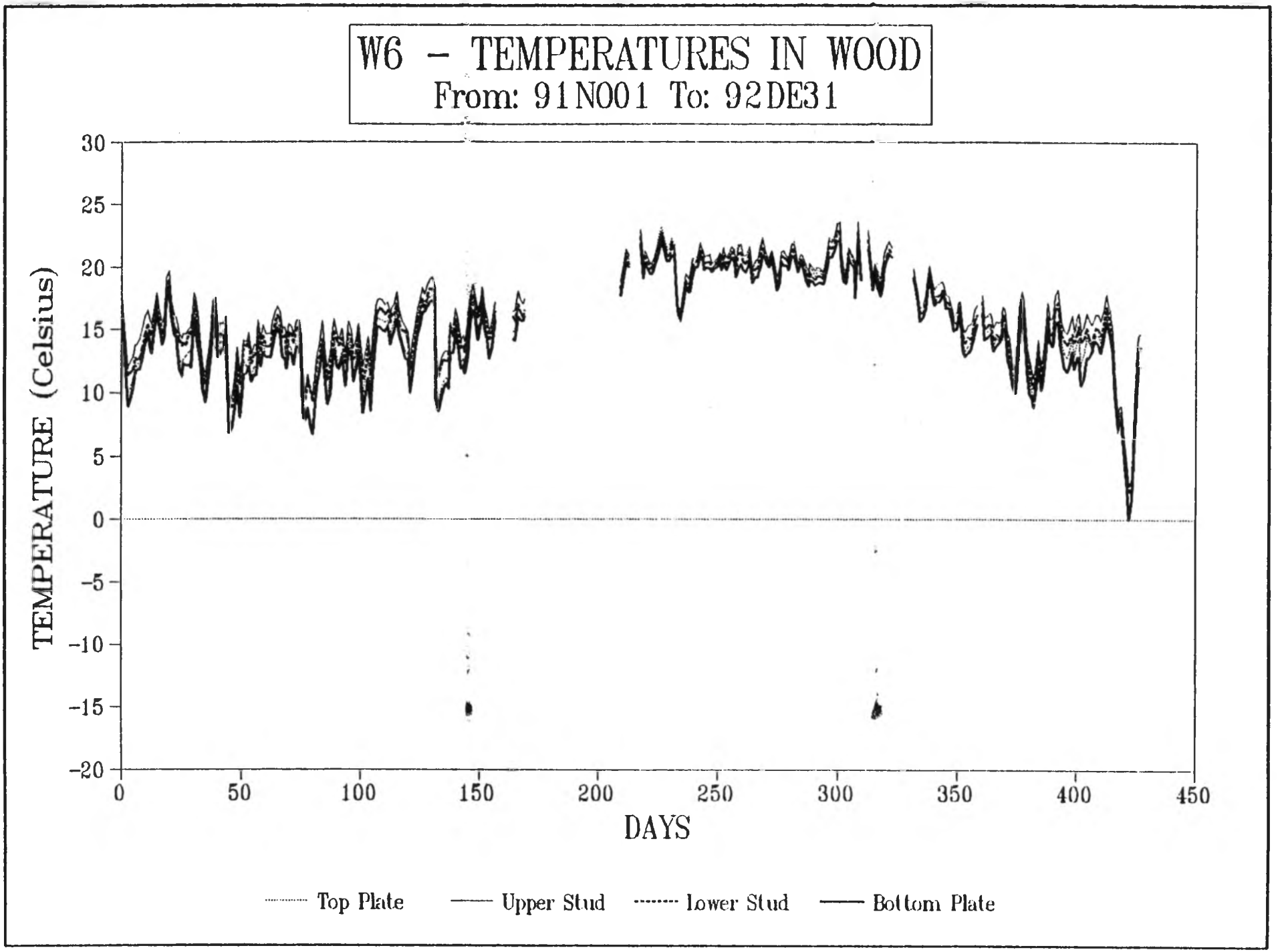
W6 - TEMPERATURES IN WOOD
From: 91N001 To: 92DE31
TEMPERATURE (Celsius)
30
25
20
15
10
5
0
-5
-10
-15
-20
0
50
100
150
200
250
300
350
400
450
DAYS
Top Plate
Upper Stud
Lower Stud
Bottom Plate

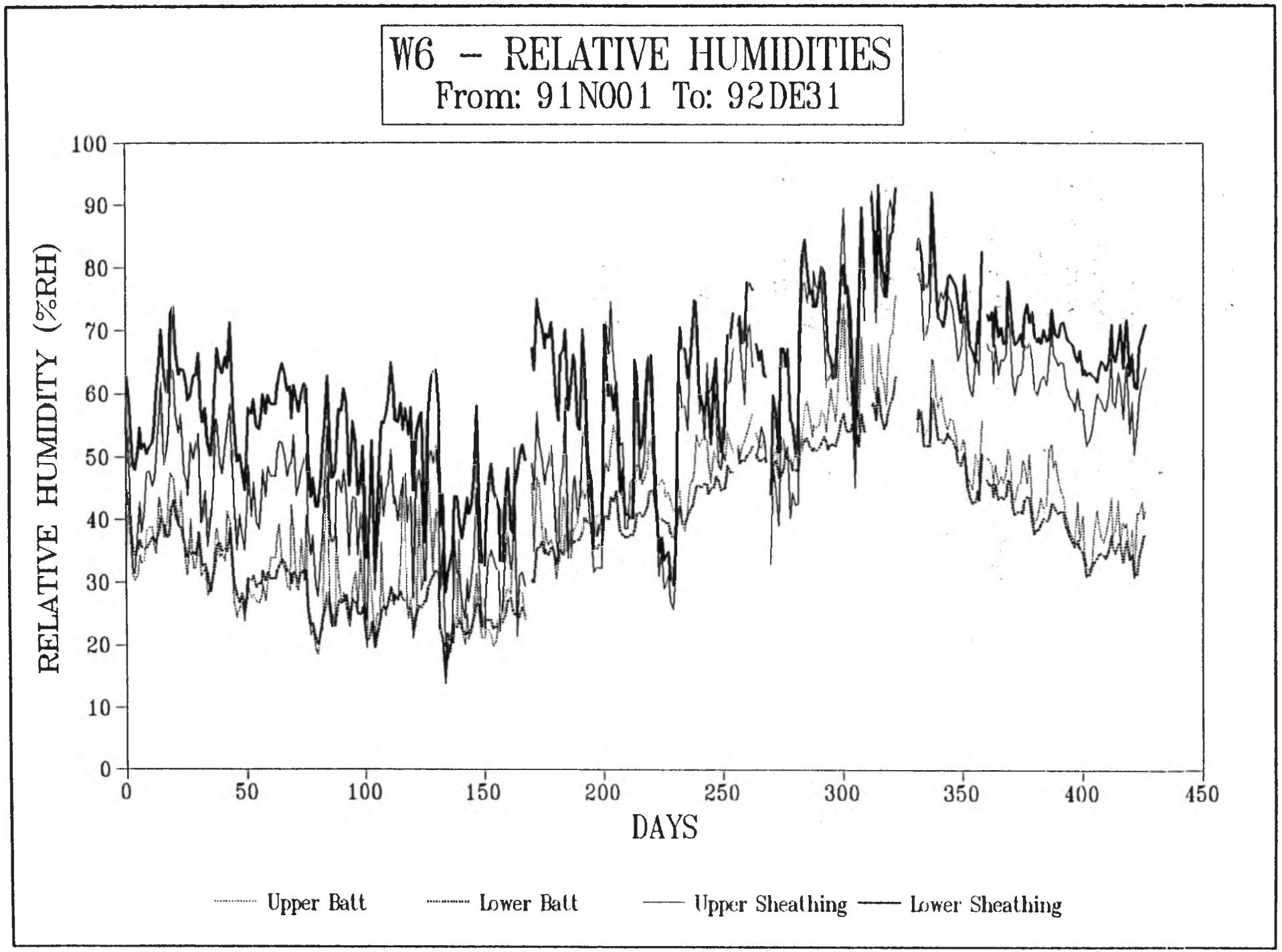
W6 – RELATIVE HUMIDITIES
From: 91N001 To: 92DE31
RELATIVE HUMIDITY (%RH)
100
90
80
70
60
50
40
30
20
10
0
0
50
100
150
200
250
300
350
400
450
DAYS
Upper Batt
Lower Batt
Upper Sheathing
Lower Sheathing

W6 – WOOD MOISTURE CONTENT
From: 91N001 To: 92DE31

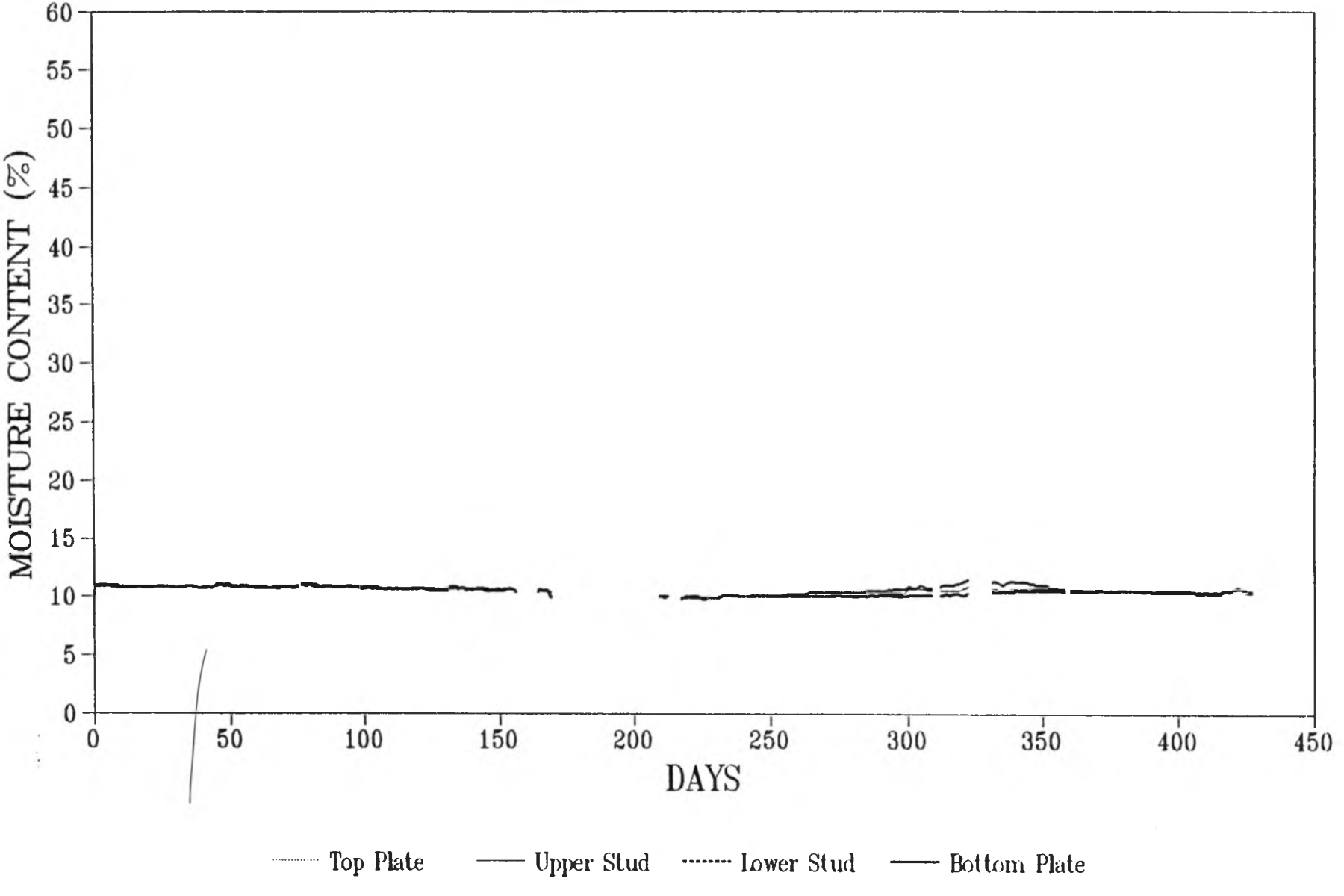

Appendix B

Graphed Data

Daily Variations

February 9, 1992

and

July 24, 1992

92JL24.Temp.E4

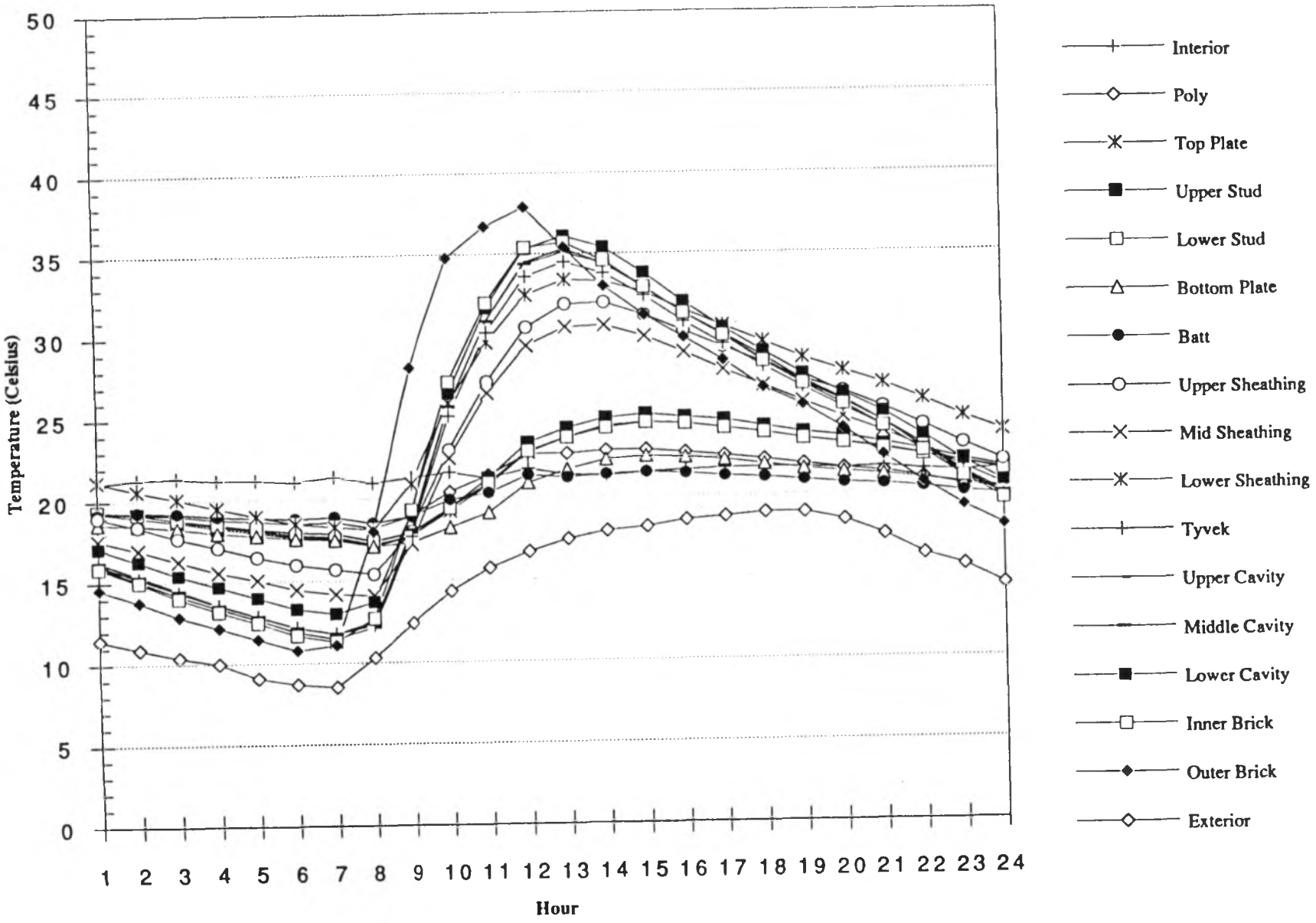

92JL24.Temp.W4

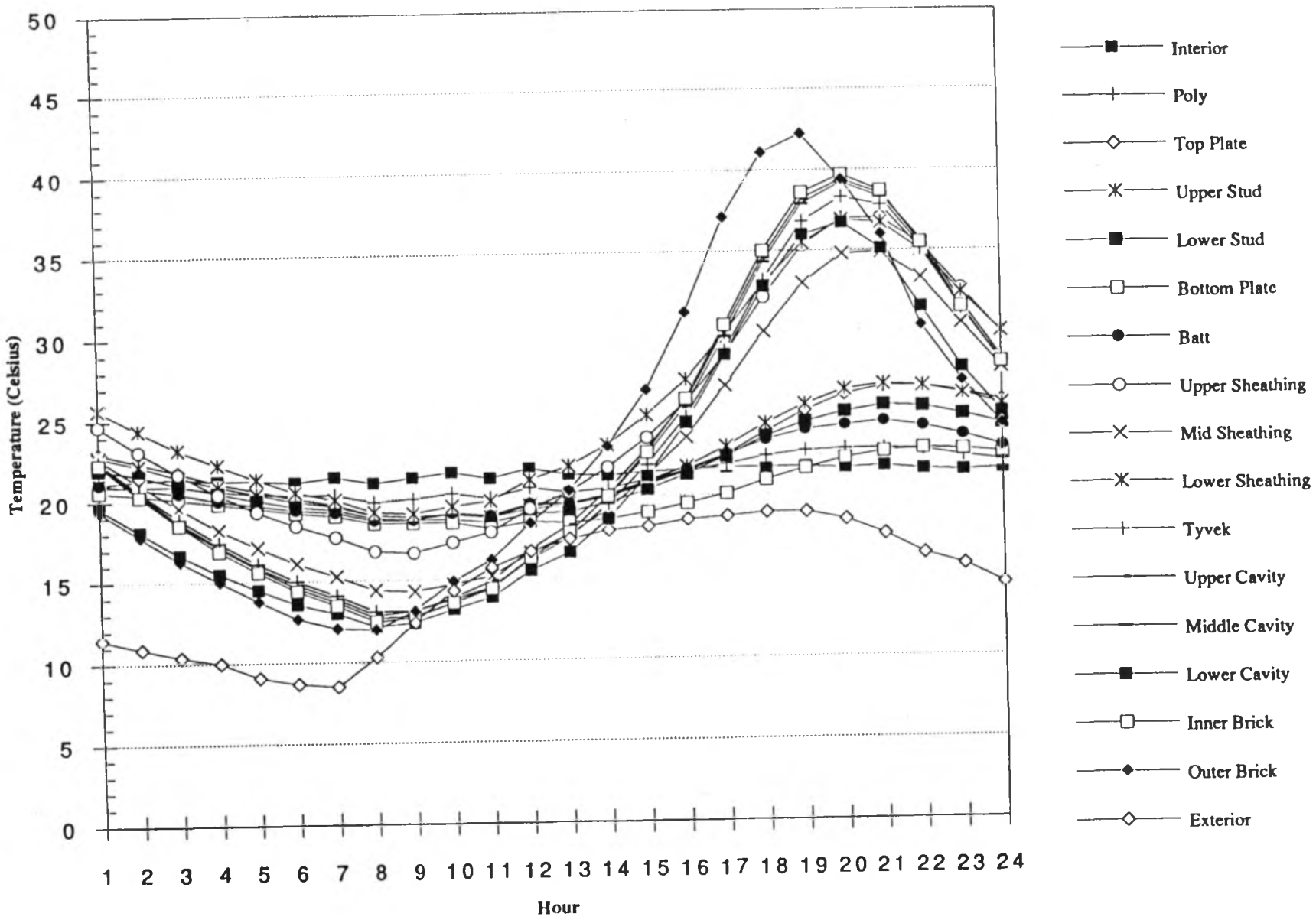

92JL24.Temp.W5

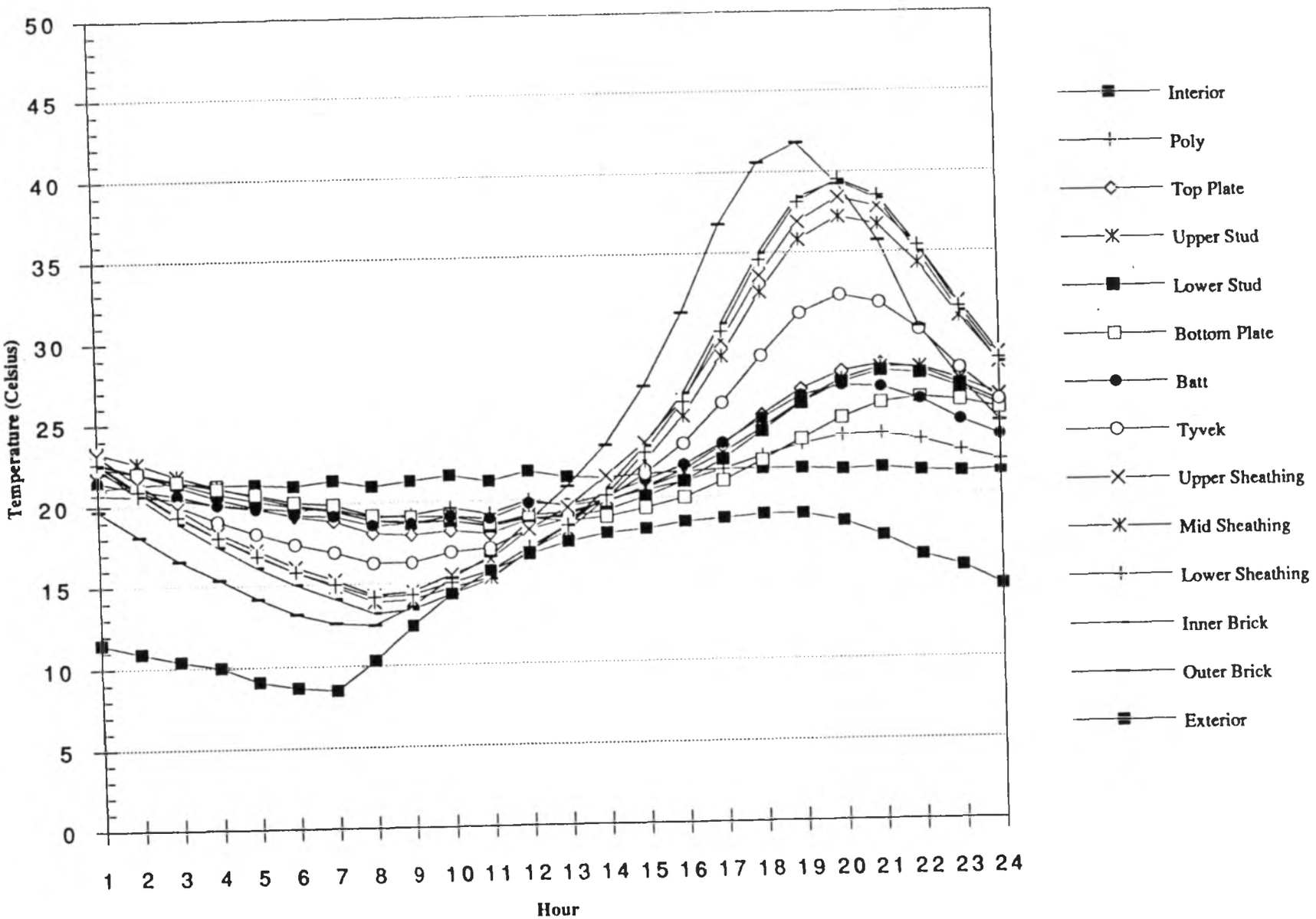

92JL24.Temp.E5

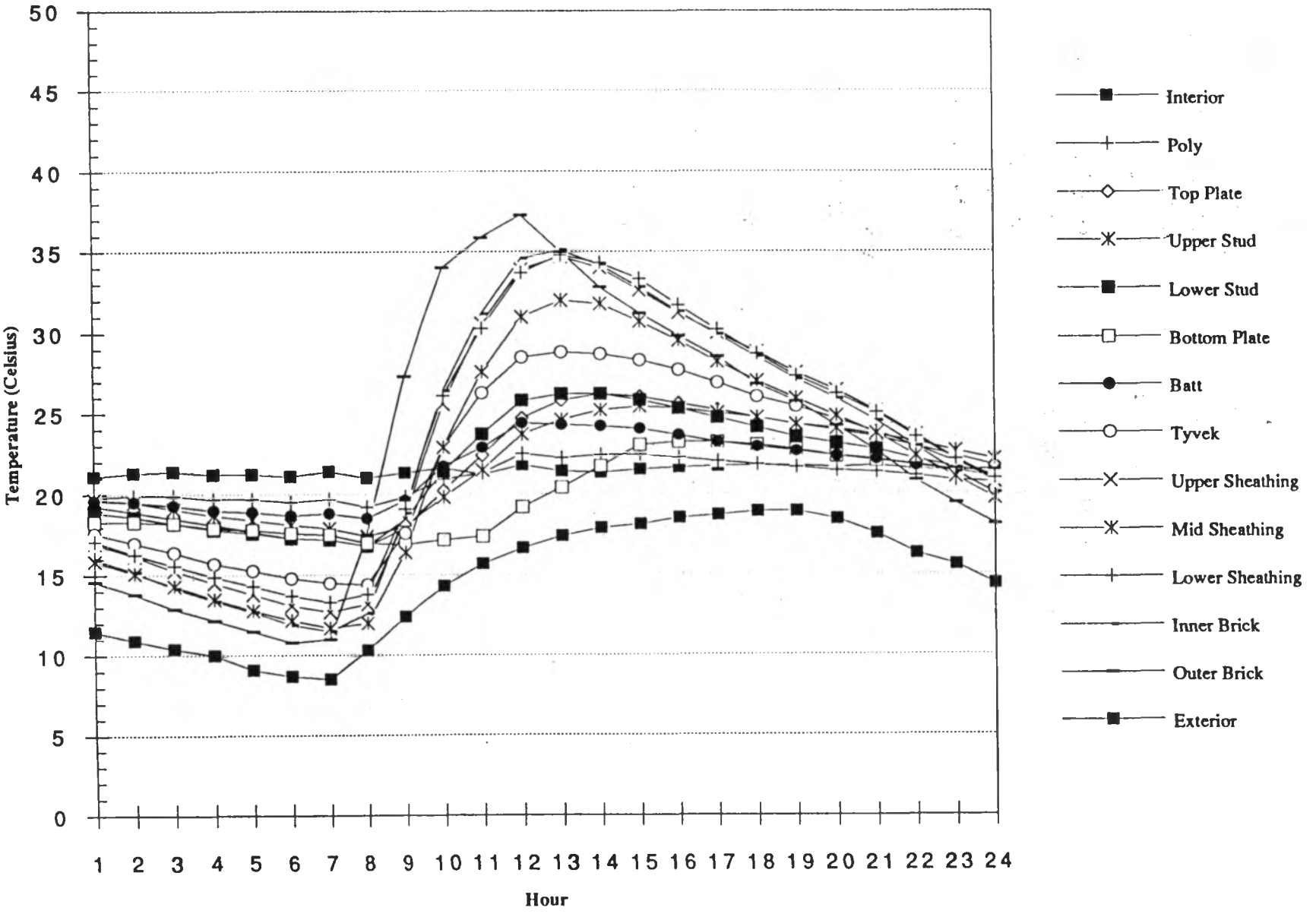

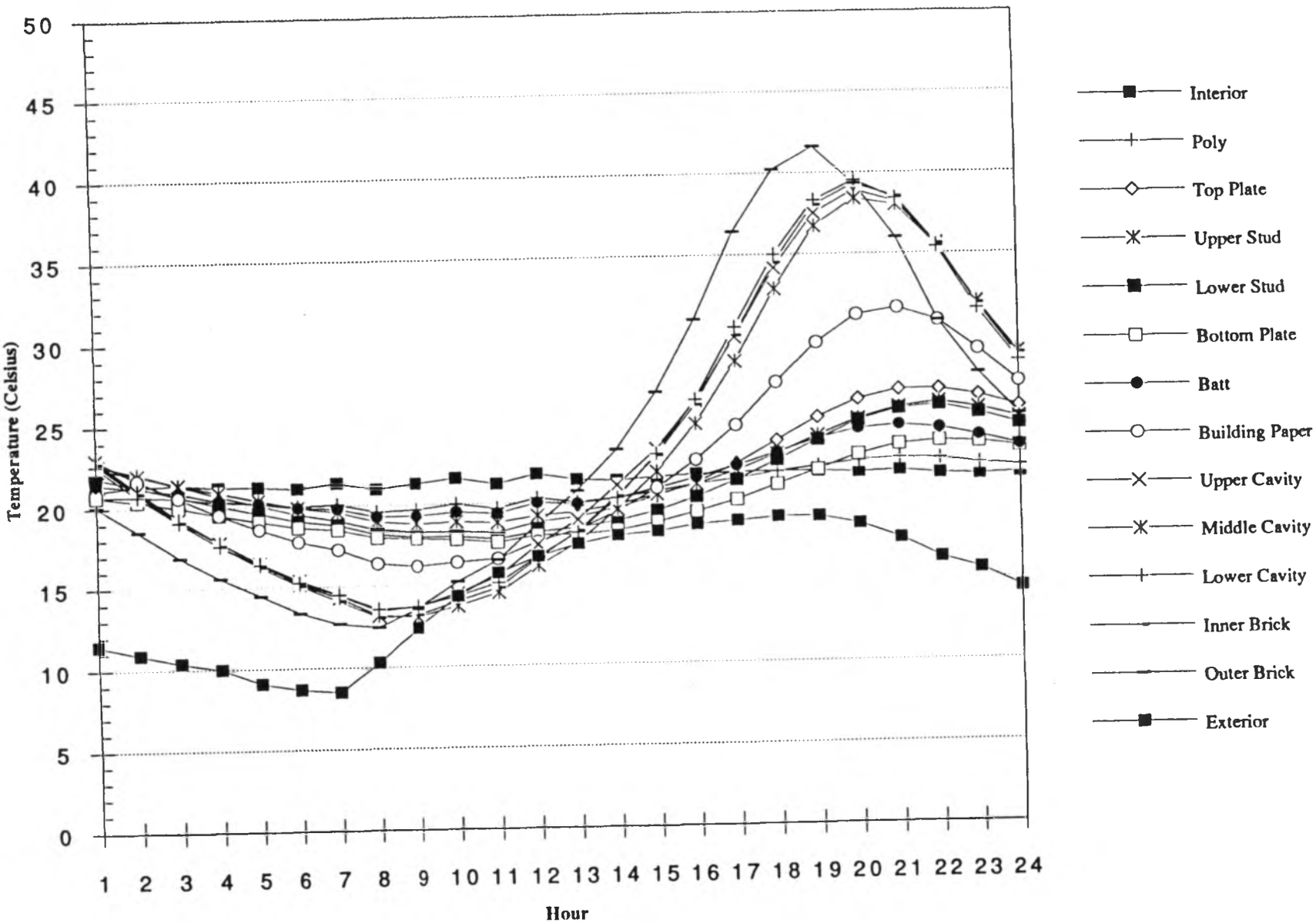
50
45
40
35
30
25
20
15
10
5
0
Temperature (Celsius)
1 2 3 4 5 6 7 8 9 10 11 12 13 14 15 16 17 18 19 20 21 22 23 24
Hour
Interior
Poly
Top Plate
Upper Stud
Lower Stud
Bottom Plate
Batt
Building Paper
Upper Cavity
Middle Cavity
Lower Cavity
Inner Brick
Outer Brick
Exterior

92JL24.Temp.E6

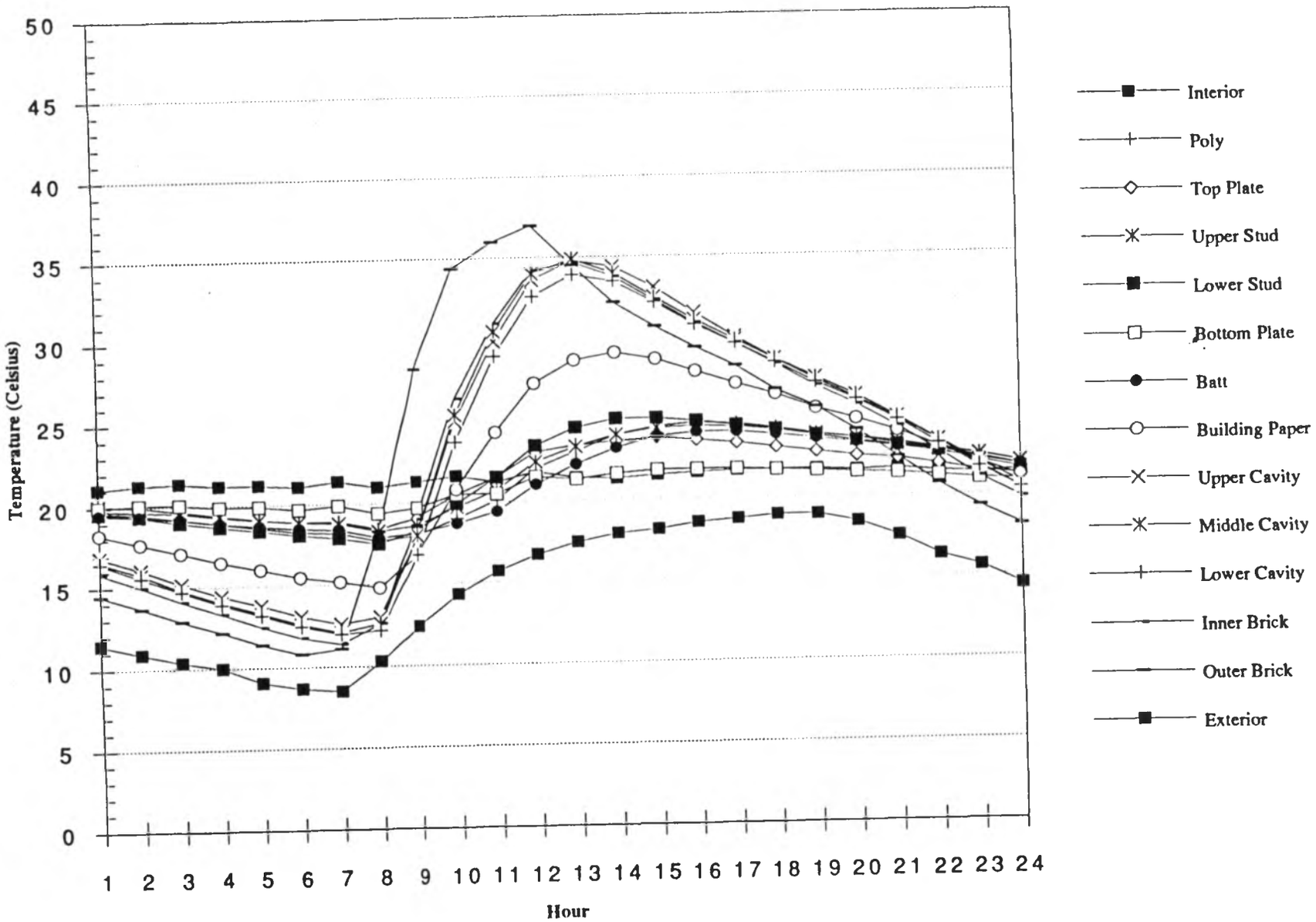

92JL24.RH.E4

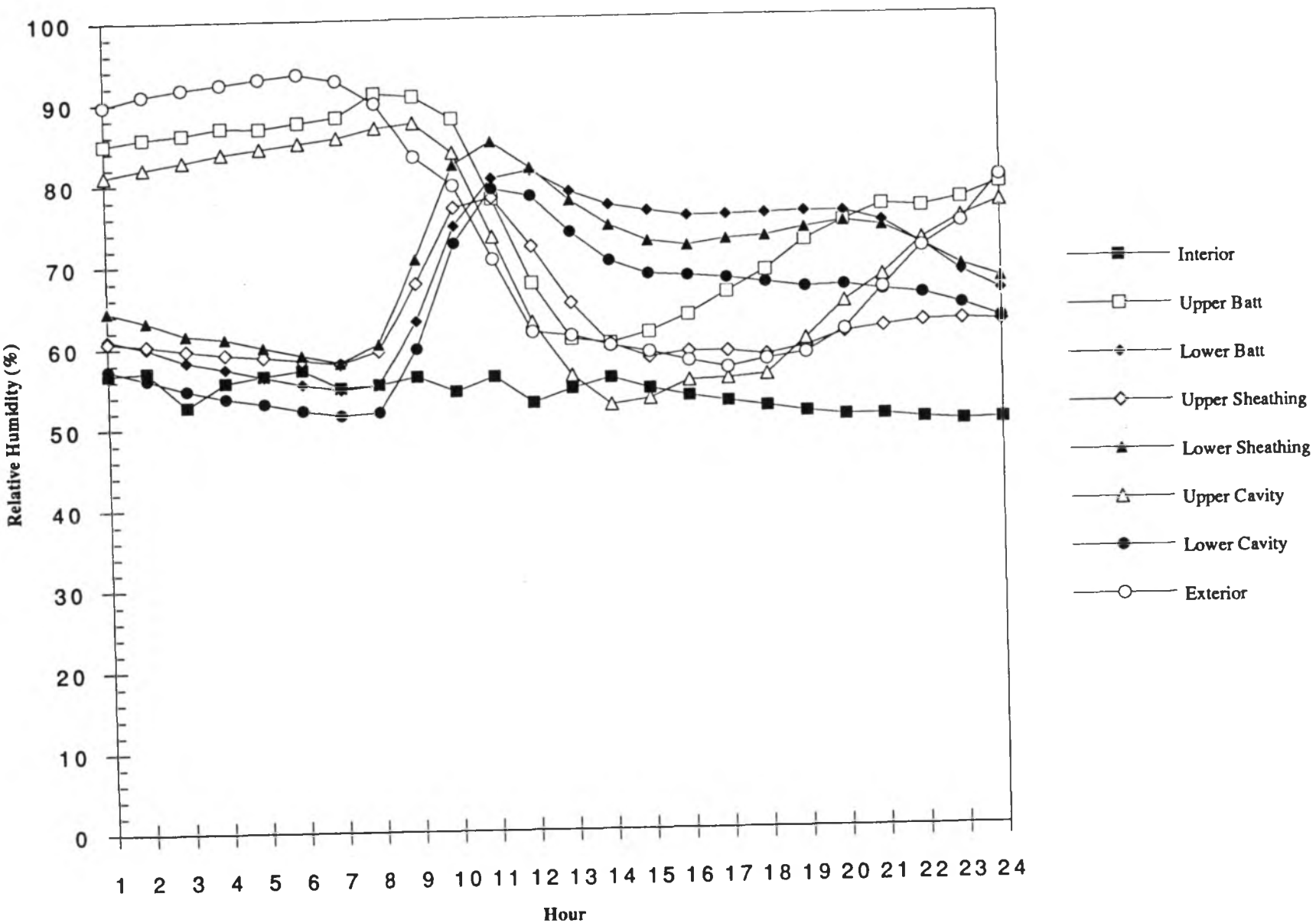
100
90
80
70
60
50
40
30
20
10
0
Relative Humidity (%)
1 2 3 4 5 6 7 8 9 10 11 12 13 14 15 16 17 18 19 20 21 22 23 24
Hour
Interior
Upper Batt
Lower Batt
Upper Sheathing
Lower Sheathing
Upper Cavity
Lower Cavity
Exterior

92JL24.RH.W4

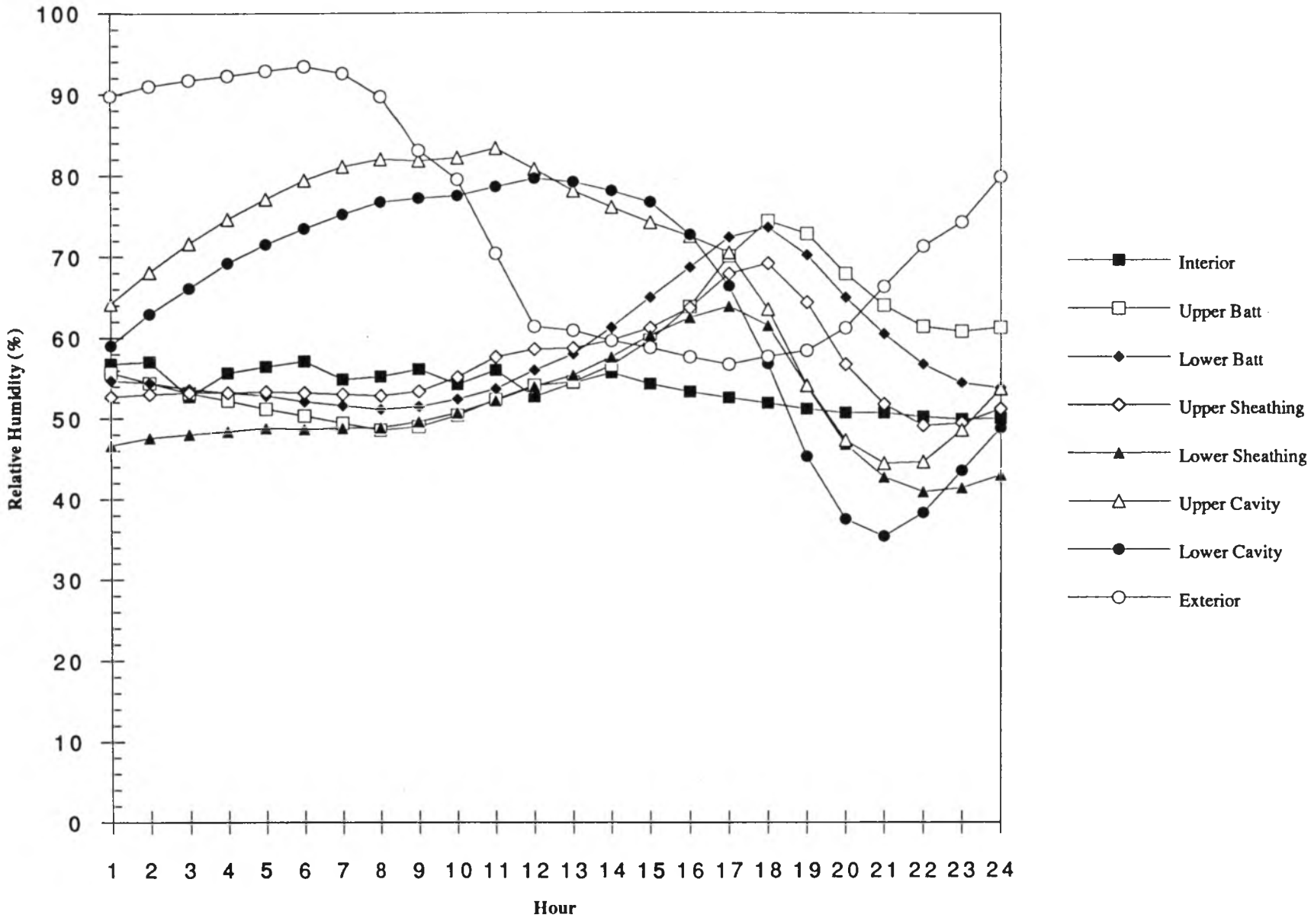
Relative Humidity (%)
100
90
80
70
60
50
40
30
20
10
0
1 2 3 4 5 6 7 8 9 10 11 12 13 14 15 16 17 18 19 20 21 22 23 24
Hour
Interior
Upper Batt
Lower Batt
Upper Sheathing
Lower Sheathing
Upper Cavity
Lower Cavity
Exterior

92JL24.RH.E5

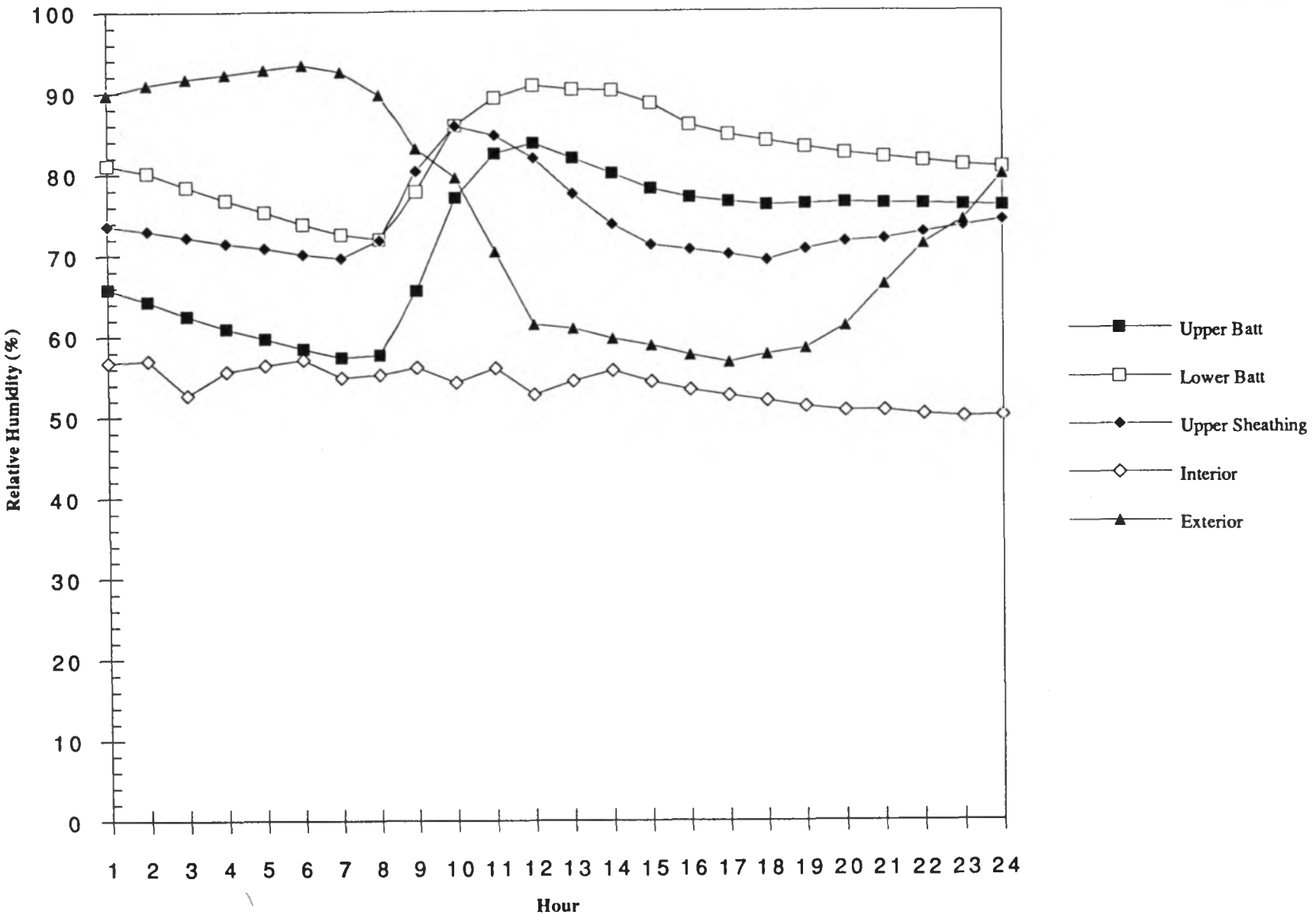
100
90
80
70
60
50
40
30
20
10
0
Relative Humidity (%)
1 2 3 4 5 6 7 8 9 10 11 12 13 14 15 16 17 18 19 20 21 22 23 24
Hour
Upper Batt
Lower Batt
Upper Sheathing
Interior
Exterior

92JL24.RH.W5

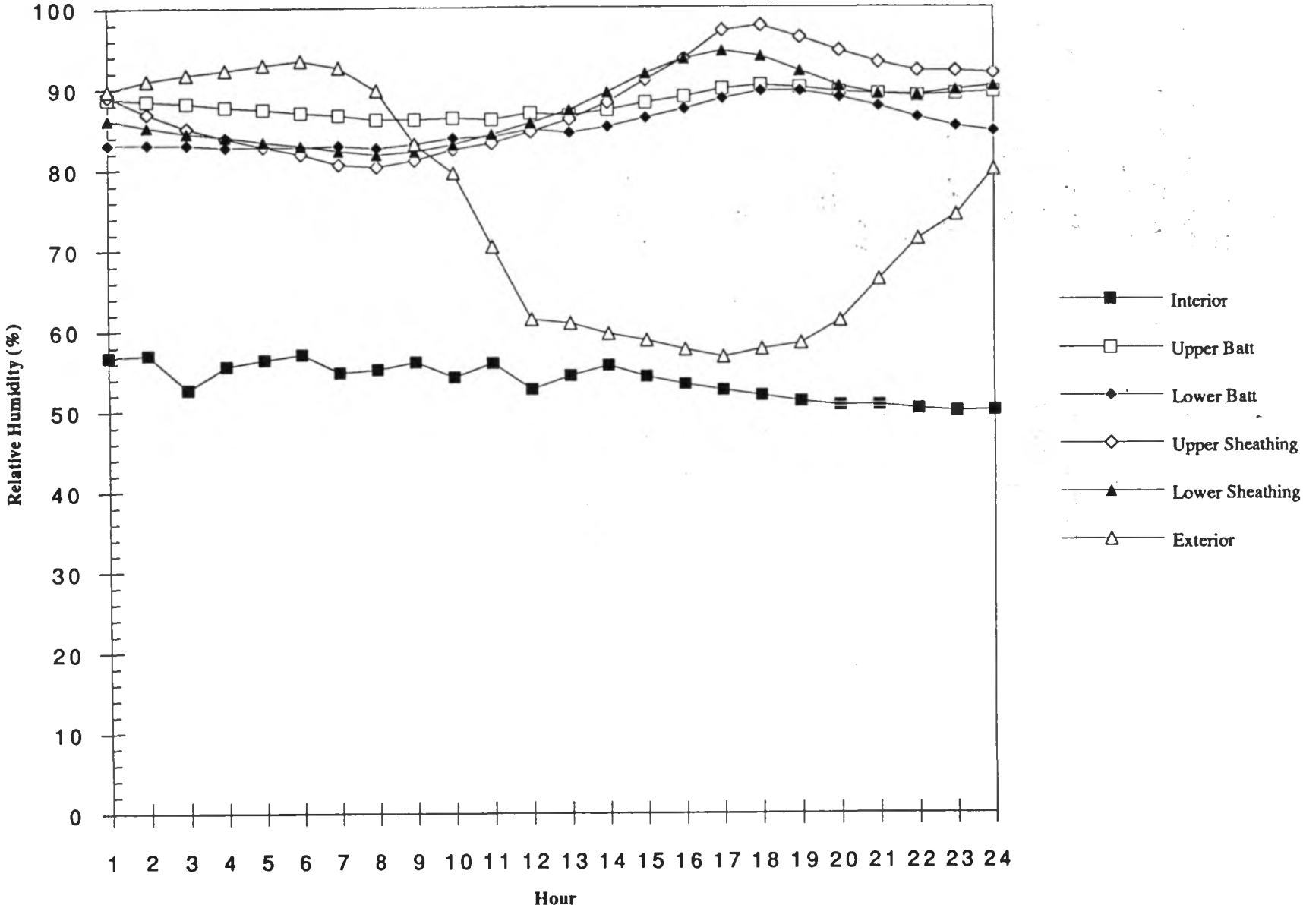
100
90
80
70
60
50
40
30
20
10
0
Relative Humidity (%)
1 2 3 4 5 6 7 8 9 10 11 12 13 14 15 16 17 18 19 20 21 22 23 24
Hour
Interior
Upper Batt
Lower Batt
Upper Sheathing
Lower Sheathing
Exterior

92JL24.RH.W6

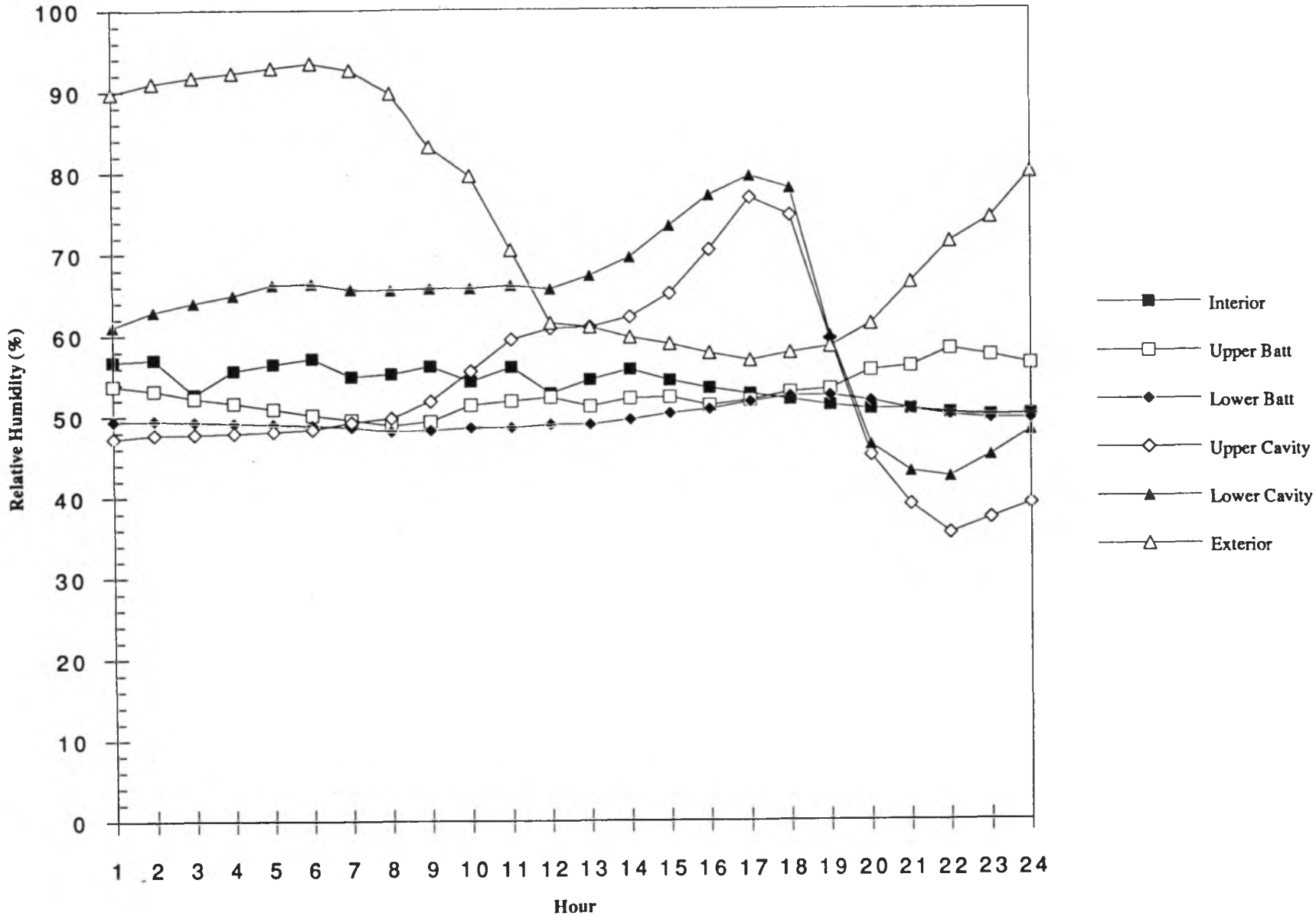
100
90
80
70
60
50
40
30
20
10
0
Relative Humidity (%)
1 2 3 4 5 6 7 8 9 10 11 12 13 14 15 16 17 18 19 20 21 22 23 24
Hour
Interior
Upper Batt
Lower Batt
Upper Cavity
Lower Cavity
Exterior

92JL24.RH.E6

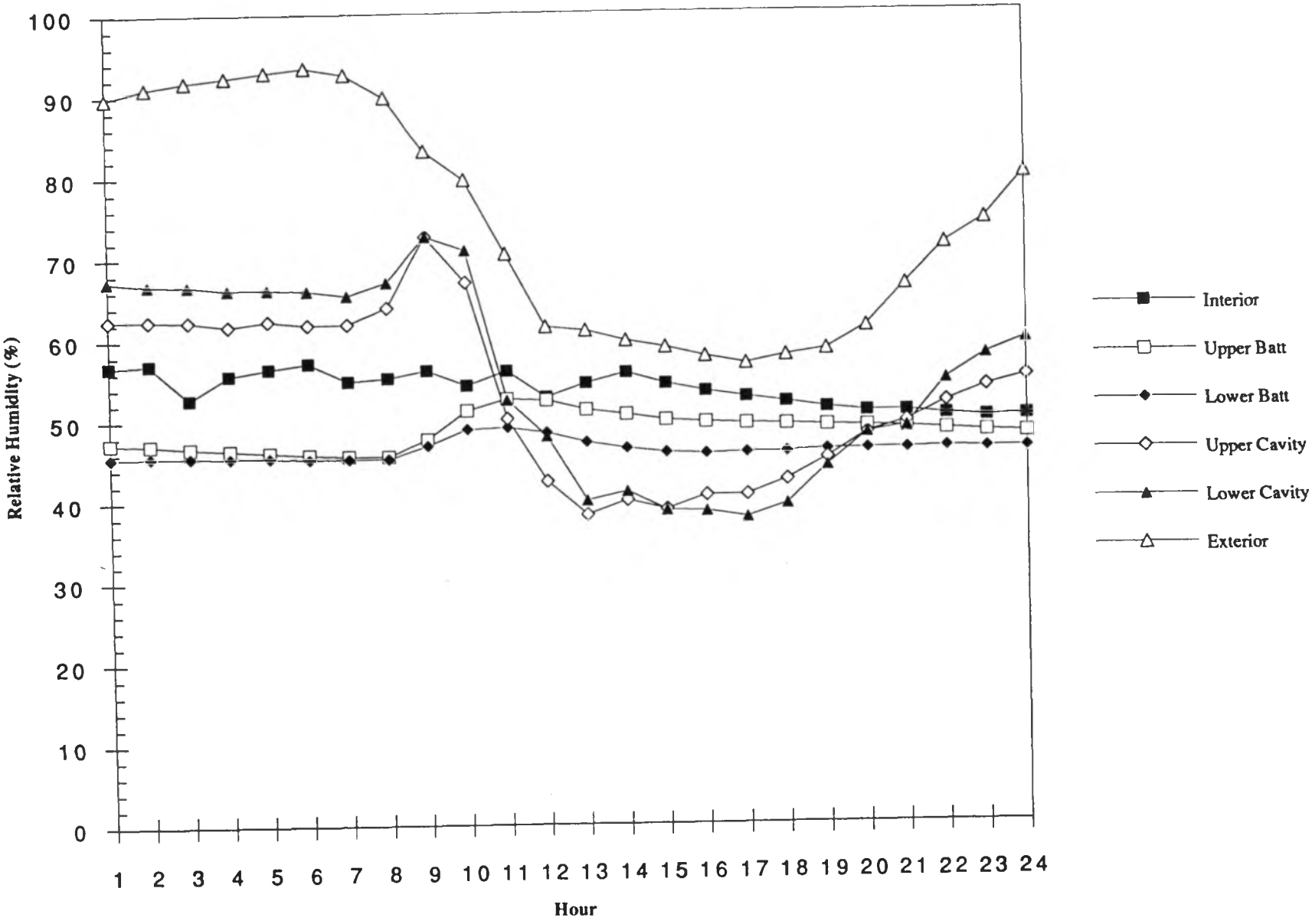
100
90
80
70
60
50
40
30
20
10
0
Relative Humidity (%)
1 2 3 4 5 6 7 8 9 10 11 12 13 14 15 16 17 18 19 20 21 22 23 24
Hour
Interior
Upper Batt
Lower Batt
Upper Cavity
Lower Cavity
Exterior

92JL24.Vapour.E4

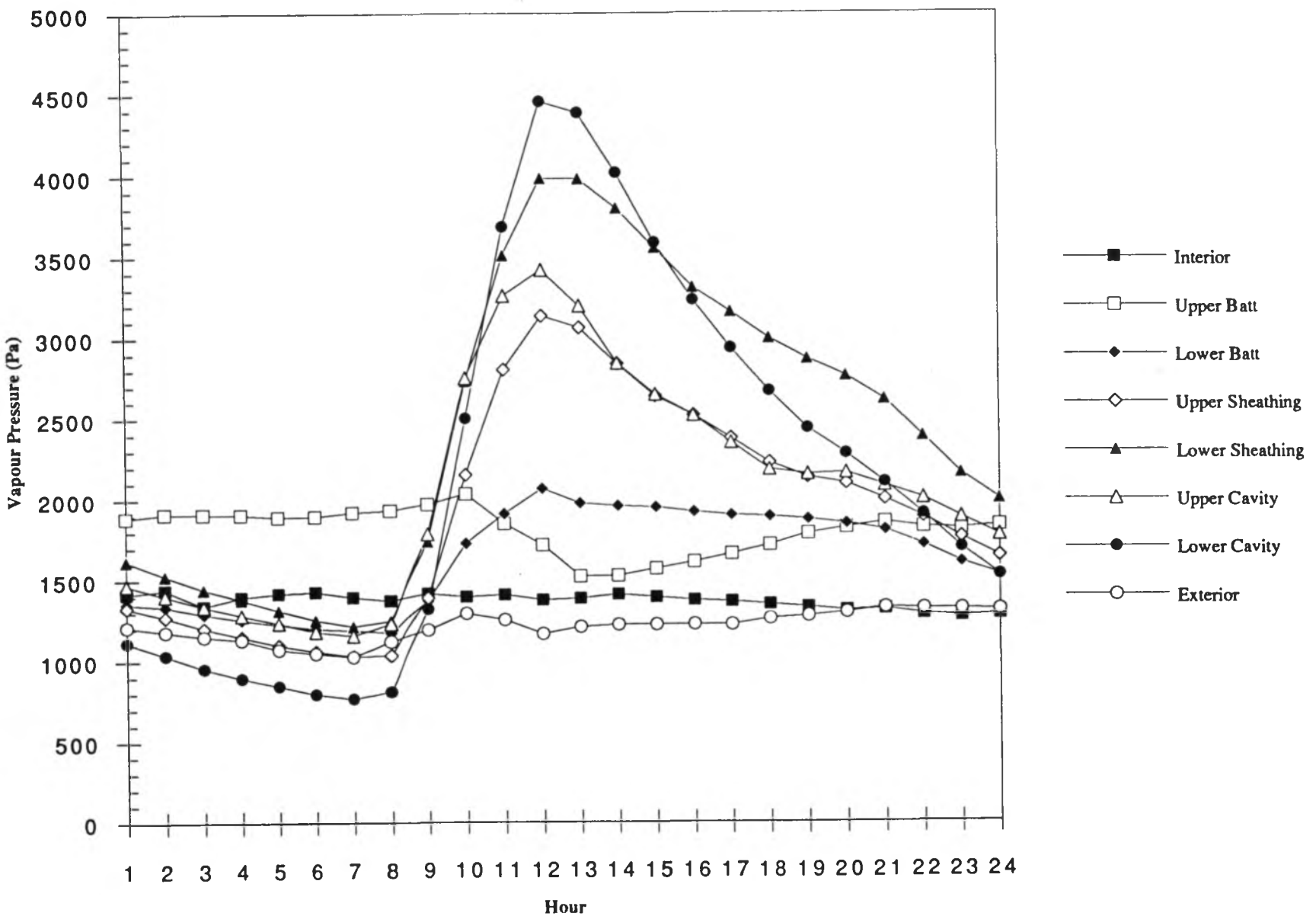

92JL24.Vapour.E5

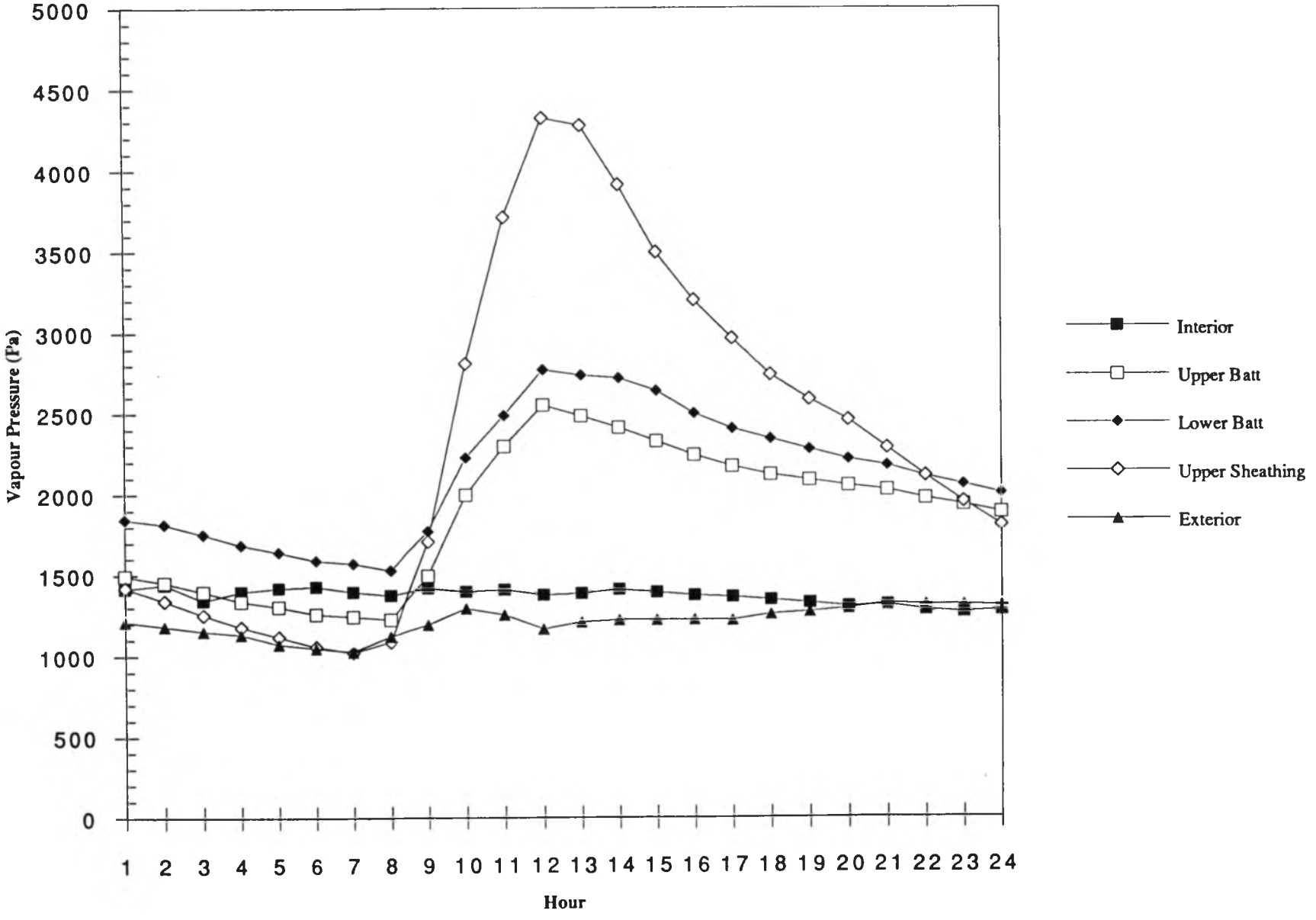

92JL24.Vapour.E6

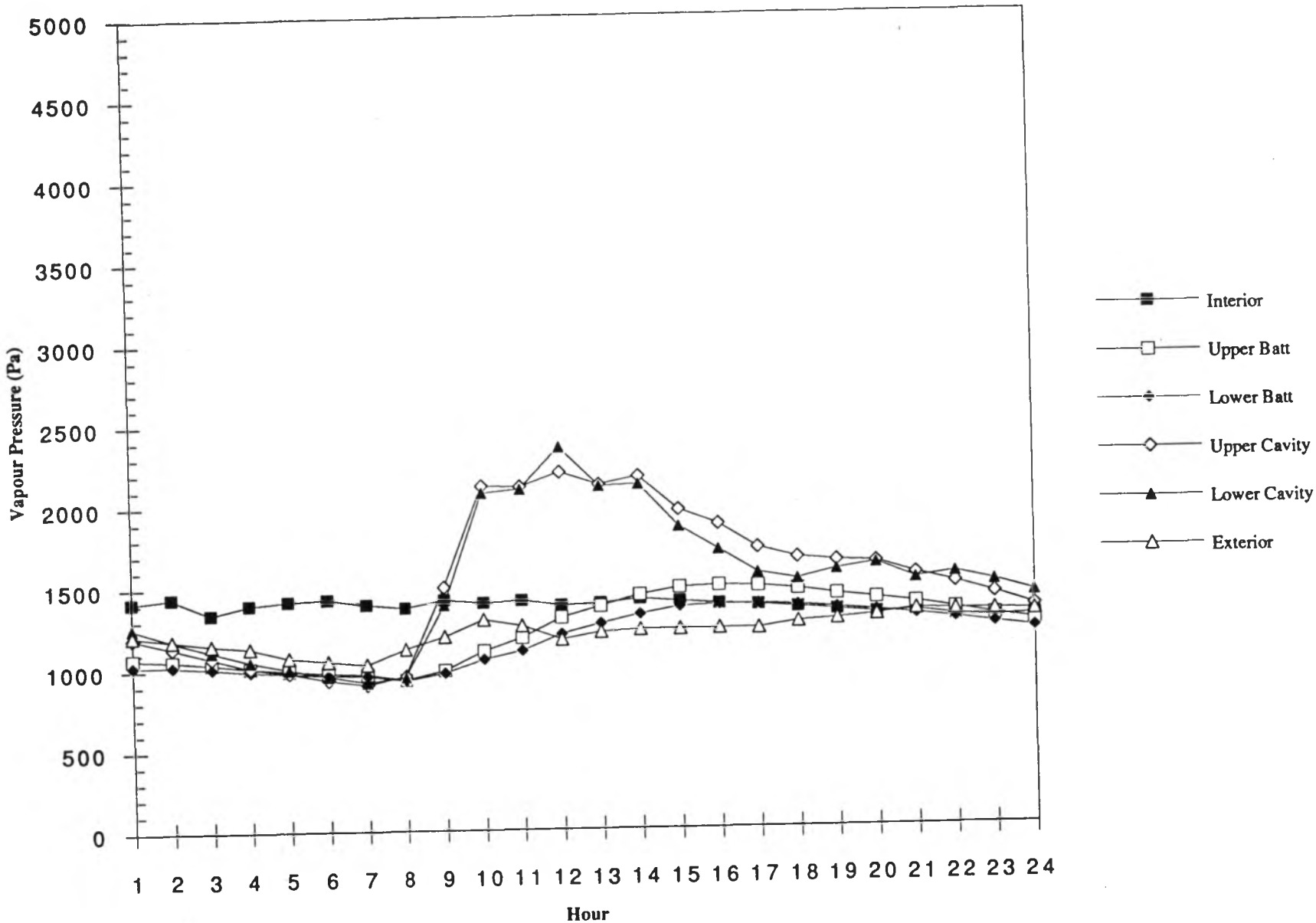

92FE09.Temp.E5

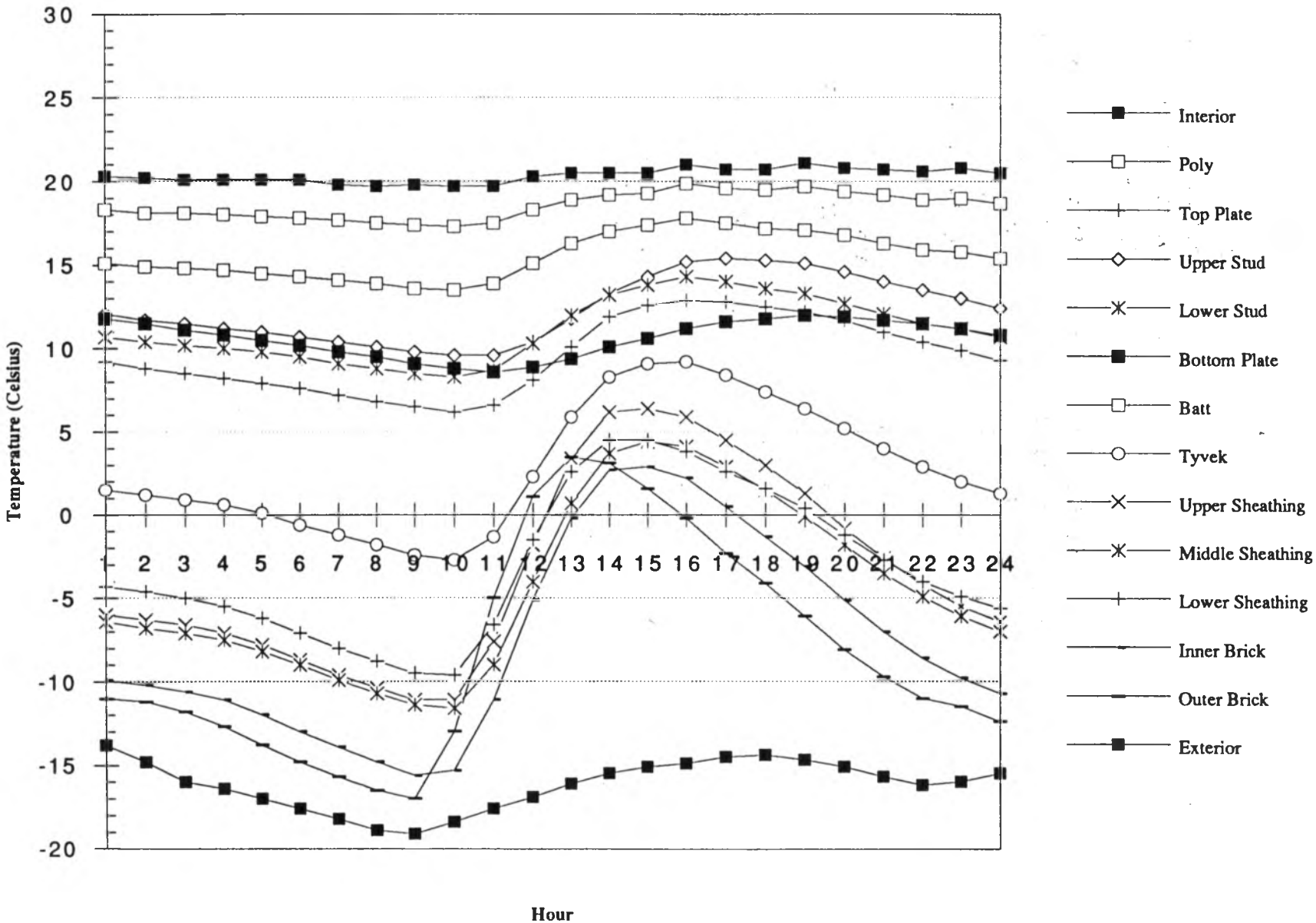

92JL24.Vapour.W5

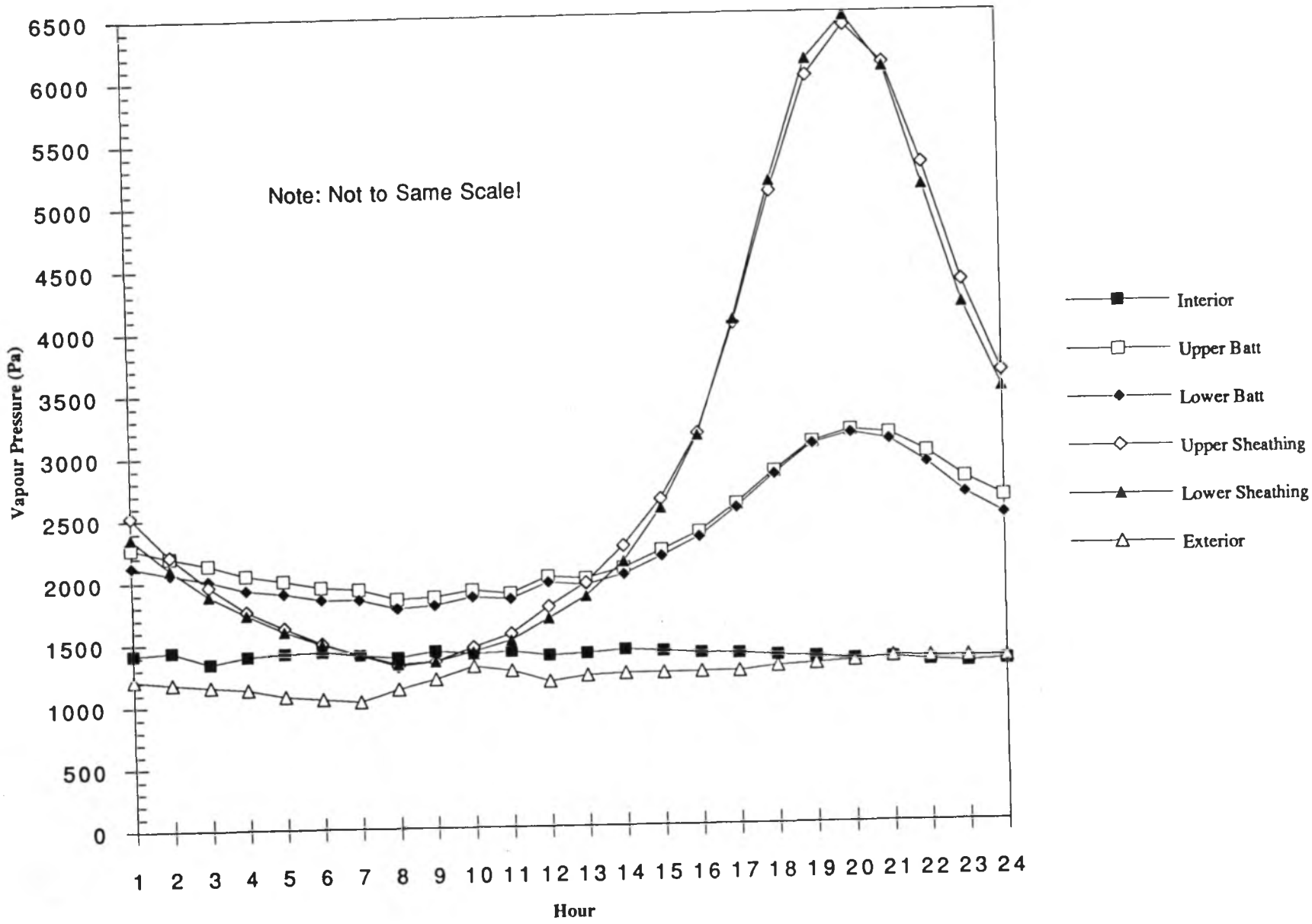

92JL24.Vapour.W6

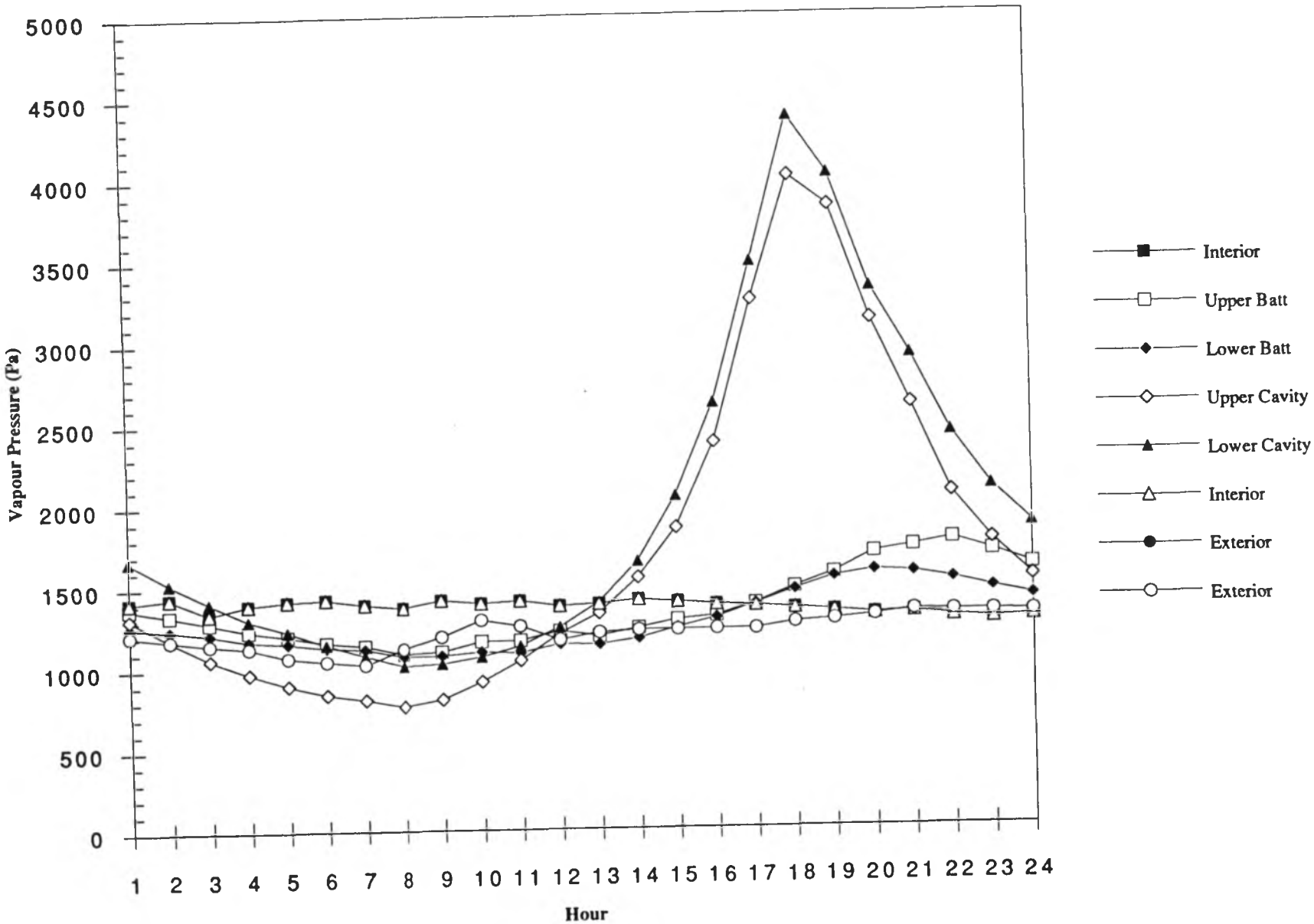

92JL24.Sol-Air.Datum

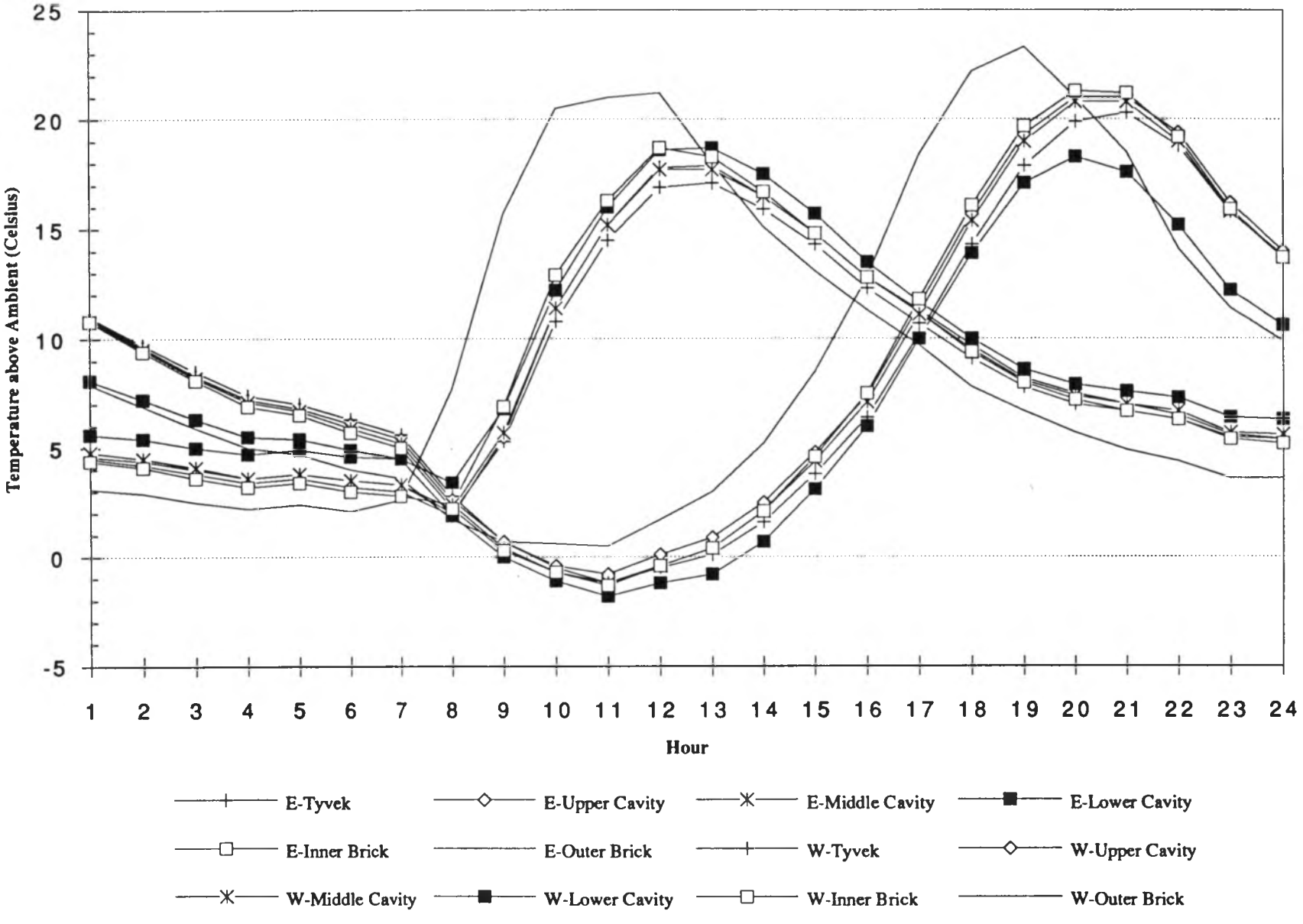

92JL24.Sol-Air.Dow

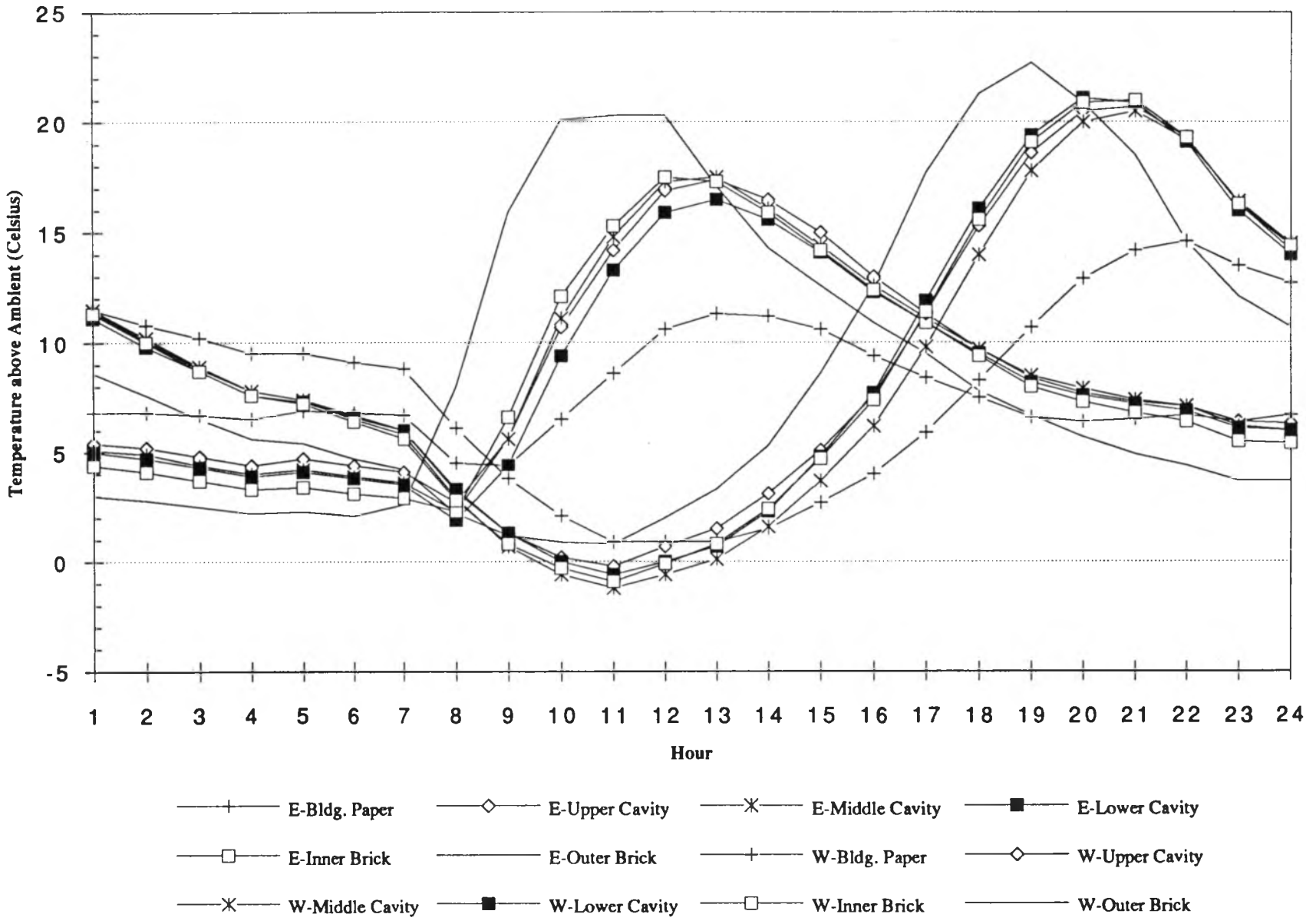

92JL24.Sol-Air.ZeroCav

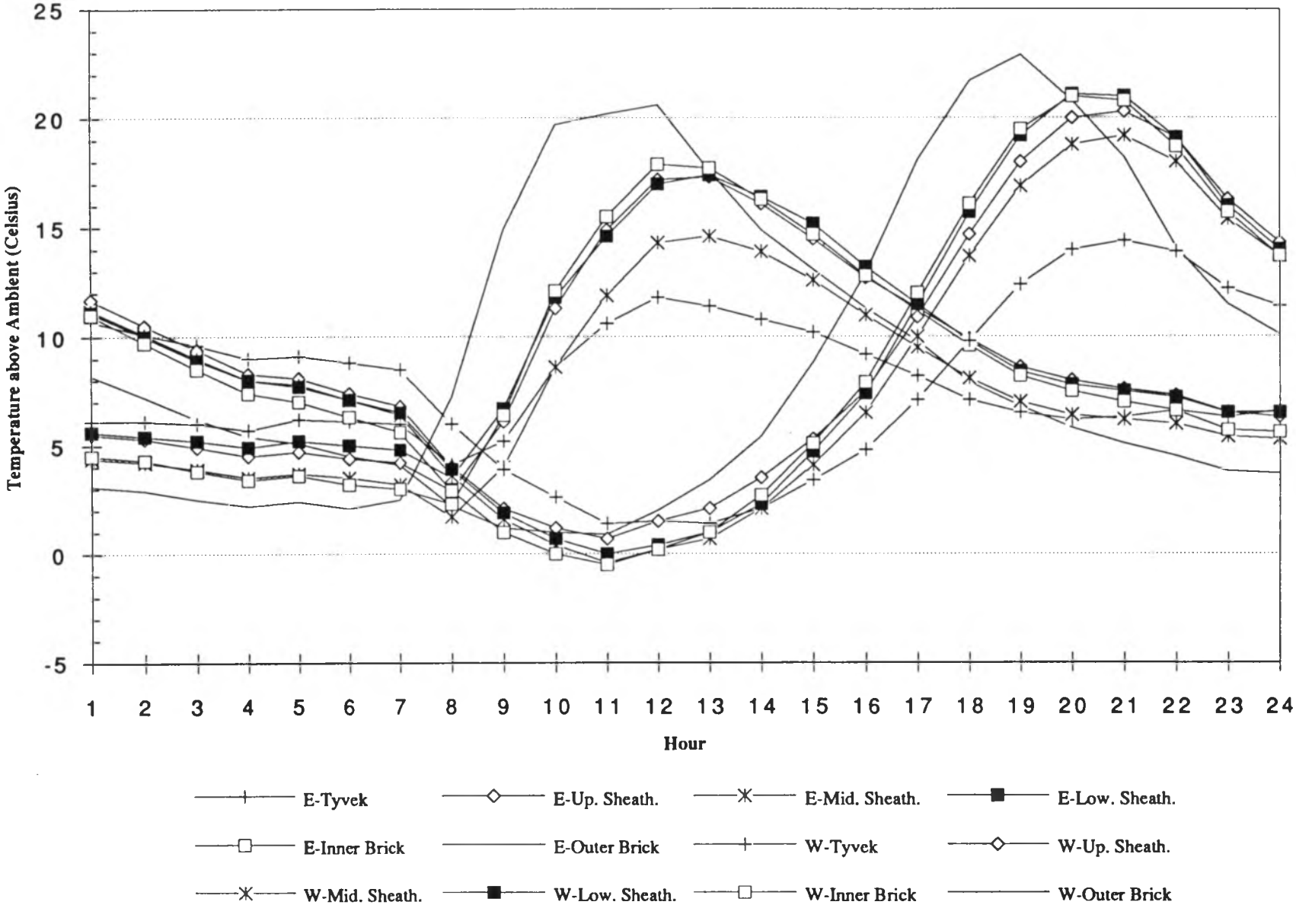

92FE09.Temp.E4

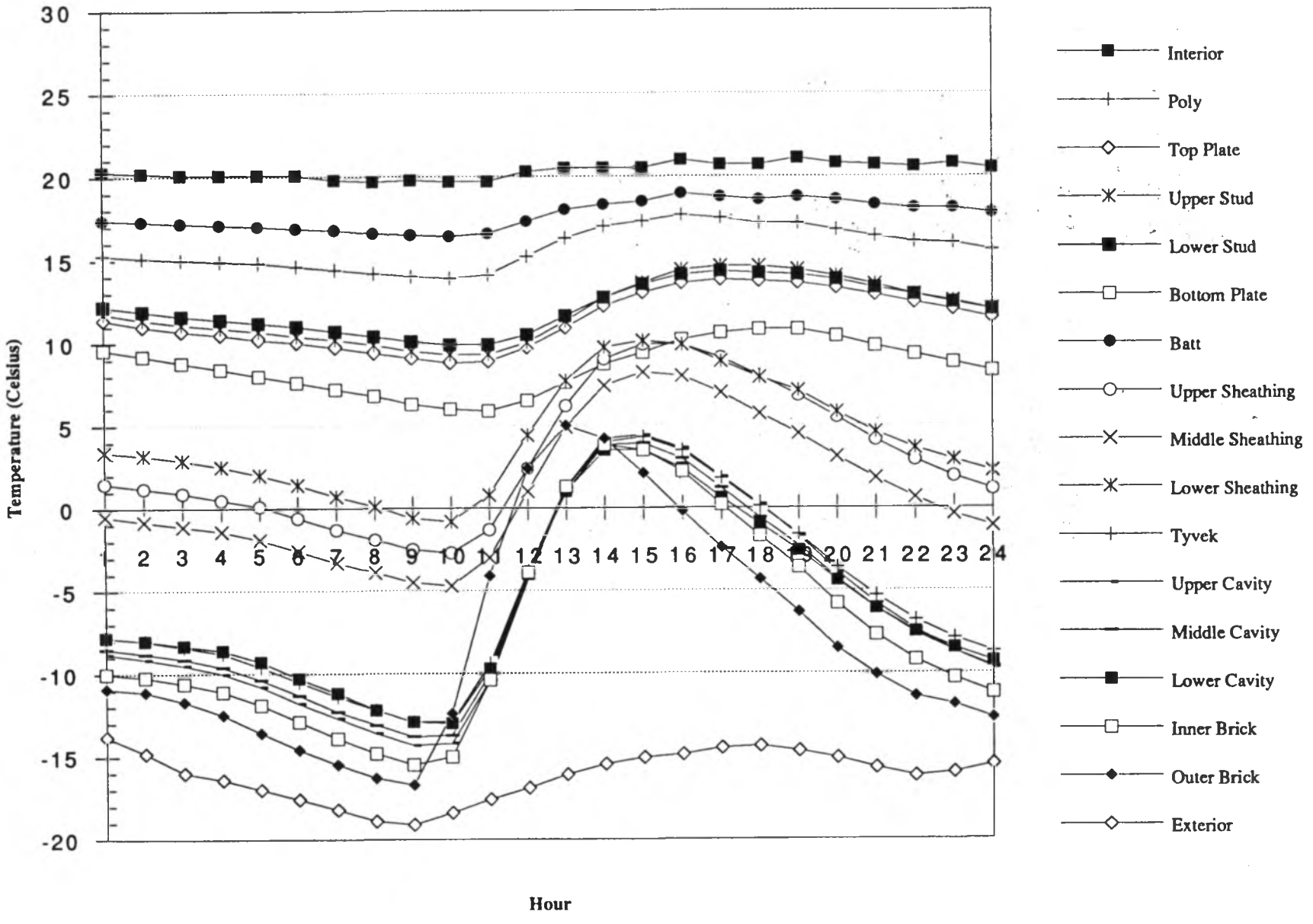

92FE09.Temp.W4

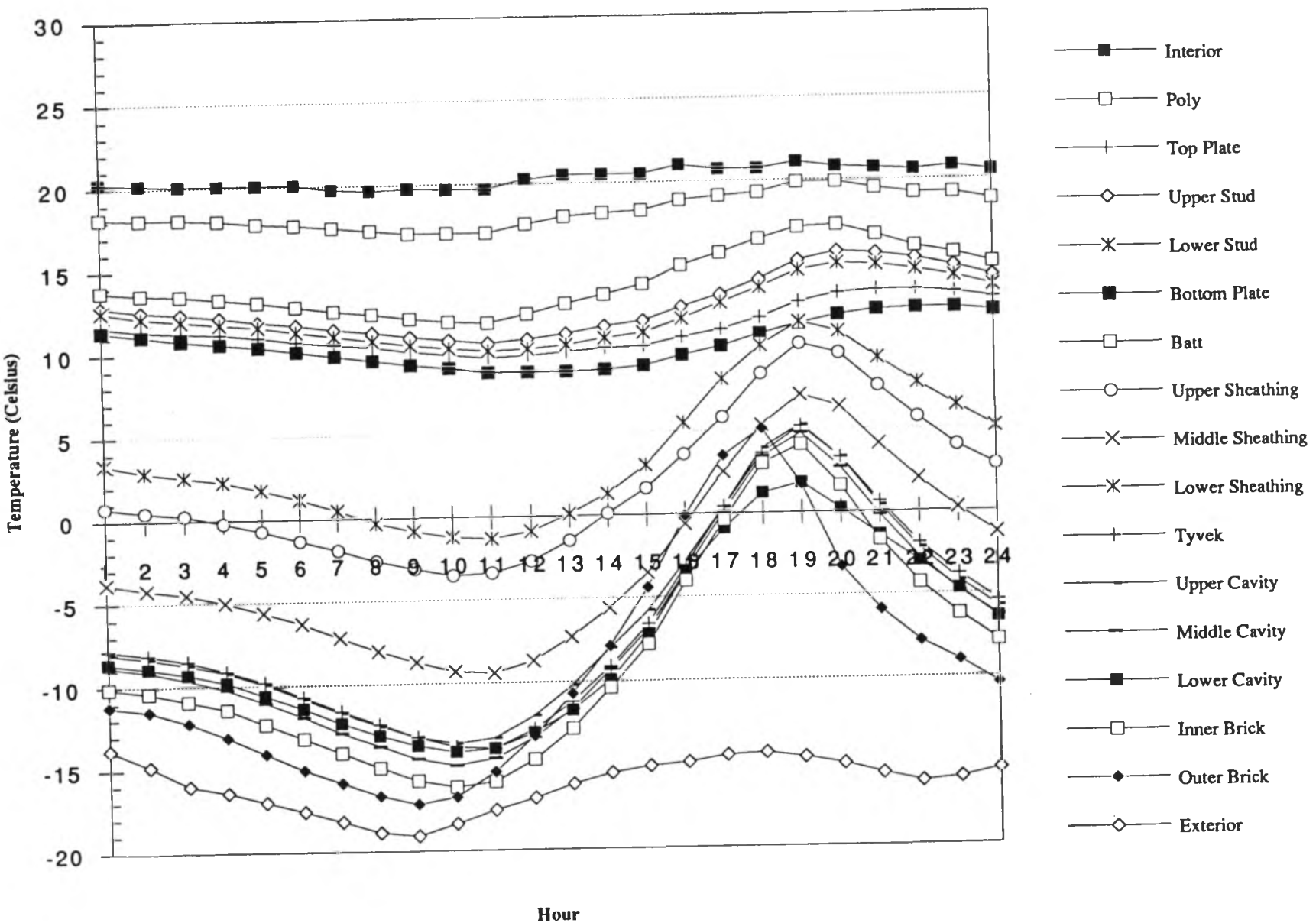

92FE09.Temp.W5

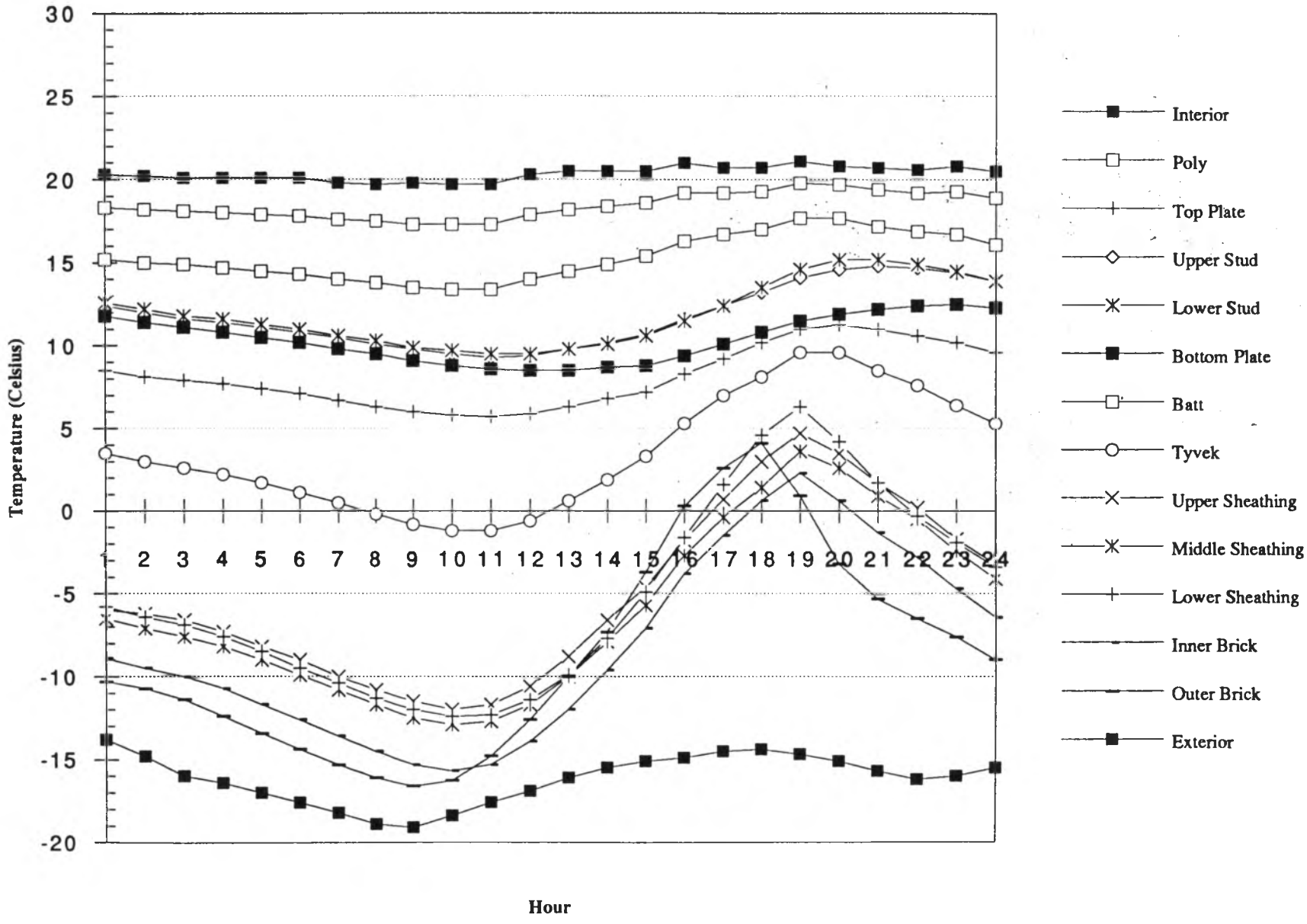

92FE09.Temp.E6

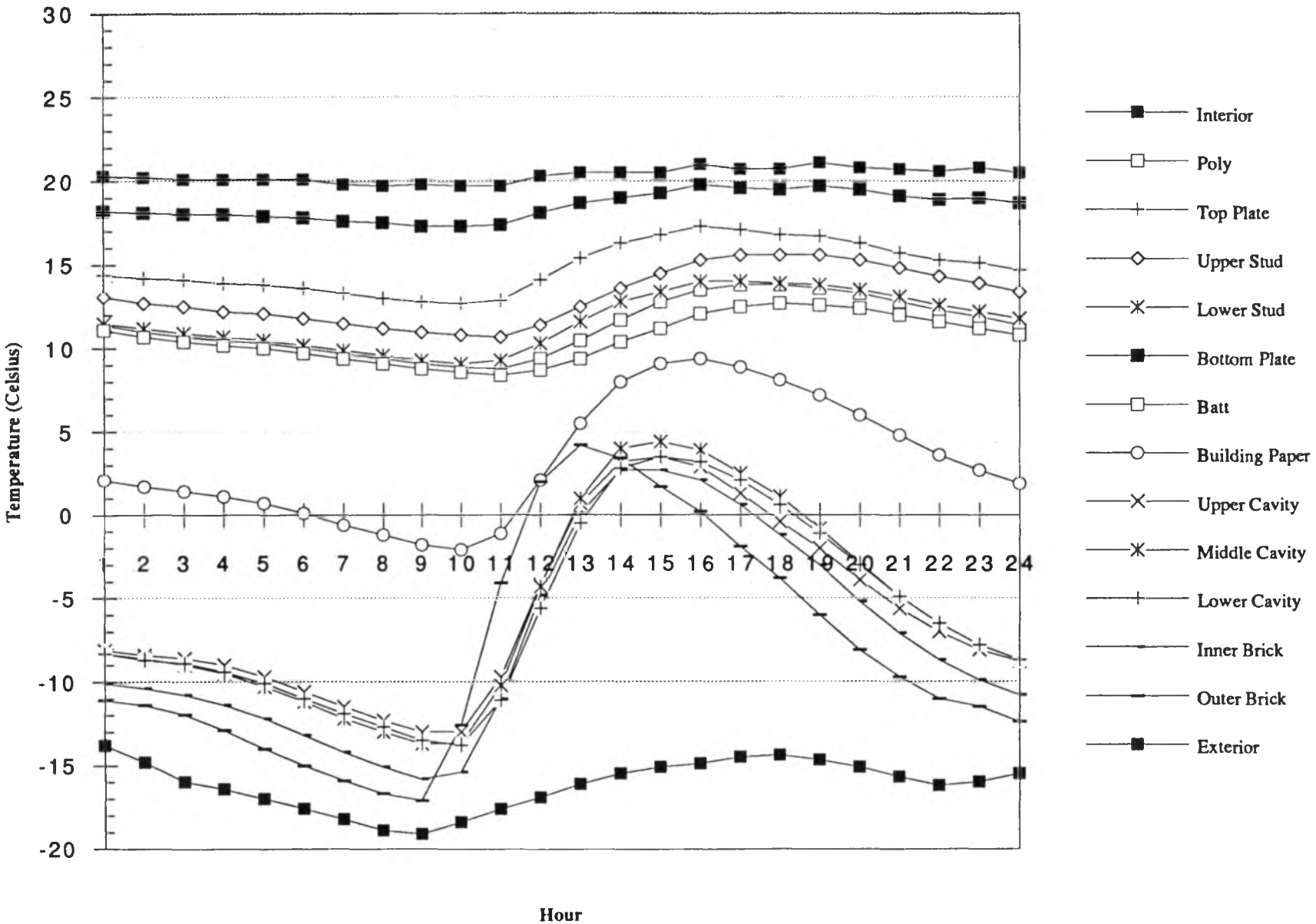

92FE09.Temp.W6

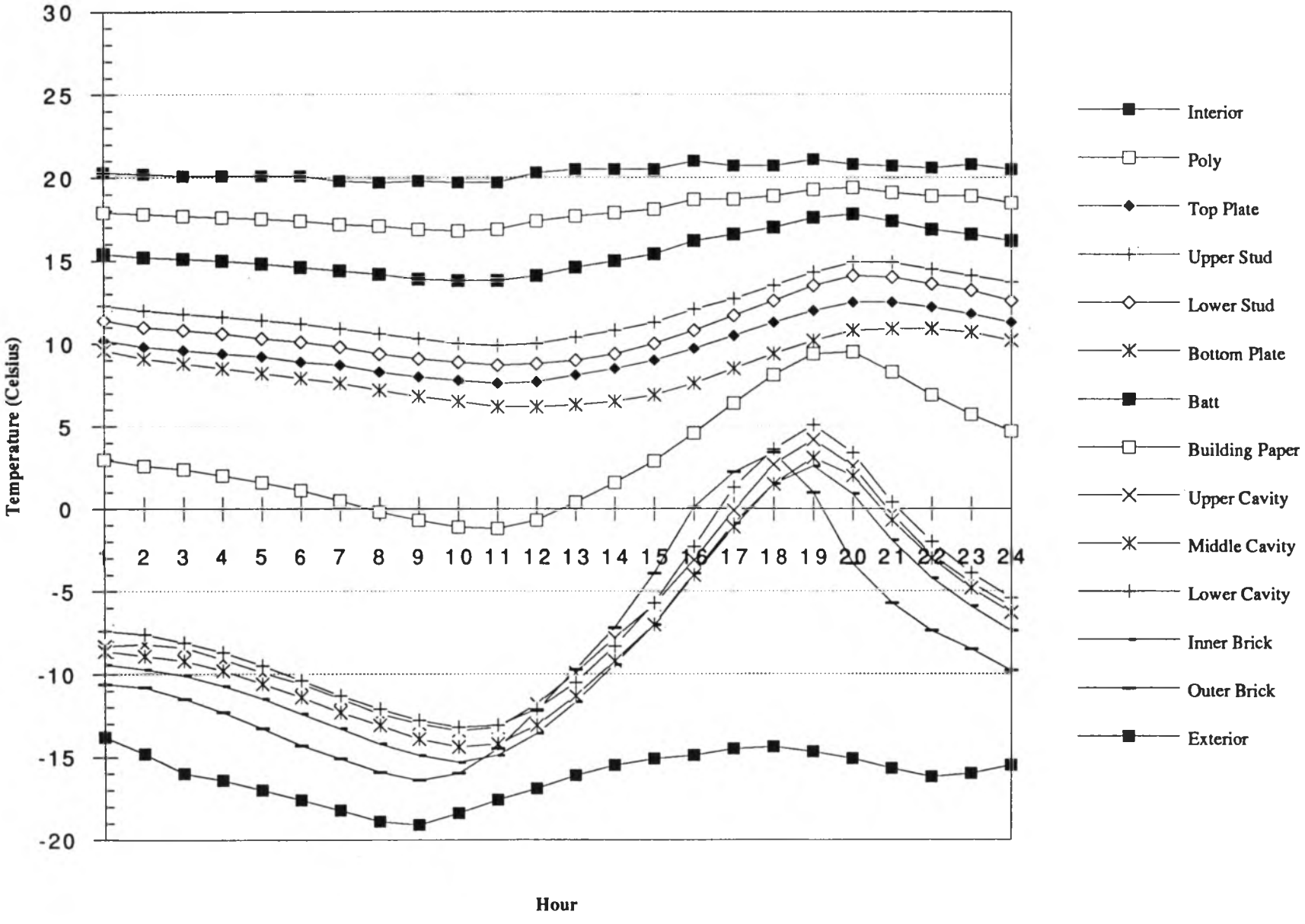

92FE09.RH.E4

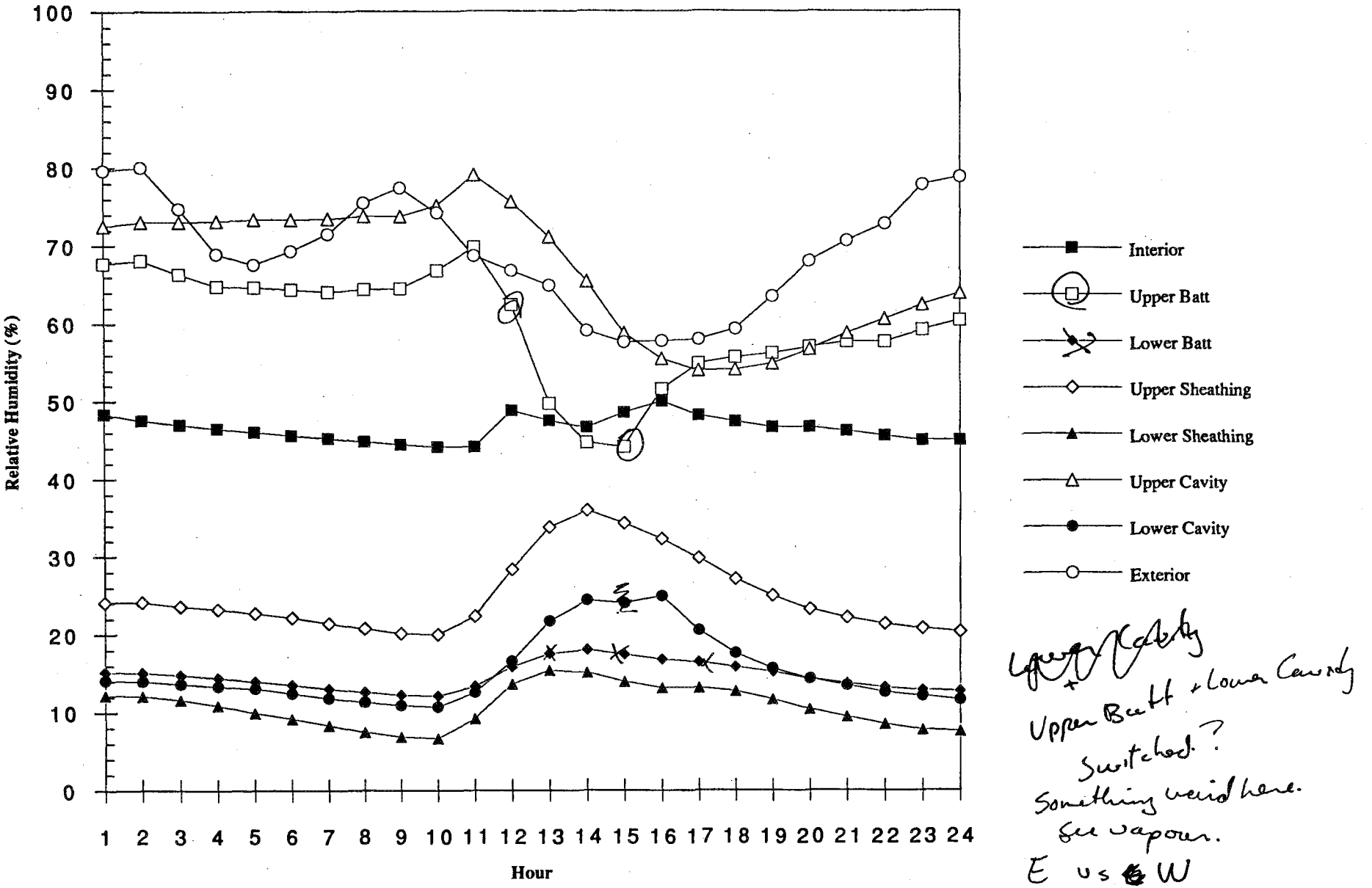

Upper Cavity + Lower Cavity
Upper Batt + Lower Cavity
Switched?
Something weird here.
See vapour.
E vs W

92FE09.RH.E5

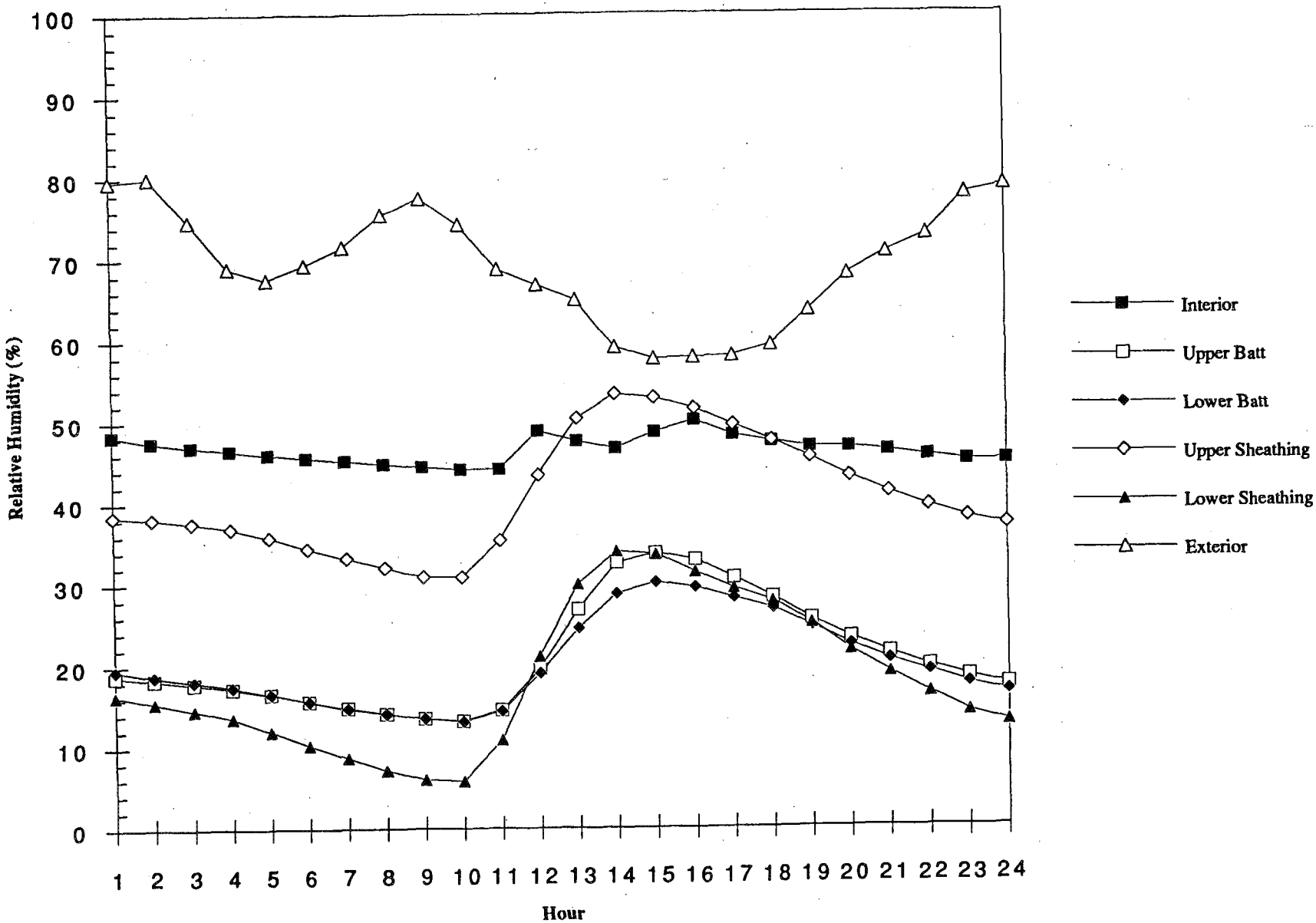
100
90
80
70
60
50
40
30
20
10
0
Relative Humidity (%)
1 2 3 4 5 6 7 8 9 10 11 12 13 14 15 16 17 18 19 20 21 22 23 24
Hour
Interior
Upper Batt
Lower Batt
Upper Sheathing
Lower Sheathing
Exterior

92FE09.RH.E6

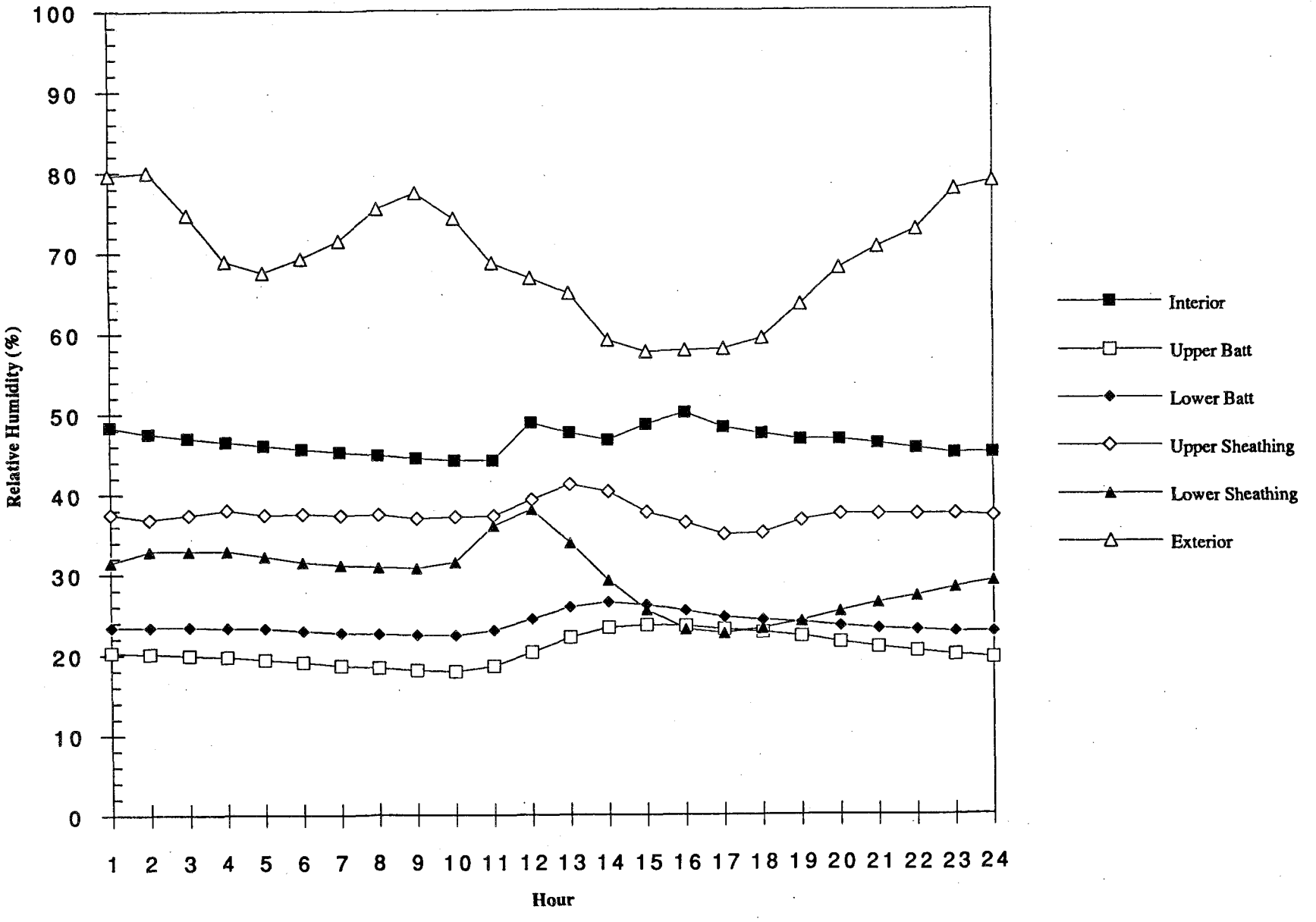
100
90
80
70
60
50
40
30
20
10
0
Relative Humidity (%)
1 2 3 4 5 6 7 8 9 10 11 12 13 14 15 16 17 18 19 20 21 22 23 24
Hour
Interior
Upper Batt
Lower Batt
Upper Sheathing
Lower Sheathing
Exterior

92FE09.RH.W4

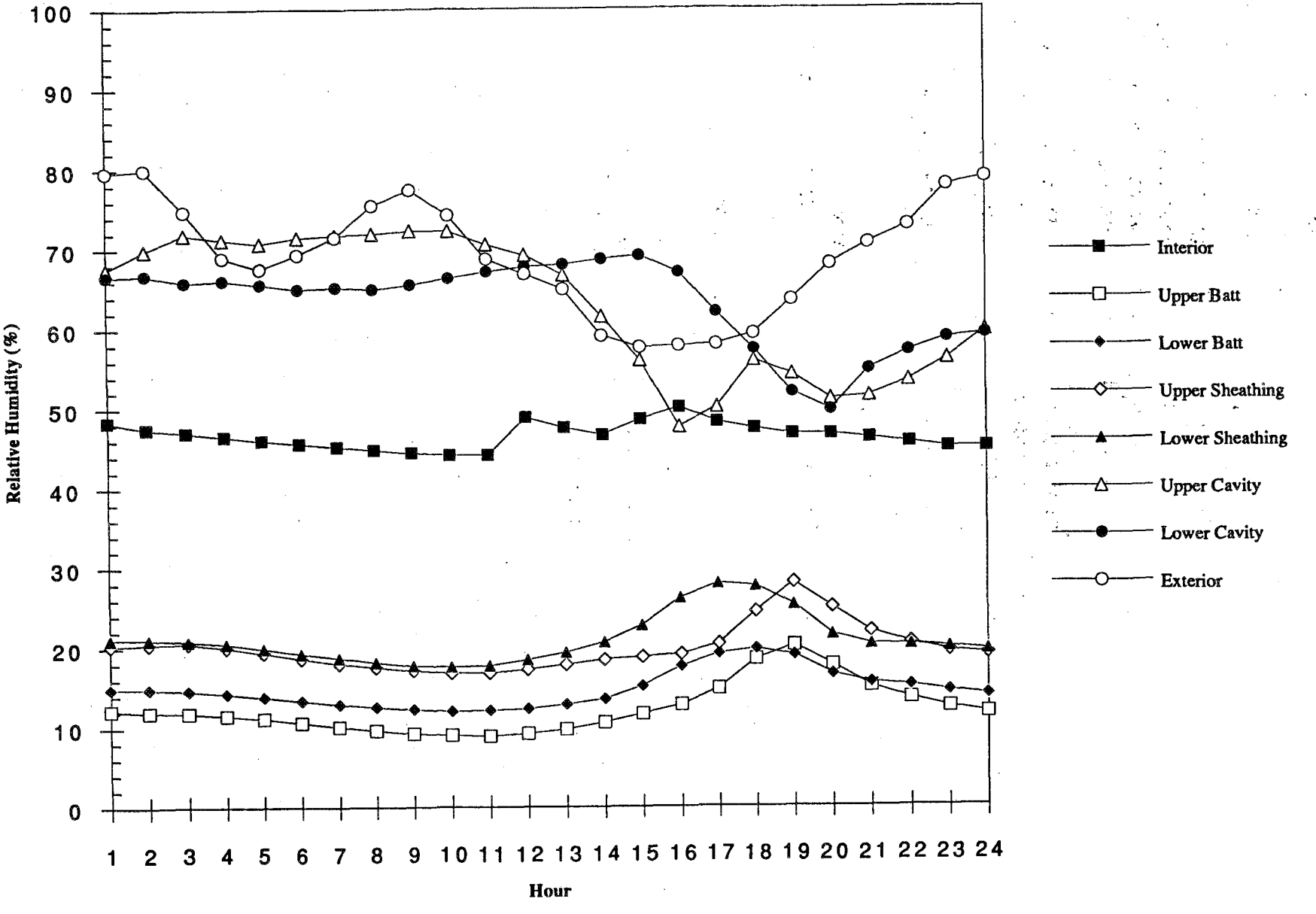
100
90
80
70
60
50
40
30
20
10
0
Relative Humidity (%)
1 2 3 4 5 6 7 8 9 10 11 12 13 14 15 16 17 18 19 20 21 22 23 24
Hour
Interior
Upper Batt
Lower Batt
Upper Sheathing
Lower Sheathing
Upper Cavity
Lower Cavity
Exterior

92FE09.RH.W5

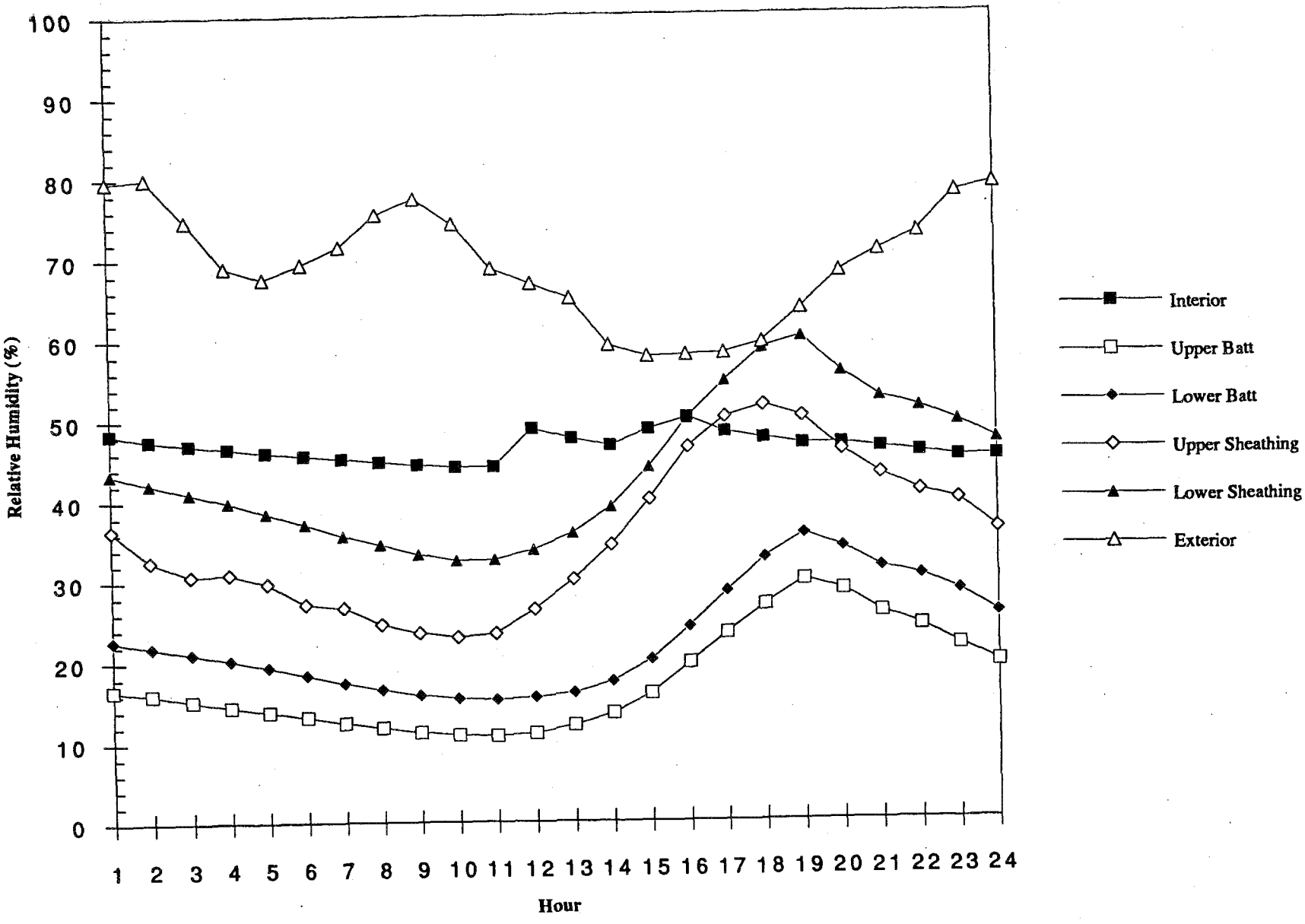
100
90
80
70
60
50
40
30
20
10
0
Relative Humidity (%)
1 2 3 4 5 6 7 8 9 10 11 12 13 14 15 16 17 18 19 20 21 22 23 24
Hour
Interior
Upper Batt
Lower Batt
Upper Sheathing
Lower Sheathing
Exterior

92FE09.RH.W6

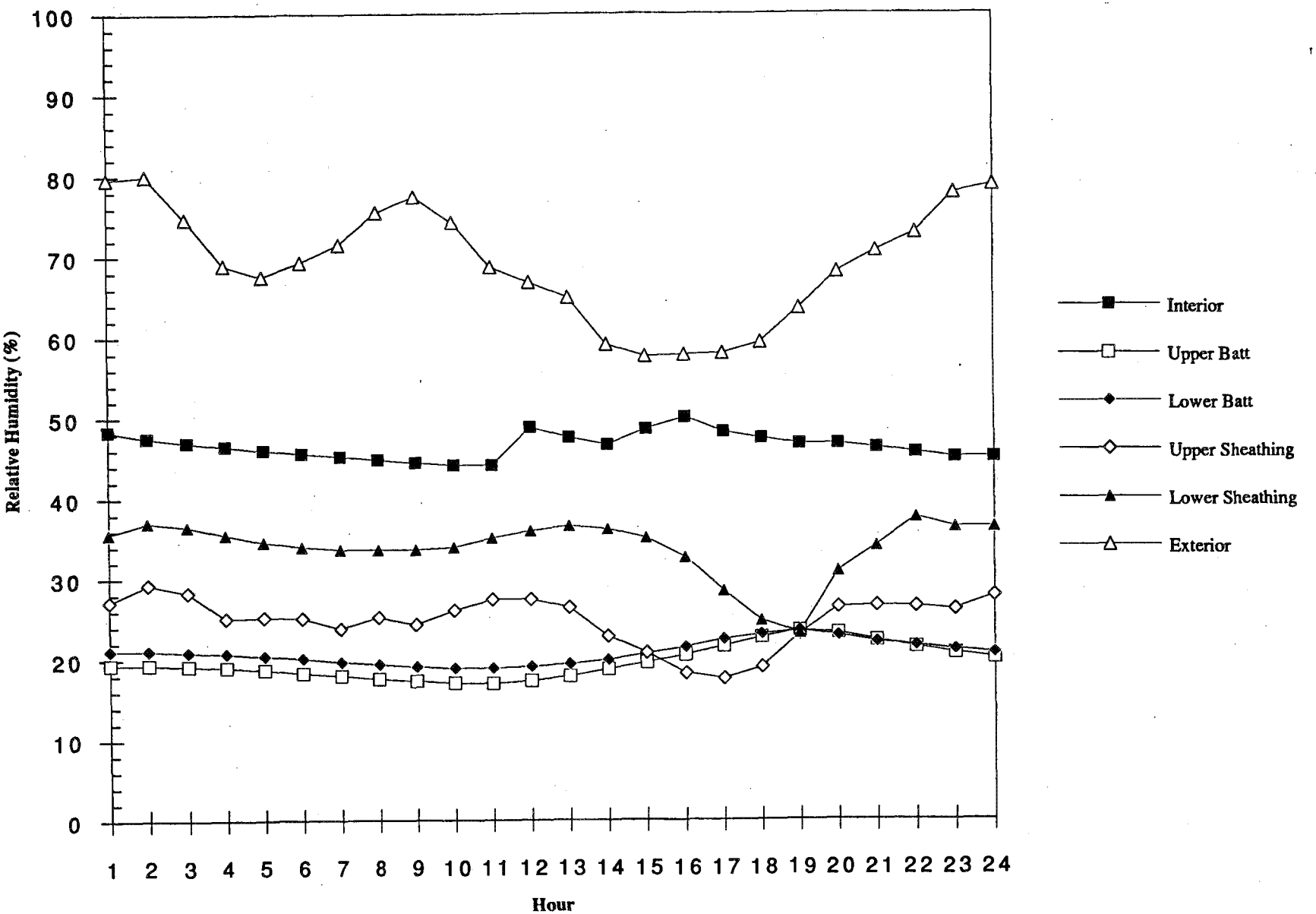
100
90
80
70
60
50
40
30
20
10
0
Relative Humidity (%)
1 2 3 4 5 6 7 8 9 10 11 12 13 14 15 16 17 18 19 20 21 22 23 24
Hour
Interior
Upper Batt
Lower Batt
Upper Sheathing
Lower Sheathing
Exterior

92FE09.Vapour.E4

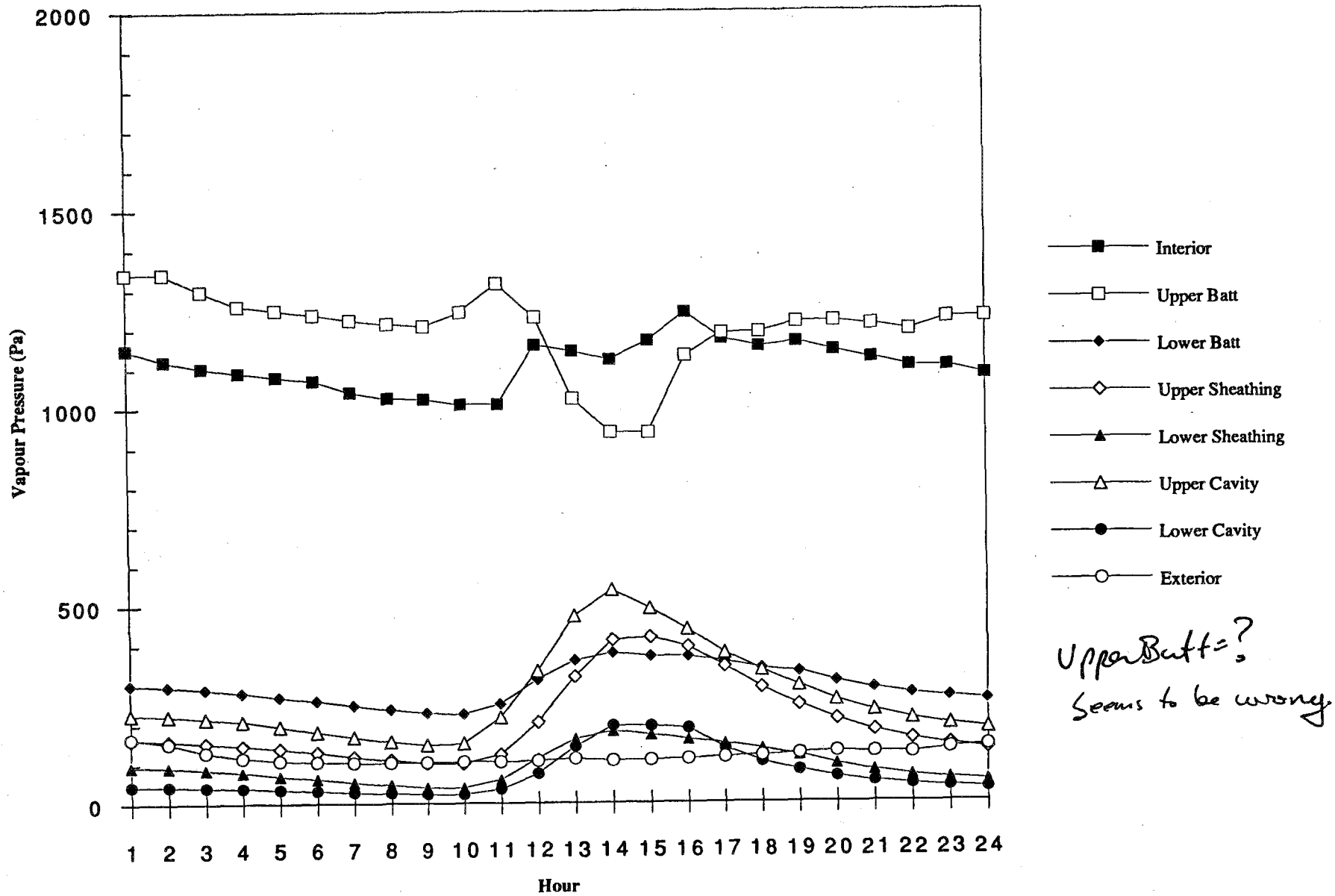

UpperButt=?
Seems to be wrong.

92FE09.Vapour.E5

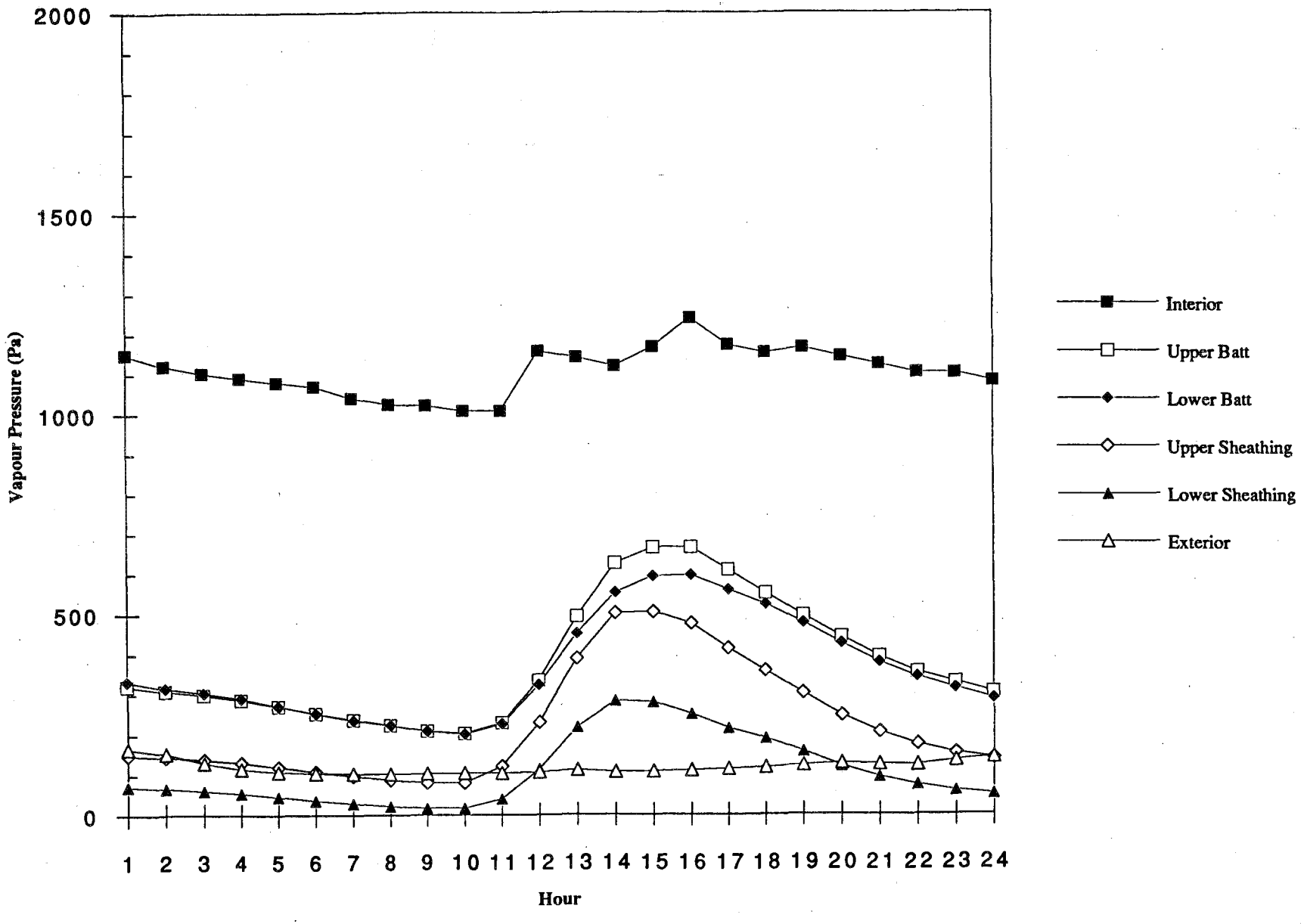

92FE09.Vapour.E6

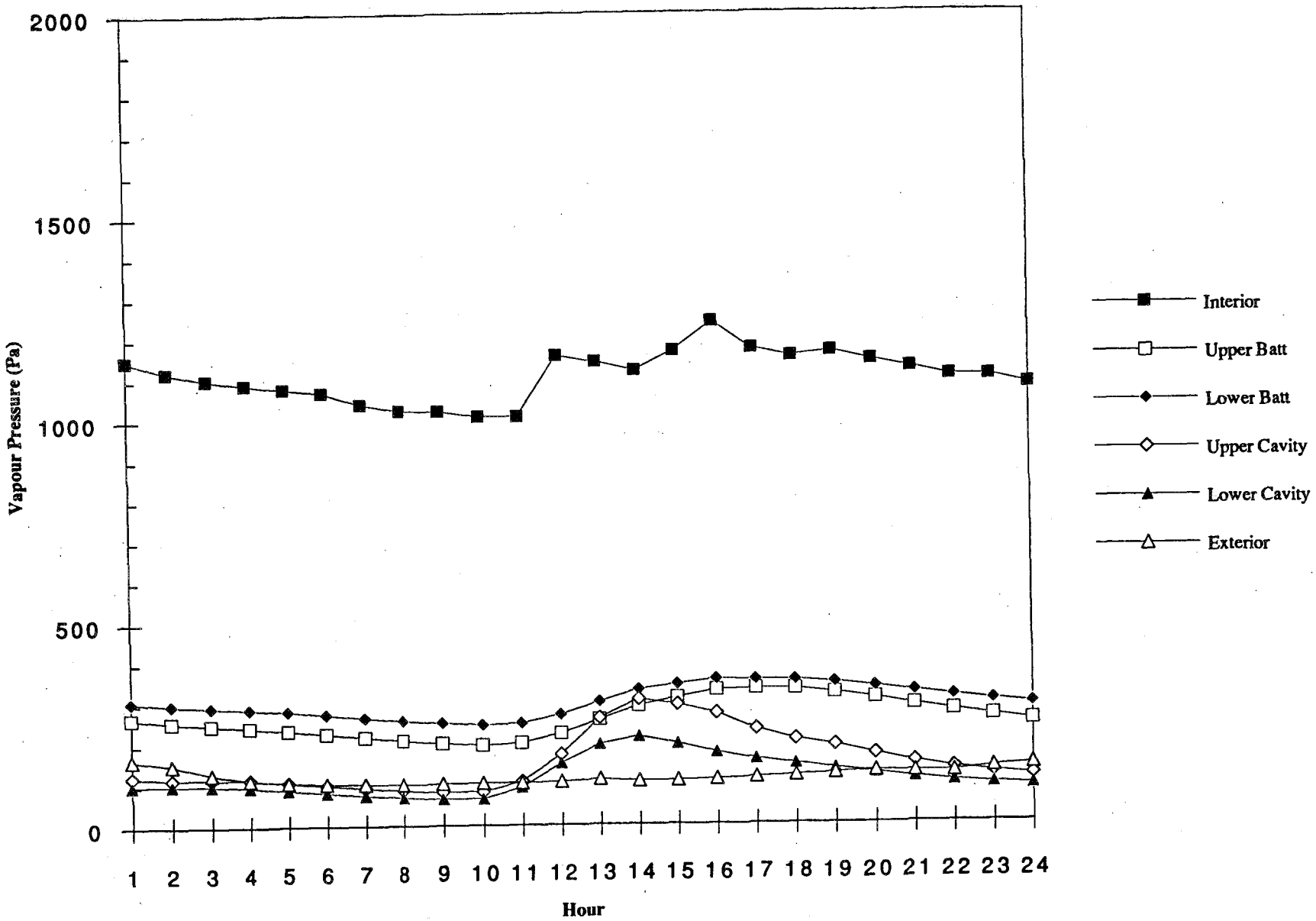

92JL24.Vapour.W4

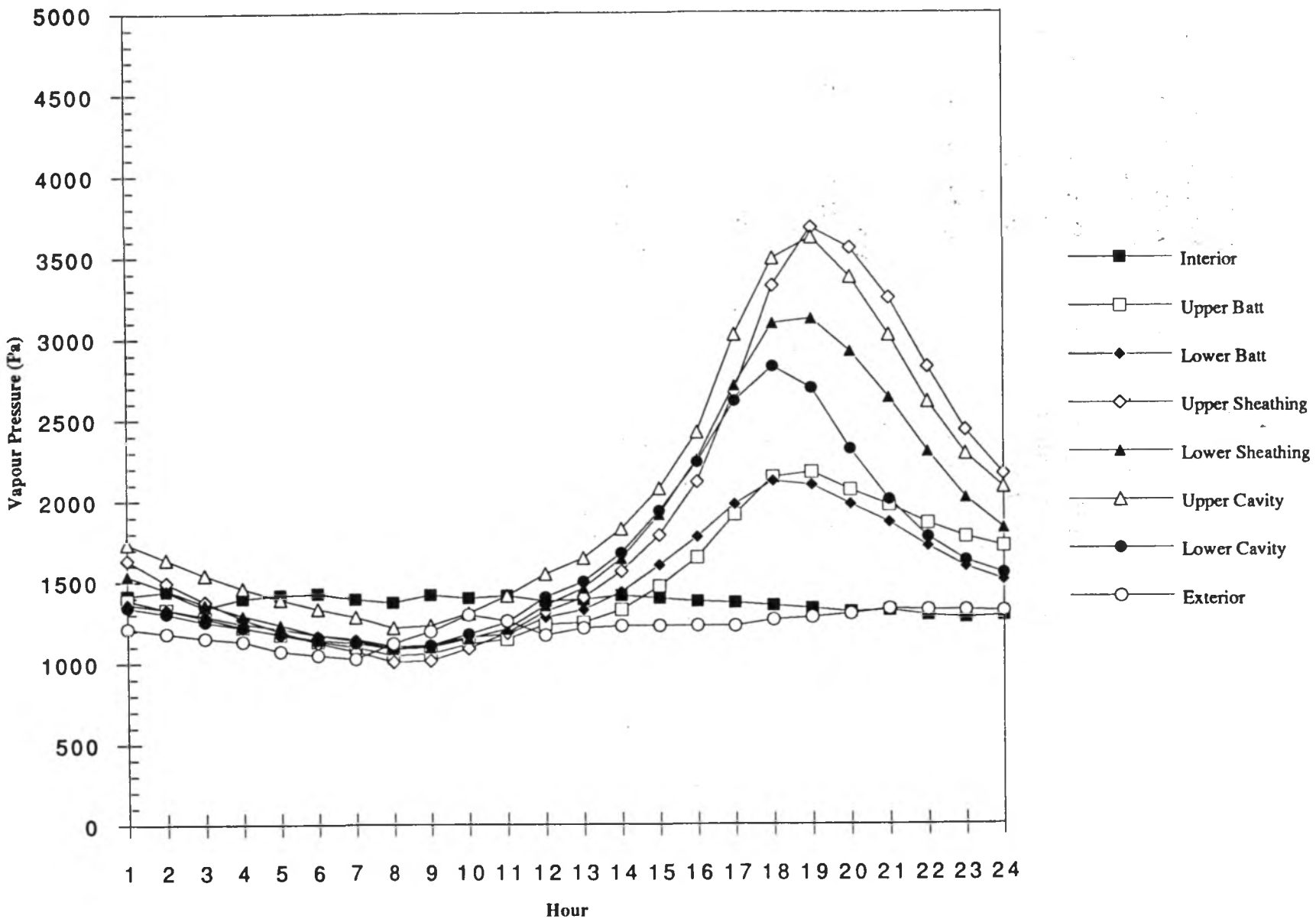

92FE09.Vapour.W4

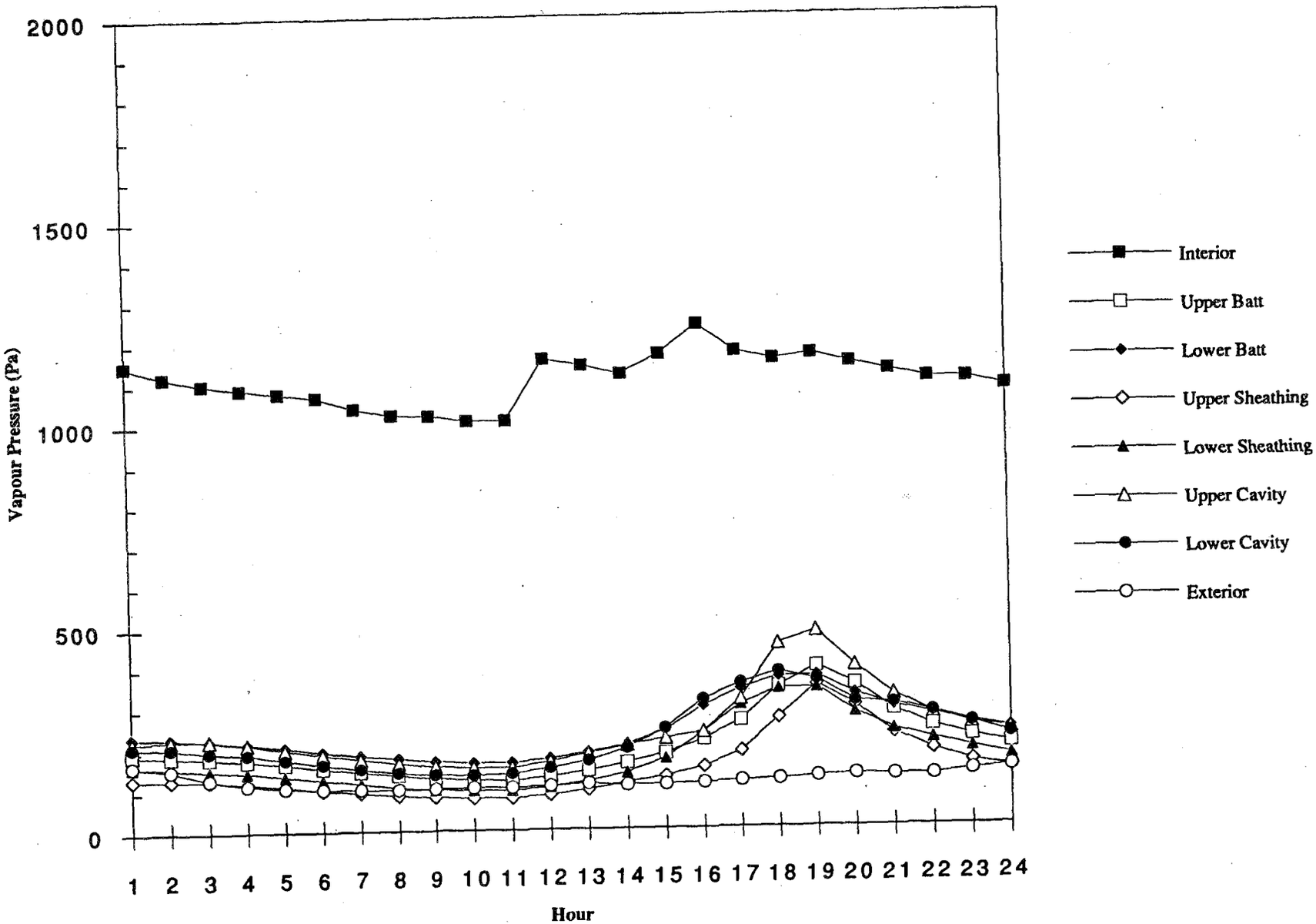

92FE09.Vapour.W5

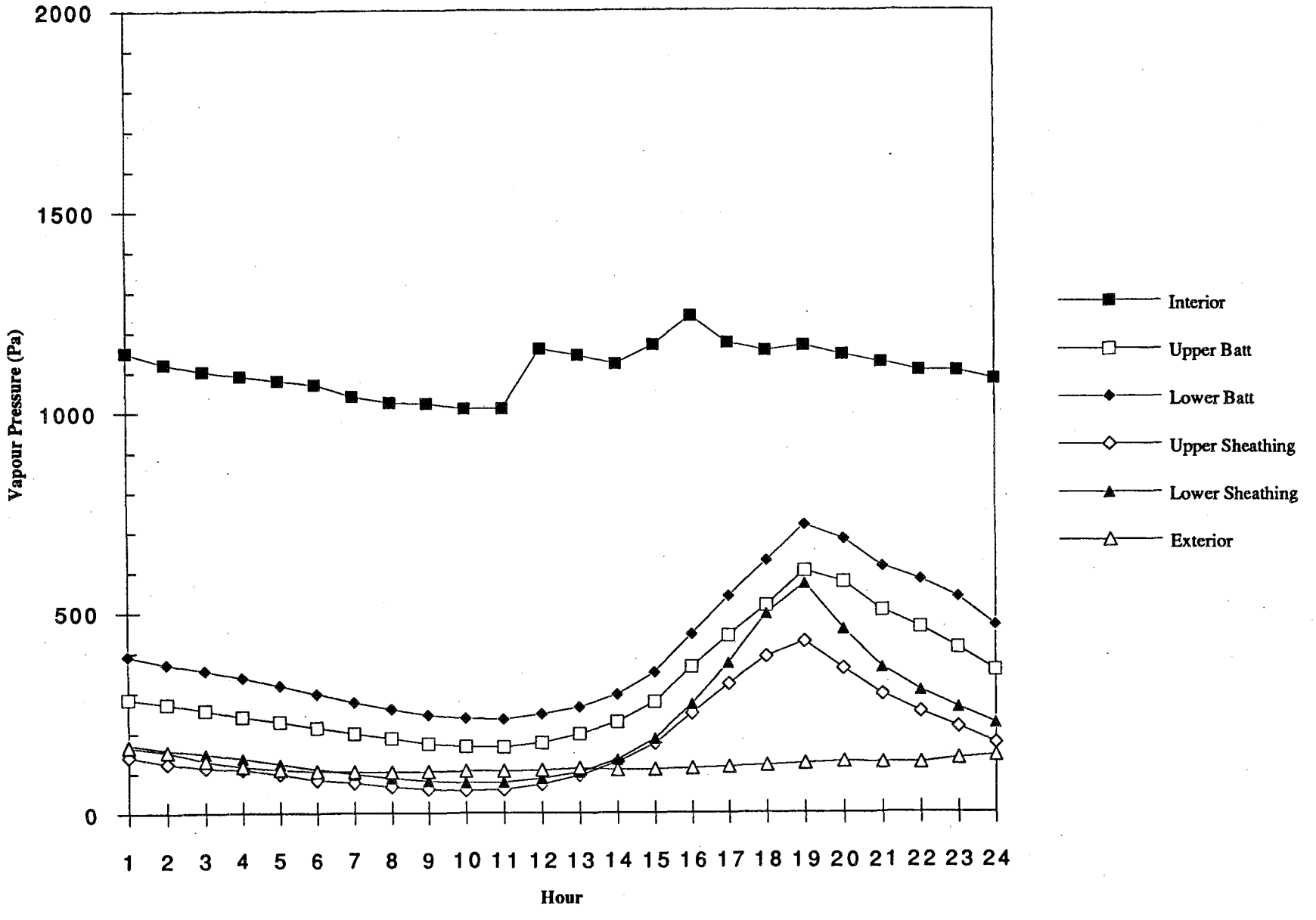

92FE09.Vapour.W6

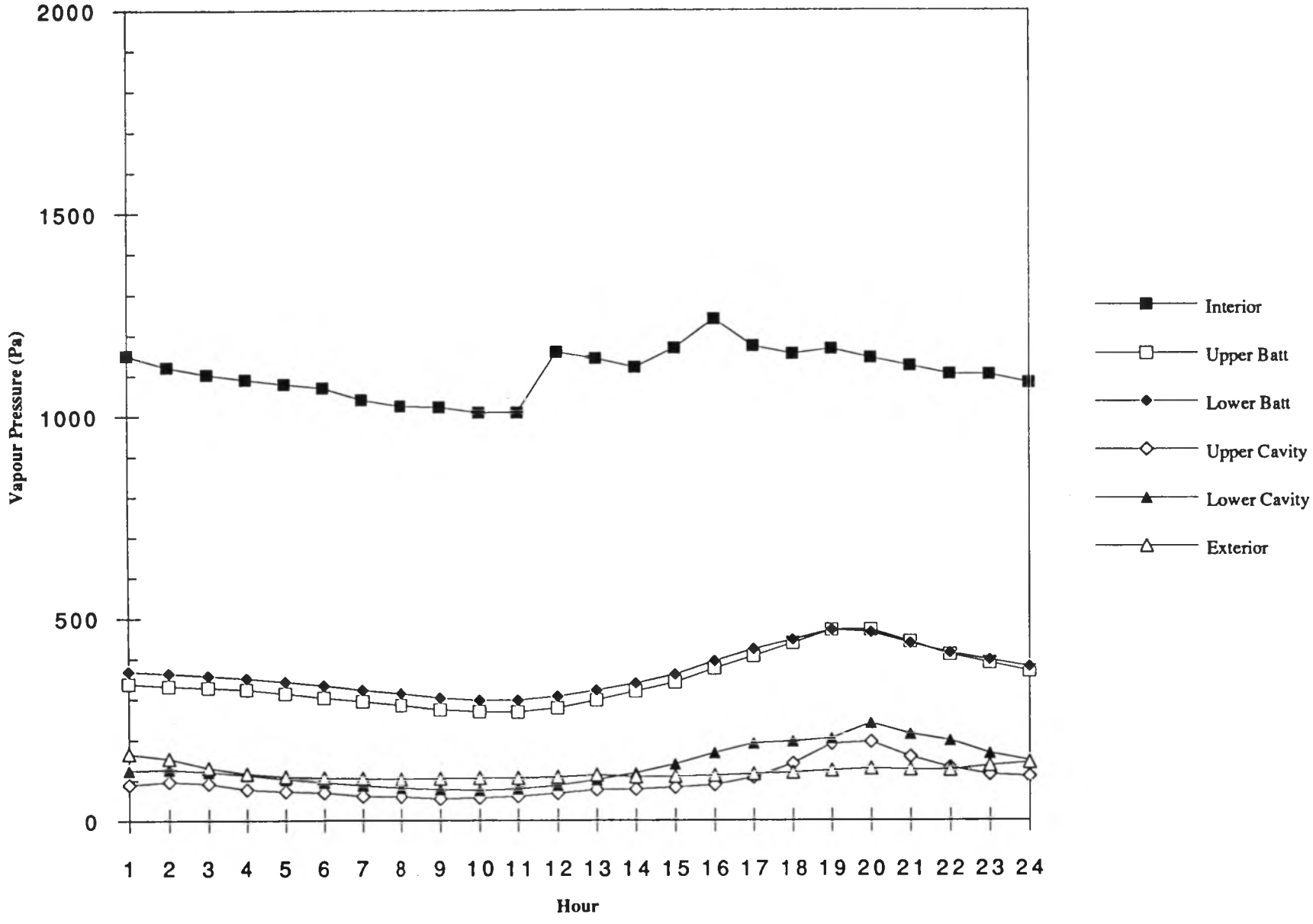

Appendix C

Statistical Data

Winter Period: Dec 14, 1991 To: February 1, 1992

and

Summer Period: June 1, 1992 To: August 14, 1992

Weather

Monitoring Period from June 1,1992 to August 14, 1992

Statistics of Daily Averages of Readings Taken Every 5 Minutes

	Exterior				Interior			
	Mean	S.D.	Max	Min	Mean	S.D.	Max	Min
Temp.	13.96	*3.02*	20.70	3.70	21.21	*0.20*	21.60	20.90
RH%	69.68	*13.89*	92.10	37.10	50.19	*2.33*	56.80	43.50

Brick Temperatures

Measured at 10 mm from the inner and outer faces repectively

	W4		E4		Datum Mean	
	Mean	S.D.	Mean	S.D.	Mean	S.D.
inner	20.49	*3.50*	21.47	*3.97*	20.98	*3.74*
outer	20.37	*3.66*	21.48	*4.14*	20.93	*3.90*
mean	20.43	*3.58*	21.48	*4.05*	**20.95**	***3.82***

Cavity Temperatures

Measured in middle of air cavity

	W4		E4		Datum Mean	
	Mean	S.D.	Mean	S.D.	Mean	S.D.
upper	20.58	*3.40*	21.40	*3.91*	20.99	*3.65*
middle	20.37	*3.45*	21.48	*3.82*	20.93	*3.63*
lower	19.85	*3.30*	22.17	*3.63*	21.01	*3.46*
mean	20.27	*3.38*	21.68	*3.78*	**20.97**	***3.58***

Sheathing Temperatures

Measured in middle of insulated sheathing layer

	W4		E4		Datum Mean	
	Mean	S.D.	Mean	S.D.	Mean	S.D.
upper	22.66	*2.57*	22.45	*2.79*	22.55	*2.68*
middle	20.44	*2.83*	21.18	*2.80*	20.81	*2.81*
lower	24.72	*2.27*	24.20	*2.46*	24.46	*2.36*
mean	22.61	*2.56*	22.61	*2.68*	**22.61**	***2.62***

Tyvek Temperatures

Measured at the outside of the Tyvek/Building Paper at panel mid-height

	W4		E4		Datum Mean	
	Mean	S.D.	Mean	S.D.	Mean	S.D.
middle	20.48	*3.31*	21.21	*3.72*	**20.84**	***3.51***

Note: The Tyvek is installed on the exterior side of the sheathing in the Datum panels

Wood Framing Temperatures

See text for locations

	W4		E4		Datum Mean	
	Mean	S.D.	Mean	S.D.	Mean	S.D.
top	21.28	*1.29*	20.92	*1.48*	21.10	*1.38*
upper	21.42	*1.15*	21.00	*1.43*	21.21	*1.29*
lower	21.17	*1.13*	20.75	*1.18*	20.96	*1.16*
bottom	20.12	*1.06*	19.73	*1.14*	19.92	*1.10*
mean	21.00	*1.16*	20.60	*1.31*	**20.80**	***1.23***

Fibreglass Batt Temperatures

Measured in the middle of the batt layer at panel mid-height

	W4		E4		Datum Mean	
	Mean	S.D.	Mean	S.D.	Mean	S.D.
middle	20.70	*0.84*	20.10	*0.52*	**20.40**	***0.68***

Vapour Barrier Temperature

Measured on the exterior side of poly at panel mid-height

	W4		E4		Datum Mean	
	Mean	S.D.	Mean	S.D.	Mean	S.D.
middle	21.02	*0.46*	20.54	*0.83*	**20.78**	***0.65***

Datum Panel Summer Period Temperatures

Weather

Monitoring Period from June 1,1992 to August 14, 1992

Statistics of Daily Averages of Readings Taken Every 5 Minutes

	Exterior				Interior			
	Mean	S.D.	Max	Min	Mean	S.D.	Max	Min
Temp.	13.96	*3.02*	20.70	3.70	21.21	*0.20*	21.60	20.90
RH %	69.68	*13.89*	92.10	37.10	50.19	*2.33*	56.80	43.50

Brick Temperatures

Measured at 10 mm from the inner and outer faces repectively

	W5		E5		Zero Cavity Mean	
	Mean	S.D.	Mean	S.D.	Mean	S.D.
inner	20.83	*3.40*	21.50	*3.94*	21.16	*3.67*
outer	20.73	*3.52*	21.37	*4.13*	21.05	*3.83*
mean	20.78	*3.46*	21.43	*4.04*	**21.11**	***3.75***

Sheathing Temperatures

Measured in middle of insulated sheathing layer

	W5		E5		Zero Cavity Mean	
	Mean	S.D.	Mean	S.D.	Mean	S.D.
upper	21.34	*3.21*	22.02	*3.64*	21.68	*3.43*
middle	20.73	*3.22*	20.52	*3.45*	20.62	*3.34*
lower	21.53	*3.25*	22.05	*3.37*	21.79	*3.31*
mean	21.20	*3.23*	21.53	*3.49*	**21.36**	***3.36***

Tyvek Temperatures

Measured at the outside surface of the Tyvek paper

	W5		E5		Zero Cavity Mean	
	Mean	S.D.	Mean	S.D.	Mean	S.D.
middle	20.93	*2.12*	21.05	*2.56*	**20.99**	***2.34***

Note: The Tyvek is installed on the exterior side of the wood studs in the Zero Cavity panels

Wood Framing Temperatures

	W5		E5		Zero Cavity Mean	
	Mean	S.D.	Mean	S.D.	Mean	S.D.
top	20.94	*1.55*	21.45	*1.79*	21.19	*1.67*
upper	21.30	*1.35*	21.41	*1.46*	21.35	*1.40*
lower	21.26	*1.33*	21.07	*1.52*	21.17	*1.43*
bottom	21.04	*1.32*	20.04	*1.33*	20.54	*1.32*
mean	21.14	*1.39*	20.99	*1.53*	**21.06**	***1.46***

Fibreglass Batt Temperatures

Measured in the middle of the batt layer at panel mid-height

	W5		E5		Zero Cavity Mean	
	Mean	S.D.	Mean	S.D.	Mean	S.D.
middle	21.05	*0.97*	21.08	*1.01*	**21.06**	***0.99***

Vapour Barrier Temperature

Measured on the exterior side of poly at panel mid-height

	W5		E5		Zero Cavity Mean	
	Mean	S.D.	Mean	S.D.	Mean	S.D.
middle	20.56	*0.59*	20.76	*0.59*	**20.66**	***0.59***

Zero-Cavity Panel Summer Period Temperatures

Weather

Monitoring Period from June 1,1992 to August 14, 1992

Statistics of Daily Averages of Readings Taken Every 5 Minutes

	Exterior				Interior			
	Mean	S.D.	Max	Min	Mean	S.D.	Max	Min
Temp.	13.96	*3.02*	20.70	3.70	21.21	*0.20*	21.60	20.90
RH%	69.68	*13.89*	92.10	37.10	50.19	*2.33*	56.80	43.50

Brick Temperatures

Measured at 10 mm from inner and outer faces respectively

	W6		E6		Dow Mean	
	Mean	S.D.	Mean	S.D.	Mean	S.D.
inner	20.65	*3.50*	21.59	*4.06*	21.12	*3.78*
outer	20.57	*3.62*	21.61	*4.21*	21.09	*3.92*
mean	20.61	*3.56*	21.60	*4.14*	**21.10**	***3.85***

Cavity Temperatures

Measured in middle of air space formed by groove in EXPS

	W6		E6		Dow Mean	
	Mean	S.D.	Mean	S.D.	Mean	S.D.
upper	20.83	*3.03*	22.01	*3.77*	21.42	*3.40*
middle	20.34	*3.38*	21.90	*3.92*	21.12	*3.65*
lower	21.18	*3.36*	21.52	*3.84*	21.35	*3.60*
mean	20.78	*3.26*	21.81	*3.84*	**21.30**	***3.55***

Building Paper Temperatures

Measured at the outside of the building paper at panel mid-height

	W6		E6		Dow Mean	
	Mean	S.D.	Mean	S.D.	Mean	S.D.
middle	20.70	*2.15*	21.38	*2.53*	**21.04**	***2.34***

Note: The building paper is installed on the exterior side of the wood studs in the Dow panels

Wood Framing Temperatures

See Text for locations

	W6		E6		Dow Mean	
	Mean	S.D.	Mean	S.D.	Mean	S.D.
top	20.76	*1.34*	21.17	*0.94*	20.96	*1.14*
upper	20.83	*1.10*	21.50	*1.25*	21.16	*1.17*
lower	20.33	*1.14*	21.41	*1.54*	20.87	*1.34*
bottom	19.84	*1.08*	21.13	*1.32*	20.49	*1.20*
mean	20.44	*1.16*	21.30	*1.26*	**20.87**	***1.21***

Fibreglass Batt Temperatures

Measured in the middle of the batt layer at panel mid-height

	W6		E6		Dow Mean	
	Mean	S.D.	Mean	S.D.	Mean	S.D.
middle	20.96	*0.74*	20.85	*1.20*	**20.90**	***0.97***

Vapour Barrier Temperature

Measured on the exterior side of poly at panel mid-height

	W6		E6		Dow Mean	
	Mean	S.D.	Mean	S.D.	Mean	S.D.
middle	20.70	*0.42*	20.84	*0.43*	**20.77**	***0.43***

DPV Panel Summer Period Temperatures

Weather

Monitoring Period from June 1,1992 to August 14, 1992

Statistics of Daily Averages of Readings Taken Every 5 Minutes

	Exterior				Interior			
	Mean	S.D.	Max	Min	Mean	S.D.	Max	Min
Temp.	13.96	*3.02*	20.70	3.70	21.21	*0.20*	21.60	20.90
RH%	69.68	*13.89*	92.10	37.10	50.19	*2.33*	56.80	43.50

Batt Insulation Relative Humidity

Measured at 220 mm from the top and bottom respectively

	W4		E4		Datum Mean	
	Mean	S.D.	Mean	S.D.	Mean	S.D.
upper	55.39	*8.50*	55.84	*9.41*	55.61	*8.95*
lower	66.15	*13.57*	52.97	*9.10*	59.56	*11.33*
mean	60.77	*11.03*	54.41	*9.25*	**57.59**	***10.14***

Cavity Relative Humidity

Measured at 220 mm from the top and bottom respectively

	W4		E4		Datum Mean	
	Mean	S.D.	Mean	S.D.	Mean	S.D.
upper	71.01	*15.04*	62.85	*13.19*	66.93	*14.12*
lower	53.05	*8.85*	66.03	*14.45*	59.54	*11.65*
mean	62.03	*11.94*	64.44	*13.82*	**63.23**	***12.88***

Sheathing Relative Humidities

Measured in middle of insulated sheathing layer

	W4		E4		Datum Mean	
	Mean	S.D.	Mean	S.D.	Mean	S.D.
upper	54.01	*9.22*	53.61	*8.77*	53.81	*8.99*
lower	49.87	*8.12*	54.52	*11.87*	52.20	*10.00*
mean	51.94	*8.67*	54.07	*10.32*	**53.00**	***9.50***

Wood Framing Temperatures

See Text for locations

	W4		E4		Datum Mean	
	Mean	S.D.	Mean	S.D.	Mean	S.D.
top	9.82	*0.16*	11.56	*0.73*	10.69	*0.44*
upper	10.81	*0.61*	13.04	*1.39*	11.93	*1.00*
lower	11.26	*0.87*	11.08	*0.79*	11.17	*0.83*
bottom	10.22	*0.29*	10.84	*0.37*	10.53	*0.33*
mean	10.53	*0.48*	11.63	*0.82*	**11.08**	***0.65***

Datum Panel Summer Period Relative Humidities and Wood Moistures

Weather

Monitoring Period from June 1,1992 to August 14, 1992

Statistics of Daily Averages of Readings Taken Every 5 Minutes

	Exterior				Interior			
	Mean	S.D.	Max	Min	Mean	S.D.	Max	Min
Temp.	13.96	*3.02*	20.70	3.70	21.21	*0.20*	21.60	20.90
RH%	69.68	*13.89*	92.10	37.10	50.19	*2.33*	56.80	43.50

Batt Insulation Relative Humidity

Measured at 220 mm from the top and bottom respectively

	W5		E5		Zero Cavity Mean	
	Mean	S.D.	Mean	S.D.	Mean	S.D.
upper	85.40	*5.87*	70.31	*7.81*	77.85	*6.84*
lower	82.36	*4.69*	83.05	*4.52*	82.70	*4.61*
mean	83.88	*5.28*	76.68	*6.17*	**80.28**	***5.72***

Sheathing Relative Humidities

Measured in middle of insulated sheathing

	W5		E5		Zero Cavity Mean	
	Mean	S.D.	Mean	S.D.	Mean	S.D.
upper	87.24	*4.35*	72.36	*6.45*	79.80	*5.40*
lower	85.99	*3.19*	49.51	*38.66*	67.75	*20.93*
mean	86.62	*3.77*	60.93	*22.56*	**73.78**	***13.16***

Wood Framing Moisture Contents

See Text for locations

	W5		E5		Zero Cavity Mean	
	Mean	S.D.	Mean	S.D.	Mean	S.D.
top	18.81	*1.96*	13.82	*0.85*	16.32	*1.40*
upper	23.31	*2.62*	14.78	*1.32*	19.04	*1.97*
lower	21.87	*2.25*	51.67	*92.77*	36.77	*47.51*
bottom	19.86	*1.68*	35.58	*1.82*	27.72	*1.75*
mean	20.96	*2.13*	28.96	*24.19*	**24.96**	***13.16***

Zero-Cavity Panel Summer Period Humidities and Wood Moistures

Weather

Monitoring Period from June 1,1992 to August 14, 1992

Statistics of Daily Averages of Readings Taken Every 5 Minutes

	Exterior				Interior			
	Mean	S.D.	Max	Min	Mean	S.D.	Max	Min
Temp.	13.96	*3.02*	20.70	3.70	21.21	*0.20*	21.60	20.90
RH%	69.68	*13.89*	92.10	37.10	50.19	*2.33*	56.80	43.50

Batt Insulation Relative Humidity

Measured at 220 mm from the top and bottom respectively

	W6		E6		Dow Mean	
	Mean	S.D.	Mean	S.D.	Mean	S.D.
upper	49.47	*4.17*	46.72	*4.89*	48.10	*4.53*
lower	45.76	*4.26*	42.31	*4.20*	44.03	*4.23*
mean	47.61	*4.21*	44.51	*4.54*	**46.06**	***4.38***

Cavity Relative Humidity

Measured at 220 mm from the top and bottom respectively

	W6		E6		Dow Mean	
	Mean	S.D.	Mean	S.D.	Mean	S.D.
upper	54.95	*13.53*	57.26	*12.02*	56.10	*12.78*
lower	60.82	*12.93*	54.01	*12.74*	57.41	*12.84*
mean	57.88	*13.23*	55.63	*12.38*	**56.76**	***12.81***

Wood Framing Moisture Contents

See Text for locations

	W6		E6		Dow Mean	
	Mean	S.D.	Mean	S.D.	Mean	S.D.
top	9.98	*0.08*	9.85	*0.05*	9.91	*0.06*
upper	10.08	*0.09*	9.96	*0.12*	10.02	*0.10*
lower	10.18	*0.18*	9.84	*0.11*	10.01	*0.14*
bottom	9.97	*0.08*	9.84	*0.05*	9.91	*0.06*
mean	10.05	*0.10*	9.87	*0.08*	**9.96**	***0.09***

DPV Panel Summer Period Relative Humidities and Wood Moistures

Weather

Monitoring Period from Dec. 14, 1991 to Feb. 1, 1992

Statistics of Daily Averages of Readings Taken Every 5 Minutes

	Exterior				Interior			
	Mean	S.D.	Max	Min	Mean	S.D.	Max	Min
Temp.	-6.94	*4.82*	0.40	-18.20	20.40	*1.25*	22.10	15.90
RH%	81.02	*6.84*	93.60	68.50	48.15	*2.40*	53.20	38.50

Brick Temperatures

Measured at 10 mm from inner and outer faces respectively

	W4		E4		Datum Mean	
	Mean	S.D.	Mean	S.D.	Mean	S.D.
inner	-2.53	*4.30*	-2.15	*4.33*	-2.34	*4.32*
outer	-3.15	*4.34*	-2.68	*4.43*	-2.91	*4.39*
mean	-2.84	*4.32*	-2.41	*4.38*	**-2.63**	*4.35*

Cavity Temperatures

Measured in middle of air cavity

	W4		E4		Datum Mean	
	Mean	S.D.	Mean	S.D.	Mean	S.D.
upper	-1.01	*4.01*	-1.36	*4.13*	-1.18	*4.07*
middle	-1.86	*4.12*	-1.13	*4.14*	-1.50	*4.13*
lower	-1.47	*3.93*	-0.31	*4.24*	-0.89	*4.09*
mean	-1.45	*4.02*	-0.93	*4.17*	**-1.19**	*4.09*

Sheathing Temperatures

Measured in middle of insulated sheathing layer

	W4		E4		Datum Mean	
	Mean	S.D.	Mean	S.D.	Mean	S.D.
upper	5.86	*3.24*	6.72	*3.01*	6.29	*3.13*
middle	1.80	*3.67*	4.81	*3.21*	3.30	*3.44*
lower	8.57	*3.30*	8.78	*3.15*	8.68	*3.23*
mean	5.41	*3.40*	6.77	*3.12*	**6.09**	*3.26*

Tyvek Temperatures

Measured at the outside of the Tyvek at panel mid-height

	W4		E4		Datum Mean	
	Mean	S.D.	Mean	S.D.	Mean	S.D.
middle	-1.15	*4.05*	-0.51	*4.02*	**-0.83**	*4.04*

Note: The Tyvek is on the exterior side of the sheathing in the Datum panels

Wood Framing Temperatures

See Text for locations

	W4		E4		Datum Mean	
	Mean	S.D.	Mean	S.D.	Mean	S.D.
top	13.28	*2.18*	13.07	*1.82*	13.18	*2.00*
upper	14.36	*1.92*	13.62	*1.80*	13.99	*1.86*
lower	13.95	*1.97*	14.07	*1.87*	14.01	*1.92*
bottom	12.89	*1.92*	11.64	*1.99*	12.27	*1.95*
mean	13.62	*2.00*	13.10	*1.87*	**13.36**	*1.93*

Fibreglass Batt Temperatures

Measured in the middle of the batt layer at panel mid-height

	W4		E4		Datum Mean	
	Mean	S.D.	Mean	S.D.	Mean	S.D.
middle	15.55	*1.72*	16.70	*1.44*	**16.13**	*1.58*

Vapour Barrier Temperatures

Measured on the outer surface of poly at panel mid-height

	W4		E4		Datum Mean	
	Mean	S.D.	Mean	S.D.	Mean	S.D.
middle	18.83	*1.36*	18.34	*1.25*	**18.59**	*1.30*

Datum Panel Winter Period Temperatures

Weather

Monitoring Period from Dec. 14, 1991 to Feb. 1, 1992

Statistics of Daily Averages of Readings Taken Every 5 Minutes

	Exterior				Interior			
	Mean	S.D.	Max	Min	Mean	S.D.	Max	Min
Temp.	-6.94	*4.82*	0.40	-18.20	20.40	*1.25*	22.10	15.90
RH%	81.02	*6.84*	93.60	68.50	48.15	*2.40*	53.20	38.50

Brick Temperatures

Measured at 10 mm from inner and outer faces respectively

	W5		E5		Zero Cavity Mean	
	Mean	S.D.	Mean	S.D.	Mean	S.D.
inner	-2.29	*4.22*	-2.09	*4.29*	-2.19	*4.25*
outer	-2.77	*4.28*	-2.68	*4.39*	-2.72	*4.34*
mean	-2.53	*4.25*	-2.39	*4.34*	**-2.46**	*4.30*

Sheathing Temperatures

Measured in middle of insulated sheathing layer

	W5		E5		Zero Cavity Mean	
	Mean	S.D.	Mean	S.D.	Mean	S.D.
upper	0.00	*3.98*	0.93	*3.81*	0.47	*3.89*
middle	-0.79	*3.98*	0.36	*3.79*	-0.22	*3.88*
lower	-0.17	*3.90*	1.69	*3.75*	0.76	*3.82*
mean	-0.32	*3.95*	0.99	*3.78*	**0.34**	*3.87*

Tyvek Temperatures

Measured at the outside of the Tyvek at panel mid-height

	W5		E5		Zero Cavity Mean	
	Mean	S.D.	Mean	S.D.	Mean	S.D.
middle	7.00	*2.92*	6.23	*2.97*	**6.61**	*2.94*

Note: The Tyvek is on the exterior side of the wood studs in the Zero Cavity panels

Wood Framing Temperatures

See Text for locations

	W5		E5		Zero Cavity Mean	
	Mean	S.D.	Mean	S.D.	Mean	S.D.
top	11.05	*2.37*	11.65	*2.11*	11.35	*2.24*
upper	13.77	*1.95*	13.83	*1.88*	13.80	*1.92*
lower	13.72	*1.97*	13.01	*1.97*	13.37	*1.97*
bottom	12.37	*1.97*	12.34	*1.72*	12.35	*1.84*
mean	12.73	*2.07*	12.70	*1.92*	**12.72**	*1.99*

Fibreglass Batt Temperatures

Measured in the middle of the batt layer at panel mid-height

	W5		E5		Zero Cavity Mean	
	Mean	S.D.	Mean	S.D.	Mean	S.D.
middle	16.46	*1.61*	16.65	*1.50*	**16.56**	*1.55*

Vapour Barrier Temperatures

Measured on the outer surface of poly at panel mid-height

	W5		E5		Zero Cavity Mean	
	Mean	S.D.	Mean	S.D.	Mean	S.D.
middle	19.06	*1.32*	18.97	*1.25*	**19.02**	*1.29*

Zero Cavity Panel Winter Period Temperatures

Weather

Monitoring Period from Dec. 14, 1991 to Feb. 1, 1992

Statistics of Daily Averages of Readings Taken Every 5 Minutes

	Exterior				Interior			
	Mean	S.D.	Max	Min	Mean	S.D.	Max	Min
Temp.	-6.94	*4.82*	0.40	-18.20	20.40	*1.25*	22.10	15.90
RH%	81.02	*6.84*	93.60	68.50	48.15	*2.40*	53.20	38.50

Brick Temperatures

Measured at 10 mm from inner and outer faces respectively

	W6		E6		Dow Mean	
	Mean	S.D.	Mean	S.D.	Mean	S.D.
inner	-2.31	*4.25*	-2.16	*4.25*	-2.24	*4.25*
outer	-2.88	*4.29*	-2.61	*4.35*	-2.75	*4.32*
mean	-2.60	*4.27*	-2.39	*4.30*	**-2.49**	***4.29***

Cavity Temperatures

Measured in middle of air cavity

	W6		E6		Dow Mean	
	Mean	S.D.	Mean	S.D.	Mean	S.D.
upper	-0.86	*4.07*	-0.37	*4.05*	-0.62	*4.06*
middle	-1.64	*4.08*	-0.91	*4.03*	-1.28	*4.06*
lower	-0.90	*4.02*	-1.00	*4.03*	-0.95	*4.03*
mean	-1.13	*4.06*	-0.76	*4.04*	**-0.95**	***4.05***

Building Paper Temperatures

Measured on outside surface of building paper

	W6		E6		Dow Mean	
	Mean	S.D.	Mean	S.D.	Mean	S.D.
middle	6.75	*2.86*	6.64	*2.91*	**6.70**	***2.89***

Note: The Tyvek is on the exterior side of the wood studs in the Zero Cavity panels

Wood Framing Temperatures

See text for locations

	W6		E6		Dow Mean	
	Mean	S.D.	Mean	S.D.	Mean	S.D.
top	11.81	*2.19*	12.89	*1.72*	12.35	*1.96*
upper	13.71	*1.91*	14.52	*1.76*	14.12	*1.84*
lower	12.97	*1.85*	13.24	*1.81*	13.11	*1.83*
bottom	11.36	*2.10*	13.31	*1.91*	12.34	*2.01*
mean	12.46	*2.01*	13.49	*1.80*	**12.98**	***1.91***

Fibreglass Batt Temperatures

Measured in the middle of the batt layer at panel mid-height

	W6		E6		Dow Mean	
	Mean	S.D.	Mean	S.D.	Mean	S.D.
middle	16.39	*1.52*	16.00	*1.59*	**16.20**	***1.56***

Vapour Barrier Temperatures

Measured on the outer surface of poly at panel mid-height

	W6		E6		Dow Mean	
	Mean	S.D.	Mean	S.D.	Mean	S.D.
middle	18.69	*1.26*	19.03	*1.26*	**18.86**	***1.26***

DPV Panel Winter Period Temperatures

Weather

	Exterior				Interior			
	Mean	S.D.	Max	Min	Mean	S.D.	Max	Min
Temp.	-6.94	*4.82*	0.40	-18.20	20.40	*1.25*	22.10	15.90
RH%	81.02	*6.84*	93.60	68.50	48.15	*2.40*	53.20	38.50

Batt Insulation Relative Humidity

Measured at 220 mm from the top and bottom respectively

	W4		E4		Datum Mean	
	Mean	S.D.	Mean	S.D.	Mean	S.D.
upper	24.39	*5.13*	27.65	*5.43*	26.02	*5.28*
lower	25.88	*5.24*	25.36	*5.06*	25.62	*5.15*
mean	25.14	*5.19*	26.51	*5.25*	**25.82**	***5.22***

Cavity Relative Humidity

Measured at 220 mm from the top and bottom respectively

	W4		E4		Datum Mean	
	Mean	S.D.	Mean	S.D.	Mean	S.D.
upper	81.21	*4.23*	82.52	*2.33*	81.87	*3.28*
lower	79.15	*4.05*	80.35	*4.68*	79.75	*4.37*
mean	80.18	*4.14*	81.44	*3.51*	**80.81**	***3.82***

Sheathing Relative Humidities

Measured in middle of insulated sheathing

	W4		E4		Datum Mean	
	Mean	S.D.	Mean	S.D.	Mean	S.D.
upper	34.97	*4.70*	38.19	*4.61*	36.58	*4.66*
lower	30.06	*7.92*	26.23	*6.30*	28.15	*7.11*
mean	32.52	*6.31*	32.21	*5.46*	**32.36**	***5.88***

Wood Framing Moisture Content

See text for locations

	W4		E4		Datum Mean	
	Mean	S.D.	Mean	S.D.	Mean	S.D.
top	10.66	*0.10*	10.40	*0.08*	10.53	*0.09*
upper	10.63	*0.08*	10.41	*0.08*	10.52	*0.08*
lower	10.71	*0.08*	10.65	*0.08*	10.68	*0.08*
bottom	10.94	*0.08*	10.92	*0.09*	10.93	*0.09*
mean	10.74	*0.09*	10.60	*0.08*	**10.67**	***0.08***

Datum Panel Winter Period Relative Humidities

Weather

	Exterior				Interior			
	Mean	S.D.	Max	Min	Mean	S.D.	Max	Min
Temp.	-6.94	*4.82*	0.40	-18.20	20.40	*1.25*	22.10	15.90
RH%	81.02	*6.84*	93.60	68.50	48.15	*2.40*	53.20	38.50

Batt Insulation Relative Humidity

Measured at 220 mm from the top and bottom respectively

	W5		E5		Zero Cavity Mean	
	Mean	S.D.	Mean	S.D.	Mean	S.D.
upper	26.85	*5.90*	28.82	*4.86*	27.83	*5.38*
lower	30.97	*5.48*	28.46	*5.67*	29.71	*5.58*
mean	28.91	*5.69*	28.64	*5.27*	**28.77**	***5.48***

Sheathing Relative Humidities

Measured in middle of insulated sheathing

	W5		E5		Zero Cavity Mean	
	Mean	S.D.	Mean	S.D.	Mean	S.D.
upper	46.49	*5.90*	48.47	*5.06*	47.48	*5.48*
lower	52.51	*5.48*	28.44	*7.46*	40.48	*6.47*
mean	49.50	*5.69*	38.46	*6.26*	**43.98**	***5.98***

Wood Framing Moisture Content

See text for locations

	W5		E5		Zero Cavity Mean	
	Mean	S.D.	Mean	S.D.	Mean	S.D.
top	11.01	*0.09*	10.83	*0.09*	10.92	*0.09*
upper	10.63	*0.10*	10.61	*0.09*	10.62	*0.10*
lower	10.63	*0.09*	10.64	*0.09*	10.63	*0.09*
bottom	13.93	*0.96*	23.06	*6.45*	18.49	*3.71*
mean	11.55	*0.31*	13.78	*1.68*	**12.67**	***1.00***

Zero-Cavity Panel Winter Period Relative Humidities

Weather

	Exterior				Interior			
	Mean	S.D.	Max	Min	Mean	S.D.	Max	Min
Temp.	-6.94	*4.82*	0.40	-18.20	20.40	*1.25*	22.10	15.90
RH%	81.02	*6.84*	93.60	68.50	48.15	*2.40*	53.20	38.50

Batt Insulation Relative Humidity

Measured at 220 mm from the top and bottom respectively

	W6		E6		Dow Mean	
	Mean	S.D.	Mean	S.D.	Mean	S.D.
upper	29.48	*6.07*	27.86	*3.15*	28.67	*4.61*
lower	28.47	*3.48*	30.61	*2.15*	29.54	*2.82*
mean	28.98	*4.78*	29.24	*2.65*	**29.11**	***3.71***

Cavity Relative Humidity

Measured at 220 mm from the top and bottom respectively

	W6		E6		Dow Mean	
	Mean	S.D.	Mean	S.D.	Mean	S.D.
upper	51.43	*4.70*	43.50	*6.33*	47.47	*5.52*
lower	51.92	*5.32*	55.30	*6.16*	53.61	*5.74*
mean	51.67	*5.01*	49.40	*6.25*	**50.54**	***5.63***

Wood Framing Moisture Content

See text for locations

	W6		E6		Dow Mean	
	Mean	S.D.	Mean	S.D.	Mean	S.D.
top	10.91	*0.08*	10.56	*0.06*	10.73	*0.07*
upper	10.81	*0.07*	10.64	*0.07*	10.72	*0.07*
lower	10.83	*0.07*	10.72	*0.08*	10.78	*0.07*
bottom	10.92	*0.08*	10.40	*0.04*	10.66	*0.06*
mean	10.87	*0.08*	10.58	*0.06*	**10.72**	***0.07***

DPV Panel Winter Period Relative Humiditi

Appendix D

Pressure Equalization Data:

Statistics

Frequency Analysis

Time Domain Plots

Read raw voltages from data files

$M := READPRN(E613)$ $N := READPRN(E614)$ $P := READPRN(E615)$

$size := rows(M)$ $timestep := \frac{1}{2}$ $j := 0..(size - 1)$ $time_j := j \cdot timestep$

Convert voltages to pressures using calibration values

File #1

$windspeed_m := (M)^{<3>} \cdot 180 + 4$ $wind_{m_j} := \left(\frac{windspeed_{m_j}}{3.6}\right)^2 \cdot 0.647$

$mean(wind_m) = 45.6$ $mean(direction_m) = 210.8$

$stdev(wind_m) = 26.9$ $stdev(direction_m) = 13.9$

File #2

$windspeed_n := (N)^{<3>} \cdot 180 + 4$ $wind_{n_j} := \left(\frac{windspeed_{n_j}}{3.6}\right)^2 \cdot 0.647$

$mean(wind_n) = 38.9$ $mean(direction_n) = 200.2$

$stdev(wind_n) = 22$ $stdev(direction_n) = 14.3$

File #3

$windspeed_p := (P)^{<3>} \cdot 180 + 4$ $wind_{p_j} := \left(\frac{windspeed_{p_j}}{3.6}\right)^2 \cdot 0.647$

$mean(wind_p) = 44.6$ $mean(direction_p) = 200.5$

$stdev(wind_p) = 23.2$ $stdev(direction_p) = 14$

Average the time domain values of all files and calculate some statistics.

$$V_{10} := \frac{mean(windspeed_m) + mean(windspeed_n) + mean(windspeed_p)}{3}$$

$$Pwind := (wind_m + wind_n + wind_p) \cdot \frac{1}{3}$$

$$\sigma_{wind} := (stdev(wind_m) + stdev(wind_n) + stdev(wind_p)) \cdot \frac{1}{3}$$

Present the statistics of the combined records:

$V_{10} = 28.2$ km/h

$mean(Pwind) = 43$ $\sigma_{wind} = 24$ $wind_{mean} := mean(Pwind)$

Intensity of Turbulence: $\frac{\sigma_{wind}}{wind_{mean}} = 0.56$

Now, take the Fourier transform of all both pressure variations to create pressure spectra.

$win_m := fft(wind_m)$ $win_n := fft(wind_n)$ $win_p := fft(wind_p)$

Average files in the frequency Domain

$N := \frac{size}{2}$ $k := 1..N$ $f_k := \frac{k}{N} \cdot \frac{1}{timestep}$

Note: This calculates the actual frequency which varies with the sampling rate

$$S_{wind_k} := \frac{win_{m_k} + win_{n_k} + win_{p_k}}{3}$$

Average values to smooth curves $p := 4 .. (N - 3)$ $f_p := \frac{p}{N} \cdot \frac{1}{timestep}$

$$S_{windavg_p} := \left| \frac{S_{wind_{p-1}} + S_{wind_p} + S_{wind_{p+1}} + S_{wind_{p+2}} + S_{wind_{p-2}} + S_{wind_{p-3}} + S_{wind_{p+3}}}{7} \right|$$

$$Vmean := \sqrt{\left(\frac{wind_{mean}}{0.647}\right)}$$ Calculate the velocity in m/s from the previously calculated pressure value

Vmean = 8.2 m/s

Calculate Typical Wind Pressure Spectrum Curve

Fetch length $L := 1200$ Surface drag coefficient: $k_d := 0.010$

$$wave_p := \frac{f_p}{Vmean} \qquad x_p := \frac{L \cdot f_p}{Vmean} \qquad S_{NBC_p} := \frac{4 \cdot k_d \cdot (x_p)^2}{\left[1 + (x_p)^2\right]^{\frac{4}{3}}}$$

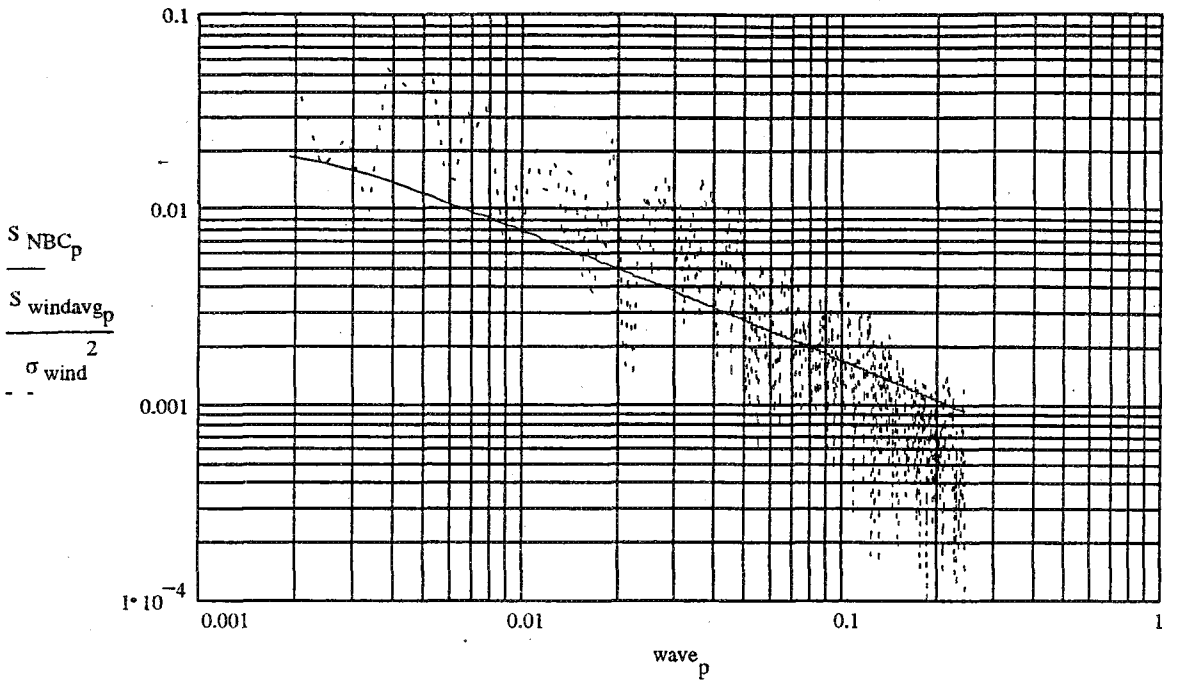

PRESSURE SPECTRUUM

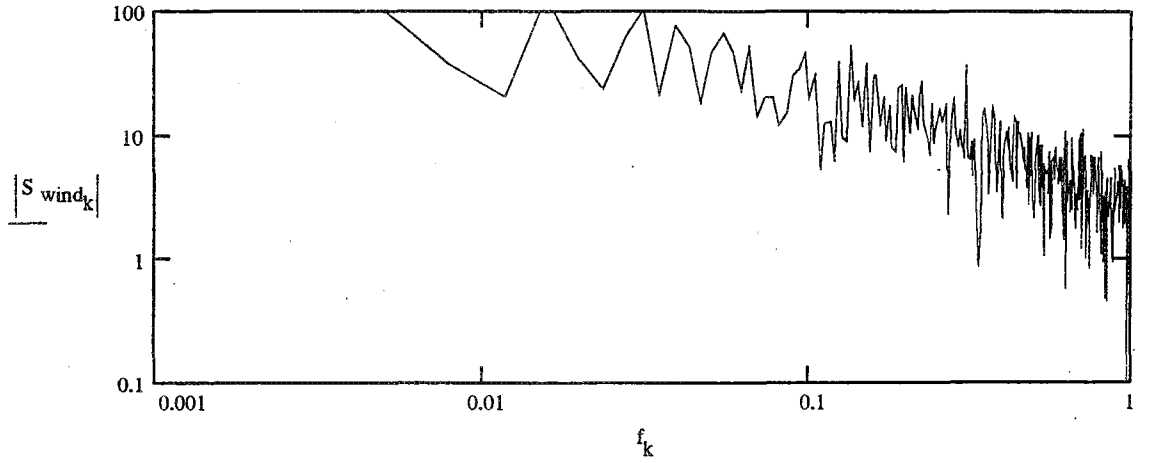

NORMALISED PRESSURE SPECTRUM

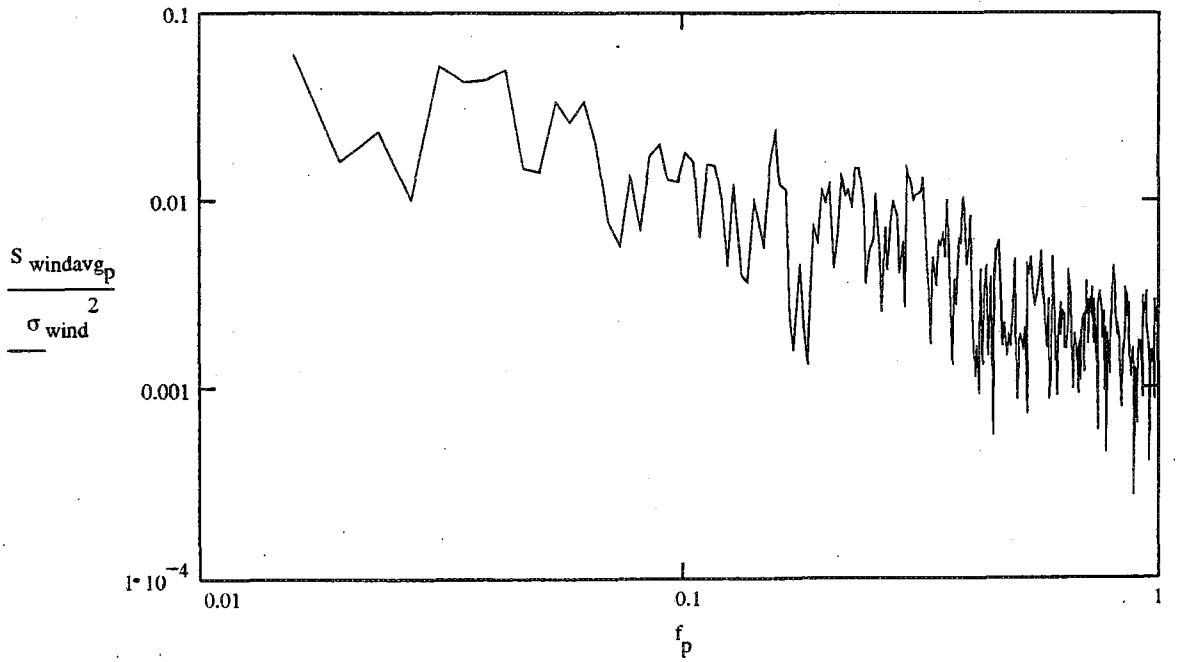

TIME DOMAIN PLOTS OF PRESSURE

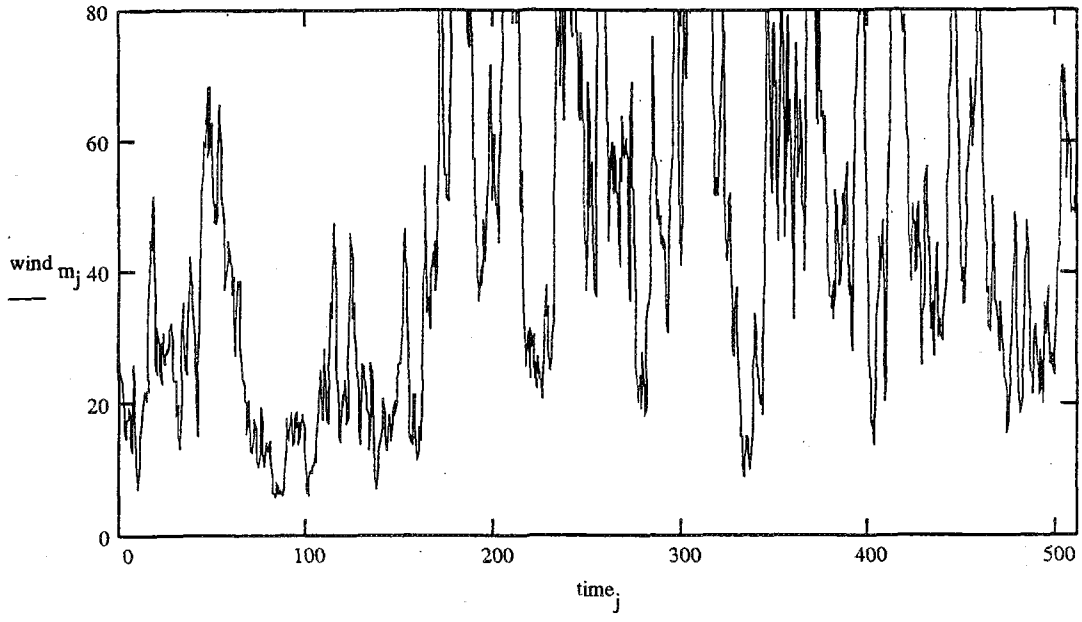

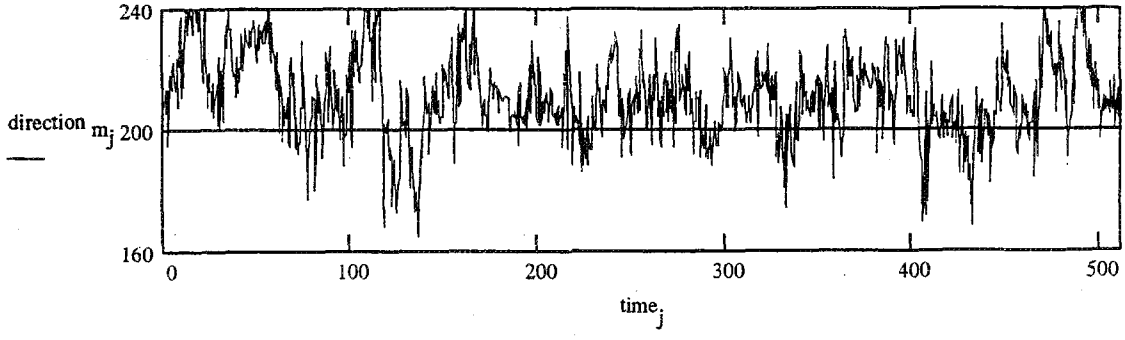

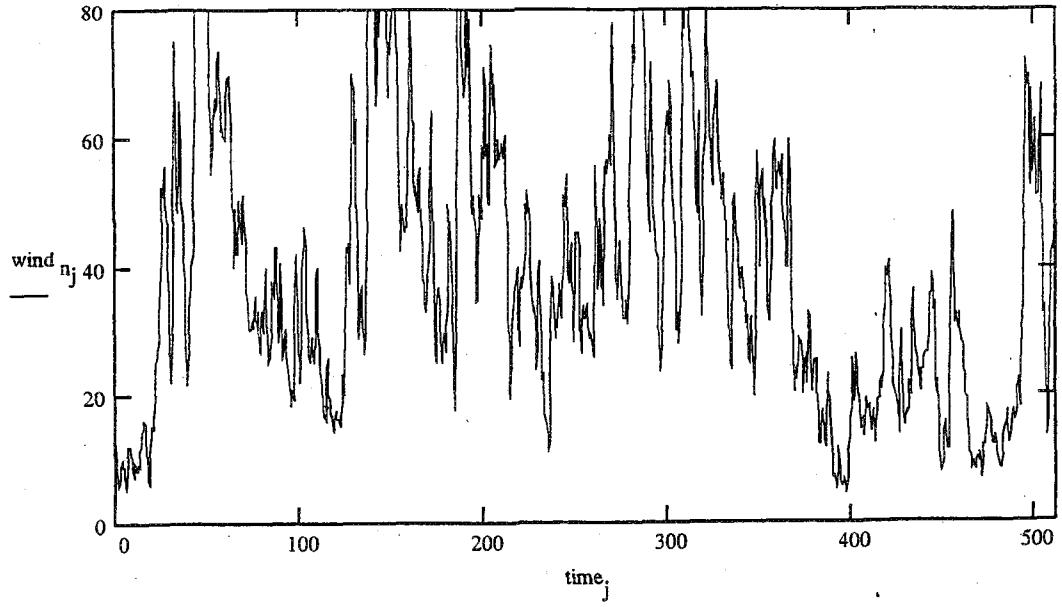

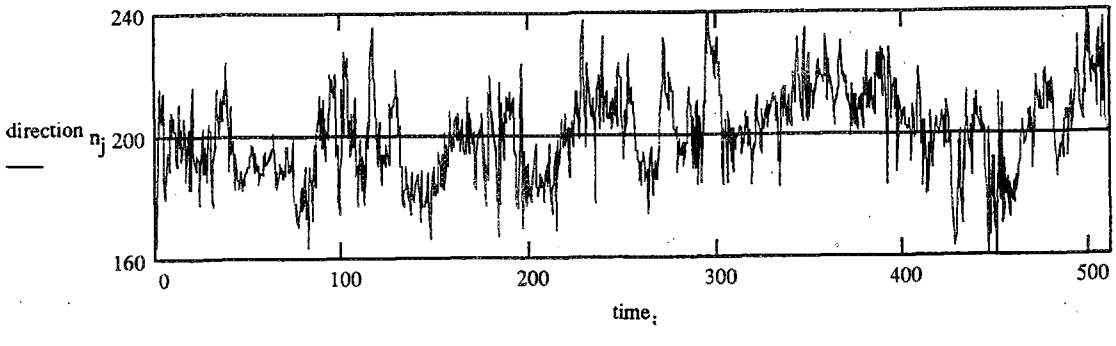

TIME DOMAIN PLOTS OF PRESSURE

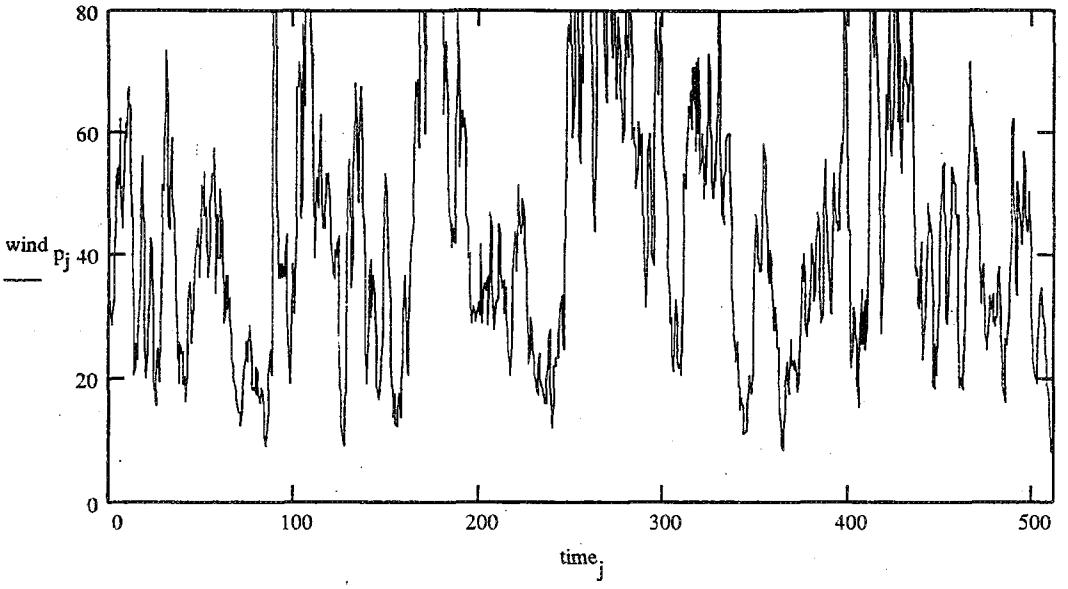

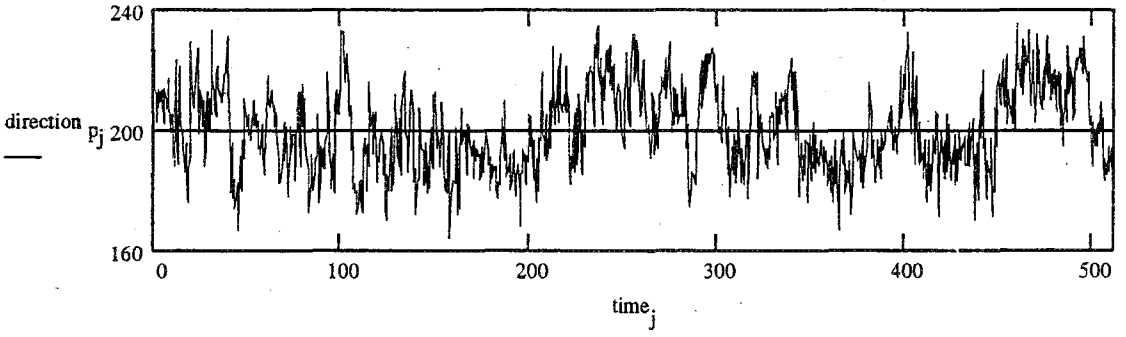

Datum Panel W4
Records W4_30, W4_31, and W4_32

Raw Pressure Spectral Density Functions (Power Spectra)

Exterior Pressures (Pa)^2

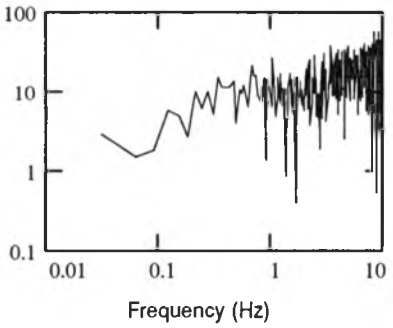

Cavity Pressures (Pa)^2

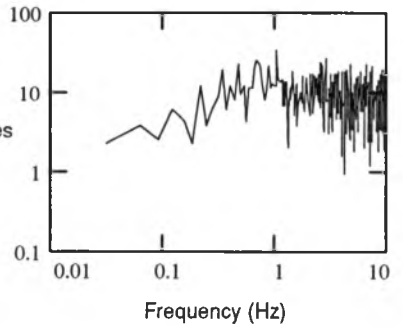

Wind Pressures (Pa)^2

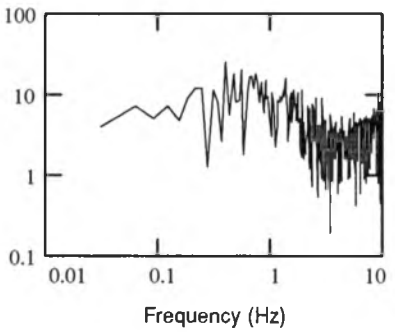

Difference Across Screen (Pa)^2

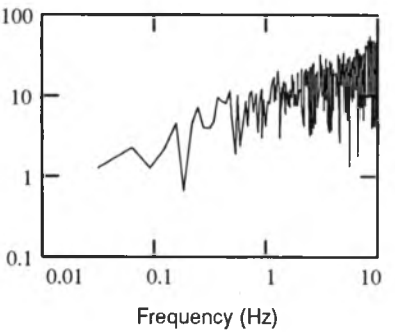

Smoothed and Normalized Pressure Spectra

Exterior Pressure

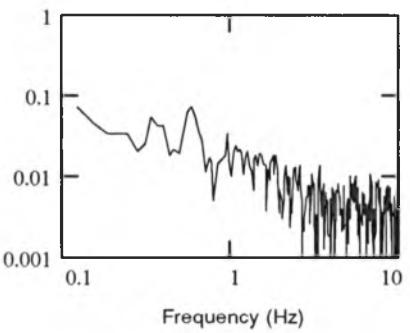

Cavity Pressure

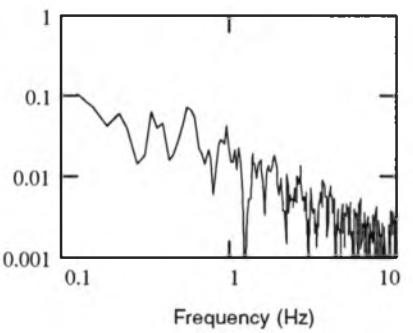

Wind Pressure

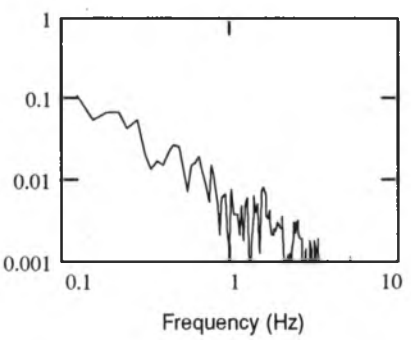

Difference Across Screen

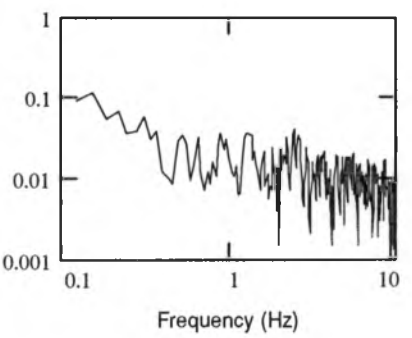

Read raw voltages from data files

$M := READPRN(W45) \qquad N := READPRN(W46) \qquad P := READPRN(W47)$

$size := rows(M) \qquad timestep := \frac{1}{16} \qquad j := 0..(size - 1) \qquad time_j := j \cdot timestep$

Convert voltages in file to pressures using calibration values

File #1

$$exterior_m := \left[(M)^{<0>} - \left(\frac{2838}{4095} \cdot 5 \right) \right] \cdot 500 \qquad cavity_m := \left[(M)^{<2>} - \left(\frac{2866}{4095} \cdot 5 \right) \right] \cdot 500$$

$$windspeed_m := (M)^{<3>} \cdot 180 + 4 \qquad wind_{m_j} := \left(\frac{windspeed_{m_j}}{3.6} \right)^2 \cdot 0.647$$

$difference_m := exterior_m - cavity_m \qquad mean(difference_m) = 3.2 \qquad stdev(difference_m) = 9.2$

$mean(exterior_m) = 17 \qquad mean(wind_m) = 39.6 \qquad mean(cavity_m) = 13.8 \qquad mean(direction_m) = 276.6$

$stdev(exterior_m) = 14 \qquad stdev(wind_m) = 16.5 \qquad stdev(cavity_m) = 12.8 \qquad stdev(direction_m) = 15.3$

File #2

$$exterior_n := \left[(N)^{<0>} - \left(\frac{2838}{4095} \cdot 5 \right) \right] \cdot 500 \qquad cavity_n := \left[(N)^{<2>} - \left(\frac{2866}{4095} \cdot 5 \right) \right] \cdot 500$$

$$windspeed_n := (N)^{<3>} \cdot 180 + 4 \qquad wind_{n_j} := \left(\frac{windspeed_{n_j}}{3.6} \right)^2 \cdot 0.647$$

$difference_n := exterior_n - cavity_n \qquad mean(difference_n) = 1.2 \qquad stdev(difference_n) = 12.6$

$mean(exterior_n) = 20 \qquad mean(wind_n) = 47 \qquad mean(cavity_n) = 18.8 \qquad mean(direction_n) = 273.3$

$stdev(exterior_n) = 16.9 \qquad stdev(wind_n) = 22.2 \qquad stdev(cavity_n) = 17.1 \qquad stdev(direction_n) = 11.7$

File #3

$$exterior_p := \left[(P)^{<0>} - \left(\frac{2838}{4095} \cdot 5 \right) \right] \cdot 500 \qquad cavity_p := \left[(P)^{<2>} - \left(\frac{2866}{4095} \cdot 5 \right) \right] \cdot 500$$

$$windspeed_p := (P)^{<3>} \cdot 180 + 4 \qquad wind_{p_j} := \left(\frac{windspeed_{p_j}}{3.6} \right)^2 \cdot 0.647$$

$difference_p := exterior_p - cavity_p \qquad mean(difference_p) = -0.8 \qquad stdev(difference_p) = 8.7$

$mean(exterior_p) = 18.3 \qquad mean(wind_p) = 37.7 \qquad mean(cavity_p) = 19.1 \qquad mean(direction_p) = 254.7$

$stdev(exterior_p) = 12.2 \qquad stdev(wind_p) = 19.8 \qquad stdev(cavity_p) = 14.6 \qquad stdev(direction_p) = 14$

Average the time domain values of all files and calculate some statistics.

$$V_{10} := \frac{mean(windspeed_m) + mean(windspeed_n) + mean(windspeed_p)}{3}$$

$$Pdiff := (difference_m + difference_n + difference_p) \cdot \frac{1}{3} \qquad Pwind := (wind_m + wind_n + wind_p) \cdot \frac{1}{3}$$

$$Pext := (exterior_m + exterior_n + exterior_p) \cdot \frac{1}{3} \qquad Pcav := (cavity_m + cavity_n + cavity_p) \cdot \frac{1}{3}$$

$$\sigma_{diff} := (stdev(difference_m) + stdev(difference_n) + stdev(difference_p)) \cdot \frac{1}{3}$$

$$\sigma_{cav} := (stdev(cavity_m) + stdev(cavity_n) + stdev(cavity_p)) \cdot \frac{1}{3}$$

$$\sigma_{ext} := (stdev(exterior_m) + stdev(exterior_n) + stdev(exterior_p)) \cdot \frac{1}{3}$$

$$\sigma_{wind} := (stdev(wind_m) + stdev(wind_n) + stdev(wind_p)) \cdot \frac{1}{3}$$

Present the statistics of the combined records:

$V_{10} = 27.8$ km/h

mean(Pdiff) = 1.2	$\sigma_{diff} = 10.1$	$diff_{mean} := mean(Pdiff)$
mean(Pcav) = 17.2	$\sigma_{cav} = 14.9$	$cav_{mean} := mean(Pcav)$
mean(Pext) = 18.4	$\sigma_{ext} = 14.4$	$ext_{mean} := mean(Pext)$
mean(Pwind) = 41.4	$\sigma_{wind} = 19.5$	$wind_{mean} := mean(Pwind)$

Intensity of Turbulence: $\frac{\sigma_{wind}}{wind_{mean}} = 0.47$ $\frac{\sigma_{cav}}{cav_{mean}} = 0.86$ $\frac{\sigma_{ext}}{ext_{mean}} = 0.78$ $\frac{\sigma_{diff}}{diff_{mean}} = 8.32$

Now, take the Fourier transform of all both pressure variations to create pressure spectra.

$ext_m := fft(exterior_m)$ $cav_m := fft(cavity_m)$ $win_m := fft(wind_m)$ $diff_m := fft(difference_m)$

$ext_n := fft(exterior_n)$ $cav_n := fft(cavity_n)$ $win_n := fft(wind_n)$ $diff_n := fft(difference_n)$

$ext_p := fft(exterior_p)$ $cav_p := fft(cavity_p)$ $win_p := fft(wind_p)$ $diff_p := fft(difference_p)$

$N := \frac{size}{2}$ $k := 1..N$ $f_k := \frac{k}{N} \cdot \frac{1}{timestep}$

Note: This calculates the actual frequency which varies with the sampling rate

Average files in the frequency Domain

$$S_{ext_k} := \frac{ext_{m_k} + ext_{n_k} + ext_{p_k}}{3} \qquad S_{cav_k} := \frac{cav_{m_k} + cav_{n_k} + cav_{p_k}}{3}$$

$$S_{wind_k} := \frac{win_{m_k} + win_{n_k} + win_{p_k}}{3} \qquad S_{diff_k} := \frac{diff_{m_k} + diff_{n_k} + diff_{p_k}}{3}$$

Average values to smooth curves $p := 4..(N - 3)$ $f_p := \frac{p}{N} \cdot \frac{1}{timestep}$

$$S_{extavg_p} := \left| \frac{S_{ext_{p-1}} + S_{ext_p} + S_{ext_{p+1}} + S_{ext_{p+2}} + S_{ext_{p-2}} + S_{ext_{p-3}} + S_{ext_{p+3}}}{7} \right|$$

$$S_{windavg_p} := \left| \frac{S_{wind_{p-1}} + S_{wind_p} + S_{wind_{p+1}} + S_{wind_{p+2}} + S_{wind_{p-2}} + S_{wind_{p-3}} + S_{wind_{p+3}}}{7} \right|$$

$$S_{cavavg_p} := \left| \frac{S_{cav_{p-1}} + S_{cav_p} + S_{cav_{p+1}} + S_{cav_{p+2}} + S_{cav_{p-2}} + S_{cav_{p-3}} + S_{cav_{p+3}}}{7} \right|$$

$$S_{diffavg_p} := \left| \frac{S_{diff_{p-1}} + S_{diff_p} + S_{diff_{p+1}} + S_{diff_{p+2}} + S_{diff_{p-2}} + S_{diff_{p-3}} + S_{diff_{p+3}}}{7} \right|$$

Calculate the Frequency Response Function function for the presure difference

$$H_{\Delta_k} := \frac{S_{diff_k}}{S_{ext_k}} \qquad K_{\Delta_k} := \left| H_{\Delta_k} \right| \qquad \phi_{\Delta_k} := atan\left(\frac{Im\left(K_{\Delta_k}\right)}{Re\left(K_{\Delta_k}\right)} \right) \cdot \frac{180}{\pi}$$

Calculate the Cavity Frequency Response function.

$$H_{c_k} := \frac{S_{cav_k}}{S_{ext_k}} \qquad K_{c_k} := \left| H_{c_k} \right| \qquad \phi_{c_k} := atan\left(\frac{Im\left(H_{c_k}\right)}{Re\left(H_{c_k}\right)} \right) \cdot \frac{180}{\pi}$$

PRESSURE SPECTRA

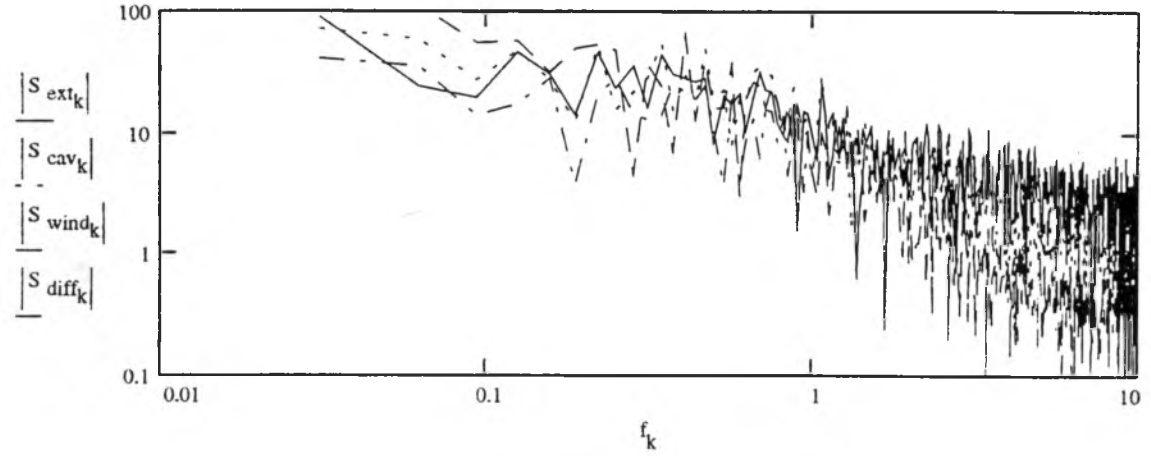

NORMALISED PRESSURE SPECTRA

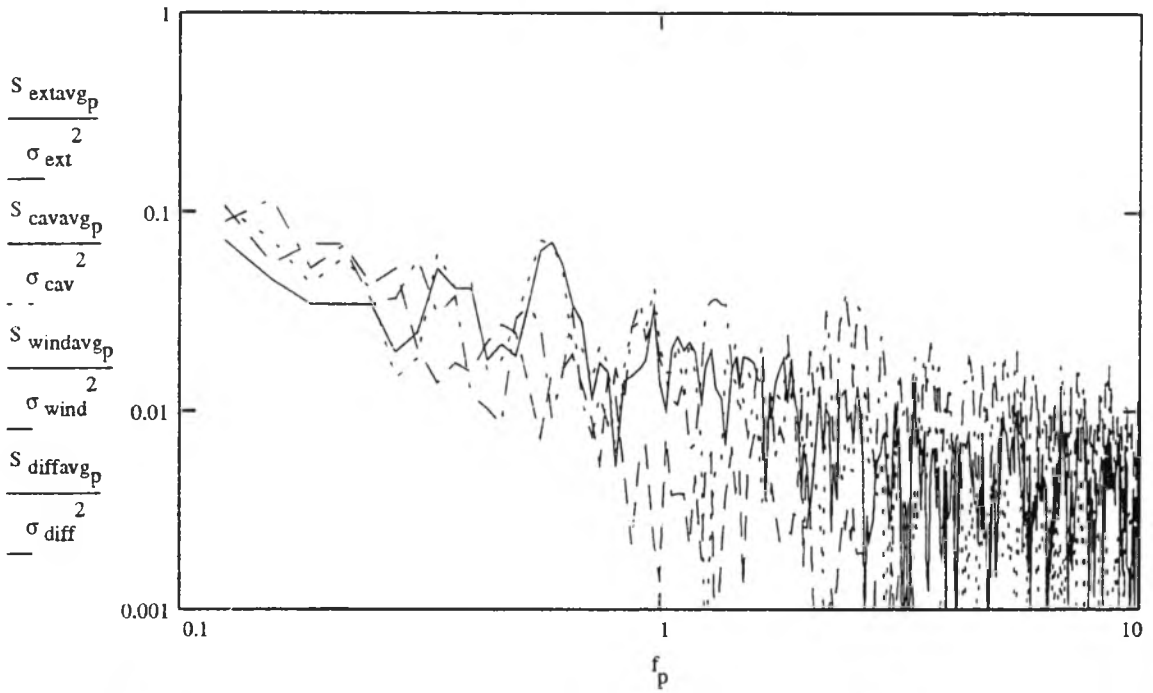

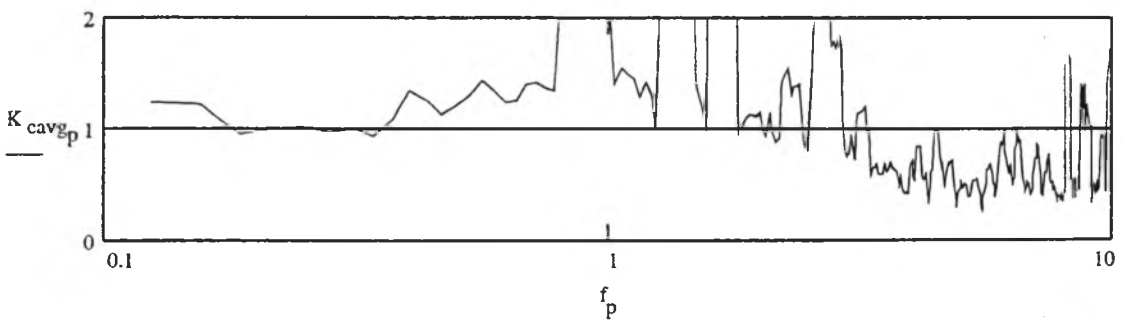

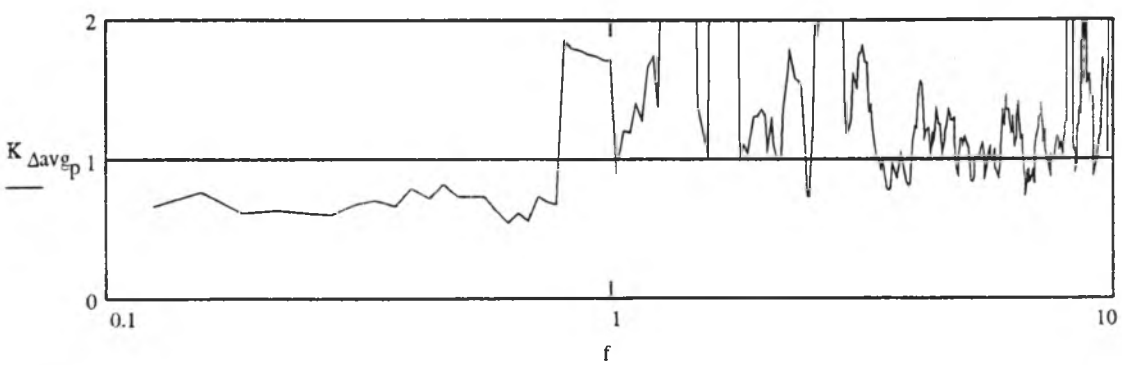

SPECTRA RELATIONSHIPS

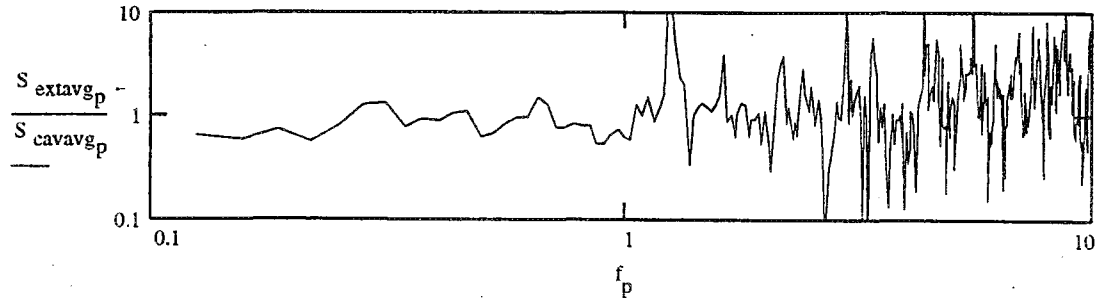

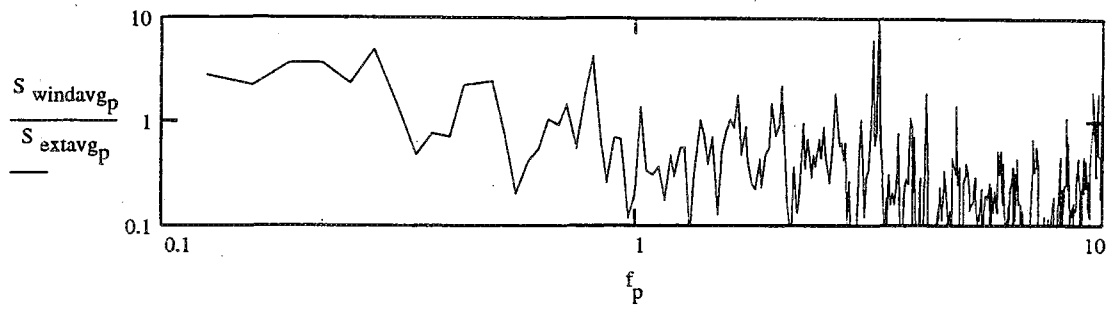

CAVITY PHASE LAG (Degrees)

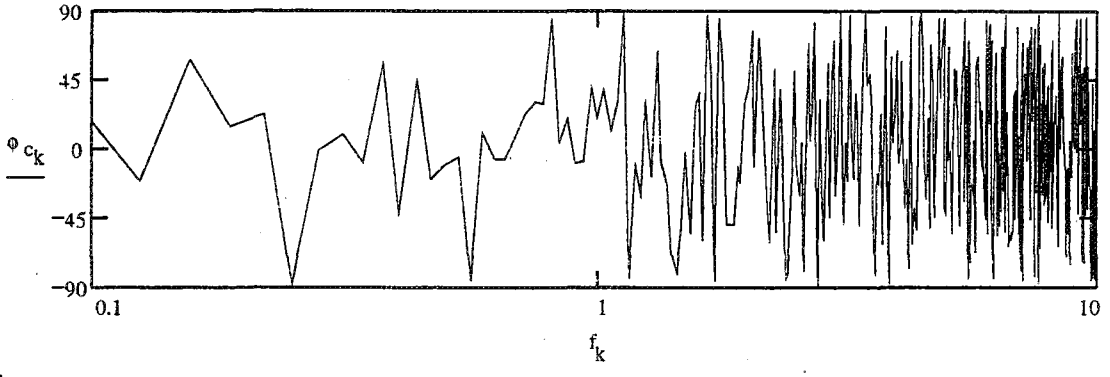

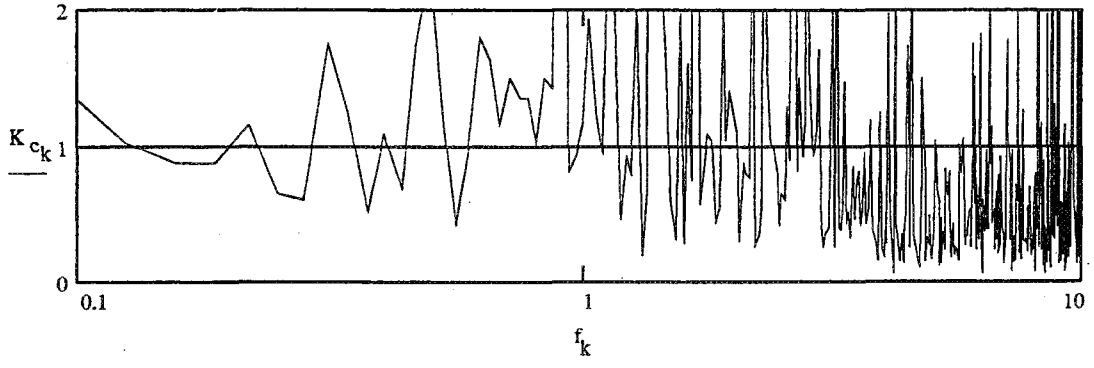

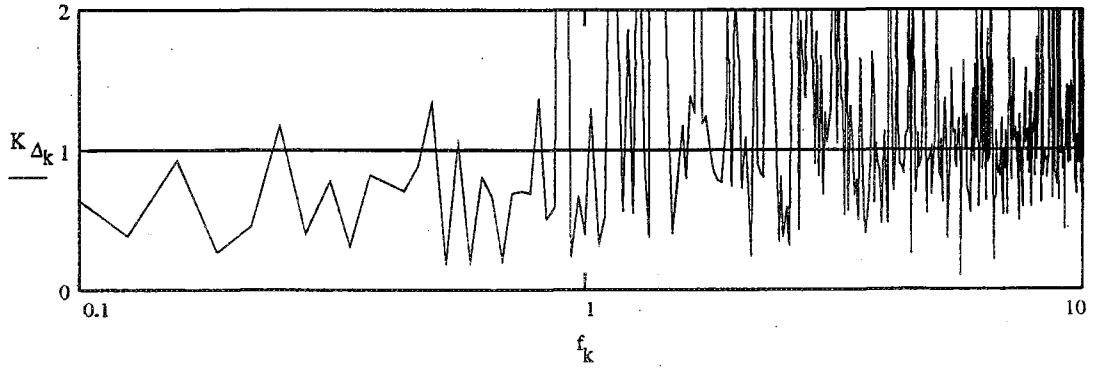

TIME DOMAIN PLOTS OF PRESSURE

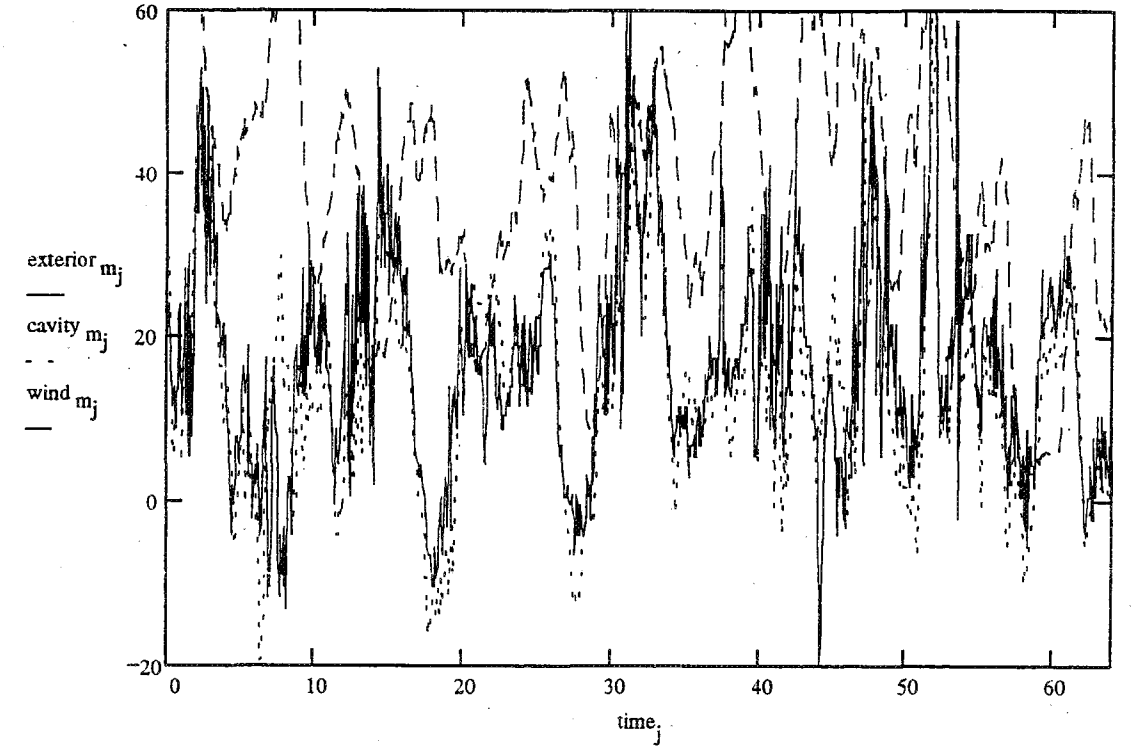

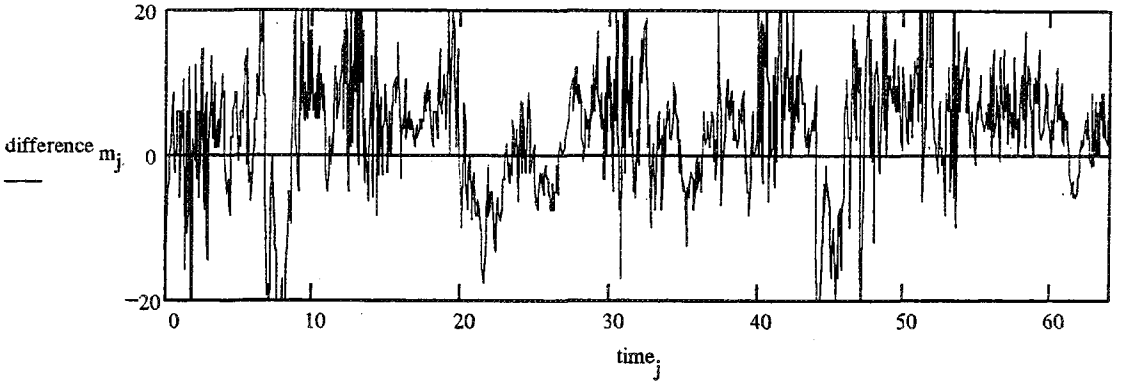

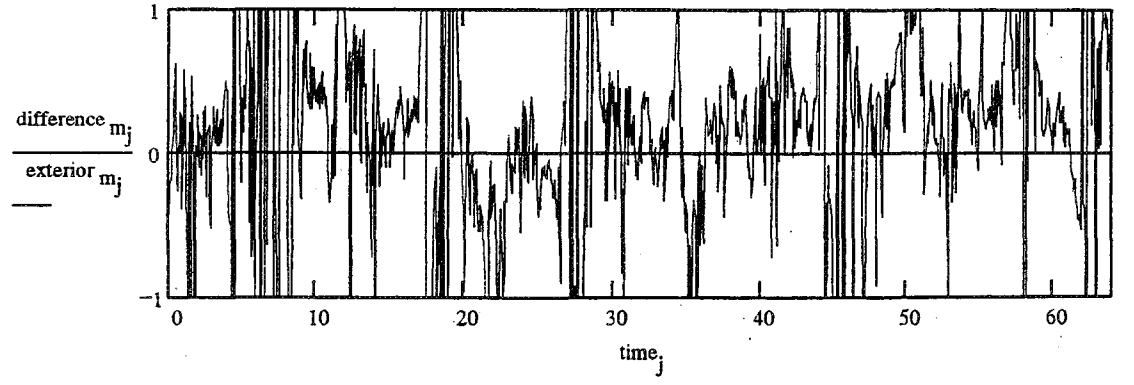

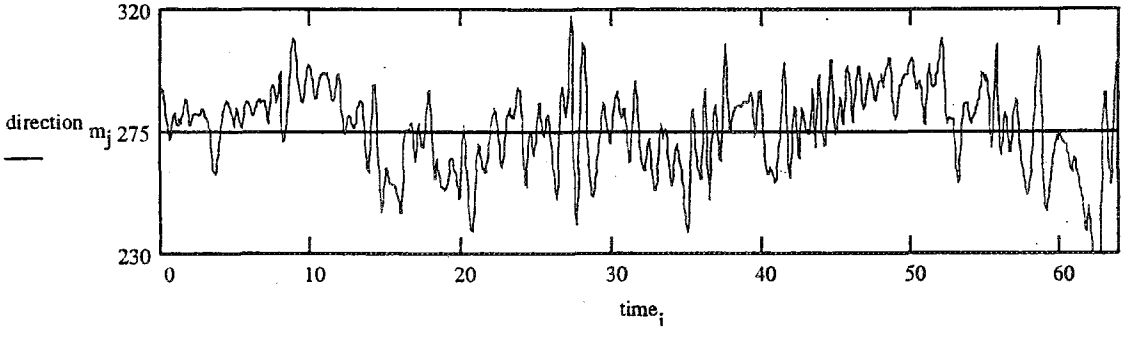

TIME DOMAIN PLOTS OF PRESSURE

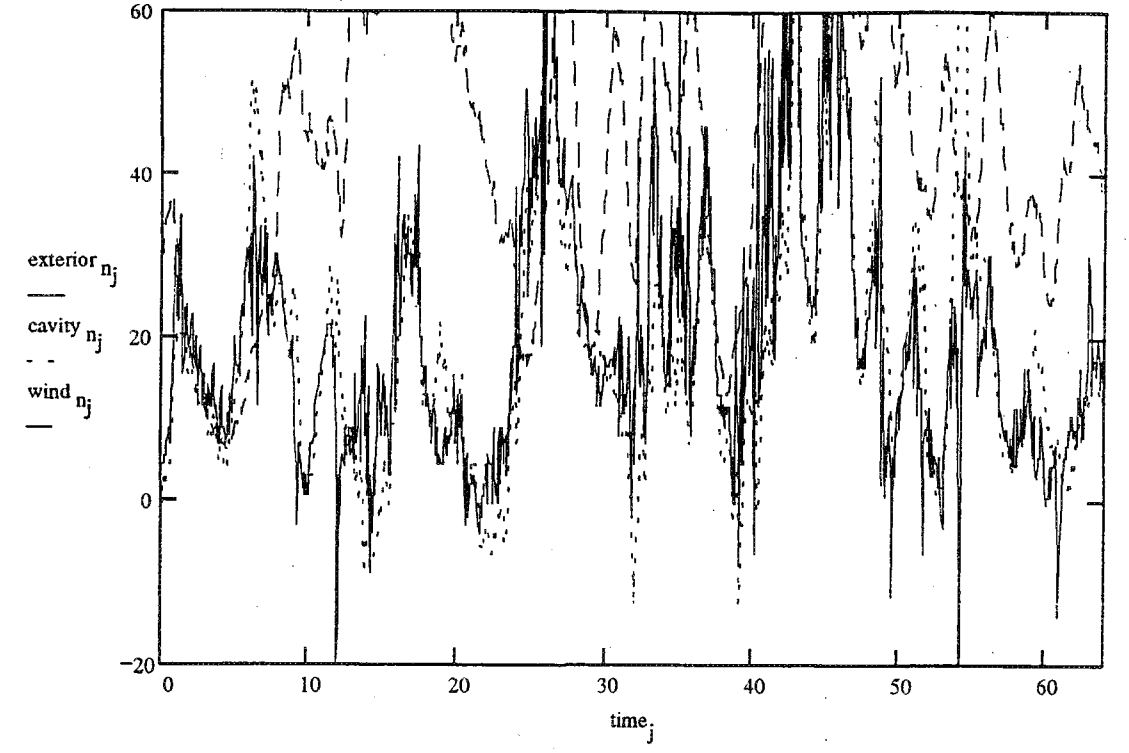

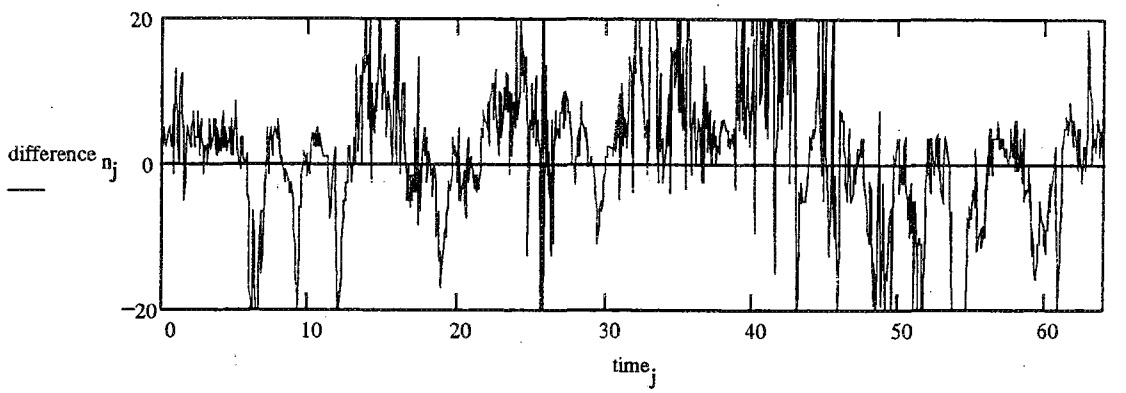

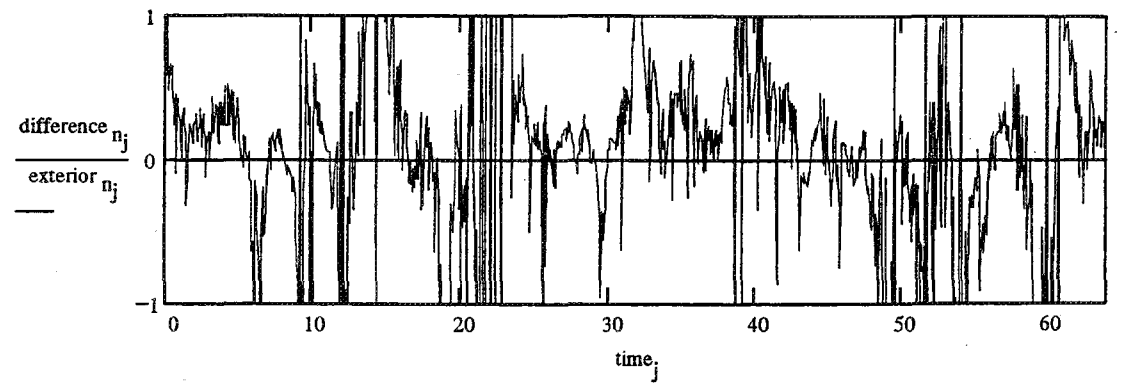

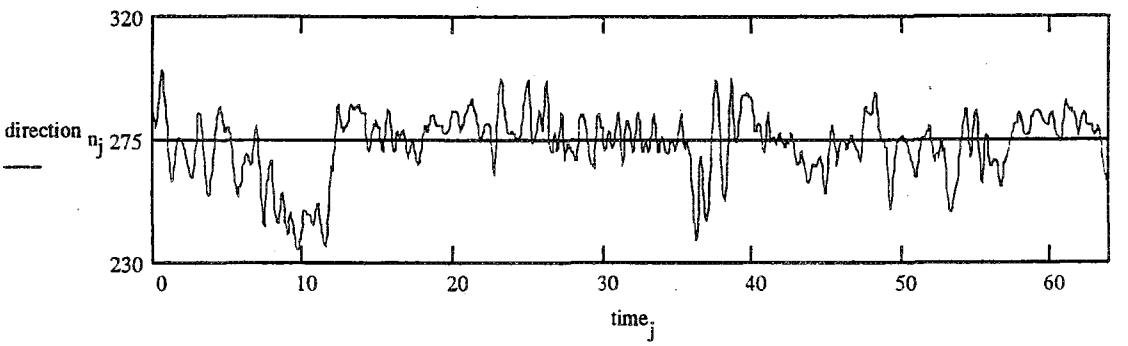

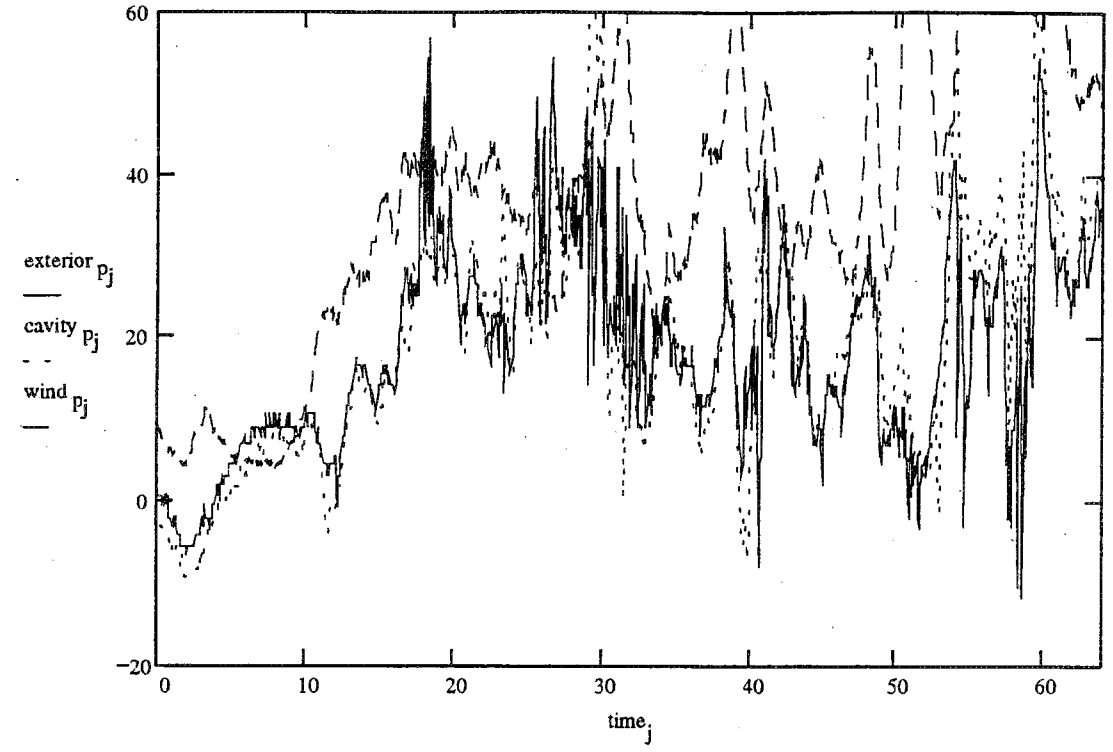
60
40
20
0
−20
exterior p_j
cavity p_j
wind p_j
0
10
20
30
40
50
60
time$_j$

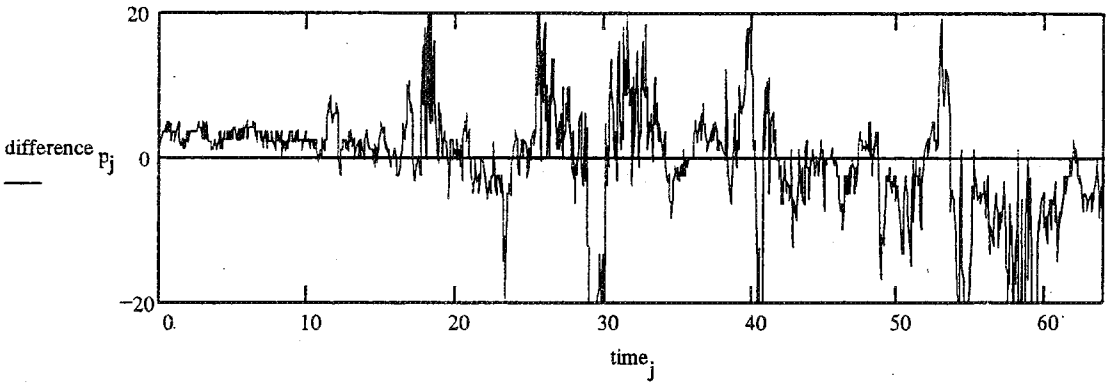
20
0
−20
difference p_j
0
10
20
30
40
50
60
time$_j$

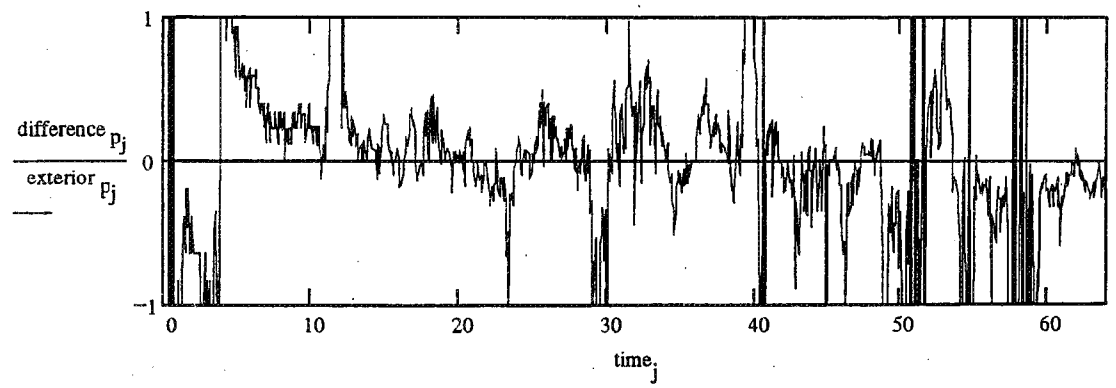
1
0
−1
difference p_j
exterior p_j
0
10
20
30
40
50
60
time$_j$

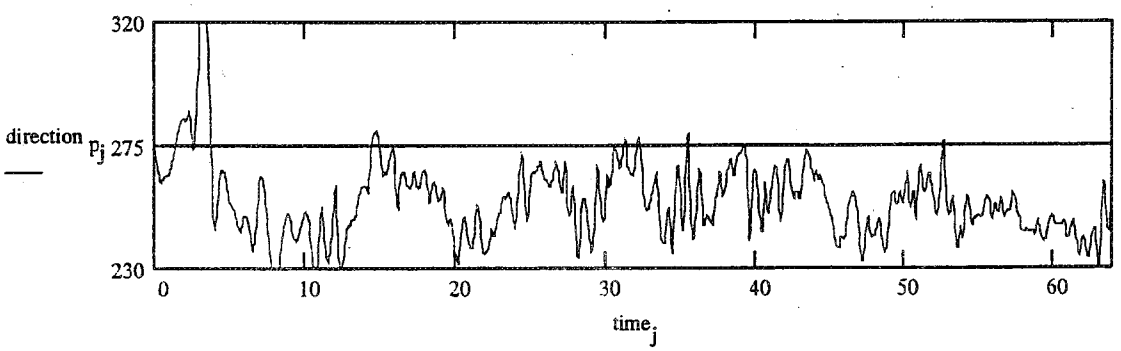
320
275
230
direction p_j
0
10
20
30
40
50
60
time$_j$

Zero-Cavity Panel W5
Records W5_30, W5_31, and W5_32

Raw Pressure Spectral Density Functions (Power Spectra)

Exterior Pressures (Pa)^2

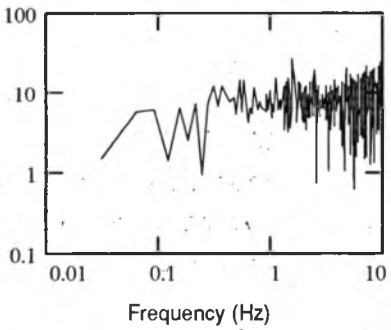

Cavity Pressures (Pa)^2

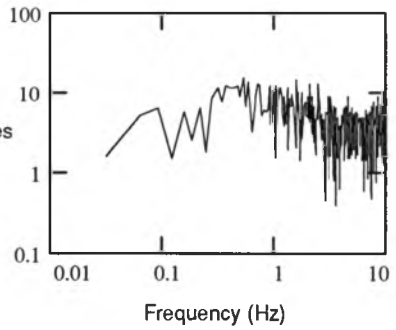

Wind Pressures (Pa)^2

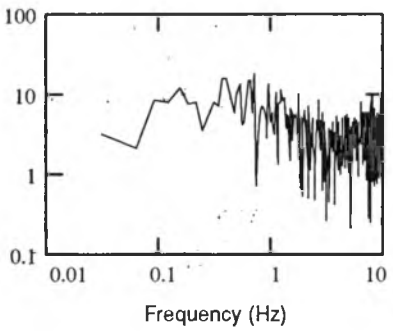

Difference Across Screen (Pa)^2

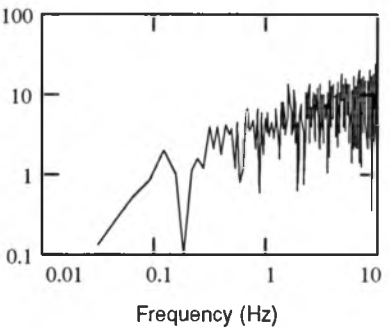

Smoothed and Normalized Pressure Spectra

Exterior Pressure

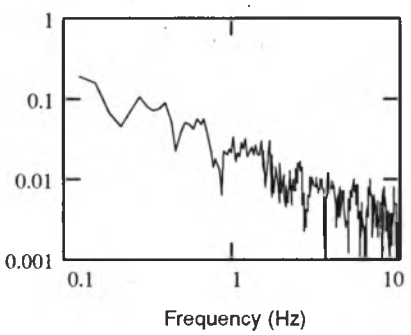

Cavity Pressure

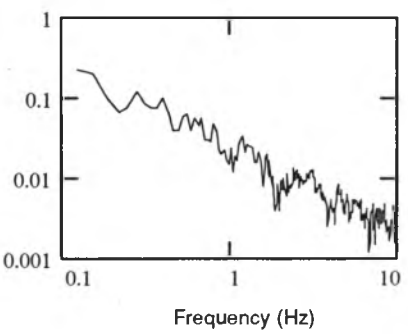

Wind Pressure

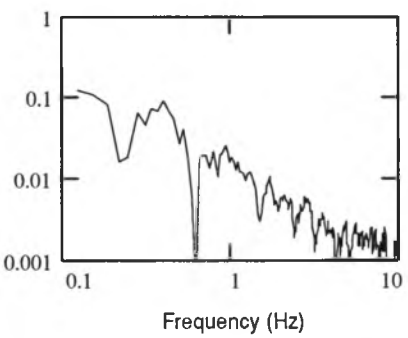

Difference Across Screen

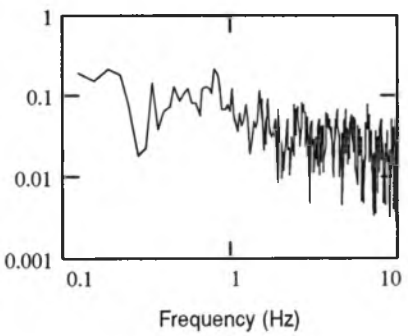

Read raw voltages from data files

$M := READPRN(W41) \qquad N := READPRN(W42) \qquad P := READPRN(W43)$

$size := rows(M) \quad timestep := \frac{1}{16} \quad j := 0..(size - 1) \quad time_j := j \cdot timestep$

Convert voltages in file to pressures using calibration values

File #1

$$exterior_m := \left[(M)^{<0>} - \left(\frac{2842}{4095} \cdot 5 \right) \right] \cdot 500 \qquad cavity_m := \left[(M)^{<2>} - \left(\frac{2866}{4095} \cdot 5 \right) \right] \cdot 500$$

$$windspeed_m := (M)^{<3>} \cdot 180 + 4 \qquad wind_{m_j} := \left(\frac{windspeed_{m_j}}{3.6} \right)^2 \cdot 0.647$$

$difference_m := exterior_m - cavity_m \qquad mean(difference_m) = 0.8 \qquad stdev(difference_m) = 3.3$

$mean(exterior_m) = 15.7 \quad mean(wind_m) = 38.5 \quad mean(cavity_m) = 15 \quad mean(direction_m) = 273.8$

$stdev(exterior_m) = 8.8 \quad stdev(wind_m) = 11.8 \quad stdev(cavity_m) = 8.2 \quad stdev(direction_m) = 7.4$

File #2

$$exterior_n := \left[(N)^{<0>} - \left(\frac{2842}{4095} \cdot 5 \right) \right] \cdot 500 \qquad cavity_n := \left[(N)^{<2>} - \left(\frac{2866}{4095} \cdot 5 \right) \right] \cdot 500$$

$$windspeed_n := (N)^{<3>} \cdot 180 + 4 \qquad wind_{n_j} := \left(\frac{windspeed_{n_j}}{3.6} \right)^2 \cdot 0.647$$

$difference_n := exterior_n - cavity_n \qquad mean(difference_n) = 1.4 \qquad stdev(difference_n) = 5.9$

$mean(exterior_n) = 20.9 \quad mean(wind_n) = 48.6 \quad mean(cavity_n) = 19.5 \quad mean(direction_n) = 276.4$

$stdev(exterior_n) = 14.4 \quad stdev(wind_n) = 21.4 \quad stdev(cavity_n) = 14.1 \quad stdev(direction_n) = 8.1$

File #3

$$exterior_p := \left[(P)^{<0>} - \left(\frac{2842}{4095} \cdot 5 \right) \right] \cdot 500 \qquad cavity_p := \left[(P)^{<2>} - \left(\frac{2866}{4095} \cdot 5 \right) \right] \cdot 500$$

$$windspeed_p := (P)^{<3>} \cdot 180 + 4 \qquad wind_{p_j} := \left(\frac{windspeed_{p_j}}{3.6} \right)^2 \cdot 0.647$$

$difference_p := exterior_p - cavity_p \qquad mean(difference_p) = 2.4 \qquad stdev(difference_p) = 3.1$

$mean(exterior_p) = 16.5 \quad mean(wind_p) = 38.5 \quad mean(cavity_p) = 14.1 \quad mean(direction_p) = 275.6$

$stdev(exterior_p) = 11.9 \quad stdev(wind_p) = 11.2 \quad stdev(cavity_p) = 11.5 \quad stdev(direction_p) = 8.6$

Average the time domain values of all files and calculate some statistics.

$$V_{10} := \frac{mean(windspeed_m) + mean(windspeed_n) + mean(windspeed_p)}{3}$$

$$Pdiff := (difference_m + difference_n + difference_p) \cdot \frac{1}{3} \qquad Pwind := (wind_m + wind_n + wind_p) \cdot \frac{1}{3}$$

$$Pext := (exterior_m + exterior_n + exterior_p) \cdot \frac{1}{3} \qquad Pcav := (cavity_m + cavity_n + cavity_p) \cdot \frac{1}{3}$$

$$\sigma_{diff} := (stdev(difference_m) + stdev(difference_n) + stdev(difference_p)) \cdot \frac{1}{3}$$

$$\sigma_{cav} := (stdev(cavity_m) + stdev(cavity_n) + stdev(cavity_p)) \cdot \frac{1}{3}$$

$$\sigma_{ext} := (stdev(exterior_m) + stdev(exterior_n) + stdev(exterior_p)) \cdot \frac{1}{3}$$

$$\sigma_{wind} := (stdev(wind_m) + stdev(wind_n) + stdev(wind_p)) \cdot \frac{1}{3}$$

Present the statistics of the combined records:

$V_{10} = 28.4$ km/h

$\text{mean}(\text{Pdiff}) = 1.5$ $\quad \sigma_{diff} = 4.1$ $\quad \text{diff}_{mean} := \text{mean}(\text{Pdiff})$

$\text{mean}(\text{Pcav}) = 16.2$ $\quad \sigma_{cav} = 11.2$ $\quad \text{cav}_{mean} := \text{mean}(\text{Pcav})$

$\text{mean}(\text{Pext}) = 17.7$ $\quad \sigma_{ext} = 11.7$ $\quad \text{ext}_{mean} := \text{mean}(\text{Pext})$

$\text{mean}(\text{Pwind}) = 41.9$ $\quad \sigma_{wind} = 14.8$ $\quad \text{wind}_{mean} := \text{mean}(\text{Pwind})$

Intensity of Turbulence: $\frac{\sigma_{wind}}{\text{wind}_{mean}} = 0.35$ $\quad \frac{\sigma_{cav}}{\text{cav}_{mean}} = 0.7$ $\quad \frac{\sigma_{ext}}{\text{ext}_{mean}} = 0.66$ $\quad \frac{\sigma_{diff}}{\text{diff}_{mean}} = 2.65$

Now, take the Fourier transform of all both pressure variations to create pressure spectra.

$\text{ext}_m := \text{fft}(\text{exterior}_m)$ $\quad \text{cav}_m := \text{fft}(\text{cavity}_m)$ $\quad \text{win}_m := \text{fft}(\text{wind}_m)$ $\quad \text{diff}_m := \text{fft}(\text{difference}_m)$

$\text{ext}_n := \text{fft}(\text{exterior}_n)$ $\quad \text{cav}_n := \text{fft}(\text{cavity}_n)$ $\quad \text{win}_n := \text{fft}(\text{wind}_n)$ $\quad \text{diff}_n := \text{fft}(\text{difference}_n)$

$\text{ext}_p := \text{fft}(\text{exterior}_p)$ $\quad \text{cav}_p := \text{fft}(\text{cavity}_p)$ $\quad \text{win}_p := \text{fft}(\text{wind}_p)$ $\quad \text{diff}_p := \text{fft}(\text{difference}_p)$

$N := \frac{\text{size}}{2}$ $\quad k := 1..N$ $\quad f_k := \frac{k}{N} \cdot \frac{1}{\text{timestep}}$

Note: This calculates the actual frequency which varies with the sampling rate

Average files in the frequency Domain

$$S_{ext_k} := \frac{\text{ext}_{m_k} + \text{ext}_{n_k} + \text{ext}_{p_k}}{3} \qquad S_{cav_k} := \frac{\text{cav}_{m_k} + \text{cav}_{n_k} + \text{cav}_{p_k}}{3}$$

$$S_{wind_k} := \frac{\text{win}_{m_k} + \text{win}_{n_k} + \text{win}_{p_k}}{3} \qquad S_{diff_k} := \frac{\text{diff}_{m_k} + \text{diff}_{n_k} + \text{diff}_{p_k}}{3}$$

Average values to smooth curves $\quad p := 4..(N-3)$ $\quad f_p := \frac{p}{N} \cdot \frac{1}{\text{timestep}}$

$$S_{extavg_p} := \left| \frac{S_{ext_{p-1}} + S_{ext_p} + S_{ext_{p+1}} + S_{ext_{p+2}} + S_{ext_{p-2}} + S_{ext_{p-3}} + S_{ext_{p+3}}}{7} \right|$$

$$S_{windavg_p} := \left| \frac{S_{wind_{p-1}} + S_{wind_p} + S_{wind_{p+1}} + S_{wind_{p+2}} + S_{wind_{p-2}} + S_{wind_{p-3}} + S_{wind_{p+3}}}{7} \right|$$

$$S_{cavavg_p} := \left| \frac{S_{cav_{p-1}} + S_{cav_p} + S_{cav_{p+1}} + S_{cav_{p+2}} + S_{cav_{p-2}} + S_{cav_{p-3}} + S_{cav_{p+3}}}{7} \right|$$

$$S_{diffavg_p} := \left| \frac{S_{diff_{p-1}} + S_{diff_p} + S_{diff_{p+1}} + S_{diff_{p+2}} + S_{diff_{p-2}} + S_{diff_{p-3}} + S_{diff_{p+3}}}{7} \right|$$

Calculate the Frequency Response Function function for the presure difference

$$H_{\Delta_k} := \frac{S_{diff_k}}{S_{ext_k}} \qquad K_{\Delta_k} := \left| H_{\Delta_k} \right| \qquad \phi_{\Delta_k} := \text{atan}\left(\frac{\text{Im}\left(K_{\Delta_k}\right)}{\text{Re}\left(K_{\Delta_k}\right)} \right) \cdot \frac{180}{\pi}$$

Calculate the Cavity Frequency Response function.

$$H_{c_k} := \frac{S_{cav_k}}{S_{ext_k}} \qquad K_{c_k} := \left| H_{c_k} \right| \qquad \phi_{c_k} := \text{atan}\left(\frac{\text{Im}\left(H_{c_k}\right)}{\text{Re}\left(H_{c_k}\right)} \right) \cdot \frac{180}{\pi}$$

PRESSURE SPECTRA

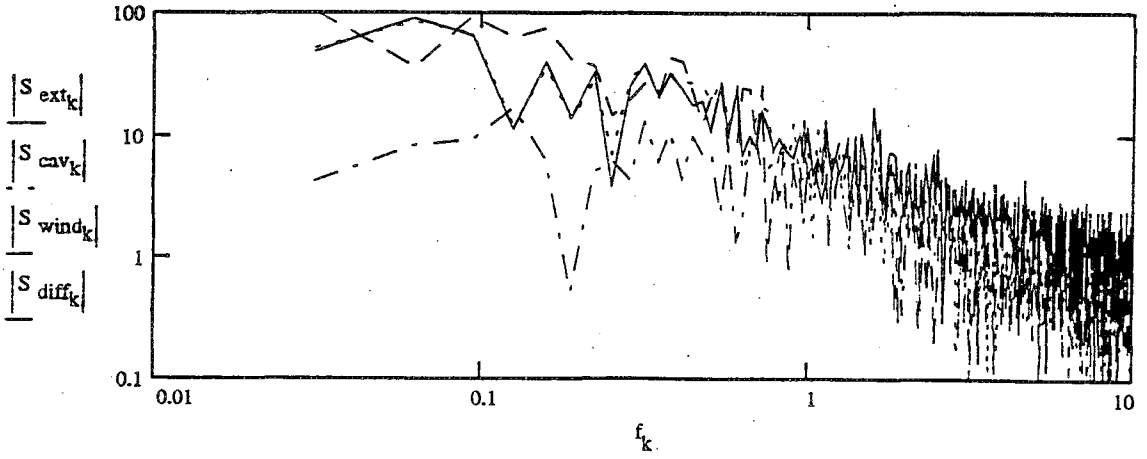

NORMALISED PRESSURE SPECTRA

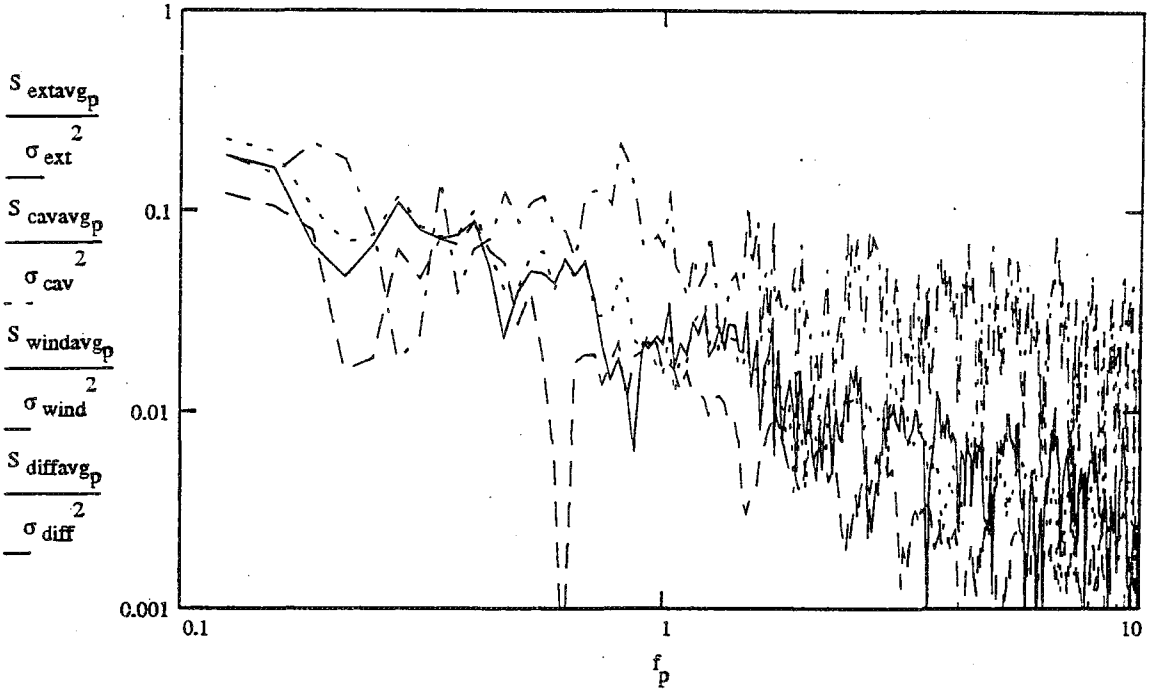

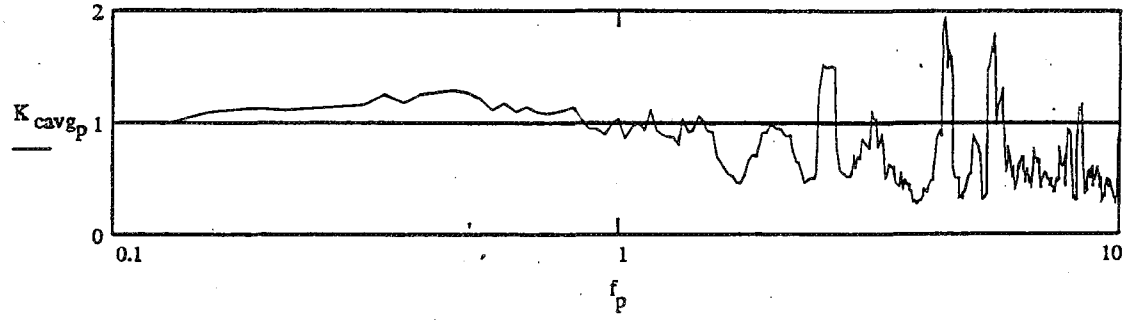

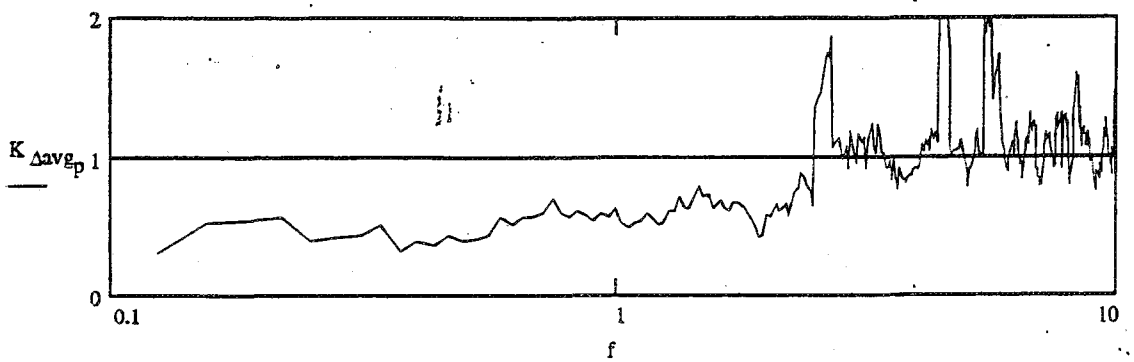

SPECTRA RELATIONSHIPS

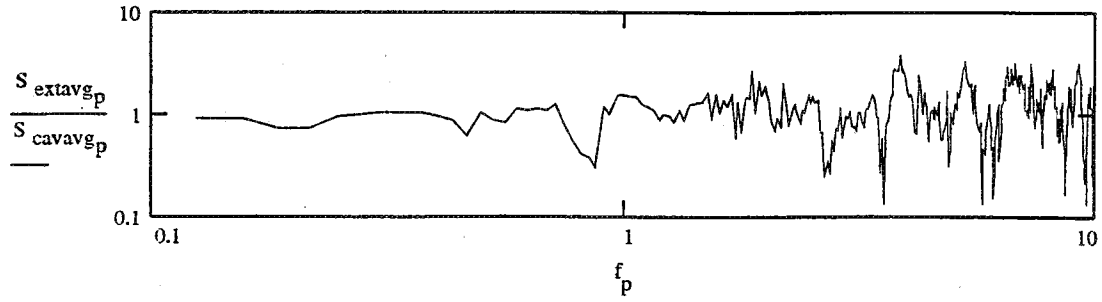

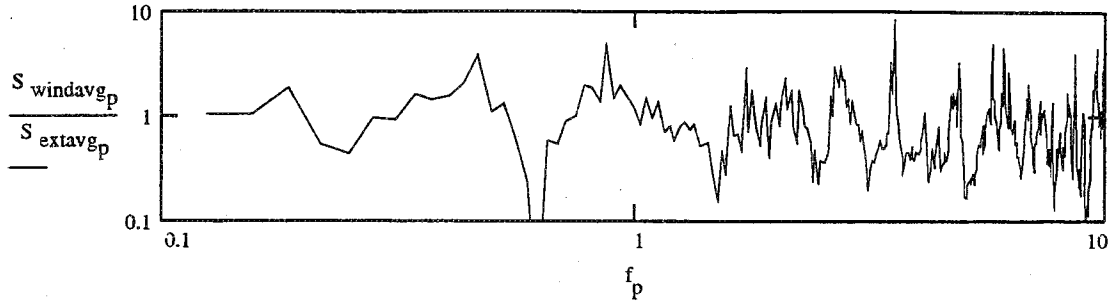

CAVITY PHASE LAG (Degrees)

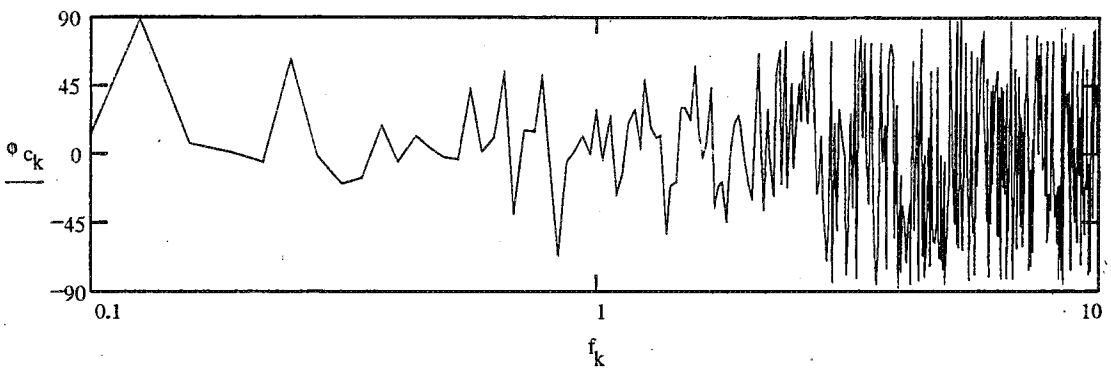

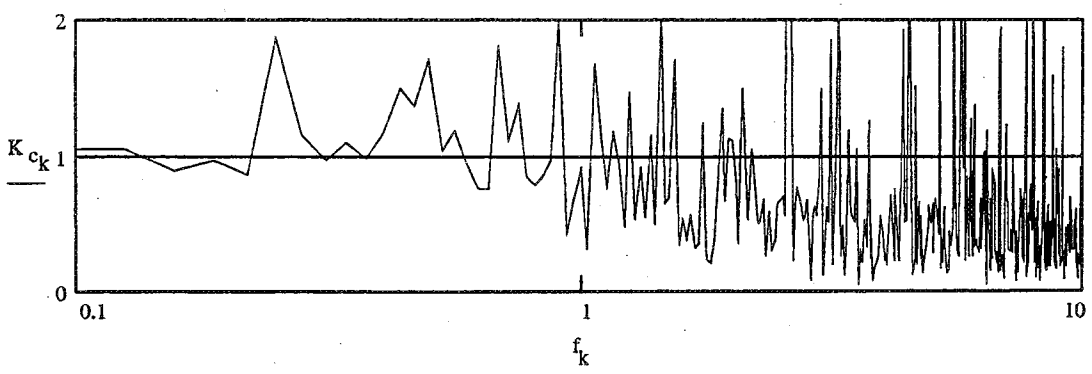

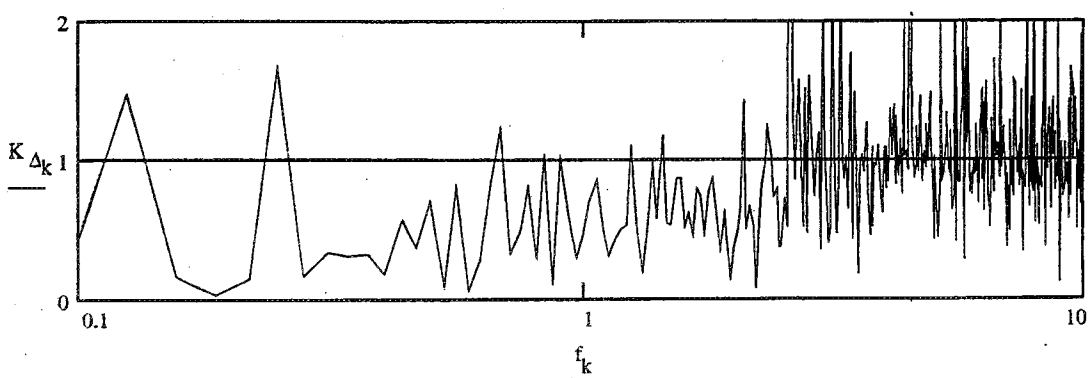

TIME DOMAIN PLOTS OF PRESSURE

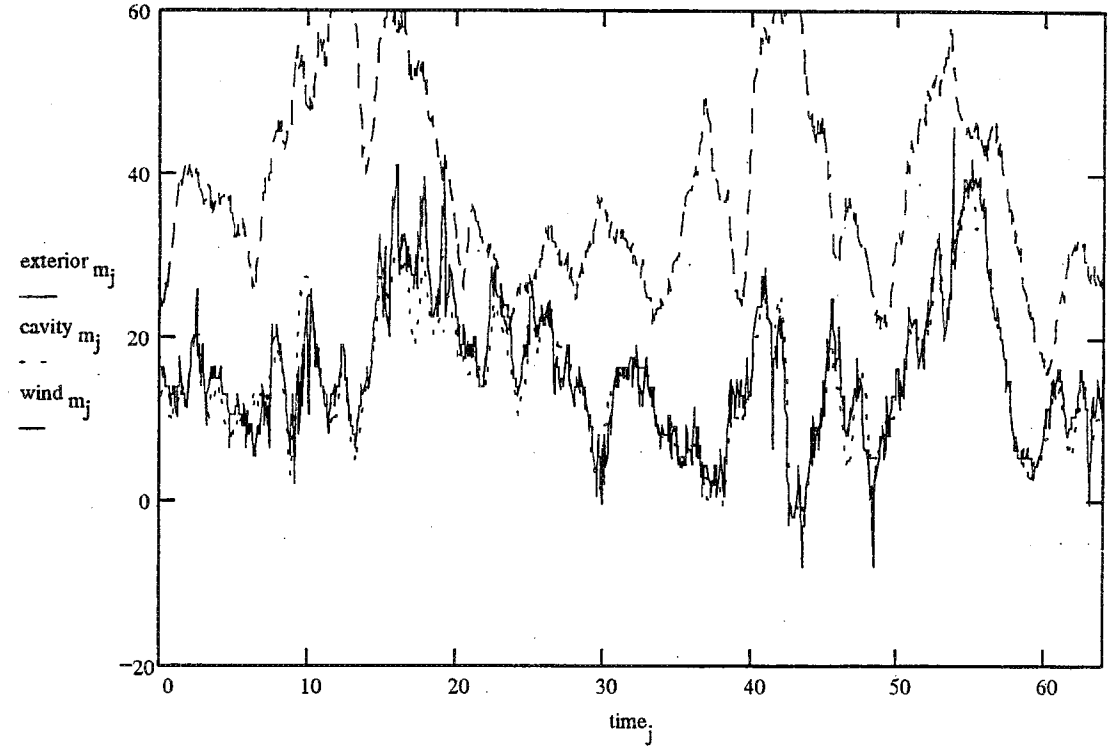

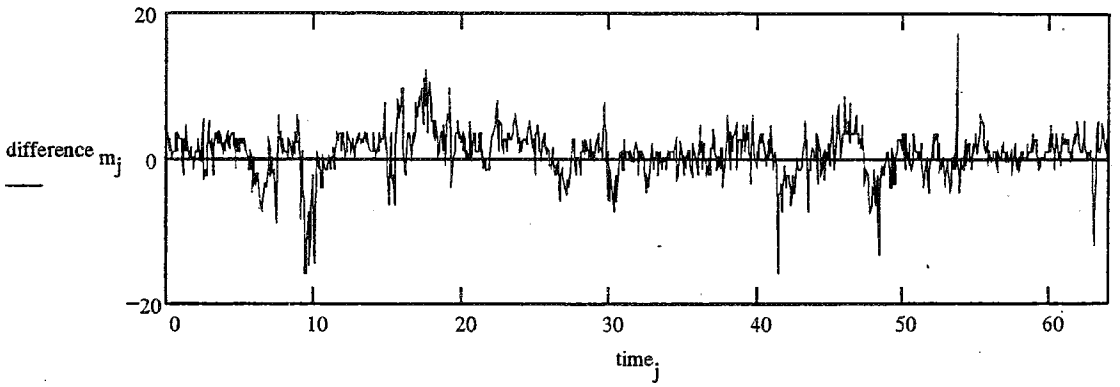

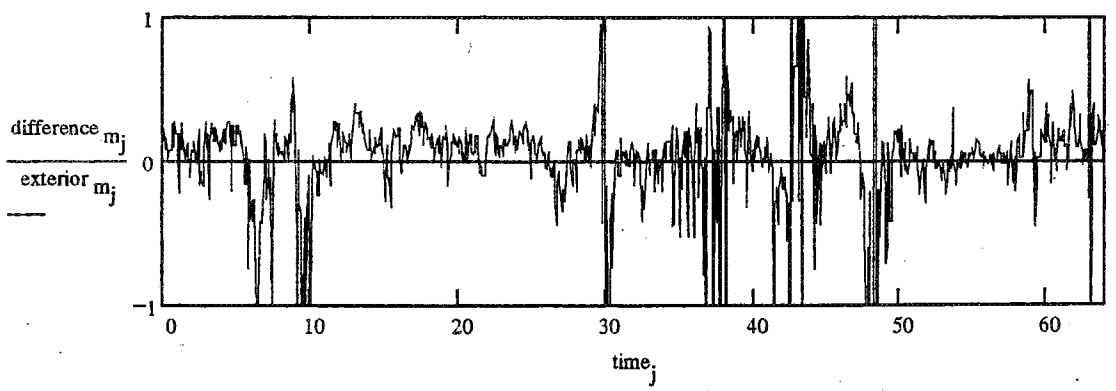

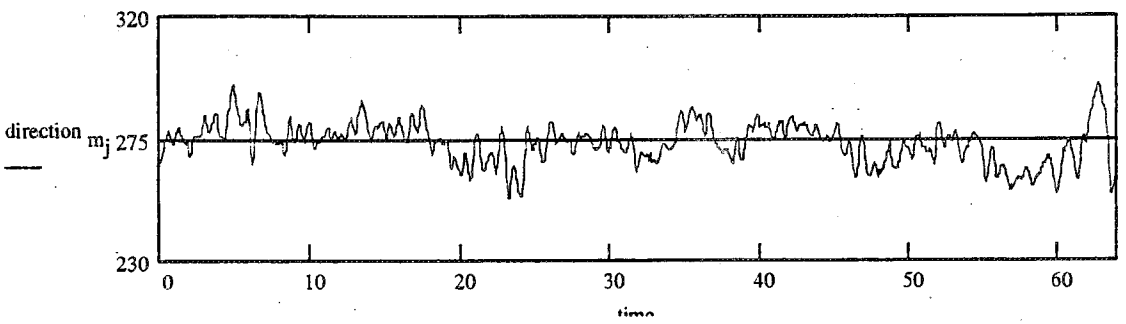

TIME DOMAIN PLOTS OF PRESSURE

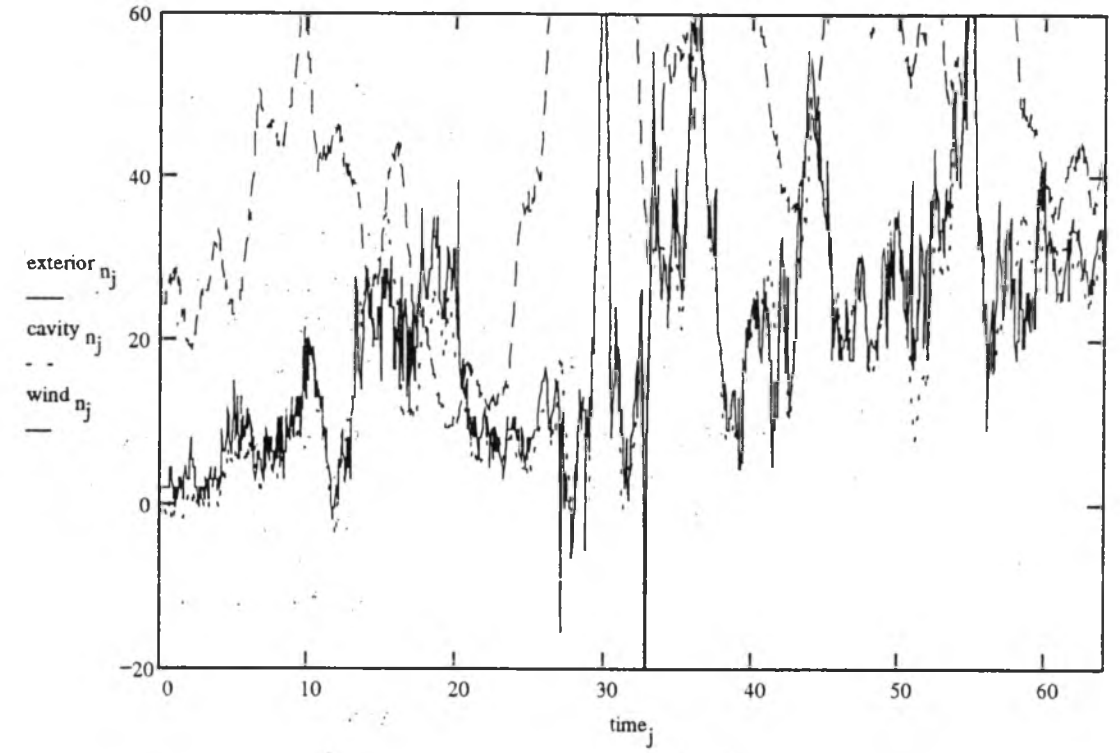

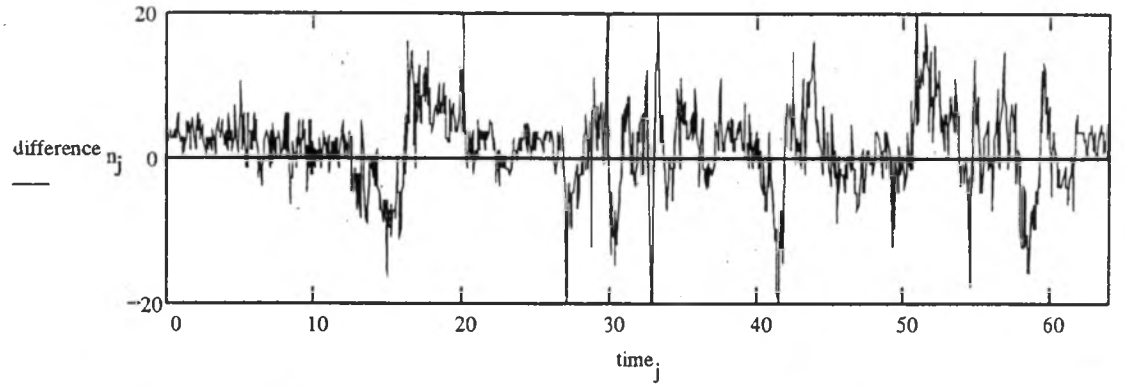

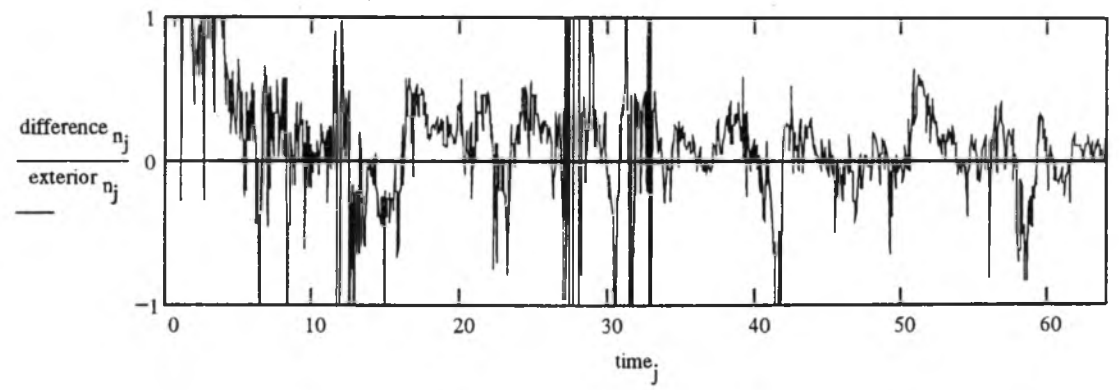

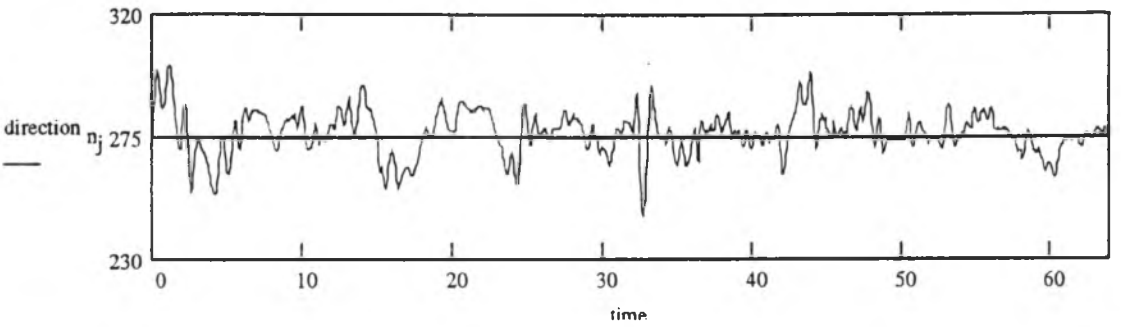

TIME DOMAIN PLOTS OF PRESSURE

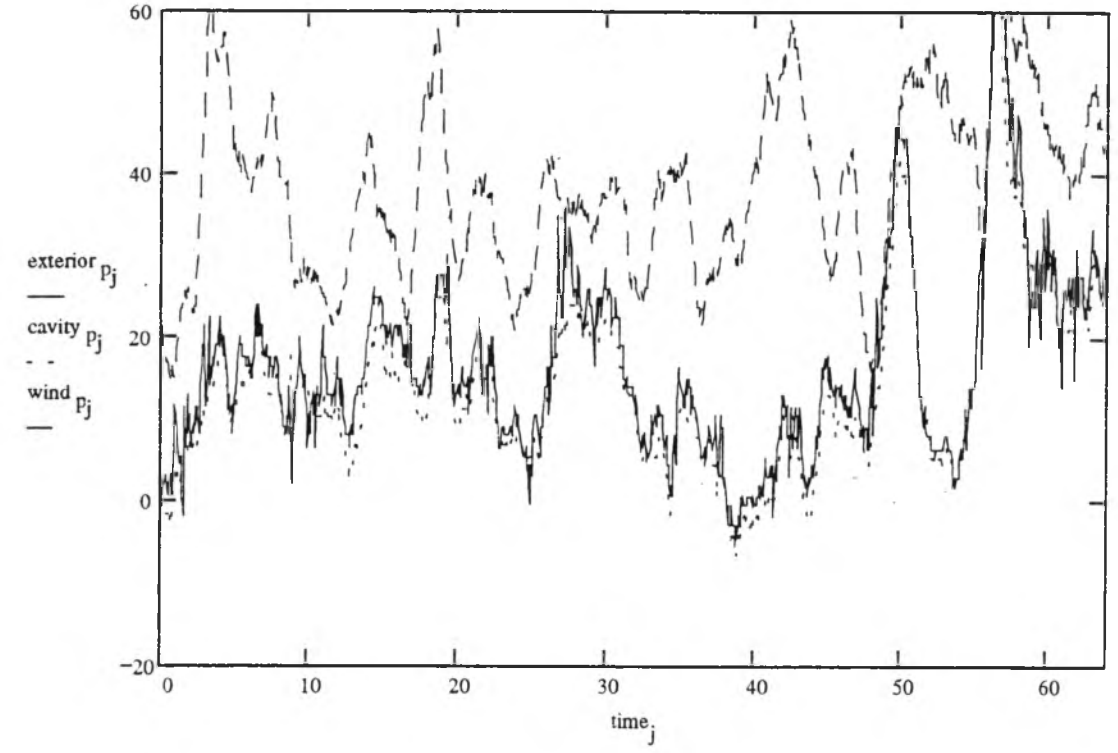

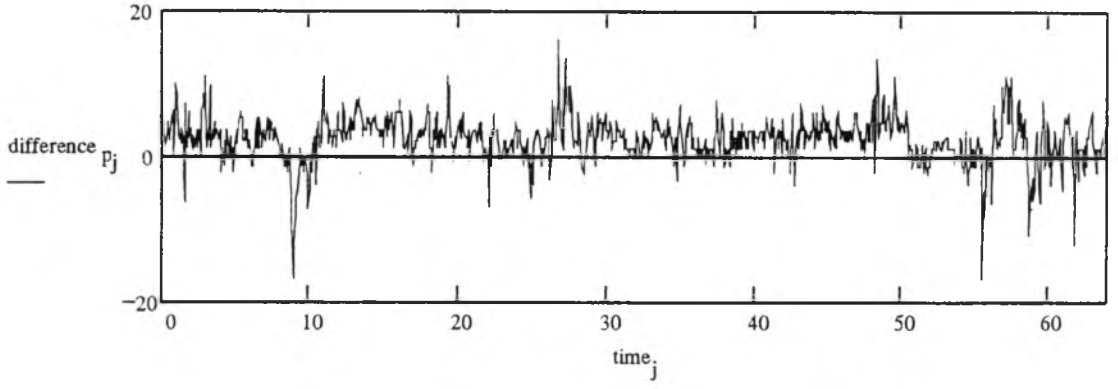

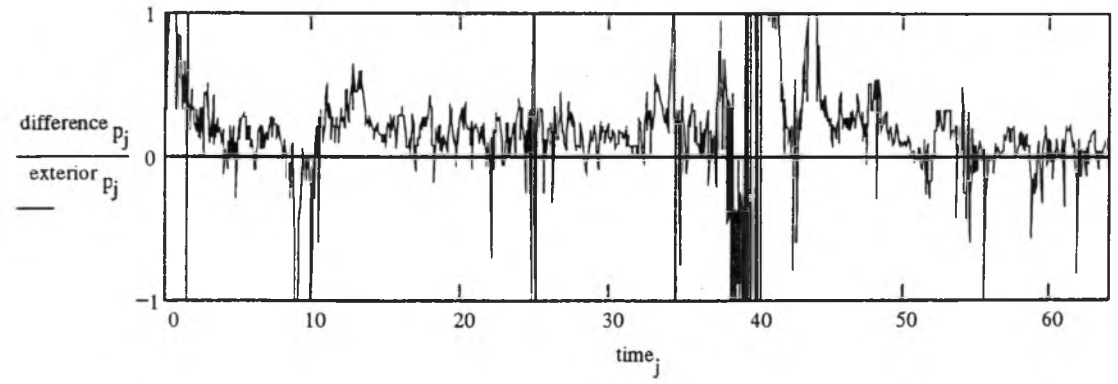

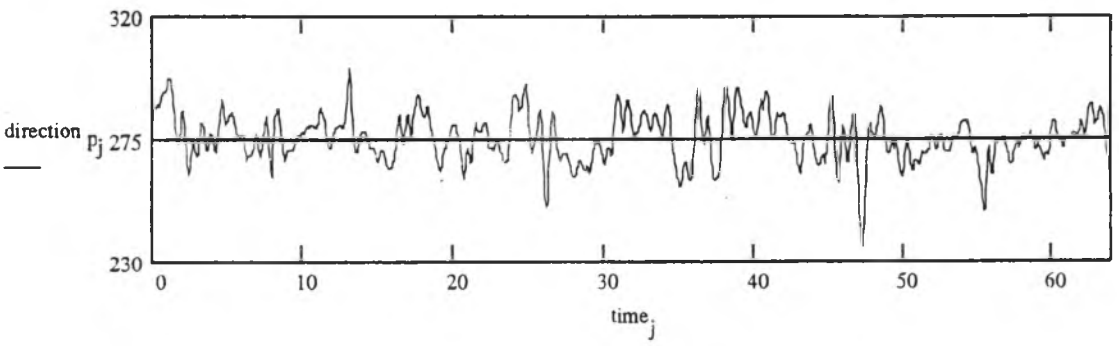

Read raw voltages from data files

$M := READPRN(E511)$ $N := READPRN(E512)$ $P := READPRN(E513)$

$size := rows(M)$ $timestep := \frac{1}{16}$ $j := 0..(size - 1)$ $time_j := j \cdot timestep$

Convert voltages in file to pressures using calibration values

File #1

$$exterior_m := \left[(M)^{<0>} - \left(\frac{2838}{4095} \cdot 5 \right) \right] \cdot 500 \qquad cavity_m := \left[(M)^{<2>} - \left(\frac{2866}{4095} \cdot 5 \right) \right] \cdot 500$$

$$windspeed_m := (M)^{<3>} \cdot 180 + 4 \qquad wind_{m_j} := \left(\frac{windspeed_{m_j}}{3.6} \right)^2 \cdot 0.647$$

$difference_m := exterior_m - cavity_m$ $mean(difference_m) = 5$ $stdev(difference_m) = 5.5$

$mean(exterior_m) = 15.3$ $mean(wind_m) = 32$ $mean(cavity_m) = 10.3$ $mean(direction_m) = 52.8$

$stdev(exterior_m) = 9.7$ $stdev(wind_m) = 14.8$ $stdev(cavity_m) = 9$ $stdev(direction_m) = 16.6$

File #2

$$exterior_n := \left[(N)^{<0>} - \left(\frac{2838}{4095} \cdot 5 \right) \right] \cdot 500 \qquad cavity_n := \left[(N)^{<2>} - \left(\frac{2866}{4095} \cdot 5 \right) \right] \cdot 500$$

$$windspeed_n := (N)^{<3>} \cdot 180 + 4 \qquad wind_{n_j} := \left(\frac{windspeed_{n_j}}{3.6} \right)^2 \cdot 0.647$$

$difference_n := exterior_n - cavity_n$ $mean(difference_n) = 0.1$ $stdev(difference_n) = 5.8$

$mean(exterior_n) = 20.5$ $mean(wind_n) = 32.6$ $mean(cavity_n) = 20.4$ $mean(direction_n) = 69.8$

$stdev(exterior_n) = 8.7$ $stdev(wind_n) = 11.5$ $stdev(cavity_n) = 9.1$ $stdev(direction_n) = 9.8$

File #3

$$exterior_p := \left[(P)^{<0>} - \left(\frac{2838}{4095} \cdot 5 \right) \right] \cdot 500 \qquad cavity_p := \left[(P)^{<2>} - \left(\frac{2866}{4095} \cdot 5 \right) \right] \cdot 500$$

$$windspeed_p := (P)^{<3>} \cdot 180 + 4 \qquad wind_{p_j} := \left(\frac{windspeed_{p_j}}{3.6} \right)^2 \cdot 0.647$$

$difference_p := exterior_p - cavity_p$ $mean(difference_p) = 2.2$ $stdev(difference_p) = 6.9$

$mean(exterior_p) = 28.3$ $mean(wind_p) = 41.5$ $mean(cavity_p) = 26.2$ $mean(direction_p) = 56.1$

$stdev(exterior_p) = 13.1$ $stdev(wind_p) = 17.8$ $stdev(cavity_p) = 13.1$ $stdev(direction_p) = 10.4$

Average the time domain values of all files and calculate some statistics.

$$V_{10} := \frac{mean(windspeed_m) + mean(windspeed_n) + mean(windspeed_p)}{3}$$

$$Pdiff := (difference_m + difference_n + difference_p) \cdot \frac{1}{3} \qquad Pwind := (wind_m + wind_n + wind_p) \cdot \frac{1}{3}$$

$$Pext := (exterior_m + exterior_n + exterior_p) \cdot \frac{1}{3} \qquad Pcav := (cavity_m + cavity_n + cavity_p) \cdot \frac{1}{3}$$

$$\sigma_{diff} := (stdev(difference_m) + stdev(difference_n) + stdev(difference_p)) \cdot \frac{1}{3}$$

$$\sigma_{cav} := (stdev(cavity_m) + stdev(cavity_n) + stdev(cavity_p)) \cdot \frac{1}{3}$$

$$\sigma_{ext} := (stdev(exterior_m) + stdev(exterior_n) + stdev(exterior_p)) \cdot \frac{1}{3}$$

$$\sigma_{wind} := (stdev(wind_m) + stdev(wind_n) + stdev(wind_p)) \cdot \frac{1}{3}$$

Present the statistics of the combined records:

$V_{10} = 26$ km/h

mean(Pdiff) = 2.4 $\quad \sigma_{diff} = 6.1 \quad diff_{mean} := mean(Pdiff)$

mean(Pcav) = 19 $\quad \sigma_{cav} = 10.4 \quad cav_{mean} := mean(Pcav)$

mean(Pext) = 21.4 $\quad \sigma_{ext} = 10.5 \quad ext_{mean} := mean(Pext)$

mean(Pwind) = 35.4 $\quad \sigma_{wind} = 14.7 \quad wind_{mean} := mean(Pwind)$

Intensity of Turbulence: $\frac{\sigma_{wind}}{wind_{mean}} = 0.42 \quad \frac{\sigma_{cav}}{cav_{mean}} = 0.55 \quad \frac{\sigma_{ext}}{ext_{mean}} = 0.49 \quad \frac{\sigma_{diff}}{diff_{mean}} = 2.53$

Now, take the Fourier transform of all both pressure variations to create pressure spectra.

$ext_m := fft(exterior_m) \quad cav_m := fft(cavity_m) \quad win_m := fft(wind_m) \quad diff_m := fft(difference_m)$

$ext_n := fft(exterior_n) \quad cav_n := fft(cavity_n) \quad win_n := fft(wind_n) \quad diff_n := fft(difference_n)$

$ext_p := fft(exterior_p) \quad cav_p := fft(cavity_p) \quad win_p := fft(wind_p) \quad diff_p := fft(difference_p)$

$N := \frac{size}{2} \qquad k := 1..N \qquad f_k := \frac{k}{N} \cdot \frac{1}{timestep}$

Note: This calculates the actual frequency which varies with the sampling rate

Average files in the frequency Domain

$$S_{ext_k} := \frac{ext_{m_k} + ext_{n_k} + ext_{p_k}}{3} \qquad S_{cav_k} := \frac{cav_{m_k} + cav_{n_k} + cav_{p_k}}{3}$$

$$S_{wind_k} := \frac{win_{m_k} + win_{n_k} + win_{p_k}}{3} \qquad S_{diff_k} := \frac{diff_{m_k} + diff_{n_k} + diff_{p_k}}{3}$$

Average values to smooth curves $\qquad p := 4..(N-3) \qquad f_p := \frac{p}{N} \cdot \frac{1}{timestep}$

$$S_{extavg_p} := \left| \frac{S_{ext_{p-1}} + S_{ext_p} + S_{ext_{p+1}} + S_{ext_{p+2}} + S_{ext_{p-2}} + S_{ext_{p-3}} + S_{ext_{p+3}}}{7} \right|$$

$$S_{windavg_p} := \left| \frac{S_{wind_{p-1}} + S_{wind_p} + S_{wind_{p+1}} + S_{wind_{p+2}} + S_{wind_{p-2}} + S_{wind_{p-3}} + S_{wind_{p+3}}}{7} \right|$$

$$S_{cavavg_p} := \left| \frac{S_{cav_{p-1}} + S_{cav_p} + S_{cav_{p+1}} + S_{cav_{p+2}} + S_{cav_{p-2}} + S_{cav_{p-3}} + S_{cav_{p+3}}}{7} \right|$$

$$S_{diffavg_p} := \left| \frac{S_{diff_{p-1}} + S_{diff_p} + S_{diff_{p+1}} + S_{diff_{p+2}} + S_{diff_{p-2}} + S_{diff_{p-3}} + S_{diff_{p+3}}}{7} \right|$$

Calculate the Frequency Response Function function for the presure difference

$$H_{\Delta_k} := \frac{S_{diff_k}}{S_{ext_k}} \qquad K_{\Delta_k} := \left| H_{\Delta_k} \right| \qquad \phi_{\Delta_k} := atan\left(\frac{Im(K_{\Delta_k})}{Re(K_{\Delta_k})} \right) \cdot \frac{180}{\pi}$$

Calculate the Cavity Frequency Response function.

$$H_{c_k} := \frac{S_{cav_k}}{S_{ext_k}} \qquad K_{c_k} := \left| H_{c_k} \right| \qquad \phi_{c_k} := atan\left(\frac{Im(H_{c_k})}{Re(H_{c_k})} \right) \cdot \frac{180}{\pi}$$

PRESSURE SPECTRA

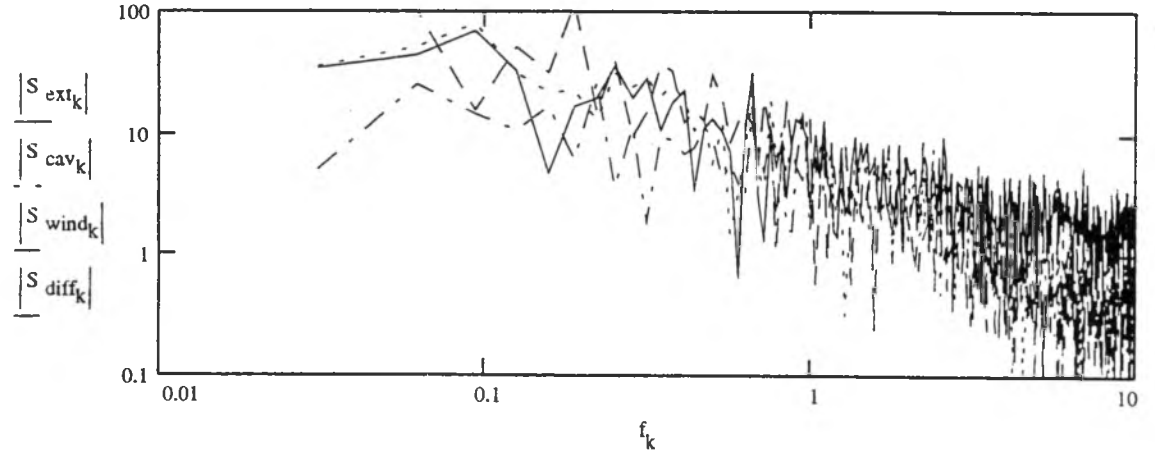

NORMALISED PRESSURE SPECTRA

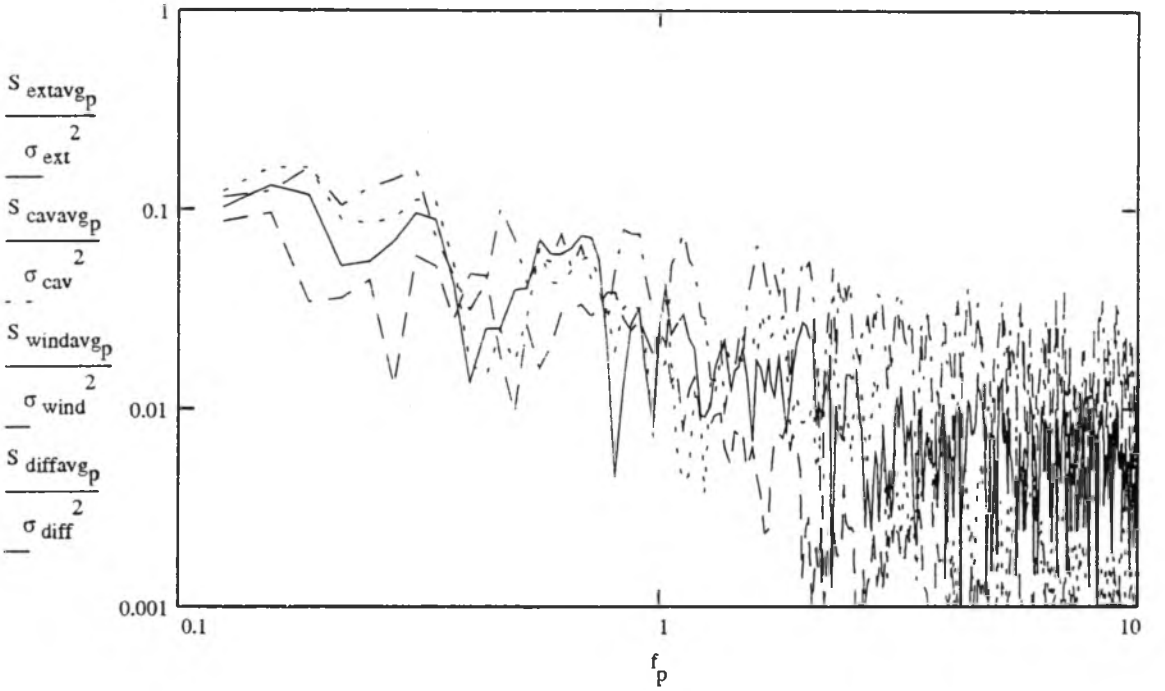

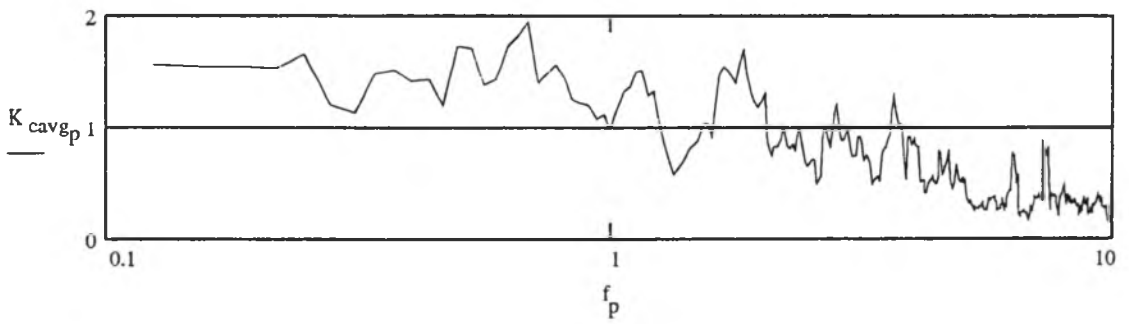

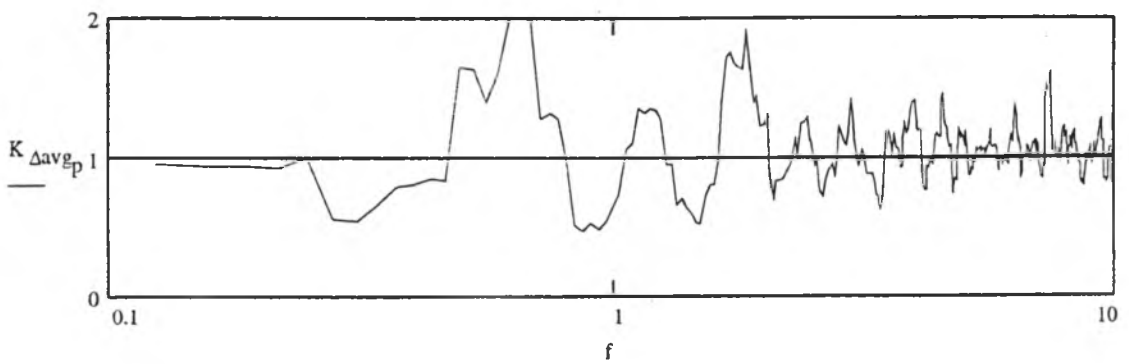

SPECTRA RELATIONSHIPS

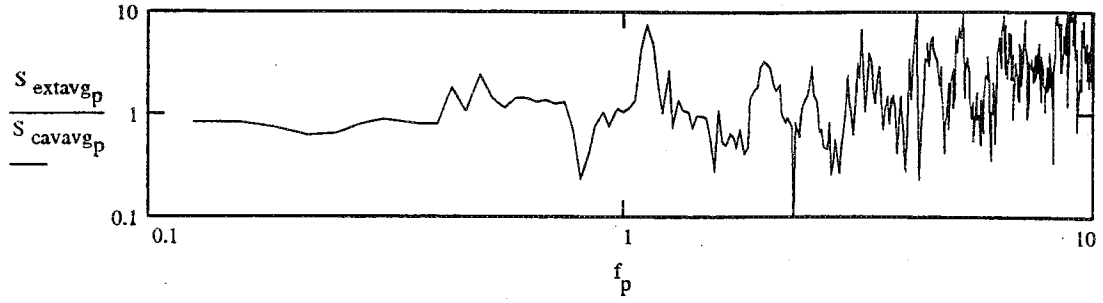

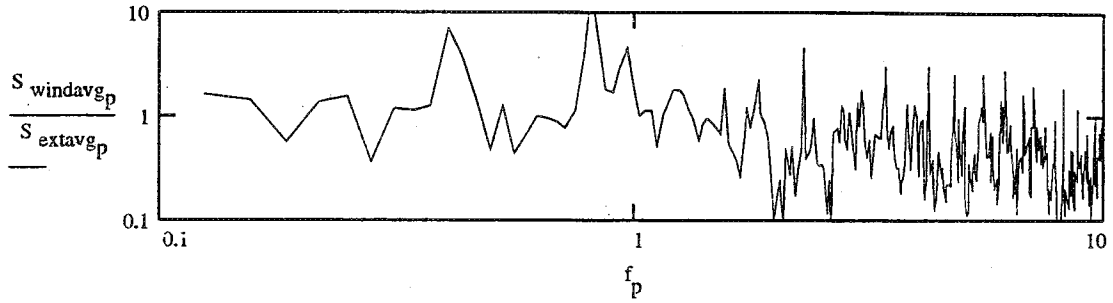

CAVITY PHASE LAG (Degrees)

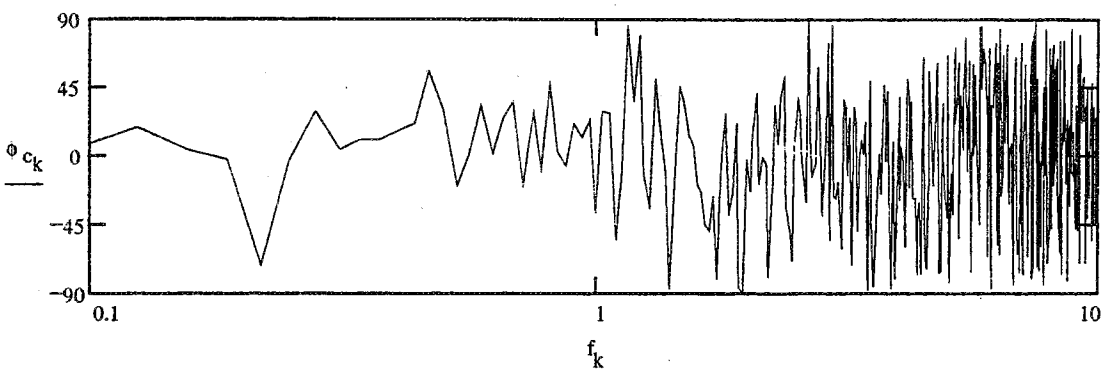

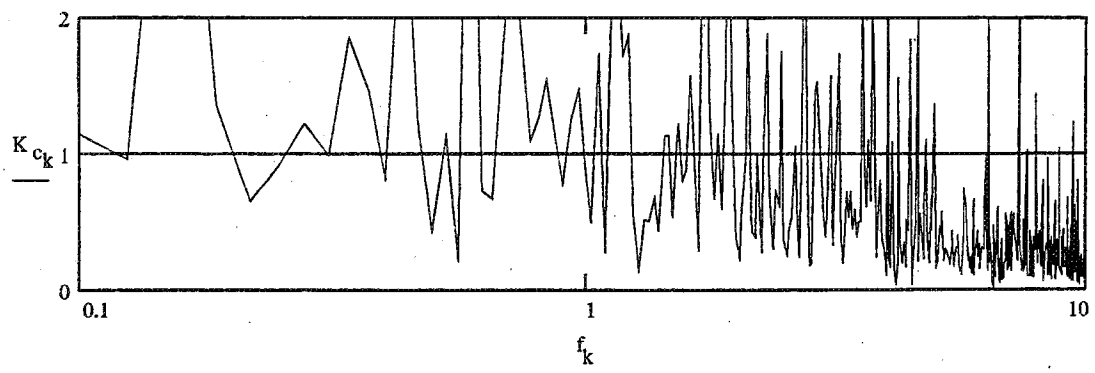

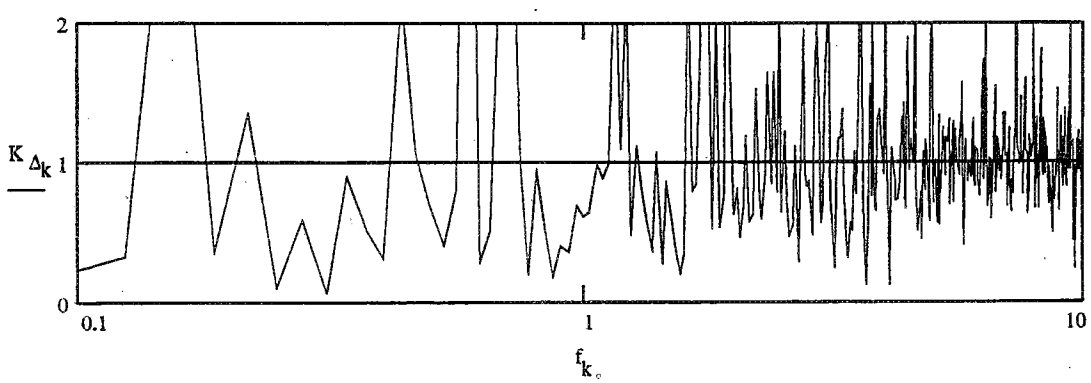

TIME DOMAIN PLOTS OF PRESSURE

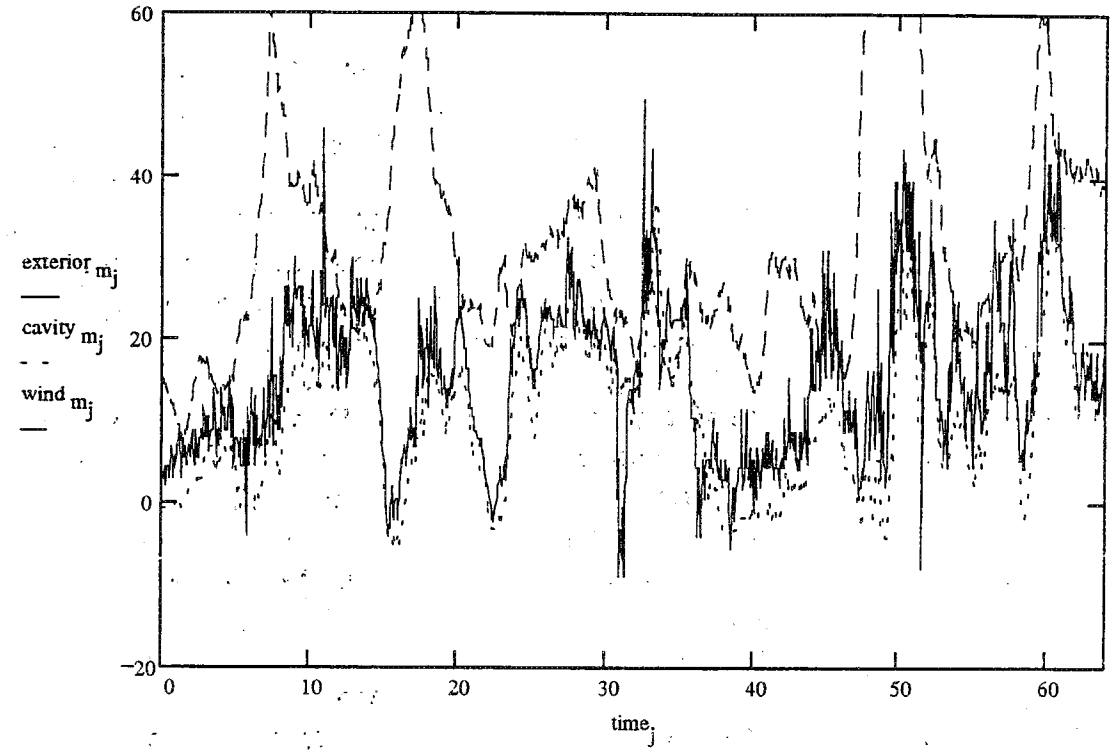

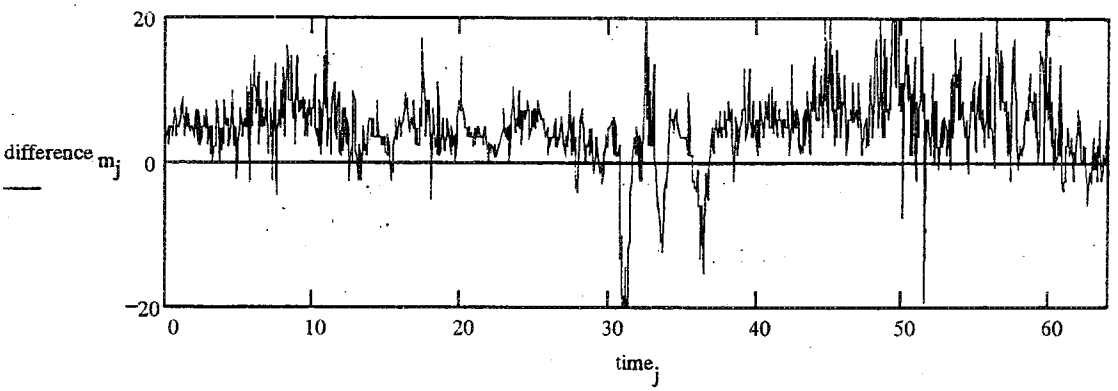

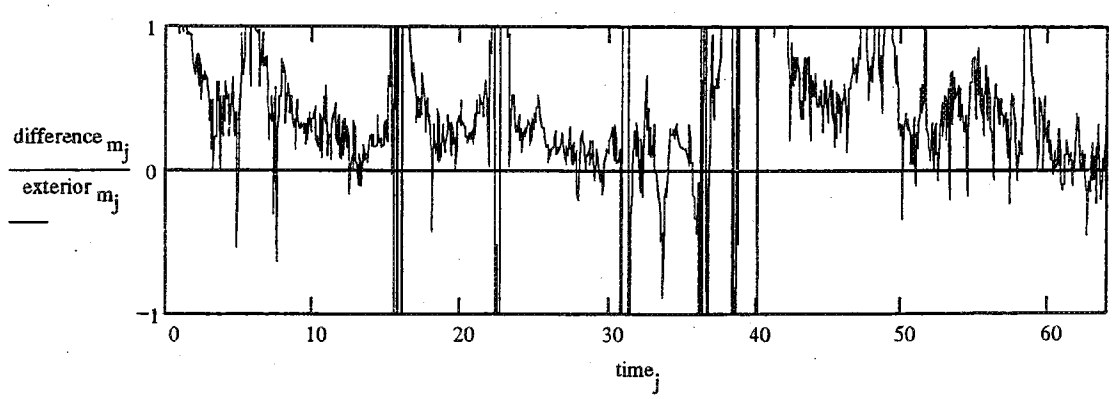

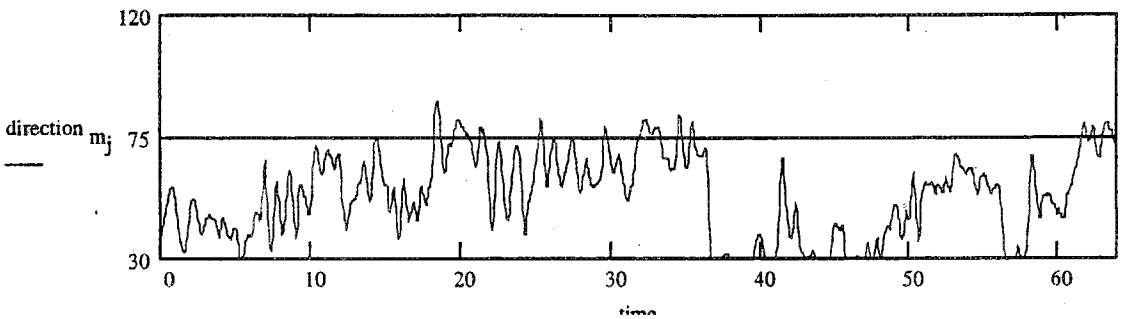

TIME DOMAIN PLOTS OF PRESSURE

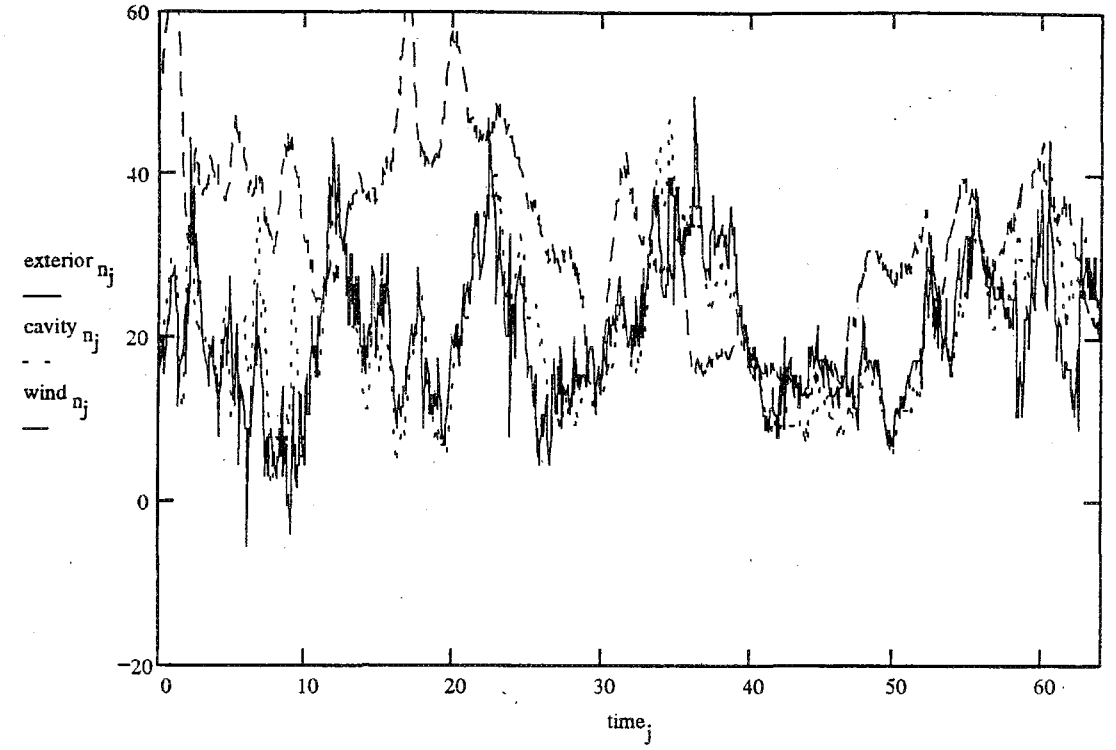

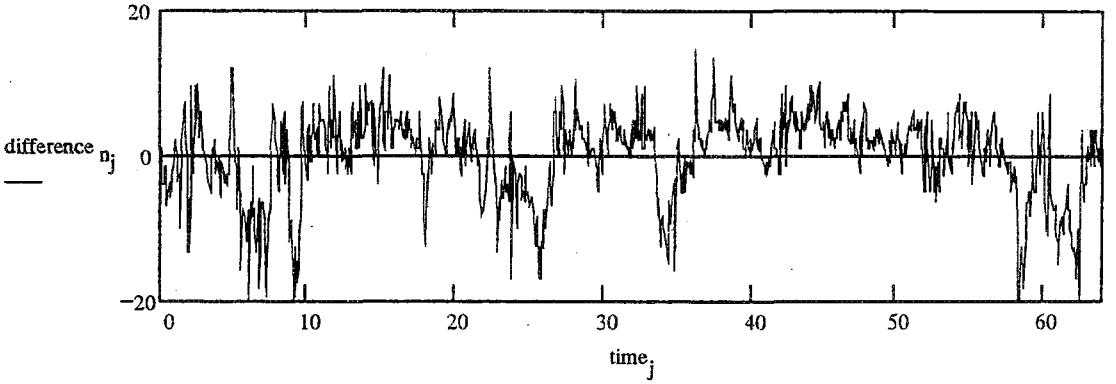

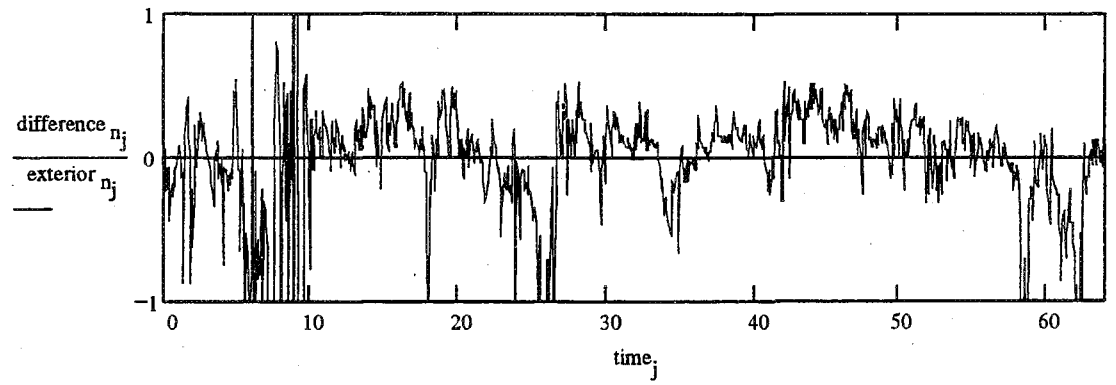

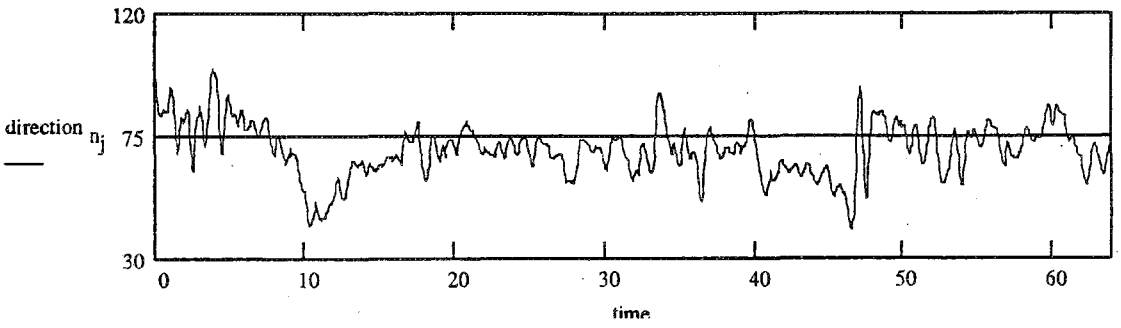

TIME DOMAIN PLOTS OF PRESSURE

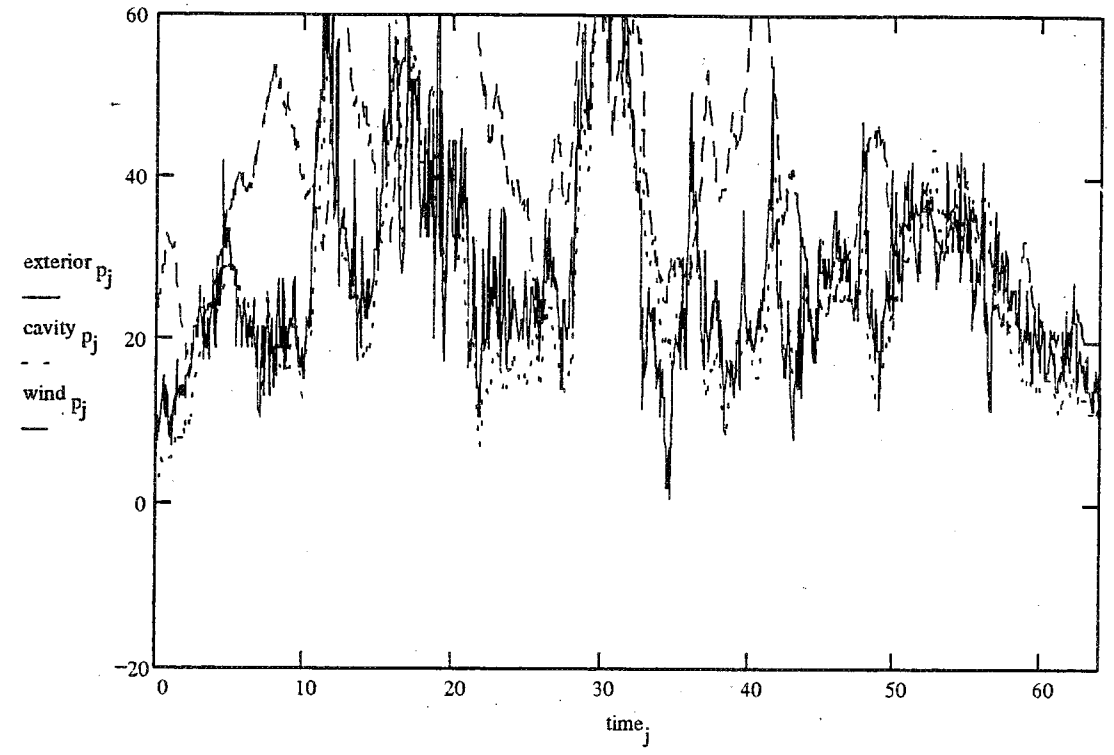

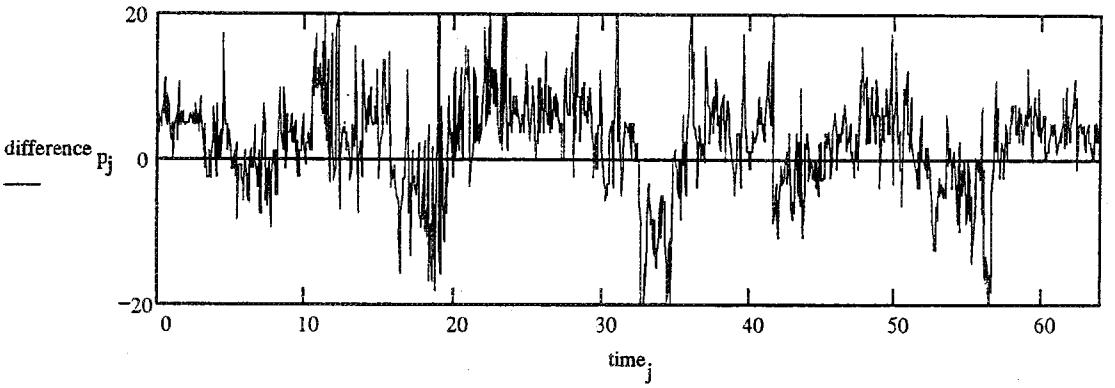

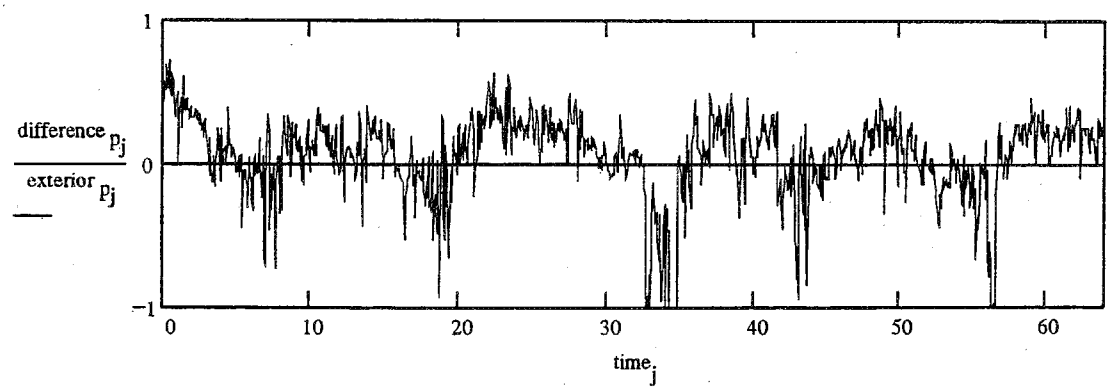

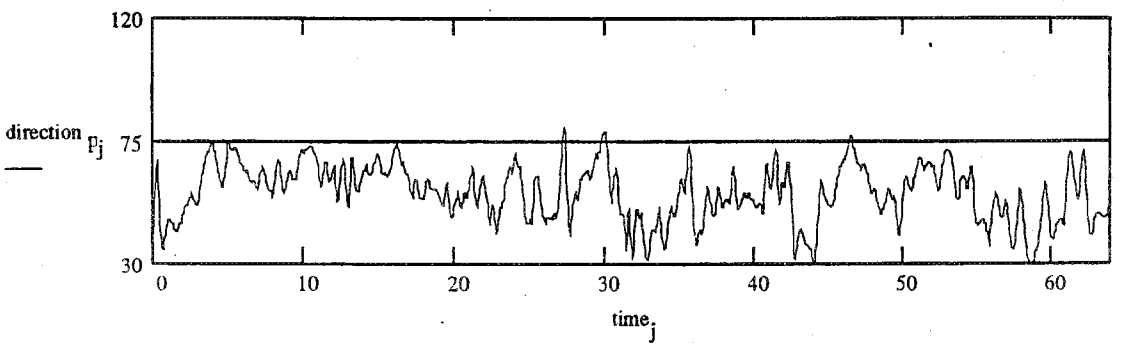

Read raw voltages from data files

$M := READPRN(W45) \qquad N := READPRN(W46) \qquad P := READPRN(W47)$

$size := rows(M) \qquad timestep := \frac{1}{16} \qquad j := 0..(size - 1) \qquad time_j := j \cdot timestep$

Convert voltages in file to pressures using calibration values

File #1

$$exterior_m := \left[(M)^{<0>} - \left(\frac{2838}{4095} \cdot 5 \right) \right] \cdot 500 \qquad cavity_m := \left[(M)^{<2>} - \left(\frac{2860}{4095} \cdot 5 \right) \right] \cdot 500$$

$$windspeed_m := (M)^{<3>} \cdot 180 + 4 \qquad wind_{m_j} := \left(\frac{windspeed_{m_j}}{3.6} \right)^2 \cdot 0.647$$

$difference_m := exterior_m - cavity_m \qquad mean(difference_m) = 1.1 \qquad stdev(difference_m) = 7.5$

$mean(exterior_m) = 8.5 \qquad mean(wind_m) = 35.3 \qquad mean(cavity_m) = 7.4 \qquad mean(direction_m) = 280.6$

$stdev(exterior_m) = 8.5 \qquad stdev(wind_m) = 15.9 \qquad stdev(cavity_m) = 7.3 \qquad stdev(direction_m) = 20.3$

File #2

$$exterior_n := \left[(N)^{<0>} - \left(\frac{2838}{4095} \cdot 5 \right) \right] \cdot 500 \qquad cavity_n := \left[(N)^{<2>} - \left(\frac{2860}{4095} \cdot 5 \right) \right] \cdot 500$$

$$windspeed_n := (N)^{<3>} \cdot 180 + 4 \qquad wind_{n_j} := \left(\frac{windspeed_{n_j}}{3.6} \right)^2 \cdot 0.647$$

$difference_n := exterior_n - cavity_n \qquad mean(difference_n) = 1.3 \qquad stdev(difference_n) = 9.8$

$mean(exterior_n) = 9.7 \qquad mean(wind_n) = 43.3 \qquad mean(cavity_n) = 8.4 \qquad mean(direction_n) = 285.3$

$stdev(exterior_n) = 12.4 \qquad stdev(wind_n) = 19.5 \qquad stdev(cavity_n) = 9.4 \qquad stdev(direction_n) = 8.4$

File #3

$$exterior_p := \left[(P)^{<0>} - \left(\frac{2838}{4095} \cdot 5 \right) \right] \cdot 500 \qquad cavity_p := \left[(P)^{<2>} - \left(\frac{2860}{4095} \cdot 5 \right) \right] \cdot 500$$

$$windspeed_p := (P)^{<3>} \cdot 180 + 4 \qquad wind_{p_j} := \left(\frac{windspeed_{p_j}}{3.6} \right)^2 \cdot 0.647$$

$difference_p := exterior_p - cavity_p \qquad mean(difference_p) = 3.2 \qquad stdev(difference_p) = 7.5$

$mean(exterior_p) = 8.9 \qquad mean(wind_p) = 25.6 \qquad mean(cavity_p) = 5.7 \qquad mean(direction_p) = 280.8$

$stdev(exterior_p) = 9.5 \qquad stdev(wind_p) = 10.9 \qquad stdev(cavity_p) = 7.2 \qquad stdev(direction_p) = 15.4$

Average the time domain values of all files and calculate some statistics.

$$V_{10} := \frac{mean(windspeed_m) + mean(windspeed_n) + mean(windspeed_p)}{3}$$

$$Pdiff := (difference_m + difference_n + difference_p) \cdot \frac{1}{3} \qquad Pwind := (wind_m + wind_n + wind_p) \cdot \frac{1}{3}$$

$$Pext := (exterior_m + exterior_n + exterior_p) \cdot \frac{1}{3} \qquad Pcav := (cavity_m + cavity_n + cavity_p) \cdot \frac{1}{3}$$

$$\sigma_{diff} := (stdev(difference_m) + stdev(difference_n) + stdev(difference_p)) \cdot \frac{1}{3}$$

$$\sigma_{cav} := (stdev(cavity_m) + stdev(cavity_n) + stdev(cavity_p)) \cdot \frac{1}{3}$$

$$\sigma_{ext} := (stdev(exterior_m) + stdev(exterior_n) + stdev(exterior_p)) \cdot \frac{1}{3}$$

$$\sigma_{wind} := (stdev(wind_m) + stdev(wind_n) + stdev(wind_p)) \cdot \frac{1}{3}$$

Present the statistics of the combined records:

$V_{10} = 25.5$ km/h

mean(Pdiff) = 1.9	$\sigma_{diff} = 8.3$	$diff_{mean} := mean(Pdiff)$
mean(Pcav) = 7.2	$\sigma_{cav} = 8$	$cav_{mean} := mean(Pcav)$
mean(Pext) = 9	$\sigma_{ext} = 10.1$	$ext_{mean} := mean(Pext)$
mean(Pwind) = 34.7	$\sigma_{wind} = 15.4$	$wind_{mean} := mean(Pwind)$

Intensity of Turbulence: $\frac{\sigma_{wind}}{wind_{mean}} = 0.44$ $\frac{\sigma_{cav}}{cav_{mean}} = 1.11$ $\frac{\sigma_{ext}}{ext_{mean}} = 1.12$ $\frac{\sigma_{diff}}{diff_{mean}} = 4.41$

Now, take the Fourier transform of all both pressure variations to create pressure spectra.

$ext_m := fft(exterior_m)$ $cav_m := fft(cavity_m)$ $win_m := fft(wind_m)$ $diff_m := fft(difference_m)$

$ext_n := fft(exterior_n)$ $cav_n := fft(cavity_n)$ $win_n := fft(wind_n)$ $diff_n := fft(difference_n)$

$ext_p := fft(exterior_p)$ $cav_p := fft(cavity_p)$ $win_p := fft(wind_p)$ $diff_p := fft(difference_p)$

$N := \frac{size}{2}$ $k := 1..N$ $f_k := \frac{k}{N} \cdot \frac{1}{timestep}$

Note: This calculates the actual frequency which varies with the sampling rate

Average files in the frequency Domain

$$S_{ext_k} := \frac{ext_{m_k} + ext_{n_k} + ext_{p_k}}{3} \qquad S_{cav_k} := \frac{cav_{m_k} + cav_{n_k} + cav_{p_k}}{3}$$

$$S_{wind_k} := \frac{win_{m_k} + win_{n_k} + win_{p_k}}{3} \qquad S_{diff_k} := \frac{diff_{m_k} + diff_{n_k} + diff_{p_k}}{3}$$

Average values to smooth curves $p := 4..(N-3)$ $f_p := \frac{p}{N} \cdot \frac{1}{timestep}$

$$S_{extavg_p} := \left| \frac{S_{ext_{p-1}} + S_{ext_p} + S_{ext_{p+1}} + S_{ext_{p+2}} + S_{ext_{p-2}} + S_{ext_{p-3}} + S_{ext_{p+3}}}{7} \right|$$

$$S_{windavg_p} := \left| \frac{S_{wind_{p-1}} + S_{wind_p} + S_{wind_{p+1}} + S_{wind_{p+2}} + S_{wind_{p-2}} + S_{wind_{p-3}} + S_{wind_{p+3}}}{7} \right|$$

$$S_{cavavg_p} := \left| \frac{S_{cav_{p-1}} + S_{cav_p} + S_{cav_{p+1}} + S_{cav_{p+2}} + S_{cav_{p-2}} + S_{cav_{p-3}} + S_{cav_{p+3}}}{7} \right|$$

$$S_{diffavg_p} := \left| \frac{S_{diff_{p-1}} + S_{diff_p} + S_{diff_{p+1}} + S_{diff_{p+2}} + S_{diff_{p-2}} + S_{diff_{p-3}} + S_{diff_{p+3}}}{7} \right|$$

Calculate the Frequency Response Function function for the presure difference

$$H_{\Delta_k} := \frac{S_{diff_k}}{S_{ext_k}} \qquad K_{\Delta_k} := \left| \sqrt{H_{\Delta_k}} \right| \qquad \phi_{\Delta_k} := atan\left(\frac{Im(H_{\Delta_k})}{Re(H_{\Delta_k})} \right) \cdot \frac{180}{\pi}$$

Calculate the Cavity Frequency Response function.

$$H_{c_k} := \frac{S_{cav_k}}{S_{ext_k}} \qquad K_{c_k} := \left| \sqrt{H_{c_k}} \right| \qquad \phi_{c_k} := atan\left(\frac{Im(H_{c_k})}{Re(H_{c_k})} \right) \cdot \frac{180}{\pi}$$

PRESSURE SPECTRA

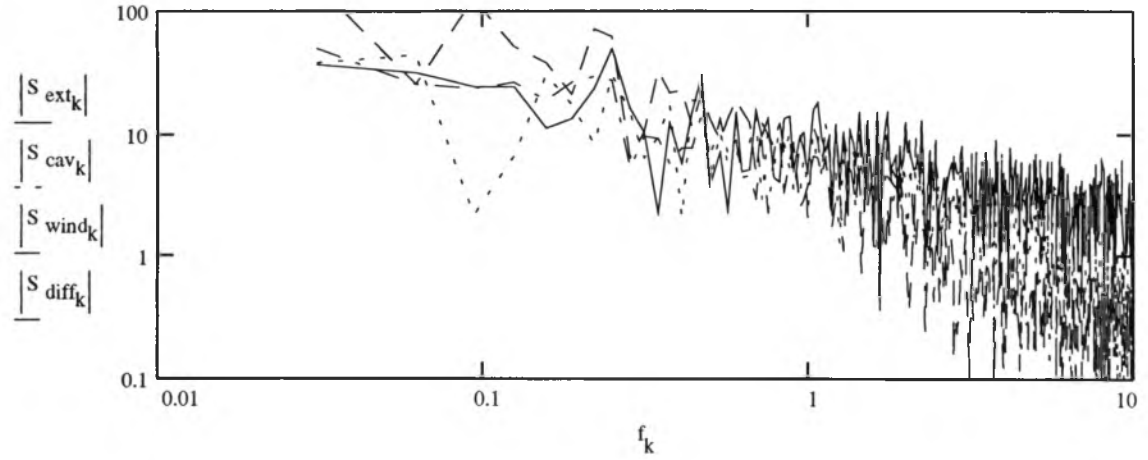

NORMALISED PRESSURE SPECTRA

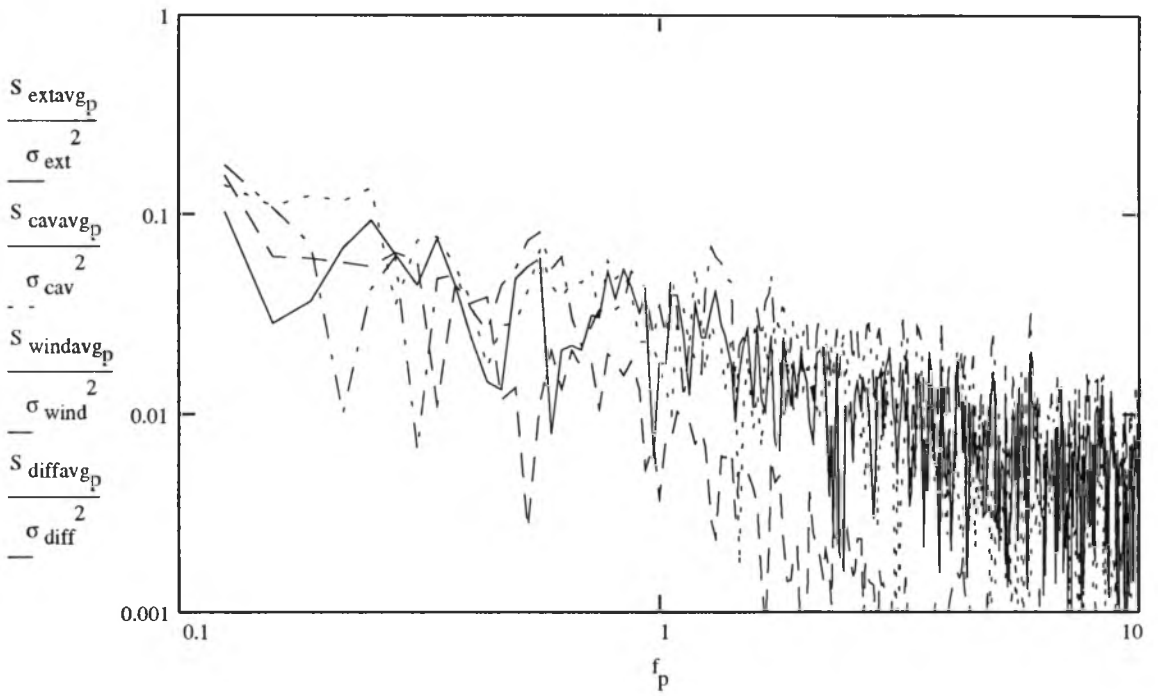

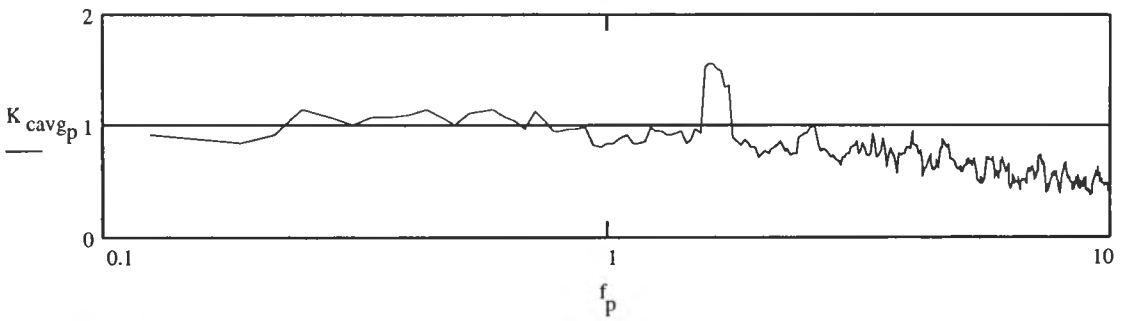

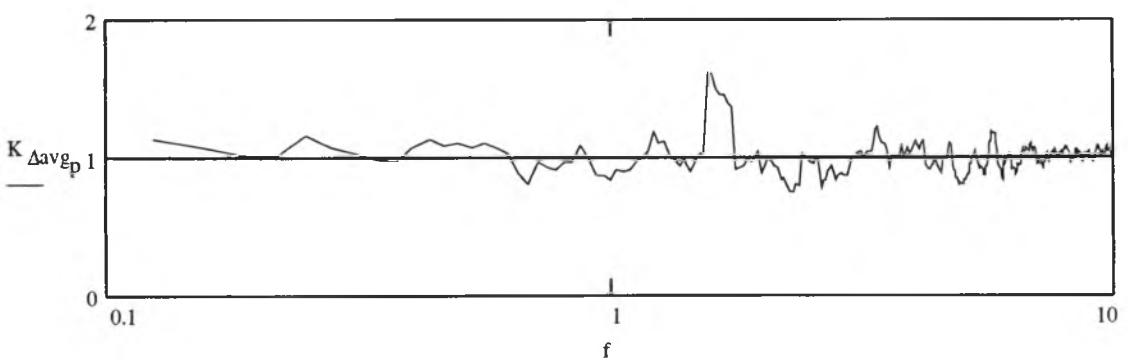

SPECTRA RELATIONSHIPS

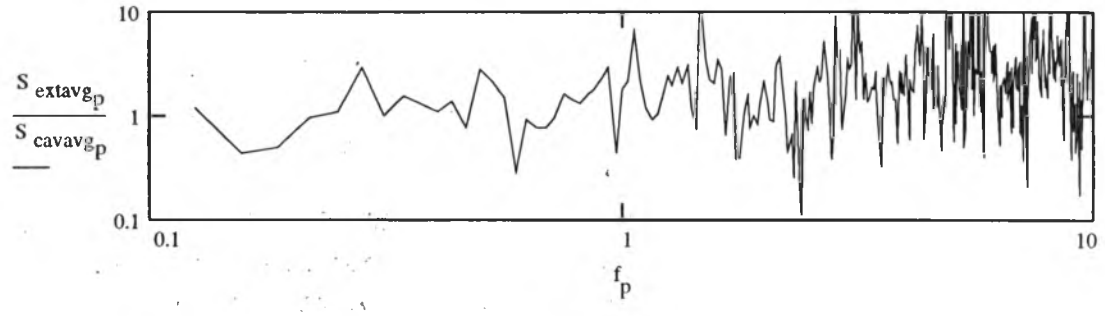

$\frac{S_{extavg_p}}{S_{cavavg_p}}$

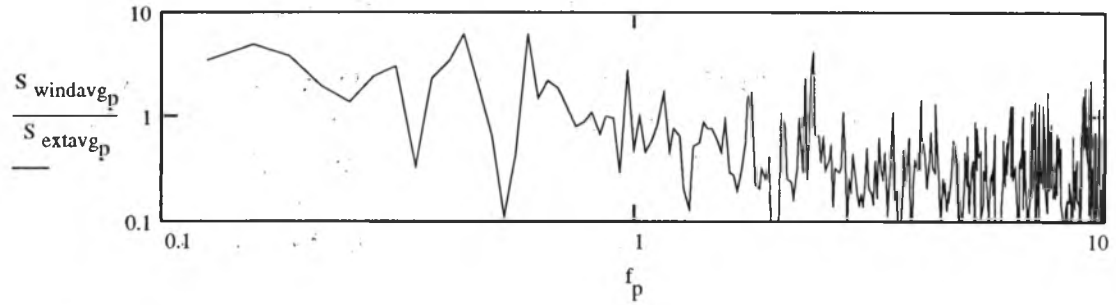

$\frac{S_{windavg_p}}{S_{extavg_p}}$

CAVITY PHASE LAG (Degrees)

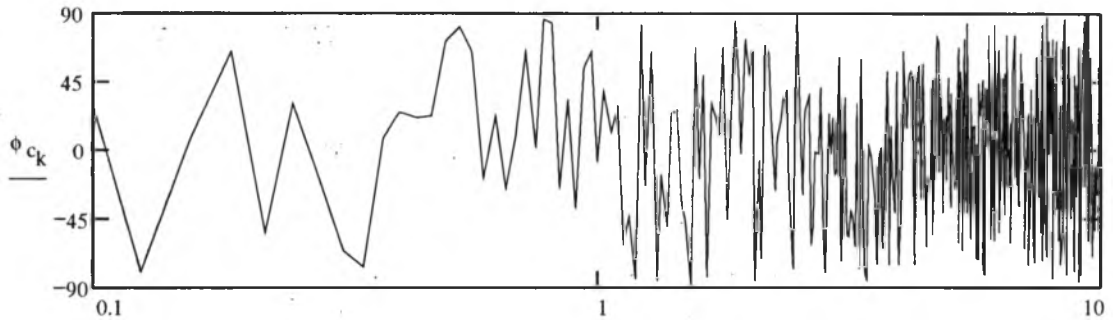

ϕ_{c_k}

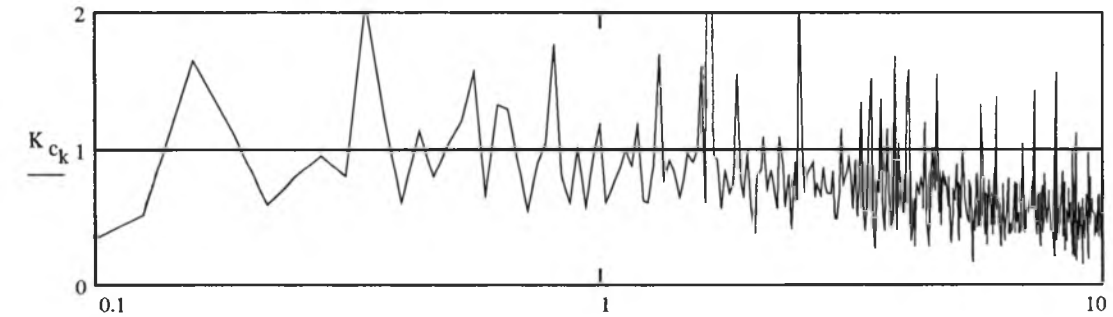

K_{c_k} 1

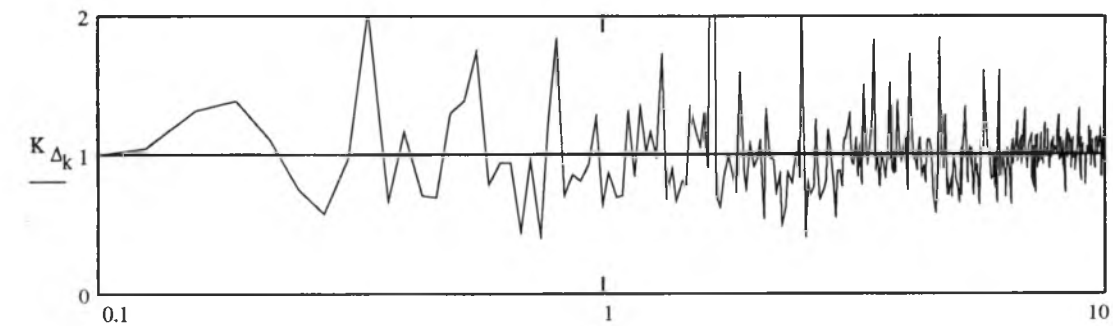

K_{Δ_k} 1

TIME DOMAIN PLOTS OF PRESSURE

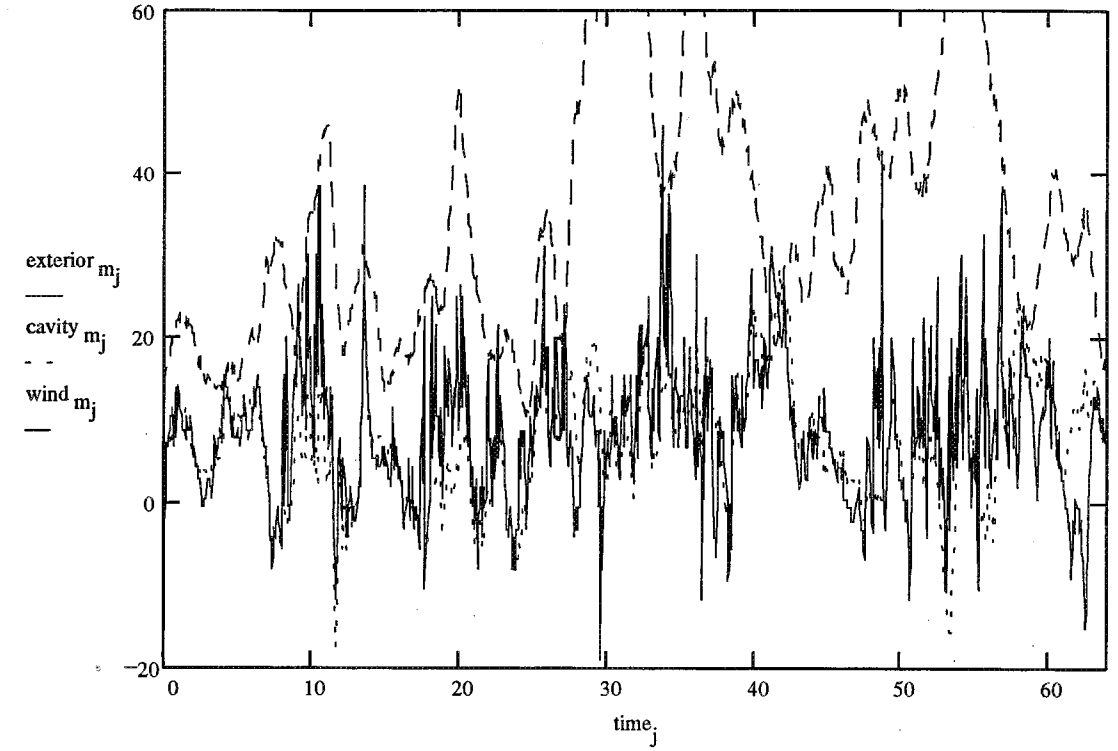

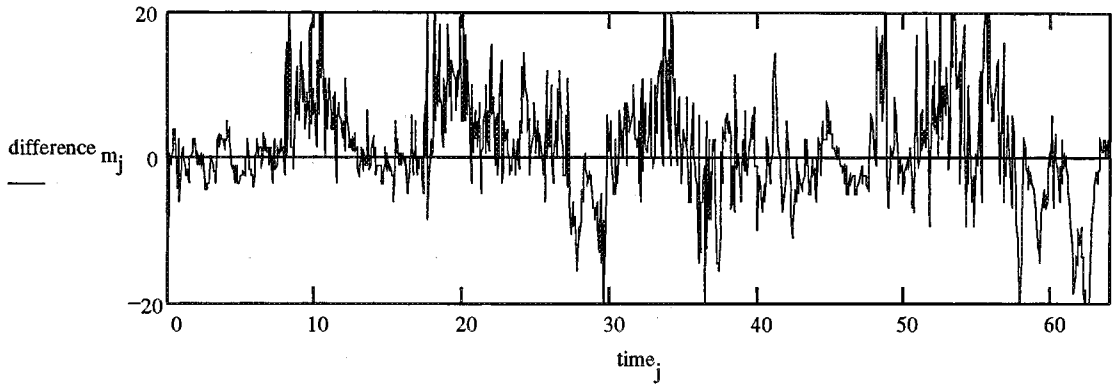

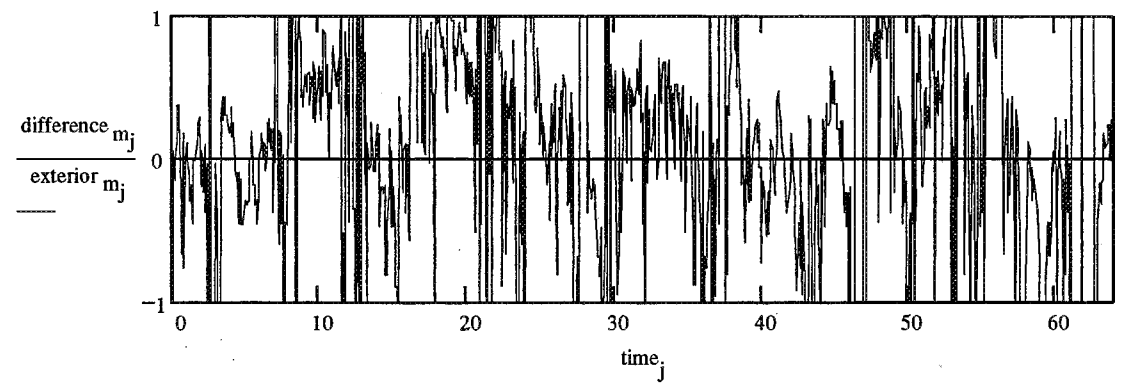

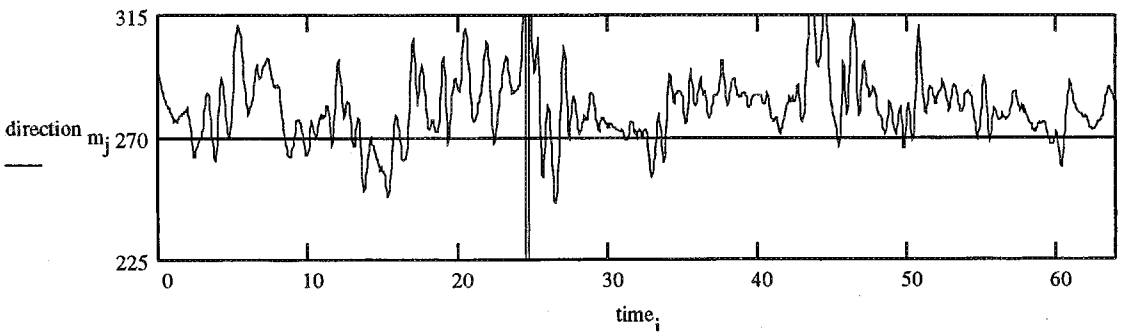

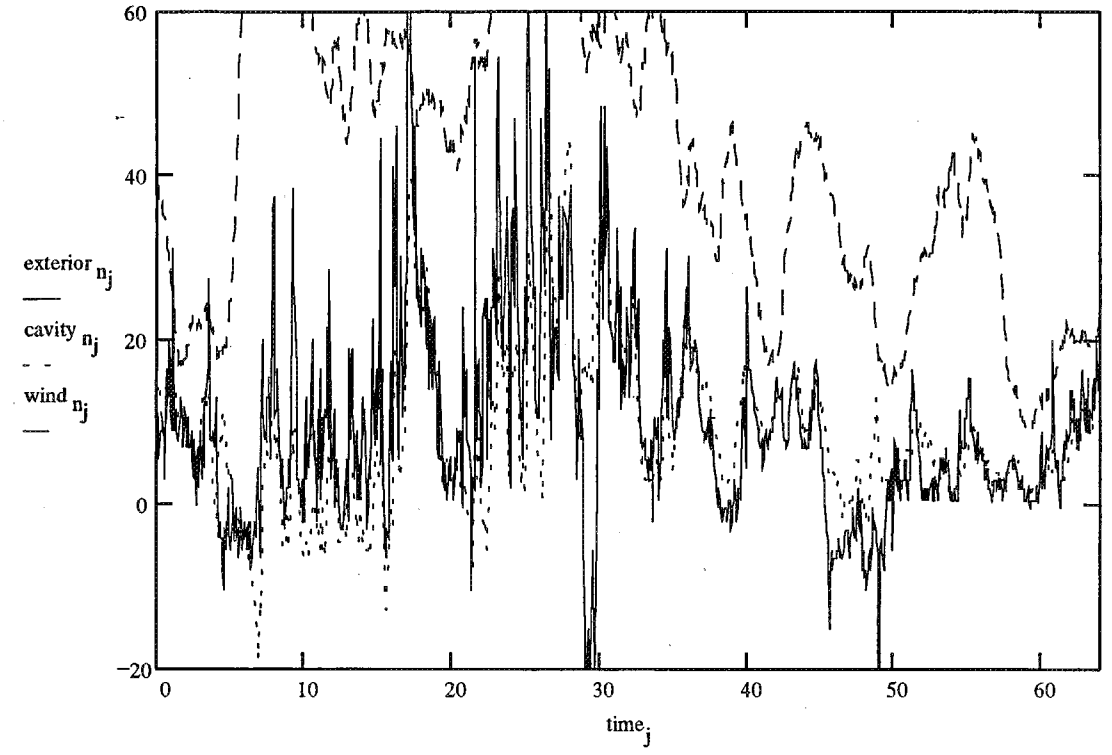
60
40
20
0
−20
0
10
20
30
40
50
60
exterior $_{n_j}$
cavity $_{n_j}$
wind $_{n_j}$
time$_j$

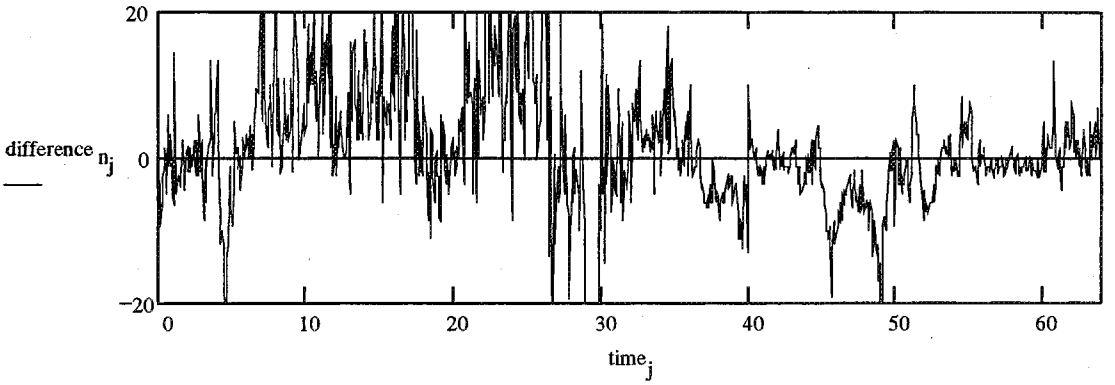
20
0
−20
0
10
20
30
40
50
60
difference $_{n_j}$
time$_j$

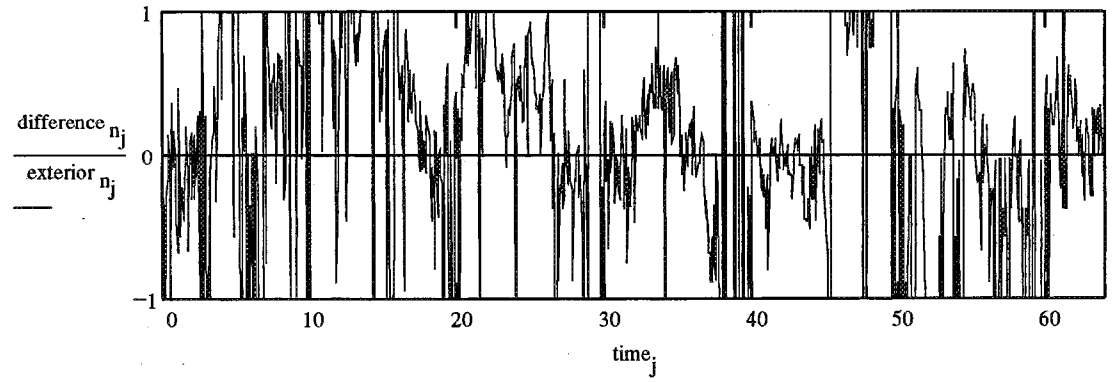
1
0
−1
0
10
20
30
40
50
60
difference $_{n_j}$ / exterior $_{n_j}$
time$_j$

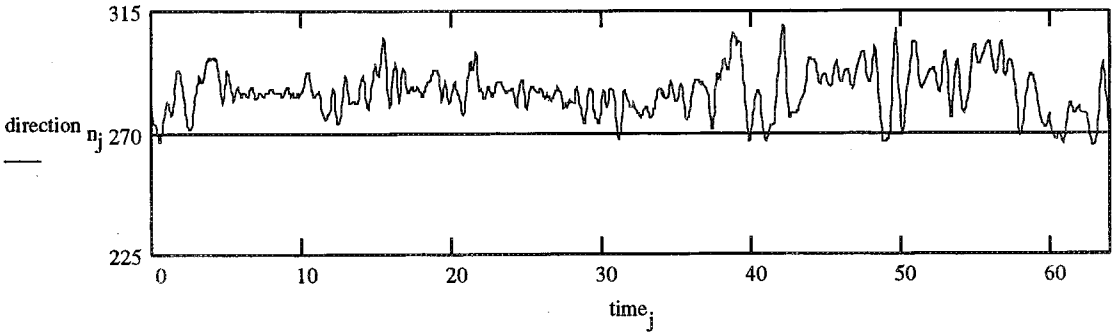
315
270
225
0
10
20
30
40
50
60
direction $_{n_j}$
time$_j$

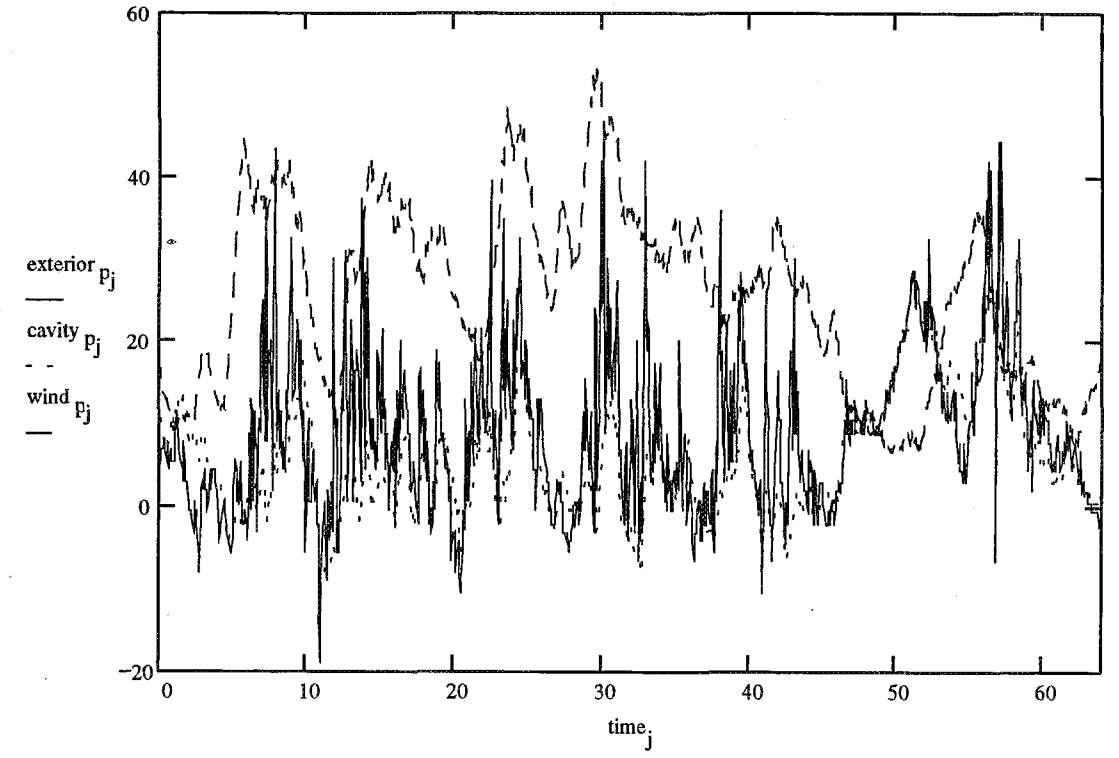
exterior p_j
cavity p_j
wind p_j
60
40
20
0
−20
0
10
20
30
40
50
60
time$_j$

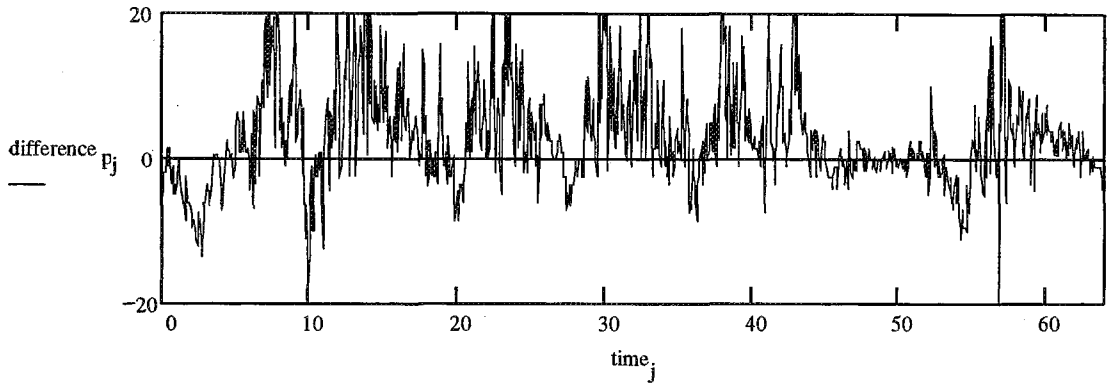
difference p_j
20
0
−20
0
10
20
30
40
50
60
time$_j$

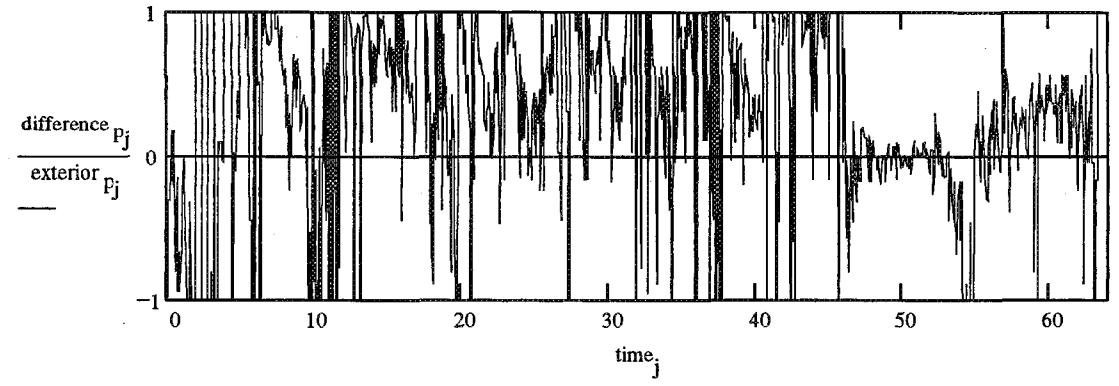
difference p_j / exterior p_j
1
0
−1
0
10
20
30
40
50
60
time$_j$

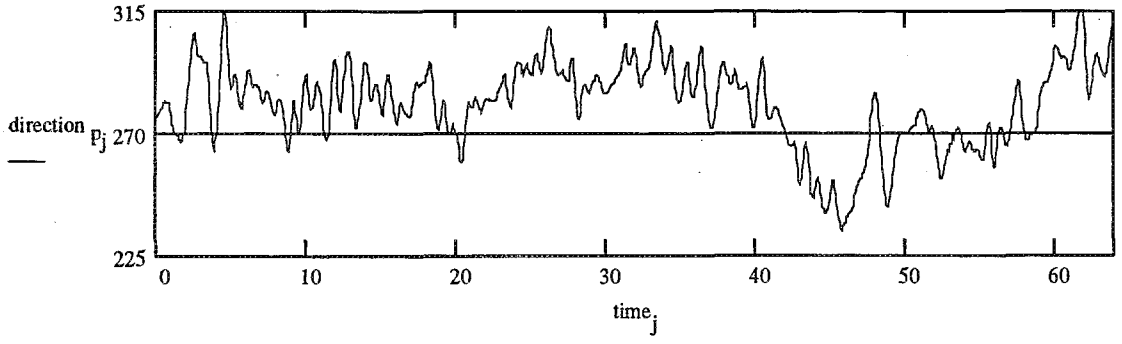
direction p_j
315
270
225
0
10
20
30
40
50
60
time$_j$

Appendix E

Information on:

Data Aquisition Equipment

and

Instrumentation

MODEL 05103
WIND MONITOR

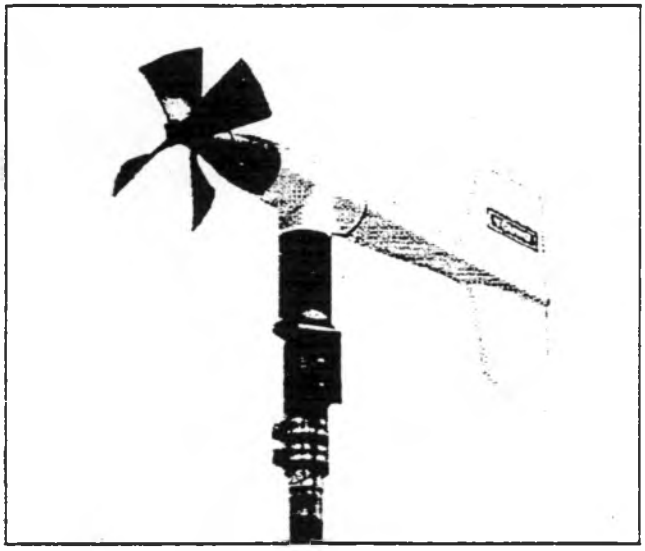

WIND SPEED SPECIFICATION SUMMARY:

Range	0 to 60 m/s (130 mph), gust survival 100 m/s (220 mph)
Sensor	18 cm diameter 4-blade helicoid propeller molded of polypropylene
Pitch	29.4 cm
Distance Constant	2.7 m (8.9 ft.) for 63% recovery
Threshold Sensitivity	1.0 m/s (2.2 mph)
Transducer	Centrally mounted stationary coil, 4K ohm nominal DC resistance
Transducer Output	AC sine wave signal induced by rotating magnet on propeller shaft. 100 mV p-p at 60 rpm. 20 V p-p at 12000 rpm.
Output Frequency	3 cycles per propeller revolution (0.098 m/s per Hz)

WIND DIRECTION (AZIMUTH) SPECIFICATION SUMMARY:

Range	360° mechanical, 355° electrical (5° open)
Sensor	Balanced vane, 38 cm (15 in) turning radius.
Damping Ratio	0.25
Delay Distance	1.3 m (4.3 ft) for 50% recovery
Threshold Sensitivity	1.0 m/s (2.2 mph) at 10° displacement 1.5 m/s (3.4 mph) at 5° displacement
Damped Natural Wavelength	7.4 m (24.3 ft)
Undamped Natural Wavelength	7.2 m (23.6 ft)
Transducer	Precision conductive plastic potentiometer, 10K ohm resistance (±20%), 0.25% linearity, life expectancy 50 million revolutions, rated 1 watt at 40° C, 0 watts at 125° C
Transducer Excitation Requirement	Regulated DC voltage, 15 VDC max
Transducer Output	Analog DC voltage proportional to azimuth angle with regulated excitation voltage applied across potentiometer.

INTRODUCTION

The Wind Monitor measures horizontal wind speed and direction. Originally developed for ocean data buoy use, it is rugged and corrosion resistant yet accurate and light weight. The main housing, nose cone, propeller, and other internal parts are injection molded U.V. stabilized plastic. The nose cone assembly threads directly into the main housing contacting an o-ring seal. Both the propeller and vertical shafts use stainless steel precision grade ball bearings. Bearings have light contacting teflon seals and are filled with a low torque wide temperature range grease to help exclude contamination and moisture.

Propeller rotation produces an AC sine wave signal with frequency proportional to wind speed. This AC signal is induced in a stationary coil by a six pole magnet mounted on the propeller shaft. Three complete sine wave cycles are produced for each propeller revolution.

Vane position is transmitted by a 10K ohm precision conductive plastic potentiometer which requires a regulated excitation voltage. With a constant voltage applied to the potentiometer, the output signal is an analog voltage directly proportional to azimuth angle.

The instrument mounts on standard one inch pipe, outside diameter 34 mm (1.34"). An orientation ring is provided so the instrument can be removed for maintenance and reinstalled without loss of wind direction reference. Both the mounting post assembly and the orientation ring are secured to the mounting pipe by stainless steel band clamps. Electrical connections are made at the terminals in a junction box at the base. A variety of devices are available for signal conditioning, display, and recording of wind speed and direction.

INITIAL CHECK-OUT

When the Wind Monitor is unpacked it should be checked carefully for any signs of shipping damage. Remove the plastic nut on the propeller shaft. Install the propeller on the shaft so the letter markings on the propeller face forward (into the wind). Although the instrument is aligned, balanced and fully calibrated before shipment, it should be checked both mechanically and electrically before installation. The vane and propeller should easily rotate 360° without friction. Check vane balance by holding the instrument base so the vane surface is horizontal. It should have near neutral torque without any particular tendency to rotate. A slight imbalance will not degrade performance.

The potentiometer requires a stable DC excitation voltage. Do not exceed 15 volts. When the potentiometer wiper is in the 5° deadband region, the output signal is "floating" and may show varying or unpredictable values. To prevent false readings, signal conditioning electronics should clamp the signal to excitation or reference level when this occurs. Avoid a short circuit between the azimuth signal line and either the excitation or reference lines. Although there is a 1K ohm current limiting resistor in series with the wiper for protection, damage to the potentiometer may occur if a short circuit condition exists.

Before installation, connect the instrument to an indicator as shown in the wiring diagram and check for proper wind speed and azimuth values. Position the vane over a sheet of paper with 30° or 45° crossmarkings to check vane alignment. To check wind speed, temporarily remove the propeller and connect the shaft to a synchronous motor. Details appear in the CALIBRATION section of this manual.

TECHNICAL DATA

HUMIDITY TRANSMITTERS-HMD/W 30 UB
HUMIDITY AND TEMPERATURE TRANSMITTERS-HMD/W 30YB

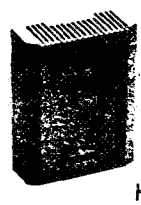

HMW 30 UB/YB

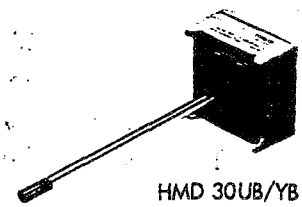

HMD 30UB/YB

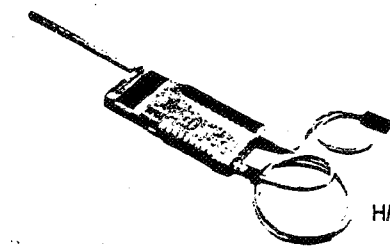

HMK 20

General

Output DC	Supply Voltage DC	AC
0 to 1V	10 to 35V	9 to 24V
0 to 5V	13 to 35V	11 to 24V
0 to 10V	18 to 35V	15 to 24V
0 to 20mA	10 to 35V	9 to 24V (R_L = 0 ohm)
0 to 20mA	19 to 35V	16 to 24V (R_L =500 ohm)

Electrical connections: Screw terminals for wires 0.5 to 1.5 mm² (AWG 20 to 16)

Housing material:

Duct mounted box (HMD 30): Cast aluminum, class IP 65 (NEMA 4)

Bushing: Metal bushing (PG 11) for cable diameter 7 to 12 mm (1/4" to 1/2")

Wall mounted box: (HMW 30): ABS plastic

Sensor protection:

Duct mounted probe (HMD 30): Membrane filter or sintered filter (optional)

Operating temperature range:

Duct mounted (HMD 30): -20 to +80 °C (-4 to +176 °F)

Wall mounted (HMW 30): -5 to +55 °C (+23 to +131°F)

Relative Humidity (HMD/W 30UB and HMD/W 30YB)

Measuring range: 0 to 100% RH

Accuracy at +20°C: ±2% RH (0 to 90% RH)
±3% RH (90 to 100% RH)
(includes calibration uncertainty, non-linearity, non-repeatability)

Temperature coefficient: ±0.04% RH/°C

90% response time: 15 sec with protective filter

Sensor: HUMICAP®

Temperature (HMD/W 30YB)

Electronics accuracy at +20°C: ±0.2 °C

Temperature coefficient: ±0.02°/°C

Linearity: better than 0.1 °C

Sensor: Pt 100 1/3 DIN 43760B

ELECTRONIC CALIBRATOR HMK 20

Operating temperature: -5 to +55 °C (+23 to +131 °F)

Measuring range: 0 to 100% RH

One point calibration range: 0 to 90% RH

Reference probe accuracy: ±2% RH (0 to 90% RH)
±3% RH (90 to100% RH)

One point calibration accuracy: ±2.2% RH (0 to 90% RH)
±3.2% RH (90 to 100% RH)

Specifications subject to change without notice.

Dimensions in mm

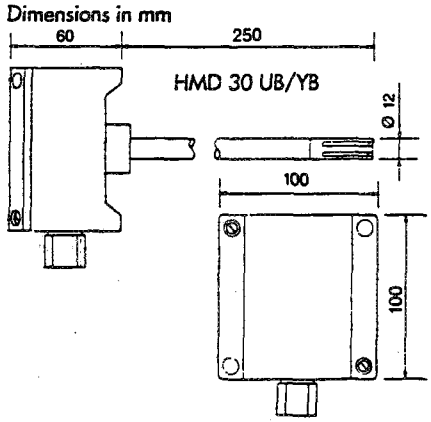

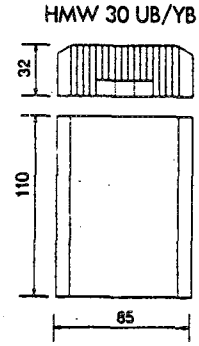

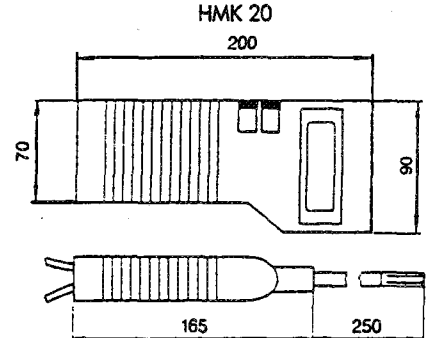

VAISALA
SENSOR SYSTEMS

Vaisala Inc., 100 Commerce Way, Woburn, MA 01801 Phone (617) 933-4500 TWX: 710-348-1332 Telefax: (617) 933-8029

TECHNICAL DATA

HUMIDITY TRANSMITTERS-HMD/W 20 UB
HUMIDITY/TEMPERATURE TRANSMITTERS-HMD/W 20YB

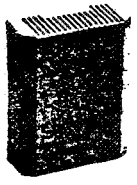

HMW 20 UB/YB

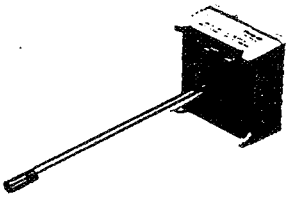

HMD 20 UB/YB

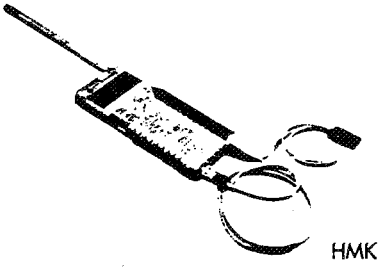

HMK 20

General

Input voltage:	10 to 35 VDC (R_L=0 ohms) 20 to 35 VDC (R_L=500 ohms)
Output signals:	4 to 20 mA
Electrical connections:	Screw terminals for wires 0.5...1.5 mm² (AWG 20 ... 16)
Housing material:	
Duct mounted box (HMD 20):	Cast aluminum, class IP 65 (NEMA 4)
Bushing:	Metal bushing (PG 11) for cable diameter 7...12 mm (1/4" ..1/2")
Tubing:	Stainless steel
Wall mounted box: (HMW 20):	ABS plastic
Sensor protection:	
Duct mounted probe (HMD 20):	ø12 mm membrane filter or sintered filter (optional)
Operating temperature range:	
Duct mounted (HMD 20):	-20 to +80 °C (-4 to +176 °F)
Electronics:	-5 to +55°C (+23 to +131°F)
Wall mounted (HMW 20):	-5 to +55°C (+23 to +131°F)

Relative Humidity (HMD/W 20UB and HMD/W 20YB)

Measuring range:	0 to 100% RH
Accuracy at +20°C:	±2% RH (0 to 90% RH) ±3% RH (90 to 100% RH) (includes calibration uncertainty, non-linearity, non-repeatability)
Temperature coefficient:	±0.04% RH/°C
90% response time:	15 sec with protective filter
Sensor:	HUMICAP®H-Sensor

Temperature (HMD/W 20YB)

Electronics accuracy at +20°C:	±0.2 °C
Temperature coefficient:	±0.02°/°C
Linearity:	better than 0.1 °C
Sensor:	Pt 100 1/3 DIN 43760B

ELECTRONIC CALIBRATOR HMK 20

Operating temperature:	-5 to +55 °C (+23 to +131 °F)
Measuring range:	0 to 100% RH
One point calibration range:	0 to 90% RH
Reference probe accuracy:	±2% RH (0 to 90% RH) ±3% RH (90 to100% RH)
One point calibration accuracy:	±2.2% RH (0 to 90% RH) ±3.2% RH (90 to 100% RH)
Probe dimensions:	ø 12 mm, Length: 250 mm

Specifications subject to change without notice.

Dimensions in mm

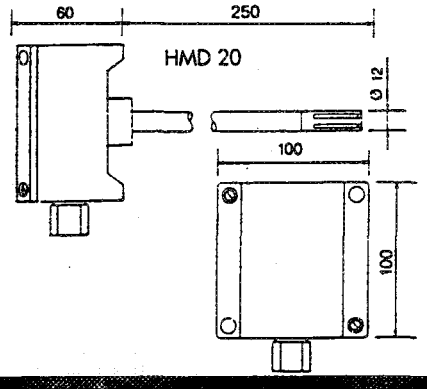

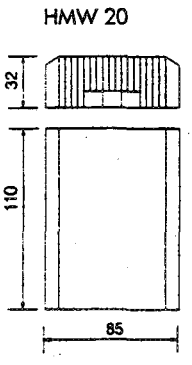

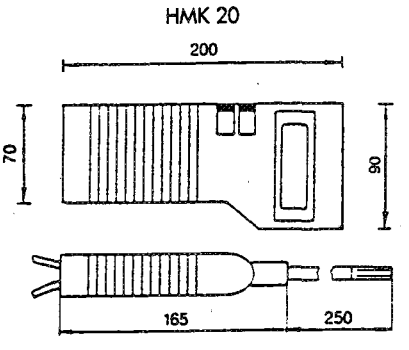

VAISALA
SENSOR SYSTEMS

Vaisala Inc., 100 Commerce Way, Woburn, MA 01801 Phone (617) 933-4500 TWX: 710-348-1332 Telefax: (617) 933-8029

Details of Moisture Content Measurement Technique Using the Electrical-Resistance Method

The following is a description of the method used in this study for measurement of the moisture content of wood. An explanation of the measurement technique is given, followed by the conversion of the measured voltage into a moisture content. These values must then be corrected for both temperature and species. The method of correcting for these is also described.

It is known that if a voltage is applied between two pins (Delmhorst 496C insulated contact pins) the drop in voltage can be measured, translated into a resistance, and subsequently translated into a moisture content. The circuit for this procedure can be shown schematically (from Sciemetric Notes, Oct. 24, 1989, N. Sheaff):

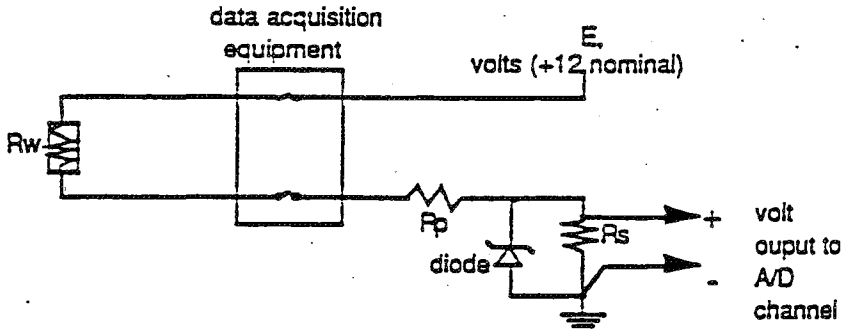

where Rw is the resistance of the wood; Rp is the protection resistor (in case pins are shorted); the triangle is the protection diode which "clamps" the voltage to a 5.1V maximum if pins are shorted; Rs is the sensing resistor; E is the supply voltage; the data acquisition equipment represents the location where the panels are connected to the monitoring equipment.

The above diagram can be simplified to:

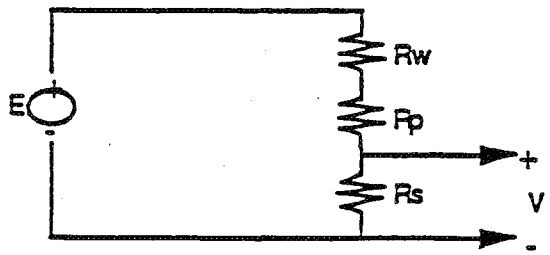

so that in terms of Ohm's Law we can say that:

$$E = IR_{tot}$$

$$E = I(R_w + R_p + R_s)$$

$$I = E/(R_w + R_p + R_s) \quad (1)$$

and

$$V = IR_s$$

$$I = V/R_s \quad (2)$$

For the same current (I), equate equations (1) and (2):

$$\frac{V}{E} = \frac{R_s}{R_w + R_p + R_s} \quad (3)$$

where E is the known constant voltage input and R_s and R_p are known resistors. Therefore, in terms of the resistance of the wood:

$$R_w = R_s\left(\frac{E}{V}\right) - R_p - R_s \quad (4)$$

In our case, R_p = 100180 Ω, R_s = 100250 Ω and E 13.324 V.

In order to translate the resistance of wood into a moisture content, a Delmhorst Meter was used. The Delmhorst Meter (model RC-1D) involves, in simple terms, the probe and the meter. The probe hooks up to the meter and consists of two pins. When the pins penetrate wood, a voltage is passed through them and a moisture content is read directly from the meter. Since water is a conductor, the principle is: the more moisture, the lower the resistance.

In order to find the relationship between resistance and moisture content, a series of resistors was used. The exact resistance across the resistors was measured. The resistors were then placed across the pins of the Delmhorst meter and the associated moisture content read. The results from this calibration were plotted (moisture content (%) versus the log (base 10) of the resistance (kΩ)). Now, given a resistance, R_w, a moisture content can be established, and later corrected. A fifth-order polynomial equation was found to fit the curve when $\log(R_w)$is less than 4. When $\log(R_w)$ is greater than or equal to 4 a linear approximation was established.

For $\log(R_w) < 4$

$$M = 622.34 - 896.79(\log(R_w)) + 535.02(\log(R_w)^2 - 156.95(\log(R_w))^3 + 22.441(\log(R_w)^4 - 1.2503(\log(R_w))^5 \quad (5)$$

For $\log(R_w) \geq 4$

$$M = 30.75403 - 3.68473(\log(R_w)) \quad (6)$$

7.7.1 Species and Temperature Correction

In order to calculate the corrected moisture contents, the following equations were used [5]:

$$M_C = (S - 0.0081\ t)\ M + (.57 - .043\ t) \quad (7)$$

if M is below fibre saturation

$$M_C = (3 - 0.028\ t)\ M - 25$$

if M is above fibre saturation

where M is the uncorrected moisture content (eq. (5) or eq. (6)), t is the measured temperature at that location and S is the appropriate species correction factor, where S=1.515 for Jack Pine [5], S=1.45 for Spruce [2] and S=1.261 for Balsam Fir [5]. It should be noted that, on the advise of Dr. Don Onysko at Forintek Canada Corp., the above equation for M above fibre saturation was altered slightly from the one given originally [5].

$$M_C = (3 - 0.028\ t)\ M - 24.63 \quad (8)$$

if M is above fibre saturation

The change allows for the fact that the majority of the wood studs are Jack Pine, and the equation used in the paper [5] accommodates the fact that it is difficult to identify whether the wood is spruce, pine or fir (S-P-F). The resulting difference in moisture content between the equation used and that given for SPF is only 0.37% moisture content.

The geometric breakpoint (which is the intersection of two linear lines and is not the fibresaturation point, as shown in Figure 7.6) is found by equating the above two equations, where

$$B = \frac{(-25.2 + 0.043\ t)}{(S - 3 + .0199\ t)} \quad (9)$$

Equation 9 is used if M is less than B, and equation 10 is used if M is greater than B.

Variation in the Supply Voltage, E

The value of the supply voltage is not perfectly constant. As this value (E) is not stored on disc, it was determined that E=13.324 V is correct 'most of the time'. Even so, the small fluctuations that do occur in this value (between approximately 13 V and 13.5 V) are not critical in the calculation of wood moisture, as shown below:

If, for example, the measured output voltage is V = .04 volts, and E = 13.324 volts, S = 1.515, at 20°C, calculate R_W:

$$R_W = 100.25\left(\frac{13.324}{0.04}\right) - 100.18 - 100.25 = 33192.845\ k\Omega \qquad (4)$$

$$\log (R_W) = 4.521$$

$$M = 30.75403 - 3.68473\ (\log (R_W)) = 14.095 \qquad (6)$$

Now find the breakpoint (B) where t = 20°C:

$$B = \frac{(-25.2 + .043\ t)}{(S - 3 + .0199\ t)} = 22.39 \qquad (9)$$

since M < B

$$M_C = (1.515 - .0081\ (20))(14.095) + (.57 - .043\ (20)) = 18.78\ \% \qquad (7)$$

If the measured output voltage is V = .04 volts, and E = 13.5 volts (variation of 0.176 V or 1.3%), S = 1.515, at 20°C, calculate R_W:

$$R_W = 100.25\left(\frac{13.5}{.04}\right) - 100.18 - 100.25 = 33633.945\ k\Omega \qquad (4)$$

$$\log (R_W) = 4.5268$$

$$M = 30.75403 - 3.68473\ (\log (R_W)) = 14.074 \qquad (6)$$

B = 22.39 @ t = 20°C (as before)

since M < B

$$M_C = (1.515 - .0081\ (20))(14.074) + (.57 - .043\ (20)) = 18.75\ \% \qquad (7)$$

If the measured output voltage is V = .04 volts, and E = 13.0 volts (a variation of 0.324 V or 2.4%), S = 1.515, at 20°C, calculate R_w:

If, E = 13.0 volts and V = .04 volts, calculate R_w:

$$R_w = 100.25\left(\frac{13.0}{.04}\right) - 100.18 - 100.25 = 32380.82\ k\Omega \quad (4)$$

$$\log(R_w) = 4.5103$$

$$M = 30.75403 - 3.68473(\log(R_w)) = 14.135 \quad (6)$$

since $M < B$ @ $t = 20°C$

$$M_c = (1.515 - .0081\ (20))(14.135) + (.57 - .043\ (20) = 18.83\ \% \quad (7)$$

The difference in moisture contents, as calculated above, are relatively small when considering that each moisture content per hour is an average of ten readings, and these hourly averages are further averaged over one day.

Appendix F

Data Loss Diary

From: November 1, 1991 To: December 31, 1992

Data Diary
Nov 1,1991 to December 31, 1992

BEG001: Computer monitoring Temperatures and Relative Humidity
BEG003: Computer monitoring Relative Humidity, Supply Air Properties, and Climate

November

1 Monitoring Day =1
4 Accidental power shutdown for one hour
28 BEG003 lost 2 hours; disk I/O error.

December

1 Monitoring Day =31
16 BEG003 lost 11 hours
17 BEG003 lost 17 hours, BEG001 lost 9 hours; unknown reason.
18 BEG001 lost 16 hours.
30 BEG001 computer lost 9 hours, BEG003 lost 9 hours,why?
31 Both computers saved no data; power failure with no reboot?

January

1 Monitoring Day =62
Both computers saved no data
2 Both computers lost 10 hours of data, presumably all due to the power failure.
6 BEG003 lost one hour. Accidental power shutdown for one hour.
7 BEG003 lost 12 hours.
Panel Dosing Begins at 11:00 a.m.
8 BEG003 lost 10 hours.
14 BEG001 lost 1 hours and BEG003 lost 11 hours. Bad supply voltage as well. Power spikes caused failures.
15 BEG003 lost 12 hours.
20 BEG003 lost 10 hours. Disk I/O error .

February

1 Monitoring Day =93
4 BEG003 lost 2 hours. Disk I/O error.
5 BEG003 lost 17 hours. Same disk I/O error.
7 BEG003 lost 9 hours while computer brought away and replaced.
8 BEG003 lost 19 hours since 'new' computer not saving to disk.
10 BEG003 lost 1 hour.
11 BEG003 lost 14 hours.
12 BEG003 lost 1 hour.
15 Both computers down for 4 hours due to large area power outage.
19 BEG003 lost 10 hours.

March

1 Monitoring Day =122
BEG003 lost 3 hours.

17 No data was recorded for this date.
18 BEG001 lost 21 hours.The lost time on BEG001 was caused when a very large number of errors were saved to disk. The software problem in Copilot was fixed.
20 BEG003 lost 15 hours. Typical Disk I/O error.
21 BEG003 lost 9 hours. As above.
26 Both computers lost one hour while diagnostics were run. Multiplexer reads a correct value again starting at 16:00.
27-30 Supply voltage falls within range again for these days; cards reconnected.
31 Supply voltage out of range. Multiplexer card goes bad again as of 10:00.

June

1 Monitoring Day =214
3 BEG003 lost 8 hours. Disk error. Bad cards disconnected at 17:00.
4 BEG001 lost 6 hours and BEG003 lost 22 hours.
Supply voltage normal because errant cards were again disconnected since problem was finally discovered. Swap with other non-NRC cards was made while the cards were fixed.
Panel temperature and wood moisture data return to normal.
5 Both computers were down for 9 hours. Disk drive problems while running diagnostics caused these problems. Power supply checks and multiplexer cards swapped to minmise data loss. Supply voltage out of range.
22 BEG003 lost 14 hours.

July

1 Monitoring Day =244
BEG003 lost 14 hours. Disk error started at 11:00.
2 BEG003 lost 8 hours. Disk error fixed at morning check.
10 Took other readings and suspended BEG003. Vacuums down & replaced.
11 BEG003 lost 16 hours.
12 BEG003 lost 24 hours.
13 BEG003 17 hours.
19 BEG003 lost 2 hours.
20 BEG003 lost 24 hours
21 BEG003 lost 8 hours. Vaccuum down @8:30, replaced 14:00 on the 24th.
25 BEG003 lost 11 hours.
26 BEG003 lost 24 hours.
27 BEG003 lost 17 hours. Disk save error.
30 BEG003 lost 15 hours.
31 BEG003 lost 8 hours. Disk save error from yesterday to today check.

August

1 Monitoring Day =275
3 BEG003 lost 7 hours.
4 BEG003 lost 8 hours. Disk error since 18:00
At the end of August and into September the vacuums failed to provide enough heat at intervals. This caused the A/C to freeze and affect supply air properties.

September

1 Monitoring Day =306
2 BEG003 and BEG001 lost 10 hours.
3 BEG003 and BEG001 lost 14 hours. 24 hour test resulted in monitoring freeze.
4 BEG003 and BEG001 lost 13 hours.
5-6 Monitoring suspended for two days during other testing.
7 BEG003 and BEG001 lost 12 hours.
9 BEG003 lost 13 hours.
10 BEG003 lost 14 hours.
15 BEG001 lost 1 hours.
16 BEG003 lost 10 hours.
17 BEG003 lost 18 hours.
18 BEG003 lost 1 hours.
19 BEG003 lost 10 hours. The errors from the 9th were all unnoticed at the time and rectified themeselves.
20-22 Monitoring suspended for three days for other testing.
23 BEG003 lost 10 hours. New vacuums installed. No more significant freezing problems.
24 BEG001 lost 13 hours. No file for BEG003.
25 Testing interrupted monitoring.
26 BEG003 and BEG001 lost 15 hours.
27 BEG003 lost 1 hours.
28 BEG003 lost 9 hours. Disk save error from 23:00 to 9:00.

October

1 Monitoring Day =336
BEG003 lost 5 hours.
2 BEG003 lost 7 hours.
5 BEG003 lost 1 hour.
7 BEG003 lost 1 hour.
13 BEG003 lost 1 hour.
22 BEG003 lost 9 hours. All of the above errors self-corrected.
23 BEG003 lost 8 hours and BEG001 lost 16 hours.
Disk error overnight and on the 24th on BEG003 and the video card blew on BEG001.
25 BEG001 lost 21 hours.Video card replaced by 21:00.
28 BEG003 lost 15 hours.
29 BEG003 lost 10 hours. Did not save from last check.

November

1 Monitoring Day =367
No Data Loss. But more problems with vacuum power level. This caused considerable freezing over of the A/C at times. The vacuums were replaced on the 20th but required tuning before all was smooth again on the 23rd @ 23:00.
The North panel flow was shut off from Nov 6 @16:30 until Nov. 24 @18:00. to ensure the proper flow to the other panels.

December

1	Monitoring Day =397
19	Vacuum died again. Conditioning of supply air stopped.
31	Monitoring Day 427.BEG003 lost 7 hours.